UNIVERSITI SAINS MALAYSIA

Laporan Akhir Projek Penyelidikan Jangka Pendek

Ductility Demands Of Inelastic Structures Affected By Repeated Earthquakes

by
Assoc. Prof. Dr. Taksiah A Majid
Assoc. Prof. Dr. Choong Kok Keong
Dr. Lau Tze Liang
Dr. Shaharudin Shah Zaini

2014

	Date :

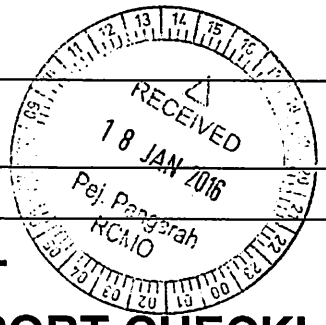

UNIVERSITI SAINS MALAYSIA

RU GRANT
FINAL REPORT CHECKLIST

Please use this checklist to self-assess your report before submitting to RCMO.
Checklist should accompany the report.

NO.	ITEM	PLEASE CHECK (✓)		
		PI	JKPTJ	RCMO
1	Completed Final Report Form	✓		✓
2	Project Financial Account Statement (e-Statement)	✓		✓
3	Asset/Inventory Return Form *(Borang Penyerahan Aset/Inventori)*	–		TIADA ASET
4	A copy of the publications/proceedings listed in Section D(ii) (Research Output)	✓		✓
5	Comprehensive Technical Report	✓		✓
6	Other supporting documents, if any			
7	Project Leader's Signature	✓		✓
8	Endorsement of PTJ's Evaluation Committee	✓		✓
9	Endorsement of Dean/ Director of PTJ's			✓

Project Code :
(for RCMO use only)

RU GRANT
FINAL REPORT FORM

Please email a softcopy of this report to rcmo@usm.my

A	**PROJECT DETAILS**
i	**Title of Research:** **DUCTILITY DEMANDS OF INELASTIC STRUCTURES AFFECTED BY REPEATED EARTHQUAKES**
ii	**Account Number:** **1001/PAWAM/814115**
iii	**Name of Research Leader:** **ASSOC. PROF. DR. TAKSIAH A.MAJID**
iv	**Name of Co-Researcher:** 1. ASSOC. PROF. DR. CHOONG KOK KEONG 2. DR. LAU TZE LIANG 3. DR. SHAHARUDIN SHAH ZAINI
v	**Duration of this research:** **a) Start Date : 1 Jan 2011** **b) Completion Date : 31 Dec 2013** **c) Duration : 2 years** **d) Revised Date (*if any*) : 31 Dec 2014**
B	**ABSTRACT OF RESEARCH**
	This research work investigated the influence of repeated earthquakes on the maximum roof and story ductility demands of the 3-dimensional inelastic reinforced concrete frames. A total of 8400 nonlinear time history analyses had been conducted using generic frames with number of story, N equal to 3, 6, 12, and 18.. Each model is assigned to have behaviour factors of 1, 1.5, 2, 4, and 6 referring to Eurocode 8 to represent ductility class low, medium, and high. The plastic hinge of members considered the stiffness and strength degrading hysteresis rule to represent reinforced concrete structure. The single, double, and triple events of synthetic repeated earthquakes were considered with a total of twenty ground motions for each event. Some interesting findings are provided showing that repeated earthquakes significantly increase the story ductility demand of inelastic concrete frames. On average, relative increment of maximum story ductility demand is experienced 1.4 and 1.3 times when double and triple events of repeated earthquakes are induced, respectively. Empirical relationships are also provided to predict these increments where their efficiency is presented examining characteristic 3- and 8-story reinforced concrete buildings.

C BUDGET & EXPENDITURE

i

Total Approved Budget : RM 240,300.00

Yearly Budget Distributed

Year 1 : RM 18,150.00
Year 2 : RM 108,850.00
Year 3 : RM 113,300.00

Total Expenditure : RM 240,189.70

Balance : RM 110.30

Percentage of Amount Spent (%) : 99.95%

 # Please attach final account statement (eStatement) to indicate the project expenditure

ii **Equipment Purchased Under Vot 35000**

No.	Name of Equipment	Amount (RM)	Location	Status
	-	-	-	-

 # Please attach the Asset/Inventory Return Form (Borang Penyerahan Aset/Inventori) – Appendix 1

D RESEARCH ACHIEVEMENTS

i **Project Objectives** *(as stated/approved in the project proposal)*

No.	Project Objectives	Achievement
1	To identify the effect of FFGM and NFGM in repeated earthquakes on the ductility demand of the 3D generic MDOF systems.	Completed
2	To identify the effect of oscillatory character, γ, and pulse period, T_p, of repeated NFGM coupled orthogonally with non-pulse NFGM on the ductility demand of 3D generic MDOF systems.	Completed

3	To identify the effect of structure's fundamental period and number of story, force reduction factor, type of material of MDOF frame, on the ductility demand of 3D generic MDOF system.	Completed
4	To develop and propose empirical relation formula for ductility demand of 3D generic MDOF system due to repeated earthquake taking into account the effect of structure's fundamental period and number of story, force reduction factor, type of material of MDOF frame, repeated FFGM or NFGM, oscillatory character and pulse period of repeated NFGM, and seismic sequence cases.	Completed

ii Research Output

a) Publications in ISI Web of Science/Scopus

No.	Publication (authors,title,journal,year,volume,pages,etc.)	Status of Publication (published/accepted/ under review)
1	Tan, C.G., Majid, T.A., Ariffin, K.S., Muhammad Bunnori, N., (2012), Site-Specific Empirical Correlation between Shear Wave Velocity and Standard Penetration Resistance using MASW Method, 2012 IEEE Colloquium on Humanities, Science and Engineering Research, (CHUSER), 3-4 Dec 2012, Sutera Harbour Resort, Kota Kinabalu, Sabah	Published
2	Mohd Zaid, M.Z.A., Majid, T.A., and Ade Faisal, (2012), Effect of repeated near field earthquake to the high-rise RC building, Australian Journal of Basic and Applied Sciences (AJBAS), 6 (10), pp129-138	Published
3	Tan, C.G., Majid, T.A., Ariffin, K.A. and Bunnori, N.M. (2013) Effects of Site Classification on Empirical Correlation between Shear Wave Velocity and Standard Penetration Resistance for Soils, *Applied Mechanics and Materials*, 284-287, pp. 1305-1310	Published
4	Ade Faisal., Majid, T.A., and Hatzigeorgiou, G.D. (2013). Investigation of story ductility demands of inelastic concrete frames subjected to repeated earthquakes. *Soil Dynamics and Earthquake Engineering*, 44, pp.42-53.	Published
5	Adiyanto, M.I., and Majid, T.A. (2014). Seismic design of two storey reinforced concrete building in Malaysia with low class ductility, *Journal of Engineering Science and Technology*, 9(1), pp.27-46.	Published
6	Tan, C.G., Majid, T.A., Ariffin, K.S. and Bunnori, N.M. (2014), Seismic microzonation for Penang using geospatial contour mapping, Natural Hazards, Springer, Feb 2014, Vol 73 (2), pp 657-670, ISSN 0921-030X, (DOI) 10.1007/s11069-014-1093-8	Published
7	Fadzli Mohamed Nazri, Tan Chee Ghuan, Shahrul Nizam Hussin and Taksiah A. Majid (2015), Evaluation of soil flexibility of the reclaimed area in Penang using the non-destructive method, Natural Hazards, DOI 10.1007/s11069-015-1770-2	Published
8	Adiyanto, M.I, Majid, T.A., and Nazri, F.M. (2016). Comparison study of seismic design of RC frame in East Malaysia with	Under review

	various behavior factor. *Jurnal Teknologi.*	
9	Majid, T.A., Hamid, N.H.A., Adiyanto, M.I., and Nazri, F.M. (2016). Visual damage observation of cyclic loading test on RC frame designed to EC8. *Journal of Earthquakes and Structures.*	Under review

b) Publications in Other Journals

No.	Publication (authors,title,journal,year,volume,pages,etc.)	Status of Publication (published/accepted/ under review)
1	Adiyanto, M.I., and Majid, T.A. (2013). Influence of behaviour factor on seismic design of two storey reinforced concrete building in Malaysian seismic region, *Australian Journal of Basic and Applied Sciences*, 7(8), pp.411-419.	Published
2	Majid, T.A., Adiyanto, M.I., and Nazri, F.M. (2014). Nonlinear response of low rise hospital RC building in Malaysia due to far and near field earthquake, *Journal of Civil Engineering Research*, 4(3A), pp.130-134.	Published
3	Tan, C. G., Majid, T. A., Ariffin, K. S. and Bunnori, N. M. (2014). The Effect of Site Classification on Incremental Dynamic Analysis for RC Buildings without Seismic Provision in Penang. Journal of Civil Engineering Research 4(3A): 154-158. doi:10.5923/c.jce.201402.23 (Scientific and Academic Publishing)	Published

c) Other Publications
(book,chapters in book,monograph,magazine,etc.)

No.	Publication (authors,title,journal,year,volume,pages,etc.)	Status of Publication (published/accepted/ under review)

d) Conference Proceeding

No.	Conference (conference name,date,place)	Title of Abstract/Article	Level (International/National)
1	Proceedings of the International Conference on Engineering and Technology Innovation (ICETI2012), 2-6 Nov 2012, Kaohsiung, Taiwan	Effects of Site Classification on Empirical Correlation between Shear Wave Velocity and Standard Penetration Resistance for Soils	International
2	AWAM International Conference on Civil Engineering (AICCE'12), Penang, 28-30 August, 2012, pp 830-839	Seismic Performance of 3 Storey Irregular Reinforced Concrete (RC) Frames Under Repeated Earthquakes,	International
3	Conference on Advances in Civil, Structural, Environmental, & Bio-Technology, 7-8 Mac 2014, Kuala Lumpur, Malaysia	Effect of behaviour factor on column design of reinforced concrete frame.	International
4	International Congress on Natural Sciences and Engineering, 5-7 May 2014,	Seismic performance of three storey hospital RC frame subjected to multiple earthquake in	International

	Kyoto, Japan.	moderate seismic region.	
5	The 5th Asia Conference on Earthquake Engineering, 16 – 18 October 2014, Taipei, Taiwan.	Cost optimization of seismic design of low rise hospital RC frame in Malaysia.	International

 # Please attach a full copy of the publication/proceeding listed above

iii **Other Research Ouput/Impact From This Project**
(patent, products, awards, copyright, external grant, networking, etc.)

- Networking with UiTM for laboratory testing
- Networking with DPRI for Disaster Risk Management (Earthquake)

E **HUMAN CAPITAL DEVELOPMENT**

a) Graduated Human Capital

Student	Nationality (No.)		Name
	National	International	
PhD	1	1	1. Ade Faisal (2012) 2. Tan Chee Ghuan (2014)
MSc	4		1. Mohd Irwan Adiyanto 2. Mohd Zulham Affandi Mohd Zahid 3. Muhammad Khairul Azuan Muhammad 4.Sabila Ahmad Basir 5. Hamed Fazli Manoochehr
Undergraduate			1. Zarina Yahya 2. Alvin Leong Chee Wei 3. Wong Zi Min 4. Chen Siew Siew

	15		5. Tahara Ramadzan Md Kassim 6. Tan Kai Hong 7. Nur Soleha Abdul Rahim 8. Ling Nieng Chen 9. Tan Kah Beng 10. Seah Ivy 11. Thoo Wei Bing 12. Law Kar Wen 13. Ng Acying 14. Soo Wei Jie 15. Amanina Nabilah binti Mohamed Kamal

b) On-going Human Capital

Student	Nationality (No.)		Name
	National	International	
PhD	2	1	1. Mohd Irwan Adiyanto – viva 6 Jan 2016 2. Tahara Ramadzan Md Kassim 3. Omid Hassanshani
MSc			1. 2.
Undergraduate			1. 2.

c) Others Human Capital

Student	Nationality (No.)		Name
	National	International	
Post Doctoral Fellow	1		1. Tan Chee Ghuan (April – August 2016)
Research Officer			1. 2.
Research Assistant			1. Mohd Irwan Adiyanto 2. Tahara Ramadzan Md Kassim 3. Omid Hassanshani 4. Muhammad Khairul Azuan Muhammad 5. Tan Chee Ghuan
Others (.....)			1. 2.

F COMPREHENSIVE TECHNICAL REPORT

Applicants are required to prepare a comprehensive technical report explaining the project. The following format should be used (this report must be attached separately):

- Introduction
- Objectives
- Methods
- Results

	• Discussion • Conclusion and Suggestion • Acknowledgements • References
G	**PROBLEMS/CONSTRAINTS/CHALLENGES IF ANY**
	(Please provide issues arising from the project and how they were resolved) The initial proposal in 2010 on experimental work at Canterburry University was changed to UiTM laboratory (simpler set up – static push over loading and slight modification of the research objective no 3) due to Canterburry Earthquake on 4th September 2010. This caused delay and extention of research period to another 1 year.
H	**RECOMMENDATION**
	(Please provide recommendations that can be used to improve the delivery of information, grant management, guidelines and policy, etc.)

Project Leader's Signature:

.....

Name : TAKSIAH A. MAJID

Date : 5 Jan 2016

I	COMMENTS, IF ANY/ENDORSEMENT BY PTJ'S RESEARCH COMMITTEE

This research study has successfully yielded beneficial outcomes for effect of repeated earthquakes on RC structures. Human capital development/training has also been achieved. Networking with other research bodies/institutes has also been established for further expansion of the research study. This research study has successfully achieved its objectives.

Signature and Stamp of Chairperson of PTJ's Evaluation Committee

Assoc. Prof. Dr. Choong Kok Keong
Deputy Dean (Research)
School of Civil Engineering
Engineering Campus
Universiti Sains Malaysia

Name :

Date :

Prof. Dr. Ahmad Farhan Mohd Sadullah
Dekan
Pusat Pengajian Kejuruteraan Awam
Kampus Kejuruteraan
Universiti Sains Malaysia

14/1/16

Signature and Stamp of Dean/ Director of PTJ

Name :

Tarikh Cetakan : 04/12/2015

UNIVERSITI SAINS MALAYSIA

JABATAN BENDAHARI

PENYATA PERBELANJAAN SEHINGGA 4 DISEMBER 2015

Projek :

No. Akaun : 1001.PAWAM.814115.

Vot	Nama Vot	Peruntukan Projek	Perbelanjaan Terkumpul Sehingga Thn Lalu	Baki Peruntukan Tahun Lalu	Peruntukan Thn Semasa	Jumlah Peruntukan Thn Semasa	Tanggungan Semasa	Bayaran Thn Semasa	Jum Belanja Thn Semasa	Baki Projek
111	GAJI	34,775.36	0.00	34,775.36	0.00	34,775.36	0.00	2,881.40	2,881.40	31,893.96
221	PERJALANAN DAN SARA HIDUP	82,236.72	0.00	82,236.72	0.00	82,236.72	1,025.00	2,058.53	3,083.53	79,153.19
222	PENGANGKUTAN BARANG-BARANG	8,000.00	0.00	8,000.00	0.00	8,000.00	0.00	0.00	0.00	8,000.00
223	PERHUBUNGAN DAN UTILITI	424.40	0.00	424.40	0.00	424.40	0.00	0.00	0.00	424.40
224	SEWAAN	-1,136.00	0.00	-1,136.00	0.00	-1,136.00	0.00	0.00	0.00	-1,136.00
226	BEKALAN BAHAN MENTAH	27,730.00	0.00	27,730.00	0.00	27,730.00	0.00	0.00	0.00	27,730.00
227	BEKALAN DAN BAHAN LAIN	-53,975.98	0.00	-53,975.98	0.00	-53,975.98	0.00	49,703.30	49,703.30	-103,679.28
228	PENYELENGGARAN & PEMBAIKAN KECIL	1,000.00	0.00	1,000.00	0.00	1,000.00	0.00	0.00	0.00	1,000.00
229	PERKHIDMATAN IKTISAS & HOSPITALITI	-42,352.37	0.00	-42,352.37	0.00	-42,352.37	800.00	95.60	895.60	-43,247.97
552	PERBELANJAAN LAIN	-28.00	0.00	-28.00	0.00	-28.00	0.00	0.00	0.00	-28.00
	Jumlah	**56,674.13**	**0.00**	**56,674.13**	**0.00**	**56,674.13**	**1,825.00**	**54,738.83**	**56,563.83**	**110.30**

Penyata ini adalah cetakan komputer tiada tandatangan diperlukan

Penyata ini adalah dianggap tepat jika tiada maklumbalas dalam tempoh masa 14 hari dari tarikh penyata

UNIVERSITI SAINS MALAYSIA

Pusat Pengajian Kejuruteraan Awam
School Of Civil Engineering

Kampus Kejuruteraan
Engineering Campus
Universiti Sains Malaysia
Seri Ampangan, 14300 Nibong Tebal
Seberang Perai Selatan
Pulau Pinang
Malaysia
T : 04-599 6201
F : 04-594 1009
W : www.civil.eng.usm.my

Tarikh : 11 Januari 2016

Pengarah
Pejabat Pengurusan & Kreativiti Penyelidikan
Bahagian Penyelidikan & Inovasi
Universiti Sains Malaysia

Tuan,

LAPORAN AKHIR GERAN PENYELIDIKAN UNIVERSITI (RU)

Dengan hormatnya perkara di atas mohon dirujuk.

Bersama-sama ini disertakan perkara berikut untuk perhatian dan tindakan pihak tuan selanjutnya.

Laporan Akhir Geran Penyelidikan Universiti (RU)

Bil.	Nama Penyelidik	Tajuk Penyelidikan
1	Prof. Madya Dr. Taksiah A Majid	*'Ductility Demands of Inelastic Structures Affected by Repeated Earthquakes* '

Sekian, kerjasama tuan saya dahului dengan ucapan terima kasih.

'BERKHIDMAT UNTUK NEGARA'
'Memastikan Kelestarian Hari Esok'

PROF. MADYA DR. CHOONG KOK KEONG
Timbalan Dekan [Penyelidikan]

s.k. Prof. Madya Dr. Taksiah A Majid

ckk/ zss...

Ea. Iqram
Utk semakan dan tindakan lanjut. TK.
20/1/16

UNIVERSITI SAINS MALAYSIA

BORANG PENYERAHAN ASET / INVENTORI

==========

A. BUTIR PENYELIDIK

1. NAMA PENYELIDIK :PROF MADYA DR TAKSIAH A.MAJID
2. NO STAF : AE 50131
3. PTJ :P.P.KEJ.AWAM
4. KOD PROJEK : 1001/PAWAM/814115
5. TARIKH TAMAT PENYELIDIKAN : 31 DEC 2015

RECEIVED 18 JAN 2016 Pej. Pengarah RCMO

B. MAKLUMAT ASET / INVENTORI

BIL	KETERANGAN ASET	NO HARTA	NO. SIRI	HARGA (RM)
	-			

C. PERAKUAN PENYERAHAN

Saya dengan ini menyerahkan aset/ inventori seperti butiran B di atas kepada pihak Universiti:

.....

(TAKSIAH A.MAJID) Tarikh: 5 Jan 2016

D. PERAKUAN PENERIMAAN

Saya telah memeriksa dan menyemak setiap alatan dan didapati :

☐ Lengkap
☐ Rosak
☐ Hilang : Nyatakan.....
☐ Lain-lain : Nyatakan .....

Tiada alat

Diperakukan Oleh :

.....

Tandatangan
Pegawai Aset PTJ

Nama : Zulkefly Hussin
Tarikh : 14/1/16

*Nota : Sesalinan borang yang telah lengkap perlulah dikemukakan kepada Unit Pengurusan Harta, Jabatan Bendahari dan Pejabat RCMO untuk tujuan rekod.

CHUSER

2012 IEEE Colloquium on Humanities, Science and Engineering Research

3rd-4th December 2012

Sutera Harbour Resort, Kota Kinabalu, Sabah, Malaysia

Sponsors:

IEEE Malaysia IEEE Malaysia PES IEEE Malaysia PEL/IE/IA Joint Chapter

www.mypels.org/mypels

CONTENTS

WELCOME MESSAGE

On behalf of the Organizing Committee of CHUSER 2012 it gives me great pleasure in welcoming all delegates to Kota Kinabalu, Malaysia.

The event is held from 3 to 4 December 2012 at the The Magellan Sutera Resort, Kota Kinabalu, Malaysia and is jointly sponsored by the IEEE Malaysia, the IEEE Malaysia Power Electronics (PEL)/Industrial Electronics (IE)/ Industrial Applications (IA) Joint Chapter and the IEEE Malaysia Power and Energy Chapter.

The occasion creates a forum for scientists, engineers and practitioners on the varied Humanities, Science & Engineering related areas and its associated applications.

We have received approximately some 406 paper submissions from 18 countries for the event. In line with the quality control emphasis in recent IEEE initiatives; over 2500 reviewers worldwide volunteered to evaluate papers of which finally only 171 papers are to be presented with up to 6 parallel technical sessions. The ISCAIE 2012 &PECON 2012, which runs concurrently, provides a combined 8 parallel technical sessions , 3 parallel tutorial sessions and four (4) distinguished keynote speaker with another 230 technical papers giving a total of over 400 papers.

Appreciating international participation we have created a special gala dinner with a cultural show. Throughout these events, we hope to create an opportunity for old friends and colleagues to get together, and more importantly, to welcome new peers in diverse areas of expertise.

On behalf of the organizing committee we would like to take this opportunity to express our gratitude to all reviewers who have been working hard to finish reviews on time and hence ensured the success of this event. We would like to thank all authors, session chairpersons, reviewers and delegates for your great support and contribution to the event. Last but not least are the Organizing Committee, colleagues and friends who have been working behind-the-scenes; who deserve special mention. Without their unfailing cooperation, hard work and dedication, this event would simply not be possible.

I understand that many delegates are here in Malaysia for the first time. I would like to encourage you to explore the beautiful sights of Malaysia during your stay and do enjoy the conference.

Zulhabri Ismail, General Chair (CHUSER 2012)
Mustafar Kamal Hamzah, Co-Chair (PECON 2012)
Habibah Hashim, Co-Chair (ISCAIE 2012)

ORGANIZING COMMITTEE

General Chairs
Zulhabri Ismail
Mustafar Kamal Hamzah

General Co-Chair
Habibah Hashim

Technical Program Chair
Oskar Hasdinoor Hassan

Publication Chair :
Mohammad Nawawi Seroji

Publicity & Website Chair :
Syed Abdul Mutalib Al Junid

Technical Program Committee :
Azilah Saparon, Universiti Teknologi MARA
Biswajeet Pradhan, Universiti Putra Malaysia
Ezlina Ahnuar, International Islamic University
Habibah Hashim, Universiti Teknologi MARA
Mohd Khairul Mohd Salleh, Universiti Teknologi MARA
Nurul Zahirah Mokhtar Azizi, Limkokwing University of Creative Technolgy
Rosmadi Fauzi, Universiti Malaya
Kamal Zuhairi Zamli, Universiti Sains Malaysia
Oskar Hasnidor Hassan, Universiti Teknologi MARA
Yee Hooi Min, Universiti Teknologi MARA

11:20 ***Site-Specific Empirical Correlation Between Shear Wave Velocity and Standard Penetration Resistance Using MASW Method***

Chee Ghuan Tan (Universiti Sains Malaysia, Malaysia); Taksiah A. Majid (Coordinator of Disaster Research Nexus, Malaysia); Kamar Shah Ariffin (Assoc. Prof, Lecturer, Malaysia); Norazura Muhamad Bunnori (Universiti Sains Malaysia & USM, Malaysia)

In seismic engineering, dynamic property of the soil is one of the most important aspects in ground response analysis. It is significantly affected by the presence soil deposits of the site. Generally, the average shear wave velocity at top 30 m (Vs30) of soil deposit is used to represent stiffness of the soil and is one of the important parameters to determine the soil amplification factor on the ground surface and site classification. Vs30 is usually determined by carry out wave propagation test on the field. However, it is not economically feasible to conduct test at all sites. Therefore, a reliable empirical correlation between shear wave velocity and standard penetration resistance (Nspt) would be useful since the ease of obtaining the Nspt from site investigation report. Although there are quite a number of these empirical correlations available in literature, but they are region specific and cannot be applicable to all region. In this study, Multichannel Analysis of Surface Wave (MASW) is employed to obtain the shear wave velocity profile of site which needed to develop the empirical regression equations between Vs and Nspt for sand, silt and clay. MASW test has been carried out on the twenty sites which posses of Nspt profiles around Penang Island. The empirical regression equations developed by the study area are exhibit good prediction performance. It can be used for the area which consist of soft to stiff clay and silt and loose to dense sand.

11:40 ***Throughfall, Stemflow and Interception Loss of Artificial Tropical Forest***

Azinoor Azida Abu Bakar (Universiti Teknologi MARA, Malaysia); Aminuddin Baki (Universiti Teknologi MARA, Malaysia); Nurakmal Hamzah (Universiti Teknologi MARA, Malaysia); Zulkifli Yusop (Universiti Teknologi Malaysia, Malaysia); Muhammad Khairudin Khalil (Depatrment of Irrigation and Drainage Malaysia, Malaysia)

An interception study of man-made forest was carried out in Bukit Lagong Reserved Forest. Out of 18 rainfall event recorded, all 18 events produce throughfall but only 15 events with measured stemflow. Two plots of 20m x 20m each were established to measure the distribution of interception (gross rainfall, Pg, throughfall, Tf and stemflow, Sf) and identify the percentage of forest canopy cover over the plotted area. Hemispherical photography method using fisheye lens was applied to capture canopy cover image over the plots. The forest plots were occupied with mixed dipterocarp trees consist of two canopy levels with 90% to 98% of canopy cover. The range of interception loss for this study is 1% to 73% with average of 30% of total gross rainfall. The relationship between interception loss and gross rainfall show a moderate correlation with r2 values of 0.3002. The canopy cover does impose significant effect to the loss of rainfall interception. From point-correlation, the interception loss (%) is increase proportionally to the canopy cover (%) with r2 values of 0.4559.

12:00 ***Use of Multi-Temporal Remote Sensing Data and GIS for Wetland Change Monitoring and Degradation***

Yasser Ghobadi (Geospatial Information Science Research Center, Faculty of Engineering, University Putra Malaysia, Malaysia); Biswajeet Pradhan (University Putra Malaysia (UPM) & Institute of Advanced Technology, Malaysia); Keivan Kabiri (Geospatial Information Science Research Center, Faculty of Engineering, University Putra Malaysia & Department of Satellite Oceanography, National Institute for Oceanography (INIO), Malaysia); Saied Pirasteh (Faculty of Environment, University of Waterloo, Canada); Helmi Shafri (Universiti Putra Malaysia, Malaysia); Gholamabbas Sayyad (Soil Science Group, Shahid Chamran University of Ahvaz, Iran)

Wetlands are transitional lands between Terrestrial and aquatic system that provide many goods and services including flood water retention, water quality maintenance, wildlife habitat, and soil erosion control. To prevent further loss of wetlands, and conserve existing wetland ecosystem for biodiversity and ecosystem services and goods, it is important to inventory and monitor wetlands and their adjacent uplands. During last decade remotely sensed data have been utilized for inventorying and monitoring wetlands. Satellite remote sensed data can also provide information on surrounding land use and their change over the time. The main objective of this study is assessment of wetland change and degradation using time series satellite data, GIS and ancillary data in Hoor Al Azim wetland. Study area is located in the southwest of Iran bordering with Iraq and lies within the latitude 31°28′4″ N and longitude 47° 56′ 57″ E in north of Persian Gulf. This wetland is mainly feed by Karkheh River. In this study, four images were used for 1985 (Landsat MSS), 1999 (Landsat ETM+), 2002 (Landsat ETM+) and 2011 (Landsat ETM+). Landsat image acquired in 2002 geometrically was registered by Google earth and was chosen as the reference image and other images were geometrically registered based on this image. Subsequently, image analysis and processing was performed on mentioned images. Then all the resultant maps were assessed in GIS framework. The results showed spatial reduction in the studied wetland has occurred ~72% due to increase in agricultural land, increase in water demands and also anthropogenic activities in the upstream areas of wetland.

Site-Specific Empirical Correlation between Shear Wave Velocity and Standard Penetration Resistance using MASW Method

Chee-Ghuan Tan
School of Civil Engineering, Universiti Sains Malaysia, Penang, Malaysia
tuc_kheen@hotmail.com

Taksiah A. Majid
Disaster Research Nexus, School of Civil Engineering, Universiti Sains Malaysia, Penang, Malaysia

Kamar Shah Ariffin
School of Material and Mineral Resources, Universiti Sains Malaysia, Penang,Malaysia

Norazura Mohamad Bunnori
School of Civil Engineering, Universiti Sains Malaysia, Penang, Malaysia
Malaysia

Abstract—**In seismic engineering, dynamic property of the soil is one of the most important aspects in ground response analysis. It is significantly affected by the presence soil deposits of the site. Generally, the average shear wave velocity at top 30 m (V_{s30}) of soil deposit is used to represent stiffness of the soil and is one of the important parameters to determine the soil amplification factor on the ground surface and site classification. V_{s30} is usually determined by carry out wave propagation test on the field. However, it is not economically feasible to conduct test at all sites. Therefore, a reliable empirical correlation between shear wave velocity and standard penetration resistance (N_{spt}) would be useful since the ease of obtaining the N_{spt} from site investigation report. Although there are quite a number of these empirical correlations available in literature, but they are region specific and cannot be applicable to all region. In this study, Multichannel Analysis of Surface Wave (MASW) is employed to obtain the shear wave velocity profile of site which needed to develop the empirical regression equations between V_s and N_{spt} for sand, silt and clay. MASW test has been carried out on the twenty sites which posses of N_{spt} profiles around Penang Island. The empirical regression equations developed by the study area are exhibit good prediction performance. It can be used for the area which consist of soft to stiff clay and silt and loose to dense sand.**

Keywords- Shear wave velocity profile, Multichannel analysis of surface wave (MASW), Standard penetration resistance, Empirical correlation

I. INTRODUCTION

The most important aspect in earthquake engineering is to determine the dynamic soil properties. The dynamics soil properties able to provide the important information of the dynamic response of the soil-structure which needed in dynamic structural analysis of the superstructures. The local soil structure also play a major role in the seismic soil amplification of a site which is a critical factor affecting the level of ground shaking [1]. However, lacking of understanding the geological information of the site often responsible for structure and environmental failure occurred. The soil stiffness and soil amplification factor on ground surface are always presented by V_{s30}.

Field measurement of shear wave velocity includes cross-hole test, downhole test, suspension logging, seismic reflection, seismic refraction and surface wave. However, surface wave test is simpler and efficient technique compared to other in-situ test in measuring the shear wave velocity. It is not economically feasible to conduct test at all sites. Therefore, a reliable empirical correlation between shear wave velocity and standard penetration resistance (N_{spt}) would be useful since the ease of obtaining the N_{spt} from site investigation report. Several researchers have proposed empirical correlation for shear wave velocity based on standard penetration test [2-5]. However, these empirical correlations are region specific and cannot be applicable to all regions.

II. SURFACE WAVE METHOD

Surface wave geophysical methods have been developed few decades ago and lots of application in geotechnical engineering. Surface wave geophysical methods able to determine dynamic properties of soil, particularly the shear wave velocity profile as well as the shear modulus. These properties are main parameters in estimating the soil response and soil-structure interaction to seismic loading [6]. Surface wave methods offer advantages over other surface based in-situ seismic techniques is rapid, cost effective, noninvasive and ability to detect low velocity layer underneath higher velocity layer of deposit provides more accurate site characterization.

A. Multichannel Analysis of Surface Waves (MASW)

Spectral analysis of surface wave (SASW) method was introduced by Stokoe and Nazarian [7] which focuses on analyzing the ground roll dispersion relation to produce near-surface S-wave velocity profile. The main drawbacks are time consuming and inherent difficulties when evaluating and distinguishing signal from noise with only a pair of receivers. To overcome the few drawbacks of the SASW method, a new technique Multichannel Analysis of Surface Waves (MASW) was developed by four-phase research project team from Kansas Geological Survey. Multi-station recording permits a single survey of a broad depth range and higher levels of redundancy with a single field configuration compared with SASW [8]. A multichannel shot gather decomposed into a swept frequency record allows the fast generation of an accurate dispersion curve. This dispersion curve is then used to determine the shear-wave velocity profile for the shallow-depth layer of soil [9].

This study was supported by the Postgraduate Research Grant Scheme given by Universiti Sains Malaysia.

B. Field Test Set up and Procedure

Extensive MASW tests were carried out in the Penang Island as shown in Fig. 1. GEOMETRICS-24 channels seismograph (Geode) with single geode operating software (SGOS) is used for the MASW tests. 24 units of vertical geophones with natural frequency of 4.5 Hz were used to receive the wave signal generated by an active source of 8 kg sledgehammer vertically hit on a striker plate. Geophones were deployed linearly with equal spacing in the range of 0.5 to 2 m interval as suggested by Maheswari et al. [1]. The nearest source to geophone offsets are in the range of 5 to 15 m to meet the requirement of different type of soil hardness suggested by Xu et al. [10]. The planer characteristic of surface waves evolve only after some distant from the source and hence it normally need to be greater than half of the maximum desired wavelength. The field configuration of MASW is illustrated in Fig. 2. The acquired wave data from the field measurement were analysis using SeisImager software and can be summarized to two main steps: (i) develop the dispersion curves of Rayleigh wave phase velocity and (ii) inversion of dispersion curve to obtain the shear wave velocity profiles. At first, the raw wiggle plot obtained from the field test was filtered to reduce the random noise effect and interference with other waves as shown in Fig. 3(a). After filtered, only surface wave is used in generating the dispersion curve analysis. The amplitude of body wave and higher mode of Rayleigh wave may dominate over the fundamental mode at high frequencies range if the raw data is not well filtered. Only fundamental mode of Rayleigh wave is picked from the frequencies of 5-8 to 40-50 Hz as shown in Fig. 3(b) to generate dispersion curve with signal to noise ratio (S/N) (Fig. 3(c)). The dispersion curve was inverted to estimate the shear wave velocity profile as shown in Fig. 4. Fig. 5 shows the typical shear wave velocity profile and N_{spt}.

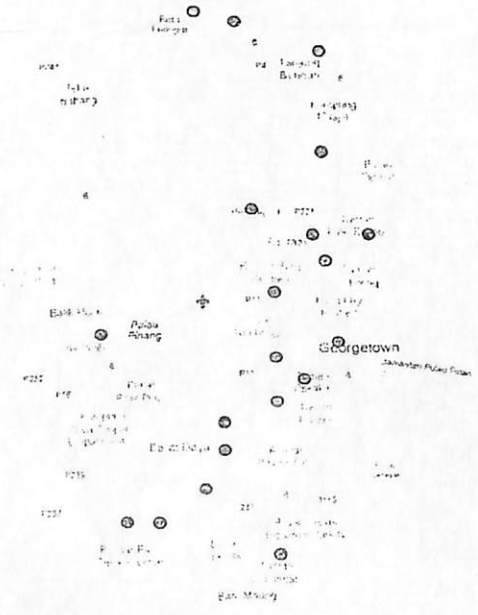

Figure 1. Location of geophysical investigation

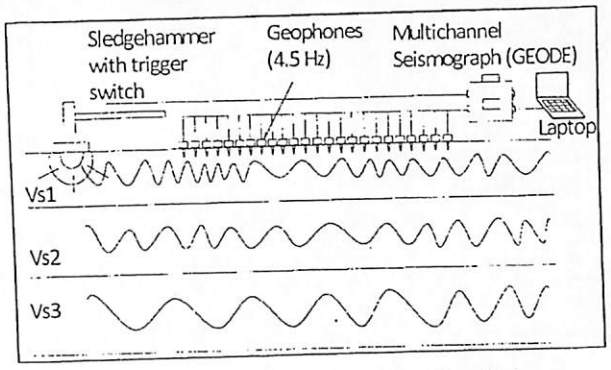

Figure 2. Field configuration of MASW method

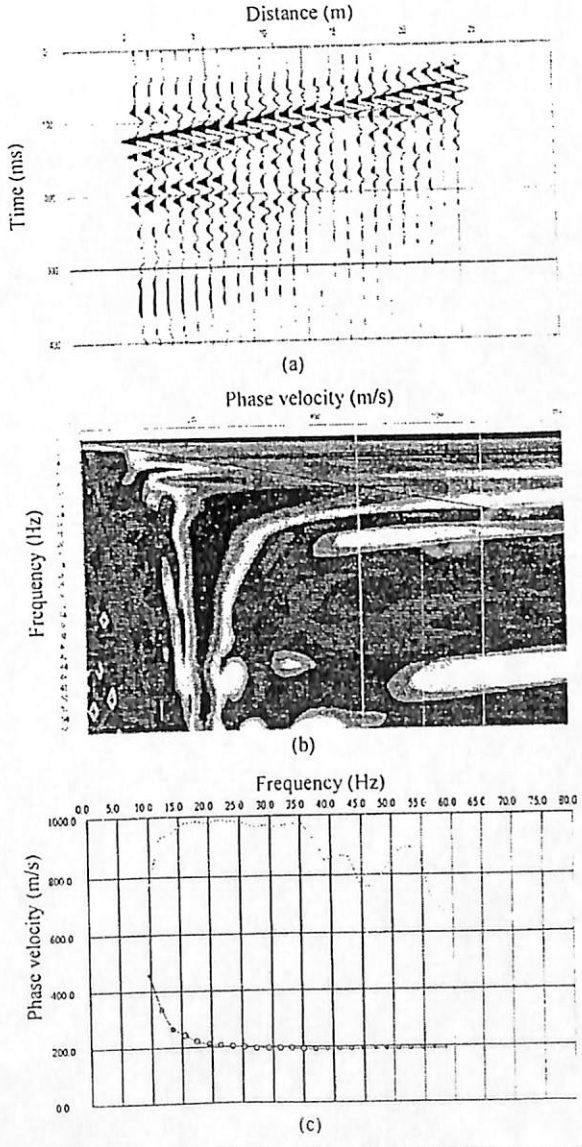

Figure 3. Development of the dispersion curves: (a) typical raw wiggle plot obtained from the field test (b) picking of maximum wave signal (c) dispersion curve with quality curve (signal to noise ratio)

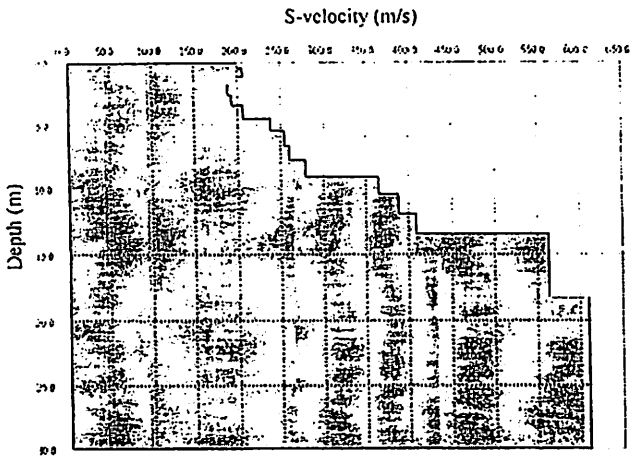

Figure 4. Typical shear wave velocity profile obtained from MASW test

III. Development of Empirical Correlations for V_S and N_{SPT}

In-situ test to determine the shear wave velocity profile is always preferable but it is not economically feasible to conduct test at all sites. A reliable empirical correlation between V_s and N_{spt} would be in advantage. In this study, V_s and N_{spt} data were collected from twenty sites in the generation of its empirical correlations. Simple regression analysis was used to develop these correlations. The new empirical correlations with their correlation coefficient (R^2) for sand, silt and clay are proposed as follows:

$$Vs = 150.00\ N_{spt}^{0.2292} (R^2 = 0.6874), \text{Sand} \quad (1)$$

$$Vs = 111.62\ N_{spt}^{0.3233} (R^2 = 0.7175), \text{Silt} \quad (2)$$

$$Vs = 118.33\ N_{spt}^{0.3276} (R^2 = 0.7142), \text{Clay} \quad (3)$$

Fig. 6 shows the V_s-N_{spt} raw data and the regression correlations for sand, silt and clay. The results proved the previous finding that N_{spt} is main parameter while soil material gives less significant effect on shear wave velocity estimation.

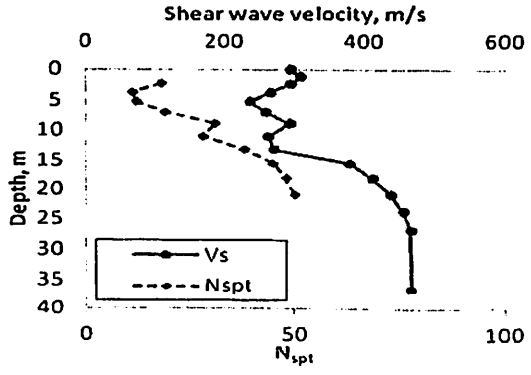

Figure 5. Typical shear wave velocity profile and N_{spt} variation for site

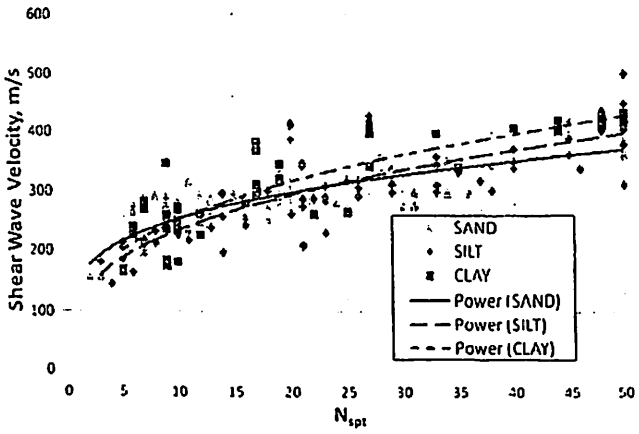

Figure 6. Correlation between V_s and N_{spt} for sand, silt and clay

The shear wave velocity obtained from Equation 1-3 for sand, silt and clay are compared with some selected correlations proposed by earlier researcher which have closest correlation curve with the proposed equation (Table 1) as shown in Fig. 7. However, the correlation for clay gives slightly higher shear wave velocity compared to existing correlation. Some discrepancy between the proposed and previous correlations may due to different site geotechnical conditions and the procedures during carry out the MASW survey in site.

IV. Conclusion

In summary, an extensive measurement of shear wave velocity by employing MASW geophysical technique was carried out in Penang Island. The correlations between V_s and N_{spt} for sand, silt and clay were developed. The results proved the previous finding that N_{spt} is the main parameter to determine shear wave velocity. Generally the shear wave velocity curves proposed are closely lying to the existing correlation. Therefore, the proposed correlations for sand, silt and clay are recommended to be used in the studied area.

TABLE I. CORRELATIONS BETWEEN VS AND NSPT

No.	Authors (year)	Vs Correlation		
		Sand	*Silt*	*Clay*
1	Okamato et al. (1989)	$Vs = 125\ N^{0.3}$		
2	Lee (1990)		$Vs = 105.6\ N^{0.32}$	$Vs = 114.4\ N^{0.31}$
3	Hanumantharao and Ramana (2008)	$Vs = 79\ N^{0.43}$	$Vs = 86.0\ N^{0.42}$	
4	Maheswari and Boominathan (2009)			$Vs = 89.3\ N^{0.36}$

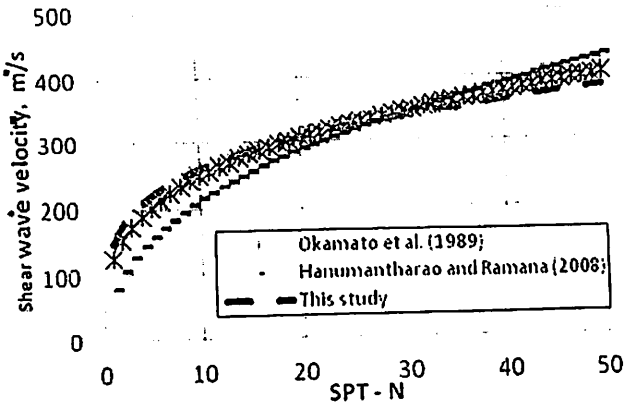

(a)

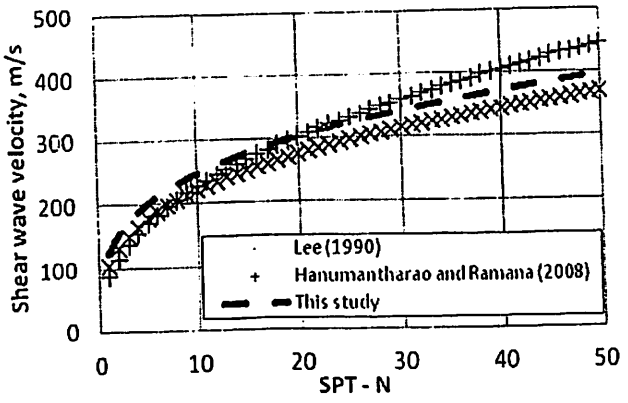

(b)

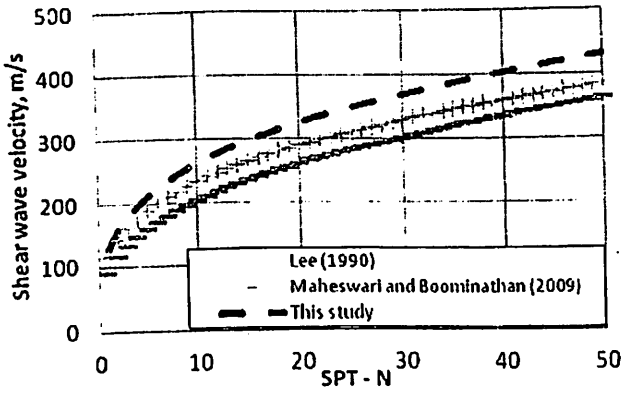

(c)

Figure 7. Comparison between proposed and existing correlations for V_s and N_{spt} for: (a) sand (b) silt (c) clay

ACKNOWLEDGEMENTS:

This study was supported by the Postgraduate Research Grant Scheme given by Universiti Sains Malaysia. The authors would like to extend their gratitude to the Ministry of Education of Malaysia for permission to collect data from both primary and secondary schools.

REFERENCES

[1] R. U. Maheswari, A. Boominathan, and G. R. Dodagoudar, "Seismic site classification and site period mapping of Chennai City using geophysical and geotechnical data," Journal of Applied Geophysics, vol. 72, pp 152–168, 2010.

[2] T. Okamoto, T. Kokusho, Y. Yoshida, and K. Kusuonoki, "Comparison of surface versus subsurface wave source for P–S logging in sand layer," Proc. 44th Ann. Conf. JSCE, vol. 3, pp. 996–997, 1989.

[3] S. H. Lee, "Regression models of shear wave velocities," J. Chin. Inst. Eng., vol. 13, pp. 519–532, 1990.

[4] C. Hanumantharao, and G. V. Ramana, "Dynamic soil properties for microzonation of Delhi. India," Journal of Earth Systen Science, vol. 117 (S2), pp. 719–730, 2008.

[5] R. U. Maheswari, and A. Boominathan, "Use of surface waves in statistical correlations of shear wave velocity and penetration resistance of Chennai soils," Journal of Geotechnical and Geological Engineering, vol. 28, pp. 119-137, 2009.

[6] R. Luna, and H. Jadi, 2000, "Determination of dynamic soil properties using geophysical methods," Proceedings of the First International Conference on the Application of Geophysical and NDT Methodologies to Transportation Facilities and Infrastructure, St. Louis, MO, 2000.

[7] K. H. Stokoe, and S. Nazarian, "Effectiveness of ground improvement from spectral analysis of surface waves," Proc. 8th European Conference on Soil Mechanics and Foundation Engineering, Helsinki, Finland, vol. 1, pp. 91–94, 1983.

[8] C. P. Lin, C. C. Chang, and T. S. Chang, "The use of MASW method in the assessment of soil liquefaction potential," Journal of Soil Dynamics and Earthquake Engineering, vol. 24, pp. 689–698, 2004.

[9] G. K. Yu, and J. F. Chien, "Study of the S-wave velocity and its error as derived from different microtremor observations," Proc. International Conference on Electric Technology and Civil Engineering (ICETCE), IEEE Conference Publications, TBD Lushan, China, pp. 5498 – 5505, 2011.

[10] Y. X. Xu, J. H. Xia, and R. D. Miller, "Quantitative estimation of minimum offset for multichannel surface-wave survey with actively exciting source. Journal of Applied Geophysics, vol. 59, pp. 117–125, 2006.

Australian Journal of Basic and Applied Sciences, 6(10): 129-138, 2012
ISSN 1991-8178

Effect Of Repeated Near Field Earthquake To The High-Rise Rc Building

[1]Mohd Zulham Affandi bin Mohd Zahid, [2]Taksiah A. Majid and [2]Ade Faisal

[1]School of Environmental Engineering, Universiti Malaysia Perlis, 02600 Arau, Perlis, Malaysia
[2]Disaster Research Nexus, School of Civil Engineering, Universiti Sains Malaysia, 14300, Nibong Tebal, Pulau Pinang, Malaysia

Abstract: Nowadays, most of the analyst and designer consider 'rare' single earthquake in seismic analysis and design. The repeated earthquakes are ignored even though the actual earthquake event occurs repetitively and the effect of the repeated earthquake is qualitatively acknowledged. Repeated earthquake is the repetition of medium-strong earthquakes at short time interval. The repeated earthquake was reported in many part of the world. This study investigates the effect of this event on the response of the reinforced concrete (RC) buildings. For that purpose, this study uses five generic RC models with different behaviour factor, q (i.e. 1, 1.5, 2, 4 and 6) in which the model with q = 1 is the strongest building and the strength of the building decreases with the increase of the q value. Furthermore, all models are 18-storey to represent high rise buildings in three dimensional in order to consider the effect of earthquake in orthogonal direction. There are 40 repeated near field ground motions which were combined randomly from 20 single near field ground motions employed in this study and 20 residual ground motion records. These repeated earthquakes are divided into two case, i.e. case 2 and case , in which case 2 has two consecutive earthquake(i.e. main shock and aftershock) and case 3 has three consecutive earthquakes (i.e. foreshock, main shock and aftershock). The duration between two consecutive earthquakes is 100s which is enough for the model to cease the motion. The near field earthquake contains special characteristic which is known as pulse effect that far field earthquake do not has, therefore, this study investigates also the effect of pulse period on the response of the RC buildings. The displacement ductility and storey ductility demand were considered to assess the response of the RC models and they are computed by using nonlinear time history analysis. It was found that repeated near field earthquake give significant effect to the respond of high-rise RC buildings compared to single near field earthquake.

Key words: high-rise building, RC building, repeated earthquake, near field earthquake

INTRODUCTION

The current practice is using 'rare' single earthquake in seismic design and analysis. The current seismic codes also ignore the influence of the repeated earthquake even though the effect of the repeated earthquake is qualitatively acknowledged (Hatzigeorgiou and Liolios, 2010). Repeated earthquake is characterized by the repetition of strong-medium earthquake ground motions after short interval of time. In these cases, the structures are already damaged in first earthquake and yet to be repaired, can be inadequate capacity to withstand subsequent earthquake. This accumulation of damage depends on the strength capacity of the building and on the characteristic of seismic events (Amadio *et al.*, 2003).

A few researchers have studied the effect of repeated earthquake on the buildings. Amadio *et al* (2003) showed that repeated earthquake can cause significant accumulation of damage and a consequent reduction in q-factor. Hartzigeorgiou has extensively study the effect of repeated earthquake to the buildings. Hatzigeorgiou and Liolios (2010) found that repeated earthquake lead to larger demand in comparison with corresponding single event. Furthermore, they also estimated the cumulative ductility demands of repeated earthquake using appropriate combinations of the corresponding demands of single earthquake and the proposed combination of ductility demands of single events is in good agreement with the results obtained from dynamic inelastic analysis.

In near field seismic region, the structures are excited by pulse like ground motion and non-pulse like ground motion or also known as residual ground motion in orthogonal direction (Baker, 2007). Since this study deals with near field ground motion, the both pulse like and non-pulse like motions are considered and therefore the RC building need to be modeled in three dimension (3D) instead of two dimension (2D) as used in previous research in investigating the influence of repeated near field earthquake, i.e: Hatzigeorgiou and Liolios (2010), Amadio *et al* (2003) and among others.

Corresponding Author: Mohd Zulham Affandi bin Mohd Zahid, School of Environmental Engineering, Universiti Malaysia Perlis, 02600 Arau, Perlis, Malaysia
E-mail: mohdzulham@unimap.edu.my,

The primary objective of this study to investigate the response of the high rise RC building under repeated near field earthquake. Therefore the response of the 18 storey building under single and repeated earthquake will be compared and the demand parameters used in evaluating the response of the buildings are displacement ductility and storey ductility demand. To be more detail, the influence of the building strength or the behaviour factor, q under repeated near field earthquake excitation will be investigated. Furthermore, since this study focuses on the near field earthquake, the effect of the pulse period, T_p under single and repeated earthquake excitation to the building response also will be evaluated.

MATERIALS AND METHODS

The 18-storey single bay model proposed by Ade Faisal (2011) was considered in this study as shown pictorially in Figure 1. This generic frame model has constant storey height of 3.6 m and 7.2 m of bay width. Moreover, this 3D model are extended from 2D models used by Medina and Krawinkler (2003) and Ruiz-Garcia and Miranda (2005). Note that the validation of 2D model was carried out by Medina and Krawinkler (2003).

The seismic assessment of this building model was carried out with reference to five values of behavior factor or q value: the q values vary between q = 1 (strong building) and q = 6 (weak building). Note that the q values were estimated with reference to the ductility level i.e DCL, DCM and DCH for the seismic design of RC buildings as proposed by Eurocode 8.

It should be noted that, the fundamental period of the buildings are computed based on equation 3.6 as proposed by Eurocode 8. In order to achieve targeted building fundamental period, the weight at each floor and the moment inertia of the structural member need to be tuned. The result from the tune process, the weights at every floor for all models are assumed to be 1240kN and irregularity in mass along the height is not taken into account as there is no significant effect on the response of the structure (Wood, 1992: Al-Ali and Krawinkler, 1998: Miranda and Taghavi, 2005). This study adopts the beam to column ratio equal to 1.3 as proposed by Eurocode 8.

Besides that, this study also adopts overstrength factor of $\alpha_u/\alpha_1 = 1.3$ as suggested by Eurocode 8 for multi-storey multi-bay frame. Since the Eurocode 8 provisions do not explain on how to distribute the factor, in this study the factor was distributed uniformly along the height of the buildings.

The reduction of the stiffness along the height of the buildings *S(z/H)* is followed the method by Miranda and Reyes (2002) and the ratio of lateral stiffness at the top to the bottom storey, δ is equal to 0.25 as proposed by Ruiz-Garcia and Miranda (2006). For the purpose of having more realistic distribution of lateral stiffness, a decreasing stepwise distribution of lateral stiffness which followed parabolic stiffness distribution was used in this study. The lateral stiffness of the global structure changes for every three stories. The lateral stiffness was calculated using the equivalent cantilever method as explained by Taranath (2010).

This study employs a single component model which was developed with inelasticity along the member is lumped at both end of each member. In order to simulate the cyclic behaviour of reinforced concrete building, this study uses modified-Takeda hysteresis curve as proposed by Zarein and Krawinkler (2009). The moment at yield point, M_y is defined following Medina and Krawinkler (2003) method in which the maximum moment resulted from the linear elastic static lateral analysis is assigned as the M_y at the hinges location. FEMA-P695 recommends a constant value of 1.13 for M_c/M_y, hence, for this study this value is used for hardening stiffness. The yield rotation can be determined by the ratio of M_y to the elastic rotation stiffness (K_o = 6EI/L) as shown in Figure 2.

The yield rotation (Θy) is obtained by the ratio of M_y with elastic rotation stiffness (K_o) and the rotation capacity, i.e. plastic rotation capacity (Θp) and post-capping rotation capacity (Θpc) is equal to 0.04 and 0.06 as proposed by Zarein and Krawinkler (2009). Furthermore, Θu is the rotation ultimate, Θc rotation capacity and M_c is the moment capacity or capping moment. Besides that, r is the post yield stiffness ratio or bi-factor which is estimated based on the ratio of capping moment and yield moment (M_c/M_y) and ductility of plastic rotation capacity (μ_Θ).

The unloading and reloading parameters (α and β) in hysteresis rule are assumed to be 0.3 and 0.6, for beam and column member respectively following the recommendation by LESSLOSS (2007) and Priestley *et al.* (2007). Moreover, this study considers member strength degradation based on the rotation ductility from Zarein and Krawinkler (2009) backbone curve, which is developed on hysteresis rule of Ibarra *et al* (2005).

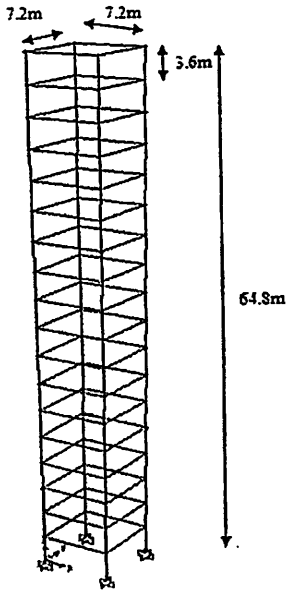

Fig. 1: 18-storey model

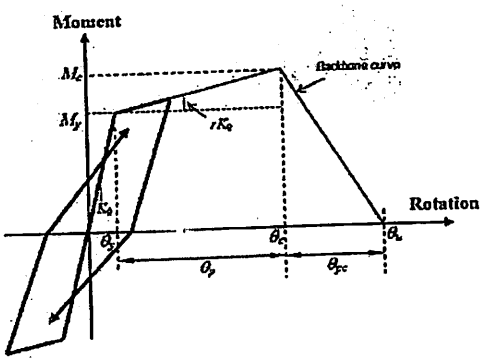

Fig. 2: Modified-Takeda hysteresis and backbone curve (Zarein and Krawinkler, 2009)

In this analytical study, two types of near field ground motion are used: i.e. natural near field earthquake (GM2) and synthetic near field earthquake or also known as residual ground motion (GM3). The original 20 natural near field earthquake records are downloaded from PEER NGA database with reference to the records published by Baker (2007) as shown in Table 1. The residual ground motions are extracted from natural near field earthquakes by removing the pulse component.

In order to study the effect of repeated ground motion, based on Hartzigeorgiou's (2010) method, the above ground motions were combined to become ground motion Case 2 and Case 3. Generally, Cases 1 to 3 can be considered as triple earthquakes, where everyone of their discrete part is multiplied with appropriate factors as follows:

Case 1: (0.0000, 1.0000, 0.0000) as shown in Figure 3 (a)
Case 2: (0.0000, 1.0000, 1.0000) as shown in Figure 3 (b)
Case 3: (0.8526, 1.0000, 0.8526) as shown in Figure 3 (c)

It should be noted that, this study adopts the Ade Faisal's (2011) combination of repeated near field earthquake in which the fore-shock and after-shock are residual ground motion and only main shock is near field ground motion. This combination of ground motions are used in fault-normal component to observe the effect of pulse period on the response of the building. In fault-parallel component, the combination of repeated earthquake consists of residual ground motion only. On top of that, the fore-shock and after-shock are randomly selected using random function in MS-EXCEL to match them with main-shock.

Moreover, all the ground motions used in this study will be scaled to the spectral acceleration ordinate at fundamental period of the building, $Sa(T_1)$, as recommended by Shome *et al.* (1998) to make them comparable. The response spectrum use in this study is the design spectrum of Eurocode 8 for condition of soil type B with peak ground acceleration $a_g = 0.36g$. The ag value is based on 475-years return period of earthquake that reflecting the condition of Seismic Zone III at Greece (Salomos *et al.*, 2008).

RESULTS AND DISCUSSION

The 18-storey RC models were subjected to 40 single ground motions (i.e. 20 GM2 and 20 GM3) and 40 repeated near field ground motions RGM2 in orthogonal direction and the structural assessment was carried by means nonlinear time history analysis.

Table 1: List of near field earthquake

No	Year	Record Name	Station Name	PGA(g)	
				Major (Normal)	Minor (Parallel)
1	1984	Morgan Hill	Coyote Lake Dam (SW Abut)	1.080	0.814
2	1989	Loma Prieta	Gilroy-Gavilan Coll	0.294	0.414
3	1989	Loma Prieta	LGPC	0.944	0.537
4	1992	Landers	Lucerne	0.704	0.807
5	1994	Northridge-01	Jensen Filter Plant	0.518	1.068
6	1994	Northridge-01	Jensen Filter Plant Generator	0.518	1.067
7	1994	Northridge-01	Syimar-Converter Sta East	0.828	0.528
8	1994	Northridge-01	Syimar-Olive View Med FF	0.733	0.595
9	1999	Kocaeli, Turkey	Gebze	0.241	0.203
10	1999	Chi-Chi, Taiwan	CHY028	0.664	0.848
11	1999	Chi-Chi, Taiwan	TCU049	0.286	0.250
12	1999	Chi-Chi, Taiwan	TCU052	0.375	0.393
13	1999	Chi-Chi, Taiwan	TCU053	0.224	0.142
14	1999	Chi-Chi, Taiwan	TCU054	0.157	0.190
15	1999	Chi-Chi, Taiwan	TCU068	0.564	0.431
16	1999	Chi-Chi, Taiwan	TCU075	0.331	0.274
17	1999	Chi-Chi, Taiwan	TCU076	0.310	0.419
18	1999	Chi-Chi, Taiwan	TCU082	0.235	0.190
19	1999	Chi-Chi, Taiwan	TCU102	0.295	0.162
20	1999	Chi-Chi, Taiwan	TCU103	0.133	0.168

Preliminary eigenvalue analysis was carried out to determine the modal properties of the structural system. The 18-storey single-bay model has natural period equal to 1.71 s for first and second mode of vibration with an effective modal mass percentage equal to 99.957%. The computed period is similar to those relative to existing high-rise RC building (e.g. Taranath, 2010).

For the seismic performance assessments, the structural response quantities are expressed in term of global behaviour, i.e. displacement ductility, μ_d and storey ductility, μ_s. Displacement ductility demand μ_d, is the ratio of maximum displacement to the yield displacement while the storey ductility demand, μ_s is defined as the maximum interstorey drift normalized by the interstorey drifts at yield. The distributions of storey ductility demands over the height of the structure are studied to evaluate the storey response characteristics of MDOF system subjected to single and repeated near-field ground motions with forward directivity effects.

Figure 4 presents the relationship between the mean μ_d and behaviour factor, q or strength level of the structure. The designation C1, C2 and C3 represent case 1, case 2 and case 3, respectively. Note that the mean value of μ_d of RC building under GM2_C1 is higher than GM3_C1, especially when $q > 2$ and for high strength structure ($q < 2$), the variation of μ_d is very small. This is because, according to Baker (2004), the residual ground motion (GM3) has similar characteristic with far field ground motion in which there is no pulse observed in both earthquakes.

The mean of μ_s over the height of the buildings and the maximum standard deviation of the μ_s of all stories (σ_{max}) were computed and included in Figure 5. In general, the different of the building responds due to GM2_C1 and GM3_C1 increases as the q increases. To be more specific, the μ_d and μ_s increase as the q increases indicate that the weaker structure undergoes higher demands in comparison with stronger one.

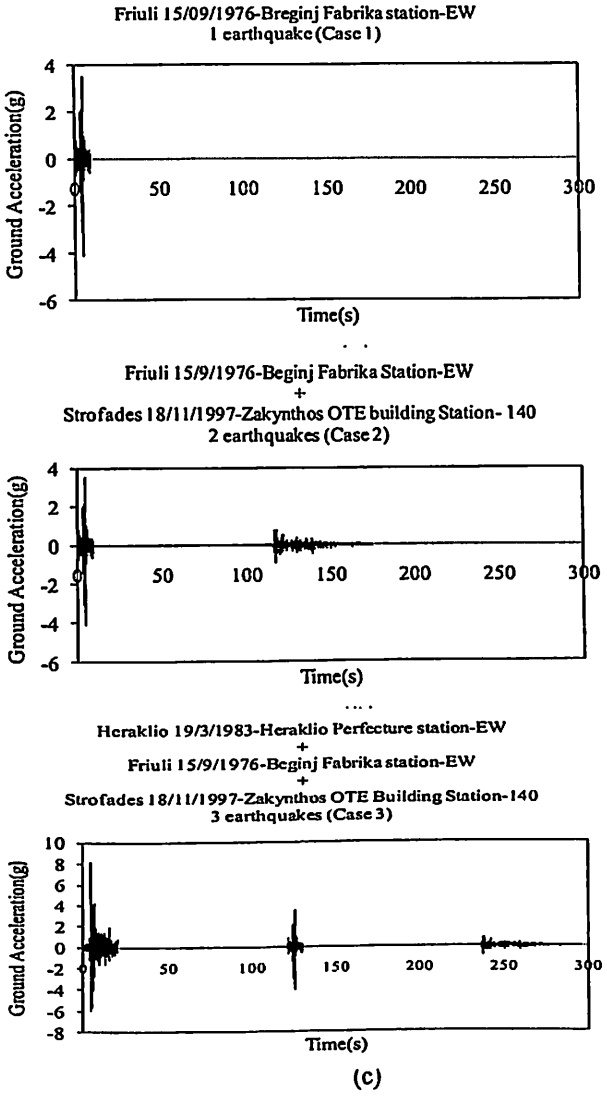

(c)

Fig. 3: Time history for single (case 1) and repeated earthquakes (case 2 and 3)

Note that the dispersion in structural response is larger for near field ground motions, as evidenced by the larger values of the maximum standard deviation of storey ductility demands when the structure is subjected to near field with forward directivity ground motions as opposed to residual ground motion and this pattern are consistent as the behaviour factor increases. Furthermore, the maximum standard deviation becomes larger as the buildings become weaker as shown in Figure 5. These findings agree with the observations made by Sehhati *et al* (2011), in which their work compared the μ_s due to near field and far field earthquakes.

Furthermore, repeated near field earthquakes i.e.: RGM2 (GM2_C2 and GM2_C3) impose higher value of μ_d compared to single earthquake as illustrated in Figure 4. Note that, the maximum μ_d of GM2_C2 and GM2_C3 are 28% and 18%, respectively, higher than GM2_C1.

Table 2 provides comparison of mean μ_s between single earthquake and repeated earthquake. The variations of mean μ_s are significant for building under repeated earthquakes (Case 2 and Case 3). Note that, the maximum μ_s tend to increase when the RGM2 is implemented in the time history analyses and the maximum μ_s increases as the q increases. For values of q corresponding to the strength of the building, the average increase of maximum mean of μ_s ranges between 36% (C2) and 90% (C3). The values computed for the frame subjected to the repeated near field earthquake can be higher than three times those computed for single near field earthquake. This finding demonstrates the importance of including the effects of RGM2 to estimate accurately the response of the building in near field area.

The number in the bracket shows the storey level where the maximum mean μ_s occurs. Note that, for the very strong building (q = 1), the maximum μ_s occurs at top storey and when the q increases the maximum μ_s migrates to bottom storey. Furthermore, the minimum μ_s always occur at the middle storey.

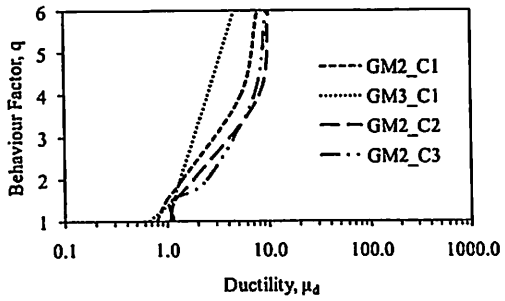

Fig. 4: Mean displacement ductility demand for 18-storey models

Pulse Period:

Since this study deals with near field earthquake, the pulse period plays a vital role in the behaviour of the building subjected to near field event, therefore, the responses of the building model are re-analyzed in order to study the influence of pulse period on storey ductility demands, μ_s. Unlike the previous research (e.g. Kalkan and Kunnath, 2006, Alavi and Krawinkler, 2004 among others), this study investigate real pulse from ground motion records.

Table 3, 4 and 5 summarized the maximum μ_s over the height of 18-storey model for various value of the ratio T_1/Tp. In order to examine the dependency of structural response to the ratio of T_1/Tp and to make it comparable with previous study, this study considers T_1/Tp from 1.8 to 0.48 because within this range the forward directivity pulse renders similar structural response to that computed for an equivalent pulse model (Sehhati et. al., 2011) and most of previous studies used equivalent pulse model to study the effect of T_1/Tp (e.g. Kalkan and Kunnath, 2006, Alavi and Krawinkler, 2004 among others).

Based on the previous study by Kalkan and Kunnath (2006), the demands are higher for T_1/Tp near 1. In this study, however, for case 1, the maximum μ_s experienced by the high rise building with $T_1/Tp = 0.55$ is higher than $T_1/Tp = 0.95$ as shown in Table 3. Therefore, further investigation is carried out and it is found that the velocity spectra ordinate at T_1 for ground motion with $T_1/Tp = 0.55$ is about 80% higher than ground motion with $T_1/Tp = 0.95$ as shown in Figure 6. This finding indicates that the real pulse from ground motion records needs to be implemented in structural analyses in order to estimate accurately the response of the building in near field area.

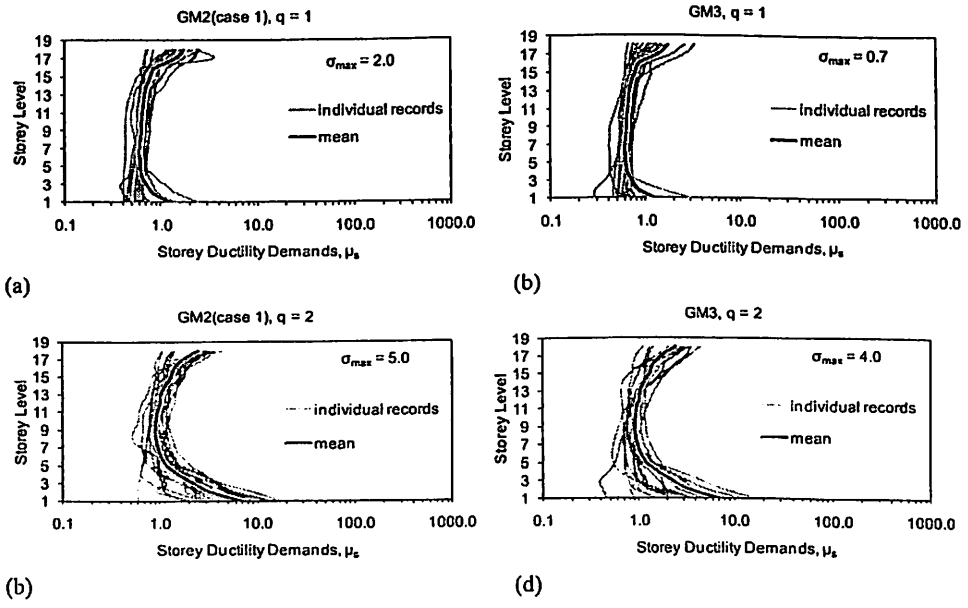

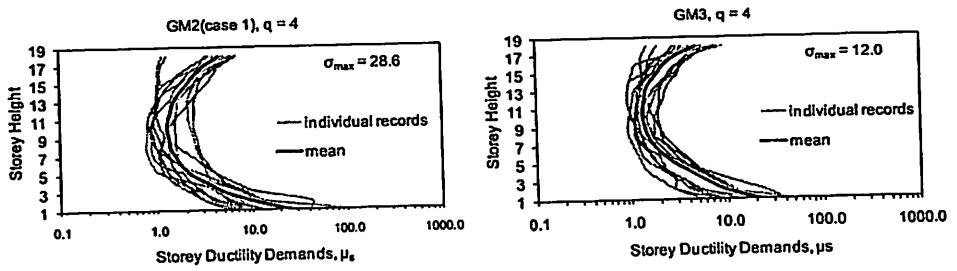

(e) (f)

Fig. 5: Storey ductility demands, μ_s

Moreover, under repeated earthquake, the maximum μ_s endured by relative weak structure (q = 4 and 6) is higher for $T_I/T_p = 0.95$ compared to $T_I/T_p = 0.55$ as shown Table 4 and 5. The average increase of maximum μ_s experienced by relative weak structures is about 190% and 33% for case 2 and case 3, respectively.

Table 2: Comparison of maximum mean storey ductility demand between single earthquake and repeated earthquakes for various level of q-value

	Behaviour factor				
	q = 1	q = 1.5	q = 2	q = 4	q = 6
C1	1.8 (18)	3.3 (1)	6.9 (1)	23.8 (1)	38.4 (1)
C2	2.1 (18)	4.2 (1)	9.0 (1)	30.4 (1)	61.2 (1)
C3	2.1 (18)	4.4 (1)	8.9 (1)	45.6 (1)	116.7 (1)
C2/C1	1.17	1.27	1.30	1.28	1.59
C3/C1	1.17	1.33	1.28	1.92	3.04

Note: Value in bracket ( ) refers to storey level.

Table 3: Comparison of maximum mean storey ductility demand between single earthquake and repeated earthquakes for various T_I/T_p for case 1

Case 1						
Behaviour Factor	T_I/T_p					
	0.48	0.49	0.55	0.81	0.95	1.8
1.0	0.8 (18)	1.6 (18)	6.8 (17)	1.0 (18)	2.6 (18)	3.3 (18)
1.5	1.3 (18)	4.8 (1)	11.1(1)	2.5 (18)	2.4 (1)	4.5 (18)
2.0	8.2 (18)	7.5 (1)	16.2 (1)	2.8 (18)	5.2 (1)	4.4 (18)
4.0	23.0 (1)	42.0 (2)	37.7 (1)	127 (1)	24.0 (1)	23.8 (2)
6.0	109.5 (1)	62.3 (1)	54.5 (1)	23.6 (1)	42.8 (1)	35.6 (1)

Table 4: Comparison of maximum mean storey ductility demand between single earthquake and repeated earthquakes for various T_I/T_p for case 2

Case 2						
Behaviour Factor	T_I/T_p					
	0.48	0.49	0.55	0.81	0.95	1.8
1.0	1.5 (18)	1.6 (18)	6.8 (16)	2.5 (18)	2.6 (18)	4.6 (17)
1.5	5.0 (1)	4.7 (1)	9.0 (17)	3.9 (18)	6.5 (1)	4.5 (18)
2.0	11.5 (1)	7.6 (1)	16.2 (1)	12.2 (1)	15.1 (1)	4.4 (18)
4.0	120.5 (1)	66.2 (1)	44.0 (2)	124.0 (1)	127.4 (1)	23.8 (2)
6.0	190.7 (1)	62.3 (1)	65.5 (2)	47.5 (1)	190.0 (1)	35.6 (1)

Table 5: Comparison of maximum mean storey ductility demand between single earthquake and repeated earthquakes for various T_I/T_p for case 3

Case 3						
Behaviour Factor	T_I/T_p					
	0.48	0.49	0.55	0.81	0.95	1.8
1.0	1.3 (18)	1.7 (17)	6.8 (17)	7.8 (18)	2.7 (18)	6.0 (17)
1.5	2.5 (18)	4.8 (1)	10.0 (1)	3.5 (18)	2.3 (1)	4.4 (18)
2.0	5.9 (1)	5.8 (1)	14.7 (1)	12.5 (17)	9.7 (1)	9.4 (1)
4.0	117.9 (1)	126.3 (1)	33.8 (1)	125.0 (1)	51.5 (1)	23.5 (1)
6.0	190.8 (1)	105 (1)	170.5 (1)	176.0 (1)	190.7 (1)	14.3 (18)

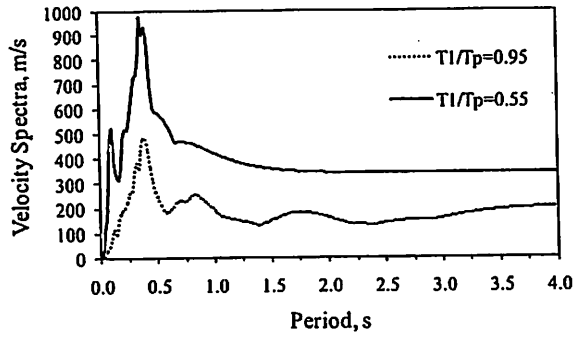

Fig. 6: Velocity spectra for ground motion with $T_I/Tp = 0.95$ and 0.55

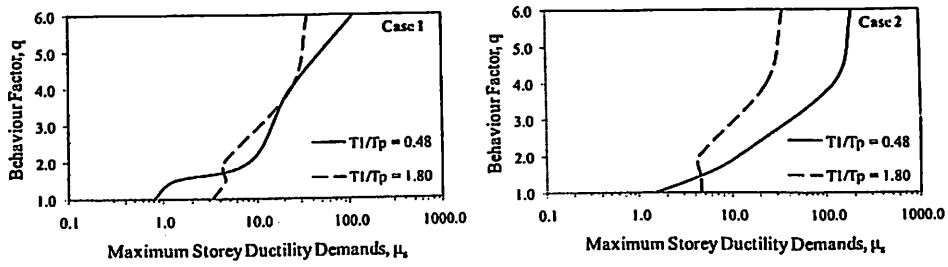

Fig. 7: Comparison of maximum storey ductility demands, μ_s for $T_I/T_p = 0.48$ and 1.80 for case 1(left) and case 2 (right)

Figure 7 illustrates the comparison between maximum μ_s due to near field ground motion with high value of pulse period with respect to fundamental period of building ($T_I/T_p = 0.48$) and high fundamental period of building with respect to the pulse period ($T_I/T_p = 1.8$). Note that, for case 1, the maximum μ_s experienced by relative strong structure (q = 1 and 1.5) under ground motion with $T_I/T_p = 1.8$ is higher than its counterpart. Then, when q increases the maximum μ_s of $T_I/T_p = 0.48$ becomes higher than $T_I/T_p = 1.8$.

This results show that the effect pulse period is significant for relative weak structure (q = 2, 4 and 6).

Furthermore, under repeated earthquake of case 2, only building with q = 1 experienced higher demands under $T_I/T_p = 1.8$ which is two times higher than $T_I/T_p = 0.48$. Then, for the rest of the structures the maximum μ_s due to $T_I/T_p = 0.48$ are higher than $T_I/T_p = 1.8$ and its gap becomes wider as the q increases. This finding indicates that the effect of pulse period may be significant for relative weak structure under repeated earthquakes.

Conclusion:

In this paper, the inelastic dynamic response of five different behavior factor, q of high rise RC buildings has been investigated to study the effect of repeated near field earthquake. A detailed study of the problem leads to the following problem:

a) The average increase of displacement ductility demands, μ_d experienced by high rise buildings under repeated near field earthquake of case 2and case 3 is 28% and 18%, respectively, higher than single near field earthquake.

b) The distribution of storey ductility demand, μ_s is significant under repeated near field earthquake. The average increase of maximum μ_s is 36% and 90% under repeated near field earthquake case 2 and case 3. The values computed for the frame subjected to the repeated near field earthquake can be higher than three times those computed for single near field earthquake. This finding demonstrates the importance of including the effects of RGM2 to estimate accurately the response of the building in near field area.

c) The increase of displacement and storey ductility demand increase as the behaviour factor, q increases.

This works also investigate the effect of pulse period on the ductility demand of the building under single and repeated near field earthquakes. It is found that the effect pulse period is significant for relative weak structure (q = 2, 4 and 6). The average increase of maximum μ_s experienced by relative weak structures is about 190% and 33% for case 2 and case 3, respectively. Furthermore, the gap of the μ_s between single and repeated near field earthquake becomes wider as the q increases. This finding indicates that the effect of pulse period may be significant for relative weak structure under repeated earthquakes.

ACKNOLEDGEMENT

Support for this work was provided by Ministry of Higher Education of Malaysia through research grant (No: 100/PAWAM/814115), UniMAP and USM Fellowship Scheme. Several people contributed to this research, including but not limited to Prof. Dr. George D. Hartzigeogiou from Democritus University of Thrace, Greece.

REFERENCES

Ade Faisal, 2011. Influence of repeated earthquake on the seismic demand of inelastic structures, Final Presentation of Research Progress (Ph.D Thesis), School of Civil Engineering, Universiti Sains Malaysia, Pulau Pinang, Malaysia

Al-Ali, A.K.A. and H. Krawinkler, 1998. Effects of vertical irregularities on seismic behavior of buildings structures, *Report No. 130*, John A. Blume Earthquake Engineering Center, Department of Civil and Environmental Engineering, Stanford University, Stanford

Alavi, B. and H. Krawinkler, 2004. Behavior of moment resisting frame structures subjected to near-fault ground motions. Earthquake Engineering and Structural Dynamics, 33(6): 687-706.

Amadio, C., M. Fragiacomo and S. Rajgelj, 2003. The effects of repeated earthquake ground motions on the non-linear response of SDOF systems. Earthquake Engineering and Structural Dynamics, 32: 291-308.

ASCE, 2006. Minimum design loads for buildings and other structures, ASCE Standard No. 007-05, American Society of Civil Engineers, Reston, VA

ASCE, 2006. Seismic rehabilitation of existing buildings, ASCE Standard No. 045-06, American Society of Civil Engineers, Reston, VA

Baker, J.W., 2007. Quantitative classification of near-fault ground motions using wavelet analysis. Bulletin of Seismological Society of America, 97(5): 1486-1501.

Blume, J.A., 1968. Dynamic Characteristics of multi-storey buildings. Journal of Structural Engineering ASCE, 120(4): 1240-1254

Carr, A.J., 2008. RUAUMOKO – inelastic dynamic analysis program. Department of Civil Engineering, University of Canterbury, Christchurch, New Zealand

CEN, 2003. Eurocode 8: Design of Structures for earthquake resistance. Part 1: General rules seismic actions and rules for buildings. Final Draft prEN 1998. European Committee for Standardization. Brussels

Chopra, A.K. and C. Chitanapakdee, 2004. Inelastic deformation ratios for design and evaluation of structures: single degree of freedom bilinear systems. *Journal of Structural Engineering*, 130(9): 1309-1319.

Chopra, A.K. and R.K. Goel, 2002. A modal pushover analysis procedure for estimating seismic demands for buildings. *Engineering and Structural Dynamics*, 31(3): 561-582.

Elnashai, A.S., L.D. Sarno, 2008. Fundamental of Earthquake Engineering. West Sussex: John Willey & Sons Ltd.

FEMA, 2000. NEHRP recommended provisions for seismic regulations for new buildings and other structures, 2000 edition, Part1: Provisions, FEMA 368, Buildings Seismic Safety Council for Federal Emergency Management Agency, Washington D.C.

FEMA, 2009. Quantification of building seismic performance factors, 2009 edition, FEMA P-695, Applied Technology Council (ATC), Redwood City

Hall, J.F., 2005. Problems encountered from the use (or misuse) of Rayleigh Damping. Earthquake Engineering Structural Dynamic, 35(5): 525-545.

Haselton, C.B., A.B. Liel, S.T. Lange, & G.G. Deierlein, 2007. Beam-column element model calibrated for predicting flexural response leading to global collapse of RC frame buildings, Report No. 2007/03, Pacific Earthquake Engineering Research Center, University of California at Berkeley, Berkeley

Haselton, C.B., A.B. Liel, S.T. Lange, G.G. Deierlein, 2009. Simulating structural collapse due to earthquakes: model idealization, model calibration and numerical solution algorithms: In: ECCOMAS Thematic Conference on Computational Methods in Structural Dynamics and Earthquake Engineering, 22-24 June 2009, Rhodes, Greece.

Hatzigeorgiou, G.D. and A.A. Liolios, 2010. Nonlinear behavior of RC frames under repeated strong ground motions, in press.

Hatzigeorgiou, G.D. and D.E. Beskos, 2009. Inelastic displacements ratios for SDOF structures subjected to repeated earthquakes. Engineering Structures, 31: 2744-55.

Hatzigeorgiou, G.D., 2010. Ductility demand spectra for multiple near- and far-field earthquakes. Soil Dynamics Earthquake Engineering, 30: 170-83.

Ibarra, L., R.A. Medina and H. Krawinkler, 2006. Hysteresis model that incorporate strength and stiffness deterioration. Earthquake Engineering Structural Dynamic, 34(12): 1489-511.

Ibarra, L.F. and H. Krawinkler, 2005. Global collapse of frame structures under seismic excitations, *Report No. TR152*, John A. Blume Earthquake Engineering Center, Department of Civil and Environmental Engineering, Stanford University, Stanford

Kalkan, E. and S.K. Kunnath, 2006. Effects of fling step and forward directivity on the seismic response of buildings. Earthquake Spectra, 22(2): 367-390

LESSLOSS, 2007. Guidelines for displacement-based design of buildings and bridges. Editor: Fardis, M. *LESSLOSS report No. 2007/05*. IUSS, Pavia.

Medina, R.A. and H. Krawinkler, 2003. Seismic demands for non-deteriorating frame structures and their dependence on ground motions. *Report No. TR144*, John A. Blume Earthquake Engineering Center, Department of Civil and Environmental Engineering, Stanford University, Stanford

Miranda, E. and C.J. Reyes, 2002. Approximate lateral drift demands in multistory buildings with nonuniform stiffness. Journal of Earthquake Engineering ASCE, 128(7): 840-849.

Miranda, E. and S. Taghavi, 2005. Approximate floor acceleration demands in multistory buildings with nonuniform stiffness. Journal of Earthquake Engineering ASCE, 131(2): 203-211.

Miranda, E., 1999. Approximate seismic lateral deformation demands in multistory buildings. Journal of Earthquake Engineering ASCE, 125(4): 417-425.

Miranda, E., 2000. Inelastic displacement ratios for structures on firm sites. Journal of Structural Engineering, 126(10): 1150-1159.

Nakashima, M., K. Ogawa and K. Inoue, 2002. Generic frame model for simulation of earthquake responses of steel frames. Earthquake Engineering and Structural Dynamics, 31: 671-692.

Panagiotakos, T.B. and M.N. Fardis, 2001. Deformations of reinforced concrete members at yielding and ultimate. ACI Structural Journal, 98(2): 135-148.

PEER, 2008. PEER NGA Database, available at http://peer.berkeley.edu/nga/.

Priestly, M.J.N., M. Calvi and M.J. Kowalsky, 2007. Displacement-based seismic design of structures, IUSS Press, Pavia.

Rodriguez-Marek, A. and J.D. Bray., 2006. Seismic site effects for near-fault forward directivity ground motions. *Journal of Geotechnical and Geoenviromental Engineering ASCE,* 132(12): 1611-1620.

Ruiz-Garcia, J. and E. Miranda, 2006. Evaluation of residual drift demands in regular multi-story frames for performance-based seismic assessment. Earthquake Engineering and Structural Dynamics, 35: 1609-1629.

Salomos, G., A. Pinto, S. Dimova, 2008. A review of the seismic zonation in national building codes in the context of Eurocode 8. EUR23563 EN-2008. Joint Research Centre, Ispra.

SAP2000, 2005. Analysis Reference Manual. Computers and Structures, Ins., Berkeley.

Sehhati, R., A. Rodriguez-Marek, M. ElGawady and W.F. Cofer, 2011. Effects of near-field ground motions and equivalent pulses on multi-story structures. Engineering Structures, 33(2011): 767-779.

Seismosoft, 2007. SeismoSignal, available at: http://www.seismosoft.com/.

Shome, N., C.A. Cornell, P. Bazzuro, J.E. Carballo, 1998. Earthquake records and nonlinear MDOF responses. Earthquake Spectra, 14(3): 469-500.

Taranath, B.S., 2010. Reinforced concrete design of tall buildings, CRC Press, Boca Raton

Wood, S.L., 1992. Seismic response of R/C frame with irregular profiles. Journal of Structure and Earthquake Engineering ASCE, 118(2): 545-566.

Yi, W.J., H.Y. Zhang and S.K. Kunnath, 2007. Probabilistic constant-strength ductility demand spectra. Journal of Earthquake Engineering ASCE, 133(4): 740-75.

Zarein, F. and R.A. Medina, 2010. A practical method for proper modelling of structural damping in inelastic plane structural system. *Computers and Structures*, 88: 45-53.

Zarein, F., and H. Krawinkler, 2009. Simplified performance-based earthquake engineering. *Report No. 169*, John A. Blume Earthquake Engineering Center, Department of Civil and Environmental Engineering, Stanford University, Stanford.

(3)

Documents

Tan, C.G., Majid, T.A., Ariffin, K.S., Bunnori, N.M.
Effects of site classification on empirical correlation between shear wave velocity and standard penetration resistance for soils
(2013) *Applied Mechanics and Materials*, 284-287, pp. 1305-1310.

Document Type: Conference Paper
Source: Scopus

Applied Mechanics and Materials Vols. 284-287 (2013) pp 1305-1310
© (2013) Trans Tech Publications, Switzerland
doi:10.4028/www.scientific.net/AMM.284-287.1305

Effects of Site Classification on Empirical Correlation between Shear Wave Velocity and Standard Penetration Resistance for Soils

Chee Ghuan Tan[1, a], Taksiah A. Majid[2, b], Kamar Shah Ariffin[3, c] and Norazura Mohamad Bunnori[1,d]

[1] School of Civil Engineering, Universiti Sains Malaysia, Penang, Malaysia

[2] Disaster Research Nexus, School of Civil Engineering, Universiti Sains Malaysia, Penang, Malaysia

[3]School of Material and Mineral Resources, Universiti Sains Malaysia, Penang, Malaysia

[a] tuc_kheen@hotmail.com, [b] taksiah@eng.usm.my, [c] kamarsha@eng.usm.my, [d] cenorazura@eng.usm.my

Keywords: Shear wave velocity profile, Multichannel analysis of surface wave (MASW), Standard penetration resistance, Empirical correlation.

Abstract. In seismic engineering, the dynamic property of the soil is one of the most important aspects in ground response analysis. Dynamic property is significantly affected by local soil deposits. Shear wave velocity (V_s) of soil is one of the main parameters in determining the amplification factor on ground surface. It is not economically feasible to measure V_s for all sites. Therefore, a reliable empirical correlation between V_s and standard penetration resistance (N_{spt}) will be useful since N_{spt} data are easily obtainable in construction industry. This study aims to develop an empirical correlation between V_s and N_{spt} for all soils by considering the effect of site classification according to the Uniform Building Code. New empirical correlations for all soils are presented in this study and well compared with the previous study to evaluate prediction capability. Results show that site classification has a significant impact on the V_s estimation, and that the proposed correlations are the most appropriate for estimating the V_s profile in the studied area compared with existing correlations.

Introduction

In seismic engineering, the most important aspect is determining the dynamic properties of the soil structure. Dynamic soil properties provide important information on the dynamic response of the soil structure needed for the dynamic structural analysis of superstructures. Local soil structure also plays a major role in the seismic soil amplification of a site, a critical factor affecting the level of ground shaking [1]. However, the lack of understanding on the geological information of the site often leads to structural and environmental failure. Field measurement of shear wave velocity (V_s) includes cross-hole test, down-hole test, suspension logging, seismic reflection, seismic refraction, and surface wave. However, surface wave test is a simpler and more efficient technique compared with other in-situ tests used in measuring V_s. It is not economically feasible to conduct the surface wave test at all sites. Hence, a reliable empirical correlation between V_s and standard penetration resistance (N_{spt}) will be useful since N_{spt} data are easily obtainable in the construction industry. Many researchers have been proposed an empirical correlation for V_s based on a standard penetration test. However, these empirical correlations are region-specific and cannot be applicable to all regions.

In contrast to the existing correlations, the current paper presents the development of correlations between V_s and N_{spt} by considering the effect of site classification according to the Uniform Building Code (UBC) (Table 1) on soil in Penang, located at the northwestern area of peninsular Malaysia. Measurement of the V_s profile was carried out extensively using Multichannel Analysis of Surface Waves (MASW) at the site where N_{spt} data are available. Based on statistical assessment and site classification, empirical correlations for V_s and N_{spt} were developed and compared with the existing correlations from previous studies to evaluate the prediction capability of the correlations.

Table 1: UBC Site Classification

Site class	Soil type	V_{s30} [m/s]
Class A	Hard rock	$V_{s30} > 1500$
Class B	Rock	$760 \leq V_{s30} \leq 1500$
Class C	Very dense soil/soft rock	$360 \leq V_{s30} \leq 760$
Class D	Stiff soil	$180 \leq V_{s30} \leq 360$
Class E	Soft soil	$V_{s30} < 180$
Class F	Soils requiring site specific evaluation	Non-applicable

Geology of study area

The total area of Penang Island is approximately 300 km^2 and is composed entirely of Pre-Quaternary granite locally covered with unconsolidated sand, silt, and clay of the Pleistocene and Holocene ages (Fig. 1). It has no sedimentary rocks and most of the island is underlain by igneous rocks (also called granite). Generally, the granite hills are raised from the sea to the highest point at 830 m from seawater level, except where Pleistocene and Holocene deposits are found. The Pleistocene deposits are found on the slopes and at the foot of granite hills, consisting of the products of weathering from granite. Sand, gravel, clay, silt, and peat of Pleistocene age were laid down by fluvial processes as channel fill, over-bank, and flood-basin deposits [2].

Surface Wave Method

Surface wave geophysical methods have been used for many years by researchers and engineers in soils and foundation applications. These methods not only provide the properties of soils, but are also used to determine the dynamic properties of soils, particularly the soil's shear wave velocity profile and shear modulus. These properties are key parameters in predicting the soil response and soil-structure systems to seismic loading [3]. Surface wave methods offer advantages over other surface-based in-situ seismic techniques because they are rapid, cost-effective, noninvasive, and have the ability to detect a low-velocity layer underneath a higher-velocity layer of deposit, thus providing more accurate site characterization.

Field Test Set up and Procedure

MASW tests were carried out using Geometrics 24 channels seismograph (Geode) with single geode operating software (SGOS). A total of 24 units of vertical geophones with 4.5 Hz natural frequency were used to receive the wave signal generated by an active source of 8 kg sledgehammer vertically hit on a striker plate. Geophones were deployed linearly with equal spacing, ranging from 0.5 m to 2 m interval as suggested by Maheswari [1]. The nearest source to the geophone offsets is in the range of 5 m to 15 m to meet the requirement of different types of soil hardness suggested by Xu et al. [4]. The field configuration of MASW is illustrated in Fig. 2.

Development of Empirical Correlations for V_s and N_{spt}

Conducting an in-situ test to determine the V_s profile is always preferable, but it is not economically feasible to conduct at all sites. A reliable empirical correlation between V_s and N_{spt} will be an advantage. Several existing correlations have been proposed as listed in Table 2.

Proposed Empirical Correlation between V_s and N_{spt} by considering the UBC Site Classification

In this study, an analysis of 40 sites was carried out through MASW in the development of empirical correlations between V_s and N_{spt} values using simple regression analysis. The new empirical correlations with their correlation coefficient (r^2) for three site classifications are proposed as follows:

$$V_s = 128.05\ N^{0.4081}\ (r^2 = 0.73),\ \text{Class C} \quad (1)$$

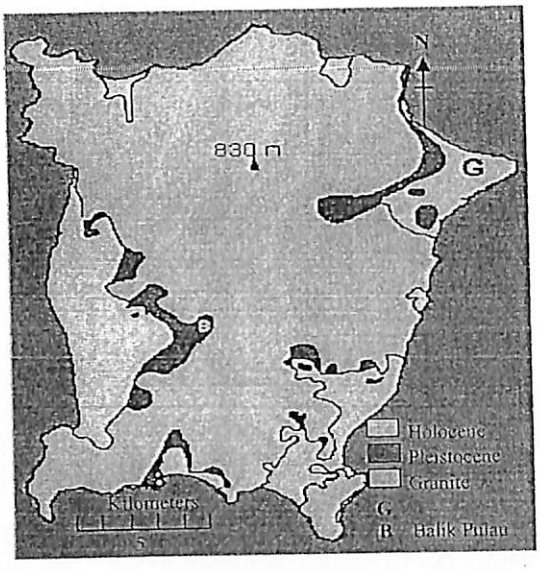

Fig. 1 Geological map of studied site

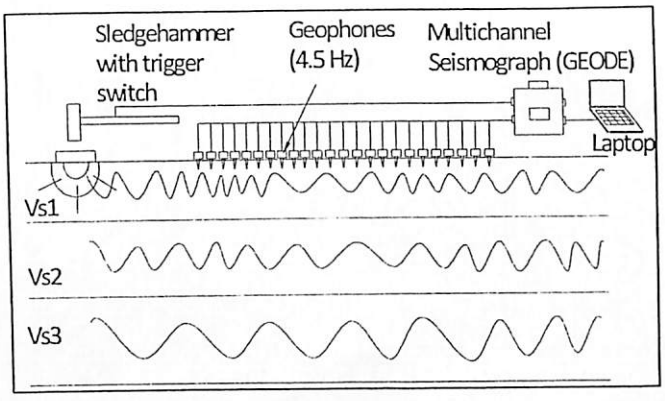

Fig. 2 The field configuration of MASW

$$V_s = 128.71\ N^{0.2833}\ (r^2 = 0.65),\ \text{Class D} \quad (2)$$

$$V_s = 101.34\ N^{0.2364}\ (r^2 = 0.83),\ \text{Class E} \quad (3)$$

The correlations curve from Eqs. 1 to 3 and their raw data were plotted (Fig. 3) to investigate the effect of site classification. In Fig. 3, site classification is indicated to have a significant effect on these correlations. The great differences between these correlations were not only due to the specific geotechnical conditions of the studied site, the quantity of processed data, and the procedures used in undertaking the MASW test, but were also significantly affected by the site classification. Class C consistently gave the highest value of V_s as N_{spt} increased followed by classes D and E. The V_s predicted from Eqs. 1 to 3 were compared with the measured V_s as presented in Fig. 4. The data were scattered between lines 1:0.5 and 1:2 slopes.

Table 2 Existing correlations for V_s and N_{spt}

No	Author (year)	Correlation
1	Imai and Yoshimura (1970)	$V_s = 76N^{0.33}$
2	Ohsaki and Iwasaki (1973)	$V_s = 82N^{0.39}$
3	Seed and Idriss (1981)	$V_s = 61N^{0.5}$
4	Athanasopoulos (1995)	$V_s = 108N^{0.36}$
5	Jafari et al. (1997)	$V_s = 22N^{0.85}$
6	Kiku et al. (2001)	$V_s = 68.3N^{0.292}$
7	Hasancebi and Ulusay (2006)	$V_s = 90N^{0.309}$
8	Hanumantharao and Ramana (2008)	$V_s = 82.6N^{0.43}$
9	Maheswari et al.(2008)	$V_s = 95.6N^{0.301}$
10	Dikmen (2009)	$V_s = 58N^{0.39}$
11	Maheswari and Boominathan (2009)	$V_s = 95.6N^{0.301}$
12	Mhaske and Choudhury (2011)	$V_s = 72N^{0.4}$

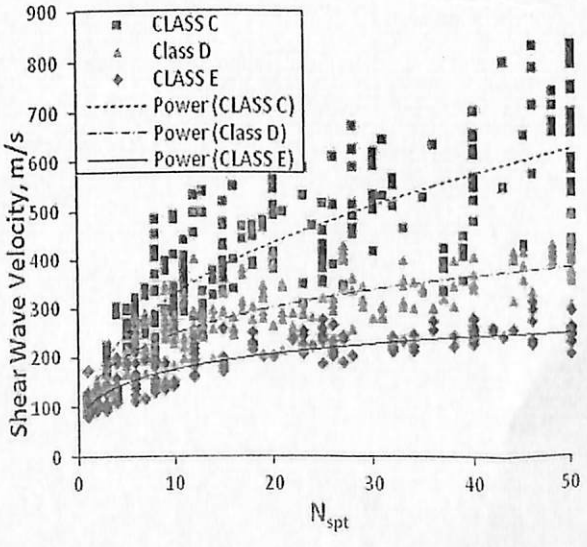

Fig. 3 Correlations for V_s and N_{spt} for all soils with Class C, Class D, and Class E site classification

Comparative Study with Published Correlation

The proposed correlations for three site classifications of all soils were compared with the earlier correlations proposed by various researchers (Fig. 5). The correlations proposed by researchers such as Imai and Yoshimura [5], Kiku et al. [6], Hasancebi and Ulusay [7], Maheswari et al. [8], Dikmen [9], Maheswari and Boominathan [10], and Mhaske and Choudhury [11] yielded similar results with the Class E correlation proposed in the current study. In comparison, correlations proposed by Ohsaki and Iwasaki [12], Athanasopoulos [13], and Hanumantharao and Ramana [14] yielded similar with Class D. The correlation of Seed and Idriss [15] generally under predicted V_s for $N_{spt} \leq 32$ and those over predicted V_s for $N_{spt} > 32$ compared with Class D correlation. The correlation presented by Jafari et al. [16] yielded lower V_s values for $N_{spt} \leq 13$ and $N_{spt} \leq 24$ but over predicted V_s values for Nspt > 13 and $N_{spt} > 24$ of Classes E and D, respectively. However, its correlation approaches Class C correlation when the N_{spt} increased to 50. Note that none of the previous correlations yielded similarly with Class C correlation. This result made sense because, normally, researchers are more interested in sites that produce higher soil amplification factor or cause higher damage to buildings (Class D and Class E) during earthquakes.

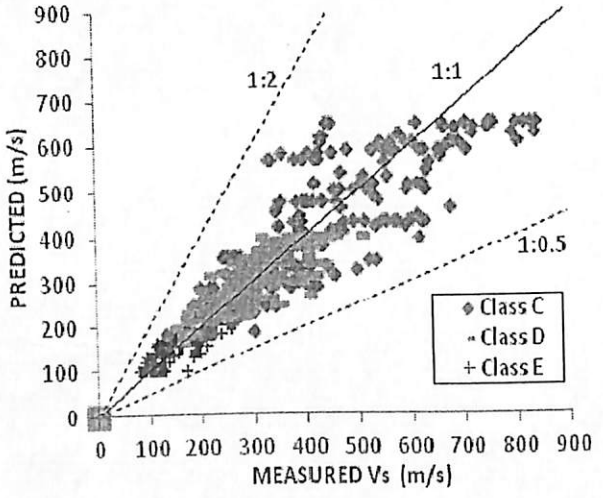

Fig. 4 Measured and predicted V_s for all soils with Class C, Class D, and Class E site classification

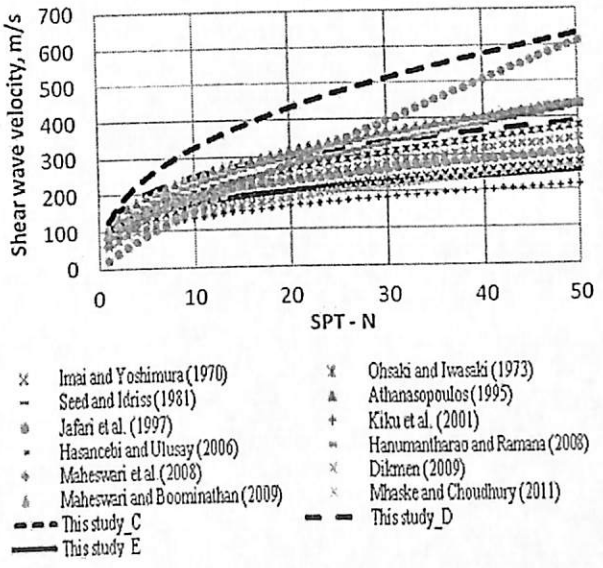

Fig. 5 Comparisons between proposed and previous correlations for all soils

Scaled Percent Error versus Cumulative Frequency

To further investigate the prediction capability of the proposed correlations, the scaled percent errors versus cumulative frequency were also drawn (Fig. 6). The scaled percent error (in per cent) is given by

$$SPE = [(V_{sc} - V_{sm})/V_{sm}] \times 100 \quad (4)$$

where V_{sc} and V_{sm} are predicted and measured V_s, respectively. As depicted in Fig. 6, V_s estimated by Eq. 2 [Fig. 6(a)] is approximately 80% of the V_s values predicted within ± 20% error margin, whereas Eq. 3 [Fig. 6(b)] is approximately 75%. Note that the comparison for Eq. 1 is not shows here because none of the previous correlations yielded similarly with Class C correlation. Generally, the proposed empirical correlations in this study have better estimation power than the existing correlations in the studied site.

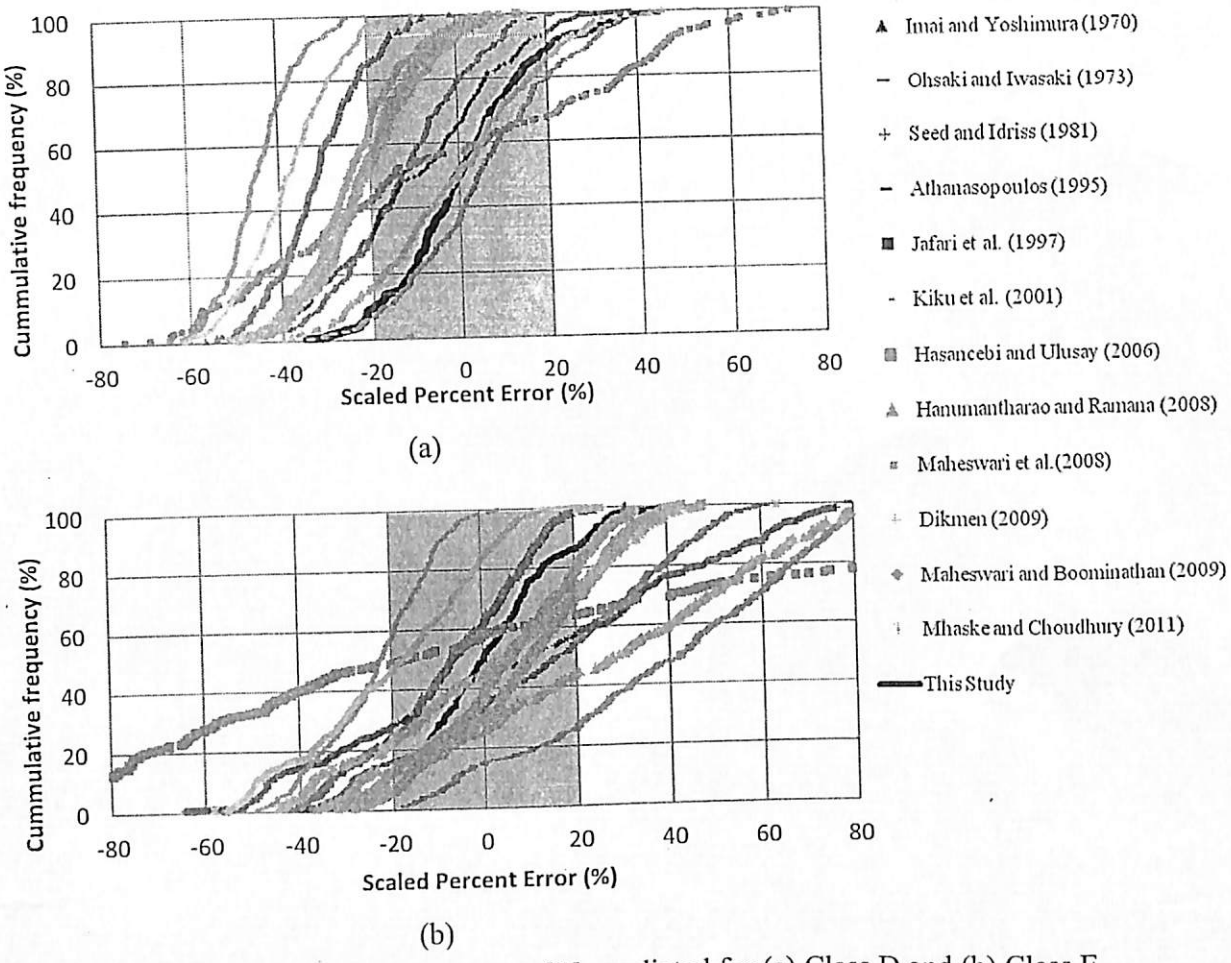

(a)

(b)

Fig. 6 Scaled percent error of V_s predicted for (a) Class D and (b) Class E

Conclusion

In summary, an extensive measurement of V_s employing the MASW geophysical technique was carried out for the Penang region. The correlations between V_s and N_{spt} for all soils with three site classifications, Class C, Class D, and Class E, were developed. Results proved the previous finding that N_{spt} is the main parameter in determining V_s. Site classification was also found to have a significant effect on these correlations. Besides site classification, the differences between proposed and existing correlations are also due to specific geotechnical conditions of the studied sites, the quantity of the processed data, and the procedures in undertaking the geo-seismic surveys. The proposed correlations in this study compare well with the previous existing correlations and exhibit good prediction capability. Therefore, the proposed correlations for all soils are recommended for use in the studied area. The developed correlations for all soils can be effectively utilized for seismic microzonation studies of the northwest region of peninsular Malaysia. However, these correlations are generally site-specific and should be verified against the measured V_s values before being used.

Acknowledgements: This study was supported by the Postgraduate Research Grant Scheme given by Universiti Sains Malaysia. The authors would like to extend their gratitude to the Ministry of Education of Malaysia for permission to collect data from both primary and secondary schools.

References

[1] R.U. Maheswari, A. Boominathan, and G.R. Dodagoudar: Journal of Applied Geophysics Vol. 72 (2010), p. 152-168.

[2] F.W. Colbourne: Tsunami Impact on the West Coast of Penang Island, Malaysia, M.S. in Physical Sciences, Emporia State University (2005)

[3] R.a.J. Luna, H. , in: First International Conference on the Application of Geophysical and NDT Methodologies to Transportation Facilities and Infrastructure, St. Louis, MO (2000).

[4] Y. Xu, J. Xia, and R.D. Miller: Journal of Applied Geophysics Vol. 59 (2006), p. 117-125.

[5] T. Imai and Y. Yoshimura: Tsuchito-Kiso Vol. 18 (1970), p. 17-22.

[6] H. Kiku, et al., in: ICSMGE/TC4 Satellite Conference on Lessons Learned From Recent Strong Earthquakes, (2001).

[7] N. Hasancebi and R. Ulusay: Bulletin of Engineering Geology and the Environment Vol. 66 (2006), p. 203-213.

[8] R. Uma Maheswari, A. Boominathan, and G. Dodagoudar, in: The 14th World Conference on Earthquake Engineering, Beijing, China (2008).

[9] Ü. Dikmen: Journal of Geophysics and Engineering Vol. 6 (2009), p. 61-72.

[10] R. Uma Maheswari, A. Boominathan, and G.R. Dodagoudar: Geotechnical and Geological Engineering Vol. 28 (2009), p. 119-137.

[11] S.Y. Mhaske and D. Choudhury: Natural Hazards Vol. 59 (2011), p. 317-327.

[12] Y. Ohsaki and R. Iwasaki: Soil Found Vol. 13 (1973), p. 61-73.

[13] G.A. Athanasopoulos, in: Proceedings of 7th International Conference on Soil Dynamics and Earthquake Engineering, A.S.Ç. Akmak, Computational Mechanics, Southampton, Chania, Crete (1995).

[14] C. Hanumantharao and G. Ramana: Journal of Earth System Science Vol. 117 (2008), p. 719-730.

[15] H.B. Seed and I.M. Idriss: ASCE National Convention (MO) Vol. (1981), p. pp. 481–544.

[16] M.K. Jafari, A. Asghari, and I. Rahmani, in: Proceedings of 4th International Conference on Civil Engineering, Tehran, Iran (1997).

Soil Dynamics and Earthquake Engineering 44 (2013) 42–53

Contents lists available at SciVerse ScienceDirect

Soil Dynamics and Earthquake Engineering

journal homepage: www.elsevier.com/locate/soildyn

Investigation of story ductility demands of inelastic concrete frames subjected to repeated earthquakes

Ade Faisal [a], Taksiah A. Majid [b,*], George D. Hatzigeorgiou [c]

[a] Fakultas Teknik, Universitas Muhammadiyah Sumatera Utara, Medan, Indonesia
[b] Disaster Research Nexus, School of Civil Engineering, Universiti Sains Malaysia, 14300 Nibong Tebal, P. Pinang, Malaysia
[c] Department of Environmental Engineering, Democritus University of Thrace, Xanthi, Greece

ARTICLE INFO

Article history:
Received 18 January 2012
Received in revised form
9 June 2012
Accepted 19 August 2012
Available online 29 September 2012

ABSTRACT

The present study focuses on the influence of repeated earthquakes on the maximum story ductility demands of three-dimensional inelastic concrete frames. A comprehensive assessment is conducted using generic frames with 3-, 6-, 12-, and 18-story structures. Each is assumed to have behaviour factors of 1.5, 2, 4, and 6 referring to Eurocode 8. Stiffness and strength degrading hysteresis rule to represent reinforced concrete structure is considered in the plastic hinge of members. Twenty ground motions are selected, and single, double, and triple events of synthetic repeated earthquakes are considered. Some interesting findings are provided showing that repeated earthquakes significantly increase the story ductility demand of inelastic concrete frames. On average, relative increment of maximum story ductility demand is experienced 1.4 and 1.3 times when double and triple events of repeated earthquakes are induced, respectively. Empirical relationships are also provided to predict these increments where their efficiency is presented examining characteristic 3- and 8-story reinforced concrete buildings.

1. Introduction

Earthquakes do not usually occur as a single event, as mostly assumed in seismic design, but as a series of shocks. Strong earthquakes have more and larger aftershocks, as well as foreshocks, and the sequences can last for years or even longer. Aftershocks are usually unpredictable and can be of large magnitude, which could collapse buildings damaged from the main shock. Repetition of medium-strength earthquake ground motions after intervals of time characterizes repeated earthquakes [1]. The interval of time can be short or long, taking several minutes, hours, days, or even years, but not more than the structure lifetime (i.e., 50 years). The combination of foreshock, mainshock, and aftershock in repeated earthquakes is illustrated in Fig. 1 and listed in Table 1. These data explain that repeated earthquakes are not a series of foreshock, mainshock, and aftershock within a 24 h period only. Furthermore, repeated earthquakes are not necessarily sourced from the same ruptured fault because it can be experienced by sites situated near active faults having various fault types and rupture mechanism (e.g., Tarzana, Los Angeles). Repeated earthquakes can be a combination of near- and far-field earthquakes containing ground motions with forward directivity (pulse) and backward directivity (no pulse) effects.

In such cases of repeated earthquakes, structures already damaged after the first earthquake ground motion and remaining unrepaired may become completely inadequate at the end of the repeated earthquakes [4]. Despite evidence that repeated earthquakes hazard is clearly threatening, the effect of repeated earthquakes on the structures has not attracted much attention [5]. To the best of the authors' knowledge, only a few studies have examined the repeated earthquakes effects on buildings. Recent studies published addressed the needs in engineering design and evaluation with some constraints. For instance, some of the studies focused on the response of single-of-degree-freedom (SDOF) systems having bilinear elastoplastic hysteresis with no stiffness and strength degradation [5–7]. In fact, real structures can be efficiently simulated with multi-degree-of-freedom (MDOF) systems comprising beams, columns, and beam–column joints those can be deformed in different manners due to cyclic loading reversals propagated by earthquake ground motion. For instance, the story ductility, as a product of interstory drift, is more sensitive than the global ductility in detecting structural damage of elements resulting from roof drift. The story ductility is also directly linked to the level of inelastic behaviour that the system experiences [8]. Moreover, the effect of having hysteresis model with stiffness degradation on the peak displacement of short period of structures is apparently significant and

* Corresponding author. Tel.: +604 5996283x6292; fax: +604 5941009.
E-mail address: taksiah@eng.usm.my (T.A. Majid).

0267-7261/$ - see front matter © 2012 Elsevier Ltd. All rights reserved.
http://dx.doi.org/10.1016/j.soildyn.2012.08.012

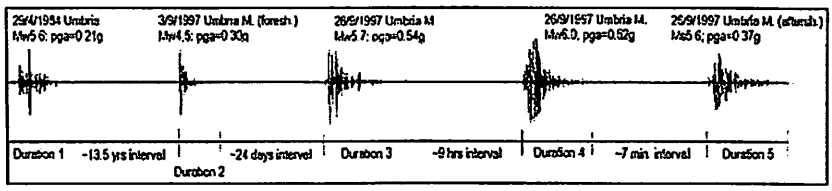

Fig. 1. Example of repeated earthquake ground motions recorded from Norcera Umbra Station, Italy.

Table 1
Examples of repeated earthquake events around the world.

No.	Station	Dir.	Earthquake name	Date	Time	Mag.	PGA (g)	Source
1	LDEO C0375VO, Turkey	NS	Duzce	07/11/1999	16:57	Mw=7.2	0.919	ESD
		NS	Duzce (aftershock)	12/11/1999	16:54	Mw=4.9	0.352	ESD
		NS	Duzce (aftershock)	13/11/1999	00:54	Ms=4.5	0.304	ESD
		NS	Duzce (aftershock)	19/11/1999	19:59	Ms=4.4	0.595	ESD
2	Norcera Umbra, Italy	NS	Umbria	29/04/1984	05:02	Mw=5.6	0.209	ESD
		NS	Umbria-Marche (foresh.)	03/09/1997	22:07	Mw=4.5	0.295	ESD
		NS	Umbria-Marche	26/09/1997	00:33	Mw=5.7	0.538	ESD
		NS	Umbria-Marche	26/09/1997	09:40	Mw=6.0	0.524	ESD
		NS	Umbria-Marche (aftersh.)	26/09/1997	09:47	Ms=5.6	0.372	ESD
3	Kalamata OTE Bldg., Greece	EW	Kalamata	13/09/1986	17:24	Ms=6.2	0.240	ESD
		EW	Kalamata (aftershock)	15/09/1986	11:41	Ms=5.4	0.240	ESD
4	IITR Berlongfer, India	NS	India-Burma Border, India	09/01/1990	18:51	Ms=6.1	0.142	Cosmos
		NS	India-Burma Border, India	06/08/1988	00:36	Ms=7.2	0.344	Cosmos
5	CHY080, Taiwan	EW	Chi-Chi	20/09/1999	17:47	Mw=7.6	0.082	Cosmos
		EW	Chi-Chi (aftershock)	20/09/1999	18:03	Mw=6.2	0.048	Cosmos
6	CSB19001 Jiashi, China	WE	Northwest China (foresh.)	05/04/1997	23:46	Mw=5.9	0.233	Cosmos
		WE	Northwest China (foresh.)	06/04/1997	04:36	Mw=5.9	0.144	Cosmos
		WE	Northwest China	11/04/1997	05:34	Mw=6.1	0.273	Cosmos
		WE	Northwest China (aftersh.)	15/04/1997	18:19	Mw=5.8	0.239	Cosmos
7	Nahanni, NWT, Sta.1, Canada	NS	Nahanni, NWT	23/12/1978	05:16	Ms=6.9	0.975	Cosmos
		NS	Nahanni, NWT (aftersh.)	23/12/1978	05:48	Ms=5.4	0.228	Cosmos
8	DGG Llolleo, Chile	NS	Valparaiso	03/03/1985	22:47	Ms=7.8	0.712	Cosmos
		NS	Valparaiso (aftershock)	03/03/1985	23:38	Ms=6.3	0.186	Cosmos
		NS	Valparaiso (aftershock)	08/04/1985	23:27	Ms=5.0	0.204	Cosmos
9	Imperial Valley, Array 9, USA	SN	El Centro	19/05/1940	04:36	Mw=6.9	0.348	Cosmos
		SN	Borrego Mountain	09/04/1968	02:28	Mw=6.5	0.130	Cosmos
		EW	Imperial Valley	15/10/1979	23:16	Mw=6.5	0.236	Cosmos
		EW	Imperial Valley (aftersh.)	15/10/1979	23:19	M_L=5.0	0.189	Cosmos
10	Cedar Hill NA, Tarzana, USA	EW	Whittier Narrows	01/10/1987	14:42	Mw=6.1	0.405	Cosmos
		EW	Northridge	17/01/1994	12:30	Mw=6.7	1.778	Cosmos
		EW	Northridge (aftershock)	20/03/1994	21:20	Mw=5.3	0.372	Cosmos

NS=North–South; EW=East–West; WE=West–East; SN=South–North.
ESD=European Strong-Motion Database [2].
Cosmos=COSMOS Virtual Data Centre [3].

larger than those experienced by structures having non-degrading hysteresis model [9].

Very recently, Hatzigeorgiou and Liolios [10] have tried to address the deficiency of the MDOF issue. They examined two regular and two irregular reinforced concrete (RC) frames with specific behaviour factors and different dynamic characteristics. All those studies were carried out using ground motion characterized based on source-to-site distance only. In fact, the characteristic of near-field ground motion would be appropriately classified by its large pulse and permanent shifts contained in the motion. These pitfalls can increase the uncertainty of nonlinear dynamic analysis. Therefore, a more comprehensive study pertaining to repeated earthquake hazard on the system having a broad range of fundamental period of vibration and strengths, as well as an appropriate classification of ground motion, is needed. Furthermore, the pertinent literature had focused on SDOF or two-dimensional MDOF systems while this study examines for the first time three-dimensional frames under horizontal bi-directional seismic excitation. Consequently, the findings can be used as general insight and a tool in seismic evaluation. The present study aims to determine the effect of far-field repeated earthquakes on maximum story ductility demands and to develop empirical relationship of maximum story ductility demands on the inelastic RC frames due to repeated earthquakes.

2. Inelastic RC frame modelling

2.1. Simplified frames

Sixty moment-resisting frame systems in the form of generic frame models with three-dimensional multi-story single-bay configuration are evaluated in this study. They are developed based on the concept of Ruiz-Garcia and Miranda [11], previously proposed by Medina and Krawinkler [8]. These types of generic frames have been also used by Ibarra et al. [12] and extended to

multi-bays by Zareian and Krawinkler [13]. The simplified single-bay frame is adequate to represent the global seismic response (e.g., roof drift and maximum interstory drift) exhibited by regular multi-bay frame at different level of inelasticity [8,11,12]. The extension from two-dimensional to three-dimensional generic models was mainly intended to incorporate the bi-directional seismic action so that the near-field ground motion with forward directivity effect (FDE) can be rationally simulated because large pulse in FDE did not occur in both orthogonal directions [14]. In fact, many FDE motions having a large pulse in one direction were recorded in which the other component direction contained a motion with no large pulse as regular as the far-field ground motion.

The present study focuses on the regular geometric system using 3-, 6-, 12-, and 18-story single-bay frame models (Fig. 2), which comply with Eurocode 8 [15] and ASCE 7-05 [16] as a regular horizontal and vertical system. The weight is lumped at the center of each story and arranged to remain constant at each story. The fundamental periods considered for the models are $T_1=0.45$, 0.75, 1.26, and 1.71 s to reflect the common multi-story moment-resisting frame, particularly from 3 to 20 building stories [17]. The shape of the floors and roof are square with size of 7.2×7.2 m and with uniform column height of 3.6 m for all stories. To model the presence of a rigid slab, a rigid diaphragm assumption for the floor/roof is utilized. The columns and beams at each story have the same stiffness to reduce uncertainty and complexity in modelling and results assessment. Most building damages due to an earthquake occur at the member ends; hence, the inelasticity is modeled with flexural plastic hinges located at the member ends (full-hinge mechanism). More specifically, according to Fardis [18], the plastic hinge length can be estimated by the following relation

$$L_{pl}=0.08\times L_s+a_{sl}(0.22d_{bl}f_{yL}) \quad (f_{yL}\text{ in MPa}) \tag{1}$$

where L_s is the member length, L_{pl} is the plastic hinge length, a_{sl} is a zero-one variable (with $a_{sl}=1$ if slippage of longitudinal bars from the anchorage zone beyond the end section is possible, and $a_{sl}=0$ if slippage is not possible) and d_{bl} the mean tension bar diameter. For the concrete frames under consideration, the above equation leads to $L_{pl}\cong0.10L_s$ and for this reason it can be assumed that $L_{pl}=10\%L_s$. The P-delta effect is considered in the current work. A 5% Rayleigh damping ratio is used at the first mode and the mode where 90% of mass participation is attained. The use of such low damping ratio is common for moment-resisting frames as regulated in many codes (e.g., Eurocode 8 and ASCE 7-05). Moreover, to avoid inaccurate estimate of displacements, apparent when the Rayleigh damping is mixed with lumped plasticity model adopted for the plastic hinge at member ends [19], a practical approach of using the Rayleigh damping according to by Zareian and Medina [20] is used in the current study.

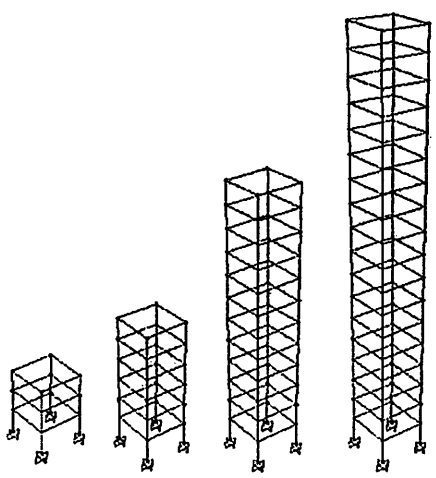

Fig. 2. Three-dimensional generic frame models representing 3-, 6-, 12-, and 18-story single-bay reinforced concrete frames.

2.2. Stiffness and strength distributions

The stiffness distribution used for the models is classified as regular stiffness according to ASCE 7-05, which means that the difference between the stiffness of adjacent stories is less than 60% of the story above or less than 70% of the average stiffness of the three stories above. This condition complies with Eurocode 8 as regular stiffness as well. The models are designed to exhibit the first-mode elastic deflected shape to be more realistic. Therefore, we used the ratio of the stiffness of all beams at the mid-height story of the frame to the sum of the stiffness of all columns at the same story based on the empirical relationship proposed by Miranda and Taghavi [21]. The stiffness distribution is tuned so that the variation of lateral stiffness along the height of the structure follows parabolic variations [22]. To have a more realistic simulation, the present study selects the decreasing stepwise distribution of lateral stiffness based on the resulting parabolic variation, and this lateral stiffness changes for every three stories. The dynamic characteristic of the models is listed in Table 2.

Four types of ductility-related behaviour factor q, namely, 1.5, 2, 4, and 6, are considered. This is done because most earthquake-resistant building designs using Eurocode 8 for moment-resisting frame have behaviour factors within the range of $1.5<q\leq4$ for medium ductility (denoted as DCM in Eurocode 8) and within the range of $4<q\leq6$ [18] for high ductility (DCH). The definition of the flexural plastic hinge is in line with the selected q using linear elastic analysis. The q factor is defined as the ratio of the ground motion intensity $S_e(T_1)/g$ to the design lateral force in the structure F_b divided by the weight of the structure W, as follows:

$$q=\frac{S_e(T_1)/g}{F_b/W} \tag{2}$$

This definition is also employed by others, including Medina and Krawinkler [8], Ruiz-Garcia and Miranda [11], and Zareian and Krawinkler [13]. Behaviour factor q affects the following modal seismic action $S_d(T)$

$$S_d(T)=S_e(T)/q \tag{3}$$

where $S_d(T)$ is the modal seismic action taken from the design spectrum response acceleration at period T, $S_e(T)$ denotes the elastic response spectrum at period T, and q is equal to q_o times the overstrength (denoted by α_u/α_1 in Eurocode 8). In the present paper, the maximum flexural bending moment is selected as the strength parameter of the member, which is obtained from the linear elastic static lateral method using horizontal force F_i derived from F_b. This strength value is assigned as the yield moment to the hinge location in a generic frame. To adopt a strong column–weak beam mechanism in an earthquake resistant system, strength ratios equal to 1.3 between columns and beams are considered ($\Sigma M_b\leq1.3\Sigma M_{col}$), as suggested by Eurocode 8,

Table 2
Fundamental period of vibration $T_{1,2}$, third-mode period of vibration T_3, and normalized modal participation factor $MPF_{1,2}$, obtained for each model.

N	$T_{1,2}$ (s)	T_3 (s)	$MPF_{1,2}$
3	0.45	0.23	1.23
6	0.75	0.37	1.34
12	1.26	0.56	1.42
18	1.71	0.62	1.41

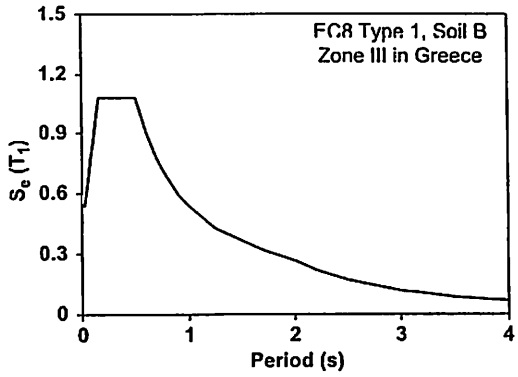

Fig. 3. Elastic spectrum acceleration of Eurocode 8 with 5% damping ratio for Type 1 and Soil B at Zone III of Greece.

in obtaining the height-wise strength distribution. The over-strength is also uniformly added with a factor of 1.3 of the available strength to represent the overstrength regulated in Eurocode 8 for real multi-story multi-bay structures. The strength is then tuned, and the mechanism is checked using pushover analysis by examining the plastic hinge progress. However, adjusting the system so that all beams will experience plastic hinges earlier than any column before the entire system collapses is neither realistic nor possible [13].

F_b is defined from ordinate design spectrum at period T_1 of the Type 1 spectrum of Eurocode 8 for Soil B condition. The elastic spectrum acceleration used in the present work with peak ground acceleration (PGA) a_g=0.36 g is shown in Fig. 3. Soil B is selected because majority of available records in the European Strong Motion Database (40.8%) are sourced from stiff soil (Soil B), as discussed by Iervolino et al. [23]. a_g is based on a 475-year return period of earthquake that reflects the condition of Seismic Zone III in Greece. Greece represents the highest seismic region in Europe, along with Turkey and Italy, whereas Zone III is the zone with highest seismicity in Greece. The model is assumed to represent ordinary building, and hence, it has an importance factor equal to 1.0.

2.3. Plastic hinge and backbone curve

The plastic hinge is represented by a moment–rotation relationship, modelled using a lumped plasticity model. To simulate the cyclic behaviour of RC members in plastic hinge under load reversals, the modified-Takeda hysteresis rule is employed (Fig. 4), where the unloading and reloading parameters (α=0.3 and β=0.6) for the beam and column members are identical, as suggested by Fardis [24]. The backbone curve proposed by Zaerian and Krawinkler [13] is used, as shown by the thin line in Fig. 4. The yield rotation θ_y of a member is obtained by the ratio of M_y to elastic rotation stiffness (K_0=6EI/L).

Plastic rotation capacity mostly affects the collapse capacity of the ductile system [12]. In an RC system, this parameter is mainly governed by the loss of confinement of the concrete core or onset of rebar buckling [25]. To represent the capacity of general RC structures, the current work employs the moment–rotation capacities of the RC beam–column members within the capacity range suggested by Haselton et al. [26] because their suggested capacity is based on the evaluation and calibration of the database from experimental testing of RC members, largely dominated by the data studied by Panagiotakos and Fardis [25]. To reflect the low, medium, and high rotation capacities of the RC members, the current work used plastic rotation capacity θ_p, namely, 0.02, 0.04, and 0.06, as proposed by Zareian and Krawinkler [13]. To the best of the authors' knowledge, the test data for the calibration of M_c/M_y and post-capping rotation θ_{pc} are insufficient because these

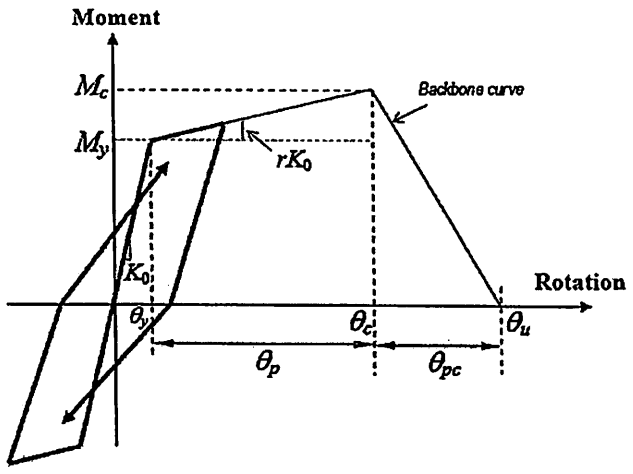

Fig. 4. Modified-Takeda hysteresis and backbone curve.

parameters are relatively new. Therefore, θ_{pc} is assumed to be equal to 0.06 based on the average value of θ_{pc} used in the Zareian and Krawinkler's study, whereas the ratio of M_c/M_y is assumed to be 1.13, as suggested by FEMA-P695 [27]. The post-yield stiffness ratio r is estimated based on M_y, capping moment, M_c, K_0, θ_y, and ductility of plastic rotation capacity $\mu_{\theta,c}$, as shown in Fig. 4.

Cyclic strength degradation can significantly increase the peak displacement demands of structures, particularly for short period of structures. The peak displacement demands are very sensitive to the changes of yield strength [28]. Therefore, the present study considers the strength degradation of the member based on rotation ductility from Zareian and Krawinkler's [13] backbone curve, developed based on the hysteresis rule proposed by Ibarra et al. [12].

In the current work, the parameters of r_k and ϑ_c are introduced in order to characterize the stiffness and capacity of ductility of the global system, respectively. The ratio of global post-yield stiffness to elastic stiffness r_K of a model and the ratio of story ductility to global ductility capacities ϑ_c of a model are defined using nonlinear static analysis. It is used as the inelastic properties of the considered concrete frame, which were governed by the fundamental period, behaviour factor, and rotation capacity of member. After regressing r_K of 60 models having varies T_1, q, and θ_p, the following expression is used to characterize the global stiffness of the considered models in the present work.

$$r_K = 10^{-0.132T_1^3 - 0.901\log(q) - 11.252\theta_p - 1.290} \quad (4)$$

Eq. (4) has coefficient of determination, denoted by R^2, and standard deviation of error in log-normal distribution, denoted as σ_{err}, of 0.972 and 0.072, respectively. The relationship explains that θ_p governs r_K compares with T_1 and q. The trend also clearly shows that as θ_p increases r_K decreases, a trend similar to that in the Zareian and Krawinkler study [13]. Only r_K with the range of 0–3% is evaluated in the current work. Moreover, the ratio of ductility capacity of the models represented by the ratio of story to global ductility capacity ϑ_c is introduced to relate the maximum global ductility (based on roof displacement) with the maximum story ductility (based on interstory drift) capacity. The following empirical relationship of ϑ_c reflects the ratio of ductility capacity of the 60 models, based on regression analysis (R^2=0.983; σ_{err}=0.028).

$$\vartheta_c = 10^{0.513T_1^3 - 0.971T_1^2 - 0.406T_1^{-1} - 0.046Log(r_K) + 1.037} \quad (5)$$

The aforesaid relationship excludes q and θ_p since both have negligible effects on ϑ_c. It also clearly indicates that as T_1 increases,

ϑ_c also increases. The models evaluated in the present work appear to have ratio of ductility capacity $1.2 \leq \vartheta_c \leq 4.9$.

3. Seismic input

3.1. Selection of ground motion record

In this work, twenty strong motion records have been examined, which have been downloaded from the European Strong Motion Database (ESD) [2], according to suggestions of Bommer and Acevedo [29]. These far-field earthquakes appear in Table 3 and are compatible with soil Type B of Eurocode 8 [23], i.e., compatible with the design process. The spectral acceleration at the fundamental period of a structure, denoted as $Sa(T_1)$, is utilized as the intensity measure of ground motion used in nonlinear response history analysis. The scaling process focuses on this intensity measure following the method proposed by Shome et al. [30], which is employed here due to its simplicity and accuracy [31].

3.2. Assembling synthetic repeated earthquakes

The main objective of this section is to provide with repeated earthquakes records, in order to examine their influence on

Table 3
Selected far-field earthquake ground motions from ESD.

No.	Date	Earthquake name	Mag. (*Mw*)	Dist. (km)	Station
1	09/15/1976	Friuli (aftersh.)	6.0	21	Breginj-Fabrika IGLI
2	09/15/1976	Friuli (aftersh.)	6.0	37	Kobarid-Osn.Skola
3	04/15/1979	Montenegro	6.9	25	Petrovac-Hotel Olivia
4	04/15/1979	Montenegro	6.9	24	Ulcinj-Hotel Olimpic
5	05/24/1979	Montenegro (aftersh.)	6.2	33	Bar-Skupstina Opstine
6	05/24/1979	Montenegro (aftersh.)	6.2	22	Kotor-Zovod
7	11/23/1980	Campano Lucano	6.9	43	Brienza
8	11/23/1980	Campano Lucano	6.9	48	Mercato San Severino
9	03/19/1983	Heraklio	5.6	40	Heraklio-Prefecture
10	10/16/1988	Kyllini	5.9	36	Armaliada-OTE Building
11	06/15/1991	Racha (aftersh.)	6.0	40	Iri
12	10/14/1997	Umbria-Marche (aftersh.)	5.6	24	Nocera Umbra
13	08/17/1999	Izmit	7.6	73	Goynuk-Devlet Hastanesi
14	09/07/1999	Athens/Ano Liosia	6.6	20	Athens 2, Chalandri District
15	06/27/1998	Adana-Ceyhan	6.3	80	Mersin-Meteoroloji Mudurlugu
16	06/17/2000	South Iceland	6.5	21	Selsund
17	11/18/1997	Strophades	6.6	38	Zakynthos-OTE Building
18	06/21/2000	South Iceland (aftersh.)	6.4	21	Hella
19	11/12/1999	Duzce 1	7.2	31	LDEO Sta. C1061
20	11/12/1999	Duzce 1	7.2	26	LDEO Sta. D0531 WF

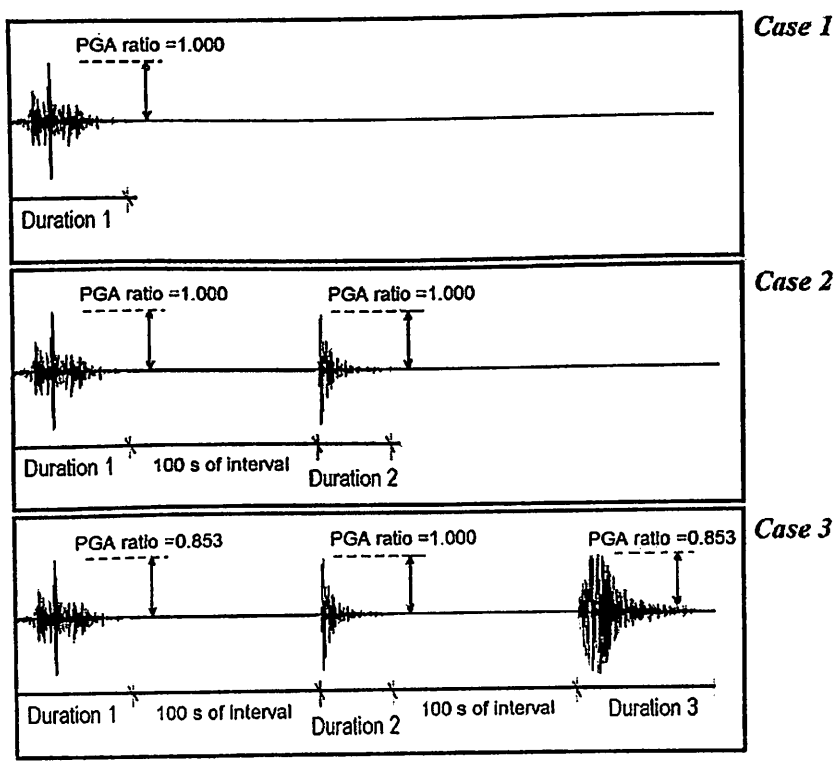

Fig. 5. Illustration of assembling the ground motion to generate synthetic repeated earthquakes.

structural behaviour, e.g., damage accumulation, in comparison with the corresponding single earthquakes. Up to now, the existent research [1,10,11] is limited to two-dimensional frames with seismic excitation in one (horizontal) direction only. In the present work, the repeated earthquakes are presented in a form of combination of the bi-directional ground motion with single, double, and triple events. Due to lack of real seismic sequences records, this paper examines only artificial sequences, where they have been generated by a rational combination of real single events. The assembly method is obtained from the study of Hatzigeorgiou and Beskos [5]. To the best of the authors' knowledge, no other practical method is found related to this issue. In this method, the amplitude ratio of the assembled ground motion is scaled based on the PGA ratio, as shown in Fig. 5, governed by the magnitude of consecutive earthquakes sourced from the same seismic region and recorded at the same site. The PGA ratio was derived using the ratio of empirical attenuation functions, which vary in magnitude [5]. The examined cases of double and triple seismic events appear to be realistic scenarios of multiply earthquakes and have been based on the findings of recognized research works on Engineering Seismology, such as the works of Gutenberg and Richter [30] and Joyner and Boore [31]. For more information, the reader can consult Refs. [5–7,10]. Thus, three types of amplitude ratios of assembled ground motion was used in the present paper, i.e., single earthquake event (mainshock only) with PGA amplitude ratio of (1.000, 0.000, 0.000) as GM Case 1, double earthquake events (foreshock–mainshock or mainshock–aftershock) with PGA amplitude ratio of (1.000, 1.000, 0.000) as GM Case 2, and triple earthquake events (foreshock–mainshock–aftershock) with PGA amplitude ratio of (0.853, 1.000, 0.853) as GM Case 3. An interval motion with zero amplitude of acceleration and 100 s duration was inserted between two consecutive ground motions. This interval is absolutely enough to achieve the state of rest of any ordinary multistory building after vibration due to inherent damping, as suggested by Hatzigeorgiou [7]. Each of the earthquake events is applied for GM Case 1 or single-event earthquake. For GM Cases 2 and 3, repeated earthquakes are assembled using different earthquake events randomly added to GM Case 1.

4. Result and discussion

The story ductility demand, defined as the mean value of maximum interstory drift from nonlinear time history analysis normalized by interstory yield from nonlinear static analysis, i.e., $\mu_s = \delta_{max}/\delta_y$, is used as the engineering demand parameter in the present paper. Figs. 6 and 7 show the trend of mean story ductility demand μ_s along the height under repeated earthquakes GM Cases 1, 2, and 3. For shorter system period, i.e., 3-story model in Fig. 6, the maximum story ductility demand $\mu_{s,max}$ due to GM Cases 1, 2, and 3 tends to appear at the top story. This is also true in the case of the 6-story model with $q<2$ in Fig. 6. This maximum demand then migrates to the bottom story as the strength decreases and as the building becomes taller. For taller models, all of $\mu_{s,max}$ due to GM Cases 1, 2, and 3 are situated at the bottom story, regardless of the type of behaviour factor and ground motion (Fig. 7), which means that the dispersion of $\mu_{s,max}$ of inelastic structures induced by repeated earthquakes of GM Cases 2 and 3 follows the same trend as that of GM Case 1. The influence of repeated earthquakes on the dispersion of $\mu_{s,max}$ is negligible. A similar trend was also found for the interstory drift on the 3- and 8-story RC frame models used by Hatzigeorgiou and Liolios [10] in evaluating the effect of repeated earthquakes. Using a different type of material (i.e., steel) and hysteresis rule, Ruiz-Garcia and Negrete-Manriquez [32] indicated that the story drift in the 4-, 8-, and 12-story inelastic models performed with the same trend as well. These two studies supported the aforesaid findings that mentioned that repeated earthquakes did not affect the dispersion of $\mu_{s,max}$ along the height. In general, the relative

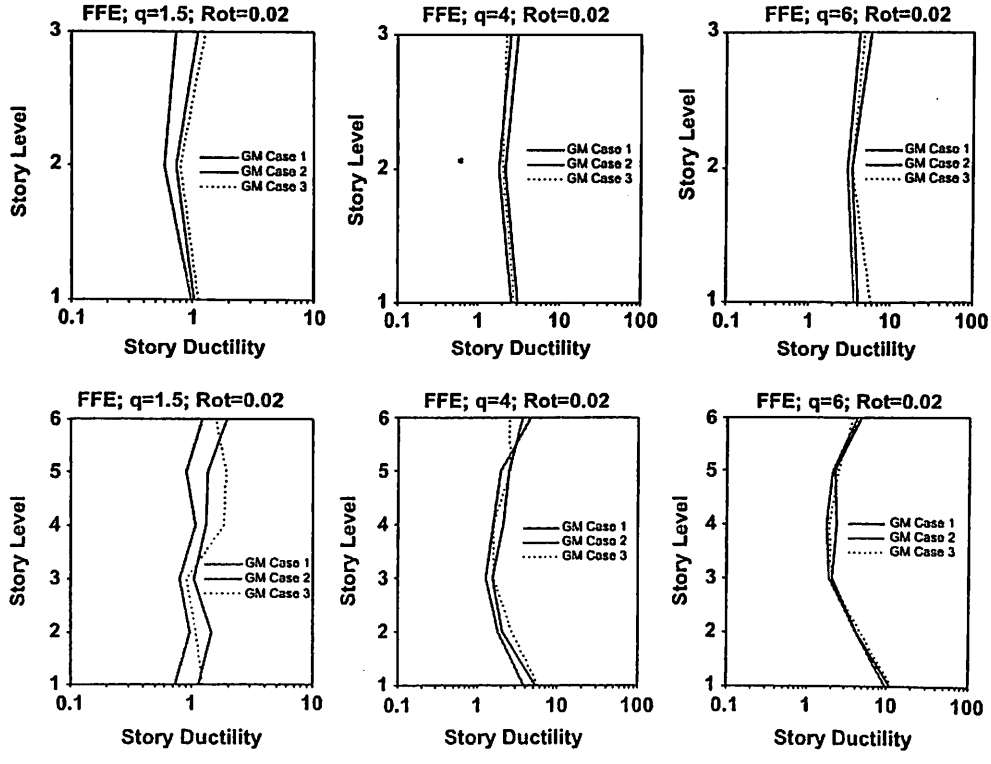

Fig. 6. Story ductility demands of 3- and 6-story inelastic concrete frames affected by repeated GM Cases 1, 2, and 3.

Table 4
$A_{r-\mu sm}$ on the models with average plastic rotation capacity and behaviour factor $1.5 \le q \le 6$ induced by repeated earthquakes.

Models	Repeated GM case	q=1.5	q=2	q=4	q=6
3-story model (T_1=0.45 s)	GM case 2	1.2	1.2	1.4	1.4
	GM Case 3	1.3	1.2	1.4	1.3
6-story model (T_1=0.75 s)	GM Case 2	1.5	1.3	1.3	1.1
	GM Case 3	1.7	1.9	1.4	1.1
12-story model (T_1=1.26 s)	GM Case 2	1.4	1.6	1.2	1.3
	GM Case 3	1.3	1.8	1.3	1.1
18-story model (T_1=1.71 s)	GM Case 2	1.5	1.4	1.2	1.2
	GM Case 3	1.5	1.7	1.6	1.5

$A_{r-\mu sm}$ on the models with fundamental period $0.45 \le T_1 \le 1.71$ s (or systems having from 3 to 18 number of stories) with average plastic rotation capacity and $q \ge 1.5$ is listed in Table 4. On average, GM Case 3 propagates an increment of $\mu_{s,max}$ on the considered concrete frames 16% larger than GM Case 2. $A_{r-\mu sm}$, regardless of GM Case 2 or 3, are found within the ranges from 1.2 to 1.6 and from 1.1 to 1.5 for the system designed with DCM (q=4) and DCH (q=6), respectively. In the system with DCM and DCH, the gaps of $A_{r-\mu sm}$ between GM Cases 3 and 2 reaches 19.2% and 12.8%, respectively. Therefore, the maximum story ductility on the system with DCM can be increased higher than the system with DCH when repeated earthquakes are propagated.

To the best of the authors' knowledge, similar studies that evaluated maximum story ductility demand on various types of fundamental period of vibration, plastic rotation capacity, and behaviour factors are not available yet. Therefore, comparison of maximum story ductility is difficult to make. Nevertheless, Hatzigeorgiou and Liolios [10] and Ruiz-Garcia and Negrete-Manriquez [32] studied the effect of repeated earthquakes on few models. The former focused on the roof ductility of 3- and 8-story regular RC frames having q=3.9. Their study graphically explained that the maximum interstory drift on the 8-story RC frame with T_1=1.23 s increased from 1.4 to 1.75 times due to repeated earthquakes, meaning that the maximum story ductility of that structure increased in the same range of values due to repeated earthquakes. Ruiz-Garcia and Negrete-Manriquez [32] evaluated 3- and 8-story inelastic structures (T_1=1.23 and 1.95 s) under real and synthetic repeated earthquakes. Their study graphically demonstrated that the increment of maximum interstory drift reached about 1.23 and 1.14 when synthetic earthquake induced the models at T_1=1.23 and 1.95 s, respectively. There was no information pertaining to the behaviour factor they have used in their article. Therefore, the average maximum story ductility demand of the system having high ductile system, i.e., q=4 to 6, were used, and the resulting increment of about 1.43 was due to the repeated near-field earthquake for system at T_1=1.26 s. This finding is reasonable because the Ruiz-Garcia and Negrete-Manriquez's findings were based on ground motions having pulse and having slightly shorter fundamental period than the current study. The maximum interstory drifts on the model considered in Hatzigeorgiou and Liolios [10] and Ruiz-Garcia and Negrete-Manriquez [32] appeared in the lower stories, which well agreed with the current study.

4.1. Predicting maximum story ductility demand

It is well-known, e.g., from Refs. [5–7,10], that multiple earthquakes leads to increased deformation demands in comparison with the corresponding single events. The main objective of this section is to provide with empirical relations to estimate the maximum story ductility demands, $\mu_{s,max}$, for sequential strong ground motions. These empirical relations will be proposed for all the examined cases of Section 3.2.

First, one must define which variables were statistically significant to the dependent variable. Thus, applying sensitivity analysis it is found that the fundamental period (or equivalently the number of floors) and behaviour factor, strongly affect $\mu_{s,max}$ when repeated earthquakes occur. Two nonlinear structural parameters were also incorporated: the ratio of post-yield stiffness r_K, and the ratio of roof ductility to maximum story ductility capacities ϑ_c. The parameter r_K reflects the stiffness condition of the system in linear and nonlinear states, and reflects that the building becomes more flexible when r_K decreases. The value of P-delta that affects the system can also be explained by this parameter because the P-delta effect on the ratio of post-yield stiffness increases as the height of the building increases.

The nonlinear multiple regression analysis was performed to obtain regression parameters. The empirical formulas used to estimate the mean maximum story ductility demand, denoted by $\mu_{s,j}$, are shown in the following. The subscript j indicates the case of repeated earthquakes, which is from 1 to 3 for repeated GM Cases 1, 2, and 3, respectively. These can be predicted as follows:

$$\ln(\mu_{s,1}) = 0.761\ln(T_1) + 0.877\ln(q) + 0.112(r_K^{-0.4}) - 0.300 \quad (6)$$

$$\ln(\mu_{s,2T_1}) = 0.785\ln() + 0.826\ln(q) + 0.501(r_K^{-0.25}) - 0.893 \quad (7)$$

$$\ln(\mu_{s,3}) = 0.720\ln(T_1) + 0.610\ln(q) + 1.843(r_K^{-0.15}) - 2.822 \quad (8)$$

where R^2 of these relationships are found to be 0.987, 0.988, and 0.974, respectively. Standard deviation of error, denoted by σ_{err}, for Eqs. (6)–(8) are found to be 0.124, 0.126, and 0.184, respectively. Eqs. (6)–(8) were ones of the simplest equations which better described the numerical data following downward and upward concave curves after testing hundreds of mathematical equations. For the system induced by seismic repetition GM Case 2 or 3, $\mu_{s,j}$, can be estimated with the relationship in Eq. (9) with R^2=0.979 and σ_{err}=0.166, as follows:

$$\ln(\mu_{s,2-3}) = 0.726\ln(T_1) + 0.659\ln(q) + 1.774(r_K^{-0.15}) - 2.694 \quad (9)$$

The efficiency of Eqs. (6)–(9) is shown in Fig. 9 where the proposed model results are compared with their counterparts from 'exact' dynamic inelastic analyses. In general, the diagonally scattered data appears in the range of $\mu_{s,j} > 20$ for all GM Cases, which is inevitable, especially at higher ductility level. It is due to the reason of selected range of behaviour factor and the P-delta effect of long-period RC models. Nevertheless, it is evident in any case that the results from predicted model obtained from this study are in good agreement based on R^2, σ_{err}, F-sig ratio, and the scatter plot of correlation between prediction model and results obtained from the dynamic inelastic analyses. Therefore, by using Eqs. (6)–(9) the effect of repeated earthquakes on $\mu_{s,max}$ of reinforced concrete frame building in form of $A_{r-\mu sm} = \mu_{s,(j>1)}/\mu_{s,1}$ can be predicted directly. These equations are valid only within the range considered in the present study.

4.2. Case studies using the prediction formulas

This section presents practical case studies in implementing the prediction formulas for the RC frame models, published by Hatzigeorgiou and Liolios [10]. Their models have been selected because they have been designed for the same region (Europe) covered in the present study. Likewise, they used these models to assess repeated earthquakes.

The models consist of 3- and 8-story moment-resisting RC frames, which represent low and medium-rise RC structures having fundamental period of vibration T_1 equal to 0.621 and 1.280 s, respectively. Both models have three equal bays with a

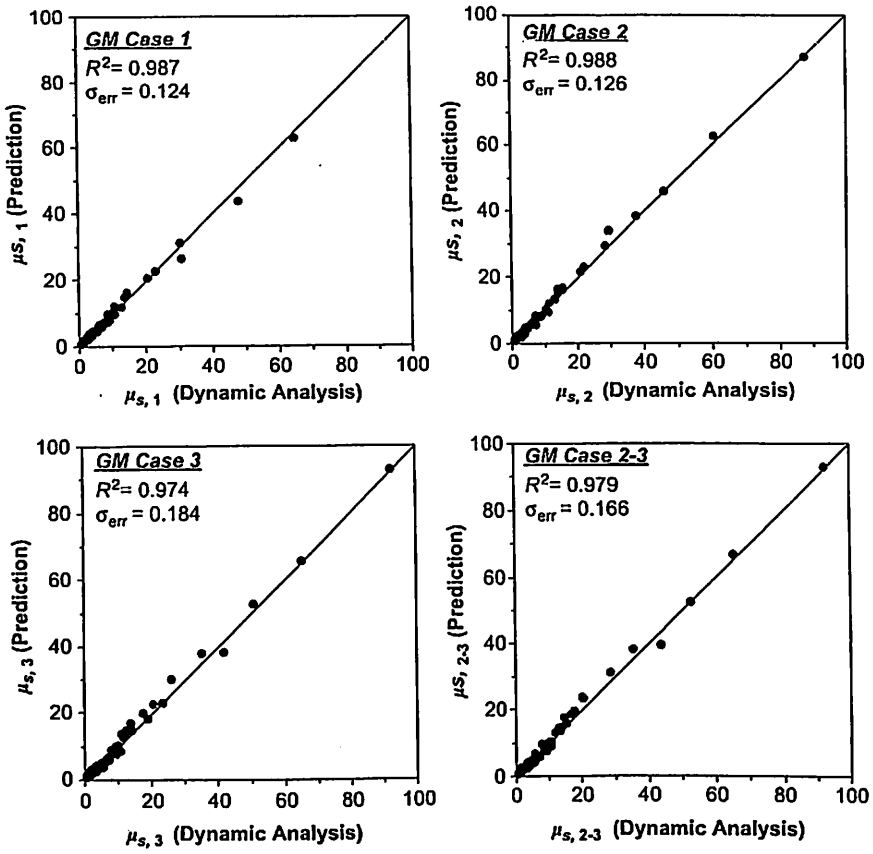

Fig. 9. Comparison of prediction model with analytical result of the mean maximum story ductility demand of inelastic concrete frames due to repeated earthquakes.

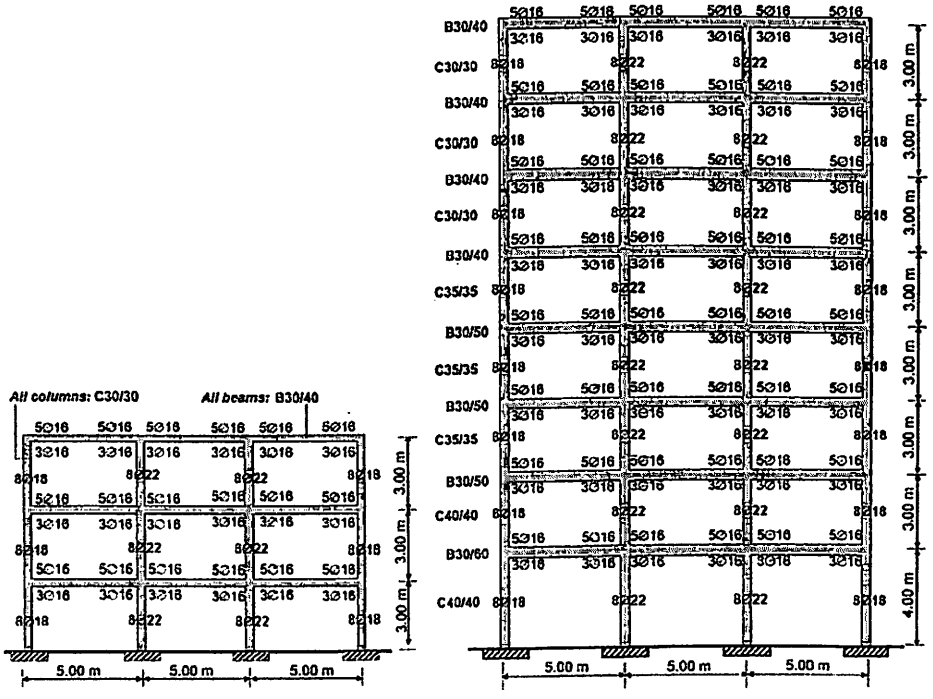

Fig. 10. Three- and eight-story moment-resisting concrete frames [10].

total length of 15 m, and all typical floor-to-floor heights are equal to 3.0 m, except for the first floor of the 8-story buildings whose height was equal to 4.0 m. The illustration of the models is shown in Fig. 10. The examined models, according to Eurocode 8 [15], are built on Class B soil located in Greece, a high-seismicity region of Europe. The model also considers both gravity and seismic loads,

Table 5
Selected far-field earthquake ground motion from ESD for the case studies.

No.	Date	Earthquake name	Mag. (*Mw*)	Epi. (km)	Station	Dir.
1	03/19/1983	Heraklio	5.6	40	Heraklio-Prefecture	EW
2	03/19/1983	Heraklio	5.6	40	Heraklio-Prefecture	NS
3	09/07/1999	Athens, Ano Liosia	6.6	20	Athens 2, Chalandri District	N126
4	09/07/1999	Athens, Ano Liosia	6.6	20	Athens 2, Chalandri District	N36
5	11/18/1997	Strofades	6.6	38	Zakynthos-OTE Building	140
6	11/18/1997	Strofades	6.6	38	Zakynthos-OTE Building	230

Table 6
Assembled ground motions as synthetic repeated earthquakes for the case studies.

GM no.	GM Case 1	GM Case 2	GM Case 3
1	GM No. 1	GM No.1–GM No.2	GM No.4–GM No.1–GM No.2
2	GM No. 3	GM No.3–GM No.4	GM No.6–GM No.3–GM No.4
3	GM No. 5	GM No.5–GM No.6	GM No.2–GM No.5–GM No.6

Table 7
Dynamic characteristics of 3- and 8-story frames.

	3-story model			8-story model		
	Mode 1	Mode 2	Mode 3	Mode 1	Mode 2	Mode 3
T_1 (s)	0.621	0.197	0.138	1.280	0.492	0.271
MPF	0.781	0.075	0.021	0.823	0.189	0.049

where a design PGA of 0.2 g is assumed. The dead loads (excluding self-weight) is equal to 20 kN/m, whereas the live load is 10 kN/m. Both loads are applied on the beams. Rigid diaphragm is assumed for all floors to represent the action of concrete slabs.

Both models have been designed for DCM class according to Eurocode 8, which has behaviour factor $q=3.9$. The effective moments of inertia I_{ef} were considered in the design, namely, $I_{ef}=0.5\ I_g$ for the beams and $I_{ef}=0.9\ I_g$ for the columns, where I_g is the moment of inertia of the corresponding cross section. The concrete compressive strength (concrete grade C20) is assumed to be 20 MPa, whereas the yield strength for both longitudinal and transverse reinforcements is 500 MPa (steel grade S500). The reinforcement arrangement can be seen in Fig. 10. The elastic and shear moduli of concrete are assumed equal to 2.885×10^4 and 1.202×10^4 MPa, respectively.

For practical purposes, the models were induced by three ground motions, and thus, the maximum response is considered as the final result. The selected ground motion is presented in Table 5, taken from ESD that originally occurred in Greece. These ground motions were assembled within the same type of ground motion to generate the repeated earthquakes. The combination of assembled ground motions is presented in Table 6.

The results of eigenvalue analysis, i.e., fundamental period of vibration T_1 and mass participation factor *MPF*, are presented in Table 7. Based on pushover analysis, the global post-yield stiffness ratio r_K was found equal to 0.003442 for the 3-story model. Using the empirical formula given in Eq. (4), r_K was found to be equal to 0.004963, based on the result of T_1 in Table 7, plastic rotation capacity $\theta_p=0.04$, and behaviour factor $q=3.9$. The selection of $\theta_p=0.04$ was based on assumption that RC members are well-detailed to avoid the loss of confinement of the concrete core or onset of rebar buckling [33]. The yield displacement was found to be equal to 0.0450 m, whereas the yield interstory drifts were equal to 0.0153, 0.0170, and 0.0127 for the first, second, and third stories, respectively. The ultimate displacement was equal to 0.573 m, whereas the ultimate interstory drifts were equal to 0.363, 0.154, and 0.018 for the first, second, and third stories, respectively. Therefore, the ductility capacity $\vartheta_c=1.863$ from the aforesaid results, which is in good agreement with 1.728 obtained from ϑ_c of Eq. (5).

The global post-yield stiffness ratio r_K was found to be equal to 0.001926 for the 8-story model based on the pushover analysis. Using the empirical formula given in Eq. (4), r_K was equal to 0.002822. The yield and ultimate displacements were found to be equal to 0.071 and 0.821 m, whereas the maximum yield and ultimate interstory drifts were equal to 0.0164 and 0.427 m, respectively. Using these findings, the ratio of ductility capacities of the 8-story model was equal to $\vartheta_c=2.251$, in good agreement with 2.099 obtained from ϑ_c of Eq. (5).

The story ductility results of the 3- and 8-story models indicate the extreme drift that occurs at the lower part. Although few cases indicate that GM Case 2 governed, most of GM Case 3 produced the maximum drift result. For the 8-story model, GM Case 3 governed all ground motions. The comparison of the analytical and prediction findings of the maximum story ductility demands for each case of repeated earthquakes (Table 6) is presented in Table 8. It is evident that very good agreement is achieved between the analytical results from dynamic inelastic analyses and the proposed empirical relations (Eqs. (6)–(8)). The relative increment of maximum story ductility demands due to repeated earthquakes is listed in Table 9. The bold values indicate the maximum analysis results from the three ground motions used. Furthermore, Table 9 shows that the prediction relationships can, in general, provide a very close estimation of the relative increment of maximum story ductility demands of the considered concrete frames excited by repeated earthquakes. Therefore, the empirical formulas produced by the current study in estimating the effect of repeated earthquakes can be used in seismic evaluation of buildings.

5. Conclusions

The present work explains the effect of repeated earthquakes on the story ductility demand of inelastic concrete frames. It concludes that the maximum story ductility demand of structures under consideration is found to be significantly affected by repeated earthquakes. However, the effect of repeated earthquakes on the maximum story ductility demand of models having behaviour factor of $q \leq 2$ tends to be small and can be neglected. The maximum story ductility demand on the structures induced by repeated earthquakes tends to appear in the upper level for a short structure, i.e., 3-story model, with low behaviour factor. This maximum demand then migrates to the bottom story as behaviour factor increases. For taller models, i.e., 6-, 12-, and 18-story models, all the maximum story ductility demands due to repeated earthquake GM Cases 1, 2, and 3 are situated at the bottom story, regardless of the type of behaviour factor. This finding means that the influence of repeated earthquakes on the dispersion of maximum story ductility demands is negligible.

Table 8
Comparison of the analytical and prediction findings for $\mu_{s,j}$

GM No.	3-story			8-story		
	GM Case 1	GM Case 2	GM Case 3	GM Case 1	GM Case 2	GM Case 3
1	3.65	5.37	5.54	9.54	11.37	12.81
2	4.37	5.76	5.90	8.98	11.23	13.84
3	4.22	5.16	5.51	8.77	11.70	12.17
Prediction	4.33	5.72	5.75	9.52	13.45	13.90
(Relative error—%)	(0.92)	(0.69)	(2.54)	(0.21)	(14.9)	(0.43)

Table 9
Comparison of the analytical and prediction findings for $A_{r-\mu sm}$.

GM No.	3-story		8-story	
	GM Case 2	GM Case 3	GM Case 2	GM Case 3
1	1.47	1.52	1.19	1.34
2	1.32	1.35	1.25	1.54
3	1.22	1.31	1.32	1.39
Prediction	1.32	1.33	1.41	1.46

On average, repeated earthquake GM Cases 2 and 3 increase the maximum story ductility demand up to 1.4 times higher than GM Case 1. On average, repeated earthquakes make the relative increment of maximum story ductility demand reach 1.4 and 1.3 times for DCM and DCH behaviour factors, respectively. In such cases, the relative increment of maximum story ductility demand due to repeated earthquake GM Cases 2 and 3 tends to decrease as behaviour factor increases. This trend is clearly evident as the number of story of the models (or fundamental period) increases, particularly in the 6- and 12-story models. These conclude that concrete frames designed with DCM have experienced higher relative increment of maximum story ductility demand than those with DCH behaviour factor when repeated earthquakes exhibited.

In the current paper, the empirical relationship used to predict the maximum story ductility demand of inelastic concrete structures under consideration affected by repeated earthquakes is also proposed. The applicability of the prediction formula is evaluated using 3- and 8-story RC buildings designed using European Code provisions. The result of relative increment of the maximum story ductility demand due to repeated earthquakes based on nonlinear analysis shows very good agreement with the predicted result.

The aforementioned conclusions appear to be new findings in the examined topic since none work in the past had not considered the effect of multiple earthquakes on the maximum story ductility demands. Furthermore, all the pertinent research works examined either SDOF systems or two-dimensional MDOF systems, while this work examines for the first time three-dimensional frames under bi-directional horizontal seismic excitation.

Finally, it should be noted that some uncovered, pertinent research topics need further study. For example the proposed method is limited to three-dimensional symmetric frames while asymmetric structures with intense torsional response can also be examined. Furthermore, other critical parameters, e.g., the roof ductility demands can also be investigated. Additionally, the response of three-dimensional frames under real seismic sequences can also be considered. All these topics are under investigation by the authors and will be presented in an oncoming research paper.

Acknowledgements

Authors are thankful to Mohd. Irwan Adiyanto, Mohd. Zulham Affandi Mohd Zahid, Mohd. Khairul Azuan Muhammad, Sabila Ahmad Basir, and Syafrina Mayang Sari for their supports during the study. The present study was supported by Research University Grant (1001/PAWAM/814115) sponsored by Universiti Sains Malaysia whereby the second author as the main investigator. The study of the first author were mainly supported by the Fellowship and Student Grant provided by Universiti Sains Malaysia and complemented by funds from Universitas Muhammadiyah Sumatera Utara. These supports are much appreciated.

References

[1] Amadio C, Fragiacomo M, Rajgelj S. The effects of repeated earthquake ground motions on the non linear response of SDOF systems. Earthquake Engineering and Structural Dynamics 2003;32:291–308.
[2] Ambraseys N, Smit P, Sigbjörnsson R, Suhadolc P, Margaris P. Internet-Site for European Strong-Motion Data. ⟨http://www.isesd.cv.ic.ac.uk⟩, EVR1-CT-1999-40008, in, European Commission, Directorate-General XII, Environmental and Climate Programme, Bruxelles, Belgium, 2001.
[3] COSMOS Virtual Data Centre. ⟨http://db.cosmos-eq.org/scripts/earthquakes.plx⟩ [last access: 2010/10/10].
[4] Muria Vila D, Toro Jaramillo AM. Effects of several events recorded at a building founded on soft soil. In: 11th European Conference on Earthquake Engineering, Paris, 1998.
[5] Hatzigeorgiou GD, Beskos DE. Inelastic displacement ratios for SDOF structures subjected to repeated earthquakes. Engineering Structures 2009;31:2744–55.
[6] Hatzigeorgiou GD. Behavior factors for nonlinear structures subjected to multiple near-fault earthquakes. Computers and Structures 2010;88:309–21.
[7] Hatzigeorgiou GD. Ductility demand spectra for multiple near- and far-fault earthquakes. Soil Dynamics and Earthquake Engineering 2010;30:170–83.
[8] Medina RA, Krawinkler H. Seismic demands for non-deteriorating frame structures and their dependence on ground motions. Report no. TR 144, John A. Blume Earthquake Engineering Centre, Stanford University, 2003.
[9] Ruiz-García J, Miranda E. Residual displacement ratios for assessment of existing structures. Earthquake Engineering and Structural Dynamics 2006;35:315–36.
[10] Hatzigeorgiou GD, Liolios AA. Nonlinear behaviour of RC frames under repeated strong ground motions. Soil Dynamics and Earthquake Engineering 2010;30:1010–25.
[11] Ruiz-Garcia J, Miranda E. Performance-based assessment of existing structures accounting for residual displacements. Report no. 153, John A. Blume Earthquake Engineering Center, Stanford University, Stanford, 2005.
[12] Ibarra L, H. Krawinkler H. Global collapse of frame structures under seismic excitations. Report no. 2005/06, Pacific Earthquake Engineering Research Center, University of California at Berkeley, Berkeley, 2005.
[13] Zareian F, Krawinkler H. Simplified performance-based earthquake engineering. Report no. 169, John A. Blume Earthquake Engineering Center, Stanford University, Stanford, 2009.
[14] Bray JD, Rodriguez-Marek A. Characterization of forward-directivity ground motions in the near-fault region. Soil Dynamics and Earthquake Engineering 2004;24:815–28.
[15] CEN. Eurocode 8: Design of structures for earthquake resistance. Part 1: General rules, seismic actions and rules for buildings. European Committee for Standardization, Brussels, 2004.
[16] American Society of Civil Engineers (ASCE). Minimum design loads for buildings and other structures. ASCE/SEI 7-05. Reston, VA: ASCE; 2005.
[17] Goel RK, Chopra AK. Period formulas for moment-resisting frame buildings. Journal of Structural Engineering 1997;123:1454–61.

(5)

Journal of Engineering Science and Technology
Vol. 9, No. 1 (2014) 27 - 46

SEISMIC DESIGN OF TWO STOREY REINFORCED CONCRETE BUILDING IN MALAYSIA WITH LOW CLASS DUCTILITY

MOHD IRWAN ADIYANTO*, TAKSIAH A. MAJID

School of Civil Engineering, Engineering Campus, Universiti Sains Malaysia,
14300, Nibong Tebal, Pulau Pinang, Malaysia
*Corresponding Author: irwano_07@yahoo.com

Abstract

Since Malaysia is not located in active seismic fault zones, majority of buildings in Malaysia had been designed according to BS8110, which not specify any seismic provision. After experienced several tremors originating from neighbouring countries especially from Sumatra, Indonesia, the Malaysian start to ask questions on integrity of existing structures in Malaysia to withstand the earthquake load. The question also arises regarding the economical effect in term of cost of construction if seismic design has to be implemented in Malaysian construction industry. If the cost is increasing, how much the increment and is it affordable? This paper investigated the difference of steel reinforcement and concrete volume required when seismic provision is considered in reinforced concrete design of 2 storey general office building. The regular office building which designed based on BS8110 had been redesigned according to Eurocode 2 with various level of reference peak ground acceleration, a_{gR} reflecting Malaysian seismic hazard for ductility class low. Then, the all frames had been evaluated using a total of 800 nonlinear time history analyses considering single and repeated earthquakes to simulate the real earthquake event. It is observed that the level of reference peak ground acceleration, a_{gR} and behaviour factor, q strongly influence the increment of total cost. For 2 storey RC buildings built on Soil Type D with seismic consideration, the total cost of material is expected to increase around 6 to 270 %, depend on seismic region. In term of seismic performance, the repeated earthquake tends to cause increasing in interstorey drift ratio around 8 to 29% higher compared to single earthquake.

Keywords: Reinforced concrete, Interstorey drift ratio, Behaviour factor, Eurocode 2, Seismic design.

Nomenclatures

As. Prov.	Area of steel provided, mm^2
a_{gR}	Reference peak ground acceleration, g
F_b	Base shear force, kN
f_{cu}	Concrete compressive strength, N/mm^2
f_y	Yield strength of steel reinforcement, N/mm^2
G_k	Dead load, kN/m
m	Total masses, kg
Q_k	Live load, kN/m
q	Behaviour factor
$Sd(T_1)$	Spectral acceleration at fundamental period of vibration, T_1, g
T_1	Fundamental period of vibration, sec
V_S	Shear wave velocity, m/s

Greek Symbols

λ	Correction factor

Abbreviations

DCL	Ductility class low
DCM	Ductility class medium
FB	Floor beam
IDR	Interstorey drift ratio, %
PGA	Peak ground acceleration, g
RB	Roof beam
RC	Reinforced concrete

1. Introduction

Malaysia is situated relatively far away from active seismic fault zone. However, it is clear that the nation is surrounded by high seismicity areas at the west, south, and east part as shown in Fig. 1 [1]. This is associated with the subduction zones between the Indo-Australian plate and Eurasian plate at the west and south part, also the subduction zones between the Eurasian and Philippines plate at the east region. Back to history, before entering the 21st century, Malaysian citizen are not totally aware of the earthquake hazard. They might hear about the catastrophic of 1996 Kobe earthquake in Japan and also the 1999 Koacaeli earthquake in Turkey, and then expressed their sympathy to the victims. After several days they forgot about the disaster and continue their business as usual. However, a large earthquake on 2004 Boxing Day which occurred west of Aceh, in Sumatra, Indonesia had became a wakeup call to all Malaysian as they felt the tremor in their home ground. The earthquake with magnitude M_w 9.0 also generated a disastrous Indian Ocean tsunami with high 'tidal' wave that struck the coast of several countries in Asian region. In Peninsular Malaysia, a total of 76 persons have been reported killed and many properties had been destroyed when the tsunami hit along the northwest coastal areas of Perlis, Kedah, Penang, and to some part of Perak [2]. Then, the tremors also had been felt in Malaysia due to earthquakes with magnitude Mw 8.6 which occurred on 28 March 2005 in Nias and 11 April 2012 in Aceh, Sumatra, Indonesia.

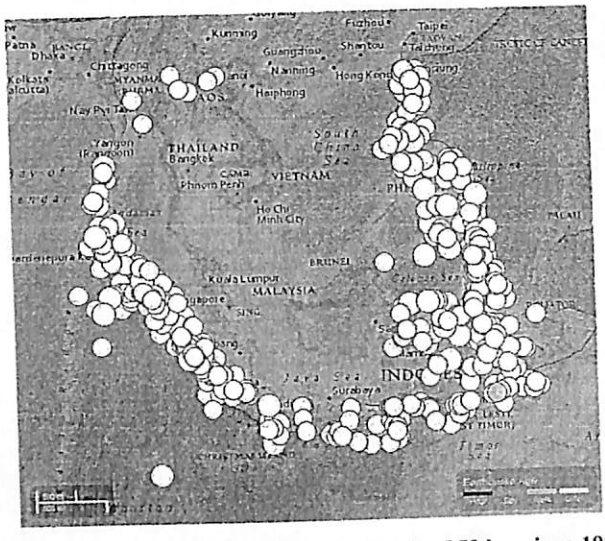

Fig. 1. Earthquake events (≥ M6.0) to a depth of 50 km since 1972 [1].

Since Malaysia is not located in active seismic fault zones, majority of buildings in Malaysia had been designed according to BS8110 [3] which not specify any seismic provision. After experienced several tremors originating from neighbouring countries, the Malaysian start to ask questions on integrity of existing structures in Malaysia to withstand the earthquake load. Based on previous investigation [2], it had been reported that most the buildings were in good condition in Peninsular Malaysia and at least 50% of selected buildings were found to experience concrete deterioration problems due to vibration during earthquake. It is also been reported that the vertical element design provision were inadequate for at least 50% of the building evaluated. Then, the Malaysian Public Work Department (JKR) suggested that it was worthwhile to consider seismic design input for new buildings located in medium-to-high risk earthquake zones. Now, the question is arises regarding the economical effect in term of cost of construction if seismic design has to be implemented in Malaysian construction industry. If the cost is increasing, how much the increment and is it affordable?

In a real earthquake event, the first tremor is always followed by other tremors. This is the nature of earthquake and may occur just a few hours after the first one, and may occur continuously to a few days. In technical views it can be called as repeated earthquake or multi event earthquake [4]. Therefore, during a great earthquake event, buildings are imposed to the action of earthquake load more than one time. The buildings may experience minor to moderate damage after being hit by the first tremor resulting in stiffness and strength degradation of the global system. For this situation, any rehabilitation action is impractical due to time constraint [5]. Then, if the not yet repaired buildings being subjected to the following tremors, the buildings are expected to experience worse damage that lead to collapse. Current provisions in earthquake engineering such as the Eurocode 8 [6] and FEMA 368 [7] only suggest to considering single earthquake

in analyses. Either in designing the new building or evaluating the existing one, this recommendation had been practised for years. However, it had been analytically proved that considering repeated earthquake phenomena in analysis requires an increase in strength with respect to single earthquake [8]. Recently, it is also reported that repeated earthquake induced 1.3 to 1.4 times increment in maximum storey ductility demand compared to the single one [9]. Therefore, the traditional seismic design procedure which is based on single earthquake should be generally reconsidered [4, 5].

This paper investigated the difference of steel reinforcement and concrete required when seismic provision is considered in reinforced concrete (RC) design of general office building. The original two storey regular office building which designed based on BS8110 [3] had been redesigned according to Eurocode 2 [10] with various level of reference peak ground acceleration, a_{gR} reflecting Malaysian seismic hazard for ductility class low (DCL). Then, the original and newly designed frames had been evaluated using nonlinear time history analysis considering single and repeated earthquakes to simulate the real earthquake event.

2. Analysis Procedure

In this paper, 2 dimensional (2D) analyses had been conducted on typical frame of two storey RC building. The frame was assumed to be designed for general office building with three equal bays of 5.0 m and typical storey height of 3.6 m as shown in Fig. 2. First of all, the generic frame was designed according to BS 8110 [3] to represent the current practice of RC design in Malaysia. The frame was designed with minimum requirement which is just to pass the demand from gravity load. Due to lower magnitude of load, the design of roof beam, RB located at top storey of the frame is differ compared to the design of floor beam, FB at first storey. Typical column design had been used in all storey. Then, the similar frame also had been designed without considering seismic load based on Eurocode 2 [10].

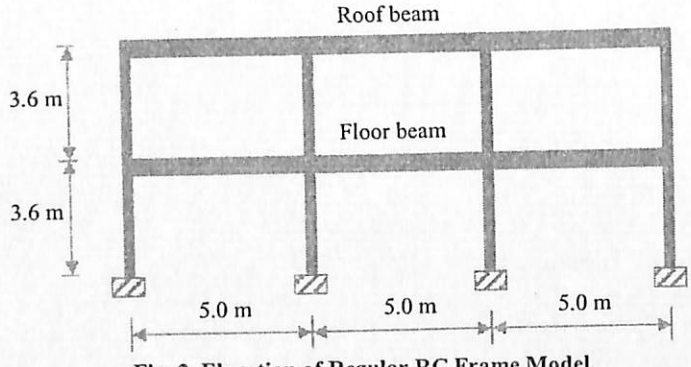

Fig. 2. Elevation of Regular RC Frame Model.

Since only the DCL had been considered in this study for seismic design, the behaviour factor, q used is equal to 1.5 as proposed in Eurocode 8 [6]. For comparison of cost, the frame also had been designed based on elastic response

spectrum where the value of behaviour factor, q is equal to 1. By referring to the seismic hazard maps of Malaysia [2, 11], the value of PGA for Peninsular Malaysia is in range of 0.02 g to 0.10 g for 500 years return period. For the same return period, the value of PGA for East Malaysia (Sabah and Sarawak) is in range of 0.06 g to 0.12 g, which is higher to the east. To cover these wide ranges of PGA for Malaysia, 3 values of PGA had been selected as reference peak ground acceleration, a_{gR} which is equal to 0.02 g, 0.06 g, and 0.12 g. Table 1 depicts all 8 frames used in this study and their design consideration. Only frame labelled as N2BS had been design based on BS 8110 [3] while the rest of it referring to Eurocode 2 [10]. In Table 1, q1.0 and q1.5 correspond to behaviour factor, q equal to 1.0 and 1.5, respectively. P1, P2, and P3 are referring to reference peak ground acceleration, a_{gR} which is equal to 0.02 g, 0.06 g, and 0.12 g, respectively. For example, model labelled with N2q1.0-P2 represents the two storey model (N2) which designed for behaviour factor, q equal to 1 (q1.0) and at reference peak ground acceleration, a_{gR} equal to 0.06 g (P2). In this work, the concrete grade C30 with compressive strength, f_{cu} = 30 N/mm^2 had been implemented in design for all frames. The yield strength, f_y of steel reinforcement for longitudinal bar and shear for frame N2BS is equal to 460 N/mm^2 and 250 N/mm^2, respectively as practiced based on BS8110 [3]. Since Eurocode 2 [10] only allows ribbed bars to be used in RC design, the yield strength, f_y for both longitudinal and shear reinforcement is equal to 460 N/mm^2. General difference for design using both codes [3, 10] is the gravitational load combination. When using BS8110 [3] for design, the gravitational load combination is equal to $1.4G_k$ + $1.6Q_k$, while for Eurocode 2 [10] is equal to $1.35G_k$ + $1.5Q_k$. G_k and Q_k correspond to dead and live load, respectively.

Table 1. List of Frames Used and Design Consideration.

No.	1	2	3	4	5	6	7	8
Frame	N2BS	N2EC2	N2 q1.0-P1	N2 q1.5-P1	N2 q1.0-P2	N2 q1.5-P2	N2 q1.0-P3	N2 q1.5-P3
Behaviour factor, q	Not Applicable		1.0	1.5	1.0	1.5	1.0	1.5
a_{gR}	Not Applicable		0.02 g		0.06 g		0.12 g	

In this paper, the lateral force method of analysis [6] had been conducted on all frames which considering seismic design. Before performing the analysis, the modal analysis was carried out in order to obtain the fundamental period of vibration (T_1) and corresponding node displacement of each storey, which will be used to determine the lateral load acting on each storey. Equation 1 [6] was adopted in order to determine the total base shear force, F_b.

$$F_b = S_d(T_1) \cdot m \cdot \lambda \quad (1)$$

where $S_d(T_1)$, m, and λ correspond to the ordinate of the design spectrum at period T_1, the total mass of the building above the foundation or above the top of a rigid basement, and the correction factor, respectively. The total masses, m of all frames had been calculated as proposed by Rozman and Fajfar [12]. Since the building used in this study only has 2 storeys, the value of λ is equal to 1.

Although Malaysia is located on a stable part of the Eurasian plate, buildings built on soft soil are occasionally subjected to tremors due to far-field earthquakes in Sumatra [13]. Therefore, the Type 1 response spectrum of Eurocode 8 [6] compatible with Soil D had been developed based on all selected PGA as mentioned in previous paragraph. Figure 3 depicts the design response spectrum for behaviour factor, $q = 1.0$ used to determine the base shear force, F_b.

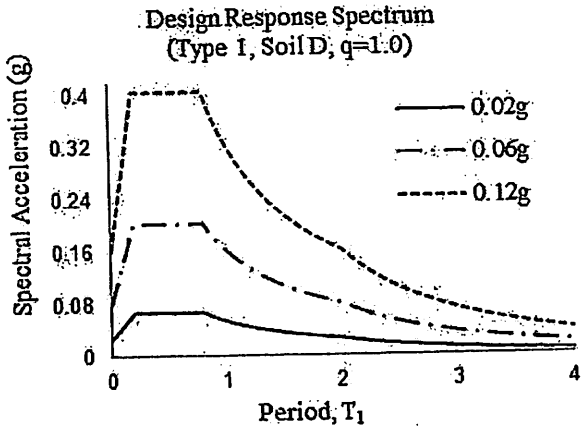

Fig. 3. Design Response Spectrum for Type 1, Soil Class D, $q = 1.0$.

In this work, all frames had been evaluated using nonlinear time history analysis with total 10 ground motion records classified as far-field earthquake as shown in Table 2. Most of it had been used in previous research [5] and are downloadable from strong motion database of the Pacific Earthquake Engineering Research (PEER) Centre [14]. All records can be said as fairly broad as its PGA ranges between 0.0103 g to 0.274 g with magnitude Mw from 6.2 to 7.6. Since only soil type D is considered in this work, all ground motions had been recorded from soft soil with shear wave velocity, $Vs < 180$ m/s.

Table 2. List of Far-Field Ground Motions.

No.	Earthquake	Station name	PGA (g)	Dist. (km)	Mag
1	Chi-Chi, Taiwan	KAU045	0.0103	119.22	6.2
2	Duzce, Turkey	Ambarli	0.038	193.3	7.1
3	Morgan Hill	58375 APEEL 1	0.046	54.1	6.2
4	Morgan Hill	58375 APEEL	0.068	54.1	6.2
5	Loma Prieta	58117 Treasure Island	0.1	82.9	6.9
6	Chi-Chi, Taiwan	TCU040	0.123	21.0	7.6
7	Chi-Chi, Taiwan	TCU040	0.149	21.0	7.6
8	Kocaeli, Turkey	Ambarli	0.184	78.9	7.4
9	Loma Prieta	1002 APEEL 2	0.22	47.9	6.9
10	Loma Prieta	1002 APEEL 2	0.274	47.9	6.9

To simulate the multiple earthquake or repeated earthquake event, the artificial ground motions had been generated. Random combination of single far-field earthquake as listed in Table 2 has been adopted to generate the artificial repeated earthquakes with appropriated scale factor as suggested [4, 9, 15, 16]. Figure 4 depicts the example of time history records of single and repeated earthquakes. Each artificial repeated earthquakes used in this work contain the fore shock, main shock, and after shock component. Very useful RUAUMOKO [17] computer software had been used to conduct the nonlinear time history analysis.

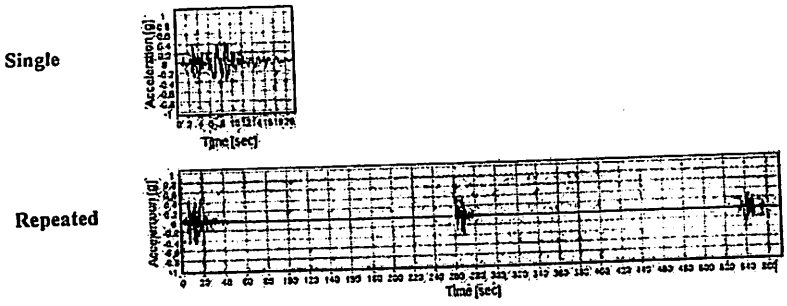

Fig. 4. Typical Profile of Generated Ground Motion.

3. Results and Discussion

3.1. Cost estimation of designed RC frames

In reality, it is hard to establish the additional cost of providing seismic resistance since buildings tend to be unique projects with different layout and requirement [18]. However, it is worth to conduct a study on seismic design and costing so the authority can plan and decide for future development. It is also important in order to give better understanding to designers on optimizing their design so the cost is affordable. In this work, one frame namely as N2BS had been design according to BS8110 [3] to represent current practice of RC design in Malaysia. One frame had been design based on Eurocode 2 [10] without seismic consideration namely as N2EC2. In order to investigate the effect of seismic design to the cost of material, six other frames had been designed based on Eurocode 2 [10] for DCL where seismic load was determined according to Eurocode 8 [6]. It is observed that all frames are differing in term of amount of materials and total cost as discussed in the following section.

3.1.1. Comparison on total volume of concrete used for all frames

The art of designing RC elements, either beam or column is quite unique where the designer have to play around with size of section and the required amount of steel reinforcement, with limitation of minimum and maximum area of total reinforcement as permitted by codes [3, 6, 10]. For example, higher depth of beam section selected by the designer will result in lower amount of steel reinforcement and vice versa. Figure 5 depicts the comparison of total volume of

concrete used in beam and column design for all frames. The size of section for RB, FB and column of N2BS frame is 200 mm × 450 mm, 200 mm × 500 mm, and 250 mm × 250 mm, respectively. It is observed that the normalised total volume of concrete for all beams is equal to one for six frames except frames designed for seismic with reference peak ground acceleration, a_{gR} equal to 0.12 g, which is the highest intensity located in Eastern part of Sabah [2, 11]. This result indicates that the size of beam is remain constant even considering seismic load with reference peak ground acceleration, a_{gR} up to 0.06 g.

However, the size of column start to increase as the reference peak ground acceleration, a_{gR} equal to 0.06 g had been used to determine the seismic load. As for beam, column for both N2q1.0-P2 and N2q1.5-P2 might be designed to have similar size of section with N2EC2 but when the amount of steel reinforcement exceeding the maximum limit at 4% of total concrete area [10], the size of section have to be enlarged. The same limit also applicable for beam designed with DCL. In this work, the total volume of concrete increases around 1.7 and 3.2 times for beam and column, respectively at region with highest seismicity. All frames which their sizes of section have to be enlarged become more rigid with lower fundamental period of vibration, T_1. Sometimes, the enlargement of section also may create conflict with architectural requirements. From Fig. 5, it is also observed that the level of behaviour factor, q not affecting the total volume of concrete used for design.

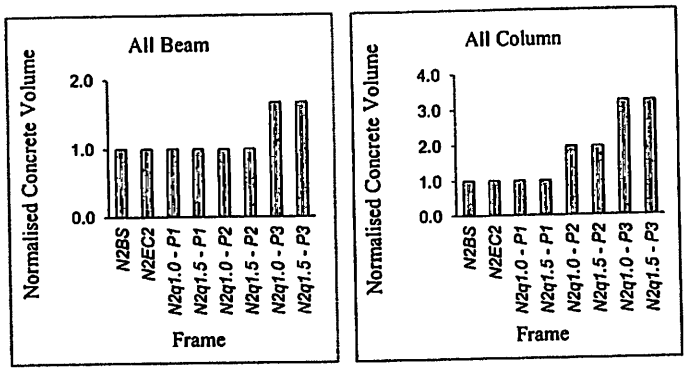

Fig. 5. Comparison of Concrete Volume Used in Design.

3.1.2. Comparison on area of steel reinforcement provided for all elements

Figures 6(a) and 6(b) depict the comparison of total area of steel reinforcement provided, As. Prov. for beam and column, respectively of all frames normalised to N2BS. In beam, near the exterior and interior support, the tension region located at top part of the section. Due to sagging moment, the tension region move to bottom part of the section at mid span. In this work, the As. Prov. is just to pass the area of steel required induced by bending moment or to exceed the minimum area of steel [10], whichever is greater.

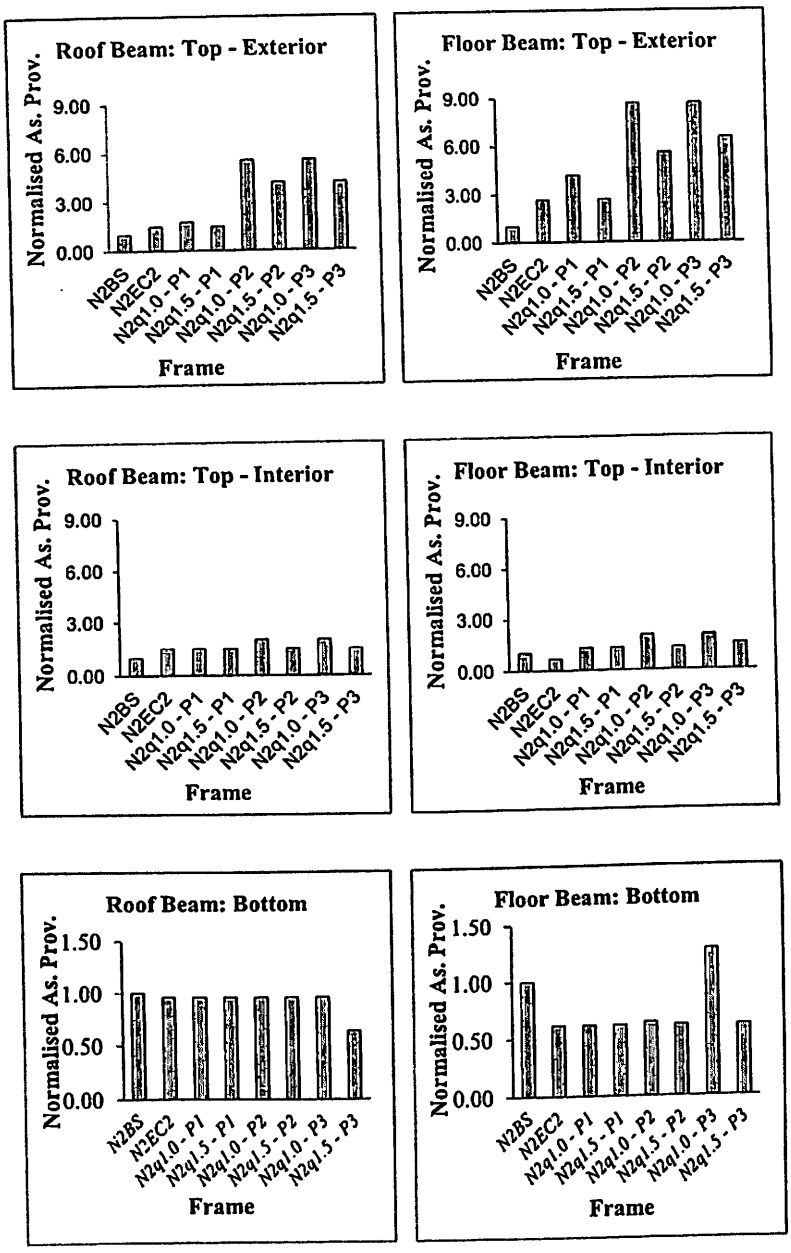

Fig. 6(a). Normalised Area of Steel Reinforcement Provided, As. Prov. for All Beams.

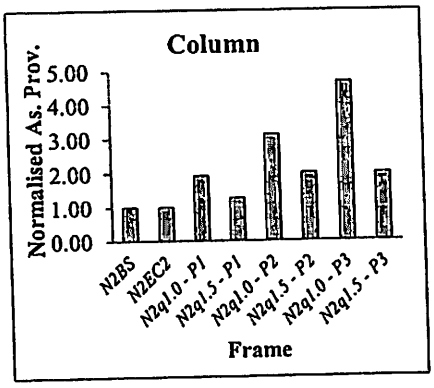

Fig. 6(b). Normalised Area of Steel Reinforcement Provided, As. Prov. for All Columns.

From Fig. 6(a), the As. Prov. as tension reinforcement for beam near exterior support is rapidly increases for both RB and FB especially when seismic load is considered in design. In this region, the As. Prov. is around 5.6 and 8.7 times higher compared to N2BS for RB and FB, respectively. The same trend also observed for As. Prov. for beam near interior support but with lower increment. This result is due to increasing of hogging moment in beam near exterior and interior support when subjected to lateral load. As previously discussed, when the size of section is constant, the number of bar or size of steel reinforcement have to be increased resulting in increment of As. Prov. Due to different size of section, similar amount of As. Prov. near exterior and interior support is observed for all beams of N2q1.0-P2 and N2q1.0-P3 frames. At these regions, higher level of behaviour factor, q considered in design resulting in lower amount of As. Prov.

In Fig. 6(a), it is also observed that total As. Prov. for tension region at mid span of RB is looked constant for all frames except N2q1.5-P3 which have lower As. Prov. associated with larger size of section. With exception for the case of N2q1.0-P3, the As. Prov. at mid span of FB for all frames is relatively around 40% lower compared to N2BS. It can be said that seismic load did not affecting the total amount of As. Prov. at mid span of beam when designed based on low level of reference peak ground acceleration, a_{gR}. For column, the total As. Prov. is rapidly increase when seismic load is considered in design especially frames with behaviour factor, q equal to 1 as shown in Fig. 6(b). Although the size of section had been enlarged as discussed in previous section, the total As. Prov. also have to be increased to resist very high moment in column induced by seismic load. Therefore, it can be concluded that total amount of As. Prov. for column and beam near exterior support is strongly influenced by intensity of seismic load.

3.1.3. Comparison on total weight of steel reinforcement provided for all frames

In RC design, the amount of steel reinforcement to be provided are strongly related to the bending moment and shear force developed from load imposed on frame. The main bar which is also known as longitudinal bar is supplied to resist

tension on concrete section due to action of bending moment. The link or transverse reinforcement is designed to resist shear force. Figure 7 presents the normalised total weight of both reinforcement in beam and column of all frames.

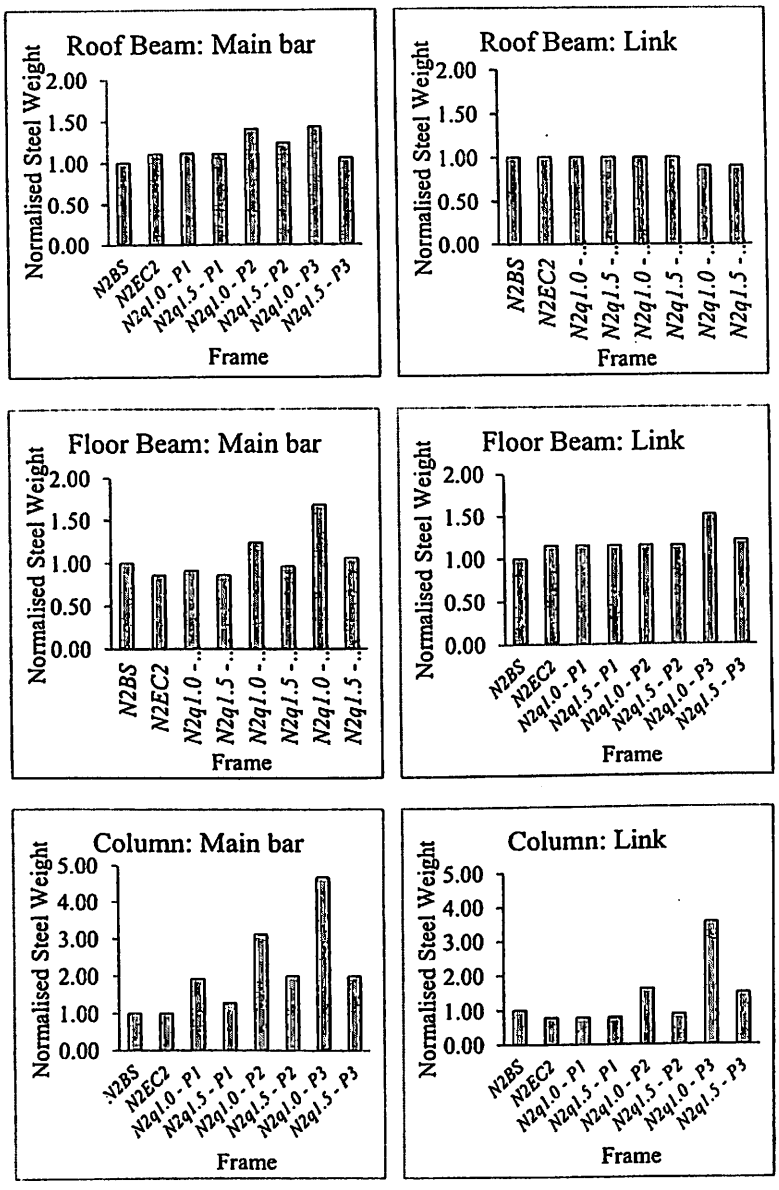

Fig. 7. Normalised Weight of Steel Provided for Each Elements.

It can be observed that total weight of main bar in RB is increase in range of 5 to 40 % higher for frames designed with seismic load. This result is strongly associated with the rapid increment of total As. Prov. at tension region in RB near exterior supports as discussed in previous section. The same trend also observed on main bar of FB especially frames which had been designed at higher level of reference peak ground acceleration, a_{gR}. As the bending moment in column increases rapidly due to action of seismic load, the total weight of main bar provided for frames with seismic design is around 1.9 to 4.7 times higher compared to non-seismic designed frames. It is clearly observed that higher level of behaviour factor, q tends to reduce the total weight of main bar provided for beam and column due to lower magnitude of base shear force, F_b distributed along the height of the frames.

From Fig. 7, total weight of link for RB are almost constant for all frames except N2q1.0-P3 and N2q1.5-P3 which is slightly lower due to larger size of section used in design. For FB, total weights of link for all frames designed based on Eurocode 2 [10], either considering seismic load or not are higher compared to N2BS. This result is in line as explained by Bhatt et al. [19], where Eurocode 2 [10] requires a greater amount of minimum links than BS 8110 [3]. Total weight of link for column is increase as the reference peak ground acceleration, a_{gR} considered for design is increase due to higher shear force to be resisted. According to Eurocode 2 [10], the size of link for column is depend on size of main bar provided, which is equal to ¼ of diameter of main bar or 6 mm, whichever is greater. Maximum spacing of link in column also influenced by 20 times diameter of main bar, dimension of column, or maximum limit at 400 mm. Then, the minimum value of the three is selected as maximum spacing.

3.1.4. Cost estimation for all frames

From total volume of concrete and steel reinforcement provided, the total cost of materials can be estimated. Figure 8 depicts the estimated cost of the whole frame normalised to the current practice represented by N2BS. As discussed in previous section, frames designed with seismic design require higher volume of concrete and weight of steel reinforcement compared to non-seismic frames. Therefore, in Fig. 8 it is observed that the total cost for frames with seismic design is around 1.06 to 2.74 times higher compared to N2BS.

The total cost is strongly influenced by the level of reference peak ground acceleration, a_{gR} and behaviour factor, q. Therefore, the same building may have different cost of material for superstructure when built in regions with different level of PGA. As an example, the increment of total cost of material of two storey RC building with seismic design built in West Coast of Peninsular Malaysia (PGA = 0.08) and East Coast of Sabah (PGA = 0.12 g) is 2.1 and 2.7, respectively when the behaviour factor, q is equal to 1. In context of Malaysian economic consideration, very high increment in total cost is unacceptable. Besides, it is not economically feasible to design structures to respond elastically during earthquake [20]. For reason of economy, most structures are designed to behave inelastically under strong earthquake. Hence, lower level of behaviour factor, q up to 1.5 is allowed for design of structure with DCL [10]. When considering behaviour factor, q equal to 1.5, the increment of total cost of the same frame at West Coast of Peninsular Malaysia and East Sabah is around 1.5 and 1.72,

respectively higher than current practice. If such increment is still unaffordable, higher class of ductility may be considered for both regions.

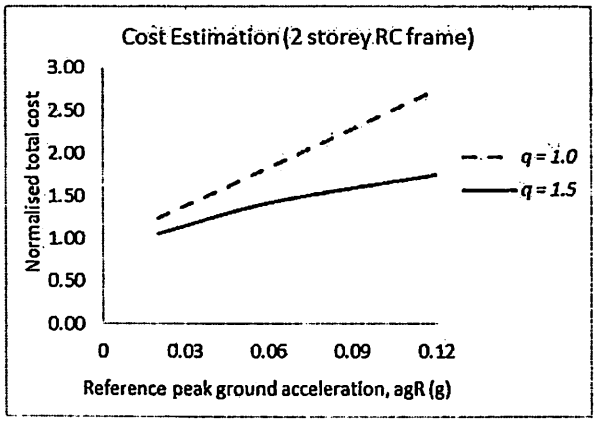

Fig. 8. Estimated Cost Normalized to Current Practice without Seismic Design.

3.2. Seismic performance of designed RC frames

Interstorey drift ratio (IDR) is a good indicator in order to evaluate the structural performance when subjected to earthquake load. The IDR corresponds to the relative lateral displacement between two adjacent storey normalized to its storey height. The accurate estimation of IDR is very important for purpose of seismic performance evaluation since the structural damage is directly related to the magnitude of IDR [7]. Thus, in this paper the mean value of IDR from 10 ground motion records had been used to present the seismic performance of all frames subjected to single and repeated earthquakes.

3.2.1. Seismic performance of RC frames designed without seismic consideration

As mentioned in earlier section, RC design in Malaysia only consider the gravity load for low rise building as used in this work. The suggestion to implement the Eurocode 2 [10] to replace current practice of BS 8110 [3] also creates an option in RC design. Thus, it is good to compare the seismic performance of similar RC frames where both codes [3, 10] had been referred for design without considering seismic action. Figure 9 depicts the IDR of both N2BS and N2EC2 frames when subjected to earthquake with PGA equal to 0.06 g.

Figure 9, it is observed that N2BS frame experienced higher IDR compared to N2EC2 frame when subjected to single earthquake excitation especially at upper level. This result is believed to be associated with higher amount of steel reinforcement near the exterior support in beam for N2EC2 frame which was designed according to Eurocode 2 [10] as discussed in previous section. One more reason is related to the design consideration where the yield strength, f_y of steel reinforcement for shear is higher for the N2EC2 frame compared to the N2BS

frame due to using ribbed bar. Therefore, the N2EC2 frame became stronger compared to another one. When subjected to repeated earthquake excitation, the magnitude of IDR experienced by both frames is relatively higher compared to the single earthquake. As shown in Fig. 5, it can be clearly observed that the repeated earthquake had caused increment in IDR around 19-24% for both frames. The magnitude of IDR for both frames also looked to become almost similar when subjected to repeated earthquake. This result indicates that the repeated earthquake is possible to cause more damage on structures as previously discussed [8].

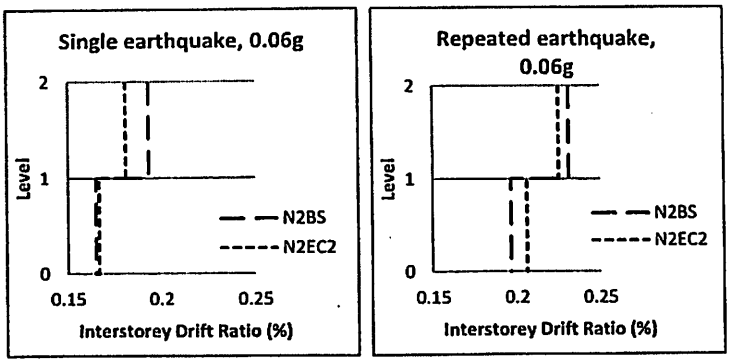

(a) (b)

Fig. 9. Interstorey Drift Ratio of Non-seismic RC Building (a) Single (b) Repeated Earthquakes.

3.2.2. Seismic performance of RC frames designed with different level of PGA

Figure 10 presents the seismic performance of two storey RC frames with seismic consideration in design when subjected to earthquake at intensity of PGA equal to 0.06 g. For comparison, the IDR for both N2BS and N2EC2 frames also presented. To cover the whole area of the nation, 3 different level of PGA had been considered as reference peak ground acceleration, a_{gR} which is equal to 0.02 g, 0.06 g, and 0.12 g as mentioned is previous section. Hence, three different frames had been designed by considering fix behaviour factor, q = 1. As discussed before, the design is strongly influenced by the level of PGA used as reference peak ground acceleration, a_{gR}. From Fig. 10, it can be observed that seismic performance, in term of IDR also strongly affected by the same parameter. All frames with seismic design performed better than non-seismic frames with lower IDR reflecting lower lateral displacement induces by earthquake. As expected, frame N2q1.0-P3 which designed based on highest level of reference peak ground acceleration, a_{gR}, experienced the lowest IDR compared to the others. This is due to higher strength designed for the frame to resist high bending moment. The frame also became stiffer as it had been designed with bigger size of section which caused the lateral displacement becomes smaller.

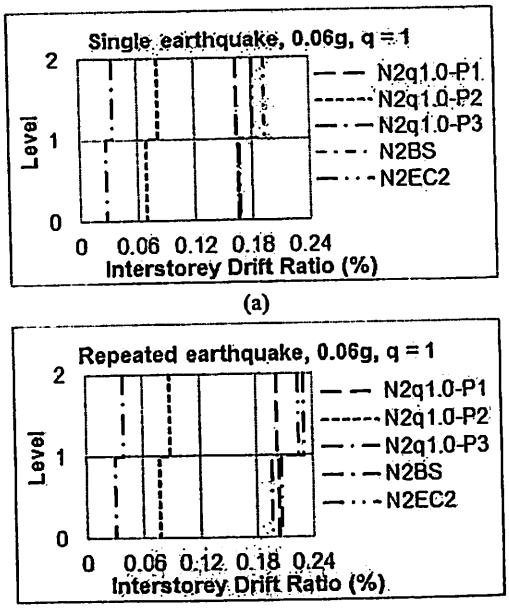

Fig. 10. Interstorey Drift Ratio for Frames with Seismic and Non-seimic Design (a) Single (b) Repeated Earthquakes.

It is also observed that the IDR of all frames with seismic design is evenly distributed along the height compared to non-seismic frames. This result indicates that the relative displacement between two adjacent storey is almost similar at level 1 and level 2 for frames with seismic design, which is not occur to frames without seismic consideration. When PGA = 0.02 g had been used as reference peak ground acceleration, a_{gR}, for design the IDR experienced by frame N2q1.0-P1 is almost similar with non-seismic frames of N2BS and N2EC2 at level 1. This result is associated with the design which is almost similar between all 3 frames, especially the size of section. However, due to higher amount of column longitudinal reinforcement provided for frame N2q1.0-P1, the IDR is evenly distributed between level 1 and level 2.

When considering the repeated earthquake excitation, the magnitude of IDR for all frames is relatively higher compared to its corresponding IDR caused by single earthquake. This result is agrees well with previous study by Hatzigeorgiou and Liolios [21] which concludes that the interstorey drift generated by repeated earthquake is larger than that caused by single earthquake. The effect of repeated earthquake on IDR is clearer for weaker frames, especially the non-seismic frames of N2BS and N2EC2 and also frame N2q1.0-P1 which consider the lowest reference peak ground acceleration, a_{gR}, in design. As all aforementioned frames have around 19-24% higher IDR when considering repeated earthquake, both frame N2q1.0-P2 and N2q1.0-P3 only experienced 10-16% increment of IDR. Hence, it can be said that the weaker structure is imposed to greater damage when subjected to repeated earthquake compared to the stronger one.

3.2.3. Effect of behaviour factor, q, on seismic performance

As discussed in previous section, increasing behaviour factor, q from 1 to 1.5 produced RC frame with lighter design in steel reinforcement although have the same size of section. Figure 11 depicts the IDR experienced by two RC frames designed with different level of behaviour factor, q when subjected to earthquake with intensity of PGA equal to 0.06 g. As observed, frame N2q1.5-P1 designed based on higher behaviour factor, q have around 8% higher IDR compared to frame N2q1.0-P1 when subjected to single earthquake. This result is as expected because adopting higher level of behaviour factor, q makes the frame becomes more ductile and allow it to sway at higher magnitude. Besides the economical reason, ductile structures is essential in seismic design which available for large absorption and dissipation of energy from earthquake action [22]. From Fig. 11, it is also observed that although using different level of behaviour factor, q the IDR is evenly distributed along the height for both frames. This result is associated with higher amount of steel reinforcement provided at critical region especially near the exterior beam ~ column joint when seismic action is considered in design. Therefore, the strength is evenly distributed to the whole structure and not concentrated at specific storey, i.e. the bottom storey as in case for non-seismic frames.

From Fig. 11, the IDR of both frames caused by repeated earthquake also higher compared to their corresponding single earthquake. Again, frame N2q1.5-P1 which had been design with higher behaviour factor, q has higher IDR. However, the increment of IDR for both frames is similar, which is around 23%. This result indicates that the level of behaviour factor, q did not affecting the increment of IDR caused by repeated earthquake at low intensity of PGA.

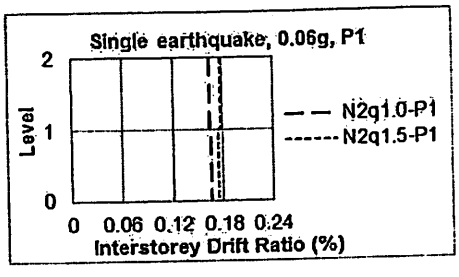

(a)

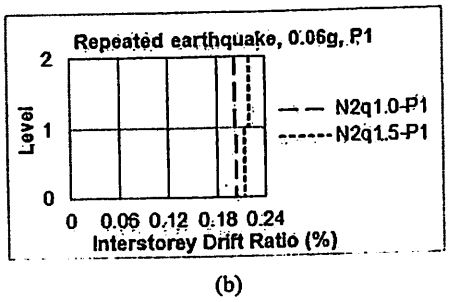

(b)

Fig. 11. Interstorey Drift ratio for Frames with Different Behaviour Factor, q, (a) Single (b) Repeated Earthquakes.

3.2.4. Maximum interstorey drift ratio at different intensity of PGA

In this work, all frames had been evaluated using nonlinear time history analysis at 4 different intensity of PGA namely as 0.02 g, 0.06 g, 0.12 g and 0.25 g to study their capacity against earthquake load, either single or repeated. Figure 12 depicts the maximum IDR for all frames at various intensity of PGA for both single and repeated earthquakes.

It can be clearly observed that the magnitude of IDR increase linearly with intensity of PGA for all frames. As expected, at same intensity of PGA the IDR of non-seismic frames are higher compared to those with seismic design. At PGA lower than 0.1 g, the IDR of N2q1.0-P1 and N2q1.5-P1 frames are looked almost similar with response of non-seismic N2BS and N2EC2 frames due to similar size of section for beam and column. When the intensity of PGA increases, the IDR of both frames with seismic design are lower due to higher amount of steel reinforcement provided. As discussed in previous section, by considering higher level of peak ground acceleration, a_{gR} for design resulting in larger section and higher amount of steel reinforcement. Therefore, the frames become more rigid and the lateral displacement due to earthquake becomes lower. This is important to ensure human comfort [22], but the cost to construct such buildings also has to be considered.

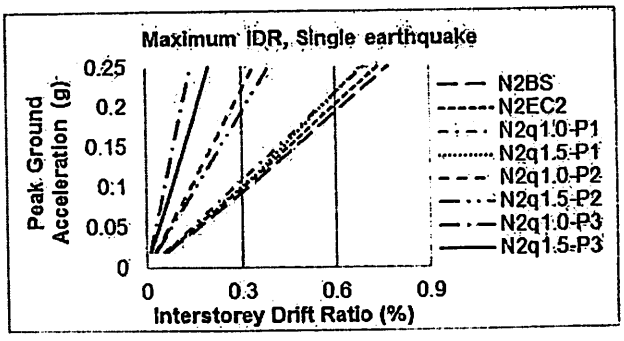

(a)

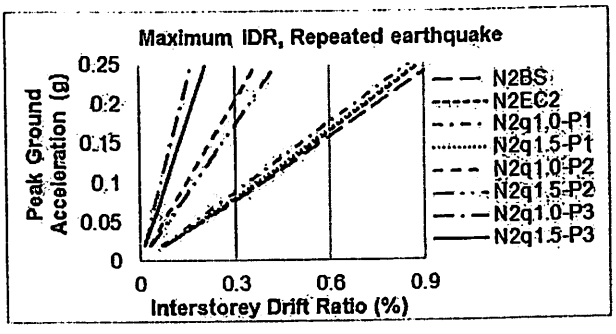

(b)

Fig. 12. Maximum IDR at Various Level of PGA (a) Single (b) Repeated Earthquakes.

If repeated earthquake is subjected, the maximum IDR of the same frame is relatively higher compared to single earthquake. This result is obtained for all frames regardless design consideration taken into account. The effect of repeated earthquake on IDR becomes clearer for weaker frames as the intensity of PGA increases, especially when the PGA greater than 0.05 g. The difference of maximum IDR for same frame designed with different level of behaviour factor, q also increases when the PGA increases.

4. Conclusions

A total 8 number of 2 storey RC buildings for general office use had been designed according to BS8110 [3] and Eurocode 2 [10] with and without seismic consideration to study the increment of cost of material if seismic design has to be implemented in Malaysia. Three different level of reference peak ground acceleration, a_{gR} had been considered in design to represent the whole seismic region in Malaysia as reported [2, 11]. Since this work only considers DCL for seismic design, the level of behaviour factor, q used is 1 and 1.5 as proposed in Eurocode 8 [6]. Then, all frames had been evaluated using nonlinear time history analysis at 4 different intensity of PGA namely as 0.02 g, 0.06 g, 0.12 g and 0.25 g to study their capacity against earthquake load. Both cases of single and repeated far-field earthquakes had been considered in the analyses.

From this work, the following conclusion may be drawn:

- The total volume of concrete is strongly influenced by the level of reference peak ground acceleration, a_{gR} used in design especially for column element. This is due to rapid increment of bending moment to be resisted by column when seismic load is considered in design.
- The same factor also affecting the increment of total weight of steel reinforcement to be provided for frames with seismic design especially in column and beam near the exterior supports.
- By considering behaviour factor, q equal to 1 in design leads to unacceptable increment in total cost of material, which is up to 270% higher compared to current practice using BS8110 [3]. When higher level of behaviour factor, q equal to 1.5 had been taken into account, it only cause the increasing of cost in range of 6 to 72% depend on seismic region. However, it is important to notice that these results had been obtained by considering response spectrum for Soil Type D according to Eurocode 8 [6] to determine the base shear force, F_b as lateral load. Lower increment of total cost of material is expected for other soil types due to lower proposed soil factor [6].
- From nonlinear time history analyses, it had been proved that the repeated earthquake tends to induce around 8 to 29% higher IDR compared to single earthquake especially on weak frames. However, the IDR looked to be similar between both cases when the intensity of PGA is lower than 0.05 6g g.
- Frames designed based on higher behaviour factor, q tend to experienced higher IDR due to lower strength provided even have the same size of section for all elements.

At the moment of this paper is written, a comprehensive work is conducted to re-design the same frame but considering other class of ductility, which is

ductility class medium (DCM) based on Eurocode 8 [6] with various level of higher behaviour factor, q. Frames with higher number of storey also will be taken into account in future works.

Acknowledgement

The authors gratefully acknowledge the facilities provided by Universiti Sains Malaysia and financial support from MyBrain15, a scholarship provided by Ministry of Education Malaysia to accomplish this study.

References

1. United States Geological Survey database (USGS). Retrieved January 8, 2014, from http://earthquake.usgs.gov/earthquakes/eqarchives/epic.
2. MOSTI (2009). Seismic and tsunami hazards and risks study in Malaysia. *Final Report*, 59-142.
3. B.S 8110 Code British Standard. (1997). Structural use of Concrete. *Code of Practice for Design and Construction, Part* 1.
4. Hatzigeorgiou, G.D. (2010). Behaviour factors for nonlinear structures subjected to multiple near-fault earthquakes. *Computers and Structures*, 88(5-6), 309-321.
5. Hatzigeorgiou, G.D.; and Beskos, D.E. (2009). Inelastic displacement ratios for SDOF structures subjected to repeated earthquakes. *Engineering Structures*, 31(11), 2744-2755.
6. CEN Eurocode 8. (2004). Design of structures for earthquake resistance, *Part* 1: *General rules, seismic actions and rules for buildings*. European Committee for Standardization, Brussels.
7. FEMA NEHRP (2000). Recommended provisions for seismic regulations for new buildings and other structures. *Part* 1: *Provisions, FEMA* 368, *Building Seismic Safety Council for the Federal Emergency Management Agency.*
8. Amadio, C.; Fragiacomo, M.; and Rajgelj, S. (2003). The effects of repeated earthquake ground motions on the non-linear response of SDOF systems. *Journal of Earthquake Engineering and Structural Dynamics*, 32(2), 291-308.
9. Faisal, A.; Majid, T.A.; and Hatzigeorgiou, G.D. (2013). Investigation of story ductility demands of inelastic concrete frames subjected to repeated earthquakes. *Soil Dynamics and Earthquake Engineering*, 44, 42-53.
10. EN 1992 Code Eurocode 2 (2004). Design of Concrete Structures. *Part* 1: *General rules and Rules for Buildings.*
11. Adnan, A.; Hendriyawan.; M.A.; and Selvanayagam, B. (2008). Development of seismic hazard maps of east Malaysia. In: *Advances in Earthquake Engineering Application*. Penerbit UTM, 1-18.
12. Rozman, M.; and Fajfar, P. (2009). Seismic response of a RC frame building designed according to old and modern practices. *Bulletin of Earthquake Engineering*, 7(3), 779-799.
13. Balendra, T.; and Li, Z. (2008). Seismic hazard of Singapore and Malaysia. *EJSE Special Issue, Earthquake Engineering in the low and moderate seismic regions of Southeast Asia and Australia*, 57-63.

Seismic microzonation for Penang using geospatial contour mapping

Chee Ghuan Tan, Taksiah A. Majid, Kamar Shah Ariffin & Norazura Mohamad Bunnori

Natural Hazards
Journal of the International Society for the Prevention and Mitigation of Natural Hazards

ISSN 0921-030X
Volume 73
Number 2

Nat Hazards (2014) 73:657-670
DOI 10.1007/s11069-014-1093-8

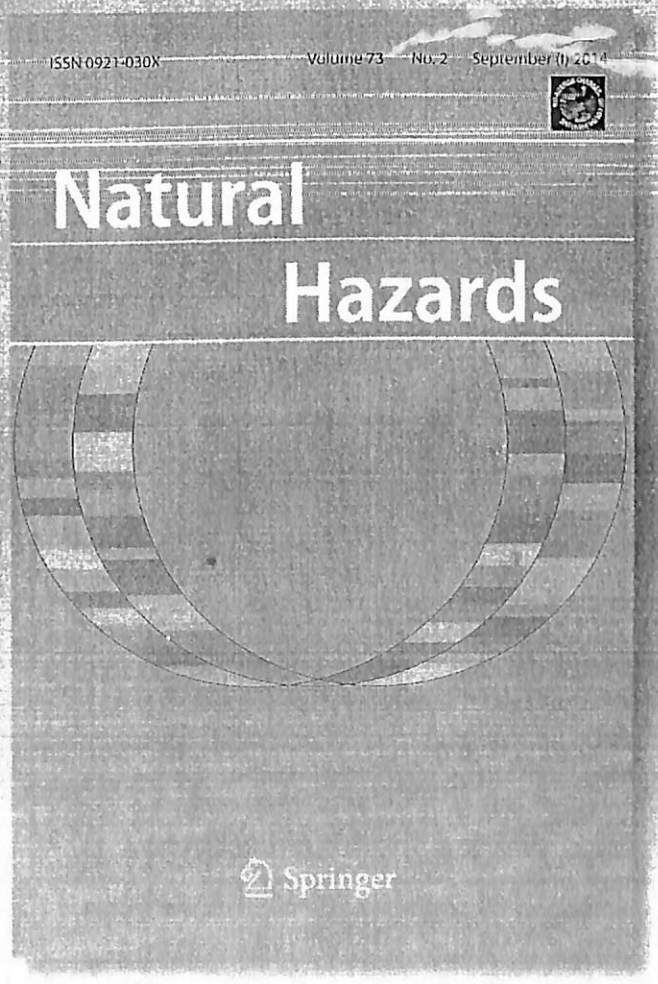

Springer

Nat Hazards (2014) 73:657–670
DOI 10.1007/s11069-014-1093-8

ORIGINAL PAPER

Seismic microzonation for Penang using geospatial contour mapping

Chee Ghuan Tan · Taksiah A. Majid · Kamar Shah Ariffin · Norazura Mohamad Bunnori

Received: 14 August 2013 / Accepted: 13 February 2014 / Published online: 21 February 2014

Abstract Shear wave velocity (V_s) and the fundamental site period of the subsurface condition are the primary parameters that affect seismic soil amplification in particular sites. Within the topmost layer of the soil, which measures 30 m, the average shear wave velocity V_{s30} is commonly used to build codes for site classification for the design of earthquake-resistant structures and to conduct microzonation studies. In this study, the development of a microzonation map for V_{s30} distribution, National Earthquake Hazard Reduction Program V_{s30} site classification, and a fundamental site period for Penang are presented. The multichannel analysis of surface wave (MASW) test was conducted for more than 50 sites with available borehole data to develop the microzonation maps. The ten selected V_s profiles measured by MASW show a good correlation with the data obtained using empirical correlations in a previous study. The highest V_s values were identified at the northeastern and southeastern parts of Penang Island, corresponding to the shallow bedrock and the outcrop zone. Conversely, the lowest V_s values were found in the northwestern and southwestern parts of the Penang mainland owing to the thick layer of soft clay and silt deposits. The site period map shows the variation in site periods, with the highest value of 1.03 s at the western part of the Penang mainland and the lowest value of 0.02 s at the eastern part of the Penang Island. The microzonation maps developed in this study are vital to studies on seismic hazard and earthquake mitigation programs in Malaysia.

Keywords Shear wave velocity · Site fundamental period · Seismic microzonation map · Multichannel analysis of surface wave · Penang

C. G. Tan (✉) · N. M. Bunnori
School of Civil Engineering, Universiti Sains Malaysia, Penang, Malaysia
e-mail: tuc_kheen@hotmail.com

T. A. Majid
Disaster Research Nexus, School of Civil Engineering, Universiti Sains Malaysia, Penang, Malaysia

K. S. Ariffin
School of Material and Mineral Resources, Universiti Sains Malaysia, Penang, Malaysia

1 Introduction

The characteristics of local soil dynamics significantly affect the propagation behavior of incoming seismic waves during an earthquake. Low flat lands along the rivers and coasts generally consist of thick layers of medium to soft clay and loose sand. Low-density soil such as alluvium deposits may amplify long-period seismic waves, thus resulting in greater danger to local infrastructures (Tuladhar et al. 2004; Mahajan 2009). This phenomenon was observed through a well-known example: the Michoacan earthquake ($M_s = 8.1$) at Mexico City in 1985. Although the earthquake source was approximately 400 km away from Mexico City, the city sustained catastrophic damages, resulting in about 20,000 fatalities owing to the substantial amplification of the long-period seismic waves by the local soft soil deposit (Seed et al. 1988; Lermo et al. 1988; Balendra et al. 1990). Thus, the strong amplification of ground motion attributed to the soft superficial deposit presents a potential earthquake hazard to high-population cities, even during a long-distance earthquake.

Penang, the state with the second highest population density in Malaysia, is located in a low seismic area. However, far-field earthquakes pose a potential hazard because of the amplification of long-period seismic waves by local soft alluvium deposits. The seismic waves generated in Sumatra have to travel over 350 km before reaching the Penang bedrock. Low period earthquake waves are quickly dampened during propagation, whereas long-period waves have higher energy dissipation, enabling them to travel long distances. Thus, long-period earthquake waves are capable of reaching the Penang bedrock and are amplified when propagating upward to the ground surface depending on the rigidity of the soil layer (Balendra and Li 2008). The amplified waves would resonate to the buildings that have close fundamental period to the site, resulting in significant building vibrations that are perceivable by occupants. The microzonation of Penang has not been explored in any study. Based on the local geological conditions, however, conducting seismic microzonation is necessary for Penang, given that such activity is beneficial to seismic hazard studies and earthquake mitigation programs in Malaysia (Mhaske and Choudhury 2011).

This study focuses on the development of a shear wave velocity (V_s) distribution and site period microzonation map for the Penang area using the multichannel analysis of surface wave (MASW) method at different sites. The MASW test was performed in more than 50 sites with available soil investigation reports to develop the microzonation maps. The MASW method is a noninvasive approach developed recently to estimate the V_s profile based on the surface wave energy. The dispersion curves determined using MASW were proven to be accurate by field comparisons conducted between the inverted shear wave velocity profile and a down-hole V_s profile (Park et al. 1999).

2 Seismicity of Penang

Malaysia lies on a stable Sunda platform on the Eurasian plate, bounded by two primary seismically active plate boundaries, namely the Indo-Australian plate and the Philippine Sea plate, as shown in Fig. 1. Although Malaysia is not located in the seismic area with active fault, buildings erected on soft soils often feel the far-field effect of earthquakes generated from Sumatran subduction and fault zones, particularly in areas on the west coast of Peninsular Malaysia, such as Penang, Johor Bharu, and Kuala Lumpur (Adnan et al. 2005; Husen et al. 2008). Figure 2 provides a record of the earthquake epicenters from neighboring countries and other locations near Penang. In the past 30 years, over 40

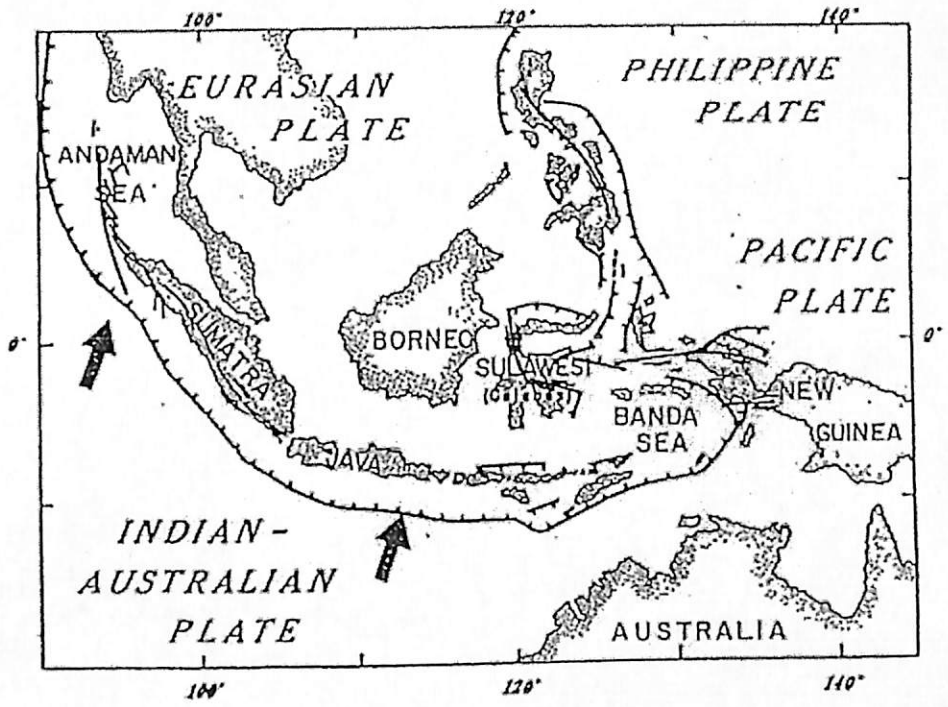

Fig. 1 Sumatran fault and subduction of the Indo-Australian Plate into the Eurasian Plate

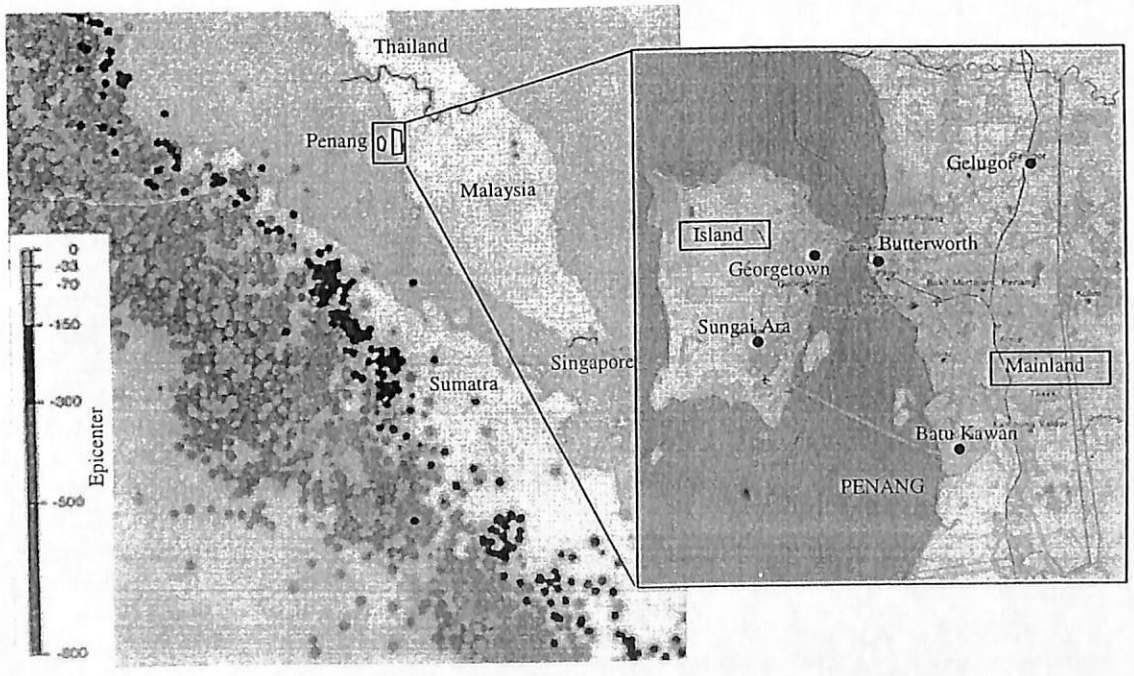

Fig. 2 Record of the earthquake epicenter and location of the study area

earthquakes originating from the Sumatra fault and subduction zone have been felt in Penang, two of which are among the greatest earthquakes in the world. Table 1 summarizes the significant earthquake events (MMI $\geq$ IV) that have been felt in Penang and have caused local citizens to panic. These earthquakes have raised public concern on the structural stability of existing buildings in Malaysia that do not have seismic designs,

Table 1 Summary of the earthquakes (MMI ≥ IV) from the Sumatran fault and subduction zone experienced by Penang (Malaysian Meteorological Department)

No.	Earthquake location	Date	Epicenter coordinate (°)	Focal depth (km)	Magnitude	Distance to Penang (km)
1	Southern Sumatra	30 Sept 2009	−0.9, 99.7	91	7.6 (M_s)	680
2	Mentawai Trough	12 Sept 2007	−4.4, 101.1	50	6.9 (m_b)	1075
3	Mentawai Strait	14 May 2005	0.8, 98.2	63	6.7 (m_b)	550
4	Nias	28 March 2005	2.0, 97.3	47	8.7 (M_w)	490
5	Aceh	26 Dec 2004	3.2, 95.9	30	9.3 (M_w)	540
6	Serba Jadi	22 Jan 2003	4.4, 97.5	33	5.7 (m_b)	320
7	Simeulu Tengah	2 Nov 2002	2.8, 96.1	30	6.2 (m_b)	540
8	Bambel	20 Aug 1997	4.3, 96.4	33	5.9 (m_b)	450
9	Lawe Alas	10 Oct 1996	3.4, 97.9	33	5.7 (m_b)	340

particularly on the capacity of such buildings to withstand the far-field effects of earthquakes.

As reported by Chiang and Mun (2011) regarding local earthquakes in Peninsular Malaysia (caused by an intra-plate fault), a new 80 km long fault line was found at Bukit Tinggi, which is located only approximately 200 km away from Penang. Alexander (2010) mentioned that a series of weak earthquakes (with magnitudes ranging from 2.9 to 3.5 M_b) in the Bukit Tinggi fault from November 2007 to May 2008 and in October 2009 were caused by the reactivation of the Bukit Tinggi fault. Given that the Bukit Tinggi fault has previously been subjected to an earthquake, more earthquakes would likely occur in the near future. An example of an intra-plate fault can be found in Australia, which has no prior records of any earthquake incidents. Previously classified as a seismic free zone, Australia suddenly experienced an earthquake of magnitude 5.5, which prompted substantial changes in the seismic design provisions of the Australian Standard (Chiang and Mun 2011). Although earthquakes generated by intra-plate faults have smaller magnitudes, such earthquakes are extremely difficult to predict and should not be underestimated.

3 Geology of Penang

Situated at the northeastern coast of Peninsular Malaysia, Penang comprises two geographically different entities, namely the Penang Island and the mainland portion, with a total area of 1,048 km^2. Penang is located between latitudes 5°7′N and 5°34′N and longitudes 100°10′E and 100°33′E (Ahmad et al. 2006). Penang is primarily composed of intrusive rocks, such as granite, marine clay, and silt, as shown in Fig. 3 (Malaysian Mineral and Geoscience Department 2007). Most of Penang Island is underlain by intrusive rock, which is also referred to as granite, and no sedimentary rock can be found in the island. The pre-quaternary granite is locally covered with unconsolidated sand, silt, and clay from the Pleistocene and Holocene ages. The granite hills are raised above the sea to the highest point from the sea water level, except where alluvium deposits (clay, silt, sand, and gravel) are found. Alluvium deposits, which are the products of the weathering of granite, can be found on the slopes and at the foot of the granite hills. Huge amounts of marine clay and silt deposits have been discovered along the coastal areas at the western area of the Penang mainland. Clay, silt, sand, and gravel were deposited through fluvial

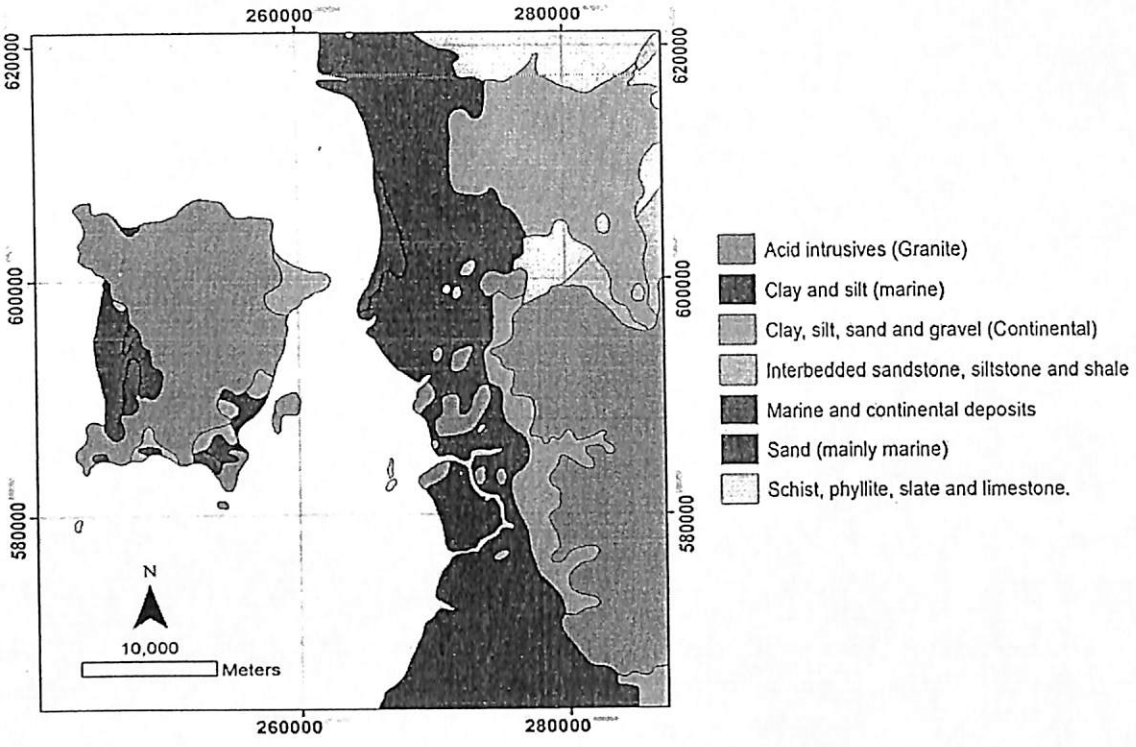

Fig. 3 Geological map of the study area (Malaysian Mineral and Geoscience Department 2007)

processes as channel fill, over-bank, and flood-basin deposits (Colbourne 2005). The alluvium deposits are found in the marine setting. These deposits resulted from the transgression of the sea about 6,500 years ago, when the sea level was approximately 2 m higher than at present owing to the peat found 3 m below the present crest of beach ridges.

4 MASW and data analysis

4.1 Development of MASW

For many years, researchers and engineers have used surface wave geophysical methods in soils and foundation applications. These methods determine the dynamic properties of soils, including the shear wave velocity profile of the soil and the shear modulus. These properties are important in predicting the soil response and soil-structure systems during seismic loading (Luna and Jadi 2000). The advantages of surface wave methods over other surface-based in situ seismic techniques include its rapid, cost-effective, noninvasive process, as well as its capacity to detect low velocity layer underneath the higher velocity layer of deposit, providing more accurate site characterization.

First introduced by Nazarian et al. (1983), the spectral analysis of surface wave (SASW) method focuses on analyzing the ground roll dispersion relation to generate near-surface S-wave velocity profiles. The main drawbacks of this method include its being time-consuming and the inherent difficulties when evaluating and distinguishing signal from noise using only a pair of receivers. To overcome these minor drawbacks, the MASW technique was developed by a four-phase research project team from Kansas Geological Survey. Unlike conventional SASW methods, multistation recording enables the single survey of a broad depth range and high levels of redundancy with a single field

configuration (Lin et al. 2004). A multichannel shot gathered and decomposed into a swept-frequency record speeds up the generation of an accurate dispersion curve. Subsequently, this dispersion curve is used to determine the shear wave velocity profile of the medium. As the frequency increases, the penetration of the surface waves decreases. Therefore, high frequencies are propagated through shallow layers, and vice versa.

4.2 Field test setup

MASW tests were performed using Geometrics 24 channels seismograph (Geode) and a single geode operating software. A total of 24 vertical geophones with a natural frequency of 4.5 Hz were used to detect the seismic waves generated by the vertical hit of an 8-kg sledgehammer on a striker plate. The 4.5-Hz geophones are selected for MASW test and are used for better detection of fundamental mode shear waves, which dominated at lower range of frequency between 4 and 50 Hz. Geophones were deployed in a linear manner, with equal spacing ranging from 0.5 to 2 m, as suggested by (Maheswari et al. 2010b). The nearest source to the geophone offsets was placed within the range of 5–15 m, to meet the requirements of the different types of soil hardness suggested by (Xu et al. 2006). The field configuration of MASW is depicted in Fig. 4.

4.3 Data acquisition and procedures

The acquired raw data from the MASW field test were analyzed using SeisImager software. The analysis can be divided into two main steps: (1) developing the dispersion curves of the Rayleigh wave phase velocity and (2) inversion of the dispersion curve to obtain the V_s profiles. The raw wiggle plot obtained from the field test was filtered within the frequency range from 3 to 107 Hz to reduce the random noise effect and the interference of other seismic waves, as shown in Fig. 5a, thereby ensuring that the surface waves are used to generate the dispersion curve. The amplitude of the body wave and the higher mode of the Rayleigh wave may dominate the fundamental mode under high-frequency ranges if the noise recorded during field test is not filtered well. Thus, as shown in Fig. 5b, only the fundamental mode of the Rayleigh wave, whose analyzable frequencies range from 4 to 75 Hz, was considered (Anbazhagan et al. 2013) in generating the dispersion curve using

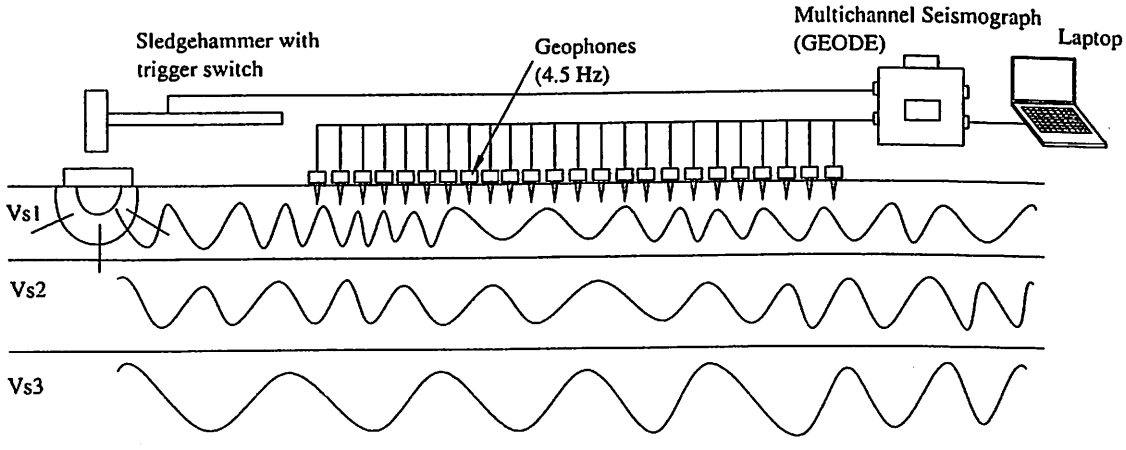

Fig. 4 MASW test field configuration

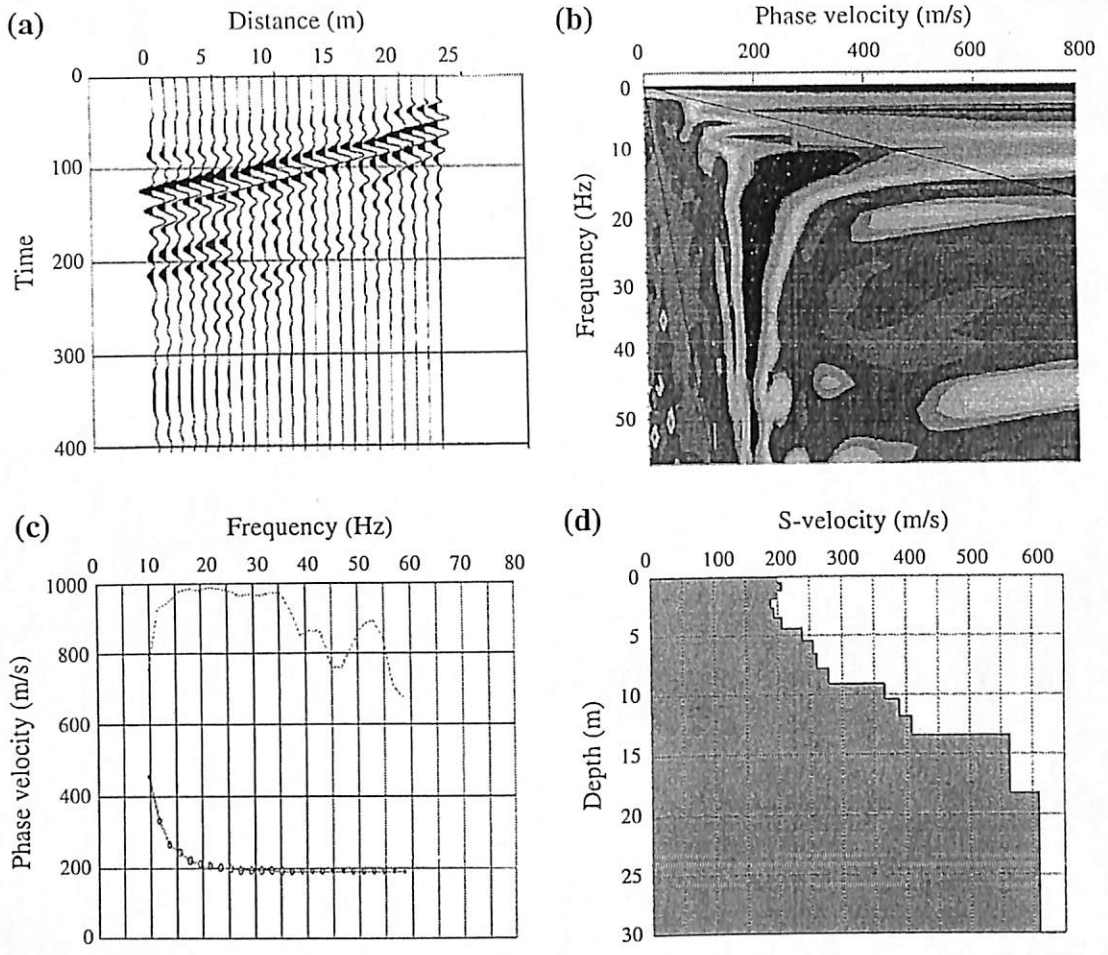

Fig. 5 Data acquisition and processing

the signal-to-noise ratio (Fig. 5c). The experimental dispersion curve was subjected to inversion analysis to develop the one-dimensional V_s profile, as illustrated in Fig. 5d.

5 Shear wave velocity distribution

The MASW test was performed in a total of 51 field sites to develop the V_s distribution and the National Earthquake Hazard Reduction Program (NEHRP) site classification maps for Penang using an integrated geographical information system (GIS) and image processing software, IDRISI Selva. The distribution of average shear wave velocity within 30 m depth, V_{s30}, is as shown in Fig. 6. The red points in the map indicate the site locations where the MASW tests were conducted. The V_{s30} distributions in Penang vary from 106.6 to 655.8 m/s. Moreover, Penang Island has higher values of V_{s30} compared with the mainland. In general, the northeastern and southeastern parts of the Penang Island have the highest V_s values, ranging from 300 to 700 m/s, which can be attributed to the shallow bedrock and the outcrop zone (i.e., granite hilly area). Conversely, the study areas in the northwestern and southwestern parts of the Penang mainland are characterized by the lowest V_s values, which are found between 106.6 and 150 m/s, which correspond to the thick layers of soft clay and silt deposits found in the area.

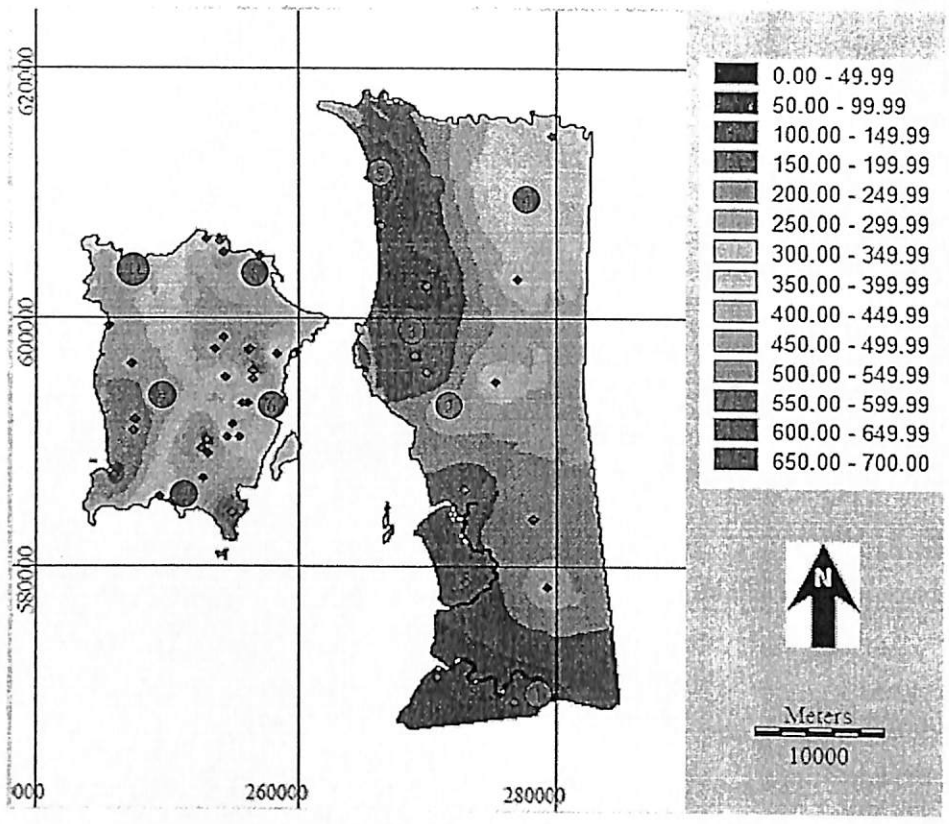

Fig. 6 V_{s30} distribution of Penang

As shown in Fig. 7, the V_s distribution map was further classified into three categories according to the NEHRP (Building Seismic Safety Council 2003). The map consists of contour lines for V_{s30} at 180, 360, and 760 m/s, which represent the boundaries for site classes E, D, and C, respectively. The areas with the highest V_{s30}, which is associated with the residual soil that categorizes site class C, are the northeastern and southeastern parts of the Penang Island, as well as a portion of the northeastern Penang mainland (red-colored zones). The transition zones, which are the western and eastern parts of the Penang Island and mainland (blue-colored zone), are categorized under site class D, which have V_s values ranging from 181 to 360 m/s. The western part of the Penang mainland (yellow-colored zone) is categorized under site class E ($V_{s30} < 180$ m/s), which can be attributed to the alluvium sediment in the low flat river and coastal areas.

6 Effect of soil profile on shear wave velocity distribution

The V_s distributions of soils generally coincided with the soil borelogs identified by geotechnical investigations. The soil profiles of ten selected different sites in Penang, indicated by the red circles in Fig. 6, are shown in Fig. 8 (1: Engineering Campus, University Sains Malaysia; 2: Bukit Minyak; 3: Seberang Jaya Hospital; 4: National School Tok Bedu; 5: Kuala Bekah; 6: Main Campus, University Sains Malaysia; 7: Teluk Kumbar; 8: Tanjung Bungah; 9: Bukit Batu Itam; and 10: Teluk Bahang). The higher V_s values were found in the soil profiles located in sites 4, 6, 7, and 8. Sites 6 and 7 are characterized by stiff silt at the topsoil, and dense sand and hard silt at end of the borelogs, respectively. Although site 8 is characterized by loose sand on its surface layer, fresh granite rock at the

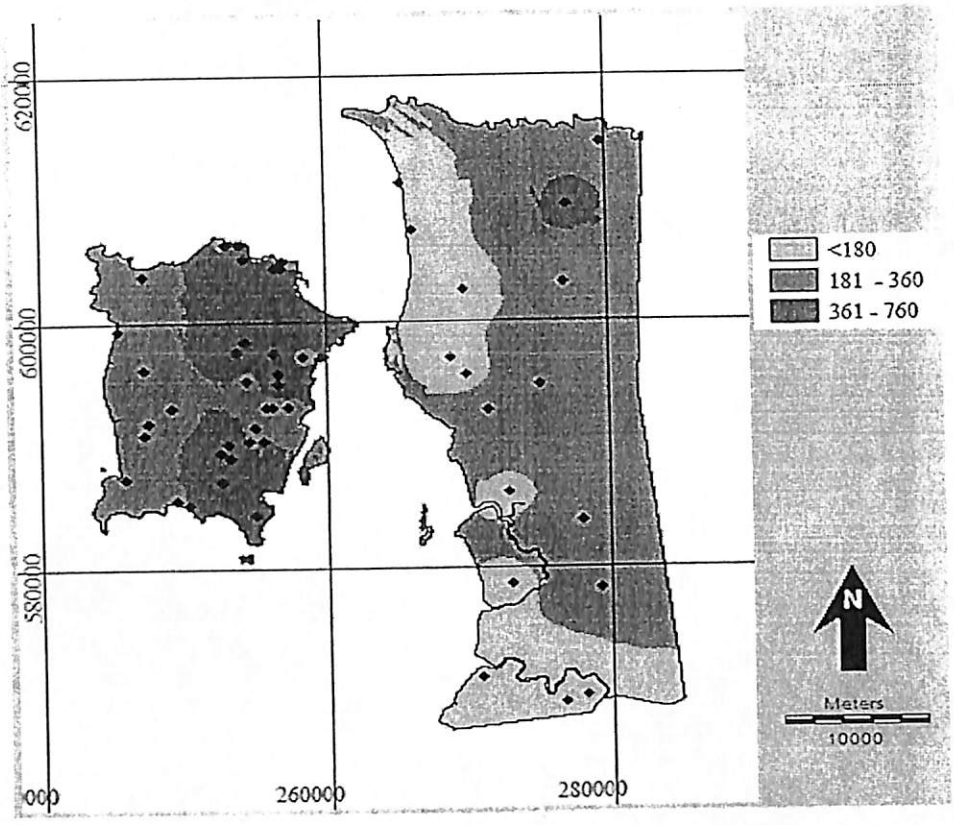

Fig. 7 Seismic site classification map according to NEHRP based on the V_{s30} distribution of Penang

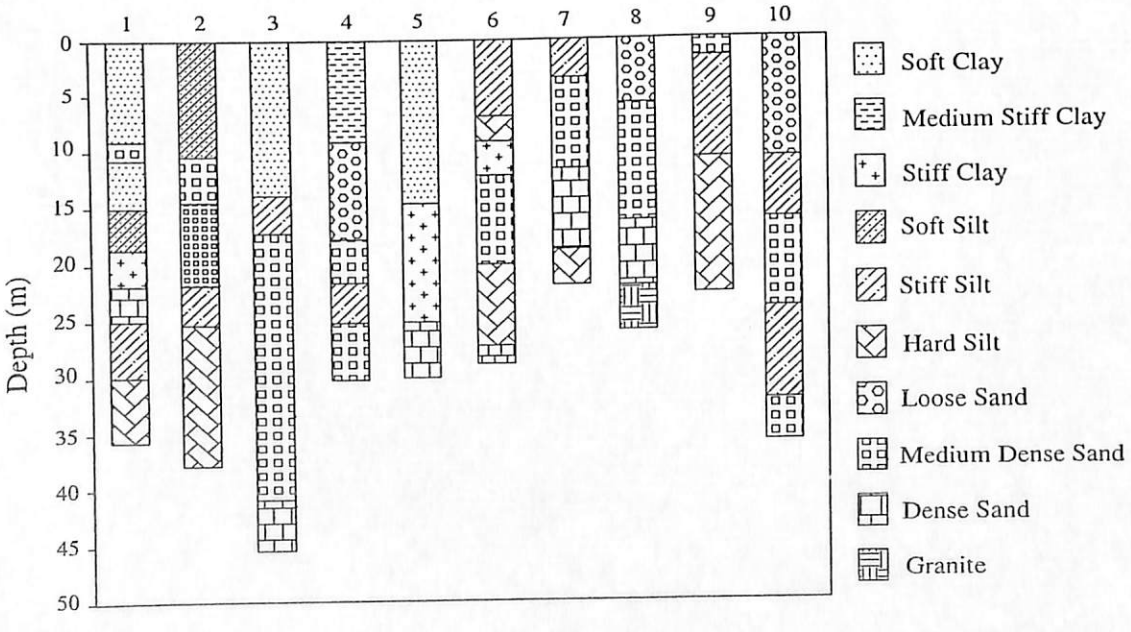

Fig. 8 Soil profile for ten selected sites in the Penang area

depth of 22 m significantly contributes to the high V_s in the local soil. Finally, sites 1, 2, 3, and 5 have the lowest V_s values. These sites consist of thick layers of either soft clay and silt or medium dense sand from the soil surface to a depth of 15–40 m. Thus, this thick layer with lower soil density resulted in the low V_s of these sites.

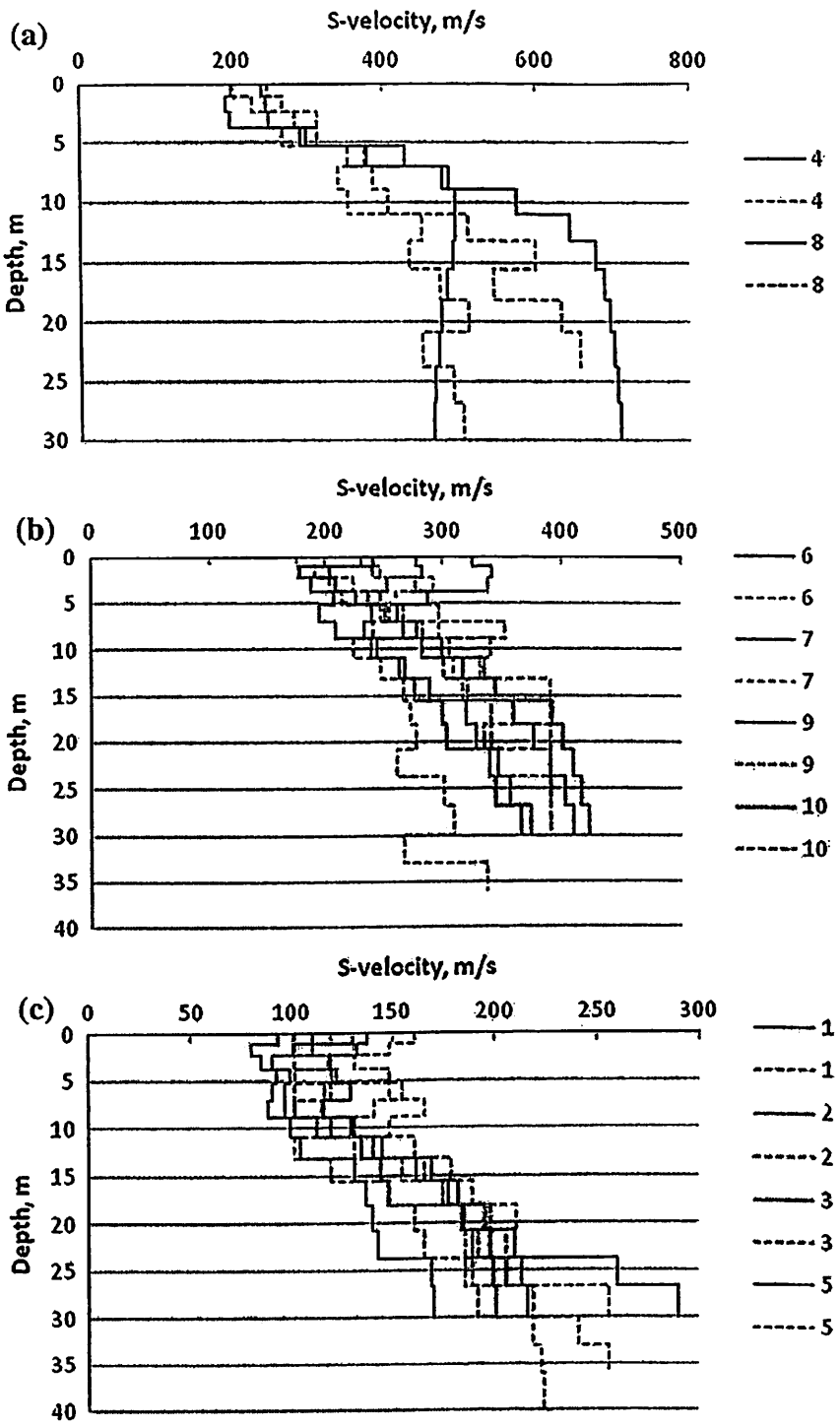

Fig. 9 Comparison of the measured and estimated shear wave velocity profiles for **a** site class C, **b** site class D, and **c** site class E (*straight line* measured, *dashed line* estimated)

The V_s profiles of the ten selected sites were verified through the empirical correlations between V_s and standard penetration resistance of soil proposed by Tan et al. (2013). The empirical correlations are developed considering the differences in the site classifications in Penang. These empirical correlations are as follows:

$$V_s = 128.05N^{0.4081}\,(\text{Site class C}) \tag{1}$$

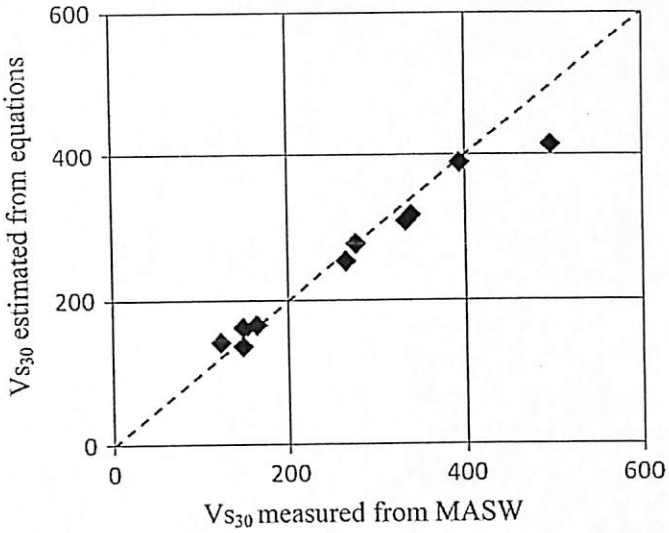

Fig. 10 Comparison of V_{s30} derived from MASW and equations

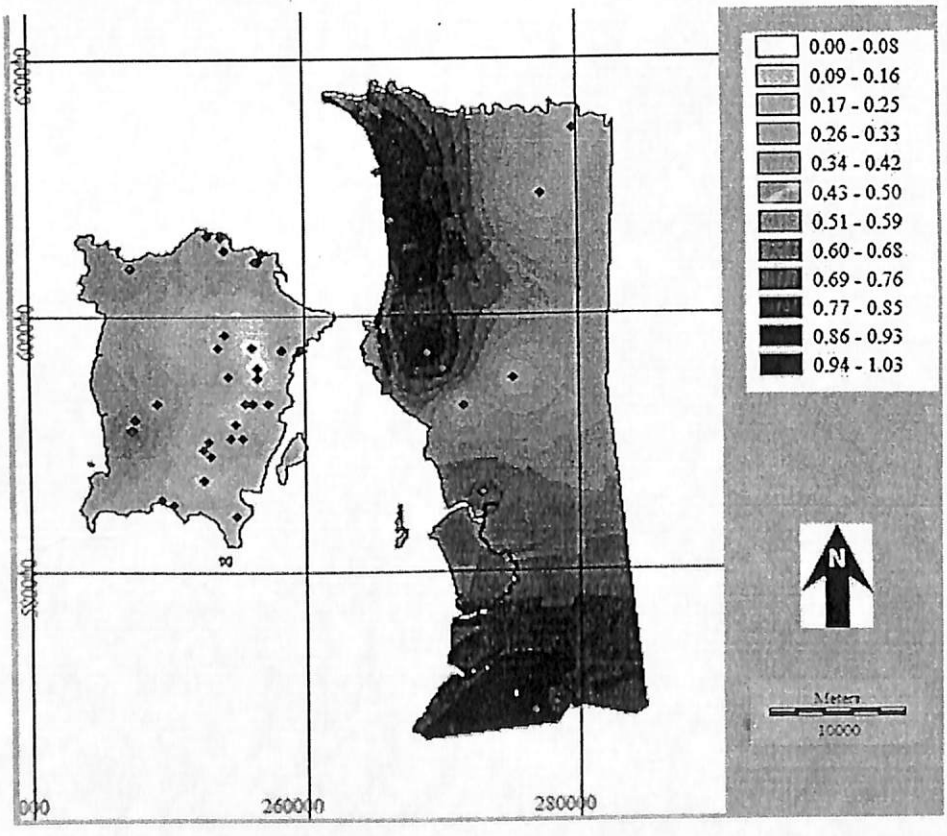

Fig. 11 Site period distribution map of Penang

$$V_s = 128.71N^{0.2833}(\text{Site class D}) \quad (2)$$

$$V_s = 101.34N^{0.2364}(\text{Site class E}) \quad (3)$$

As shown in Fig. 9, the V_s profiles of the sites with respect to site class C, D, and E were estimated by Eqs. (1–3), respectively, and compared with the shear wave profiles obtained through the MASW test. The graphs show that the measured V_s profiles yielded similar results with the V_s profiles estimated using the equations. The V_{s30} from both methods are

further compared in Fig. 10, and the result shows a good correlation between the V_{s30} estimation obtained through the MASW test and the empirical correlations above.

7 Site period distribution

Site fundamental period, represented as T_s, corresponds to the period of the first mode of soil deposit vibration, which combines the effects of seismic bedrock and shear stiffness (equivalent to V_s) in soil dynamic characterization for seismic microzonation (Antoniou et al. 2008). Site period is primarily influenced by the thickness of each soil layer and its corresponding V_s. Site period can be calculated using the following expression (Kramer 1996):

$$T_s = 4 \sum \frac{H_i}{V_{si}} \tag{4}$$

where H_i is the thickness of ith soil layer, and V_{si} is the V_s of ith layer. The developed site period distribution shown in Fig. 11 indicated that the Penang Island has a lower site period, ranging from 0.02 to 0.33 s, compared with that of the mainland, which ranges from 0.17 to 1.03 s. The low site period, particularly in the eastern part of the island, corresponds to the more shallow bedrock or the lesser thickness of overburden. Although loose or soft deposits, such as sand, silt, and clay, are distributed in the surface layer of the soil in the island (Fig. 8), the site period observed was relatively low due to the lesser thickness of these deposits coupled with the high V_s layers. The relatively thicker and softer alluvium deposit is the primary cause of the long site periods observed in mainland Penang, particularly at the northwestern and southwestern regions. In terms of site classification, the study areas in site classes C, D, and E were characterized by site periods ranging from 0.02 to 0.24, 0.25 to 0.68, and 0.69 to 1.03 s, respectively. Similar results were found by Tuladhar et al. (2004) and Maheswari et al. (2010a).

8 Conclusions

This study presented V_s distribution and site period maps, which are essential for seismic microzonation in Penang. The MASW test was conducted in over 50 sites to develop V_s distribution and site classification maps. The highest V_s values were found at the northeastern and southeastern parts of the Penang Island, which correspond to the shallow bedrock and the outcrop zones, respectively. By contrast, the lowest V_s values were found in the northwestern and southwestern parts of the Penang mainland, which can be attributed to the thick layers of soft clay and silt deposits. The V_s distribution of Penang was further grouped into three ranges (<180, 180 to 360, and 360 to 760 m/s, according to NEHRP). The seismic site classification map shows three distinct zones in Penang: Zone C corresponds to the shallow bedrock and outcrop zones (residual deposit); Zone D corresponds to dense soils with relatively shallow bedrock (transition zone); and Zone E corresponds to the soil in the river and coastal areas (alluvium sediment). The V_s profiles and its corresponding V_{s30} values obtained through the MASW method for the ten selected sites showed good correlation with the estimated results using the empirical correlation proposed by Tan et al. (2013). The site period map showed that the period varied from as high as 1.03 s at the western part of mainland Penang, to periods as low as 0.02 s at the eastern part of Penang Island. The results of the site period ranges for each site classification are proven by some of the previous studies.

As mentioned above, Penang could be affected by long-period earthquakes originating from Sumatra (>350 km to the Sumatran fault and subduction zone). Therefore, the western part of Penang mainland, which possesses long site periods due to the thicker layer of soft marine deposits, may experience higher amplification (Surve and Mohan 2010) during earthquakes, particularly the long-period structures, such as high-rise buildings and long-span bridges.

Acknowledgments This study was sponsored by the Postgraduate Research Grant Scheme provided by Universiti Sains Malaysia. The authors would like to extend their gratitude to the Ministry of Education of Malaysia for the permission to collect data from primary and secondary schools in the study area.

References

Adnan A, Hendriyawan, Marto A, Irsyam M (2005) Seismic hazard assessment for Peninsular Malaysia using Gumbel Distribution Method. Jurnal Teknologi 42 (B):57–73

Ahmad F, Yahaya AS, Farooqi MA (2006) Characterization and geotechnical properties of Penang residual soils with emphasis on landslides. Am J Environ Sci 2(4):121–128

Alexander YSW (2010) Earthquake-generating faults in Malaysia. In: National Technical Seminar on Earthquake and Tsunami, Petaling Jaya, Malaysia

Anbazhagan P, Kumar A, Sitharam TG (2013) Seismic site classification and correlation between standard penetration test N value and shear wave velocity for Lucknow City in Indo-Gangetic Basin. Pure appl Geophys 170:299–318

Antoniou AA, Papadimitriou AG, Tsiambaos G (2008) A geographical information system managing geotechnical data for Athens (Greece) and its use for automated seismic microzonation. Nat Hazards 47(3):369–395. doi:10.1007/s11069-008-9226-6

Balendra T, Li Z (2008) Seismic hazard of Singapore and Malaysia. EJSE special issue: earthquake engineering in the low and moderate seismic regions of Southeast Asia and Australia

Balendra T, Tan TS, Lee SL (1990) An analytical model for far-field response spectra with soil amplification effects. Eng Struct 12(4):263–268

Building Seismic Safety Council (2003) NEHRP recommended provisions for seismic regulations for new buildings and other structures (FEMA 450), part 1: provisions. Washington DC

Chiang CL, Mun KP (2011) Gathering of views and opinions on seismic investigations in Peninsular Malaysia—report on the IEM workshop on earthquake (part 1). In: JURUTERA, UniMap, Perlis pp 44–48

Colbourne FW (2005) Tsunami impact on the west coast of Penang Island. Emporia State University, Malaysia

Husen H, Majid TA, Nazri FM, Arshad MR, Faisal A (2008) Development of design response spectra based on various attenuation relationships at specific location. Paper presented at the International Conference on Construction and Building Technology, Kuala Lumpur, Malaysia, 16–20 June

Kramer SL (1996) Geotechnical earthquake engineering. Prentice Hall, upper Saddle River

Lermo J, Rodriguez M, Singh SK (1988) The Mexico earthquake of September 19, 1985—natural period of sites in the valley of Mexico from microtremor measurements and strong motion data. Earthq Spectra 4:805–813

Lin CP, Chang CC, Chang TS (2004) The use of MASW method in the assessment of soil liquefaction potential. Soil Dyn Earthq Eng 24(9–10):689–698. doi:10.1016/j.soildyn.2004.06.012

Luna R, Jadi H (2000) Determination of dynamic soil properties using geophysical methods. In: first international conference on the application of GEOPHYSICAL and NDT methodologies to transportation facilities and infrastructure, St. Louis, MO

Mahajan AK (2009) NEHRP soil classification and estimation of 1-D site effect of Dehradun fan deposits using shear wave velocity. Eng Geol 104:232–240

Maheswari RU, Boominathan A, Dodagoudar GR (2010a) Seismic site classification and site period mapping of Chennai City using geophysical and geotechnical data. J Appl Geophys 72(3):152–168. doi:10.1016/j.jappgeo.2010.08.002

Maheswari RU, Boominathan A, Dodagoudar GR (2010b) Use of surface waves in statistical correlations of shear wave velocity and penetration resistance of Chennai soils. Geotech Geol Eng 28(2):119–137. doi:10.1007/s10706-009-9285-9

Nat Hazards
DOI 10.1007/s11069-015-1770-2

ORIGINAL PAPER

Evaluation of soil flexibility of the reclaimed area in Penang using the non-destructive method

Fadzli Mohamed Nazri[1] · Tan Chee Ghuan[1] · Shahrul Nizam Hussin[1] · Taksiah A. Majid[1]

Received: 8 October 2014 / Accepted: 16 April 2015

Abstract Rapid development in urban area needs solutions to address scarcity of land for the development and infrastructure. Land reclamation has played an important role in the process of urban development in Malaysia especially in Penang area. However, the land reclamation usually comes along with challenges such as instability of the reclaimed platform and soil liquefaction. Furthermore, the assumption of fixed-base structure in the current building design practice is realistic only when the structure is founded on soil class B (rock). The main objective of this study was to investigate the soil classification and liquefaction potential of the reclaimed land and to study the effect of soil flexibility on low- and medium-rise structure in terms of structure drift. In this study, two areas in Penang have been used as a case study, namely Seri Tanjung Pinang (STP) and Bandar Sri Pinang (BSP). The multichannel analysis of surface wave (MASW) method was implemented to investigate the soil classification and the soil liquefaction for the two case study areas. In addition, the pushover analysis was performed in order to study the effect of soil flexibility on low- and medium-rise structures in terms of drift. Based on the shear wave velocity (Vs30) from MASW, the STP and BSP can be categorized as soil class D (stiff soil) and E (soft soil), respectively. Results also showed that the STP area has no threat to the liquefaction potential compared with BSP area. In terms of drift, it is clearly shown that the difference of flexible-base structures at STP and BSP is 6 and 19 %, respectively, and are larger than fixed-base structure.

Keywords Drift · Land reclamation · Multichannel analysis of surface waves · Soil liquefaction · Pushover analysis

✉ Fadzli Mohamed Nazri
ccfmn@usm.my

[1] Disaster Research Nexus, School of Civil Engineering, Engineering Campus, Universiti Sains Malaysia, 14300 Nibong Tebal, Penang, Malaysia

Published online: 24 April 2015

1 Introduction

Land reclamation has taken on an important role in the process of urban growth in coastal areas. The rapid development of commercial and industrial areas will directly enhance the growth of the population and typically require more area for the development and infrastructure. The maritime nations such as Singapore, Hong Kong, and Japan consider beach reclamation as the best solution to solve the problem of scarcity of land. The same situation exists in Malaysia, especially in Penang area. Penang is located in the north-west coast of Peninsular Malaysia. It is well known among tourists as the island and a thriving modern metropolis. Penang has experienced rapid growth as a consequence of positive economic development. Urban growth and infrastructure demand have increased due to population growth in the country. As a result, scarcity of land has been one of the major problems in Penang. To overcome the shortage of land, development on reclaimed land has been implemented.

Malaysia lies on a stable Sunda platform within the Eurasian plate, bounded by two primary seismically active plate boundaries, namely the Indian-Australian Plate and the Philippine Plate, as shown in Fig. 1. Although Malaysia is not located close to the seismic-prone area with active fault, buildings erected on soft soils are often exposed to the far-field earthquakes generated from along Sumatran fault and subduction zones, particularly in areas on the west coast of Peninsular Malaysia, such as in Penang, Johor Bharu, and Kuala Lumpur (Adnan et al. 2005; Husen et al. 2008). Figure 2 provides a record of the earthquake epicentres from neighbouring countries and other locations near Penang (Jeffrey 2008). In the past 40 years, 44 earthquakes originating from the Sumatra fault and subduction zone have been recorded in Penang, two of which are among the greatest earthquakes in the world. Table 1 summarizes the significant earthquake events (MMI $\geq$ IV) that have been felt in Penang. Although no casualties or damages were reported due to those earthquakes, the tremors have been causing panic to a lot of people in several cities in Peninsular Malaysia. Non-structural cracks on buildings in few cities due to these

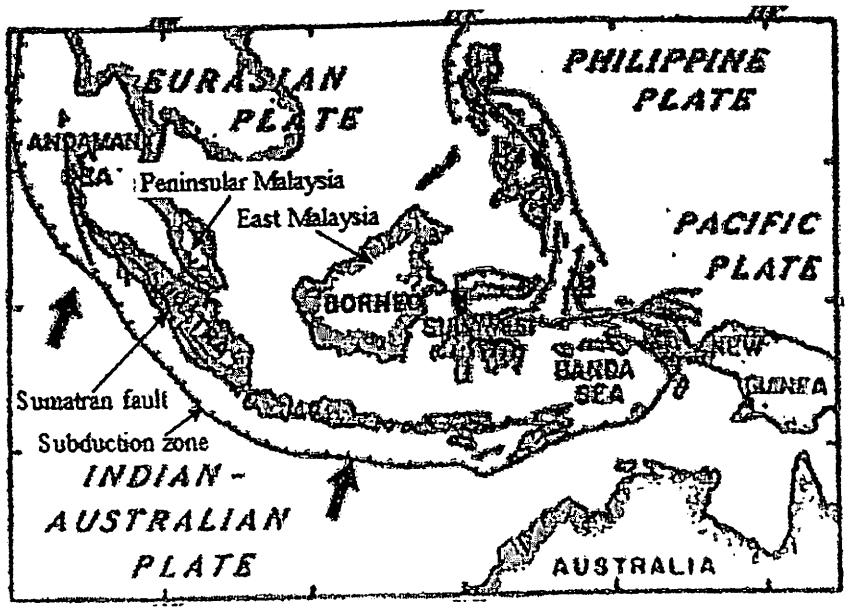

Fig. 1 Sumatran fault lines and subduction zone of the Indian-Australian Plate into the Eurasian Plate (Balendra and Li 2008)

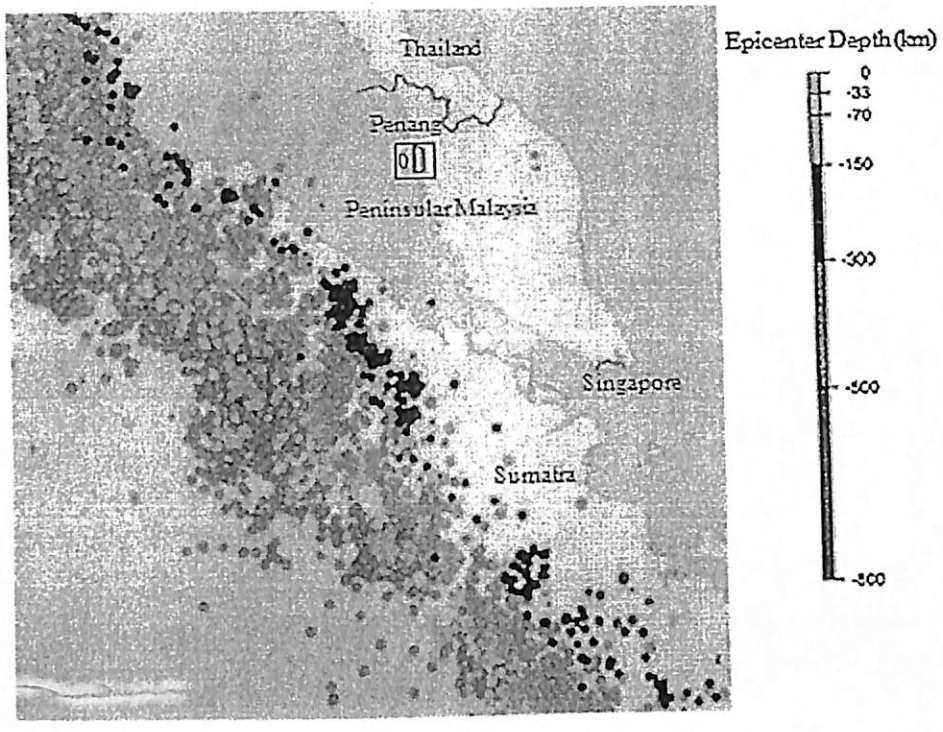

Fig. 2 Record of the earthquake epicentre (Jeffrey 2008)

Table 1 Summary of the earthquakes (MMI ≥ IV) from the Sumatran fault and subduction zone experienced by Penang (Malaysian Meteorological Department)

No.	Earthquake location	Date	Epicentre Coordinate (°)	Focal depth (km)	Magnitude	Distance to Penang (km)
1	Northern Sumatera	17 July 2013	5.4, 98.0	40	5.5 (M_w)	250
2	Southern Sumatera	30 Sept 2009	−0.9, 99.7	91	7.6 (M_s)	680
3	Mentawai Trough	12 Sept 2007	−4.4, 101.1	50	6.9 (m_b)	1075
4	Mentawai Strait	14 May 2005	0.8, 98.2	63	6.7 (m_b)	550
5	Nias	28 Mar 2005	2.0, 97.3	47	8.7 (M_w)	490
6	Aceh	26 Dec 2004	3.2, 95.9	30	9.3 (M_w)	540
7	Serba Jadi	22 Jan 2003	4.4, 97.5	33	5.7 (m_b)	320
8	Simeulu Tengah	2 Nov 2002	2.8, 96.1	30	6.2 (m_b)	540
9	Bambel	20 Aug 1997	4.3, 96.4	33	5.9 (m_b)	450
10	Lawe Alas	10 Oct 1996	3.4, 97.9	33	5.7 (m_b)	340

earthquakes also have been reported (Che Abas 2012; Adnan et al. 2004, Che Abas 2001; Hee et al. 2005).

Reclamation can be defined as the process of creating new land from the seashore, rivers, and lakes. Two different activities can be described through land reclamation. First, land reclamation is a direction to modify wetlands, streams, and convert them into useful land that could be utilized for growth purposes. It can also be a process in which damaged land restored to its original condition. In both cases, a land reclamation term used to describe a type of procedure performed essentially changes the basic characteristics of the soil in order to achieve the desired goal.

In order to evaluate the potential liquefaction for reclaimed area, a method called surface wave method has been used. A surface wave method is a non-destructive method that has often been used by researchers and engineers in geotechnical and earthquake engineering (Boore 2006; Park et al. 1999; Nazarian et al. 1983). The main principles of surface wave method are requiring energy from an impact, explosives, or a mechanical source to generate elastic waves in the ground. Surface wave method is able to provide higher vertical and lateral resolution in the shallow near surface without suffering limitation. The surface wave method will generate a shear wave velocity profile and will provide average shear wave velocity (Vs30) (Luna and Jadi 2000). Stokoe et al. (1994) stated that the shear wave velocity (V_s) profile is a standard property and key parameters to evaluate near-surface stiffness. The application of shear wave velocity is to determine the soil properties and site classification, evaluation of liquefaction potential, and spring stiffness for the foundation of a structure (Molas and Yamazaki (1995).

Site classification is a critical parameter in engineering because it might lead to safety and liability problems. In order to categorize the site criteria, all soil and rock layer in the upper 30 m of the site profile are considered. In actual cases, engineering site investigation is usually limited to the uppermost 30 m of material since that is the typical depth of borings, and it has become the standard depth for classifying sites. According to IBC (2000), three methods were mainly suggested for determining site classification: average shear wave velocity (V_s); average standard penetration resistance; and average undrained shear strength.

According to BSI (2004), the site should be classified from the value of average shear wave velocity (Vs30) if available; otherwise, the value Nspt should be applied. The site classification based on descriptions of site classes is described in Table 2. In addition, the value of average shear wave velocity (Vs30) is recommended to classify sites in recent buildings codes and for seismic design for new building (Scott et al. 2006; Dobry et al. 2000). Based on empirical studies by Xia et al. (2002), the difference between the shear wave velocity calculated by the MASW method and borehole measurements is less than 15 %. Anderson et al. (1996) stated that the shear wave velocity is an important parameter to classify of site, and the classification is more accurate from other methods.

Soil liquefaction is a phenomenon by which water-saturated sediment losses strength and stiffness due to the evaluation of pore water pressure by an earthquake. Evaluation of the liquefaction potential of soils is an important task in geotechnical and earthquake investigations. In geotechnical investigations, a standard penetration test (SPT) has been applied for evaluating liquefaction potential. As mention earlier, that method is quite

Table 2 Site classification (IBC 2000)

Site class	Soil profile name	Average properties in top 30 M		
		Shear wave velocity, V_s (m/s)	Standard penetration resistance, N	Undrained shear strength, S_u (Kpa)
A	Hard rock	$V_s > 1500$	N/A	N/A
B	Rock	$760 < V_s < 1500$	N/A	N/A
C	Very dense soil/soft rock	$360 < V_s < 760$	$N > 50$	$S_u > 100$
D	Stiff soil	$180 < V_s < 360$	$15 < N < 50$	$50 < S_u < 100$
E	Soft soil	$V_s < 180$	$N < 15$	$S_u < 50$

expensive and time-consuming. A liquefaction potential analysis using shear wave velocity has been proposed as a non-destructive method that can be performed on the surface.

Land reclamation has taken on an important role in the process of urban development. The rapid development of commercial and industrial areas will directly enhance the development of the population and typically require more area for the development and infrastructure. One of the options to create more land is to reclaim coastal land. However, the subsoil along the coastline is generally composed of silt and clay soils. Coastal land reclamation usually comes along with difficulties such as instability of the reclaimed platform, long-term excessive settlement, and soil liquefaction potential. From the engineering point of view, the land is generally not a suitable site for a civil construction project.

In the current building design practice, the foundation of the structure is assumed to be fixed. However, this assumption is realistic only when the structure is founded on soil, rock, or when the relative stiffness of the foundation soil is high compared with the superstructure. The buildings are supposed to be clumped and considered on the foundation medium and local soil conditions (soil–structure interaction) with selecting appropriate tremors records compatible with the characteristics of the soil deposit in the seismic evaluation (Saez et al. 2013). The soil–structure interaction (SSI) phenomenon which was neglected by most of the seismic codes as well as common design practices always leads to conservative results (Minasidis et al. 2014). In the pertinent literature, many research studies have confirmed the important effects of SSI (Maravas et al. 2014; Abdel Raheem et al. 2014). In order to consider the effect of soil flexibility on structure, average shear wave velocity (Vs30) of soil development is needed in the spring stiffness as the flexible base.

Therefore, the objectives of this study were to investigate the soil classification and liquefaction potential of the reclaimed land by using multichannel analysis of surface wave (MASW) method. Moreover, this work studies the effect of soil flexibility on low-rise and medium-rise structure in terms of drift based on value of Vs30.

2 Methodology

This section describes in detail the method to determine the site classification and the potential of liquefaction at the reclaimed area based on average shear wave velocity (Vs30) by using multichannel analysis of surface wave (MASW) method. In addition, the value Vs30 obtained from this method will be used to study the effect of soil flexibility on low-rise and medium-rise structures in terms of drift. Hence, this study is divided into two parts, which are the soil investigation and the structural analysis. The general flow chart of the methodology is summarized in Fig. 3.

2.1 Site selection

In this study, two sites have been selected as a case study. The reason we choose this site is because of the availability to access the site and the criteria are suitable for the objectives of this study. The first site is Seri Tanjung Pinang (STP), which is a new residential and commercial area in Tanjung Tokong, Penang. It is situated along on the northeast coast of Penang Island and bordering Gurney Drive and Tanjung Bungah. STP is a mixed-use development including luxury residential properties, shopping centres, and high-rise

condominiums. It was built on reclaimed land. The total reclamation area is approximately 980 acres and is the largest land reclamation in Penang. Reclamation works carried out in 2004 and completed in 2006 are shown in Fig. 4.

Bandar Sri Pinang (BSP) is a new residential area in Jalan Sungai Pinang Jelutong Expressway, Penang. The neighbourhood is constructed on reclaimed land that was created after the construction of the Jelutong Expressway. The neighbourhood has a mix of development, including two-storey houses, medium-cost apartments, luxury condominiums, luxury residential, and commercial areas. Reclamation works carried out in 2000 and fully completed in 2007 are shown in Fig. 4.

2.2 Multichannel analysis of surface wave

Multichannel analysis of surface wave (MASW) technique was used to obtain the shear wave velocity (V_s) at 30 m as part of soil investigation in this study. MASW test was carried out using Geometric 24 channels seismograph. The general equipment necessary to

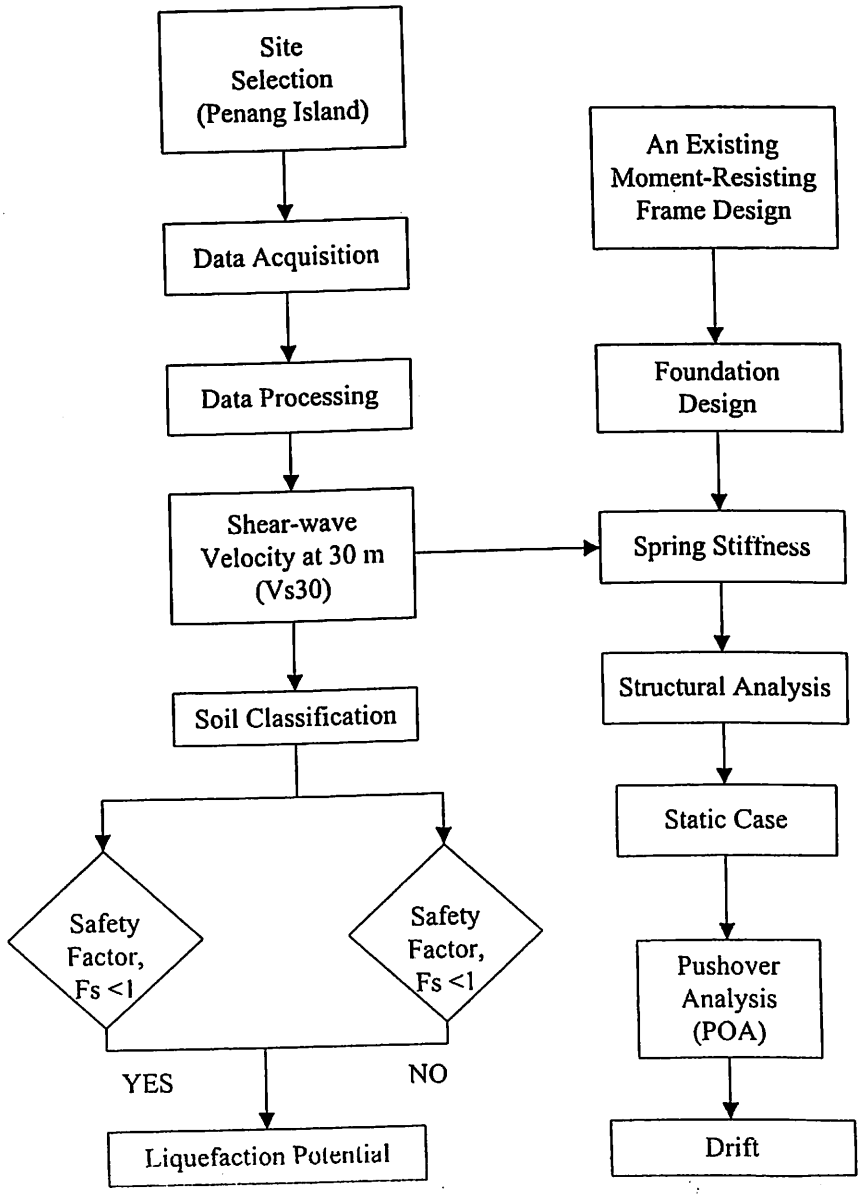

Fig. 3 General flow chart of methodology

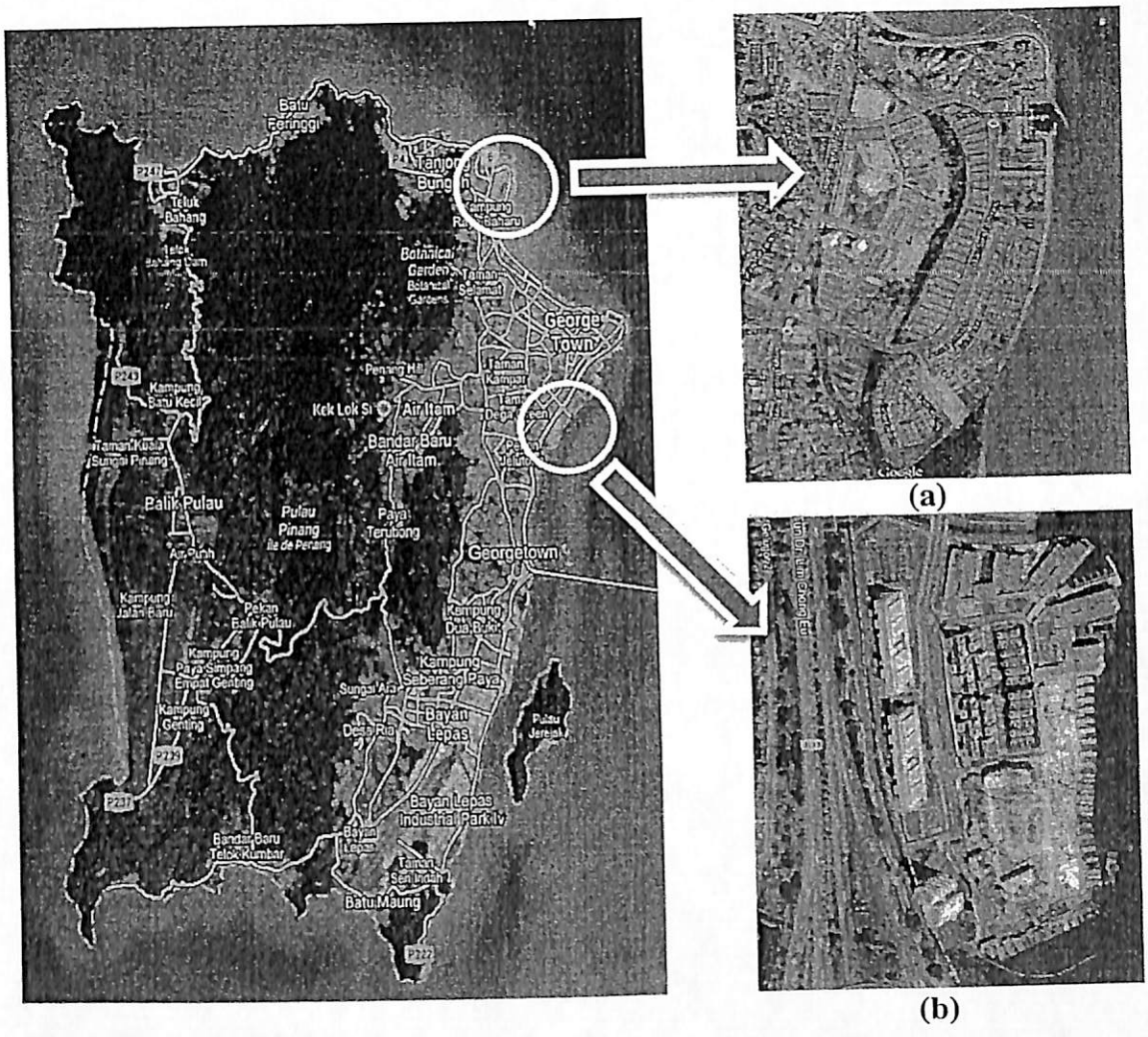

Fig. 4 Case study area

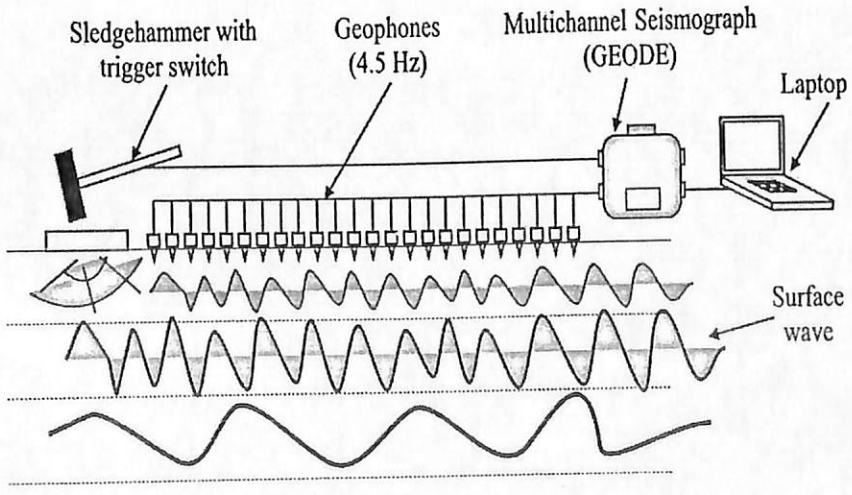

Fig. 5 Schematic illustration of MASW test field configuration

carry out a MASW includes seismograph and power supply, 24 units of vertical geophones with 4.5 Hz natural frequency, geophones cable, active source of 8 kg sledgehammer, striker plate, and associated equipments. The test was performed by deploying a linear

array of receivers on the ground surface. The field configuration of MASW is illustrated in Fig. 5.

Data acquisition is the process of acquired raw data from the selected site. The raw surface wave data are required to develop a dispersion curve to obtain shear wave velocity (V_s). Park et al. (1999) stated that to enhance ground-roll signal, parameter of data acquisition such as number of channels, source–receiver offset, and receiver interval should be set correctly. The effective distance between the receivers is in the range of 0.5 m to 2.0 m as suggested by Uma Maheswari et al. (2010). The nearest source–receiver offset to meet the requirement of different types of soil hardness is in the range of 5 m to 15 m (Xu et al. 2006). In order to obtain the best data, striker plate must be placed on firm ground and the signal is stacked in the seismograph 5 to 15 times (Tan et al. 2014). The data acquisition parameter for this study is shown in Table 3.

2.3 Site classification

The average shear wave velocity (Vs30) obtained from multichannel analysis of surface wave (MASW) method was used to determine the site classification for selected sites in this study based on the International Building Code site classification. The site classification is shown in Table 2. The density of soil was calculated using Eq. (1) (Tezcan et al. 2006).

$$\rho = 0.44 V_S^{0.25} \tag{1}$$

2.4 Liquefaction potential and factor of safety (F_s)

With the increasing popularity worldwide of shear wave velocity measurement for site characterization, the simplified procedure using the shear wave velocity (V_s) has been developed for evaluating liquefaction potential of soil (Youd 2001; Andrus and Stokoe 2000; Seed and Idriss 1971). In this study, a simplified equation by Zhang (2010) will be used as a main reference. Zhang (2010) developed the simplified method for evaluating liquefaction potential of soils. This simple method is developed by using the optimum seeking method to quantify the influence of various factors directly with no required assumptions or simplifications. The entire process to evaluate the liquefaction potential consists of five factors: the earthquake magnitude, the vertical effective overburden stress, average shear wave velocity, peak acceleration at the ground surface, and fines content.

Table 3 Data acquisition parameter

Parameter	Description
Source	8 kg sledgehammer
Drop height	1 m approx.
Vertical stack	5
Geophone/receiver	4.5 Hz vertical
No. of receiver	24
Receiver spacing	1 m
Source–receiver offset	5, 10, 15 m
Sampling interval	0.25 ms
Record length	1 s

The factor is graded according to the standard shown in Table 4. The grading standard is established by considering the possible range of the factors and their influence on the liquefaction potential of soils.

The liquefaction potential (LP) can be calculated using Eq. (2).

$$\mathrm{LP} = 35G(M) + 32G(\sigma'_v) + 71G(V_s) + 34G(a_{\max}) + 39G(\mathrm{FC}) \tag{2}$$

where M is the earthquake method; σ'_v is the effective vertical overburden stress; V_s refers to average shear wave velocity; $\alpha_{\max}$ is the peak horizontal acceleration at the ground surface, and FC is the fine content.

Meanwhile, the factor of safety (F_s) can be simply defined by Eq. (3)

$$F_s = \frac{315}{\mathrm{LP}} \tag{3}$$

Based on the empirical studies by Lin et al. (2004), the cost, limited time, and the analysis for the liquefaction potential by the simplified procedure using the shear wave velocity (V_s) were shown to be effective for estimating the extent of the potential liquefaction hazard if compared with cone penetration test (CPT).

2.5 Soil–structure interaction

During the earthquakes, the structures interact with the foundation soil and usually suffer significant damage, deformation, and collapse even newly built and designed buildings according to modern seismic codes. According to FEMA (2009), the response of a structure during an earthquake is dictated by interactions between the structure, the foundation, and the underlying soil or rock surrounding the foundations and is defined as soil–structure interaction (SSI). According to FEMA (2004), soil–structure interaction is one of the most important aspects and needs to be considered in structural analysis.

The dynamic interaction between superstructure and substructure is categorized as inertial interaction and kinematic interaction. Stewart et al. (2003) stated that soil–structure interaction (SSI) effect tends to be significant for laterally stiff structures founded on soft soils. Based on studies by Galal and Naimi (2008b), the effect of soil–structure interaction (SSI) on high-rise building is higher than on medium- and low-rise building.

The idealized analysis for soil–structure interaction (SSI) is performed by direct and substructure approaches. In a direct approach, the soil and structure are fully modelled and analysed in a single step; meanwhile, in a substructure approach, SSI is analysed in three steps. In the current structural design practice, the foundation of the structure is assumed to be fixed. However, this assumption is realistic only when the structure is founded on soil, rock, or when the relative stiffness of the foundation soil is high compared with the

Table 4 Factor grading standard (Zhang 2010)

Factor	G (*)			
	0	1	2	3
M	≤5.9	6.0–6.9	7.0–7.9	≥8.0
$\sigma'v$ (kPa)	≥120.1	59.6–120.0	30.0–59.5	≤29.9
V_S (ms^{-1})	≥177	125–176	105–124	≤104
α_{max} (g)	≤0.09	0.10–0.19	0.20–0.29	≥0.30
FC (%)	≥61	35–60	6–34	≤5

superstructure (Galal and Naimi 2008b). Spring is used in foundation to represent the SSI. In case of rigid foundation, 3 springs are used for 2D system; meanwhile, for 3D system, 6 springs are used. In the implementation of SSI system, the model is analysed using force-based procedure, displacement-based procedure, and response history procedure.

2.6 Nonlinear static analysis

Nonlinear static analysis, also commonly known as pushover analysis (POA) is defined as an analysis wherein a mathematical model directly incorporating the nonlinear load-deformation characteristics of individual components and elements of the structures is subjected to monotonically increasing lateral forces representing inertia forces until a target displacement is reached (Fajfar 2000). The target displacement limit may be set based on different criteria such as maximum allowable storey drift or member ductility limits. Alternatively, the structure may be pushed until the control node reaches collapse state. One important product of the POA is the base shear versus top displacement relationship, commonly referred as the capacity curve. This curve gives an overall summary of the performance of the structure under lateral loading. From this curve, the information such as the initial elastic stiffness, the initiation of first yielding, the stage of rapid stiffness deterioration, and ultimate strength can be obtained. A pushover analysis of a structure with a flexible base is schematically illustrated in Fig. 6.

During an earthquake, lateral forces can be imposed on structures. In terms of the lateral force-resisting system, when the lateral force is placed on structure, the structures respond and move due to the force. The movement due to the forces is known as a drift. According to FEMA (2009), drift can be defined as the difference of lateral displacement between two consecutive stories. Drift has three primary effects on a structure: the structural elements, non-structural elements, and adjacent structures. Drift was also selected as a parameter of soil–structure interaction (SSI) effect and needs to be considered in engineering design practice. As mentioned by Searer and Freeman (2004), the structures that had the greatest drift demands and would arguably be the most likely to collapse during a large earthquake are the low-rise structures. However, to prevent structural collapse, the stiffness of the structure was increased and this indirectly will reduce the ductility demands.

The percentage drift for each structure will be determined by using pushover analysis (POA), and then it will be compared with the drift limitation for structural performance

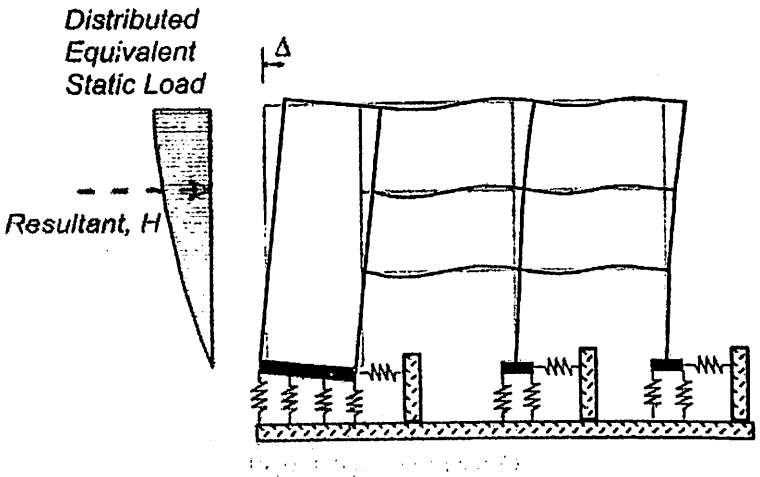

Fig. 6 Schematic illustration of pushover analysis (NERHP 2012)

level as suggested from (FEMA-356 2000) and as tabulated in Table 5. From the average drift, the effect of soil flexibility on low- and medium-rise structures will be determined.

2.7 Moment-resisting concrete frame (MRCF)

In the second part of the structural design of this study, the existing moment-resisting concrete frame (MRCF) was used to study the effect of soil flexibility on low- and medium-rise structure in terms of drift. The two types of MRCF are designed according to the Eurocode 2 and Eurocode 8. In a framed building, the basic skeleton comprises of beams, columns, joints, and foundations.

The characteristic of MRCF has two bays with span length of 6 m per bay, height of 3 m per each storey, and shallow bearing foundation. The difference between two types of MRCF is that the frame storey for low-rise structure is three storeys and for medium-rise structure is six storeys. Each type of MRCF is designed with two different cases, which is MRCF with fixed base; otherwise, it is MRCF with flexible base. The dimension of beam and column is shown in Tables 6 and 7. The design assumptions are as follows: (i) bar diameter = 20 mm; (ii) link diameter = 10 mm; (iii) concrete cover = 25 mm; (iv) concrete strength = 30 N/mm^2; and (v) steel yield stress = 460 N/mm^2. The structures are based on rigid connection as a default setting in SAP 2000 software. The types of elements used to model beam and column are based on plastic hinge element. The plastic hinge element has two nodes with local node 1 and 2. These elements are also based on a default hinge model that is defined in SAP 2000. The model behaviour is based on the simplest case of trilinear model with 5 % of damping used in this study.

Beams and columns are modelled by 3D frame elements. In order to obtain the bending moments and forces at the beam and column faces, beam–column joints are modelled by giving end-offsets to the frame elements. The beam–column joints are to be considered as rigid, and the column end of the foundation is assumed as fixed.

2.8 Shallow bearing foundation

The shallow foundation was designed as a base for the two types of moment-resisting concrete frame (MRCF). The shallow foundation was designed with concrete strength 30 N/mm^2. EsteemPlus (Esteem Innovation 1993) software was used in this study to design the shallow foundation of MRCF.

For the purpose of evaluation, effect of soil and foundation flexibility, the rigid shallow bearing foundation with respect to the supporting soil, and an uncoupled spring model are designed to represent the foundation stiffness as shown in Fig. 7. In order to evaluate the spring stiffness, the dimension of foundation should be known. The values of the stiffness of the springs are dependent on the mechanical characteristics of the soil material, the dimensions of the foundation, and its embedment depth. Based on the relative stiffness of the foundation structure and the supporting soil, the spring stiffness was calculated using Eq. (4) from FEMA-356 (2000)

Table 5 Maximum drift for structural performance levels

Limit state	Maximum drift (%)
Intermediate occupancy (IO)	1.0
Life safety (LS)	2.0
Collapse prevention (CP)	4.0

Table 6 Dimension of beam

MRCF	Size (mm × mm)	Reinforcement (area/mm^2)	Shear link
3 Storeys	300 × 700	6T25 (2950)	8 mm @ 150 mm c/c
6 Storeys	300 × 700	4T32 (3230)	8 mm @ 150 mm c/c

Table 7 Dimension of column section

MRCF	Size (mm × mm)	Reinforcement (area/mm^2)
3 Storeys	500 × 500	6T32 (4830)
6 Storeys	500 × 500	6T32 (4830)

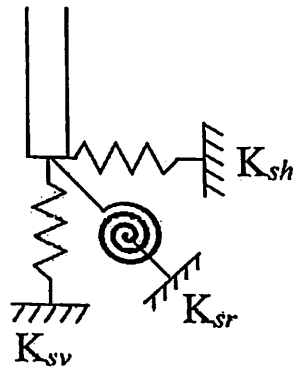

Fig. 7 Uncoupled spring model for rigid foundation (FEMA-356 2000)

$$\text{Translation along } x\text{-axis}, K_{sh} = \frac{GB}{2-\nu}\left[3.4\left(\frac{L}{B}\right)^{0.65} + 1.2\right]$$
$$\text{Translation along } z\text{-axis}, K_{sv} = \frac{GB}{1-\nu}\left[1.55\left(\frac{L}{B}\right)^{0.75} + 0.8\right] \quad (4)$$
$$\text{Translation along } y\text{-axis}, K_{sr} = \frac{GB^3}{1-\nu}\left[0.47\left(\frac{L}{B}\right)^{2.4} + 0.034\right]$$

where G = effective shear modulus; B = width of foundation; L = length of foundation ν = Poisson's ratio.

2.9 Structural analysis

For the purpose of structural analysis, the two types of moment-resisting concrete frame (MRCF) were analysed using SAP 2000 version 15 (CSI 2004). SAP 2000 is ideal for the general-purpose civil engineering software for the analysis and design or any case of structural system. It is also a purpose finite element program, which performs the static or dynamic, linear or nonlinear analysis of structural systems. Basic and advanced systems,

from 2D to 3D, simple geometry to complex, may be modelled, analysed, designed, and optimized using a practical and intuitive object-based modelling environment that simplifies and streamlines the engineering process.

The steps involve developing a computational model of the frame using SAP 2000 followed by applying the external forces based on the design load from EC8. Subsequently, the internal forces in the members of the frame can be calculated to estimate the deformations of the members and frame and finally interpret the results. MRCF is analysed for the static case by performing pushover analysis (POA) in SAP 2000.

In the implementation of the POA, the model must account for the nonlinear behaviour of the structural elements. In the present study, a point-plasticity approach is considered for modelling nonlinearity, wherein the plastic hinge is assumed to be concentrated at a specific point in the frame member under consideration.

2.10 Result and discussions

Data acquisition for multichannel analysis of surface wave (MASW) was carried out in two reclaimed areas in Penang. One is in Seri Tanjung Pinang (STP), and the other one is in Bandar Sri Pinang (BSP). Each site has four locations of data acquisition. Raw data of MASW were processed to develop the 1D shear velocity profile for all of data acquisition. The dispersion curves for STP and BSP (Figs. 8, 9) for all locations of data acquisition to generate the 1D shear velocity profile are shown in Figs. 10 and 11, respectively. From the 1D shear velocity profile, average shear wave velocity (Vs30) for each site is shown in Table 6.

2.11 Site classification

The average shear wave velocity (Vs30) obtained from multichannel analysis of surface wave (MASW) was used to characterize the site for two reclaimed areas. The site classification is based on (IBC 2000). From the result of MASW, the average Vs30 for Seri Tanjung Pinang (STP) is 246 m/s; meanwhile, for Bandar Sri Pinang (BSP) is 155 m/s. The site classification for two reclaimed areas in this study is shown in Table 5.

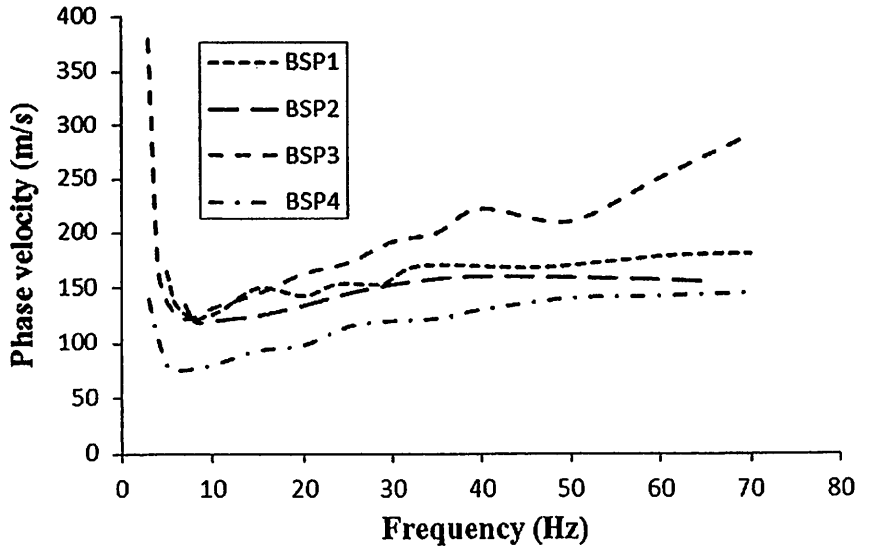

Fig. 8 Dispersion curves for Bandar Sri Pinang (BSP)

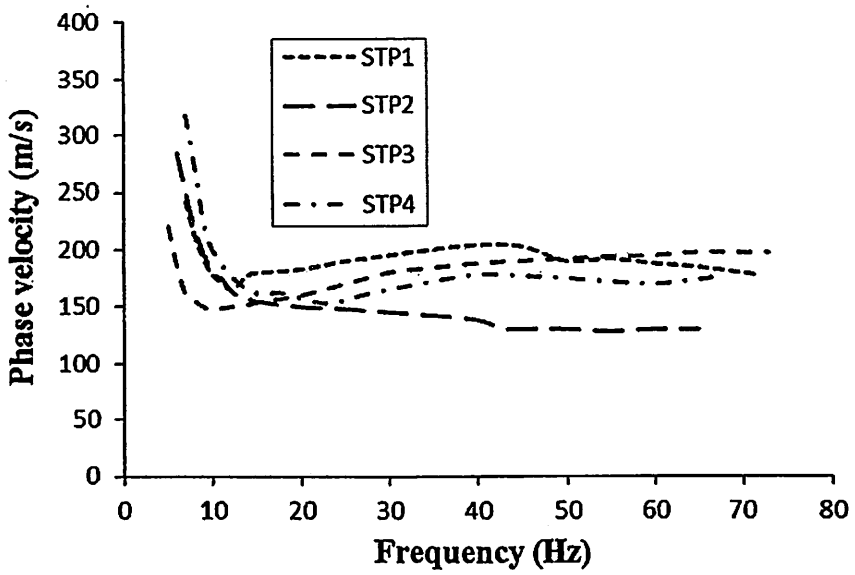

Fig. 9 Dispersion curves for Seri Tanjung Pinang (STP)

Based on the IBC site classification, STP is defined as a stiff soil. It means a soil profile consists a deposit of loose-to-medium cohesionless soil (with or without some soft cohesive layers), or of predominantly soft-to-firm cohesive soil. Meanwhile, BSP is defined as a soft soil. It means a soil profile consists of a surface alluvium layer. Based on equation state by Tezcan et al. (2006), the density and unit weight of soil for two reclaimed areas are shown in Table 6.

2.12 Liquefaction potential

The simple method of Zhang (2010) is applied to evaluate the liquefaction potential at Seri Tanjung Pinang (STP) and Bandar Sri Pinang (BSP) based on magnitude earthquake south of Bireun, Indonesia (2013), and west coast of northern Sumatra, Indonesia (2004). The details of these two earthquakes can be found in the United State Geological Services (USGS) website (http://www.usgs.gov/). The result of liquefaction potentials is shown in Tables 8, 9, 10, and 11 for various peak horizontal accelerations at the ground surface, α_{max} equals to 0.05, 0.15, 0.25, and 0.35 g, respectively.

The liquefaction is predicted to occur when the factor of safety is $(Fs) \leq 1$; otherwise, the liquefaction is predicted not to occur when $Fs \geq 1$. From the result, it shows that the soil at STP is still not potential to cause the soil liquefaction after the value of peak acceleration at the ground surface and the earthquake magnitude is increased. However, BSP has potential to cause liquefaction after the value of peak acceleration and earthquake magnitude is increased. This happens because BSP has a low shear wave velocity that represents a soil stiffness compared with STP. This indicates that when the soil has low stiffness, the potential to cause liquefaction is high. Furthermore, this study confirms that the shear wave velocity is the most important factor that influences the liquefaction potential as stated by Zhang (2010) (Table 12).

2.13 Displacement for fixed and flexible base

The fundamental periods of MRCFs with fixed and flexible base are summarized in Table 13. Compared with the fixed-base MRCFs, the result show the elongation of

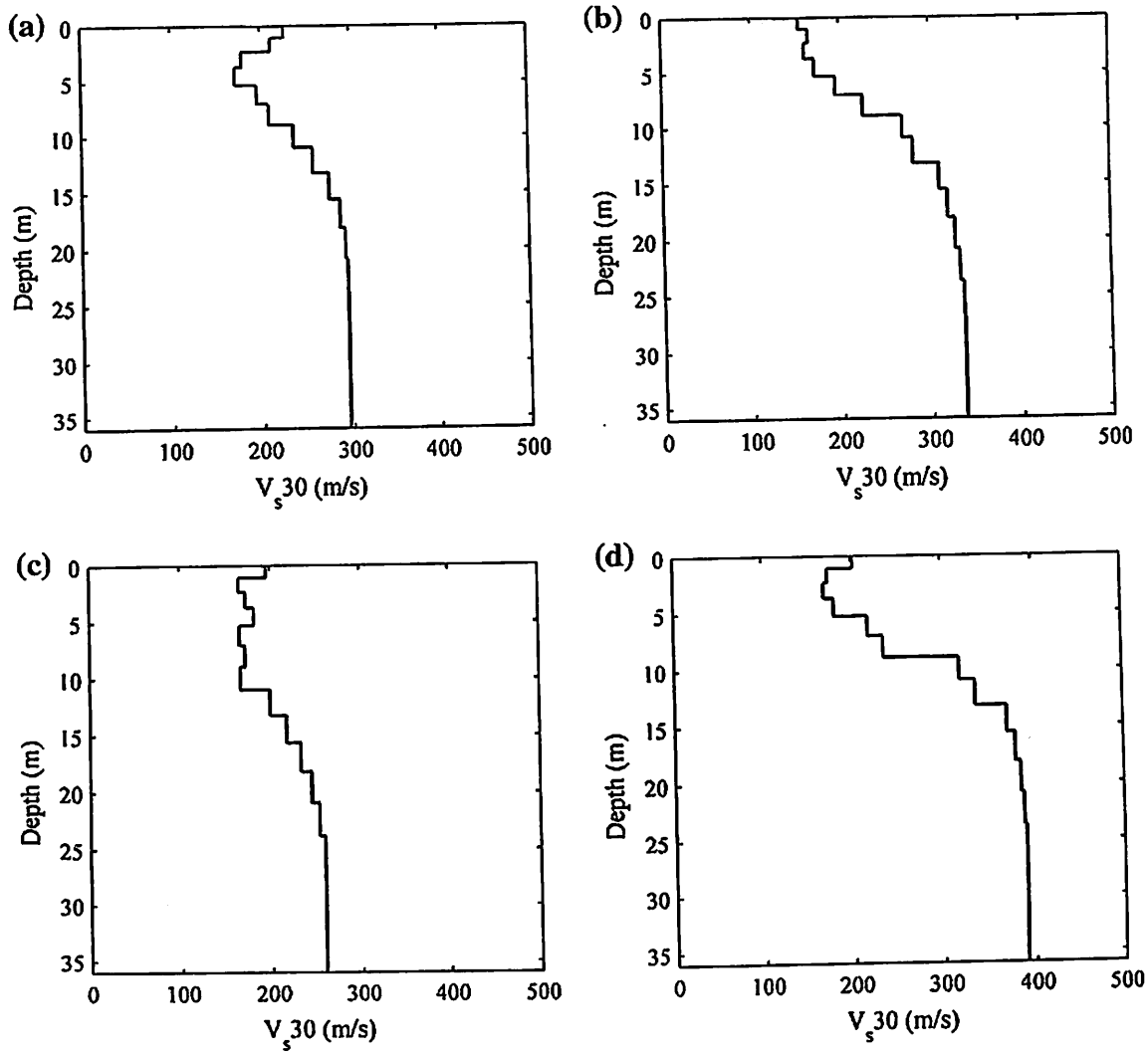

Fig. 10 1D shear velocity profile at Seri Tanjung Pinang (STP)

fundamental period in flexible-base MRCFs. The result depicted that more significant increment in fundamental period is found as the soil stiffness reduces (Class D to Class E), and hence, the effect of soil flexibility should not be ignored especially in soft soil deposits (Hatzigeorgiou and Kanapitsas 2013). The fundamental period of 3-storey MFCFs in site Class D (STP) and E (BSP) shows increment of 4.6 and 12.4 %, respectively, while 6-storey MRCFs shows 3.5 and 9.6 %, respectively. Figure 12 shows the maximum displacement due to pushover analysis with respect to the storey height of the structures that designed based on the fixed- and flexible-base case. From the figure, it can be observed that the storey displacement for 3- and 6-storey MRCFs is in the similar trend as the storey height increases. The reduction in lateral stiffness is observed as the soil stiffness reduces for both 3- and 6-storey MRCFs as mentioned by Minasidis et al. (2014); however, the percentage difference is insignificant.

2.14 Capacity curve flexible-base structure

From the pushover analysis (POA), it will generate the capacity curve and plastic hinge state. The capacity curve represents the drift and base shear for each type of frame. Drift in

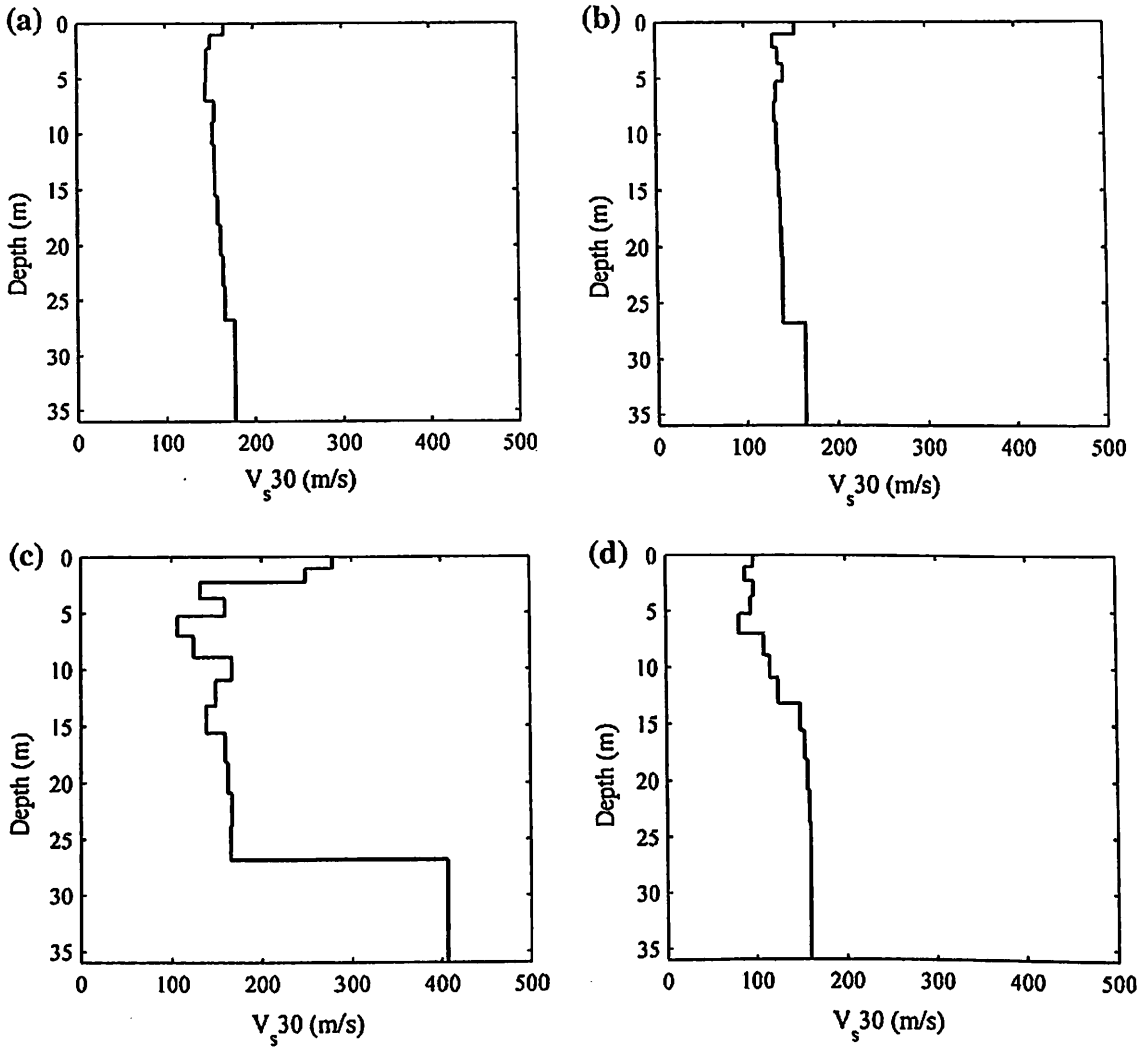

Fig. 11 1D shear velocity profile at Bandar Sri Pinang (BSP)

this study was calculated by taking the maximum displacement of the top storey and dividing it by the total number of storeys of the structures. From Figs. 13 and 14, it is shown that the base shear for 3-storey frames is greater than 6-storey frames. For example, in case of moment-resisting concrete frame (MRCF) at Seri Tanjung Pinang (STP), the base shear of 3-storey MRCF is 1368 kN, which is greater than 1065 kN base shear of 6-storey MRCF. This trend is also similar to MRCF at Bandar Sri Pinang (BSP). This indicates that low-rise structure has greater post-yield stiffness compared with the medium-rise structure. The results of this study indicate that the stiffness of the structure influences the value of base shear (Tables 14, 15).

For the 6-storey MRCF, this structure has larger drift compared with the 3-storey MRCF. For example, in the case of MRCF at STP, the drift difference of 6-storey MRCF is 12 % larger than that of the 3-storey MRCF. The same trends happen to MRCF at BSP in which the drift difference for 6-storey MRCF is 5 % larger than that for the 3-storey MRCF. This indicates that the drift for high-rise structures is larger than medium- and low-rise structures as stated by Galal and Naimi (2008a). Moreover, it is shown that 3-storey MRCF had greatest drift demand and high potential to collapse.

Table 8 Field liquefaction data ($\alpha_{max} = 0.05$ g)

Location	M	$\sigma'v$	V_s	FC	LP	FS	Liquefaction
South of Bireun earthquake							
STP 1	6.1	245.70	241.00	46.1	74	4.26	No
STP 2	6.1	249.10	247.50	46.1	74	4.26	No
STP 3	6.1	225.50	205.60	46.1	74	4.26	No
STP 4	6.1	270.20	289.70	46.1	74	4.26	No
BSP 1	6.1	194.00	158.50	37.1	145	2.17	No
BSP 2	6.1	180.30	140.80	37.1	145	2.17	No
BSP 3	6.1	220.40	197.50	37.1	74	4.26	No
BSP 4	6.1	166.00	123.90	37.1	216	1.46	No
Northern Sumatera earthquake							
STP 1	9.0	245.70	241.00	46.1	144	2.19	No
STP 2	9.0	249.10	247.50	46.1	144	2.19	No
STP 3	9.0	225.50	205.60	46.1	144	2.19	No
STP 4	9.0	270.20	289.70	46.1	144	2.19	No
BSP 1	9.0	194.00	158.50	37.1	215	1.47	No
BSP 2	9.0	180.30	140.80	37.1	215	1.47	No
BSP 3	9.0	220.40	197.50	37.1	144	2.19	No
BSP 4	9.0	166.00	123.90	37.1	286	1.10	No

Table 9 Field liquefaction data ($\alpha_{max} = 0.15$ g)

Location	M	$\sigma'v$	V_s	FC	LP	FS	Liquefaction
South of Bireun earthquake							
STP 1	6.1	245.70	241.00	46.1	108	2.92	No
STP 2	6.1	249.10	247.50	46.1	108	2.92	No
STP 3	6.1	225.50	205.60	46.1	108	2.92	No
STP 4	6.1	270.20	289.70	46.1	108	2.92	No
BSP 1	6.1	194.00	158.50	37.1	179	1.76	No
BSP 2	6.1	180.30	140.80	37.1	179	1.76	No
BSP 3	6.1	220.40	197.50	37.1	108	2.92	No
BSP 4	6.1	166.00	123.90	37.1	250	1.26	No
Northern Sumatera earthquake							
STP 1	9.0	245.70	241.00	46.1	178	1.77	No
STP 2	9.0	249.10	247.50	46.1	178	1.77	No
STP 3	9.0	225.50	205.60	46.1	178	1.77	No
STP 4	9.0	270.20	289.70	46.1	178	1.77	No
BSP 1	9.0	194.00	158.50	37.1	249	1.27	No
BSP 2	9.0	180.30	140.80	37.1	249	1.27	No
BSP 3	9.0	220.40	197.50	37.1	178	1.77	No
BSP 4	9.0	166.00	123.90	37.1	320	0.98	Yes

From all the result of capacity curves, it shows that all types of MRCF exceeded life safety (LS) level when compared to the drift limit based on structural performance level as suggested by (FEMA-356 2000). However, the 6-storey MRCF at BSP exceeded the

Table 10 Field liquefaction data ($\alpha_{max} = 0.25$ g)

Location	M	$\sigma'v$	V_s	FC	LP	FS	Liquefaction
South of Bireun earthquake							
STP 1	6.1	245.70	241.00	46.1	142	2.22	No
STP 2	6.1	249.10	247.50	46.1	142	2.22	No
STP 3	6.1	225.50	205.60	46.1	142	2.22	No
STP 4	6.1	270.20	289.70	46.1	142	2.22	No
BSP 1	6.1	194.00	158.50	37.1	213	1.48	No
BSP 2	6.1	180.30	140.80	37.1	213	1.48	No
BSP 3	6.1	220.40	197.50	37.1	142	2.22	No
BSP 4	6.1	166.00	123.90	37.1	284	1.11	No
Northern Sumatera earthquake							
STP 1	9.0	245.70	241.00	46.1	212	1.49	No
STP 2	9.0	249.10	247.50	46.1	212	1.49	No
STP 3	9.0	225.50	205.60	46.1	212	1.49	No
STP 4	9.0	270.20	289.70	46.1	212	1.49	No
BSP 1	9.0	194.00	158.50	37.1	283	1.11	No
BSP 2	9.0	180.30	140.80	37.1	283	1.11	No
BSP 3	9.0	220.40	197.50	37.1	212	1.49	No
BSP 4	9.0	166.00	123.90	37.1	354	0.89	Yes

Table 11 Field liquefaction data ($\alpha_{max} = 0.35$ g)

Location	M	$\sigma'v$	V_s	FC	LP	FS	Liquefaction
South of Bireun earthquake							
STP 1	6.1	245.70	241.00	46.1	176	1.79	No
STP 2	6.1	249.10	247.50	46.1	176	1.79	No
STP 3	6.1	225.50	205.60	46.1	176	1.79	No
STP 4	6.1	270.20	289.70	46.1	176	1.79	No
BSP 1	6.1	194.00	158.50	37.1	247	1.28	No
BSP 2	6.1	180.30	140.80	37.1	247	1.28	No
BSP 3	6.1	220.40	197.50	37.1	176	1.79	No
BSP 4	6.1	166.00	123.90	37.1	318	0.99	Yes
Northern Sumatera earthquake							
STP 1	9.0	245.70	241.00	46.1	246	1.28	No
STP 2	9.0	249.10	247.50	46.1	246	1.28	No
STP 3	9.0	225.50	205.60	46.1	246	1.28	No
STP 4	9.0	270.20	289.70	46.1	246	1.28	No
BSP 1	9.0	194.00	158.50	37.1	317	0.99	Yes
BSP 2	9.0	180.30	140.80	37.1	317	0.99	Yes
BSP 3	9.0	220.40	197.50	37.1	246	1.28	No
BSP 4	9.0	166.00	123.90	37.1	388	0.81	Yes

collapse prevention (CP) level, and it shows that the frame has higher drift compared with the other frames. Result also shows that the MRCF at BSP has higher drift compared with the MRCF at STP for each type of frame. This indicates that the low stiffness of foundation structures and the percentage drift of the structure are high.

Table 12 Average shear wave velocity (Vs30)

Site	Vs30 (m/s)
STP 1	241.00
STP 2	247.50
STP 3	205.60
STP 4	289.70
BSP 1	158.50
BSP 2	140.80
BSP 3	197.50
BSP 4	123.90

Table 13 Site classification

Site	Site class
Seri Tanjung Pinang (STP)	D
Bandar Sri Pinang (BSP)	E

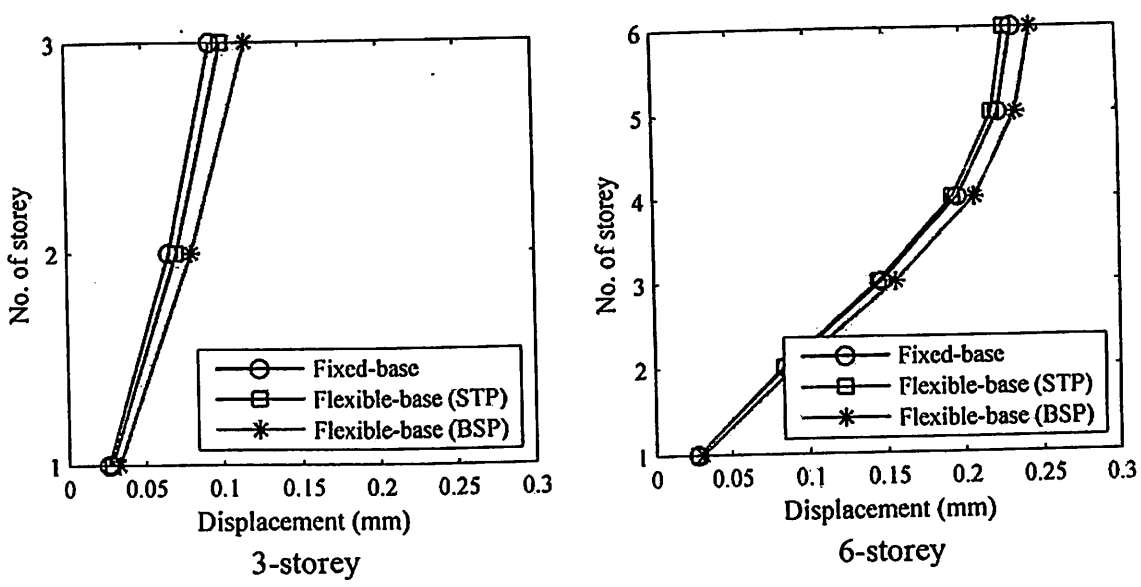

Fig. 12 Displacement over storey of structure

In the POA, the internal stresses start to accumulate when the lateral forces push the frame from the left side. This will induce the failure of the beam or column sections. Figures 15 and 16 show the distribution of the hinge deformation at the maximum drift and base shear. The hinges occurred in the section will be represented in the types of colour coding, where they are purple for Operational (O), yellow for Collapse (C), and orange for Damage (D) state. From the figures, it is shown that most of the damage state is formed at the beam section. This indicates that the potential failure starts occurring at the beam section before the column section. In Fig. 15, the hinges with damage state are deformed at all beam sections of the MRCF at BSP, but it has not fully occurred in all beam sections of the MRCF at STP. The same trends can be observed for a 6-storey MRCF cases. This indicates that MRCF at BSP with low stiffness of foundation will result high potential to collapse.

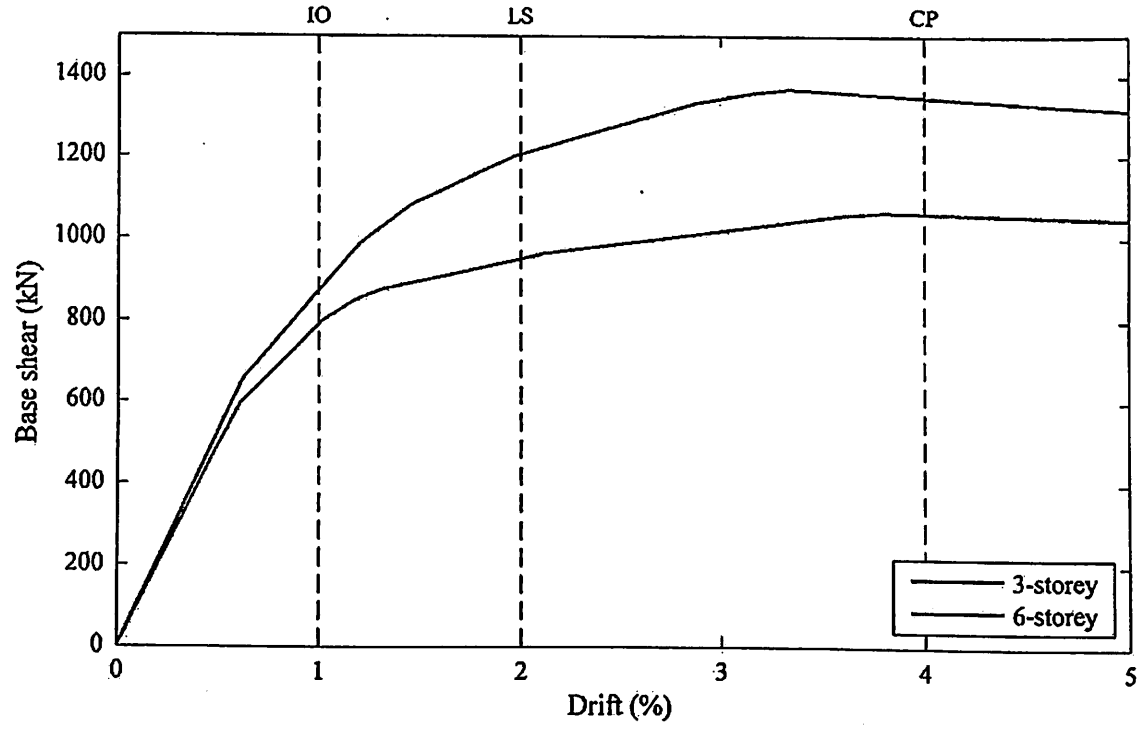

Fig. 13 Capacity curve for MRCF at Seri Tanjung Pinang (STP)

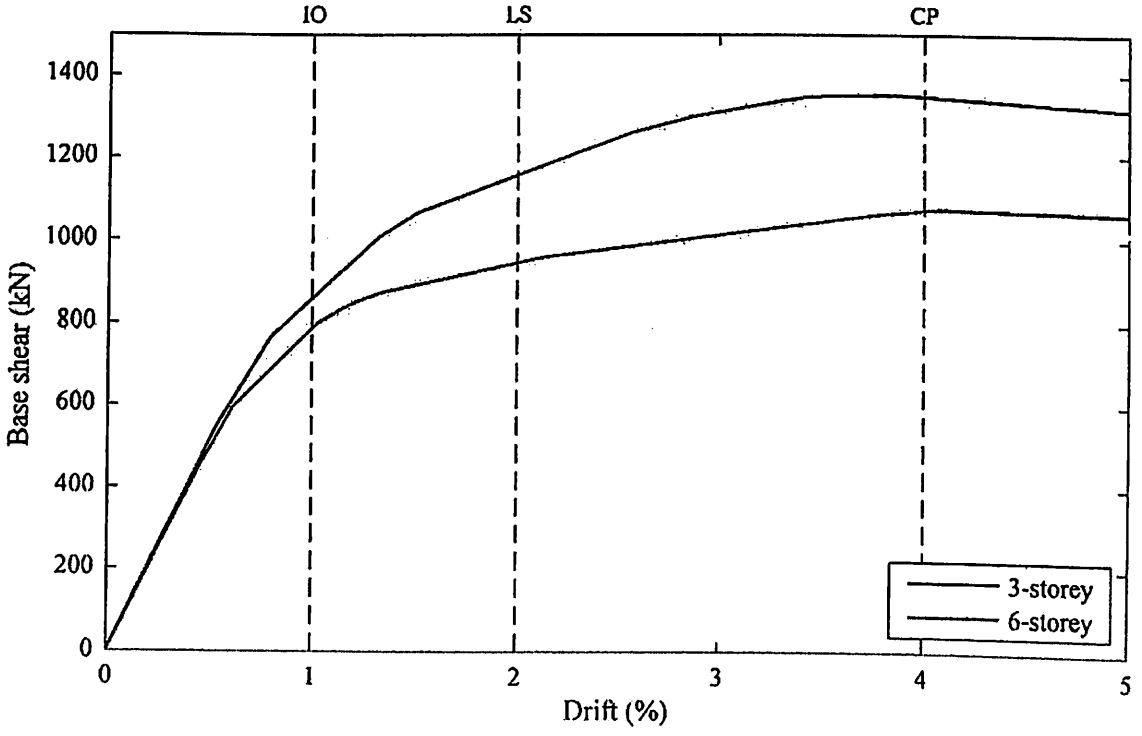

Fig. 14 Capacity curve for MRCF at Bandar Sri Pinang (BSP)

2.15 Flexible and fixed base

In this section, the moment-resisting concrete frame (MRCF) with a flexible base will be compared with the MRCF with fixed base. The MRCF fixed base was designed according

Table 14 Soil parameter

Site	Density (kg/m^3)	Unit weight (kN/m^3)
Seri Tanjung Pinang (STP)	1743	17.4
Bandar Sri Pinang (BSP)	1522	15.2

Table 15 Fundamental period of MRCF with fixed and flexible base

Foundation	Site class	Number of storey	Fundamental period, T_f (s)	Incremental (%)
Fixed base	–	3	0.153	–
		6	0.317	–
Flexible base	D (STP)	3	0.160	4.6
		6	0.328	3.5
	E (BSP)	3	0.172	12.4
		6	0.347	9.5

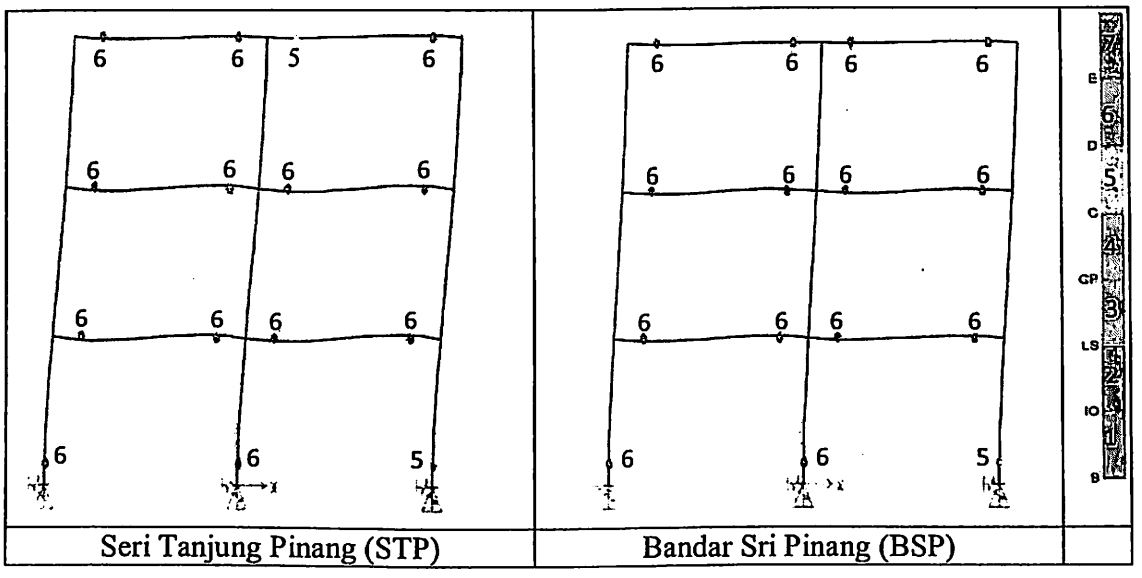

Fig. 15 Three-storey MRCF with deformed hinges

to EC2 and EC8 with the same characteristic of the MRCF flexible base. Figures 17 and 18 illustrate the drift of the cases with flexible- and fixed-base structure.

Figure 17 shows that the drift difference of 3-storey flexible-base structure at Seri Tanjung Pinang (STP) and Bandar Sri Pinang (BSP) which is 6 and 19 % is greater than in the fixed-base structure. This indicates that in terms of drift, flexible base is greater than fixed base. However, the damage to structural components and potential to collapse are smaller than those for fixed base. Furthermore, from the figure, it is shown that the flexible base at STP which is based on a relative stiff soil follows the same trends as a structure with a fixed base that was given the same value of maximum base shear. This indicates that the stiffness of the flexible base at STP is similar to fixed-base structure. However, the stiffness of flexible base at BSP which based on a relatively soft soil is low and was considered as the worst scenario for the flexible base as stated by (IBC 2000). Based on Searer and Freeman (2004), by increasing the stiffness of the structure such as increase

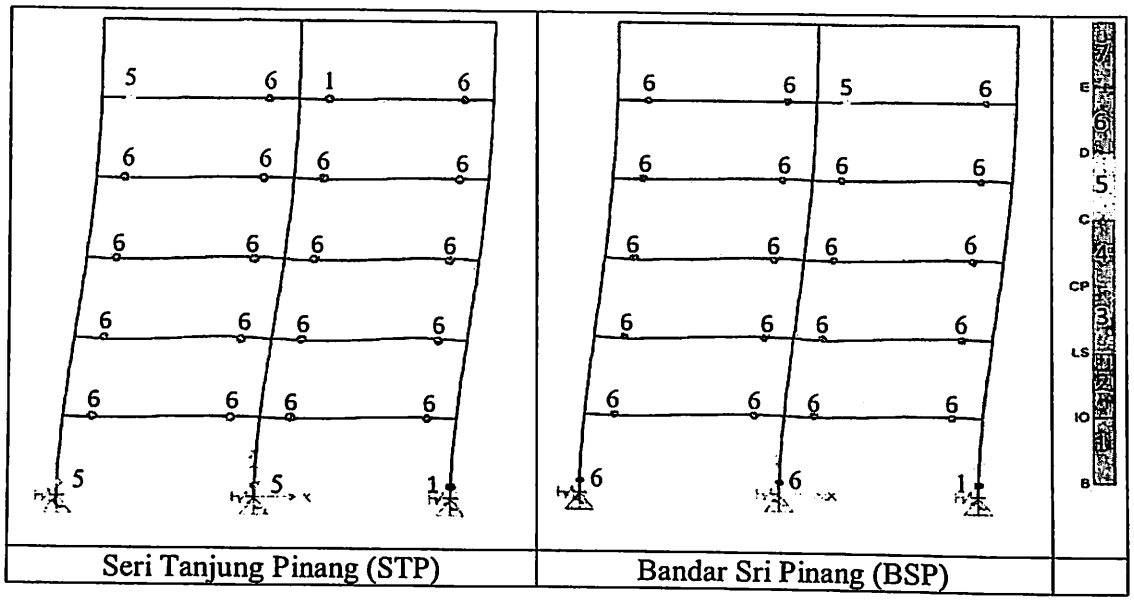

Fig. 16 Six-storey MRCF with deformed hinges

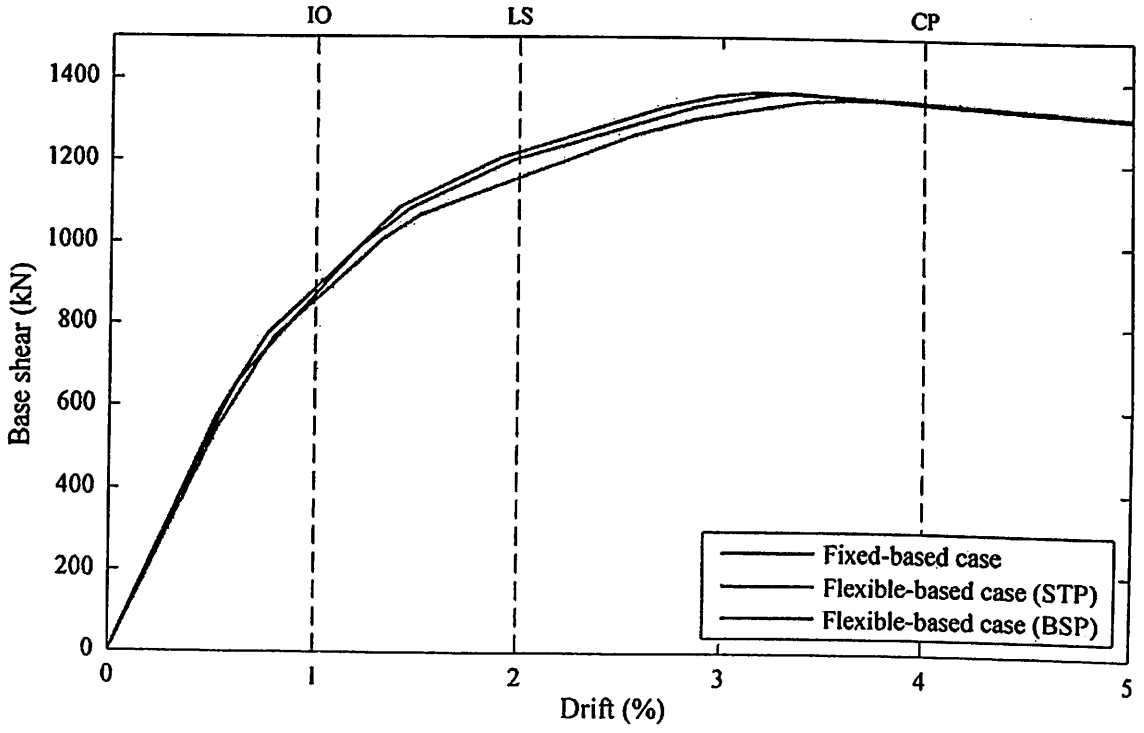

Fig. 17 Capacity curve for three-storey MRCF

section properties and stiffness of foundation will increase the strength of the structure and reduce the potential to collapse. However, in Fig. 18, it is shown that there is no significant difference found between flexible and fixed base in case of 6-storey structure. This observation is probably because the soil classification at both locations is not significantly different. Moreover, the Vs30 is not the only important factor in this particular structure. Further investigation is needed, by comparing the results with the dynamic analysis.

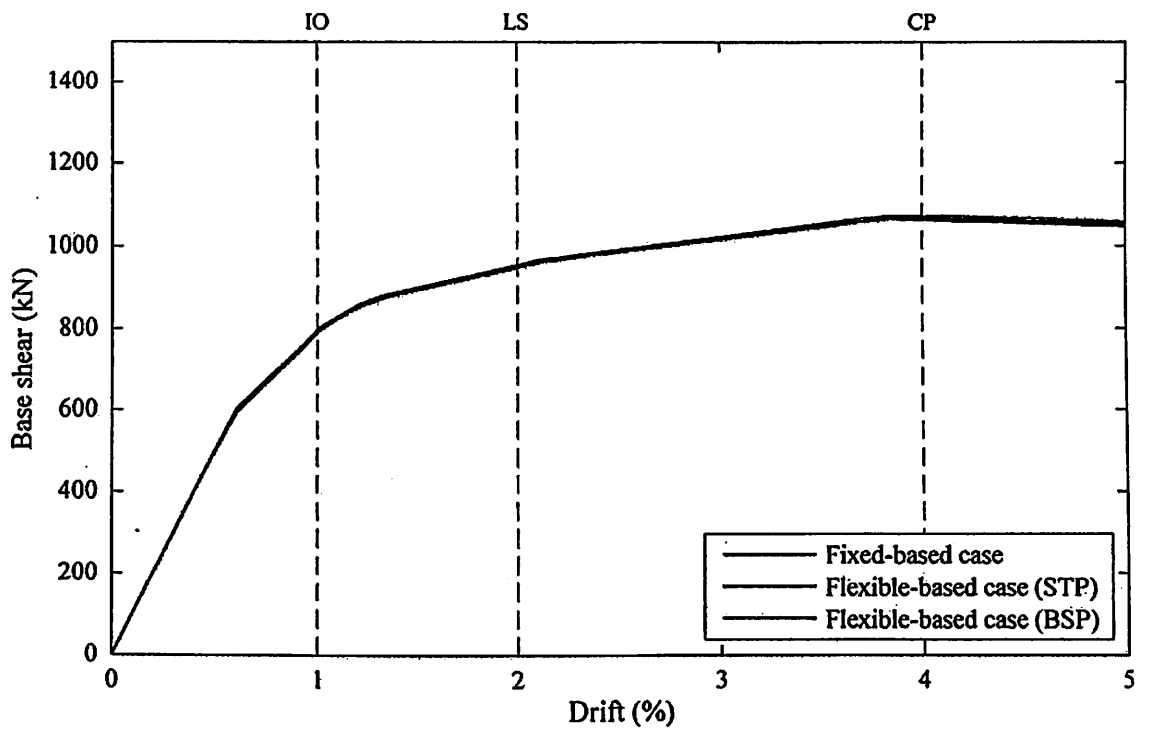

Fig. 18 Capacity curve for six-storey MRCF

3 Conclusion

This study presents the implementation of the multichannel analysis of surface wave (MASW) method to investigate the soil classification and liquefaction potential in the reclaimed area in Penang. Two areas in Penang have been used as a case study, namely Seri Tanjung Pinang (STP) and Bandar Sri Pinang (BSP). Furthermore, the value of shear wave velocity (V_s) obtained from that method was used to study the effect of soil flexibility on low- and medium-rise structure in terms of drift. The analysis of this study was done based on the pushover analysis (POA) by using SAP 2000 software. From the results and discussion, the following conclusion can be drawn from this research:

1. Based on the IBC site classification, the soil profile for STP consists a deposit of loose-to-medium cohesionless soil that falls into the category soil class D. Meanwhile, for BSP, it can be classified as a surface alluvium layer with a Vs30 is 155.00 m/s, which falls in the category soil class E. Based on the liquefaction potential, after increasing the value of peak acceleration at the ground surface and magnitude earthquake, the STP area does not have any threat of the liquefaction that will occur in that particular area. However, for BSP area, it shows that the potential of the liquefaction to occur is possible, but only when the value of peak acceleration at ground surface increasing to 0.15 g. This can be concluded that with certain area, such as, namely a few, the behaviour of the ground motion, the peak ground motion, and the soil characteristic criteria, the potential of the liquefaction to occur is quite high.
2. The displacement trend for both 3 and 6 storeys that designed based on fixed and flexible base is quite similar. In addition, their significant percentage differences between these two based designs are quite low. For the drift results, it is clearly shown

that the flexible base is greater than fixed base. However, the damage to structural component and potential to collapse are smaller than fixed base.

Acknowledgments This research was supported by Universiti Sains Malaysia under Research University (Individual) Grant (814223). We thank Dr Koichi Hayashi from Geometrics for comments that greatly improved the manuscript and anonymous reviewers for their so-called insights.

References

Abdel Raheem SE, Ahmed MM, Alazrak TM (2014) Soil-raft foundation-structure interaction effects on seismic performance of multi-story MRF buildings. Eng Struct Technol 6(2):43–61

Adnan A, Marto A, Hendriyawan H (2004) Lesson learned from the effect of recent far field Sumatra earthquakes to Peninsular Malaysia. 13th World conference on earthquake engineering, Vancouver

Adnan A, Hendriyawan H, Marto A, Irsyam M (2005) Seismic hazard assessment for Peninsular Malaysia using Gumbel Distribution Method. Jurnal Teknologi 42(B):57–73

Anderson JG, Lee YJ, Zeng YH, Day S (1996) Control of strong motion by the upper 30 meters. Bull Seismol Soc Am 86:1749–1759

Andrus RD, Stokoe KH (2000) Liquefaction resistance of soils from shear-wave velocity. J Geotech Geoenviron Eng 126:1015–1025

Balendra T, Li Z (2008) Seismic hazard of Singapore and Malaysia. EJSE Spec Issue Earthq Eng Low Mod Seismic Reg Southeast Asia Aust 57–63

Boore DM (2006) Determining subsurface shear-wave velocities : a review. 3rd International symposium on the effects of surface geology on seismic motion, 30 August 2006–1 September 2006, Grenoble

BSI (2004) Eurocode 8: design provisions for earthquake resistance of structures: part 1–1, general rules—seismic actions and general requirements for structures. BS EN: 1998-1-1: 2004. British Standards Institution, London

Che Abas MR (2001) Earthquake monitoring in Malaysia. Seismic risk seminar. Malaysia

Che Abas MR (2012) Shelter from tremors. The Star online

CSI (2004) SAP 2000 integrated finite element analysis and design of structures. v10ed. Computer and Structures Inc, Berkeley

Dobry R, Borcherdt R, Crouse C, Idriss I, Joyner W, Martin GR, Power M, Rinne E, Seed R (2000) New site coefficients and site classification system used in recent building seismic code provisions. Earthq Spectra 16:41–67

Fajfar P (2000) A nonlinear analysis method for performance-based seismic design. Earthq Spectra 16:573–592

FEMA (2009) NEHRP Recommended Seismic Provisions for New Buildings and Other Structures: FEMA P-750/2009 Edition. Federal Emergency Management Agency, Washington, DC

FEMA-356 (2000) NEHRP guidelines for the seismic rehabilitation of buildings. Building Seismic Safety Council, Washington, DC

Galal K, Naimi M (2008a) Effect of soil conditions on the response of reinforced concrete tall structures to near-fault earthquakes. Struct Des Tall Spec Build 17:541–562

Galal K, Naimi M (2008b) Effect of soil conditions on the response of reinforced concrete tall structures to near-fault earthquakes. Struct Des Tall Spec Build 17:541–562

Hatzigeorgiou GD, Kanapitsas G (2013) Evaluation of fundamental period of low-rise and mid-rise reinforced concrete buildings. Earthquake Eng Struct Dyn 42(11):1599–1616

Hee MC, Lee WO, Jeffrey C, Sooi TK, Andy GKF, Low KC, Adnan A, Teo CW, John KR, Liew SS, Ismail E (2005) Position paper on issues related to earthquake. IEM position document. Institution of Engineering, Malaysia

Husen H, Majid TA, Nazri FM, Arshad MR, Faisal A (2008) Development of design response spectra based on various attenuation relationships at specific location. International conference on construction and building technology. Kuala Lumpur

IBC (2000) International building code. Dearborn Trade Publishing

Innovation Esteem (1993) EsteemPlus: Integrated modeling, design, analysis, detailing and costing solution for reinforced concrete structure. Esteem Innovation Pte, Ltd

Jeffrey C (2008) Design for seismic action--a far field effect in Malaysia experience. The 3rd ACF international conference, 2008 Ho Chi Minh, Vietnam, pp 1191–1201

Lin CP, Chang CC, Chang TS (2004) The Use of MASW method in the assessment of soil liquefaction potential. Soil Dyn Earthq Eng 24:689–698

Luna R, Jadi H (2000) Determination of dynamic soil properties using geophysical methods. In: Proceedings of the first international conference on the application of geophysical and ndt methodologies to transportation facilities and infrastructure—geophysics, pp 3-1

Maravas A, Mylonakis G, Karabalis DL (2014) Simplified discrete systems for dynamic analysis of structures on footings and piles. Soil Dyn Earthq Eng 61:29–39

Minasidis G, Hatzigeorgiou GD, Beskos DE (2014) SSI in steel frames subjected to near-fault earthquakes. Soil Dyn Earthq Eng 66:56–68

Molas GL, Yamazaki F (1995) Attenuation of Earthquake Ground Motion in Japan Including Deep-Focus Events. Bull Seismol Soc Am 85:1343–1358

Nazarian S, Stokoe KH, Hudson WR (1983) Use of spectral analysis of surface waves method for determination of moduli and thickness of pavement systems. Transp Res Rec 930:38–45

Park CB, Miller RD, Xia JH (1999) Multichannel analysis of surface waves. Geophysics 64:800–808

Saez E, Lopez-Caballero F, Modaressi-Farahmand-Razavi A (2013) Inelastic dynamic soil–structure interaction effects on moment-resisting frame buildings. Eng Struct 51:166–177

Scott JB, Rasmussen T, Luke B, Taylor WJ, Wagoner JL, Smith SB, Louie JN (2006) Shallow shear velocity and seismic microzonation of the urban Las Vegas, Nevada, Basin. Bull Seismol Soc Am 96:1068–1077

Searer GR, Freeman SA (2004) Design drift requirements for long-period structures. 13th World conference on earthquake engineering, Vancouver, BC

Seed HB, Idriss IM (1971) Simplified procedure for evaluating soil liquefaction potential. J Soil Mech Found Div 97:1249–1273

Stewart JP, Kim S, Bielak J, Dobry R, Power MS (2003) Revisions to soil–structure interaction procedures in NEHRP design provisions. Earthq Spectra 19:677–696

Stokoe KH, Wright S, Bay J, Roesset J (1994) Characterization of geotechnical sites by SASW method. Geophys Charact Sites 15–25

Tan CG, Majid TA, Ariffin KS, Bunnori NM (2014) Seismic microzonation for Penang using geospatial contour mapping. J Nat Hazard 73:657–670

Tezcan SS, Keceli A, Ozdemir Z (2006) Allowable bearing capacity of shallow foundations based on shear wave velocity. Geotech Geol Eng 24:203–218

Uma Maheswari R, Boominathan A, Dodagoudar GR (2010) Use of surface waves in statistical correlations of shear wave velocity and penetration resistance of Chennai soils. Geotech Geol Eng 28:119–137

Xia JH, Miller RD, Park CB, Hunter JA, Harris JB, Ivanov J (2002) Comparing shear-wave velocity profiles inverted from multichannel surface wave with borehole measurements. Soil Dyn Earthq Eng 22:181–190

Xu YX, Xia JH, Miller RD (2006) Quantitative estimation of minimum offset for multichannel surface-wave survey with actively exciting source. J Appl Geophys 59:117–125

Youd T (2001) Liquefaction resistance of soils: summary report from the 1996 NCEER and 1998 NCEER/NSF workshops on evaluation of liquefaction resistance of soils. J Geotech Geoenviron Eng, p 297

Zhang L (2010) A simple method for evaluating liquefaction potential from shear wave velocity. Front Archit Civil Eng China 4:178–195

Jurnal Teknologi

Full Paper

COMPARISON STUDY OF SEISMIC DESIGN OF RC FRAME IN EAST MALAYSIA WITH VARIOUS BEHAVIOR FACTOR

Article history
Received
yyyyyy
Received in revised form
wwwwww
Accepted
zzzzzzzzzz

Mohd Irwan Adiyanto, Taksiah A. Majid*, Fadzli Mohamed Nazri

Disaster Research Nexus, School of Civil Engineering, Universiti Sains Malaysia, Penang, Malaysia.

*Corresponding author
taksiah@usm.my

Graphical abstract

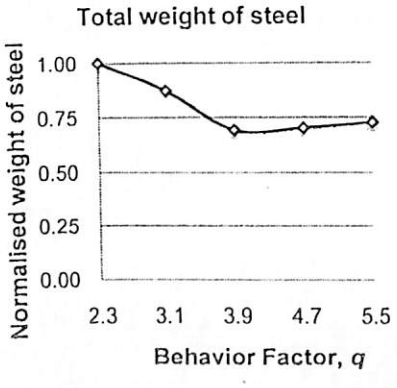

Abstract

Over the past few years, the tremors originated from Sumatra Andaman and Philippines earthquakes can be felt in Peninsular and East Malaysia, respectively. A moderate earthquake occurred in Ranau, Sabah on 5th June 2015 with M_w5.9 had caused damages on buildings. The damages became worse due to after-shocks activity. Therefore, it is important to consider seismic design for new buildings in that region. Eurocode 8 can be considered as standard reference for seismic provision. This paper investigate the influence of behavior factor, q on seismic design of reinforced concrete frame in Sabah. Ductility class medium had been considered with five different value of behavior factor, q. The total amount of steel reinforcement for each model is presented for comparison. It can be concluded that the value of behavior factor, q strongly influencing the total amount of steel reinforcement. For economical reason, higher value of behavior factor, q might be considered in design.

Keywords: Seismic design; Eurocode 8; reinforced concrete; behavior factor

Abstrak

Beberapa tahun kebelakangan ini gegaran berasal dari gempa bumi di Sumatera Andaman dan Filipina dapat dirasai di Semenanjung dan Malaysia Timur. Gempa bumi sederhana yang berlaku di Ranau, Sabah pada 5 Jun 2015 dengan kekuatan M_w5.9 telah menyebabkan kerosakan pada bangunan. Kerosakan bertambah teruk disebabkan oleh gempa-gempa susulan. Dengan itu adalah penting untuk mempertimbangkan reka bentuk seismik untuk bangunan baru di wilayah itu. Eurocode 8 boleh dipertimbangkan sebagai rujukan piawai untuk perincian seismic. Kertas teknikal ini mengkaji pengaruh faktor kelakuan ke atas reka bentuk seismik bagi kerangka konkrit bertetulang di Sabah. Kemuluran kelas pertengahan telah dipertimbangkan dengan lima nilai faktor kelakuan yang berbeza. Jumlah besi pengukuhan bagi setiap model dipersembahkan untuk perbandingan. Ia boleh disimpulkan bahawa nilai faktor kelakuan sangat kuat mempengaruhi jumlah besi pengukuhan. Atas sebab ekonomi, nilai faktor pengukuhan yang lebih tinggi boleh dipertimbangkan dalam reka bentuk.

Kata kunci: Reka bentuk seismik; Eurocode 8; konkrit bertetulang; faktor kelakuan

1.0 INTRODUCTION

In the past few decades, construction practice in Malaysia only consider gravity load for design of low rise buildings. Seismic load consideration was not taken into account since the nation is situated relatively far away from active seismic fault region [1]. Therefore, most reinforced concrete (RC) buildings had been designed according to BS 8110 [2]. After December 2004, tremors from Sumatra Andaman and Philippines earthquakes can be felt in Peninsular and East Malaysia, respectively. This situation can be said as a wakeup call for Malaysian authority since the public citizen started to ask question about the capacity of existing buildings to withstand the earthquake load. Based on research works, it come to a conclusion that it is worth to consider seismic design for new buildings located in medium to high seismic regions in Malaysia [3]. The conclusion became stronger after the M_w5.9 moderate earthquake which occurred in Ranau, Sabah on 5th June 2015. Minor to severe damages had occurred on buildings which were designed without any seismic consideration.

In seismic design, it is not economically feasible to design structures which can respond elastically during earthquake [4]. This is due to very high magnitude of lateral load representing earthquake action which will result in very large size of section with very high amount of steel reinforcement. Therefore, the seismic design always associated with a concept namely as behavior factor, q. The latter was proposed to reduce the forces obtained from a linear analysis, in order to take account for the nonlinear response of a structure [5]. In American code, similar concept is known as strength reduction factor, R [6]. In Eurocode 8 [5] there are three classes of ductility namely as ductility class low (DCL), ductility class medium (DCM), and ductility class high (DCH). Every class of ductility has different value of behavior factor, q. Based on previous research work [7, 8, 9] the value of behavior factor, q strongly influencing the performance of structures when subjected to earthquake loads.

In a recent few years, there were a lot research works which evaluated the value of behavior factor, q. There are comment that the European and American Standard are too conservative where the ductility demand which is influenced by behavior factor, q is higher than the ductility supply [10]. It is also found that the value of behavior factor, q for multi degree of freedom (MDOF) systems are significantly lower than those for single degree of freedom (SDOF) systems [11]. Therefore, the behavior factor, q computed based on SDOF system should be modified by a reduction factor so it can be used by MDOF system [12]. Regarding the soil factor, it was concluded that the behavior factor, q for soft soil should be reduced for the sake of safety [13, 14].

Due to lack of experience in dealing with seismic design, there is a lot of uncertainty regarding the class of ductility and suitable value of behavior factor, q to be used in Malaysia. According to Pappin et. al, [15] ductile detailing could be ignored by using lower behavior factor, q but higher seismic design forces has to be considered in design. In contrast, the designer may work on ductile detailing with the advantage of lower seismic design forces by adopting higher value of behavior factor, q. This paper present the influence of behavior factor, q on seismic design of three storey RC frame in East Malaysia. The total amount of steel used as flexural and shear reinforcement in beams and columns as well as within the beam-columns joints is presented for comparison and discussion.

2.0 RC FRAME MODEL

This study adopted a typical frame used in previous study [16,17]. The frame is regular in plan and elevation with storey height equal to 3.3 m. The frame has three number of bays which equal to 5.0 m each as shown in Figure 1: For RC frame, the value of behavior factor, q for DCM lies in range of $1.5 < q < 5.85$ [5]. The proposed value to be used in design is 3.9. Therefore, in order to investigate the influence of behavior factor, q on seismic design the typical frame had been designed repeatedly by considering five different value of behavior factor, q equal to 2.3, 3.1, 3.9, 4.7, and 5.5 for DCM. All frames has similar size of section for corresponding structural element. This is important so the dynamic characteristic is similar for all frames. Therefore, the fundamental period of vibration, T_1 for all frames is fixed at 0.55 sec. The size of beam labeled as B1 and B2 is equal to 250 mm x 550 mm and 300 mm x 600 mm, respectively. The column C1 has typical size of section equal to 350 mm x 350 mm regardless its position.

The designed process was conducted by referring to Eurocode 8 [5] for seismic provision. All frames had been designed based on cylinder concrete compressive strength, f_{ck} and yield strength of steel, f_y equal to 30 N/mm^2 and 500 N/mm^2, respectively. The design response spectrum compatible with Soil Type B [5] had been developed in order to determine the magnitude of base shear force, F_b. For Sabah, the reference peak ground acceleration, a_{gR} = 0.12g [18] was taken into account to develop the design response spectrum. The load combination and distribution of base shear force, F_b by using lateral force method is similar as explained in previous study [17]. Figure 2 shows the design response spectrum developed based on all five different value of behavior factor, q.

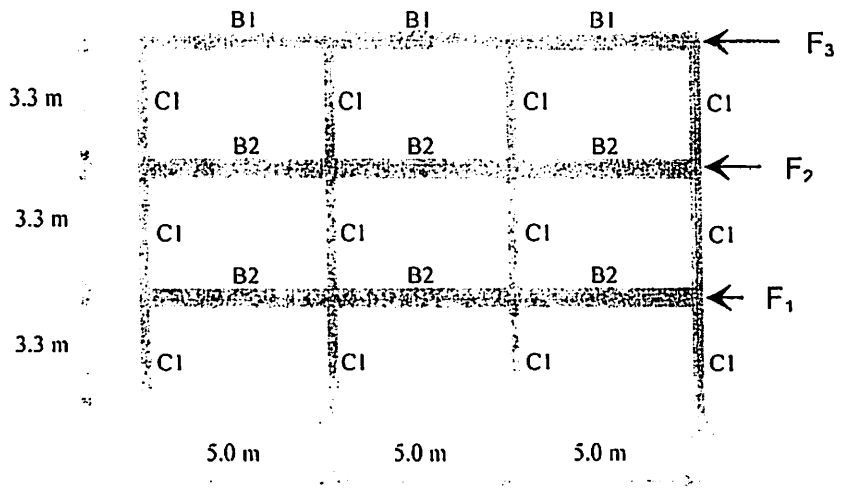

Figure 1 Elevation view of three storey RC frame

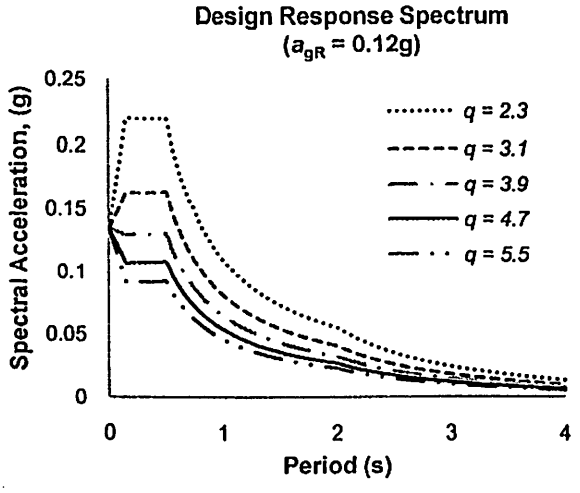

Figure 2 Design response spectrum

3.0 RESULTS AND DISCUSSION

3.1 Base shear force, F_b

Table 1 presents the influence of behavior factor, q on the magnitude of base shear force, F_b acting on all frames. It is clear that the value of behavior factor, q strongly influencing the magnitude of base shear force, F_b. The latter decreases as the former is increases and vice versa. As a result, the lateral forces acting on each storey, namely as F_1, F_2, and F_3 also decrease as the value of behavior factor, q increases. As mentioned in previous section, higher seismic design forces has to be considered if lower behavior factor, q is used in design. In contrast, lower seismic design forces is assigned in structural analysis when higher behavior factor, q is taken into account. Structural analysis had been conducted by using SAP 2000 computer software[19]. It was found that the frames with higher behavior factor, q tend to have lower magnitude of bending moment, M shear force, V and axial load, P due to lower base shear force, F_b.

Table 1: Influence of behavior factor, q on base shear force, F_b

Behavior factor, q	2.3	3.1	3.9	4.7	5.5
F_3 (kN)	156.6	116.2	92.4	76.6	65.5
F_2 (kN)	137.8	102.3	81.3	67.5	57.6
F_1 (kN)	79.3	58.8	46.7	38.8	33.1
F_b (kN)	373.7	277.3	220.4	182.9	156.3

3.2 Design of beam flexural reinforcement

In RC design, the designer has to play around with diameter of bar, d_{bL} and it number to ensure that the total area of steel provided, A_{Sprov} is larger than the total area of steel required, A_{Sreq}. Figure 3 presents

the comparison of total amount of steel used as flexural reinforcement of B2. The weight of steel for all B2 is normalizes to the weight of steel for B2 of frame with behavior factor, q = 2.3. It is clear that the total amount of steel for beam flexural reinforcement is decreases as the value of behavior factor, q is increases. Frame designed with behavior factor, q = 2.3 has the highest amount of steel as beam flexural reinforcement. The latter is reduced in range of 16% to 34% by increasing behavior factor, q from 3.1 to 5.5.

This result is strongly associated with the magnitude of bending moment, M where the latter directly influencing the total area of steel required, A_{Sreq}. Higher bending moment, M tend to induces higher stress in beam which result in higher total area of steel required, A_{Sreq} to resist the stress and vice versa. Therefore, the amount of steel as beam flexural reinforcement can be reduced by using higher value of behavior factor, q in design. In beam design with DCM, the designer has to fulfill the requirement of local ductility demand [5]. The latter is related to the reinforcement ratio in the tension zone, ρ where the maximum value is strongly influenced by the curvature ductility factor, μ_ϕ. The increasing of behaviour factor, q caused increasing on the curvature ductility factor, μ_ϕ which finally reduce the value of maximum reinforcement ratio in the tension zone, ρ_{max}. Another local ductility demand which has to be fulfilled is the diameter of flexural reinforcement, d_{bL} passing through the beam-column joints. This is important to prevent bond failure [5].

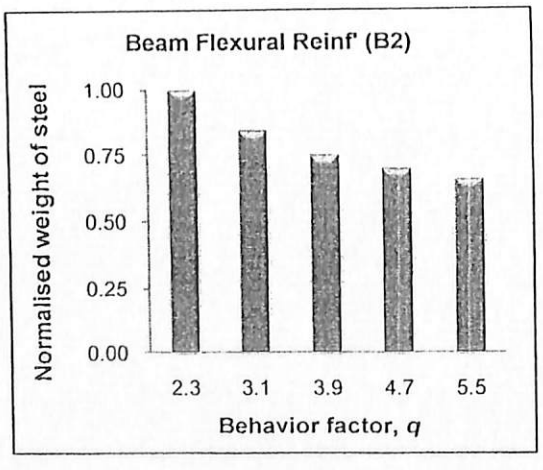

Figure 3 Influence of behavior factor, q on design of beam flexural reinforcement

3.3 Design of beam shear reinforcement

The design of RC beam is not complete without the shear reinforcement. Figure 4 shows the comparison of total amount of steel used as beam shear reinforcement for B2. It is clear that the frames with higher behavior factor, q have higher amount of steel as beam shear reinforcement. However, the amount of steel is similar for frames with behavior factor, q = 2.3 and q = 3.1. The same also obtained for frames with behavior factor, q = 3.9 to q = 5.5. This result indicates that the value of behavior factor, q did not directly influencing the design of beam shear reinforcement.

As explained in previous study [17] the design of beam shear reinforcement is directly related to the design of beam flexural reinforcement. According to Eurocode 8 [5] the maximum spacing of bar, s_{max} should be limited based on the quarter of beam depth, h_w, or 8 times the minimum diameter of flexural reinforcement, d_{bL}, or 24 times diameter of shear reinforcement, d_{bw}, whichever gives the lowest value. The maximum spacing of bar, s_{max} for beam shear reinforcement shall not exceed 225 mm. In this study, the depth of beam, h_w and the diameter of shear reinforcement, d_{bw} is similar for all frames which is equal to 600 mm and 6 mm, respectively. Therefore, the spacing of bar, s was influenced by the diameter of flexural reinforcement, d_{bL}. Frames with behavior factor, q = 2.3 and q = 3.1 have diameter of flexural reinforcement, d_{bL} equal to 16 mm. For frames with higher behavior factor, q the diameter of flexural reinforcement, d_{bL} was smaller and equal to 12 mm. Therefore, the spacing of bar, s for frames with higher behavior factor, q ≥ 3.9 was limited to 96 mm only. As a result, shear reinforcement with closer spacing was provided for that frames contributing to higher amount of steel.

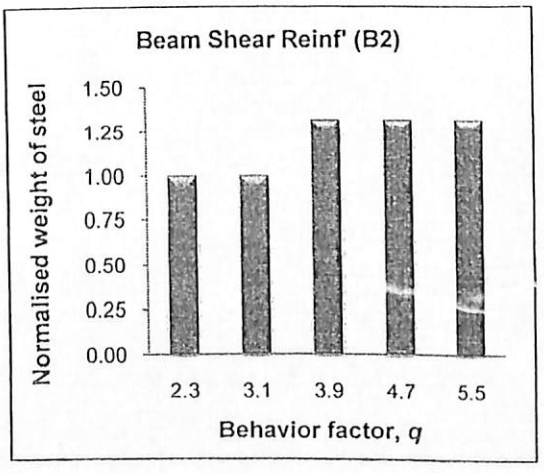

Figure 4 Influence of behavior factor, q on design of beam shear reinforcement

3.4 Design of column flexural reinforcement

For RC frame with moment resisting system as used in this study, columns play a very important role to resist gravity load before transfer it to the foundations. During earthquake the columns has to resist both gravity and lateral load. Therefore, the columns has to be designed and detailed properly. In seismic design, a concept namely as *Strong Column ~ Weak Beam* is adopted in order to ensure that the damage will occur on beams rather than on columns. In other word, the columns has to be designed stronger than the beams. For that purpose, the design moment

resistance of column, M_{Rc} is directly derived from the design moment resistance of beam, M_{Rb} at the same joint. The former has to be at least 1.3 times the latter [5]. In this case, the design moment resistance of column C1, M_{Rc} is directly derived from the design moment resistance of beam B2, M_{Rb} at the internal joint. Figure 5 depicts the comparison of total amount of steel used as column flexural reinforcement.

It is clear that the total amount of steel used as column flexural reinforcement is decreases as the value of behavior factor, q increases. By using higher value of behavior factor, q the amount of steel was reduced in range of 22% to 64%. This result is strongly associated with the design of the beam. As discussed in previous subsection, the highest amount of steel used as beam flexural reinforcement is belong to the frame with behavior factor, q = 2.3 result in highest design moment resistance of beam, M_{Rb}. Therefore, the highest design moment resistance of column, M_{Rc} automatically belong to the frame with behaviour factor, q = 2.3 result in highest total area of steel required, A_{Sreq}. For column design with DCM, the reinforcement ratio of primary column, ρ shall in range of 1% to 4% of total area of column cross section [5,20]. Therefore, similar amount of steel was used for frame with behaviour factor, q = 4.7 and q = 5.5. Mathematically, the amount of steel for frame with behaviour factor, q = 5.5 shall be the lowest due to lowest design moment resistance of column, M_{Rc}. However , the area of steel provided, A_{Sprov} has to be increased to fulfil the requirement of at least 1% of reinforcement ratio to be provided.

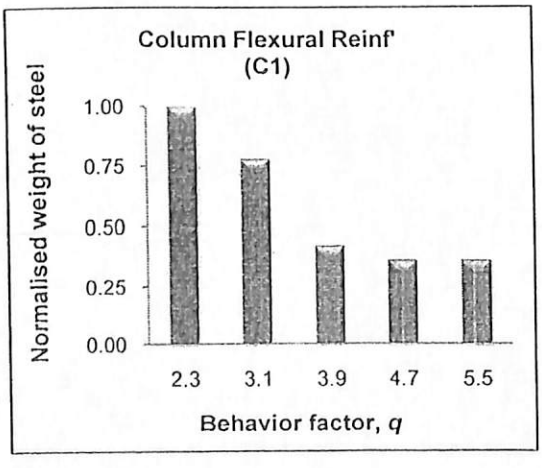

Figure 5 Influence of behavior factor, q on design of column flexural reinforcement

3.5 Design of column confinement reinforcement

The shear reinforcement in column with DCM also known as confinement reinforcement. Figure 6 depicts the comparison of total amount of steel used as column confinement reinforcement. The value of behavior factor, q directly influences the amount of steel as confinement reinforcement. The latter increases as the former is increases.

The confinement reinforcement in columns for frame with behavior factor, q = 5.5 is almost 3 times higher than the frame with behavior factor, q = 2.3. The main reason of this result is strongly relates to the requirement of confinement reinforcement for DCM column as stated in Eurocode 8 [5]. The provided mechanical volumetric ratio of confining hoops within the critical region, $\omega_{wd\ prov}$ must be higher than the required mechanical volumetric ratio of confining hoops within the critical region, $\omega_{wd\ req}$. The latter is strongly influenced by the value of curvature ductility factor, μ_ϕ which increases as the value of behaviour factor, q increases as mentioned before. Therefore, the required mechanical volumetric ratio of confining hoops within the critical region, $\omega_{wd\ req}$ is higher for frames with higher behaviour factor, q. As a result, higher amount of steel has to be provided as confinement reinforcement. For that purpose, the designer has to play around with the number of steel bar, diameter of steel bar, and its spacing, s. The best combination should be selected so the provided mechanical volumetric ratio of confining hoops within the critical region, $\omega_{wd\ prov}$ only slighty higher that the required mechanical volumetric ratio of confining hoops within the critical region, $\omega_{wd\ req}$. This is important for economic reason.

Decreasing the spacing of bar, s might be the smartest solution [17]. This is because the provided mechanical volumetric ratio of confining hoops within the critical region, $\omega_{wd\ prov}$ increases as the spacing of bar, s decreases. At the same moment, decreasing the spacing of bar, s also decreasing the required mechanical volumetric ratio of confining hoops within the critical region, $\omega_{wd\ req}$. Detail calculation was presented in a good example by Elghazouli [21].

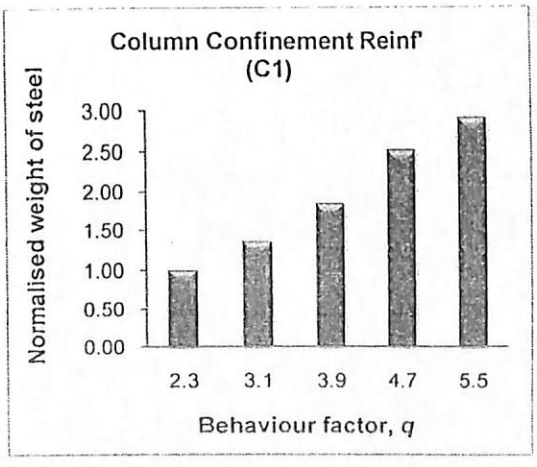

Figure 6 Influence of behavior factor, q on design of column confinement reinforcement

3.6 Design of confinement reinforcement within beam-column joints

In DCM seismic design the confinement reinforcement also has to be provided within the beam-column joints. Figure 7 shows the comparison on the total amount of steel used as confinement reinforcement within that region. It is clear that the amount of steel increases as the value of behavior factor, q increases. This means that higher amount of steel has to be provided for frames designed with higher behavior factor, q. This result is strongly associated with the design requirement itself which stated that the horizontal confinement reinforcement in joints of primary seismic beams with columns should be not less than that specified for the critical regions of columns [5]. Therefore, the design of confinement reinforcement within the beam-column joint is directly derived from the design of confinement reinforcement of its column.

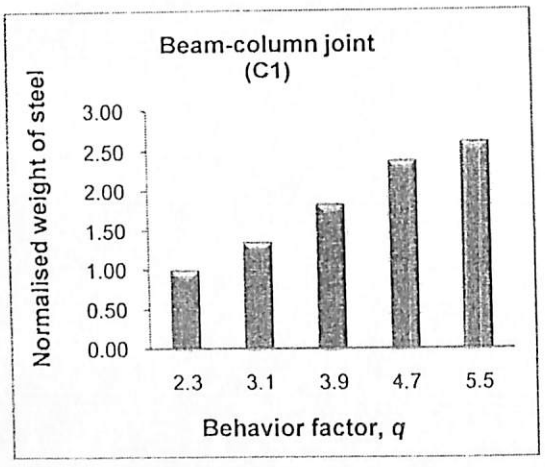

Figure 7 Influence of behavior factor, q on design of confinement reinforcement within beam-column joints

3.7 Summation of total steel reinforcement

Figure 8 presents the comparison of summation of total amount of steel reinforcement for all frames. It include the amount of steel used as beams flexural reinforcement, beams shear reinforcement, columns flexural reinforcement, columns confinement reinforcement, and also the confinement reinforcement within the beam-column joints. From Figure 8, it is clear that frame designed based on behavior factor, q = 2.3 has the highest amount of steel reinforcement compared to the others. This result is strongly contributed by the amount of steel as flexural reinforcement in beams and columns, where the frame has the highest. Then, the total amount of steel reinforcement decreases as the value of behavior factor, q increases. The total amount of steel for frames with behavior factor, q = 3.1, 3.9, 4.7, and 5.5 is approximately around 13%, 31%, 30%, and 27%, respectively lower than the total amount of steel reinforcement for frame with behavior factor, q = 2.3.

It is interesting to observe that total amount of steel reinforcement for frames with behavior factor, q = 3.9 to 5.5 is not significantly different and almost similar. The total amount of steel reinforcement for frames with higher behavior factor, q = 4.7 and 5.5 increase to be a bit higher than the frame with behavior factor, q = 3.9. This result is due to design of columns confinement reinforcement and confinement reinforcement within the beam-column joints. As discussed before, the amount of steel used as confinement reinforcement in columns and within the beam-column joints are rapidly increases as the value of behavior factor, q increases. Therefore, although has lower amount of steel for flexural reinforcement in beams and columns, high amount of steel as confinement reinforcement caused the total amount of steel reinforcement increases for both frames. It can be concluded that behavior factor, q ≥ 3.9 contributed to most economic design.

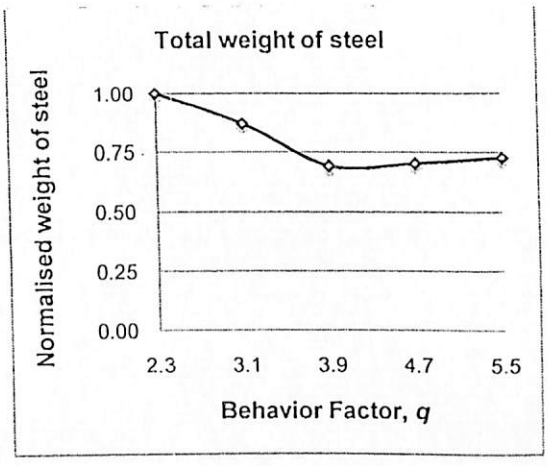

Figure 8 Influence of behavior factor, q on design of confinement reinforcement within beam-column joints

4.0 CONCLUSIONS

Since December 2004, tremors from Sumatra Andaman and Philippines earthquakes were felt rapidly in Peninsular and East Malaysia, respectively. Based on previous research, it was concluded that it is worth to consider seismic design for new buildings in medium and high seismic regions in Malaysia [3]. In seismic design, the designers have to deal with a concept namely as behavior factor, q to take into account the nonlinear response during earthquake. Therefore, this paper investigated the influence of behavior factor, q on the total amount of steel used as reinforcement for seismic design of three storey RC frame. The typical RC frame were designed repeatedly based on five value of behavior factor, q = 2.3, 3.1, 3.9, 4.7, and 5.5 for DCM by referring to Eurocode 8 [5]. The design response spectrum for Soil Type B where the value of reference peak ground acceleration, a_{gR} = 0.12g for Sabah in East Malaysia was developed in order to determine the magnitude

of base shear force, F_b. There are several conclusions can be drawn as follow:

- The amount of steel used as flexural reinforcement in beams decreases as the value of behavior factor, q increases. Similar result also obtained for the columns flexural reinforcement. However, the amount of columns flexural reinforcement is almost similar for frames with behavior factor, $q \geq 4.7$ due to requirement of minimum reinforcement ratio, ρ_{min} which has to be provided.

- The amount of steel used as beam shear reinforcement was not directly influenced by the value of behavior factor, q. This is because the design of beam shear reinforcement is strongly relates to the spacing of bar, s as specified by the code [5].

- Due to requirement of confinement reinforcement which differ for every value of behavior factor, q the amount of steel used as confinement reinforcement in columns and within the beam-column joints are rapidly increases as the value of behavior factor, q increases.

- The total amount of steel reinforcement decreases as the value of behavior factor, q increases. However, as the value of behavior factor, $q \geq 3.9$ the difference became not significant where the total amount of steel reinforcement was almost similar. Frame designed based on behavior factor, $q = 3.9$ has the most economic design compared to others.

Acknowledgement

The authors gratefully acknowledge the financial support by Research University Grant (1001/PAWAM/814115) sponsored by Universiti Sains Malaysia. The first author personally acknowledge financial support program from MyBrain15, a scholarship provided by Ministry of Education Malaysia.

References

[1] Adiyanto, M.I. and T.A. Majid. 2014. Seismic design of two storey reinforced concrete buildings in Malaysia with low class ductility. *Journal of Engineering Science and Technology*. 9(1): 27–46.

[2] BS 8110 Code British Standard. 1997. Structural use of concrete: *Code of Practice for Design and Construction, Part 1*.

[3] MOSTI. 2009. Seismic and Tsunami Hazards and Risk Study in Malaysia, *Final Report*. Ministry of Science, Technology, and Innovation of Malaysia.

[4] FEMA. 2007. NEHRP recommended provisions for new buildings and other structures: training and instructional materials. FEMA 451B. *Building Seismic Safety Council for the Federal Emergency Management Agency*. Washington D.C.

[5] CEN. 2004. Eurocode 8: Design of structures for earthquake resistance. Part 1: *General rules, seismic actions and rules for buildings*. European Committee for Standardization, Brussels.

[6] ICC. 2006. International building code. United States of America.

[7] Mwafy, A.M. and A.S. Elnashai. 2002. Calibration of force reduction factors of RC buildings. *Journal of Earthquake Engineering*. 6(2): 239–273.

[8] Krawinkler, H., R. Medina, and B. Alavi. 2003. Seismic drift and ductility demands and their dependence on ground motions. *Engineering Structures*. 25: 637–653.

[9] Ruiz-Garcia, J. and E. Miranda. 2006. Evaluation of residual demands in regular multi-storey frames for performance-based seismic assessment. *Earthquake Engineering and Structural Dynamics*. 35: 1609–1629.

[10] Borzi, B. and A.S. Elnashai. 2000. Refined force reduction factors for seismic design. *Engineering Structures*. 22: 1244–1260.

[11] Cai, J., J. Zhou, and X. Fang. 2006. Seismic ductility reduction factors for multi degree of freedom systems. *Advances in Structural Engineering*. 9(5): 591–602.

[12] Zhai, C.H. and L.L. Xie. 2006. The modification of strength reduction factors for MDOF effect. *Advances in Structural Engineering*. 9(4): 477–490.

[13] Eser, M., C. Aydemir, and I. Ekiz. 2011. Effects of soil structure interaction on strength reduction factors. *Procedia Engineering*. 14: 1696–1704.

[14] Ganjavi, B. and H. Hao. 2012. Ductility reduction factor for multi degree of freedom system with soil structure interaction. *15th World Conference on Earthquake Engineering*. October. Lisbon.

[15] Pappin, J.W., P.H.I. Yim, and C.H.R. Koo. 2011. An approach for seismic design in Malaysia following the principles of Eurocode 8. *Bulletin Jurutera*: 22–28.

[16] Adiyanto, M.I. and T.A. Majid. 2014. Seismic performance of three storey hospital RC frame subjected to multiple earthquake in moderate seismic region. *International Congress on Natural Sciences and Engineering*. May. Kyoto.

[17] Adiyanto, M.I., T.A. Majid, and F.M. Nazri. 2014. Cost optimization of seismic design of low rise hospital RC frame in Malaysia. *5th Asia Conference on Earthquake Engineering*. October. Taipei.

[18] Adnan, A., Hendriyawan, A. Marto, and P.N.N. Selvanayagam. 2008. Development of seismic hazard maps of east Malaysia. *Advances in Earthquake Engineering Applications*: 1 – 17.

[19] SAP 2000. 2002. *Analysis reference manual*. Computer and Structures, Inc., Berkeley.

[20] Acun, B., A. Athanasopoulou, A. Pinto, E. Carvalho, and M. Fardis. 2012. Eurocode 8: Seismic Design of Buildings Worked Examples, *European Commission Joint Research Center*. Ispra.

[21] Elghazouli, A.Y. 2009. *Seismic Design of Buildings to Eurocode 8*. London and New York: Spon Press.

Visual damage observation of cyclic loading test on RC frame designed to EC8

Taksiah A. Majid*[1], Nor Hayati Abdul Hamid[2a], Mohd Irwan Adiyanto[1b], Fadzli Mohamed Nazri[1c]

[1]*School of Civil Engineering, Universiti Sains Malaysia, Penang, Malaysia*
[2]*Faculty of Civil Engineering, Universiti Teknologi Mara, Shah Alam, Malaysia*

(Received keep as blank , Revised keep as blank , Accepted keep as blank)

Abstract. The damages caused by earthquake always occurred to the non-engineered structures or the buildings which were not designed with seismic load consideration. The damages on such buildings usually caused by the *Weak Column~Strong Beam* design, poor quality of concrete, and lack of confinement reinforcement in beams and columns. The use of unribbed steel reinforcement also caused severe damages which lead to collapse. All aforementioned damages were observed during the in-situ field investigation after the real earthquake events including the M_w5.9 Ranau earthquake in Sabah, Malaysia on June 2015. Such observation also important in research and development works. An experimental work namely as cyclic loading test can be considered for that purpose. The damage and failure mechanism can be investigated for improvement. This paper presents the step by step visual damage observation from cyclic loading test on a 3 dimension half scale double bay RC frame. The RC frame was designed with seismic consideration by referring to Eurocode 8 and properly constructed by using available construction materials in Malaysia. Damage started by the formation of hairline cracks at the beams first then followed by the columns. This observation indicates that the *Strong Column ~ Weak Beam* design capacity concept was fully adopted. Greater damages such as longer cracks and spalling of concrete cover were observed as the level of target drift was increased. In this experimental work, heavy damages such as the buckling of longitudinal reinforcement and crushing of concrete cover was prevented by the existence of adequate confinement reinforcement in the critical regions.

Keywords: Cyclic loading test; seismic damage; displacement control; reinforced concrete; Eurocode 8

1. Introduction

Earthquake excitation always induced damage and collapse on structures especially the strong event like the 1996 Japan Kobe earthquake, 1999 Taiwan Chi Chi earthquake, and many more. The damages caused by earthquake always occurred to the non-engineered structures or the buildings which were not designed with seismic load consideration. According to Bayraktar *et al.* (2013) the

*Corresponding author, Associate Professor, E-mail: taksiah@usm.my
[a] Associate Professor, E-mail: norha454@salam.uitm.edu.my
[b] Ph.D. Student, E-mail: irwano_07@yahoo.com
[c] Ph.D., E-mail: cefmn@usm.my

damages on such reinforced concrete (RC) buildings usually caused by the *Weak Column~Strong Beam* design, poor quality of concrete, and lack of confinement reinforcement in beams and columns. In addition, in-situ field investigation of structural damages due to 2011 Van, Turkey earthquake found that the confinement reinforcement did not exist in beam-column joints as reported by Ates *et al.* (2013). It was also found that the use of unribbed steel reinforcement also caused severe damages which lead to collapse. Other in-situ field investigations also reported similar findings (Tapan *et al.* 2013, Romao *et al.* 2013). Since majority of RC buildings in Malaysia were designed for gravity and wind loads only, the potential of experiencing similar damages is high if subjected to earthquake load. That was proven during the recent M_w5.9 Ranau earthquake in Sabah region which occurred on 5th June 2015. Fig. 1 presents selected damage on structural elements prior to that event. The occurrence of after-shock events caused greater damage. This can be called as the effect of repeated earthquake on buildings which usually induces higher displacement and interstorey drift ratio as reported in previous researches (Hatzigeourgiou and Beskos 2009, Ade Faisal *et al.* 2013, Adiyanto and Majid 2014).

Other than stiffness and strength degradation, the level of damage also has become a behavior of interest in seismic evaluation. All behaviors can be determined using analytical procedures such as pushover analysis. For a better result with high level of confidence, experimental work such as cyclic loading test can be conducted (Park, 1994). It is suitable either for the whole structure, or only on the sub-assemblages such as beam, column, and beam-column joint. Damage observation occurred on the specimens during the test has been widely reported in previous works. As an example, Kuang and Wang (2014) reported that the flexural cracks occurred at hogging moment regions of beams and columns under low drift around 0.4%. Then, the shear cracks occurred at columns and beam-column joints when the drift up to 1.2%. Similar observation also reported by Ma *et al.* (2013) which stated that at the early stage of loading, no cracks were found on the specimens which indicates the elastic structural response. At 30% - 40% of the maximum lateral load, tiny cracks developed at the bottom part of the column and extended when the magnitude of lateral load was increased. Generally the damages of RC beams and columns is started by spalling of concrete cover, buckling of longitudinal reinforcement, failure on anchorage hook, and crushing of concrete core (Giao *et al.* 2014, Eom *et al.* 2014). The beam-column joints detail strongly influences the behavior of tested specimens (Tawfik et al. 2014). Visual damage observation due to cyclic loading test on RC models without seismic design in Malaysia also reported in previous works (Kay Dora and Abdul Hamid 2012, Abdul Hamid and Mohamad 2013).

This paper presents the step by step visual damage observation from cyclic loading test on a 3 dimension half scale double bay RC frame. The RC frame was designed with seismic consideration by referring to Eurocode 8 (2004) and properly constructed by using available construction materials in Malaysia. To the best of authors' knowledge, the cyclic loading test on such frame did not conducted yet. Therefore, the test is worth to be conducted to study the suitability of the Eurocode 8 (2004) to be referred for seismic design of new buildings in Malaysia.

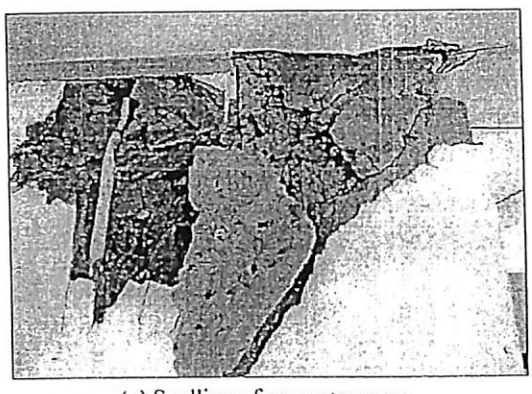

(a) Spalling of concrete cover

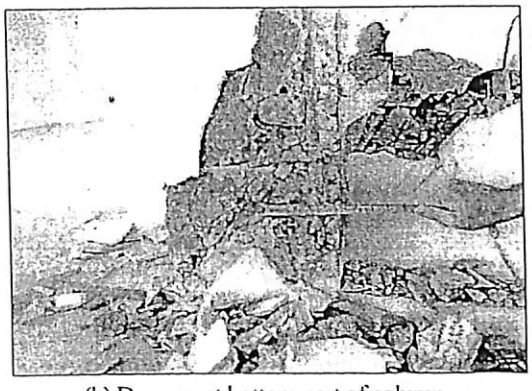

(b) Damage at bottom part of column

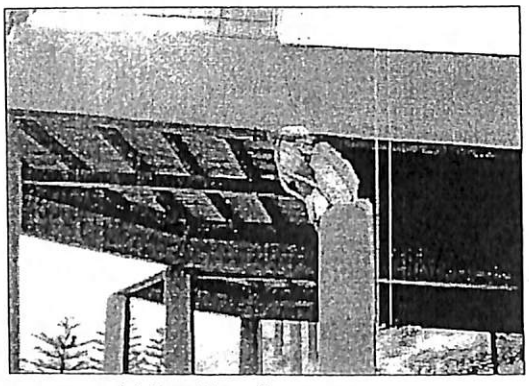

(c) Crushing of concrete core

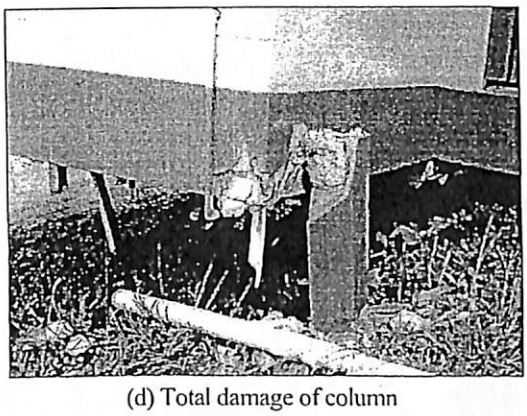

(d) Total damage of column

Fig. 1: Damages on nonseismic columns due to 2015 Ranau earthquake, Sabah, Malaysia

2. Description of model and experimental setup

2.1.Description of the RC frame model

In this experimental work, a 3 dimension half scale RC frame namely as N2-DB model was used in cyclic loading test. The full scale RC frame was scaled down based on similarity rule as proposed in previous works (Harris and Sabnis 1999, Kalman and Sigmun 2009, Zovkic *et al.* 2013). The N2-DB model has double bay and two storey as shown in Fig. 2. The structural configuration of N2-DB model is close to the previous model used by Filiatrault *et al.* (1998). Such structural configuration has its own advantage which allow for detail evaluation on the seismic performance of exterior and interior beam-column joints. The span of main beam is 2250 mm while the storey height is 1650 mm. The size of main and transverse beams is equal to 175mm width and 250 mm depth. All six columns has size of cross section equal to 200 mm square.

As mentioned before, the N2-DB model was designed with seismic consideration by referring to Eurocode 8 (2004) for ductility class medium (DCM). The cylinder concrete compressive strength, f_{ck} and the yield strength of steel reinforcement, f_y is equal to 30 N/mm^2 and 500 N/mm^2, respectively. The full scale model was designed based on peak ground acceleration, a_{gR} = 0.12g which represent the medium seismic region is East Sabah, Malaysia (Adnan *et al.* 2008). The N2-

DB model adopting the *Strong Column~Weak Beam* design capacity as proposed for seismic design (Elnashai and Sarno 2008, Kirtas and Kakaletsis 2013). By following this concept, it is expected that the plastic hinge should be formed in beam first rather than column (Giao *et al.* 2014). In Eurocode 8 (2004), this provision can be referred in Clause 4.4.2.3 (4).

The confinement reinforcement also provided within the beam-column joints as proposed in seismic detailing. All steel used for reinforcement are ribbed bar. Fig. 2 also presents the setup of steel reinforcement for beams, columns, and within the beam-column joints.

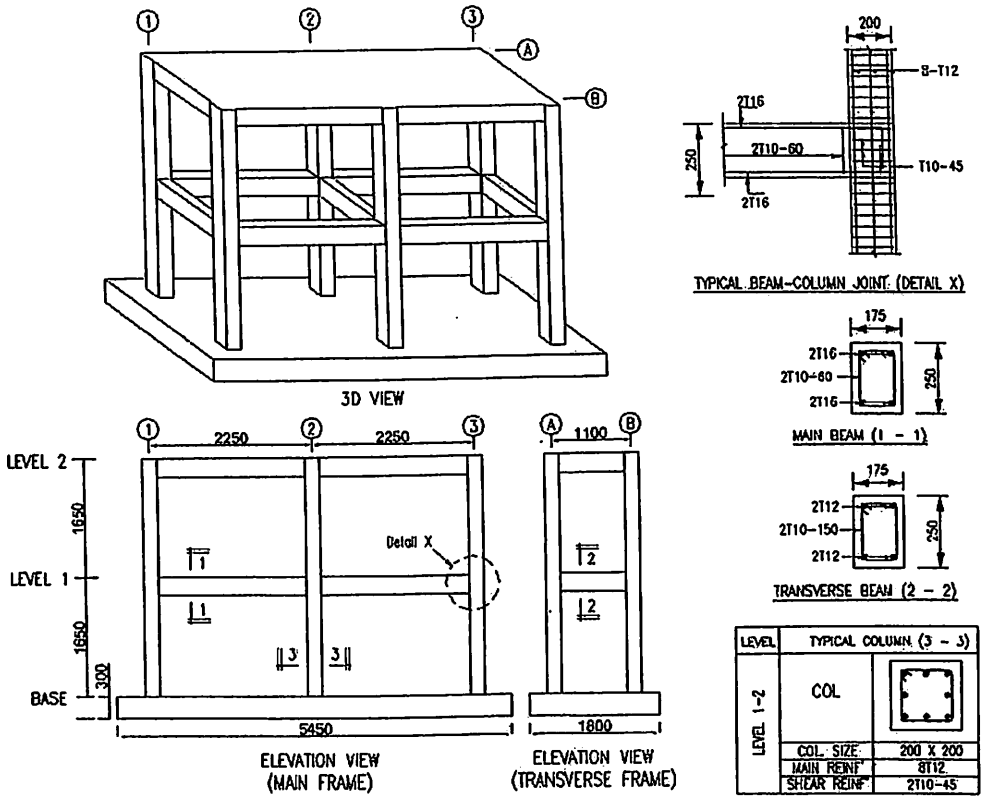

Fig. 2: Detail design of N2-DB model

2.2. *Experimental setup*

The cyclic loading test on N2-DB model was conducted based on displacement control. This method also used in previous works (Kirtas and Kakaletsis 2013, Tawfik *et al.* 2014, Eom *et al.* 2014). Based on displacement control method, the lateral load is imposed by actuator on the top of the N2-DB model parallel to the main frame until it displace to a specific distant namely as target drift. The latter is started from 0.10% and increased up to 3.25% of the total height of the N2-DB model. Therefore, the displacement was increased and the lateral load imposed to achieve the

corresponding displacement was recorded by the load cell before being transferred to the computer. In this work, the action of lateral load which cause the N2-DB model sway to the left and right is called as pushing and pulling, respectively as shown in Fig. 3. A complete cycle consist of pushing, pulling, and then back to original position. Two complete cycle is repeated for each target drift before the magnitude of target drift was increased. The magnitude of displacement due to both action is recorded by the Linear Variables Displacement Transducer (LVDT) which was attached horizontally at the top of N2-DB model. The schematic loading regime based on displacement control is shown in Fig. 4. After every cycle, the crack and damage occurred on the N2-DB model was observed and marked. For that purpose, the red and blue in color permanent marker was used for pushing and pulling action, respectively.

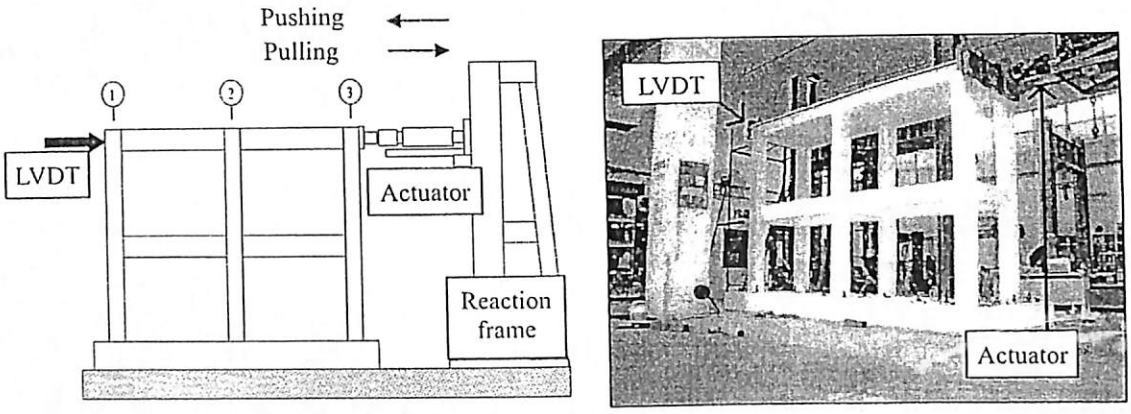

Fig. 3: Final experimental setup of N2-DB model

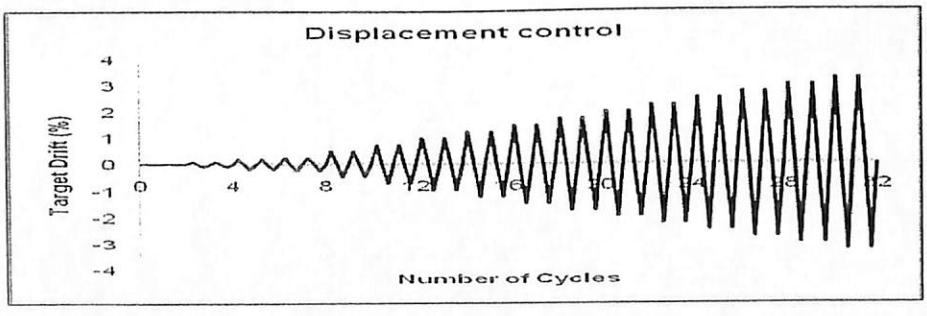

Fig. 4: Loading regime for cyclic loading test

3. Visual damage observation for each target drift

As mentioned in previous section, the cyclic loading test was conducted based on displacement control where the displacement is increased from one cycle to other cycles. The test was started with low target drift at 0.10% which is around 3.2 mm lateral displacement. At this very low displacement, no crack observed on the N2-DB model. As the target drift increased to 0.25% and 0.50%, the N2-DB model still maintain its original condition as before the test. This means that the structure still respond in its elastic range. At 0.75% target drift, the appearance of hairline cracks were observed at the main beams as shown in Fig. 5. This indicates that the flexural crack started to develop. At the same target drift, the hairline cracks also occurred at the beam-column joints while columns maintain its original undamaged condition. When the target drift was increased to 1.00%, the hairline cracks started to occur at first level of columns, especially all four exterior columns. In this study, it was clear that the hairline cracks firstly occurred on beams, then followed by the columns. This result is a good indicator that the *Strong Column~Weak Beam* design capacity concept had been fully adopted, which is a good characteristic of seismic resistant structure. This result also valid with the damage type in FEMA 356 (2000) which stated that at 1.00% drift the hairline cracks started to occur on structural elements. The performance level at this stage is belong to Immediate Occupancy (IO).

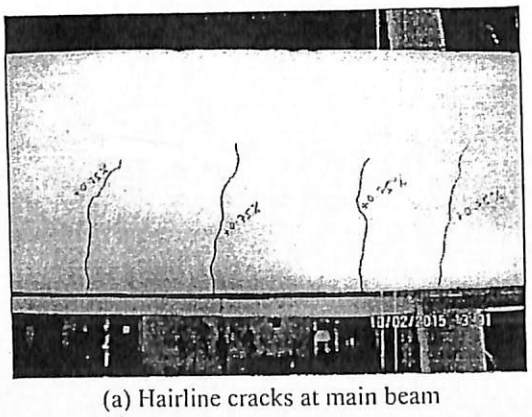

(a) Hairline cracks at main beam

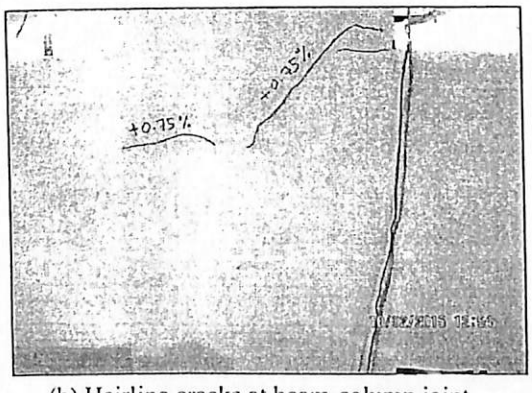

(b) Hairline cracks at beam-column joint

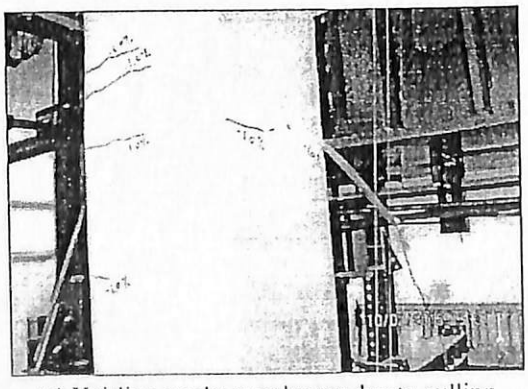

(c) Hairline cracks at columns due to pulling

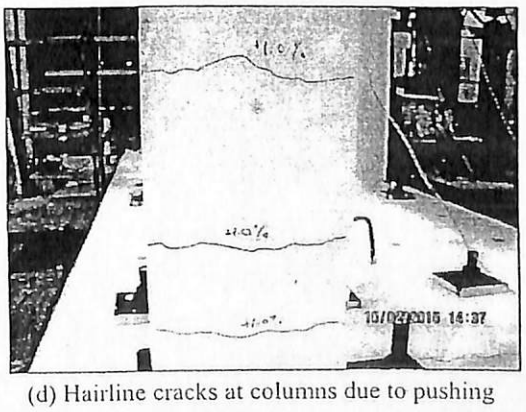

(d) Hairline cracks at columns due to pushing

Fig. 5: Formation of hairline cracks due to 0.75% and 1.00% target drift

The visual damage observed for target drift at 1.25% and 1.50% is presented in Fig. 6. The lateral displacement at top floor of N2-DB corresponding to these target drift is equal to 39.7 mm and 47.6 mm, respectively. It was observed that the increasing of target drift result in increasing number of cracks. At 1.25% target drift, the cracks at beams occurred previously were elongated and extended to the middle of the beam depth, which is around 125 mm length. Then, the number of cracks at columns became higher at 1.50% target drift. Similar damage also observed at the beam-column joints due to both pushing and pulling action. This result indicates that the damage has become worse at reported in previous work by Ma *et al.* (2013).

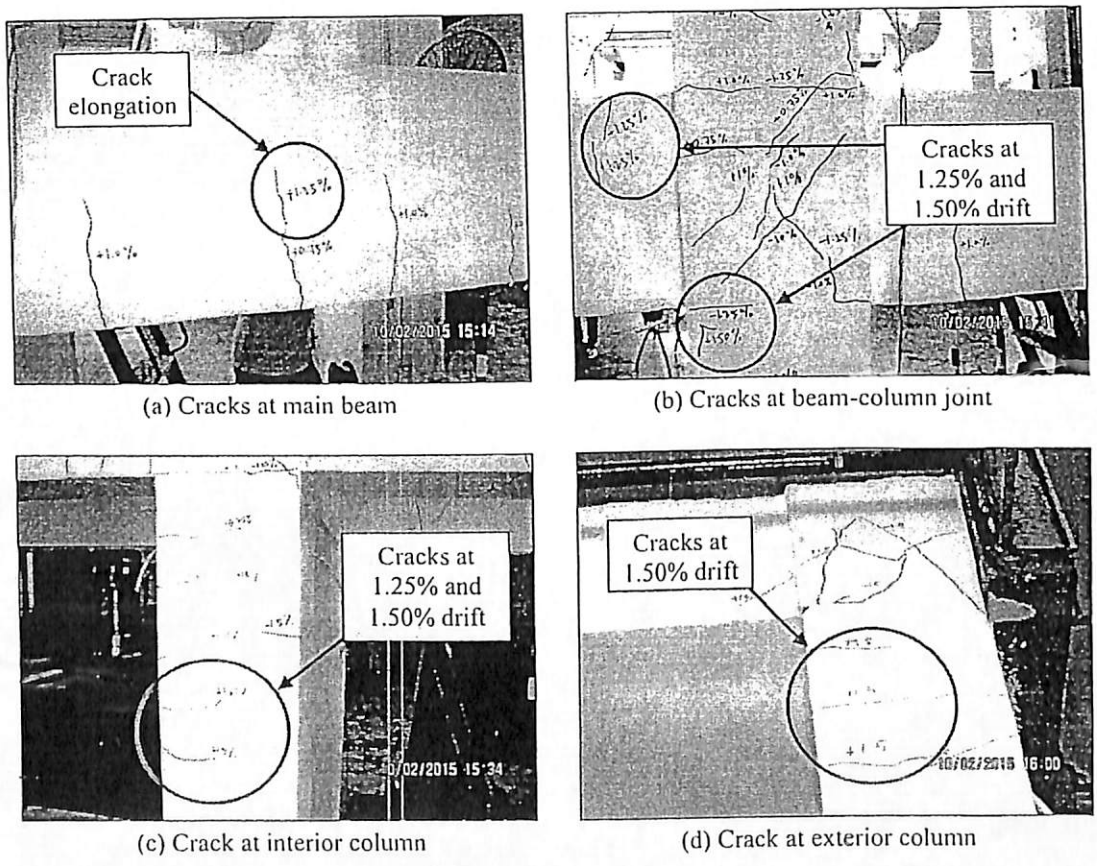

(a) Cracks at main beam

(b) Cracks at beam-column joint

(c) Crack at interior column

(d) Crack at exterior column

Fig. 6: Hairline cracks due to 1.25% and 1.50% target drift

Severe and longer cracks were observed at 1.75% and 2.00% target drift as shown in Fig. 7. This observation were occurred at all main beams, columns, and beam-column joints. When subjected to lateral displacement corresponding to 2.00% target drift, the concrete cover started to spall from the structural elements. In this study, the first spalling of concrete cover was occurred at the top of the interior column. The length of the concrete cover is about 110 mm. This damage observation is in good agreement with the standard of FEMA 356 (2000) which stated that at

2.00% drift the concrete cover is expected to spall from the main structural elements. The performance level at this target drift is correspond to Life Safety (LS).

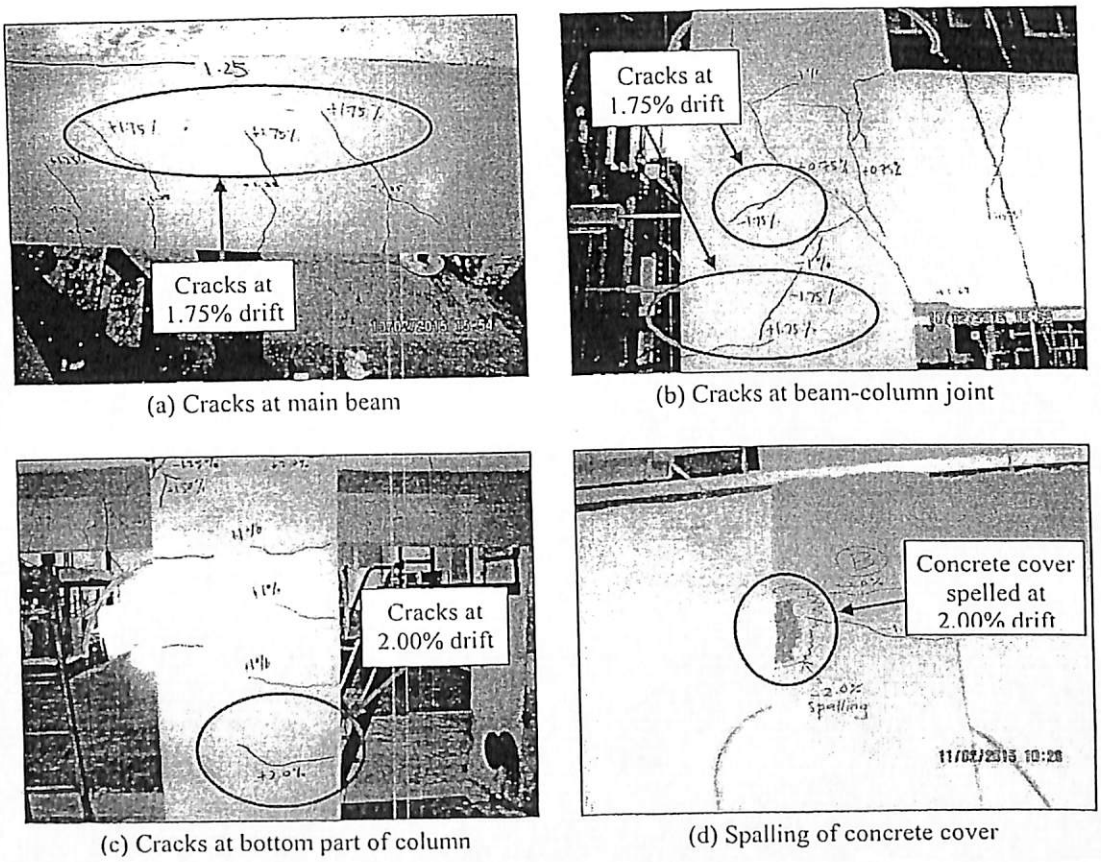

(a) Cracks at main beam

(b) Cracks at beam-column joint

(c) Cracks at bottom part of column

(d) Spalling of concrete cover

Fig. 7: Damage observation due to 1.75% and 2.00% target drift

At 2.25% and 2.50% target drift, the cracks occurred at main beams, columns, and beam-column joints propagated, extended, and linked together. Fig. 8 presents the visual damage occurred at these target drift. At 2.25% target drift, the cracks actively occurred at first level of both interior columns. The damage became severe at 2.50% target drift where the concrete cover spell out at the interior beam-column joint at first level. Verticality check on column showed that all columns did not return to fully 90 degrees vertical position when the imposed lateral load is equal to zero. This condition indicates that the columns experienced permanent displacement. At this target drift, the cracks from beam-column joints propagated to the transverse beams.

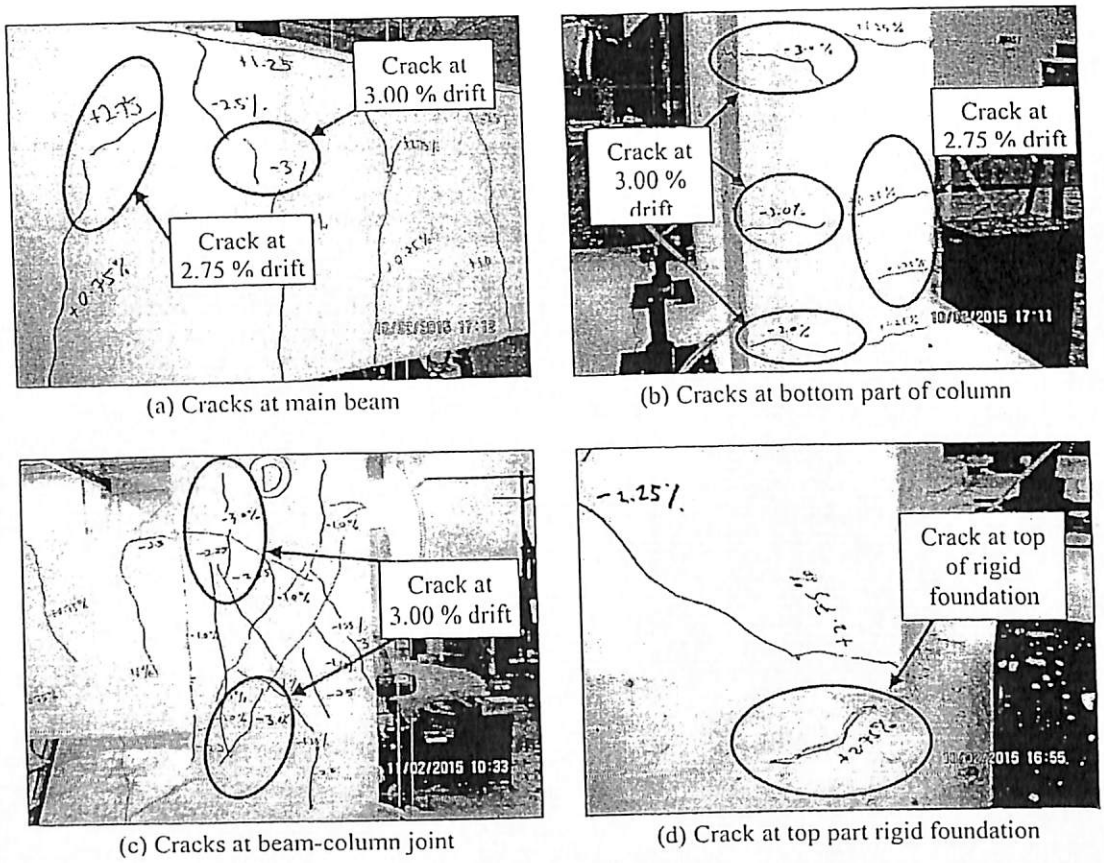

(a) Cracks at main beam

(b) Cracks at bottom part of column

(c) Cracks at beam-column joint

(d) Crack at top part rigid foundation

Fig. 9: Damage observation due to 2.75% and 3.00% target drift

At 3.25% of target drift, the actuator stopped automatically at the first pushing action indicated that the N2-DB model experienced sudden strength degradation. At this stage, the model no longer able to resist imposed lateral load. Therefore, the test was stopped for safety purpose.

4. Post-test damage assessment

After the cyclic loading test was stopped, the post-test assessment also conducted on the N2-DB model. This is important to evaluate the overall crack pattern and damage. One of the post-test assessment was the damage on beam-column joints at first level as shown in Fig. 10. It can be clearly observed that the cracks occurred on all 6 beam-column joints were in similar pattern. The cracks were in diagonal shape due to pushing and pulling actions. Heavier damage with longer and wider cracks occurred at exterior beam-column joints compared to the interior part. This is due to higher stress experienced in the beam-column joints to resist the lateral load. Calvi *et al.* (2002) also observed similar damage in the same region. In this study, greater damage was prevented by the existence of confinement reinforcement as discussed in previous section which is in good

agreement with Tawfik *et al.* (2014). According to Adiyanto *et al.* (2014) the design and amount of confinement reinforcement in critical region of column and beam-column joint strongly influenced by the value of behavior factor, q considered in design.

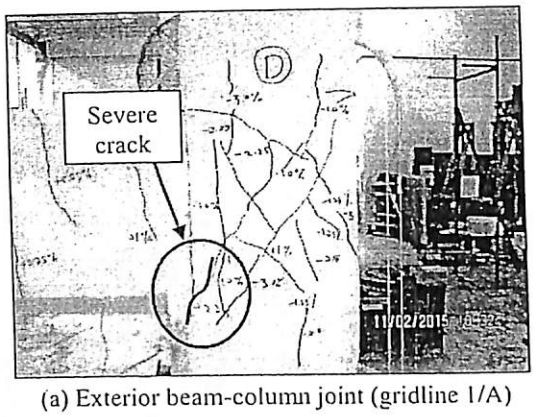

(a) Exterior beam-column joint (gridline 1/A)

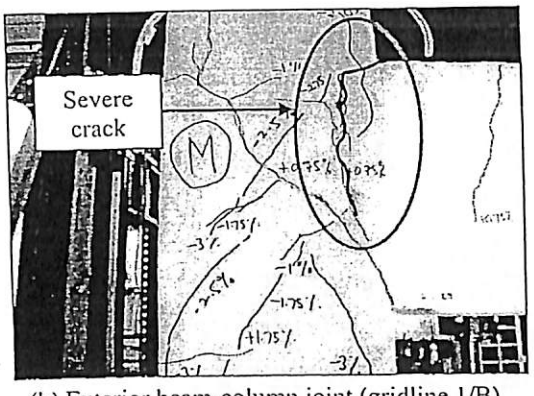

(b) Exterior beam-column joint (gridline 1/B)

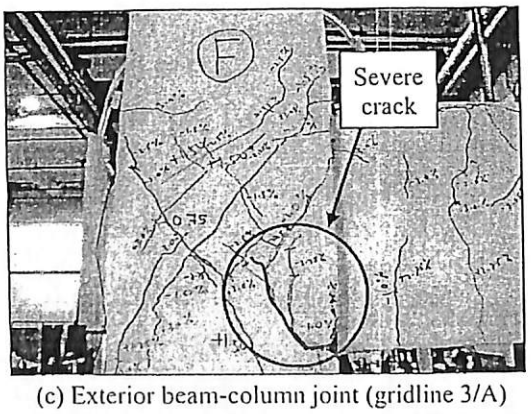

(c) Exterior beam-column joint (gridline 3/A)

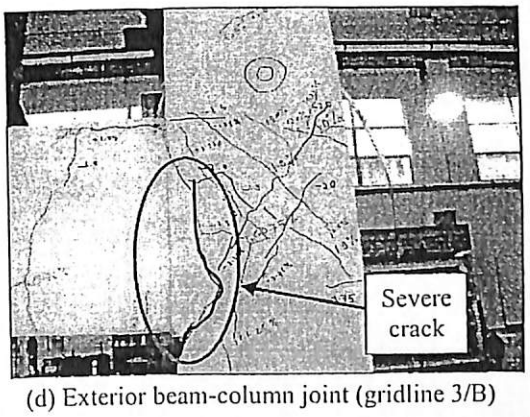

(d) Exterior beam-column joint (gridline 3/B)

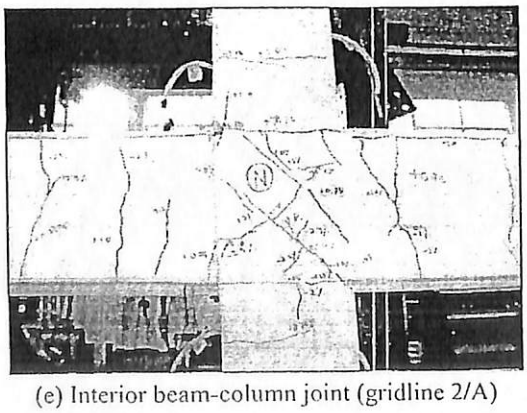

(e) Interior beam-column joint (gridline 2/A)

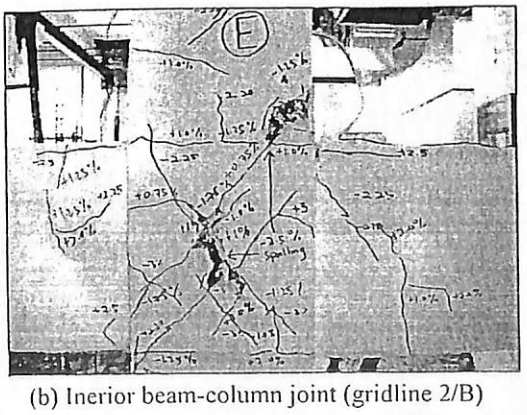

(b) Inerior beam-column joint (gridline 2/B)

Fig. 10: Post-test assessment on beam-column joints

The post-test damage assessment also focused on the spall of concrete cover from structural elements as shown in Fig. 11. It can be clearly observed that the spalling of concrete cover occurred in the critical regions which is located near the beam-column joints. In this study, the concrete cover spell out from the structural elements as the target drift greater than about 2.00%. As discussed in previous section, this damage correspond to LS performance level. According to Eom *et al.* (2014) the spalling of concrete cover tends to lead to severe damage such as buckling of longitudinal reinforcement and crushing of concrete core. The latter was observed on the buildings without seismic design as reported based on in-situ field investigations (Bayraktar *et al.* 2013, Ates *et al.* 2013, Tapan *et al.* 2013). The N2-DB model used in the cyclic loading test did not experienced such damage even subjected to as high as 3.00% target drift. This result is contributed by proper seismic design and detailing.

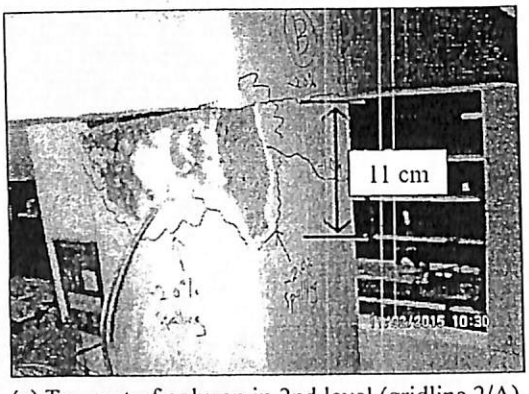

(a) Top part of column in 2nd level (gridline 2/A)

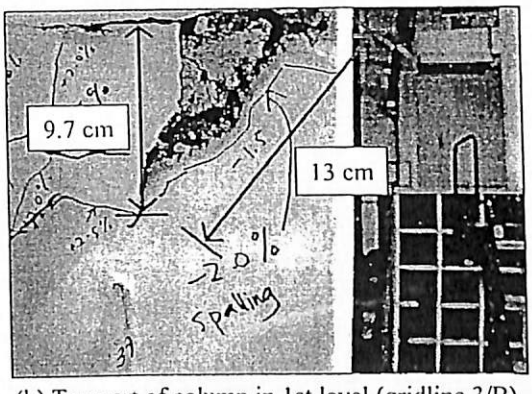

(b) Top part of column in 1st level (gridline 3/B)

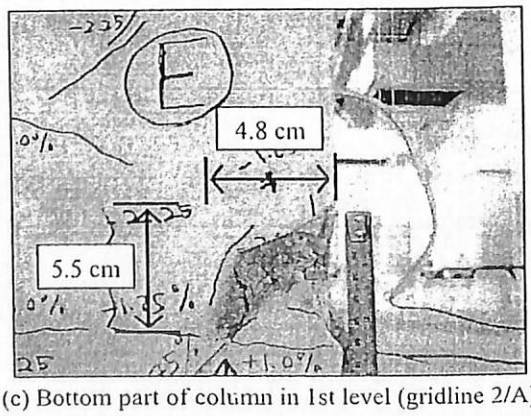

(c) Bottom part of column in 1st level (gridline 2/A)

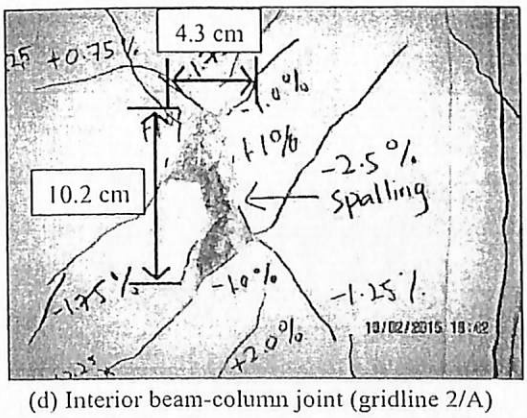

(d) Interior beam-column joint (gridline 2/A)

Fig. 11: Post-test assessment on spell of concrete cover

5. Conclusions

An experimental work namely as cyclic loading test was conducted in the laboratory. A 3 dimension half scale RC frame was constructed as the model for the test. The latter was designed based on peak ground acceleration, a_{gR} = 0.12g represent the medium seismic region in East Sabah, Malaysia. Full seismic design for DCM was taken into account by referring to Eurocode 8 (2004). The N2-DB model was constructed using available construction materials in Malaysia and compatible with the Eurocode 8 (2004) including the use of ribbed bar as steel reinforcement. Based on the damage observation, the following conclusions can be drawn:

- At as low as 0.10% to 0.50% target drift, no cracks were observed on any structural elements of the N2-DB model. This result indicates that the structure still in its elastic response.
- The *Strong Column ~ Weak Beam* design capacity concept proposed for seismic design was fully adopted by the N2-DB model. This was proven by formation of cracks at beams first then followed by columns at target drift of 0.75% and 1.00%, respectively.
- When the level of target drift is increased, the number of cracks also increased, extended, and linked together.
- The hairline cracks occurred at beams, columns, and beam-column joints at target drift of 0.75% and 1.00%. At target drift more than about 2.00%, the concrete cover spell out from structural elements. Therefore, this experimental work is valid with the standard level of damage as promoted by FEMA 356.
- Diagonal cracks and spalling of concrete cover were observed at beam-column joints. The existence of adequate confinement reinforcement within that region prevented the occurrence of greater damage such as buckling of longitudinal reinforcement and crushing of concrete core. The use of ribbed bar as steel reinforcement also contributed to this performance.
- RC frame with full seismic design and detailing performed well when subjected to lateral load compared to the nonseismic design. Therefore, it is worth to consider seismic design for new buildings in Malaysia to prevent greater loss due to future earthquake. For that purpose, the Eurocode 8 can be referred as seismic provision code.

At the moment this paper is written, further analysis related to seismic behavior of the N2-DB model based on cyclic loading test is conducted and the result will be published soon.

Acknowledgments

The authors gratefully acknowledge the financial support by Research University Grant (1001/PAWAM/814115) sponsored by Universiti Sains Malaysia. All authors also acknowledge the facilities provided in the Heavy Structure Laboratory in Universiti Teknologi Mara for the conducted test. Special thanks also acknowledged to Rusdiana Rusdin, Norain, Anis Azmi, Muhammad Syazwan, Allim Abdullah, Fendy, and Muhammad Tarmizi Ismail for their help and support to accomplish this experimental work. The third author personally acknowledge financial support program from MyBrain15, a scholarship provided by Ministry of Education Malaysia.

References

Abdul Hamid, N.H. and Mohamad, N.M. (2013), "Seismic assessment of a full-scale double-storey residential house using fragility curve", *Procedia Engineering*, 54, 207-221.

Ade Faisal., Majid, T.A. and Hatzigeorgiou, G.D. (2013), "Investigation of story ductility demands of inelastic concrete frames subjected to repeated earthquakes", *Journal of Soil Dynamics and Earthquake Engineering*, 44, 42-53.

Adiyanto, M.I. and Majid, T.A. (2014), "Seismic design of two storey reinforced concrete building in Malaysia with Low Class Ductiltiy", *Journal of Engineering Science and Technology*, 9(1), 27-46.

Adiyanto, M.I., Majid, T.A. and Nazri, F.M. (2014), "Cost optimization of seismic design of low rise hospital RC frame in Malaysia", *Proceedings of the 5th Asia Conference on Earthquake Engineering*, Paper reference 148, Taipei, Taiwan, October.

Adnan, A., Hendriyawan., Marto, A. and Selvanayagam, P.N.N. (2008), "Development of seismic hazard maps of east Malaysia", *Advances in Earthquake Engineering Applications*, 1-17.

Ates, S., Kahya, V., Yurdakul, M. and Adanur, S. (2013), "Damages on reinforced concrete buildings due to consecutive earthquakes in Van", *Journal of Soil Dynamics and Earthquake Engineering*, 53, 109-118.

Bayraktar, A., Altunisik, A.C. and Pehlivan, M. (2013), "Performance and damages of reinforced concrete buildings during the October 23 and November 9, 2011 Van, Turkey, earthquakes", *Journal of Soil Dynamics and Earthquake Engineering*, 53, 49-72.

Calvi, G.M., Magenes, G. and Pampanin, S. (2002), "Experimental test on a three storey RC frame designed for gravity only", *Proceedings of the 12th European Conference on Earthquake Engineering*, Paper reference 727, London, United Kingdom, September.

CEN (2004). *Eurocode 8: Design of structures for earthquake resistance*, Part 1: General rules, seismic actions and rules for buildings, European Committee for Standardization, Brussels.

Elnashai, A.S. and Sarno, L.D. (2008), *Fundamentals of earthquake engineering*, John Wiley & Sons, West Sussex, UK.

Eom, T.S., Kang, S.M., Park, H.G., Choi, T.W. and Jin, J.M. (2014), "Cyclic loading test for reinforced concrete columns with continuous rectangular and polygonal hoops", *Journal of Engineering Structures*, 67, 39-49.

FEMA (2000). *FEMA 356: Prestandard and commentary for the seismic rehabilitation of buildings, 2000 Edition*, Building Seismic Safety Council for the Federal Emergency Management Agency, Washington D.C.

Filiatrault, A., Lachapelle, E. and Lamontagne, P. (1998), "Seismic performance of ductile and nominally ductile reinforced concrete moment resisting frames; I Experimental study", *Canadian Journal of Civil Engineering*, 25, 331-341.

Giao, R., Lucio, V. and Chastre, C. (2014), "Assessing the behaviour of RC beams subject to significant gravity loads under cyclic loads", *Journal of Engineering Structures*, 59, 512-521.

Harris, H.G. and Sabnis, G.M. (1999), *Modelling and Experimental Techniques* (2nd Edition), CRC Press, Florida, USA.

Hatzigeorgiou, G.D. and Beskos, D.E. (2009), "Inelastic displacement ratios for SDOF structures subjected to repeated earthquakes", *Journal of Engineering Structures*, 31, 2744-2755.

Kalman, T. and Sigmund, V. (2009), "Seismic capacity of infilled frames using neural networks", *Proceedings of the 6th ICCSM*, Zagreb, Croatia.

Kay Dora, A.G. and Abdul Hamid, N.H. (2012), "Seismic performance of SFRC beam-column joint with corbel under reversible lateral cyclic loading", *IACSIT International Journal of Engineering and Technology*, 4(1), 76-80.

Kirtas, E. and Kakaletsis, D.J. (2013), "Numerical investigation of influential parameters concerning the experimental testing of RC frames under cyclic loading", *The Open Construction and Building Technology Journal*, 7, 230-243.

Kuang, J.S. and Wang, Z. (2014), "Cyclic loading tests of frame with column-isolated masonry infills",

Australian Journal of Basic and Applied Sciences, 7(8): 411-419, 2013
ISSN 1991-8178

Influence Of Behaviour Factor On Seismic Design Of Two Storey Reinforced Concrete Building In Malaysian Seismic Region

[1]Mohd Irwan Adiyanto, [2]Taksiah A. Majid

[1]Postgraduate Student, Universiti Sains Malaysia, Penang, Malaysia
[2]Disaster Research Nexus, Universiti Sains Malaysia, Penang, Malaysia

Abstract: Malaysia is situated relatively far away from active seismic fault zone. However, it is clear that the nation is surrounded by high seismicity areas at the west, south, and east part as. This is associated with the subduction zones between the Indo-Australian plate and Eurasian plate at the west and south part, also the subduction zones between the Eurasian and Philippines plate at the east region. In Malaysian construction industry, the British Standard of BS 8110 had been implemented as reference for reinforced concrete design. For low rise buildings, the designers only consider gravitational load only since Malaysia is situated relatively far away from active seismic fault zone. However, over the past decade tremors induced by seismic activities from Sumatra Andaman and Philippines earthquake had been felt in Malaysian soil. There are several questions on implementation of seismic design in Malaysia such as the class of ductility to be adopted and the increment of cost. This paper investigated the difference of steel reinforcement and concrete required when seismic provision is considered in reinforced concrete design of general office building. The original two storey regular office building which designed based on BS8110 had been redesigned according to Eurocode 2 and Eurocode 8 provision with various level of reference peak ground acceleration, $_{agR}$ reflecting Malaysian seismic hazard for ductility class Medium (DCM). It is observed that the level of behaviour factor, q strongly influences the total cost of material for the whole frame. For such class of ductility, the increment of cost of material is extremely high which lie in range of 1.7 to 3.3 times higher compared to nonseismic frame design.

Key words: Reinforced concrete, Eurocode 8, behaviour factor, ductility class medium, seismic design.

INTRODUCTION

In Malaysian construction industry, the British Standard of BS8110 (1997) had been implemented as reference for reinforced concrete (RC) design. For low rise buildings, the designers only consider gravitational load only since Malaysia is situated relatively far away from active seismic fault zone. However, over the past decade tremors induced by seismic activities from Sumatra Andaman and Philippines earthquake had been felt in Malaysian soil. From 1984 to 2007, a total of 35 seismic events originating from Sumatra, Indonesia and 9 other events originating from Bukit Tinggi area, Pahang were reported to have been felt in various parts of the country (MOSTI, 2009). Within the same period, a total of 32 seismic events originating from Philippines, Indonesia, and local region were felt in East Malaysia (Sabah and Sarawak). The unforgettable one of course belongs to the earthquake with magnitude Mw 9.0 on 2004 Boxing Day which occurred west of Aceh in Sumatra, Indonesia. The earthquake also generated a disastrous Indian Ocean tsunami with high 'tidal' wave that struck the coast of several countries in Asian region including several parts of west coast of Peninsular Malaysia. The tremors also caused vibration on buildings and created panic situation. It had been reported that most buildings were in good condition in Peninsular Malaysia and at least 50% of selected buildings were found to experience concrete deterioration problems due to vibration during earthquake (MOSTI, 2009). The Malaysian Public Work Department (JKR) suggested that it was worthwhile to consider seismic design input for new buildings located in medium – to – high risk earthquake zones. For design, the classification of ductility class low (DCL) or even ductility class medium (DCM) may be considered in Peninsular Malaysia (Jeffrey and Peng, 2011). For low rise buildings with lower fundamental period of vibration, T_1 ductile detailing could be ignored but at the expense of using a lower behaviour factor, q which will result in higher seismic design forces. Therefore, the designer may still wish to use ductile detailing to take advantage of the lower seismic design forces resulting from using a higher behaviour factor, q (Pappin *et al.*, 2011).

In earthquake engineering, it is important for designers to understand the concept of stiffness, strength, and ductility, as well as behaviour factor, q for design purposes. Stiffness, strength, and ductility correspond to the ability of a component to resist deformations when subjected to actions, capacity of component for load resistance at a given response, and ability of a component to deform beyond the elastic limit (Elnashai and Sarno, 2009). In seismic design, it is not economically feasible to design structures which can respond elastically during earthquake (FEMA 451B, 2007). Thus, for economic reason most structures are designed to

Corresponding Author: Mohd Irwan Adiyanto, Postgraduate Student, Universiti Sains Malaysia, Penang, Malaysia
E-mail: irwano_07@yahoo.com

behave inelastically due to tremors. In order to achieve this target, the concept of behaviour factor, q had been promoted in seismic design. The behaviour factor, q is a factor which used for design purposes to reduce the forces obtained from a linear analysis, in order to account for the nonlinear response of a structure (Eurocode 8, 2004). The same concept namely as force or strength reduction factor, R is implemented in American code for the same purpose (FEMA 451B, 2007). The level of behaviour factor, q to be applied in design depends on the material, type of structures, and class of ductility (Eurocode 8, 2004). Over the past few years, the value of behaviour factor, q proposed by the codes had been scientifically re-evaluated and commented. As an example, Gillie *et al.*, (2010) commented that common design specification which is based on non-pulse forward directivity ground motions cannot be directly applied to deal with pulse-type forward directivity ground motions. In their work, they also found that the strength reduction factor, R resulting from forward directivity ground motions is smaller than those from non-forward directivity ground motions. For conservative design of structures in near-fault regions, the simple and effective modification is needed to replace the current value of strength reduction factor, R (Jalali and trifunac ,2008). Borzi and Elnashai (2000) concluded that both European and American standards are too conservative where the ductility demand which corresponds to the behaviour factor, q is higher than the ductility supply. If not supported by high overstrength, the demand could have exceeds the supply thus leading to unsafe situation in terms of deformation capacity. The behaviour factor, q also had been evaluated due to excitation of repeated earthquake (Hatzigeorgiou and Beskos, 2009, Hatzigeorgiou, 2010, Ade Faisal *et al.*, 2013). However, in previous works mentioned above, the effect of behaviour factor, q on cost of materials was not discussed.

Therefore, this paper investigated the difference of steel reinforcement and concrete required when seismic provision is considered in reinforced concrete (RC) design of general office building. The original two storey regular office building which designed based on BS8110 (1997) had been redesigned according to Eurocode 2 (2004) and Eurocode 8 (2004) with various level of reference peak ground acceleration, $_{agR}$ reflecting Malaysian seismic hazard for ductility class Medium (DCM). Then, the cost of materials for frames with seismic design had been presented alongside the factors influencing the design.

MATERIAL AND METHODS

To investigate the effect of behaviour factor, q on cost of material, a frame of two storey RC building regular in plan and elevation had been used in analysis and design. As shown in Figure 1, the frame has typical storey height of 3.6 m and three equal bays of 5.0 m for general office use. The same frame also had been used by Adiyanto and Majid (2013) to study seismic design for ductility class low (DCL). To represent existing RC building and current construction practice in Malaysia, the frame had been designed for gravitational load only based on BS 8110 (1997) namely as N2BS. Then, by referring to European standard practices (Eurocode 2, 2004, Eurocode 8, 2004) the same frame had been redesigned with considering seismic action for ductility class medium (DCM). For such class of ductility, the proposed behaviour factor, q is lies in range of 1.5 to 4.5 depend on structural system (Eurocode 8, 2004). For RC frame system, the behaviour factor, q is proposed to be equal to 3.9. Hence, in this study four different level of behaviour factor, q in DCM had been used in design of the similar frame which is equal to 1.5, 2.7, 3.9, and 4.5. Since this study focus on seismic design in Malaysian seismic region, the seismic hazard maps for Malaysia had been referred. For 500 years return period, the value of peak ground acceleration (PGA) for Peninsular Malaysia is lies in range of 0.02g to 0.10g (Adnan *et al.*, 2008, MOSTI, 2009). For East Malaysia (Sabah & Sarawak), the value of PGA is around 0.06g to 0.12g which is increasing toward the eastern part like Tawau, Lahad Datu, and Semporna. A total 3 value of these PGA had been selected as reference peak ground acceleration, a_{gR} which is equal to 0.02g, 0.06g, and 0.12g to develop the response spectrum. In this study, all frames had been designed based on concrete compressive strength, f_{cu} = 30 N/mm^2 and the yield strength of steel, f_y = 460 N/mm^2. Table 1 presents the list of all 13 frames. Except for N2BS, all frames had been designed based on the following suggested load combinations (Eurocode 1, 2002, Eurocode 8, 2004) which also had been used in previous work (Hatzigeorgiou and Liolios, 2010).

i) CASE 1 $= 1.0G + \psi_2 Q + 1.0E$
ii) CASE 2 $= 1.0G + \psi_2 Q - 1.0E$
iii) CASE 3 $= 1.35G + 1.50Q$

where G, Q and E represent the dead, live, and earthquake loads, respectively. Since the frame is designed for general office use, the quasi-permanent value of a variable action, ψ_2 which had been applied to the live load, Q in Case 1 and Case 2 is equal to 0.3 (Eurocode, 2002, Acun *et al.*, 2012).

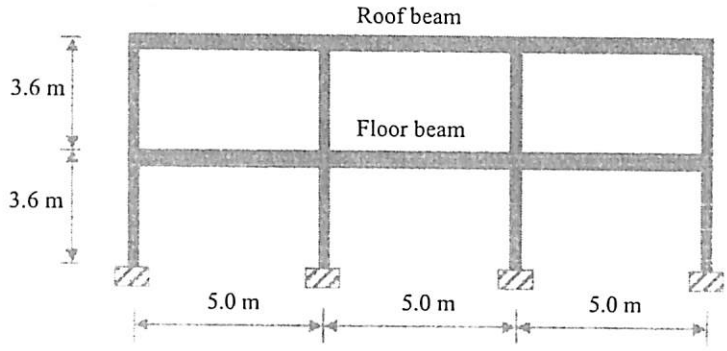

Fig. 1: Elevation of regular RC frame model

Table 1: List of frames used and design consideration

No.	Frame	Behaviour factor, q	agR (g)
1	N2BS	-	-
2	q1.5 – P1	1.5	0.02
3	q2.7 – P1	2.7	
4	q3.9 – P1	3.9	
5	q4.5 – P1	4.5	
6	q1.5 – P2	1.5	0.06
7	q2.7 – P2	2.7	
8	q3.9 – P2	3.9	
9	q4.5 – P2	4.5	
10	q1.5 – P3	1.5	0.12
11	q2.7 – P3	2.7	
12	q3.9 – P3	3.9	
13	q4.5 – P3	4.5	

For frames with seismic design, the lateral force method (Eurocode 8, 2004) had been conducted in analysis. In this method, the designers are required to determine the action of earthquake load on building and assign it as lateral load acting on each storey joint. For this purpose, the base shear force, F_b had been determined by using the following equation (Eurocode 8, 2004):

$$F_b = S_d(T_1) \cdot m \cdot \lambda \quad (1)$$

where $S_d(T_1)$, m, and λ correspond to the ordinate of the design spectrum at period T_1, the total mass of the building above the foundation or above the top of a rigid basement, and the correction factor, respectively.

Due to far-field earthquakes from Sumatra, buildings built on soft soil are occasionally subjected to tremors although Malaysia is situated on a stable part of the Eurasian plate (Balendra and Li, 2008). Hence, in this study the Type 1 response spectrum compatible with Soil D (Eurocode 8, 2004) had been developed to determine the spectral acceleration at fundamental period of vibration, $Sd(T_1)$. Figure 2 depicts the response spectrum developed based on reference peak ground acceleration, a_{gR} equal to 0.12g at various level of behaviour factor, q.

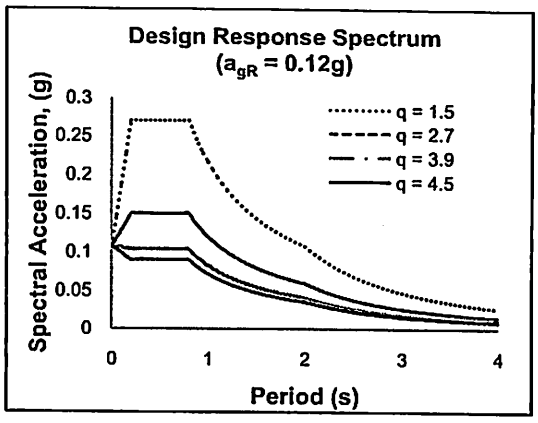

Fig. 2: Design response spectrum for type 1, soil class D, a_{gR} = 0.12g

RESULTS AND DISCUSSION

Effect Of Behaviour Factor, Q On Base Shear Force, F_b:

As discussed in previous section, the main function of behaviour factor, q is to reduce the lateral load act on structure so it wills response inelastically due to earthquake excitation. Figure 3 shows the base shear force, F_b acting on 2 storey RC building used in this study. It is clearly observed that the magnitude of base shear force, F_b is decreases when the level of behaviour factor, q increases. In all cases of reference peak ground acceleration, a_{gR} considered in this study, the base shear force, F_b is reduced around 40%, 58%, and 62% when the level of behaviour factor, q is increased from 1.5 to 2.7, 3.9, and 4.5, respectively. Lower magnitude of base shear force, F_b means lower magnitude of distributed lateral load acting on each storey. Therefore, the bending moment developed from seismic action also becomes lower. The design of frame with higher level of behaviour factor, q is expected to be lighter compared to the lower one.

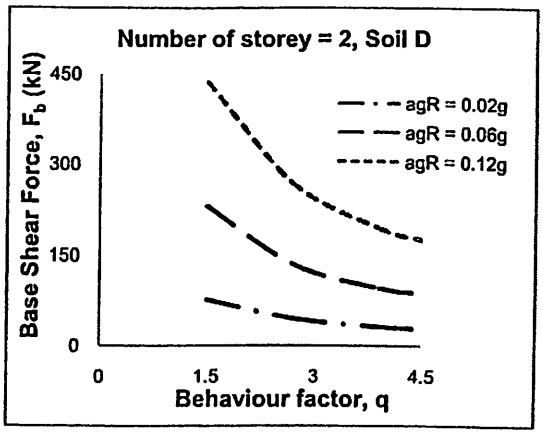

Fig. 3: Comparison base shear force, F_b acting on building

Effect Of Behaviour Factor, Q On Beam Design Of Flexural Reinforcement:

In RC design, the designers have to play around with concrete and steel reinforcement. Size of section, size of steel bar, and the number of steel bar have to be selected and adjusted smartly in order to fulfil the flexural demand from bending moment. The total concrete volume and weight of flexural steel reinforcement of floor beam designed with different level of behaviour factor, q considering fixed reference peak ground acceleration, a_{gR} equal to 0.02g is depicted in Figure 4. It is clearly observed that the total concrete volume of floor beam is constant except for frame q1.5-P1, which has lower concrete volume due to smaller size of section. On the other hand, higher level of behaviour factor, q seems to increase amount of steel used for flexural reinforcement. This result is quite contra with what has been discussed in previous section where lower level of behaviour factor, q induces higher magnitude of base shear force, F_b and heavier frame design is expected. From equivalent static

load analysis, the maximum bending moment used for design of frame q1.5-P1 was developed from Case 1 and Case 2 of load combination, which considering the seismic load. For other frames, maximum bending moment was developed from Case 3, which is gravitational load only due to decreasing of base shear force, F_b.

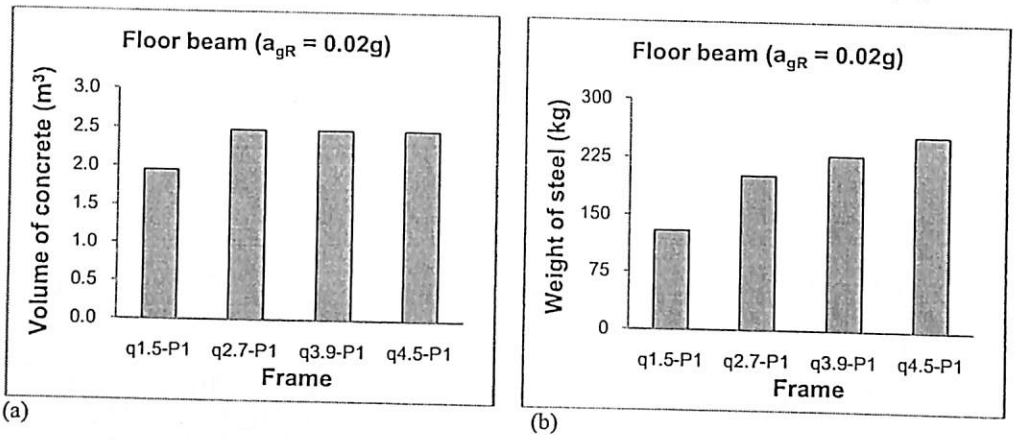

Fig. 4: Effect of behaviour factor, q on floor beam design, (a) volume of concrete (b) weight of steel

However, there is a reasonable answer for this result which is strongly associated by requirement to fulfil the local ductility demand. According to Eurocode 8 (2004), for DCM structures, the reinforcement ratio of the tension zone, ρ does not exceed a value of ρ_{max} as expressed in the following equation:

$$\rho_{max} = \rho' + \left[\frac{(0.0018 \cdot fcd)}{(\mu_\theta \cdot \varepsilon_{sy.d} \cdot f_{yd})}\right] \quad (2)$$

Where ρ', μ_θ, $\varepsilon_{sy.d}$, f_{cd}, and f_{yd} is the reinforcement ratio in compression zone, curvature ductility factor, design value of tension steel strain at yield, design value of concrete compressive strength, and design value of yield strength of steel, respectively. Eurocode 8 (2004) also states that if the tension zone includes a slab, the amount of slab reinforcement parallel to the beam within the effective flange width should be included in the reinforcement ratio in tension zone, ρ. As a result, the latter becomes larger compared to those contributed by amount of steel reinforcement of beam only.

Since the value of $\varepsilon_{sy.d}$, f_{cd}, and f_{yd} is fixed, the ρ_{max} is strongly influence by curvature ductility factor, μ_θ which is determined by:

$$\mu_\theta = 1 + 2\left[(q_0 - 1) \cdot \left(\frac{T_c}{T_1}\right)\right] \quad (3)$$

where q_0, T_C, and T_1 represent the basic value of behaviour factor, period at the upper limit of the constant acceleration region of the response spectrum, and fundamental period of building, respectively. From equation (3) above, it is clear that the curvature ductility factor, μ_θ is increases as the level of basic behaviour factor, q_0 is increases. Inversely, the maximum reinforcement ratio, ρ_{max} is decrease. As a result, the amount of steel reinforcement at tension zone has to be reduced. However, reducing the steel reinforcement may cause the area of steel required, As_{req} due to action of bending moment cannot be fulfilled. One more option is to increasing the size of section so the area of steel required, As_{req} can be reduced. However, promoting large size of beam may create conflict with architectural requirement such as aesthetic value and the need of space. Therefore, in order to maintain the size of beam without reducing the steel of reinforcement at tension zone, the amount of steel reinforcement at compression zone has to be increase so that the reinforcement ratio in compression zone, ρ' is increase. Hence, the maximum reinforcement ratio, ρ_{max} also increase as explained in equation (2). It can be concluded that although designed based on lower base shear force, Fb as well as lower bending moment, frames with higher level of behaviour factor, q tends to have higher amount of steel reinforcement due to local ductility demand.

Effect Of Behaviour Factor, Q On Column Design Of Flexural Reinforcement:

In order to prevent the formation of soft storey mechanism, the design values of the moments of resistance of the columns framing the joint, M_{Rc} should be greater than or equal to 1.3 times the design values of the moments of resistance of the beams, M_{Rb} framing the same joint (Eurocode 8, 2004). This concept of design is

known as *Strong Column ~ Weak Beam* philosophy where the capacity of column must be greater than the beam (Elnashai and Sarno, 2009). As explained by Elghazouli (2009), the magnitude of moment to be resisted by column is derived from the design moment of resistance of the beams, M_{Rb}. Therefore, in this study the column design is strongly influence by the corresponding beam design. Figure 5 presents the total concrete volume and weight of flexural steel reinforcement of column designed with different level of behaviour factor, q considering fixed reference peak ground acceleration, a_{gR} equal to 0.02g.

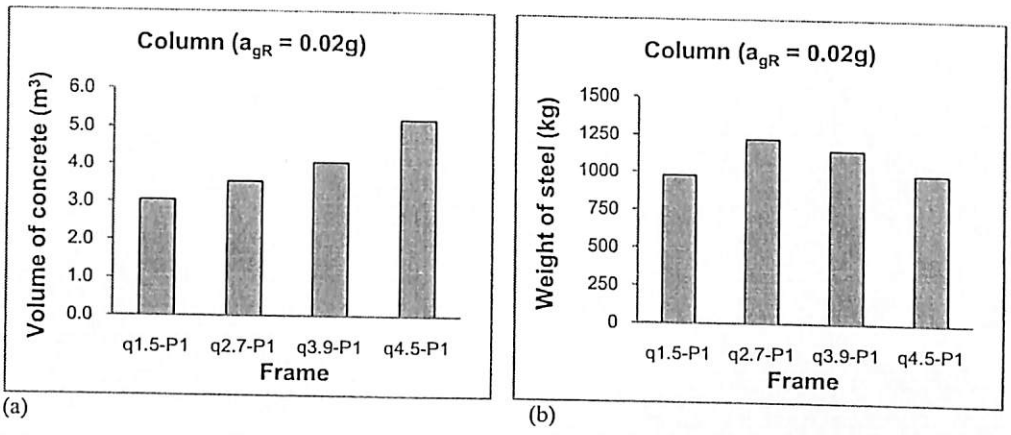

Fig. 5: Effect of behaviour factor, q on column design, (a) volume of concrete (b) weight of steel

From Figure 5, the total concrete volume for column is strongly influence by the level of behaviour factor, q. When the latter is increases, the concrete volume also increases. This result is fully associated with beam design as discussed in previous section. Higher level of behaviour factor, q tends to cause higher amount of steel reinforcement in beam. As a result, the design moment of resistance of the beam, M_{Rb} becomes high. Then, the latter had been amplified around 1.3 times as the design moment of resistance of the column, M_{Rc}. Sufficient amount of steel reinforcement have to be supplied to fulfil the area of steel required, As_{req} which had been determined by using appropriate design chart for column (Beeby and Narayanan, 1995). For DCM structures, the total amount of steel reinforcement in primary column shall lies between 1 to 4% of total area of column cross section (Eurocode 8, 2004, Fardis, 2009, Acun *et al.*, 2012). Besides, symmetrical reinforcement should be provided with at least 3 bars per side in symmetrical cross section. When total area of steel provided, As_{prov} exceeds the limit of 4%, the size of column should be enlarged. Therefore, the concrete volume of column for frame q4.5-P1 is the highest due to largest design moment of resistance of the column, M_{Rc}. In term of steel reinforcement, the amount of the latter is in range of 975 to 1222 kg for all four frames considered. Except frame q1.5-P1, total amount of steel reinforcement is decreases as the level of behaviour factor, q increases due to larger size of cross section. For DCM structures, it can be concluded that the column design is fully depends on beam design. If beam had been designed with high amount of steel reinforcement contributing to high capacity of moment resistance, the column also had to be designed to achieve high capacity of moment resistance either increasing the amount of steel reinforcement of enlarging the size of cross section. Again, higher level of behaviour factor, q contributes to heavier design.

Effect Of Behaviour Factor, Q On Shear Reinforcement:

In RC design, the designers not only have to design the flexural reinforcement to resist bending moment, but also have to design the reinforcement for shear load which is also known as link or transverse reinforcement. Figure 6 depicts the total amount of link in floor beam and column when designed at reference peak ground acceleration, a_{gR} equal to 0.06g. For floor beam, the level of behaviour factor, q only slightly influences the total amount of link. According to Eurocode 8 (2004), the spacing of link, s depends on the diameter of link, d_{bw} which shall be not less than 6 mm, minimum longitudinal bar diameter, d_{bL} and the beam depth, h_w as stated in the following equation:

$$s = \min\{hw/4;\ 24dbw;\ 225;\ 8dbL\} \tag{4}$$

from equation (4) above, the spacing of link, s can be increased if the diameter of link, d_{bw} diameter of longitudinal bar, d_{bL}, and beam depth, h_w is increased. Since the beam design is almost similar in term of size of section, and only differ in number of longitudinal bar for all frames, the total amount of link used is only slightly differ.

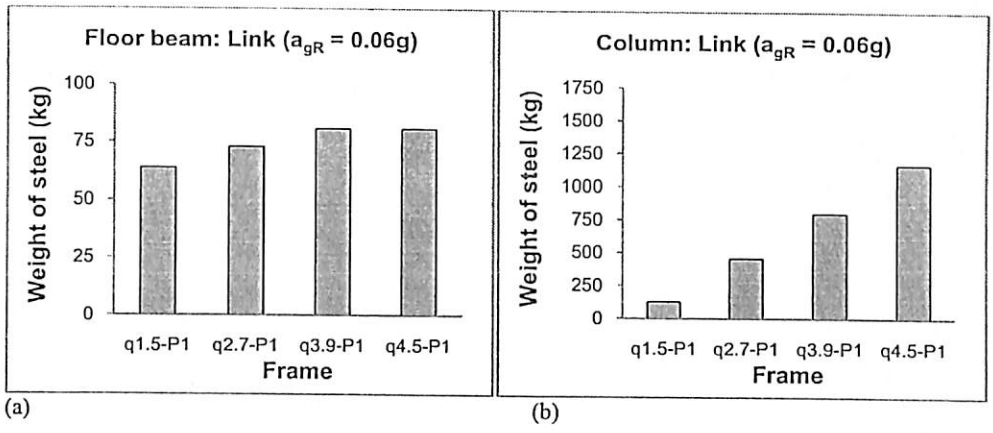

Fig. 6: Effect of behaviour factor, q on shear reinforcement, (a) floor beam (b) column

For column element, the level of behaviour factor, q is strongly influences the total amount of link. The latter increases rapidly as the level of behaviour factor, q increases. This result is strongly associated with the requirement of confinement reinforcement as stated in Eurocode 8 (2004) by the following equation:

$$\alpha \cdot \omega_{wd} \geq \left(30 \cdot \mu_{\phi} \cdot \nu_{d} \cdot \varepsilon_{sy,d} \cdot \frac{b_c}{b_0}\right) - 0.035 \quad (5)$$

Where α is the confinement effectiveness factor which is strongly influenced by the spacing of link, s (Eurocode 8, 2004). Other parameters like μ_{ϕ}, ν_d, $\varepsilon_{sy,d}$, b_c, and b_0 represent the curvature ductility factor, normalised design axial force, design value of tension steel strain at yield, gross cross-sectional width, and the width of confined core, respectively. In order to fulfil the requirement of confinement reinforcement, the mechanical volumetric ratio of confining hoops within the critical regions, ω_{wd} shall be sufficiently provided. From equation (5) above, it is clear that the main parameter which strongly influencing the required mechanical volumetric ratio of confining hoops within the critical regions, $\omega_{wd\ req}$ among other is the curvature ductility ratio, μ_{ϕ}, and the normalised design axial force ν_d. As discussed in previous section, the curvature ductility ratio, μ_{ϕ} is increases as the level of behaviour factor, q increases. Therefore, frame designed with high level of behaviour factor, q tends to require higher amount of link as confinement reinforcement due to high curvature ductility ratio, μ_{ϕ}. This situation had been proven in this study as shown in Figure 6. As explained by Elghazouli (2009), the designers have to play around with area of link, A_{sv} and spacing of link, s to provide sufficient mechanical volumetric ratio of confining hoops within the critical regions, ω_{wd}. In this study, it had been found that the spacing of link, s is the most powerful parameter that influencing the requirement of confinement reinforcement. The decreasing of spacing of link, s tends to decrease the confinement effectiveness factor, α which automatically decreasing the required mechanical volumetric ratio of confining hoops within the critical regions, $\omega_{wd\ req}$ as presented by equation (5) above. At the same moment, decreasing the spacing of link, s will increase the provided mechanical volumetric ratio of confining hoops within the critical regions, $\omega_{wd\ prov}$ as explained in previous work (Elghazouli, 2009). Decreasing the spacing of link, s had caused the space between two adjacent links become closer and higher amount of steel is required to complete the confinement reinforcement of the whole column. Therefore, frame q4.5-P1 has the highest amount of steel reinforcement as link due to highest required mechanical volumetric ratio of confining hoops within the critical regions, $\omega_{wd\ req}$ as a result of highest level of behaviour factor, q. In this study, all frames have the total amount of link in exterior column lesser than interior column regardless the level of behaviour factor, q and reference peak ground acceleration, a_{gR}. This result is associated with the normalised design axial force, ν_d which will increase the required mechanical volumetric ratio of confining hoops within the critical regions, $\omega_{wd\ req}$. Generally, the magnitude of axial force, N in exterior column is lower than that in the interior column. Therefore, the interior column requires higher confinement reinforcement compared to the exterior column.

Cost Estimation Of The Whole Frame:

In reality, it is hard to establish the additional cost of providing seismic resistance since buildings tend to be unique projects with different layout and requirement. However, it is worth to conduct a study on seismic design and costing so the authority can plan and decide for future development (Booth and Key, 2006). The total cost of material for the whole frame can be estimated from the sum of total concrete volume and weight of steel reinforcement, including the link. The estimated cost of the whole frame normalised to the existing frame

designed based on BS8110 (1997) is presented in Figure 7. As discussed in previous section, the frames which had been designed based on high level of behaviour factor, q require higher amount of material, especially the steel reinforcement. From Figure 7, it can be clearly observed that the total cost of the whole frame is increases as the level of behaviour factor, q increases. This result is similar for all level of reference peak ground acceleration, a_{gR}. When the level of behaviour factor, q is fixed, the estimated cost of the whole frame is only slightly increases when the reference peak ground acceleration, a_{gR} is increase. This result is associated with almost similar bending moment and axial force used for design which is dominated by the Case 3 of gravitational load only, except for behaviour factor, q equal to 1.5. This means that if DCM is considered in design with fixed level of behaviour factor, q the difference of total cost of material is not significant even built in different seismic region. As an example, the increment of total cost of material for the same RC building built in West Coast of Peninsular Malaysia (PGA = 0.08g) is not much differ compared to the same building built in East Coast of Sabah (PGA = 0.12g). Logically, the total cost of material should be lower for frames designed with higher level of behaviour factor, q due to lower magnitude of base shear force, F_b acting laterally on building. However, the requirements of local ductility demand in beam and confinement reinforcement in column which have to be fulfilled in DCM structures contribute to this inverse result.

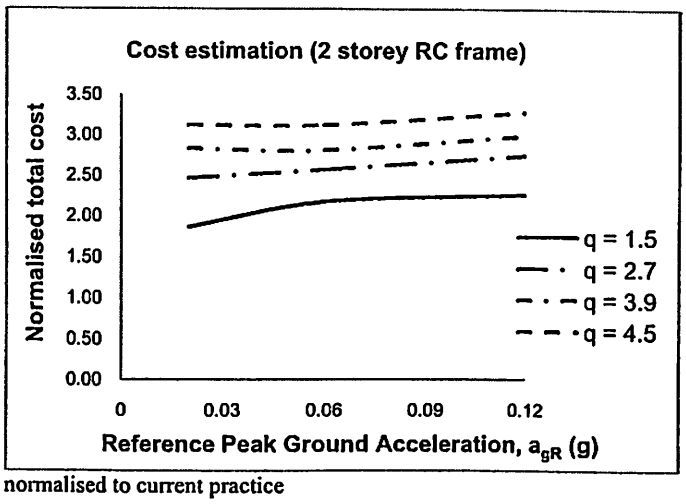

Fig. 7: Estimated cost normalised to current practice

Conclusion:

In this study, a total 13 typical frames of double storey RC general office buildings had been designed based on BS 8110 (1997) and Eurocodes (Eurocode 2, 2004, Eurocode 8, 2004) to investigate the increment of total cost of material if seismic design has to be implemented in Malaysia. Since this study considered DCM in seismic design, four different level of behaviour factor, q which compatible with such class of ductility had been adopted equal to 1.5, 2.7, 3.9, and 4.5. To represent the seismicity in Malaysian region, three different level of reference peak ground acceleration, a_{gR} in range of 0.02g to 0.12g had been considered during development of response spectrum for determination of base shear force, F_b. From this study, several conclusions might be drawn as follow:

- Level of behaviour factor, q strongly influence the design of structural members. In beam design, for the same reference peak ground acceleration, a_{gR} frames with higher level of behaviour factor, q tends to have higher amount of steel reinforcement due to local ductility demand.
- In order to fulfil the requirement of Strong Column ~ Weak Beam concept for DCM structures, the column design is directly associated with beam design. If beam had been designed with high amount of steel reinforcement contributing to high capacity of moment resistance, the column also had to be designed to achieve high capacity of moment resistance either increasing the amount of steel reinforcement of enlarging the size of cross section. Again, higher level of behaviour factor, q contributes to heavier design.
- In order to fulfil the requirement of confinement reinforcement in column, the mechanical volumetric ratio of confining hoops within the critical regions, ω_{wd} shall be sufficiently provided. The latter is higher when higher level of behaviour factor, q is assigned in design. The best option to fulfil this requirement is to use closer spacing of link, s. Therefore, frames designed with high level of behaviour factor, q require higher amount of link as transverse reinforcement.
- The DCM approach is not practical to be implemented for seismic design in Malaysia for low rise RC building with low fundamental period of vibration, T_1. This is due to extremely high increment of total cost of materials in range of 1.7 to 3.3 times compared to current practice regardless the seismic region.

ACKNOWLEDGEMENT

The authors gratefully acknowledge the facilities provided by Universiti Sains Malaysia and financial support from MyBrain15 to accomplish this study.

References

Acun, B., A. Athanasopoulou., A. Pinto., E. Carvalho and M. Fardis, 2012. Eurocode 8: Seismic design of buildings worked examples. Ispra Italy: European commission joint research center.

Ade Faisal., T.A. Majid and G.D. Hatzigeorgiou, 2013. Investigation of story ductility demands of inelastic concrete frames subjected to repeated earthquakes. Journal of Soil Dynamics and Earthquake Engineering, (44): 42-53.

Adiyanto, M.I and T.A. Majid, 2013. Seismic design of two storey reinforced concrete building in Malaysia with low class ductility. Accepted for publication in Journal of Engineering, Science, and Technology.

Adnan, A., Hendriyawan., A. Marto and P.N.N. Selvanayagam, 2008. Development of seismic hazard maps of east Malaysia. Advances in Earthquake Engineering Applications, 1-17.

Balendra, T and Z. Li, 2008. Seismic Hazard of Singapore and Malaysia. EJSE Special Issue, Earthquake Engineering in the low and moderate seismic regions of Southeast Asia and Australia, 57-63.

Beeby, A.W and R.S. Narayanan, 1995. Designers' handbook to Eurocode 2, Part 1.1: Design of concrete structures. London: Thomas Telford.

Booth, E and D. Key, 2006. Earthquake design practice for buildings (2nd edition). London: Thomas Telford.

Borzi, B and A.S. Elnashai, 2000. Refined force reduction factors for seismic design. Journal of Engineering Structures, (22): 1244-1260.

BS 8110, 1997. Code British Standard: Structural use of concrete. Part 1: Code of practice for design and construction.

CEN, 2002. Eurocode 1: Actions on structures. Part 1-1: General actions, densities, self weight, imposed loads for buildings, European Committee for Standardization, Brussels.

CEN, 2002. Eurocode: Basis of structural design, European Committee for Standardization, Brussels.

CEN, 2004. Eurocode 2: Design of concrete structures. Part 1-1: General rules and rules for buildings, European Committee for Standardization, Brussels.

CEN, 2004. Eurocode 8: Design of structures for earthquake resistance. Part 1: General rules, seismic actions and rules for buildings, Final Draft prEN 1998, European Committee for Standardization, Brussels.

Elghazouli, A.Y., 2009. Seismic design of buildings to Eurocode 8. New York: Taylor & Francis.

Elnashai, A.S and L.D. Sarno, 2008. Fundamentals of earthquake engineering. West Sussex: John Wiley & Sons Ltd.

Fardis, M.N., 2009. Seismic design, assessment and retrofitting of concrete buildings. London: Springer.

FEMA, 2007. NEHRP recommended provisions for new buildings and other structures, 2006 Edition, Design Examples, FEMA 451B, Building Seismic Safety Council for the Federal Emergency Management Agency, Washington D.C.

Gillie, J.L., A.R. Marek and M.D. Cole, 2010. Strength reduction factors for near-fault forward-directivity ground motions. Journal of Engineering Structures, (32): 273-285.

Hatzigeorgiou, G.D and A.A. Liolios, 2010. Nonlinear behaviour of RC frames under repeated strong ground motions. Soil Dynamics Earthquake Engineering, doi:10.1016/j.soildyn.2010.04.013.

Hatzigeorgiou, G.D and D.E. Beskos, 2009. Inelastic displacement ratios for SDOF structures subjected to repeated earthquakes. Journal of Engineering Structures, (31): 2744-2755.

Hatzigeorgiou, G.D., 2010. Behaviour factors for nonlinear structures subjected to multiple near-fault earthquakes. Journal of Computers and Structures, (88): 309-321.

Jalali, R.S and M.D. Trifunac, 2008. A note on strength-reduction factors for design of structures near earthquake faults. Journal of Soil Dynamics and Earthquake Engineering, (28): 212-222.

Jeffrey, C.C.L and M.K. Peng, 2011. Gathering of views and opinions on seismic investigations in Peninsular Malaysia – Report on the IEM workshop on earthquake (Part 1). Bulletin Jurutera October 2011: 44-47.

MOSTI, 2009. Seismic and tsunami hazards and risks study in Malaysia, Final Report.

Pappin, J.W., P.H.I. Yim and C.H.R Koo, 2011. An approach for seismic design in Malaysia following the principles of Eurocode 8. Bulletin Jurutera October 2011: 22-28.

Journal of Civil Engineering Research 2014, 4(3A): 130-134
DOI: 10.5923/c.jce.201402.22

Nonlinear Response of Low Rise Hospital RC Building in Malaysia Due to Far and Near Field Earthquake

Taksiah A. Majid[1], Mohd Irwan Adiyanto[2], Fadzli Mohamed Nazri[1,*]

[1]Disaster Research Nexus, School of Civil Engineering, Universiti Sains Malaysia, Penang, Malaysia
[2]Postgraduate Student, School of Civil Engineering, Penang, Malaysia

Abstract Geographically, Malaysia is situated in relatively far away from active seismic fault zones. Therefore, the earthquake hazard is not exist in Malaysian dictionary of life before the new century. Therefore, seismic consideration is not required in public buildings design. However, since a shock from a gigantic Mw 9.0 earthquake in Aceh, Indonesia on 26 December 2004, Malaysian authority and public citizen become aware of that hazard. The possibility to implement the seismic design start to be discussed at least for important structures such as bridge and dam. Hospital also cannot be ignored in discussion since the buildings is very important and must secure during disaster such as earthquake. This paper presents the study on the nonlinear response of three storey hospital reinforced concrete moment resisting frame designed for medium seismic region in Sabah, Malaysia. The typical frame had been designed according to Eurocode 8 for ductility class medium. The nonlinear response history analysis had been conducted on all five frames with far field and near field earthquake ground motion records as input. The result shows that the magnitude of interstorey drift ratio is strongly influenced by the value of behavior factor, q used in the design. The former is increases around 23% - 52% and 44% - 65% when subjected to the far field and near field earthquakes, respectively as the value of behavior factor, q is increases.

Keywords Hospital, Reinforced concrete, Eurocode 8, Bchaviour factor, Interstorey drift ratio

1. Introduction

Since the gigantic Mw 9.0 earthquake in Aceh, Indonesia on 26 December 2004 which also triggered tsunami in the Indian Ocean, Malaysian authority and public citizen start to rethink about the earthquake hazard toward the nation. After 10 years, the number of tremors which can be felt in Malaysian soil due to Sumatra Andaman and Philippines earthquakes is rising. A lot of researches had been conducted related the that field including the possibility of considering seismic design. According to Mosti report [1], it is worth to consider seismic design for construction of new structures located in medium to high seismic region. Experience from the past earthquakes gave a very useful lesson that hospitals and health care facilities are considered as the most important facilities which must remain safe and operable after the disaster [2]. Damages on the non-structural elements and equipment also can make the building inoperable. As an example, in the 1999 ChiChi Taiwan earthquake, the whole Shiu-Tuwan hospital was closed due to damages of non-structural elements even the damages on structure was not severe. After a significant earthquake, the victims turn to hospitals where they expect to receive treatment for any injuries during the event. Therefore, in every community's post disaster plan, hospitals require special attention and should be the safest place because people's lives depend on its functionality [3, 4].

To implement the seismic design in a developing country like Malaysia, the increment of cost also has to be taken into account. Due to economical reason, it is not practical to design structures that can behave elastically during earthquake [5]. This mean that the use of lateral force which had been derived based on elastic response spectrum for design purpose will result in very high cost of construction. Therefore, the concept of behaviour factor, q is proposed to reduce the force obtained from a linear analysis, in order to take into account the nonlinear response of a structure [6]. In American code [7], the concept of behaviour factor, q also proposed namely as force or strength reduction factor, R. The behaviour factor, q strongly influencing the class of ductility, namely as low, medium and high. According to Borzi and Elnashai [8], both European and American codes are too conservative where the ductility demand which corresponds to the behaviour factor, q is higher than the ductility supply. The forward directivity ground motions require smaller value of strength reduction factor, R compared to the non-forward directivity ground motions [9]. Therefore, Jalali and Trifunac [10] suggested that the simple and effective modification is needed to replace the current

* Corresponding author:
takziah@usm.my (Fadzli Mohamed Nazri)
Published online at http://journal.sapub.org/jce

value of behaviour factor, q.

This paper presents the nonlinear response of low rise hospital reinforced concrete (RC) building when subjected to the near and far field earthquakes. The typical three storey moment resisting frame (MRF) had been designed repeatedly based on different value of behaviour factor, q for ductility class medium (DCM). The seismic response is evaluated based on the value of interstorey drift ratio (IDR).

2. Material and Method

2.1. 2 Dimensional MRF Model

In this study, the nonlinear response history analysis had been conducted on the three storey RC MRF. A total of five typical model had been designed based on five different value of behaviour factor, q. According to Eurocode 8 [6], the value of behaviour factor, q for ductility class low (DCL) is equal to 1.5. for DCM structure, the value of behaviour factor, q lies in range of $1.5 < q < 5.85$ depend on the type of structure and material. The behaviour factor, $q \geq 5.85$ is used for the ductility class high (DCH). Therefore, the typical frame had been designed repeatedly based on five value of behaviour factor, q equal to 2.3, 3.1, 3.9, 4.7, and 5.5 for DCM. The typical frame is regular in plan and elevation where the floor to floor height is equal to 3.3 m for each stories. The frame is completed by three equal bays of 5.0 m. since this study focus on hospital building, the typical frame is classified into important class IV where the importance factor, γ_I used for design is equal to 1.4. All frames had been designed based on reference peak ground acceleration, a_{gR} equal to 0.12g to represent to the medium seismic region in Sabah, Malaysia [1, 11].

The size of beam located at top storey is equal to 250 mm x 550 mm while at the first and second storey is equal to 300 mm x 600 mm. The size for all columns is equal to 375 mm x 375 mm regardless its position either interior or exterior column. All five frames had been designed based on the aforementioned size of sections so that the dynamic characteristic of all frames is similar with fundamental period of vibration, T_1 equal to 0.5 sec. All frames had been designed with seismic provision based on Eurocode 8 [6] with concrete compressive strength, f_{cu} and steel yield strength, f_y is equal to 30 N/mm^2 and 500 N/mm^2, respectively. The detail of steel reinforcement for all frames can be found elsewhere [12].

Table 1. List of Selected Far Field Ground Motion Records

No	Event	Comp	Station	PGA [g]	PGV [cm/s]	Mw
1	Duzce	ATS 030	Ambarli	0.038	7.4	7.1
2	Duzce	ATS 030	Ambarli	0.025	7.1	7.1
3	Morgan Hill	A01040	58375 Apeel 1	0.046	3.4	6.2
4	Morgan Hill	A01310	58375 Apeel 1	0.068	3.9	6.2
5	Chi Chi	CHY069 N	CHY 069	0.039	10.3	7.6
6	Chi Chi	CHY069 W	CHY 069	0.047	10.9	7.6
7	Chi Chi	TAP026 N	TAP 026	0.073	14.3	7.6
8	Chi Chi	TAP026 E	TAP 026	0.077	11.7	7.6
9	Chi Chi	KAU074 N	KAU 074	0.028	10.0	7.6
10	Chi Chi	KAU074 W	KAU 074	0.032	6.7	7.6
11	Chi Chi	CHY054 N	CHY 054	0.097	19.3	7.6
12	Chi Chi	CHY054 W	CHY 054	0.094	17.9	7.6
13	Chi Chi	KAU010 N	KAU 010	0.034	16.6	7.6
14	Chi Chi	KAU010 W	KAU 010	0.034	11.3	7.6
15	Chi Chi	TAP006 N	TAP 006	0.071	14.1	7.6
16	Chi Chi	TAP008 N	TAP 008	0.061	14.2	7.6
17	Chi Chi	ILA042 W	ILA 042	0.085	21.6	7.6
18	Chi Chi	TAP014 N	TAP 014	0.073	19.4	7.6
19	Chi Chi	TAP095 W	TAP 095	0.098	18.8	7.6
20	Chi Chi	CHY090 W	CHY 090	0.079	14.5	7.6
21	Chi Chi	KAU063 W	KAU 063	0.039	12.5	7.6
22	Chi Chi	TAP013 E	TAP 013	0.094	19.7	7.6
23	Loma Prieta	MEN360	Foster City Menhaden Court	0.098	17.2	6.9
24	Loma Prieta	LKS360	Larkspur Ferry Terminal	0.12	18.6	6.9
25	Loma Prieta	TRI090	Treasure Island	0.13	20.1	6.9

2.2. Nonlinear Response History Analysis

In order to study the nonlinear response of low rise hospital RC MRF in Malaysia, the nonlinear response time history analysis had been conducted on all frames using Ruaumoko program [13]. The nonlinear response history analysis simulates the response of the frames when subjected to the real earthquake represented by dynamic load which varies against time. For that purpose, the program requires input in form of ground acceleration against time known as ground motion records. A total of 25 ground motion records which had been downloaded from PEER database [14] is shown in Table 1. The list of near field ground motion records can be found elsewhere [15].

All ground motion records were recorded on soft soil with shear wave velocity, Vs < 180 m/s. Before being assembled as input in Ruaumoko program, all ground motion records had been scaled based on the spectral acceleration with damping ratio of 5% at the fundamental period of vibration, $Sa(T_1,5\%)$. The scaling process was referred to the Type 1 response spectrum of Eurocode 8 [6] for Soil Type D developed based on the reference peak ground acceleration, a_{gR} as mentioned in previous subsection.

3. Result and Discussion

The action of earthquake induces lateral displacement on the structures. Large lateral displacement will cause damage to the non-structural and structural elements and then lead to collapse. Performance-Based Earthquake Engineering (PBEE) concept proposed four different performance level which might be experienced by structures due to action of earthquake load. The performance level is namely as Operational (OP), Immediate Occupancy (IO), Life Safety (LS), and Near Collapse (NC) [16]. All performance levels can be evaluated through the magnitude of IDR, which can be expressed as the relative lateral displacement between two adjacent stories normalized to its storey height. The magnitude of IDR equal to 0.5%, 1.0%, 2.0%, and 4.0% indicates the OP, IO, LS, and NC performance level, respectively. Hospitals and health care facilities are considered as the most important facilities which must remain safe and operable after the disaster [2]. Hence, such buildings should be categorized as IO performance level. According Eurocode 8 [6], the IDR for structures in important class IV, such as hospital in this study is limited to 1.25%.

Fig. 1(a) shows the distribution of IDR over the height of all three storey RC MRF used in this study when subjected to the far field earthquakes. Since a total of 25 ground motion records had been used in the nonlinear response history analysis, the magnitude of IDR presented here is the mean value. The frames designed based on lower behaviour factor, q experienced lower magnitude of IDR compared to the same frame designed with higher behaviour factor, q. For example, at the bottom storey, the IDR of frames designed with behaviour factor, q = 2.3 and q = 3.9 is equal to 0.56% and 0.72%, respectively. When designed based on behaviour factor, q = 5.5, the magnitude of IDR at same storey is rising to 0.85%. This trend is clear and indicates that frames designed with higher value of behaviour factor, q experienced larger lateral displacement compared to the frames designed with lower behaviour factor, q. This result is in good agreement with previous study which stated that the increase of force reduction factor, R always leads to an increase of the inelastic displacement ratio [17].

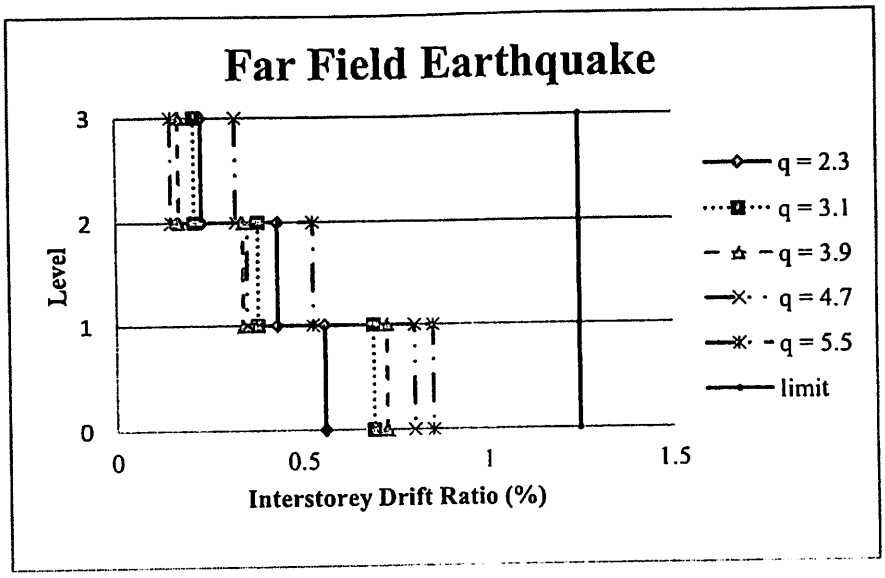

(a)

found that the magnitude of IDR caused by both far field and near field earthquakes is lower than the limit of 1.25% regardless the value of behaviour factor, q used in design. Therefore, in term of seismic performance, the design of all frames are acceptable. However, the design also has to consider the total cost of material which is discussed elsewhere [12].

4. Conclusions

This paper presents the study on the nonlinear response of three storey hospital RC MRF designed for medium seismic region in Sabah, Malaysia. The typical frame had been designed according to Eurocode 8 [6] for DCM. Five different value of behaviour factor, q had been used for designed which is equal to 2.3, 3.1, 3.9, 4.7, and 5.5. Then, the nonlinear response history analysis had been conducted on all five frames with far field and near field ground motion records as input. The following conclusions can be drawn from this study:

- The value of behaviour factor, q used in design strongly influencing the magnitude of IDR where the latter is increases as the former is increases and concentrated at the bottom storey.
- Due to far field earthquake, the magnitude of IDR is increases in range of 23% to 52% as the value of behaviour factor, q used in design is increases.
- Due to near field earthquake, the magnitude of IDR is increases in range of 44% to 65% as the value of behaviour factor, q used in design is increases.
- For all frames, it is observed that the action of near field earthquake caused greater IDR compared to the far field earthquake.
- In this study, the magnitude IDR for all frames is below than the limit regardless the type of earthquake ground motion records, either far field or near field. Therefore, the design of all frames is acceptable in term of seismic performance. The cost evaluation is needed to find the most economic design.

ACKNOWLEDGEMENTS

The authors gratefully acknowledge the facilities provided by Universiti Sains Malaysia and financial support from MyBrain15, a scholarship provided by Ministry of Education Malaysia to accomplish this study.

REFERENCES

[1] MOSTI. Seismic and tsunami hazards and risks study in Malaysia. Final Report, 2009.

[2] M. Hossain Nazer, and F. Nateghi Elahi. Seismic vulnerability of nonstructural components of hospitals. *Proc. of 13th World Conference on Earthquake Engineering.* Canada. 2004, paper no. 1250.

[3] J. Lewis, and M. Wang. Seismic risk mitigation of operational and functional components in hospitals – the British Columbia experience. *Proc. of 13th World Conference on Earthquake Engineering.* Canada. 2004, paper no. 1636.

[4] E.A. Tingatinga, and R.W. Arriesgado. Earthquake response analysis and simulation of sensitive hospital equipment in the Philippines. *Proc. of 15th World Conference on Earthquake Engineering.* Lisbon. 2012.

[5] FEMA NEHRP. Recommended provisions design examples, Topic 7: Concepts of Seismic-Resistant Design, FEMA 451B, *Building Seismic Safety Council for the Federal Emergency Management Agency.* 2006.

[6] CEN Eurocode 8. Design of structures for earthquake resistance, *Part 1: General rules, seismic actions and rules for buildings*, Brussels. 2003.

[7] ICC. International Building Code, United States of America. 2006.

[8] B. Borzi, and A. S. Elnashai. Refined force reduction factors for seismic design. *Engineering Structures.* 2000, 22: 1244 – 1260.

[9] J. L. Gillie, A. R. Marek, M. D. Cole. Strength reduction factors for near-fault forward-directivity ground motions. *Engineering Structures.* 2010, 32: 273 - 285

[10] R.S. Jalali, and M.D. Trifunac. A note on strength-reduction factors for design of structures near earthquake faults. *Soil Dynamics and Earthquake Engineering.* 2008, 28: 212-222.

[11] A. Adnan, Hendriyawan, A. Marto, P.N.N. Selvanayagam. Development of seismic hazard maps of east Malaysia. *Advances in Earthquake Engineering Applications.* 2008: 1-17.

[12] M.I. Adiyanto, T.A. Majid, F.M. Nazri. Cost optimization of seismic design of low rise hospital RC frame in Malaysia. *Submitted to the15th Asia Conference on Earthquake Engineering.* Taiwan. 2014.

[13] A.J. Carr. RUAUMOKO 2D-user manual for the 2-dimensional version. *Department of Civil Engineering, University of Canterbury,* Christchurch. 2007.

[14] Pacific Earthquake Engineering Research Center. *PEER strong motion database,* [accessed 08.12.13] *http://peer.berkeley.edu/smcat.*

[15] M.I. Adiyanto, and T.A. Majid. Seismic performance of three storey hospital RC frame subjected to multiple earthquake in moderate seismic region. *Proc. of International Congress on Natural Sciences and Engineering.* Kyoto. 2014.

[16] M.N. Fardis. *Seismic design, assessment, and retrofitting of concrete buildings.* Springer. New York. 2009.

[17] G.D. Hatzigeorgiou. and D.E. Beskos. Inelastic displacement ratios for SDOF structures subjected to repeated earthquakes. *Engineering Structures.* 2009, 31: 2744-2755.

Journal of Civil Engineering Research 2014, 4(3A): 154-158
DOI: 10.5923/c.jce.201402.27

The Effect of Site Classification on Incremental Dynamic Analysis for RC Buildings without Seismic Provision in Penang

Chee-Ghuan Tan[1,*], Taksiah A. Majid[2], Kamar Shah Arriffin[2], Norazura Mohamad Bunnori[1]

[1]School of Civil Engineering, Universiti Sains Malaysia, Penang, Malaysia
[2]School of Material and Mineral Resources, Universiti Sains Malaysia, Penang, Malaysia

Abstract Malaysia has been long term subjected to far field from neighboring country and local earthquake although it is not located in the active fault region. Local soil condition or site classification may play a major role in the soil dynamic characteristic correspond to the tremors. This study is to evaluate the effect of site classification on seismic response to the non-seismic design existing RC buildings in Penang. Five types of moment resistance RC building with 3, 8, 12, 16 and 20 storey are evaluated by using Incremental Dynamic Analysis (IDA). IDA result show that the non-seismic designed RC frames behaved low ductility and collapse at relatively lower IDR_{max} which between the performance level of Immediate Occupancy, IO (1%) and Life Safety, LS (2%). 20 storey buildings give the highest IDR_{max} followed by 8 storey buildings for every type of site classification. This phenomenon is more obvious in harder soil (Class B) and the effect reduces in softer soil condition by observing the slope reduction of the IDR_{max} vs T_1 curves.

Keywords Site classification, Incremental dynamic analysis, Maximum interstorey drift ratio

1. Introduction

Dynamic soil properties provide important information on the dynamic response of the soil structure needed for the dynamic structural analysis of superstructures. Local site classification always plays a major role in the seismic soil amplification of a site, a critical factor affecting the level of ground shaking [1]. Although Malaysia is not located close to the seismic prone area with active fault, buildings erected on soft soils often exposed to the far-field earthquakes generated from along Sumatran fault and subduction zones, particularly in areas on the west coast of Peninsular Malaysia, such as in Penang, Johor Bharu, and Kuala Lumpur [2, 3].

In the past 30 years, over 40 earthquakes originating from the Sumatra fault and subduction zone have been recorded in Penang, two of which are among the greatest earthquakes in the world [4]. Table 1 summarises the most recent significant earthquake events (MMI ≥ IV) that have been felt in Penang and have caused panic to the local citizens. Malaysian Meteorological Department has recorded that a series of local earthquakes (intra-plate fault) in Peninsular Malaysia and Sabah in the past 5 years as shown in Table 2.

Malaysia has been long term subjected to far field and local earthquake, this have been raised questions on the structural stability and the integrity of the existing building which is not designed seismically in Malaysia in tackling of the far field earthquakes effect from Sumatra and local earthquakes. The vulnerability of these non-seismic BS designed buildings either a distance earthquake originated from at Sumatra or local source may also increase due the low performance of its joint ductility. This study is to evaluate the effect of site classification on seismic response to the existing reinforced concrete (RC) buildings in Penang.

2. Consideration of Site Classification in Structural Analysis

2.1. Models

Five types of RC building with storey height of 3, 8, 12, 16 and 20-storey were selected for the analysis in this study. The selections of these buildings are intended to consider the low, medium and the high-rise buildings in order to cover the wider range of building's fundamental period from 0.2 s to 1.4 s in the analysis. The selected frame which has 2 bays framing and 3.0 m storey height was structurally designed by using EsteemPlus software. British Standard 8110 [5] was adopted as the design code since the aim of the study is to evaluate the seismic resistance for the non-seismic designed RC buildings in Malaysia. The design parameters for the RC building are tabulated in Table 3.

* Corresponding author:
tuc_khcon@hotmail.com (Chee-Ghuan Tan)
Published online at http://journal.sapub.org/jce

Table 1. Recent earthquakes (MMI ≥ IV) from the Sumatran fault and subduction zone experienced by Penang (Malaysian Meteorological Department)

No.	Earthquake location	Date	Epicenter Coordinate (°)	Focal depth (km)	Magnitude	Distance to Penang (km)
1	Northern Sumatera	17 July 2013	5.4, 98.0	40	5.5 (M_w)	250
2	Southern Sumatera	30 Sept 2009	-0.9, 99.7	91	7.6 (M_s)	680
3	Mentawai Trough	12 Sept 2007	-4.4, 101.1	50	6.9 (m_b)	1075
4	Mentawai Strait	14 May 2005	0.8, 98.2	63	6.7 (m_b)	550
5	Nias	28 Mar 2005	2.0, 97.3	47	8.7 (M_w)	490
6	Aceh	26 Dec 2004	3.2, 95.9	30	9.3 (M_w)	540

Table 2. Recent local earthquakes in Malaysia (Mb ≥ 3.8) (Malaysian Meteorological Department)

No.	Location	Date	Epicenter Coordinate (°)	Magnitude (M_b)
1	Baling	20 Aug 2013	5.6, 100.9	3.8
2	Tasik Temenggor	20 Aug 2013	5.4, 101.4	4.1
3	Kudat	23 July 2013	6.8, 117.8	4.2
4	Kunak	29 May 2012	4.6, 118.3	4.4
5	Lahat Datu	21 Aug 2010	5.4, 118.4	4.2
6	Bukit Tinggi	07 Oct 2009	3.4, 101.8	4.2

Table 3. Design parameter of RC frames

Design Parameter	Description
Code of Practice for RC	BS8110
Concrete grade for slab, beam and column	30 N/mm^2
Concrete grade for foundation	35 N/mm^2
Characteristic strength for main reinforcement	460 N/mm^2
Characteristic strength for stirrup and link	250 N/mm^2
Statutory live load	2.0 kN/m^2
Superimposed dead load as floor finishes	1.0 kN/m

Table 4. Expression for spring stiffness and their corresponding embedment factor for pile cap [6]

Mode	Stiffness Coefficient	Embedment factor
Horizontal	$K_x = \frac{GB}{2-\nu}[1.2+3.4\left(\frac{L}{B}\right)^{0.65}]$	$\beta_x = \left(1+0.21\sqrt{\frac{D}{B}}\right).[1+0.16(\frac{hd(B+L)}{BL^2})^{0.4}]$
Vertical	$K_z = \frac{GB}{1-\nu}[0.8+1.55\left(\frac{L}{B}\right)^{0.75}]$	$\beta_z = \left(1+\frac{D}{21B}\left(2+2.6\frac{B}{L}\right)\right).[1+0.32(\frac{d(B+L)}{BL})^{0.67}]$
Rotational	$K_\theta = \frac{GB^3}{1-\nu}[0.+0.47\left(\frac{L}{B}\right)^{2.4}]$	$\beta_\theta = 1+1.4(\frac{d}{L})^{0.6}\ [1.5+3.7\left(\frac{d}{L}\right)^{1.9}\left(\frac{d}{D}\right)^{-0.6}]$

Note: G is the effective shear modulus; ν is poisson's ratio; L is the length of the pile cap; B is the width of the pile cap; d is thickness of the pile cap; D is the embedment depth of the pile cap.

2.2. Soil-Structure Presentation

Pile foundations are considered since the buildings in this study consist of low, medium and high-rise buildings. According to Fema356 [6], the footing uncouple spring model shall be represented by a various spring stiffness in difference axes. The pile cap spring stiffness was expressed in the horizontal, vertical and rotational springs since the two dimensional frame were considered. The embedment of the pile caps are represented by the spring stiffness which is multiplied by the embedment factor according as shown in Table 4. The vertical axial spring stiffness, k_{sv} and rotational spring stiffness, k_{sr} of the pile group are shown in Table 5.

Table 5. Expression for spring stiffness of pile group [6]

Mode	Stiffness Coefficient
Axial spring stiffness	$K_{sv} = \sum_{n=1}^{N} \frac{AE}{L}$
Rocking spring stiffness	$K_{sr} = \sum_{n=1}^{N} k_{vn} S_n^{\,2}$

Note: A is cross-section area of a pile; E is modulus of elasticity of piles; L is length of piles; N is number of pile in group; k_{vn} is axial stiffness of nth pile; S_n is distance between nth pile and axis of rotation.

3. Incremental Dynamic Analysis

Incremental dynamic analysis (IDA) involves implementing a series of nonlinear time history analyses to a structure for multiple ground motion records by scaling every record to several levels of intensity to discover the full range of the structure's behaviour from elastic to yielding, nonlinear inelastic and eventually leading to global instability [7]. To comply with the minimum requirement of the codes, seven ground motions were used for the nonlinear time history analysis as tabulated in Table 6. Tan el al. [4] had concluded that the site classification of Penang consists of Soil Type B (V_s = 360 - 800 m/s), C (V_s = 180 - 360 m/s) and D (V_s < 180 m/s) as defined in Eurocode 8 [8], hence only ground motion records with these three soil types were selected. Moreover, far field ground motion records were selected due to the studied area only subjected to far field earthquakes. IDA carried out have covered (i) five types of fundamental period of moment resistance frame (MRF); (ii) four types of foundations (three flexible and one fixed); (iii) seven ground motions; (iv) fourteen types peak ground accelerations by using SAP2000. Total numbers of 1960 nonlinear time history analyses have been carried out in the IDA.

3.1. The Effect of the Site Classification on IDA

Figure 1 shows the IDA curves for 3, 8, 12, 16 and 20 storey buildings. Noted that the parameter of peak ground acceleration (PGA) was used as the intensity of seismic action in the IDA instead of the first mode spectral acceleration, Sa(T_1) because of PGA is more familiar and applicable to the academic and industry sectors in Malaysia. The results indicated that the increase of the building storey height and lower soil hardness had reduced the stiffness of the IDA curves. IDA curves show that buildings in Class D site have comparable much higher maximum interstorey drift ratios, IDR_{max} for the same PGA than other sites.

The typical performance levels and the associated damages state according to FEMA indicated that the concrete frame is expected to collapse at 3% to 4 % of the drift. However, all IDA curves found the non-seismic designed RC frames behaved low ductility and collapse at relatively lower IDR_{max} which between the performance level of Immediate Occupancy, IO (1%) and Life Safety, LS (2%). The discrepancy of this result can be explained by the finding of the Ghobarah [9]. He concluded that the drift limits in current available codes are found not suitable for the structures which designed without seismic detailing as in this study. The MRF of this structure behave in a non-ductile manner and often suffer in brittle failure modes due to poor confinement of lap splices, lack of shear reinforcement in the beam-column joint and inadequate embedment. More importantly, he had established the drift ratio limits associated with damage levels for various types of structures as shown in Table 7. His result concluded that the collapse of non-ductile MRF structures would happen at more than 1.0% IDR which fully support the finding of the current study.

3.2. IDR_{max} with Respective to Storey Height RC Buildings

IDR_{max} versus building fundamental period (T_1) with respect to various site classification and PGA are plotted as shown in Figure 2. The T_1 for 3, 8, 12, 16 and 20 storeys are 0.236 s, 0.567 s, 0.824 s, 1.071 s and 1.333 s, respectively. It noted that the maximum PGA plotted in these graphs are up to 0.7 g, 0.4 g and 0.125 g for Class B, Class C and Class D, respectively. The results show that the 20 storey buildings give the highest IDR_{max} followed by 8 storey buildings for every type of site classification. This phenomenon is more clearly observed in harder soil (Class B) and the effect reduces as the soil become soft by observing the slope reduction of the curves.

Table 6. Selected far-field ground motion records for nonlinear time history analysis (PEER)

No.	Earthquake	Year	Magnitude (M_w)	PGA (g)	Depth (km)	V_{s30} (m/s)	Time step size (s)	No. of time step
1	Morgan Hill	1984	6.2	0.067	8.5	158.80	0.005	5665
2	Hector Mine	1999	7.1	0.194	5.0	271.40	0.02	3000
3	Whittier Narrows	1987	6.0	0.038	14.6	332.80	0.02	1834
4	Landers	1992	7.3	0.119	7.0	370.80	0.02	2000
5	Northridge	1994	6.7	0.153	17.5	405.20	0.01	2999
6	Northridge Aftershock	1994	5.5	0.044	6.0	508.10	0.02	1000
7	N. Palm Springs	1986	6.1	0.099	11.0	684.90	0.005	4077

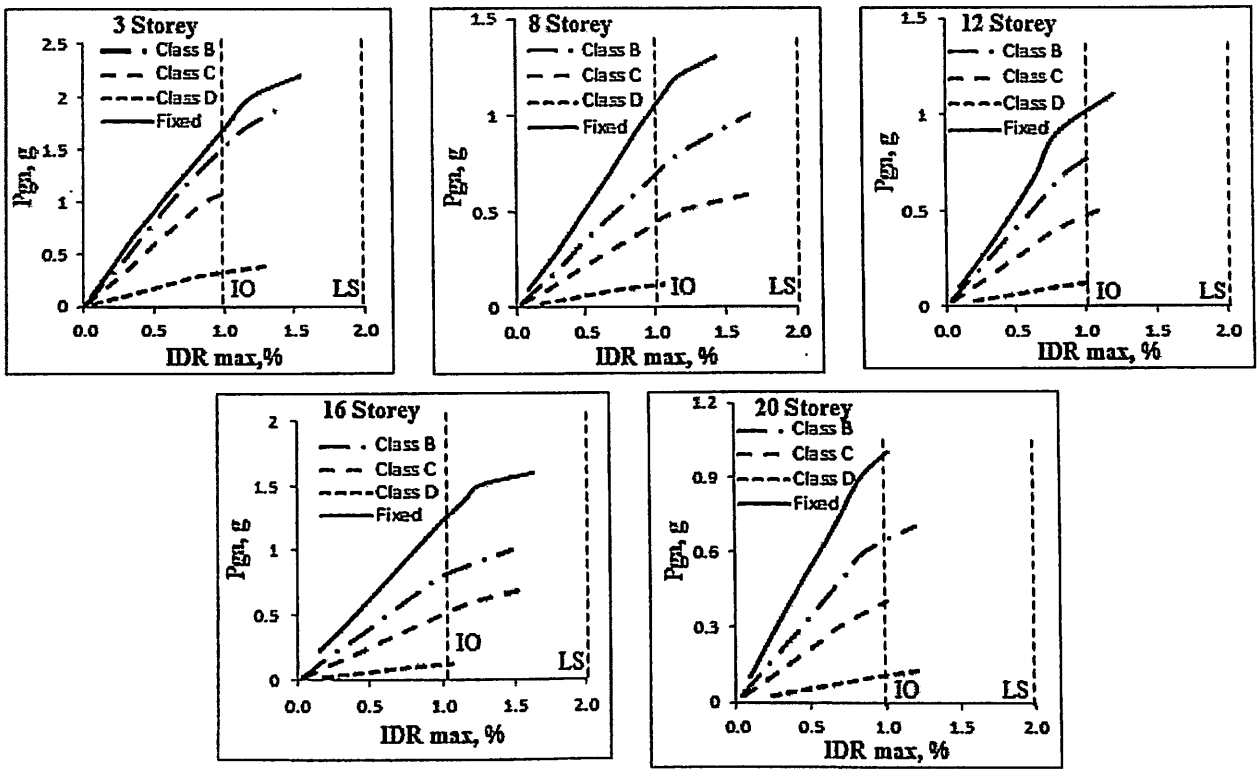

Figure 1. IDA curves for 3, 8, 12, 16 and 20 storey buildings

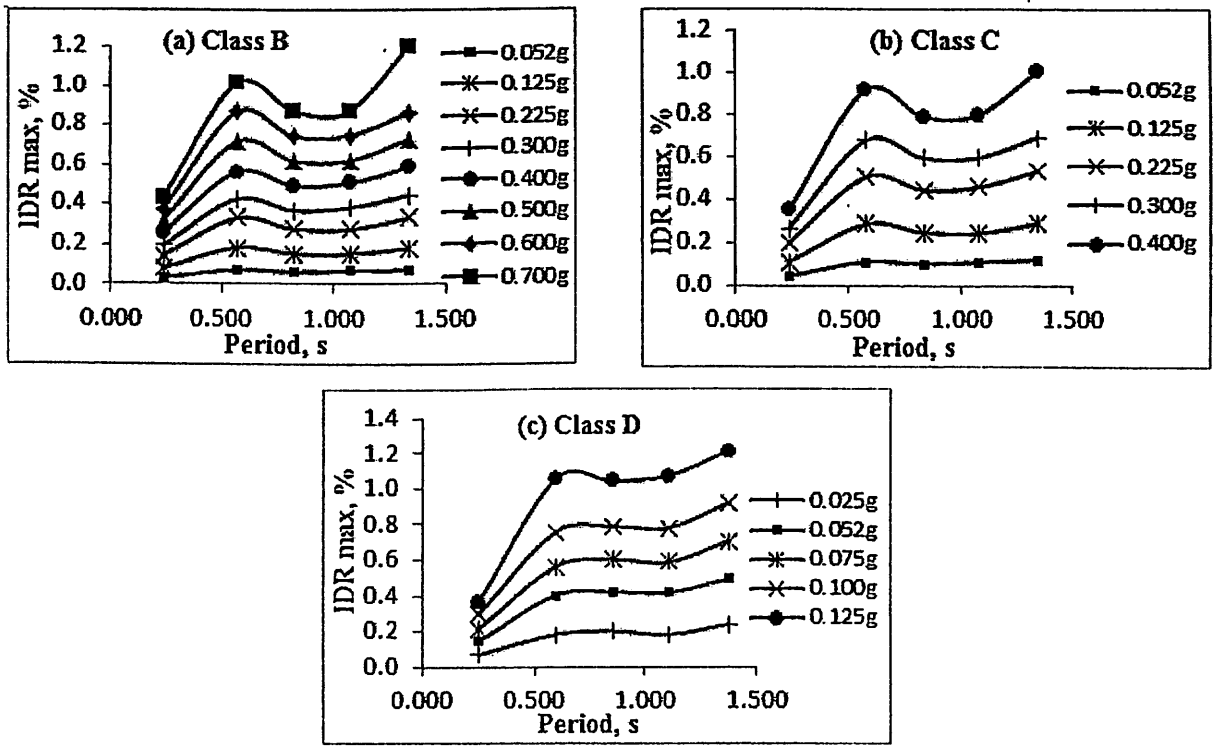

Figure 2. The IDR_{max} plot with respect to T_1 of the buildings for (a) Class B, (b) Class C and (c) Class D

Table 7. IDR_{max} associated with various damage level [%] [9]

State of Damage	Ductile MRF	Non-ductile MRF	MRF with Infills	Ductile Walls	Squat Walls
No Damage	< 0.2	< 0.1	< 0.1	< 0.2	< 0.1
Repairable Damage	< 1.0	< 0.5	< 0.4	< 0.8	< 0.4
Irreparable Damage	> 1.0	> 0.5	> 0.4	> 0.8	> 0.4
Severe Damage	1.8	0.8	0.7	1.5	0.7
Collapse	> 3.0	> 1.0	> 0.8	> 2.5	> 0.8

4. Conclusions

Total numbers of 1960 nonlinear time history analyses have been carried out to produce the IDA curves for 3, 8, 12, 16 and 20 storey non-seismic designed RC buildings. IDA curves found the non-seismic designed RC frames behaved low ductility and collapse at relatively lower IDR_{max} which between the performance level of Immediate Occupancy (1%) and Life Safety, LS (2%). This may due to the non-seismic resistance RC structure behave in a non-ductile manner and often suffer in brittle failure modes due to poor confinement of lap splices, lack of shear reinforcement in the beam-column joint and inadequate embedment. IDA results shows that the 20 storey buildings (T_1 = 1.33 s) give the highest IDR_{max} followed by 8 storey buildings (T_1 = 0.57 s) for every type of site classification.

ACKNOWLEDGEMENTS

This study was sponsored by the Postgraduate Research Grant Scheme provided by Universiti Sains Malaysia. The authors would like to extend their gratitude to the Ministry of Education of Malaysia for the permission to collect MASW data from primary and secondary schools in the study area.

REFERENCES

[1] R.U. Maheswari, A. Boominathan, and G.R. Dodagoudar, Seismic site classification and site period mapping of Chennai City using geophysical and geotechnical data. *J. Appl. Geophys.*, 2010. 72(3): pp. 152-168. DOI: 10.1016/j.jappgeo.2010.08.002.

[2] A. Adnan, et al., Seismic hazard assessment for Peninsular Malaysia using Gumbel Distribution Method. *Jurnal Teknologi*, 2005. 42 (B): pp. 57-73.

[3] H. Husen, et al. Development of design response spectra based on various attenuation relationships at specific location. *International Conference on Construction and Building Technology*. Kuala Lumpur, Malaysia 2008 pp. 511-518.

[4] C.G. Tan, et al., Seismic microzonation for Penang using geospatial contour mapping. *Natural Hazards*, 2014.DOI: 10.1007/s11069-014-1093-8.

[5] British Standard 8110, *Part 1. Structural use of concrete: Code of Practice for Design and Construction*, 1997: Milton Keynes.

[6] FEMA356, *Prestandard and Commentary for the Seismic Rehabilitation of Buildings*, in *Federal Emergency Management Agency* 2000: Washington, D. C.

[7] D. Vamvatsikos and C.A. Cornell, Direct estimation of seismic demand and capacity of multidegree-of-freedom systems through incremental dynamic analysis of single degree of freedom approximation. *Journal of Structural Engineering*, 2005. 131(4): pp. 589-599.

[8] CEN., *Eurocode 8: Design of structures for earthquake resistance. Part 1: General rules, seismic actions and rules for buildings*, 2004, European Committee for Standardization: Brussels.

[9] A. Ghobarah. On Drift Limits Associated with Different Damage Levels. *International Workshop on Performance-Based Seismic Design*. McMaster University 2004.

ICETI 2012

Proceedings of the International Conference on Engineering and Technology Innovation 2012

November 2-6, 2012
Kaohsiung, Taiwan

International Journal of Engineering and Technology Innovation (IJETI, ISSN Print: 2223-5329, ISSN Online: 2226-809X) is an international, multidiscipline, peer-reviewed scholarly journal, published quarterly for researchers, developers, technical managers, and educators in the field of engineering and technology Innovation. Articles of original research, reports, reviews, and commentaries are welcomed by IJETI. The goal of this journal is to provide a platform for scientists and academicians all over the world to promote, share, and discuss various new issues and developments in all areas of engineering and technology innovation.

All manuscripts must be prepared in English, and are subject to a rigorous and fair peer-review process. Decisions will be made as rapidly as possible, and the journal strives to return reviewers' comments to authors within 6 weeks. Currently, *there are no page charges for authors*. Accepted papers will immediately appear online followed by printed hard copy. The journal publishes original papers including but not limited to the following fields:

- Automation Engineering
- Civil Engineering
- Control Engineering
- Electric Engineering
- Electronic Engineering
- Green Technology
- Information Engineering
- Mechanical Engineering
- Material Engineering
- Mechatronics and robotics Engineering
- Nanotechnology
- Optic Engineering
- Sport Science and Technology
- Other Engineering and Technology related topics

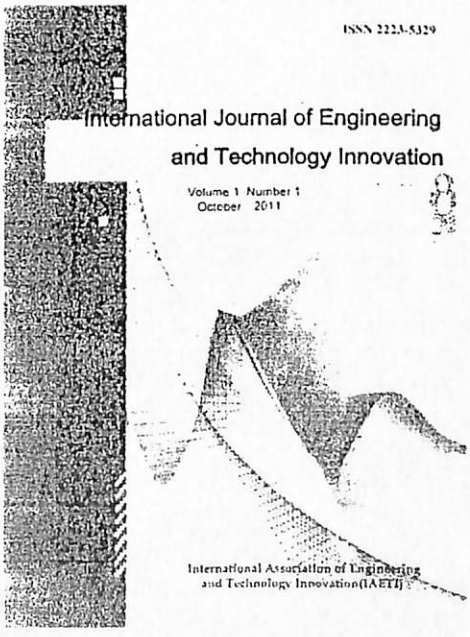

For more information, please visit http://sparc.nfu.edu.tw/~ijeti

Publisher: *Taiwan Association of Engineering and Technology Innovation* (TAETI)

Oral Sessions I
13:00~15:00

3F Room D (Rose)	3F Room E (Orchid)	3F Room F (Narcissus)
D1.Computer & Information Engineering *Chih-Chien Yang, National Taichung University of Education, Session Chair* *Shu-Ching Wang, Chaoyang University of Technology, Co-Chair*	**E1. Computer & Information Engineering Intelligent Computing and Application** *Hsiang-Chuan Liu, Asia University, Session Chair* *Yen-Lin Chen, National Taipei University of Technology, Co-Chair*	**F1. Green Technology & Civil Engineering Nanotechnology** *Chung-Fah Huang, National Kaohsiung Univ. of Applied Sciences, Sessioin Chair* *Yit-Jin Chen, Chung Yuan Christian University, Co-Chair*
D1-1. 13:00	E1-1. 13:00	F1-1. 13:00
F1001 - Reaching Agreement in a Dual Fallible Cluster-based Wireless Sensor Network *Shu-Ching Wang, Kuo-Qin Yan, Chin-Ling Ho, Shun-Sheng Wang*	M1043 - A Critical Review into the Evolution of Japanese Project Management: A Comparative Approach *Foon Siang Low, Heap Yih Chong*	G1012 - Effects of Site Classification on Empirical Correlation between Shear Wave Velocity and Standard Penetration Resistance for Soils *Chee-Ghuan Tan, Taksiah A. Majid, Kamar Shah Ariffin, Norazura Mohamad Bamori*
D1-2. 13:12	E1-2. 13:12	F1-2. 13:12
F1011 - An Adaptively-guiding Web-based E-learning System Based on Competency-based Learning Theory *Wei-Chih Hsu, Cheng-Hsin Li*	F1025 - JokerBot - An Android-Based Botnet *Ruei-Min Jiang, Jia-Sian Jhang, Fu-Hau Hsu, YanLing Hwang, Peiwen Huang, Yung-Hoh Shen*	G1020 - Seismic Analysis of the Condensate Storage Tank in a Nuclear Power Plant *Wei-Ting Lin, Meng-Hsin Hsieh, Yuan-Chieh Wu, Chin-Cheng Huang*
D1-3. 13:24	E1-3. 13:24	F1-3. 13:24
V1008 - An Implementation Model of RFID Information Security and Privacy *Chih-Yung Chen, Jih-Fu Tu*	F1308 - Modulations of Amplitude in Acoustical Heritage *Chen Kim Lim, Kian Lam Tan, Abdullah Zawawi Talib*	G1019 - Energy Consumption and Potential Retrofitting of Rest and Service Areas (RSAs) in Malaysia Case Study *R. Zakaria, F. Ainee, K.S.Foo, M. Z. Abd. Majid, R. Mohamad Zin, M. R. Hainin, H. Yaacob, A. Adnan, H Md. Nor, N. Hamzah, S. O. Babubaid, A. N. Mazlan, Ismail M. A., Y. S. Yazid, H. Haidar, N. Aifa, M. BujangHasrul Haidar Ismail, Norhaliza Hamzah, Muhd Zaimi Abd. Majid*
D1-4. 13:36	E1-4. 13:36	F1-4. 13:36
F1014 - Neighbor-Index Method for Continuous Window Queries over Wireless Data Broadcast *Jun-Hong Shen, Ching-Ta Lu, Ming-Shen Jian*	F17033 - Video Quality Adjustment Model Supporting Mobility for Seamless Multimedia Service Delivery *Suh, Dongjun*	G1028 - Evaluation of Tip Capacity Analysis Model for Drilled Shafts in Gravelly Soils *Yit-Jin Chen, Maria Cecile M Marcos, Tsu-Hung Chu, Hao-Wei Wu*
D1-5. 13:48	E1-5. 13:48	F1-5. 13:48
F1016 - Defend a System against Keyloggers with a Privilege-limited Account *Chien-Wei Hung, Fu-Hau Hsu, Shih-Jen Chen, Yan-Ling Hwang, Chang-Kuo Tso, Li-Pin Hsu*	N1026 - Supply Chain Pricing Strategy for Short-lived Ramp-type Demand Models *Yini Lin*	G1035 - Curriculum Innovation for Fostering Green Building Literacy in General Education *Ko-Yu Shiao, Ming-Liang Lin, Qua-Cheng Sung*
D1-6. 14:00	E1-6. 14:00	F1-6. 14:00
F1021 - Full Multiplexers Implementation of Dual Basis Multiplier over GF(2^m) *Hung Wei Chang, Che Wun Chiou, Wen-Yew Liang and Jeng-Haur Wang*	N1033 - Building a Post-search Academic Search Engine based on a Serial of Clustering Methods *Lin-Chih Chen*	G1036 - Establishment of a Removable Experiment Platform for VAWT *Sheam-Chyun Lin, Fu-Sheng Chuang, Harki Apri Yanto*

Analytical Simulation of Axial Behavior of RCFT Wall

Jiho Moon[1], Dawn E. Lehman[2], Heejung Ko[1], Hak-Eun Lee[1]

[1]*School of Civil, Environmental & Architectural Engineering, Korea University, Seoul, South Korea.*
[2]*Department of Civil & Environmental Engineering, University of Washington, Seattle WA, USA.*

Abstract

Rectangular concrete-filled tubes (RCFTs) have been widely used as columns of building and piers due to several advantages such as their strength-to-size efficiency and facilitation of rapid uction. Recently, some researchers have tried to use RCFT as a wall system in a building. RCFT ave a high aspect ratio while the aspect ratio of the RCFT column is usually one. Thus, the or of the RCFT wall is clearly different from that of RCFT column and it needs to be investigated. study, the axial behavior of the RCFT wall was investigated through analytical simulation, and ects of the aspect ratio, internal stud, and through rebar on axial behavior of the RCFT wall were ed. From the results, it was found that axial load capacity is decreased with increasing aspect ue to local buckling of the steel tube, and this local buckling can be efficiently prevented by using through rebar. Finally, long-term behavior of RCFT wall under axial load was discussed.

rds: RCFT, Composite structure, Analytical simulation, Finite element analysis.

fects of Site Classification on Empirical Correlation between Shear Wave Velocity and Standard Penetration Resistance for Soils

Chee Ghuan Tan[1], Taksiah A. Majid[2], Kamar Shah Ariffin[3], Norazura Mohamad Bunnori[1]

[1]*School of Civil Engineering, Universiti Sains Malaysia, Penang, Malaysia.*
Disaster Research Nexus, School of Civil Engineering, Universiti Sains Malaysia, Penang, Malaysia.
[3]*School of Material and Mineral Resources, Universiti Sains Malaysia, Penang, Malaysia.*

Abstract

n seismic engineering, the dynamic property of the soil is one of the most important aspects in response analysis. Dynamic property is significantly affected by local soil deposits. Shear wave (V_s) of soil is one of the main parameters in determining the amplification factor on ground It is not economically feasible to measure V_s for all sites. Therefore, a reliable empirical ion between V_s and standard penetration resistance (N_{spt}) will be useful since N_{spt} data are easily ble in construction industry. This study aims to develop an empirical correlation between V_s and all soils by considering the effect of site classification according to the Uniform Building Code. pirical correlations for all soils are presented in this study and well compared with the previous evaluate prediction capability. Results show that site classification has a significant impact on estimation, and that the proposed correlations are the most appropriate for estimating the V_s n the studied area compared with existing correlations.

rds: Shear wave velocity profile, Multichannel analysis of surface wave (MASW), Standard ion resistance, Empirical correlation.

Effects of Site Classification on Empirical Correlation between Shear Wave Velocity and Standard Penetration Resistance for Soils

Chee Ghuan Tan[1, a], Taksiah A. Majid[2, b], Kamar Shah Ariffin[3, c] and Norazura Mohamad Bunnori[1,d]

[1] School of Civil Engineering, Universiti Sains Malaysia, Penang, Malaysia

[2] Disaster Research Nexus, School of Civil Engineering, Universiti Sains Malaysia, Penang, Malaysia

[3]School of Material and Mineral Resources, Universiti Sains Malaysia, Penang, Malaysia

[a] tuc_kheen@hotmail.com, [b] taksiah@eng.usm.my, [c] kamarsha@eng.usm.my, [d] cenorazura@eng.usm.my

Keywords: Shear wave velocity profile, Multichannel analysis of surface wave (MASW), Standard penetration resistance, Empirical correlation.

Abstract. In seismic engineering, the dynamic property of the soil is one of the most important aspects in ground response analysis. Dynamic property is significantly affected by local soil deposits. Shear wave velocity (V_s) of soil is one of the main parameters in determining the amplification factor on ground surface. It is not economically feasible to measure V_s for all sites. Therefore, a reliable empirical correlation between V_s and standard penetration resistance (N_{spt}) will be useful since N_{spt} data are easily obtainable in construction industry. This study aims to develop an empirical correlation between V_s and N_{spt} for all soils by considering the effect of site classification according to the Uniform Building Code. New empirical correlations for all soils are presented in this study and well compared with the previous study to evaluate prediction capability. Results show that site classification has a significant impact on the V_s estimation, and that the proposed correlations are the most appropriate for estimating the V_s profile in the studied area compared with existing correlations.

Introduction

In seismic engineering, the most important aspect is determining the dynamic properties of the soil structure. Dynamic soil properties provide important information on the dynamic response of the soil structure needed for the dynamic structural analysis of superstructures. Local soil structure also plays a major role in the seismic soil amplification of a site, a critical factor affecting the level of ground shaking [1]. However, the lack of understanding on the geological information of the site often leads to structural and environmental failure. Field measurement of shear wave velocity (V_s) includes cross-hole test, down-hole test, suspension logging, seismic reflection, seismic refraction, and surface wave. However, surface wave test is a simpler and more efficient technique compared with other in-situ tests used in measuring V_s. It is not economically feasible to conduct the surface wave test at all sites. Hence, a reliable empirical correlation between V_s and standard penetration resistance (N_{spt}) will be useful since N_{spt} data are easily obtainable in the construction industry. Many researchers have been proposed an empirical correlation for V_s based on a standard penetration test. However, these empirical correlations are region-specific and cannot be applicable to all regions.

In contrast to the existing correlations, the current paper presents the development of correlations between V_s and N_{spt} by considering the effect of site classification according to the Uniform Building Code (UBC) (Table 1) on soil in Penang, located at the northwestern area of peninsular Malaysia. Measurement of the V_s profile was carried out extensively using Multichannel Analysis of Surface Waves (MASW) at the site where N_{spt} data are available. Based on statistical assessment and site classification, empirical correlations for V_s and N_{spt} were developed and compared with the existing correlations from previous studies to evaluate the prediction capability of the correlations.

Table 1: UBC Site Classification

Site class	Soil type	V_{s30} [m/s]
Class A	Hard rock	$V_{s30} > 1500$
Class B	Rock	$760 \leq V_{s30} \leq 1500$
Class C	Very dense soil/soft rock	$360 \leq V_{s30} \leq 760$
Class D	Stiff soil	$180 \leq V_{s30} \leq 360$
Class E	Soft soil	$V_{s30} < 180$
Class F	Soils requiring site specific evaluation	Non-applicable

Geology of study area

The total area of Penang Island is approximately 300 km^2 and is composed entirely of Pre-Quaternary granite locally covered with unconsolidated sand, silt, and clay of the Pleistocene and Holocene ages (Fig. 1). It has no sedimentary rocks and most of the island is underlain by igneous rocks (also called granite). Generally, the granite hills are raised from the sea to the highest point at 830 m from seawater level, except where Pleistocene and Holocene deposits are found. The Pleistocene deposits are found on the slopes and at the foot of granite hills, consisting of the products of weathering from granite. Sand, gravel, clay, silt, and peat of Pleistocene age were laid down by fluvial processes as channel fill, over-bank, and flood-basin deposits [2].

Surface Wave Method

Surface wave geophysical methods have been used for many years by researchers and engineers in soils and foundation applications. These methods not only provide the properties of soils, but are also used to determine the dynamic properties of soils, particularly the soil's shear wave velocity profile and shear modulus. These properties are key parameters in predicting the soil response and soil-structure systems to seismic loading [3]. Surface wave methods offer advantages over other surface-based in-situ seismic techniques because they are rapid, cost-effective, noninvasive, and have the ability to detect a low-velocity layer underneath a higher-velocity layer of deposit, thus providing more accurate site characterization.

Field Test Set up and Procedure

MASW tests were carried out using Geometrics 24 channels seismograph (Geode) with single geode operating software (SGOS). A total of 24 units of vertical geophones with 4.5 Hz natural frequency were used to receive the wave signal generated by an active source of 8 kg sledgehammer vertically hit on a striker plate. Geophones were deployed linearly with equal spacing, ranging from 0.5 m to 2 m interval as suggested by Maheswari [1]. The nearest source to the geophone offsets is in the range of 5 m to 15 m to meet the requirement of different types of soil hardness suggested by Xu et al. [4]. The field configuration of MASW is illustrated in Fig. 2.

Development of Empirical Correlations for V_s and N_{spt}

Conducting an in-situ test to determine the V_s profile is always preferable, but it is not economically feasible to conduct at all sites. A reliable empirical correlation between V_s and N_{spt} will be an advantage. Several existing correlations have been proposed as listed in Table 2.

Proposed Empirical Correlation between V_s and N_{spt} by considering the UBC Site Classification

In this study, an analysis of 40 sites was carried out through MASW in the development of empirical correlations between V_s and N_{spt} values using simple regression analysis. The new empirical correlations with their correlation coefficient (r^2) for three site classifications are proposed as follows:

$$V_s = 128.05\, N^{0.4081}\ (r^2 = 0.73),\ \text{Class C} \qquad (1)$$

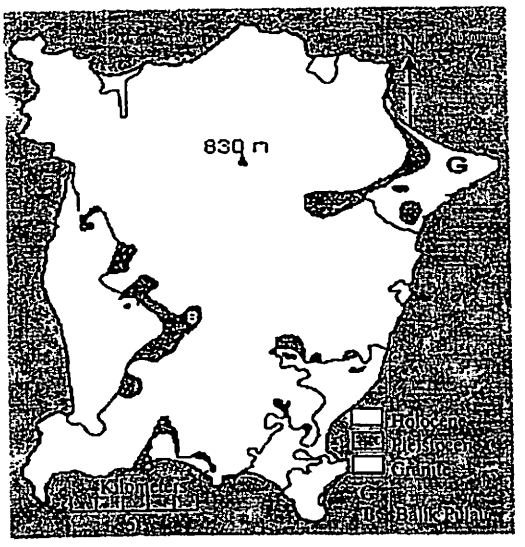

Fig. 1 Geological map of studied site

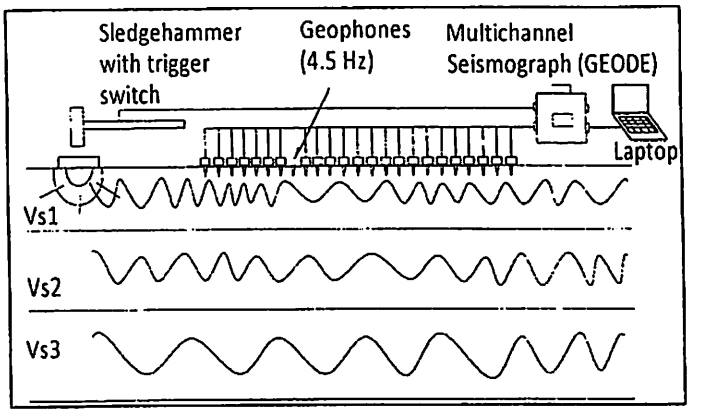

Fig. 2 The field configuration of MASW

$V_s = 128.71\ N^{0.2833}$ ($r^2 = 0.65$), Class D (2)

$V_s = 101.34\ N^{0.2364}$ ($r^2 = 0.83$), Class E (3)

The correlations curve from Eqs. 1 to 3 and their raw data were plotted (Fig. 3) to investigate the effect of site classification. In Fig. 3, site classification is indicated to have a significant effect on these correlations. The great differences between these correlations were not only due to the specific geotechnical conditions of the studied site, the quantity of processed data, and the procedures used in undertaking the MASW test, but were also significantly affected by the site classification. Class C consistently gave the highest value of V_s as N_{spt} increased followed by classes D and E. The V_s predicted from Eqs. 1 to 3 were compared with the measured V_s as presented in Fig. 4. The data were scattered between lines 1:0.5 and 1:2 slopes.

Table 2 Existing correlations for V_s and N_{spt}

No	Author (year)	Correlation
1	Imai and Yoshimura (1970)	$V_s = 76N^{0.33}$
2	Ohsaki and Iwasaki (1973)	$V_s = 82N^{0.39}$
3	Seed and Idriss (1981)	$V_s = 61N^{0.5}$
4	Athanasopoulos (1995)	$V_s = 108N^{0.36}$
5	Jafari et al. (1997)	$V_s = 22N^{0.85}$
6	Kiku et al. (2001)	$V_s = 68.3N^{0.292}$
7	Hasancebi and Ulusay (2006)	$V_s = 90N^{0.309}$
8	Hanumantharao and Ramana (2008)	$V_s = 82.6N^{0.43}$
9	Maheswari et al.(2008)	$V_s = 95.6N^{0.301}$
10	Dikmen (2009)	$V_s = 58N^{0.39}$
11	Maheswari and Boominathan (2009)	$V_s = 95.6N^{0.301}$
12	Mhaske and Choudhury (2011)	$V_s = 72N^{0.4}$

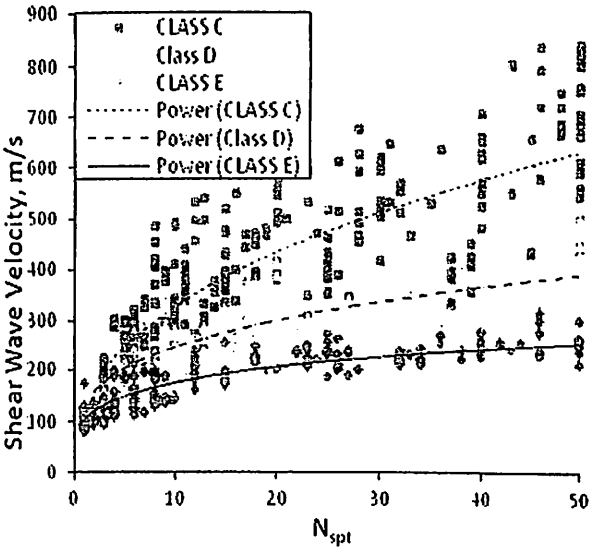

Fig. 3 Correlations for V_s and N_{spt} for all soils with Class C, Class D, and Class E site classification

Comparative Study with Published Correlation

The proposed correlations for three site classifications of all soils were compared with the carlier correlations proposed by various researchers (Fig. 5). The correlations proposed by researchers such as Imai and Yoshimura [5], Kiku et al. [6], Hasancebi and Ulusay [7], Maheswari et al. [8], Dikmen [9], Maheswari and Boominathan [10], and Mhaske and Choudhury [11] yielded similar results with the Class E correlation proposed in the current study. In comparison, correlations proposed by Ohsaki and Iwasaki [12], Athanasopoulos [13], and Hanumantharao and Ramana [14] yielded similar with Class D. The correlation of Seed and Idriss [15] generally under predicted V_s for $N_{spt} \leq 32$ and those over predicted V_s for $N_{spt} > 32$ compared with Class D correlation. The correlation presented by Jafari et al. [16] yielded lower V_s values for $N_{spt} \leq 13$ and $N_{spt} \leq 24$ but over predicted V_s values for Nspt > 13 and $N_{spt} > 24$ of Classes E and D, respectively. However, its correlation approaches Class C correlation when the N_{spt} increased to 50. Note that none of the previous correlations yielded similarly with Class C correlation. This result made sense because, normally, researchers are more interested in sites that produce higher soil amplification factor or cause higher damage to buildings (Class D and Class E) during earthquakes.

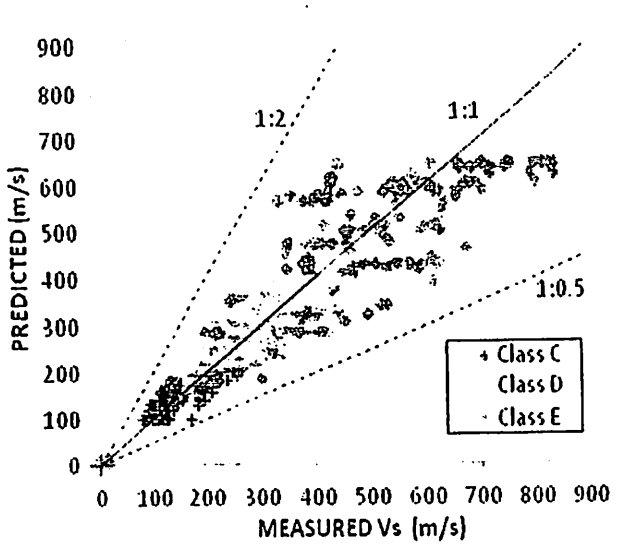

Fig. 4 Measured and predicted V_s for all soils with Class C, Class D, and Class E site classification

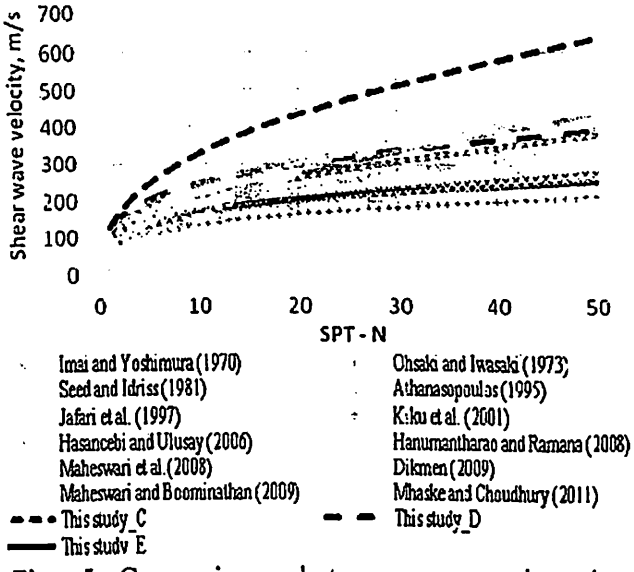

Fig. 5 Comparisons between proposed and previous correlations for all soils

Scaled Percent Error versus Cumulative Frequency

To further investigate the prediction capability of the proposed correlations, the scaled percent errors versus cumulative frequency were also drawn (Fig. 6). The scaled percent error (in per cent) is given by

$$SPE = [(V_{sc} - V_{sm})/V_{sm}] \times 100 \quad (4)$$

where V_{sc} and V_{sm} are predicted and measured V_s, respectively. As depicted in Fig. 6, V_s estimated by Eq. 2 [Fig. 6(a)] is approximately 80% of the V_s values predicted within ± 20% error margin, whereas Eq. 3 [Fig. 6(b)] is approximately 75%. Note that the comparison for Eq. 1 is not shows here because none of the previous correlations yielded similarly with Class C correlation. Generally, the proposed empirical correlations in this study have better estimation power than the existing correlations in the studied site.

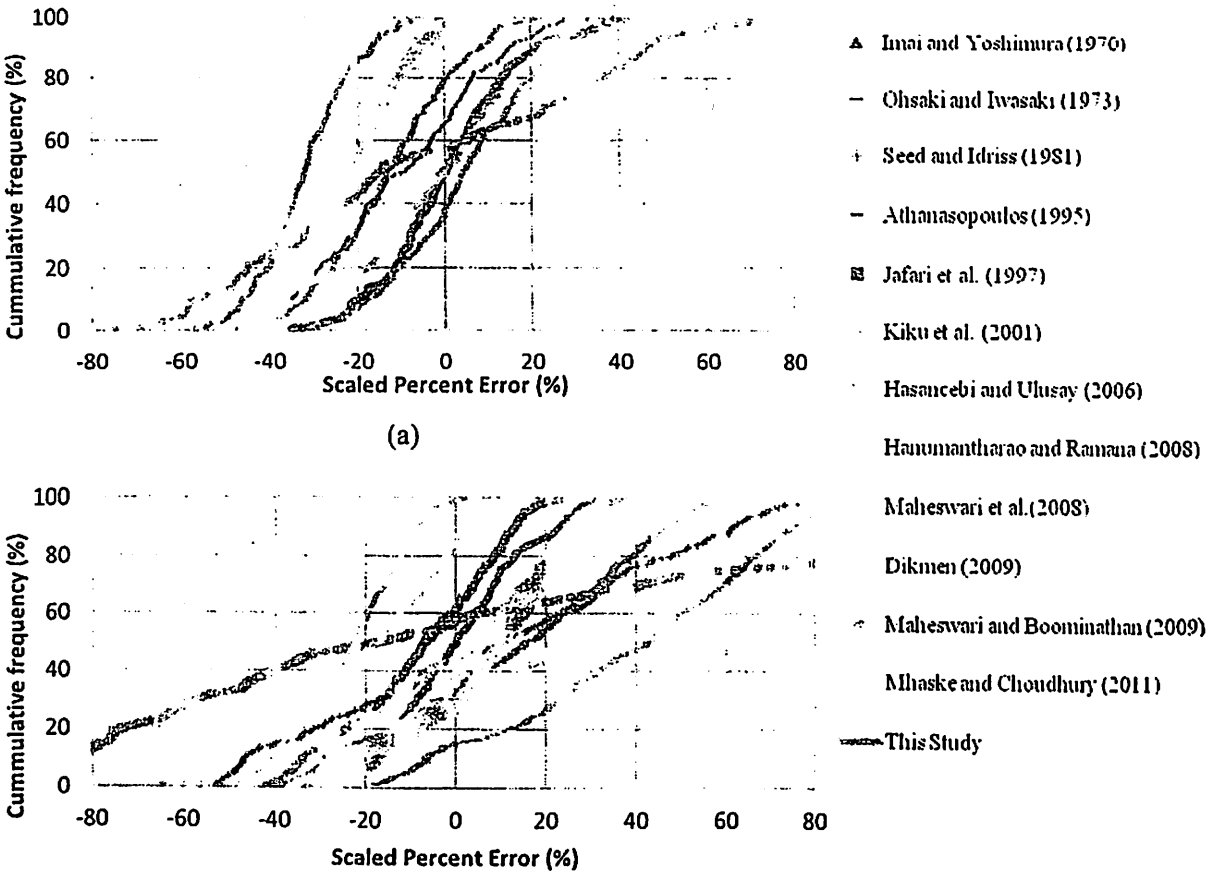

Fig. 6 Scaled percent error of V_s predicted for (a) Class D and (b) Class E

Conclusion

In summary, an extensive measurement of V_s employing the MASW geophysical technique was carried out for the Penang region. The correlations between V_s and N_{spt} for all soils with three site classifications, Class C, Class D, and Class E, were developed. Results proved the previous finding that N_{spt} is the main parameter in determining V_s. Site classification was also found to have a significant effect on these correlations. Besides site classification, the differences between proposed and existing correlations are also due to specific geotechnical conditions of the studied sites, the quantity of the processed data, and the procedures in undertaking the geo-seismic surveys. The proposed correlations in this study compare well with the previous existing correlations and exhibit good prediction capability. Therefore, the proposed correlations for all soils are recommended for use in the studied area. The developed correlations for all soils can be effectively utilized for seismic microzonation studies of the northwest region of peninsular Malaysia. However, these correlations are generally site-specific and should be verified against the measured V_s values before being used.

Acknowledgements: This study was supported by the Postgraduate Research Grant Scheme given by Universiti Sains Malaysia. The authors would like to extend their gratitude to the Ministry of Education of Malaysia for permission to collect data from both primary and secondary schools.

References

[1] R.U. Maheswari, A. Boominathan, and G.R. Dodagoudar: Journal of Applied Geophysics Vol. 72 (2010), p. 152-168.

[2] F.W. Colbourne: Tsunami Impact on the West Coast of Penang Island, Malaysia, M.S. in Physical Sciences, Emporia State University (2005)

[3] R.a.J. Luna, H. , in: First International Conference on the Application of Geophysical and NDT Methodologies to Transportation Facilities and Infrastructure, St. Louis, MO (2000).

[4] Y. Xu, J. Xia, and R.D. Miller: Journal of Applied Geophysics Vol. 59 (2006), p. 117-125.

[5] T. Imai and Y. Yoshimura: Tsuchito-Kiso Vol. 18 (1970), p. 17-22.

[6] H. Kiku, et al., in: ICSMGE/TC4 Satellite Conference on Lessons Learned From Recent Strong Earthquakes, (2001).

[7] N. Hasancebi and R. Ulusay: Bulletin of Engineering Geology and the Environment Vol. 66 (2006), p. 203-213.

[8] R. Uma Maheswari, A. Boominathan, and G. Dodagoudar, in: The 14th World Conference on Earthquake Engineering, Beijing, China (2008).

[9] Ü. Dikmen: Journal of Geophysics and Engineering Vol. 6 (2009), p. 61-72.

[10] R. Uma Maheswari, A. Boominathan, and G.R. Dodagoudar: Geotechnical and Geological Engineering Vol. 28 (2009), p. 119-137.

[11] S.Y. Mhaske and D. Choudhury: Natural Hazards Vol. 59 (2011), p. 317-327.

[12] Y. Ohsaki and R. Iwasaki: Soil Found Vol. 13 (1973), p. 61-73.

[13] G.A. Athanasopoulos, in: Proceedings of 7th International Conference on Soil Dynamics and Earthquake Engineering, A.S.Ç. Akmak, Computational Mechanics, Southampton, Chania, Crete (1995).

[14] C. Hanumantharao and G. Ramana: Journal of Earth System Science Vol. 117 (2008), p. 719-730.

[15] H.B. Seed and I.M. Idriss: ASCE National Convention (MO) Vol. (1981), p. pp. 481–544.

[16] M.K. Jafari, A. Asghari, and I. Rahmani, in: Proceedings of 4th International Conference on Civil Engineering, Tehran, Iran (1997).

Awam International Conference on Civil Engineering (AICCE'12)
Geohazard Information Zonation (GIZ'12)
Park Royal Penang Resort 28th – 30th August 2012

Seismic performance of 3 storey irregular reinforced concrete (rc) frames under repeated earthquakes

Hamed Fazli#, Taksiah A. Majid
Disaster Research Nexus, School of Civil Engineering, Universiti Sains Malaysia

Abstract

Earthquake resistance is one of the most important factors for designing a building in the seismic prone area in order to reduce the earthquake damage on buildings. After earthquake events, the number of damage on buildings with setback is increases, which exhibit inadequate behaviour though they were designed according to the current state of knowledge existing in seismic codes. Most analysis will be carried out based on single earthquake as recommended by codes of practices. In reality, this is not the case, in which earthquake can occur repeatedly in the life span of the buildings.This paper studies three storeys 2D frames with regular three storeys 2D (RC) frames and irregular in elevation (setback) (RC) frame, under repeated earthquakes. Non-linear time history (dynamic) seismic analyses of buildings were employed in this paper. The seismic performance is based on the estimation of important structural parameters such as displacements and inter-storey drifts. Results of single ground motion were compared with repeated earthquakes while the regular frame was compared with irregular frame in terms of maximum lateral displacement and inter-storey drift ratio. This paper shows that regular and irregular structures which were subjected to repeated earthquakes produce higher responds than single ground motions in term of displacement demand.

Keywords: Reinforced concrete; Irregular structure, Dynamic analysis, time history analysis, inter-storey drift ratio.

1. Introduction

Earthquakes occur when a sudden energy is released by shifting and sliding the earth tectonic plates. Earthquakes usually occur as a series of shocks and not as a single event. Repetition may destroy buildings that were damaged by the main shock. One of the main causes of failure of a building due to earthquakes is the irregularity configurations on the structures either in plan or elevation. The inelastic analysis of structures requires a non-linear dynamic time-history procedure in addition to the elastic response that is up to collapse [1].Seismic ground motions commonly chosen for the design of structure depend on sensibility of a site, engineering structure and analyses [2]. The earthquake may occur sequential and it is difficult to predict the frequency of the earthquake. The certain displacement of structure is due to the first wave of earthquake that will hit the structure. Another incoming earthquakes causes the permanent displacements are cumulate and the maximum displacement was increased [3].

Dynamic inputs are defined as a ground motion acceleration time-history which is applied regularly at all the points of the structure's base [4]. More accurate results can be obtained by analysing the structure time-history analysis and response spectrum analysis[5]. The accuracy of nonlinear dynamic time history analysis in simulating the proper behaviours of structures under earthquake actions has been accepted since 1960s. Researched by [6] performed an extensive parametric research on the inelastic response and they found that the earthquake damage for repeated earthquakes is higher than that for single ground motions.

2. Methodology

Structural models data such as the designed cross-section of columns and beams, live loads and dead loads were obtained from [6]. Regular and Irregular elevation frames were labelled

#Corresponding author e-mail: hamed.fazli62@gmail.com

as A and B, and models are presented in Fig. 1 and Fig. 2, respectively. The storey heights assumed in the model are 3 m for the first storey and top stories. The dimensions of columns are 30/30 cm. The depth of beams is 30 cm and the height of beams is 40 cm.

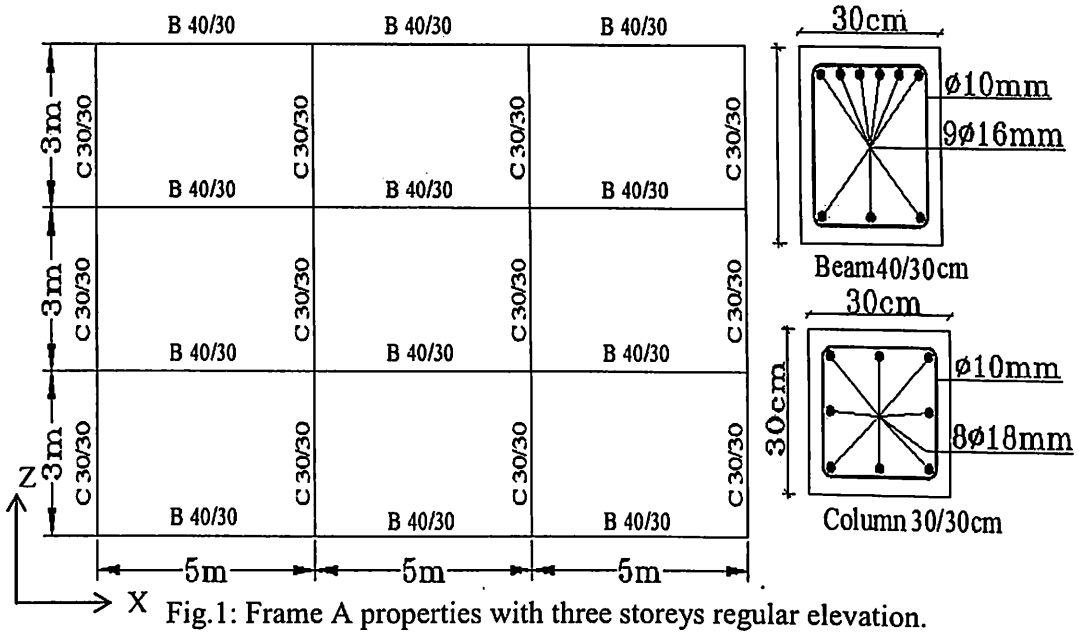

Fig.1: Frame A properties with three storeys regular elevation.

The live loads are equal to10 kN/m while the dead loads excluding the self-weight are equal to 20 kN/m. The compressive strength for concrete grade C20 is 20 MPa whereas both the longitudinal and transverse reinforcements yield strength is 500MPa. All the models consist of 3 bays with a total length of 15m. Only moment-rotation with displacement controlled is used to model hinge for all members[7].The regular and irregular frame are assumed situated at a high-seismicity area in Europe that take into consideration the gravity and seismic loads[6].

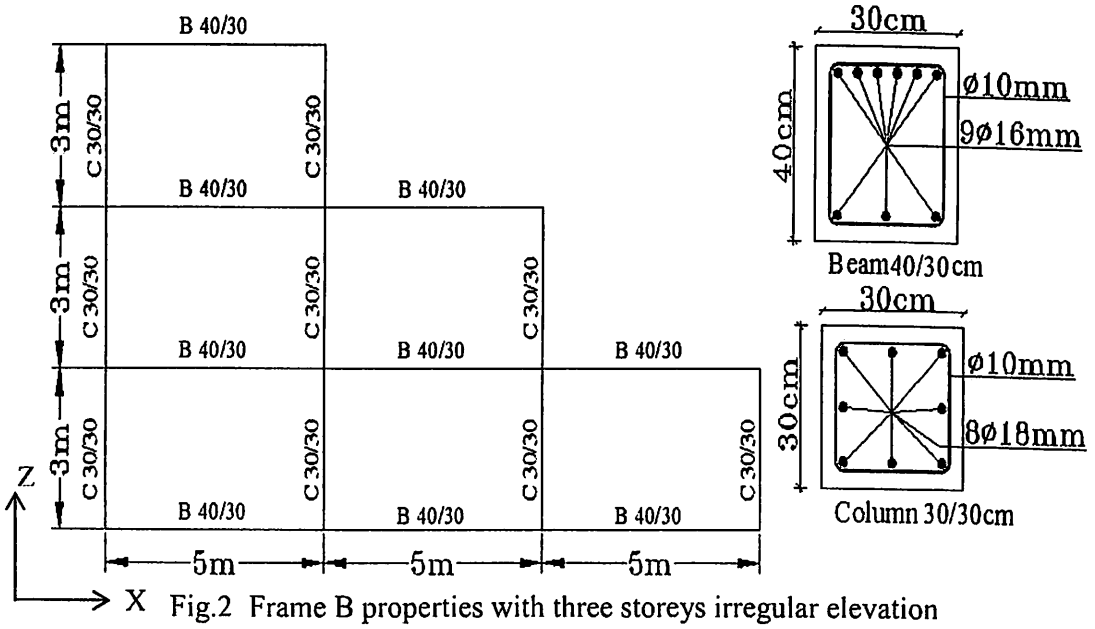

Fig.2 Frame B properties with three storeys irregular elevation

2.1 Description Input Motion

Seven ground motions in horizontal position that have different effect on the structure were utilized in this paper as input motion. The ground motion acceleration data can be obtained from international centers such as NGA-PEER database of University of California, Berkeley, ISESD (European Commission Project Site).The complete list of earthquakes is shown in Table 11 which is selected from earthquake with magnitude equal or more than 4.85. Also all ground motions were recorded compatible with the soil class B, the selected earthquakes are based on the selected ground motions[6].

Table 11: Ground motions for model

No.	Seismic sequence	Station	Comp.	Date	Time	ML	PGA (g)
1	Anza	Mountain center	360	2001-10-31	07:56	4.92	0.1042
2	Bishop	Creek - Surface	360	1984-11-23	18:08	5.82	0.1091
3	El Alamo	Centro Array #9	270	1956-02-09	14:33	6.80	0.0457
4	Gilroy	Gilroy	67	2002-05-14		4.90	0.2310
5	Imperial Valley	Centro Array #9	90	1938-06-06	02:42	5.00	0.0158
6	Imperial Valley	Centro Array #9	270	1940-05-19	04:37	6.95	0.2584
7	Mammoth Lakes	Lakes (CON)	270	1980-06-11	04:41	4.85	0.1902

Two cases of ground motion, single ground motion and repeated earthquakes were considered in this paper. Fore shock and aftershock scale factor is 0.8526 which based on the Gutenberg-Richter law for fore and aftershock ground motion [8]. Table 1 shows the combination scale of the two cases. The time gap of 100s between each repeated earthquakes was used in this study as proposed by [6].

$$N = 10^{A-BM} \tag{1}$$

where N is the number of events in a given magnitude range, M the magnitude range and A and B are coefficients, with the first one indicating the total seismicity rate of the examined region and the second one being normally equal to 1.0 [8].

Table 1: Combination of ground motion

Case	Combination Scale		
Case 1	0.00	1.00	0.00
Case 2	0.8526	1.00	0.8526

3. Element and plastic hinge properties

Element properties such as plastic moment at columns and beams are required as the inputs to be defined in the software. Plastic moment was considered for idealized and ultimate moment of each element. The CONSEC Programme [9] was used in this study to perform concrete section analysis for reinforced concrete members with or without embedded steel shapes.

Nonlinear force-displacement characteristics of frame elements can be modelled as hinges. Hinges can be defining at any number of locations such as potential yielding points along the span of the frame element as well as element ends. Non-linear behaviour of the beams and columns at both ends of the structural members were modelled by moment-rotation plastic hinges. Fig. 3 shows the tri-linear moment rotation relationship that is utilized in this study.

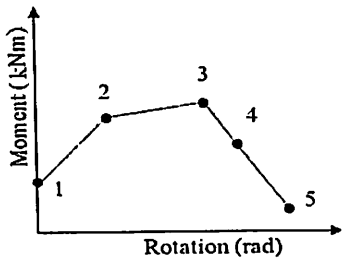

Fig. 3: Moment rotation relationship

The 5 points of moment rotation relationship shown in Fig. 3, where the first three points that are in increasing trend are the cracking concrete points.

1- The point at cracking of concrete (CR)

2- The point at yielding of reinforcement (Y)

3- The point at maximum moment (M)

4- The point at Near collapse (NC)

5- The point at Total collapse (assuming the point is 0.01 of the yield strength)

4. Results and discussions

4.1 Maximum lateral displacements:

The average values of Maximum lateral displacements in X-direction for three storey frame are presented in Fig. 4a and Fig.1b - 4b.The effect of ground motion repetition in X-direction can be observed clearly.

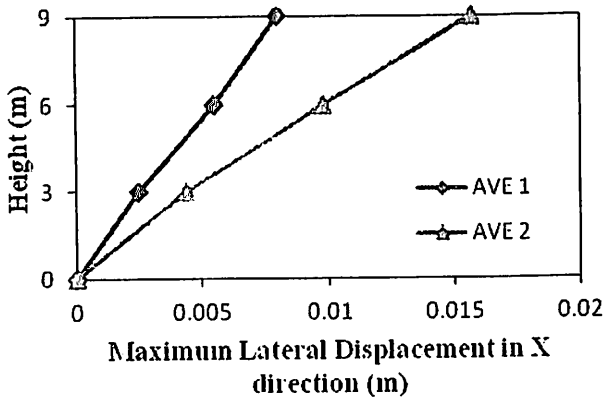

Fig.1a: Irregular three storey frame

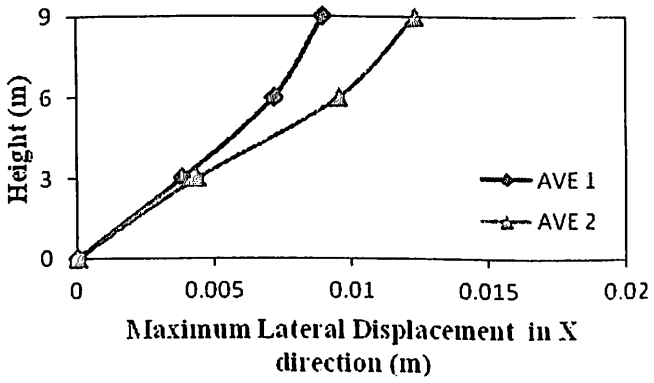

Fig.1b: Regular three storey frame

The results from time history analysis show that the maximum lateral displacement in X-direction for repeated earthquakes (AVE 2) is 27.02% higher than maximum lateral displacement in X-direction subjected to single ground motion (AVE 1). Likewise, the maximum lateral displacement in X-direction for irregular frames in repeated earthquakes

(AVE 2) is 48.77% higher than the single ground motion (AVE 1). Also results shown that the repeated earthquakes effect on irregular frame are 21.75% higher than the regular frame.

In any seismic case under consideration due to the repeated earthquakes, the displacement demands are increased. It is well known that inelastic flexible systems for single strong earthquakes, present permanent displacements. Thus, for any other oncoming earthquake, the permanent displacements are cumulated and therefore the maximum displacement obviously will be increased.

4.1 Inter-storey drift ratio:

Inter-storey drift ratio is defined as the lateral displacement difference of one floor with the adjacent floor (inter-storey drift) divided by the height of the storey. Figure 5a and 5b show the results of inter-storey drift ratio in X-direction for seismic single ground motions and repeated earthquakes.

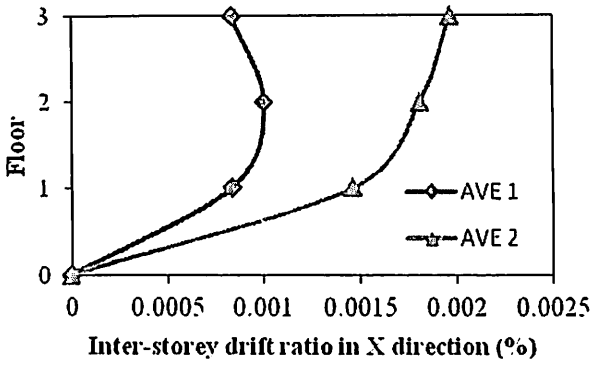

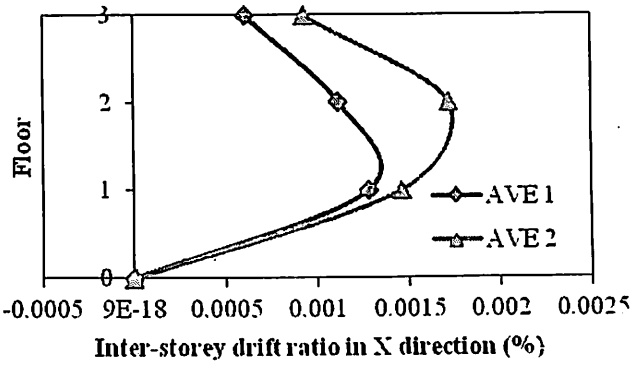

Fig.5a: Irregular three storey frame

Fig.5b: Regular three storey frame

For irregular three storey frame under single ground motion (AVE 1) the maximum inter-storey drift ratio with the mean value is 0.001 while the maximum inter-storey drift ratio for repeated earthquakes is about 0.0019 (AVE 2) and 49% higher than single ground motion. **Error! Reference source not found.**Figure 5a and 5b show that the maximum inter-storey drift ratio for regular three storey frame under single ground motion (AVE 1) with the mean value is 0.0012 and the inter-storey drift ratio under repeated earthquakes (AVE 2) is 0.0017 and 25.67% higher than single ground motion. This shows that the repeated earthquakes have higher effect on the response of structure as the inter-storey drift ratio increases when the single ground motion is changed to repeated earthquakes. Also time history results shown that the repeated earthquakes effect on irregular frame are 23.33% higher than the regular frame in terms of inter-storey drift ratio.

5. Conclusions

The maximum displacements in X-direction show significant difference between single ground motion and repeated earthquakes on regular and irregular structures. It is clearly shown that the repetition of earthquake motion has crucial effects on the damage or failure of the structures. The repeated earthquakes give the significant effect to the displacement in X-direction. Lateral displacement of the repeated earthquakes is higher than the single earthquake. Findings from this paper showed that, repeated earthquakes give the increment of 27% maximum lateral displacement for regular three frame and the value for the maximum displacement in X-direction of irregular frame under repeated earthquakes is 21.15% higher than single ground motion.

The results of time history analysis show that the maximum inter-storey drift ratio for regular and irregular frames is higher under repeated earthquakes compared to single ground motion. It is evident that repeated earthquakes leads to a higher inter-storey drift ratio as compare to the single ground motion.

6. Acknowledgement

This study was supported by the RU Grant (1001/PAWAM/814115) given by Universiti Sains Malaysia.

7. References

[1] CHOPRA, A.K., Dynamics of structures: theory and applications to earthquake engineering. 1995, Englewood Cliffs, N.J.: Prentice Hall; London: Prentice-Hall International (UK), p. 729.

[2] KRINITZSKY, E.L. 2002. How to obtain earthquake ground motions for engineering design. Engineering Geology, Vol. 65(1), pp.1-16.

[3] HATZIGEORGIOU, G.D. 2010. Behavior factors for nonlinear structures subjected to multiple near-fault earthquakes. Computers & Structures, Vol. 88(5-6), pp.309-321.

[4] ATHANASSIADOU, C.J. 2008. Seismic performance of R/C plane frames irregular in elevation. Engineering Structures, Vol. 30(5), pp.1250-1261.

[5] LEE, D.G. AND H.C. KIM. 1996. Efficient seismic analysis of multi-story buildings. Structural Engineering and Mechanics, Vol. 4(5), pp.497-511.

[6] HATZIGEORGIOU, G.D. AND A.A. LIOLIOS. 2010. Nonlinear behaviour of RC frames under repeated strong ground motions. Soil Dynamics and Earthquake Engineering, Vol. 30(10), pp.1010-1025.

[7] DOLSEK, M. 2010. Development of computing environment for the seismic performance assessment of reinforced concrete frames by using simplified nonlinear models. Bulletin of Earthquake Engineering, Vol. 8(6), pp.1309-1329.

[8] HATZIGEORGIOU, G.D. AND D.E. BESKOS. 2009. Inelastic displacement ratios for SDOF structures subjected to repeated earthquakes. Engineering Structures, Vol. 31(11), pp.2744-2755.

[9] MATTHEWS, R.C., Program Documentation for CONSEC® Concrete Section Analysis Program 2004-2005, structsource: California, USA.

Proc. of the Intl. Conf. on Advances in Civil, Structural, Environmental & Bio-Technology -- CSEB 2014

ISBN: 978-1-63248-001-9 doi: 10.15224/ 978-1-63248-001-9-02

Effect of behavior factor on column design of reinforced concrete frame

[Mohd Irwan Adiyanto, Taksiah A. Majid]

Abstract— Generally, Malaysian citizen are very fortunate because their country is situated relatively far away from active seismic fault zones. Hence, seismic consideration is not taken into account in Malaysian construction industry. However, after experiencing tremors from Sumatra Andaman and Philippines earthquakes which caused vibration on buildings, local authority start to consider about implementing seismic design for new buildings. Since have very limited experience in dealing with seismic design, there is some uncertainties among engineers about level of ductility and behavior factor, q to be used and their effect on cost of material. This paper investigated the difference of steel reinforcement when seismic provision is considered in reinforced concrete design of general office building. A total three regular moment resisting frame had been designed based on Eurocode 8 with various level of behavior factor, q for ductility class medium. From this study, it is observed that the level of behavior factor, q is strongly influencing the cost of steel reinforcement where the decrement of cost is in range of 22.1 to 42.5% lower compared to the highest one.

***Keywords*—seismic design, Eurocode 8, ductility, reinforced concrete, column**

I. Introduction

Current practice among engineers in Malaysia to design reinforced concrete (RC) structures is still by referring to BS 8110 [1] which not includes any seismic provision. This is reasonable because Malaysia is situated relatively far away from active seismic fault zone. Therefore, only gravitational load had been considered for low rise buildings. However, in the last 10 years, several tremors originating from Sumatra Andaman earthquakes had been felt in Malaysian Soil and induced vibration on buildings. Started by a large earthquake on December 2004, Nias 2005, until the latest one which just occurred on 2nd July 2013 in Aceh, Malaysian citizens start to worry about this hazard. Within the same period, seismic events originating from Bukit Tinggi, Pahang were reported to have been felt in various parts of the country [2]. Therefore, the Malaysian Public Work Department (JKR) suggested that it was worthwhile to consider seismic design input for new buildings. Since have very limited experiences in seismic design, the engineers faced a lot of uncertainties to implement it in Malaysia. In term of ductility, the ductility class low (DCL) or ductility class medium (DCM) may be recommended for Peninsular Malaysia [3].

In seismic design, engineers have to deal with a concept known of behavior factor, q. According to Eurocode 8 [4], it is a factor which used for design purposes to reduce the forces obtained from a linear analysis, in order to account for the nonlinear response of a structure. The same concept also exists in American code which known as force or strength reduction factor, R [5]. Both concepts are promoted so the structures are designed to behave inelastically due to tremors for economical reason [6]. The level of behavior factor, q to be used in design depends on the material, type of structures and class of ductility. For RC moment resisting frame structures with DCM, the level of behavior factor, q is lies in range of 1.5 to 4.5 [4]. However, over the past few years, there are several scientific evaluation and comment on the level of behavior factor, q proposed by the code. Borzi and Elnashai [7] had concluded that both European and American standards are too conservative where the ductility demand which corresponds to the behavior factor, q is higher than the ductility supply. It is also found that the strength reduction factor, R resulting from forward directivity ground motions is smaller than those from non-forward directivity ground motions [8]. When subjected to repeated earthquake, maximum storey ductility demand of low rise RC building depends on the level of behavior factor, q [9]. According to Pappin et. al, [10] using higher level of behavior factor, q resulting in lower seismic design forces but leads to ductile detailing.

This paper investigated the difference of steel reinforcement required in RC column design when seismic load is considered. A regular three storey RC frame for hospital use had been designed for DCM with various level of behavior factor, q. The comparison of flexural and shear reinforcement in column is presented.

II. Analysis Procedure

In this study, a 2 dimensional moment resisting frame of three storey RC building regular in plan and elevation had been used as model. The frame is designed for hospital use with typical storey height of 3.3 m and three equal bays of 5.0 m as shown in Figure 1. This frame is modified from two storey RC model which had been used in previous work [11,

Mohd Irwan Adiyanto
Universiti Sains Malaysia
Malaysia
irwano_07@yahoo.com

Taksiah A. majid
Disaster Research Nexus, Universiti Sains Malaysia
Malaysia
Taksiah@eng.usm.my

Proc. of the Intl. Conf. on Advances in Civil, Structural, Environmental & Bio-Technology -- CSEB 2014

ISBN: 978-1-63248-001-9 doi: 10.15224/ 978-1-63248-001-9-02

12]. The frame had been designed repeatedly with various level of behavior factor, q for DCM. Three different level of behavior factor, q had been used for design which is equal to 1.5, 3.0 and 4.5. As a result, a total three frames with different design had been produced for comparison. In term of material, the design process was performed based on concrete compressive strength, f_{cu} = 30 N/mm^2 and yield strength of steel, f_y = 500 N/mm^2. To maintain the dynamic characteristic of the frame, similar size of section for columns and beams had been used for all three frames. Therefore, the size of column is equal to 375 mm x 375 mm while the size of beam at two lower storeys is assigned as 300 mm x 600 mm. For top storey, smaller size of beam with 250 mm x 550 mm had been used. Based on modal analysis, the fundamental period of vibration, T_1 for all frames is equal to 0.50 second.

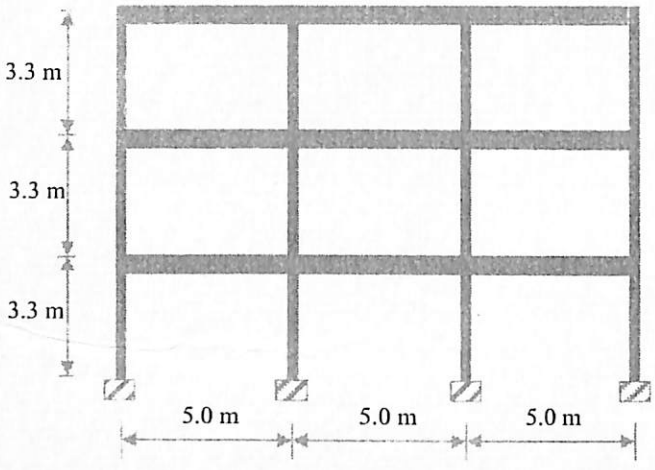

Figure 1: Elevation of three storey typical RC frame model

In order to get the magnitude of bending moment, shear force, and axial load for design of RC elements, the lateral force method analysis as proposed by Eurocode 8 [4] had been performed on each frame. In this method, the total earthquake action on building is represented by lateral load named as base shear force, F_b which had been determined using (1):

$$F_b = S_d(T_1) \cdot m \cdot \lambda \quad (1)$$

where $S_d(T_1)$, m, and λ correspond to the ordinate of the design spectrum at period T_1, the total mass of the building above the foundation or above the top of a rigid basement, and the correction factor, respectively. Since the frame has more than two storey, the correction factor, λ is equal to 0.85 [4]. Then, the base shear force, F_b is proportionally distributed on each storey as lateral load using (2):

$$F_i = F_b \cdot \frac{s_i \cdot m_i}{\sum s_j \cdot m_j} \quad (2)$$

where F_i is the horizontal force acting on storey i, m_i and m_j are the masses of storey i and j, respectively and s_i and s_j are the displacements of masses m_i and m_j, respectively in the fundamental mode shape.

The ordinate of the design spectrum at period T_1, $S_d(T_1)$ is determined by referring to the design response spectrum as shown in Figure 2. The Type 1 design response spectrum had been developed according to Eurocode 8 [4] which compatible with Soil D (v_s < 180 m/s). This is because buildings built on soft soil are occasionally subjected to tremors although Malaysia is situated on a stable part of the Eurasian plate [13]. The reference peak ground acceleration, a_{gR} used for development of design response spectrum is equal to 0.08g [2, 14] while the importance factor, γ_I is equal to 1.4 since the frame is designed for hospital and therefore classified in Class IV [4].

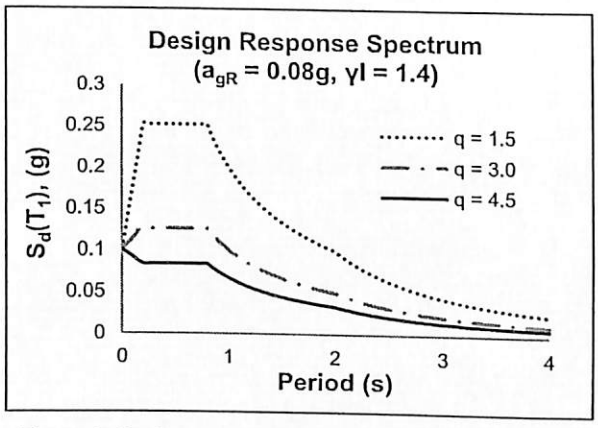

Figure 2: Design response spectrum for Type 1, Soil D

III. Result and discussion

In this study, all four frames had been subjected to similar gravitational load (dead load and live load) acting vertically on beam. But, due to different level of behavior factor, q used in developing the design response spectrum, different lateral load had been imposed on each frame. As a result, frame designed based on behavior factor, q equal to 1.5, 3.0, and 4.5 have total base shear force, F_b which are equal to 476kN, 238kN, and 162kN, respectively. As expected, higher level of behavior factor, q tends to decrease the magnitude of base shear force, F_b acting on frame. Therefore, bending moment, shear force, and axial load for frames with higher behavior factor, q should be lower and resulting in lighter reinforcement design.

When dealing with RC design, the designers have to play around with volume of concrete and amount of steel reinforcement. For example, small size of section resulting in low volume of concrete and high amount of steel reinforcement and vice versa. The designers also have to fulfill the requirement of minimum and maximum steel reinforcement as proposed by codes [1, 4]. Therefore, they

Proc. of the Intl. Conf. on Advances in Civil, Structural, Environmental & Bio-Technology -- CSEB 2014

ISBN: 978-1-63248-001-9 doi: 10.15224/ 978-1-63248-001-9-02

have to select size of section, number and size of steel bar and adjust it smartly in order to fulfill the flexural demand from bending moment. For the same section, the designers also have to consider suitable arrangement of steel reinforcement to cater for shear demand. The global stiffness that developed the fundamental period of vibration, T_1 is strongly influenced by the size of section. Therefore, the latter is not altered as long as the amount of steel for column flexural reinforcement provided is not exceeds the limit of 4% of cross sectional area. It the limit is exceeded, the size of column has to be enlarged resulting in lower fundamental period of vibration, T_1 which cause the structure become stiffer and attracts higher inertia force.

For moment resisting frame system, RC column play an important role to support the beams and slabs then transfer the loads to the foundations [15]. Therefore, it is important for RC column to be designed and detailed adequately to resist both lateral and gravity loads. For DCM structures, column design is strongly related to the beam design where the magnitude of moment to be resisted by column, M_{Rc} is derived to be 1.3 times design moment of resistance of the beam, M_{Rb} [4, 16]. This concept is known as *Strong Column ~ Weak Beam* which is promoted to prevent the formation of plastic hinges in column. In this study, the design for exterior and interior column had been conducted separately due to different strength of beam at exterior and interior section. Figure 3 presents the comparison of total amount of flexural reinforcement for column to resist the derived bending moment.

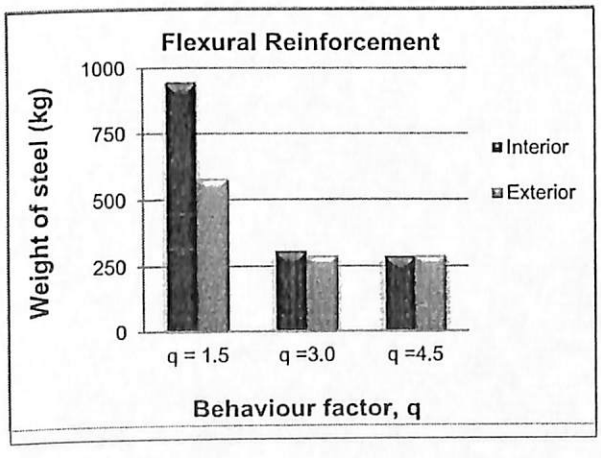

Figure 3: Effect of behavior factor, q on flexural reinforcement

In Figure 3, it is clearly observed that the amount of flexural reinforcement for both exterior and interior column decreases when the level of behavior factor, q is increases. This result is associated with the reduced lateral load for higher level of behavior factor, q. Lower bending moment obtained for beam design resulting in smaller amount of flexural reinforcement in beam which creates lower design moment of resistance of the beam, M_{Rb}. As explained in previous paragraph, the design of RC column in DCM structures is directly related to its beam design. Therefore, smaller amount of flexural reinforcement are required for columns of frames with higher level of behavior factor, q.

From Figure 3, it can be observed that for frame designed with behavior factor, q equal to 1.5, the amount of steel for flexural reinforcement is higher for interior column compared to the exterior one. This is due to higher design moment of resistance of the beam, M_{Rb} for interior section compared to the exterior. For frames designed with higher level of behavior factor, q the amount of steel reinforcement is similar for both interior and exterior column. The latter is associated with the requirement of minimum 1% of column cross sectional area must be provided in column with DCM design as proposed by the code [4]. This result indicates that as the level of behavior factor, $q \geq 3.0$, the area of steel required, As_{req} is very low due to lower design moment of resistance of the beam, M_{Rb}. Therefore, total area of steel provided, As_{prov} is at least 1% of cross sectional area of the column.

In RC design, shear or transverse reinforcement is important to resist shear forces and to avoid shear failure, to clamp together lap splices, to prevent buckling of longitudinal reinforcing bars, and to confine the concrete core to provide sufficient deformability (ductility) [15]. The comparison of total amount of steel used as shear reinforcement for interior and exterior column is shown in Figure 4. It is found that the amount of shear reinforcement is increases when the level of behavior factor, q is increases for both columns. This result is associated to the requirement of confinement reinforcement for column in DCM structures as proposed by Eurocode 8 [4].

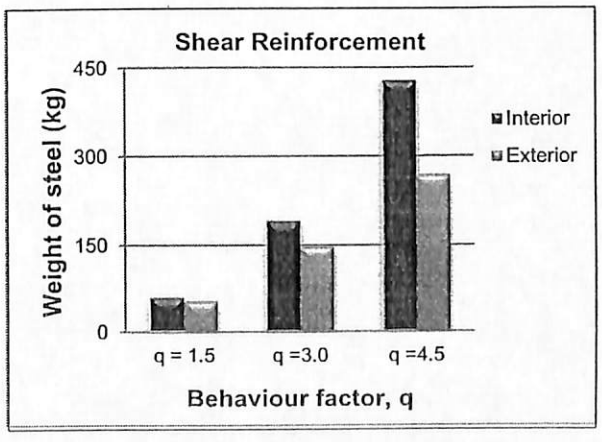

Figure 4: Effect of behavior factor, q on shear reinforcement

Among the main parameters which strongly influencing this confinement reinforcement is the gross cross-sectional width, b_c width of confined core, b_0 curvature ductility factor, μ_ϕ design value of tension steel strain at yield, $\varepsilon_{sy,d}$ and normalized design axial load, ν_d [4]. Due to higher ductility demand, higher level of behavior factor, q tends to require higher mechanical volumetric ratio of confining hoops within

Proc. of the Intl. Conf. on Advances in Civil, Structural, Environmental & Bio-Technology – CSEB 2014

ISBN: 978-1-63248-001-9 doi: 10.15224/ 978-1-63248-001-9-02

the critical regions, $\omega_{wd\,req}$. In order to fulfill this requirement, the latter shall be sufficiently provided.

As explained in a design example by Elghazouli [17], the best solution for this matter is by decreasing the spacing of shear reinforcement, s which will automatically increase the provided mechanical volumetric ratio of confining hoops within the critical regions, $\omega_{wd\,prov}$. The latter also can be increased by using higher number and/or larger diameter of steel bar. Therefore, the amount of shear reinforcement in column is higher when higher level of behavior factor, q is considered. It is also presented in Figure 4 that the amount of shear reinforcement for interior column is higher compared to exterior column regardless the level of behavior factor, q. As explained, the requirement of confinement reinforcement also influenced by the normalized design axial load, v_d. Therefore, the interior column which located at middle part of the frame requires higher confinement reinforcement due to higher axial force, N compared to the exterior column.

Since all three frames have similar size of section for all corresponding elements, the total volume of concrete also becomes similar. Hence, the cost of steel used as flexural and shear reinforcement is strongly influencing the cost of material for all frames. Figure 5 depicts the total amount of steel reinforcement used in both interior and exterior column. It can be clearly observed that the highest amount of steel reinforcement is obtained for frame which used behavior factor, q equal to 1.5 in design. This is associated with high magnitude of base shear force, F_b acting on the frame resulting in high magnitude of bending moment, shear force, and axial load. Then, total amount of steel reinforcement is decreases due to lower amount of flexural reinforcement used for higher level of behavior factor, q as discussed in previous paragraph.

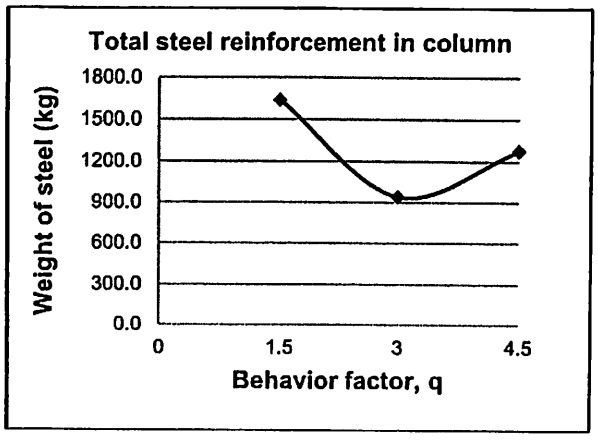

Figure 5: Effect of behavior factor, q on total steel reinforcement

However, as the behavior factor, q is greater than about 3.0; the total amount of steel reinforcement is increases. This is due to rapid increasing of total amount of shear reinforcement as the level of behavior factor, q is increases. For example, although have decrement in term of flexural reinforcement, frame designed with behavior factor, q equal to 4.5 have to use very high amount of shear reinforcement. As a result, the cost of steel for that frame becomes higher although subjected to smaller lateral load compared to frame designed with behavior factor, q equal to 3.0. Therefore, it can be concluded that in this study, the most economical design is obtained when using behavior factor, q equal to 3.0 where the cost of steel reinforcement can be saved up to 42.5% compared to the highest one.

IV. Conclusion

This study investigated the effect of behavior factor, q on seismic design of RC column. In this study, a three storey regular RC frame for hospital had been used as model. A total of three frames had been designed based on behavior factor, q equal to 1.5, 3.0, and 4.5 for ductility class medium. There are several conclusions can be drawn based on this study as follow:

- Total amount of steel provided as flexural reinforcement is decreases as the level of behavior factor, q is increases and vice versa. This is associated with the magnitude of base shear force, F_b which is strongly influenced by the level of behavior factor, q.
- Due to requirement of confinement reinforcement, total amount of steel provided as shear or transverse reinforcement is increases as the level of behavior factor, q is increases and vice versa.
- The sum of total flexural and shear reinforcement presents the total amount of steel reinforcement for design of RC column. It can be concluded that the level of behavior factor, q is strongly influencing the cost of steel reinforcement. Therefore, it is important to select the suitable behavior factor, q to obtained economic design without compromising safety.

Acknowledgment

The authors gratefully acknowledge the facilities provided by Universiti Sains Malaysia and financial support from MyBrain15, a scholarship provided by Ministry of Education Malaysia to accomplish this study.

References

16

ICNSE-798

Seismic Performance of Three Storey Hospital RC Frame Subjected to Multiple Earthquake in Moderate Seismic Region

Mohd Irwan Adiyanto*
Universiti Sains Malaysia, Malaysia
E-mail: irwano_07@yahoo.com

Taksiah A. Majid
Universiti Sains Malaysia, Malaysia
E-mail: taksiah@usm.my

Abstract

In earthquake engineering, the nonlinear time history analysis is the best method to evaluate the seismic performance of structural system. This is because the structural models are imposed to the real earthquake ground motion records. In conventional practice, only single earthquake ground motion records is considered in the analysis. However, in real earthquake event, the tremors of earthquake always occur repeatedly for several times after the first one. This is the nature of earthquake and can be technically called as repeated or multiple earthquake. In this paper, the effect of multiple earthquakes on interstorey drift ratio of three storey regular RC frame is investigated. The total of 5 similar frames had been designed based on 5 different value of behaviour factor, q for ductility class medium based on Eurocode 8. All frames are assumed to be located in moderate seismic region in Sabah, Malaysia. From a total of 250 nonlinear time history analyses, it is observed that the action of multiple earthquakes on frame tends to cause higher interstorey drift ratio compared to the action of single earthquakes. For weaker frames, the action of multiple earthquake had caused the interstorey drift ratio exceed the limit.

Keyword: Reinforced concrete, Eurocode 8, Multiple earthquake, Behaviour factor, Nonlinear time history analysis.

1. Introduction

In order to perform the nonlinear time history analysis on structural models, current practice such as Eurocode 8 [1] and FEMA 368 [2] only consider the single earthquake excitation. The latter is applicable either for design a new structure or evaluating the existing one. Recently, there is a few research works which consider more than single earthquake in nonlinear time history analysis [3-5].

Their works are reasonable because in real earthquake event, the structures might being hit by the tremors repeatedly in just a few hours after the first one. This is the nature of earthquake and it can be called as repeated or multiple earthquake [6]. The structures may experience minor to moderate damage after the first tremor of great earthquake event. Any rehabilitation or repairing work is impractical due to time constraint.

Therefore, it is reasonable to worry that the not yet repaired structures may experience greater damage which leads to collapse when subjected to the aftershock. According to Hatzigeorgiou and Liolios [7], the interstorey drift ratio (IDR) of reinforced concrete (RC) frame is higher when subjected to multiple earthquake compared to its single companion.

In seismic design, it is not economically feasible to design earthquake resisting structures that

can remain elastic when subjected to earthquake ground motion [8]. This means that a very high amount of money has to be spent to build such structures. Therefore, the structures are allowed to behave inelastically during earthquake for economical reason. For that purpose, a very useful concept known as behaviour factor, q in Eurocode 8 [1] or strength reduction factor, R in American code [9] had been promoted. Both concepts is used to reduce the forces obtained from linear analysis to take into account the nonlinear response of a structure. The value of behaviour factor, q depends on the type of structures, material, and class of ductility. Higher value of behaviour factor, q represents higher level of ductility. Therefore, the inelastic displacement ratio increases as the value of behaviour factor, q used in design increases and vice versa [6]. The inelastic lateral displacement and the distribution of IDR along the height of the structure also strongly influenced by the value of behaviour factor, q. According to Jalali and Trifunac [10], the simple and effective modification is needed to replace the current value of behaviour factor, q. In Malaysian seismic region, ductile detailing may become an option by using higher value of behaviour factor, q which reduces the seismic design force [11].

In this paper, the effect of multiple earthquakes on IDR of three storey regular RC frame is presented. The total of 5 similar frames had been designed based on 5 different value of behaviour factor, q for ductility class medium. All frames are assumed to be located in moderate seismic region in Sabah, Malaysia.

2. Material and Method

To investigate the effect of multiple earthquakes on seismic performance, a set of three storey RC frame had been used in nonlinear time history analysis. The three storey frame is regular in plan and elevation where the storey height and beam span is equal to 3.3 m and 5.0 m, respectively as shown in Figure 1.

This type of frame had been used as office building in previous studies [7, 12]. In this study, the RC frame is designed for hospital use since that structure is important and must survive during earthquake with no or minor damage which not affecting its function. Therefore, the frame is classified into important class IV with importance factor, γ_I equal to 1.4 [1].

The RC design had been performed by referring to the code [1] with concrete compressive strength, f_{cu} = 30 N/mm^2 and yield strength of steel, f_y = 500 N/mm^2. The size of all columns is equal to 375 mm x 375 mm. The size of beam at the first and second storey is 300 mm x 600 mm while the top beam has the size of section equal to 250 mm x 550 mm. The frame had been designed repeatedly using 5 different value of behaviour factor, q equal to 2.3, 3.1, 3.9, 4.7, and 5.5. Therefore, a total of 5 frames had been produced as model for nonlinear time history analysis. All 5 frames have similar size of section so that its dynamic characteristic can be maintained with fundamental period of vibration, T_1 is equal to 0.5 sec. To prevent the formation of soft storey mechanism, the *Strong Column~Weak Beam* philosophy had been implemented to all frames where the strength of column is designed to be at least 1.3 times the strength of beam [1]. In order to determine the magnitude of lateral load acting on each storey joint, the Type 1 design response spectrum had been developed as recommended by Eurocode 8 [1] where the frame is assumed to be located on soil type D (soft soil). To represent the moderate seismic region in Sabah, Malaysia the reference peak ground acceleration, a_{gR} equal to 0.12g [13,14] had been used to developed the design response spectrum.

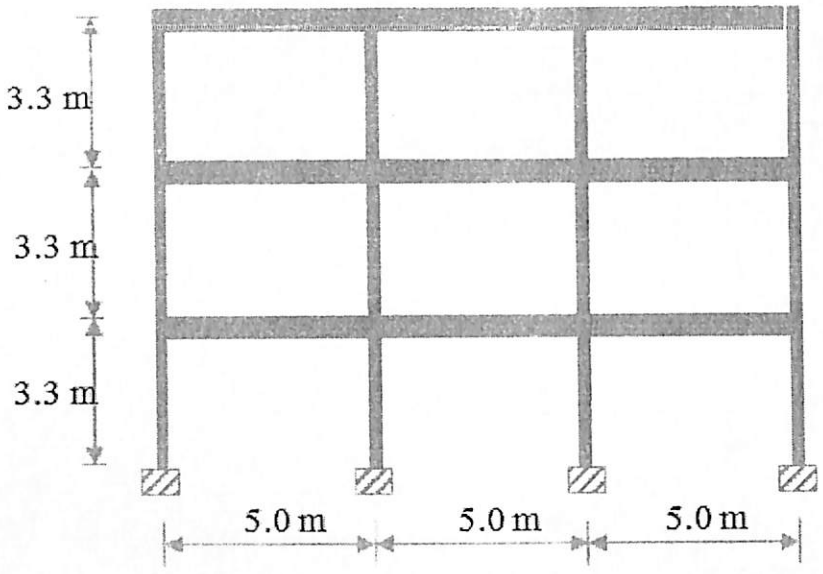

Figure 1: Elevation view of three storey RC frame.

To perform the nonlinear time history analysis, two set of ground motion records namely as single and multiple earthquakes had been used in this study. Each set has 25 number of ground motion records. Table 1 shows the list of 25 single earthquake ground motion records which can be downloaded from PEER database [15]. In this study, the multiple earthquakes ground motion records had been artificially generated from random combination of single ground motion records from Table 1.

Each multiple earthquakes ground motion record has three component namely as Fore ~ shock, Main ~ shock, and After ~ shock as used in previous studies [4,5]. Figure 2 depicts the acceleration records for both single and multiple earthquakes.

Table 1: List of selected ground motion records

No	Event	Comp	Station	PGA (g)	PGV (cm/s)	Mw
1	Imperial Valley	H-E03140	5057 El. Centro Array #3	0.266	46.8	6.5
2	Imperial Valley	H-E03230	5057 El. Centro Array #3	0.221	39.9	6.5
3	Loma Prieta	A02043	1002 APEEL2 Redwood City	0.274	53.6	6.9
4	Loma Prieta	A02123	1002 APEEL2 Redwood City	0.220	34.3	6.9
5	Chi-Chi	CHY026-N	CHY026	0.066	32.6	7.6
6	Chi-Chi	CHY026-W	CHY026	0.076	46.2	7.6
7	Chi-Chi	CHY032-W	CHY032	0.088	26.4	7.6
8	Chi-Chi	CHY041-N	CHY041	0.639	39.5	7.6
9	Chi-Chi	CHY039-N	CHY039	0.101	25.7	7.6
10	Chi-Chi	CHY039-W	CHY039	0.114	28.6	7.6
11	Chi-Chi	TCU040-N	TCU040	0.123	50.3	7.6
12	Chi-Chi	TCU040-W	TCU040	0.149	50.9	7.6
13	Chi-Chi	TCU056-N	TCU056	0.134	42.9	7.6
14	Chi-Chi	TCU056-W	TCU056	0.134	42.5	7.6
15	Chi-Chi	TCU110-N	TCU110	0.180	54.9	7.6
16	Chi-Chi	TCU110-W	TCU110	0.180	67.5	7.6
17	Chi-Chi	TCU112-N	TCU112	0.073	33.4	7.6
18	Chi-Chi	TCU112-W	TCU112	0.083	41.3	7.6
19	Chi-Chi	TCU116-N	TCU116	0.148	45.3	7.6
20	Chi-Chi	TCU116-W	TCU116	0.184	48.7	7.6
21	Chi-Chi	TCU118-N	TCU118	0.092	33.5	7.6
22	Chi-Chi	TCU118-W	TCU118	0.114	30.5	7.6
23	Chi-Chi	TCU117-N	TCU117	0.120	54.4	7.6
24	Westmoreland	WLF225	5062 Salton Sea	0.199	16.4	5.8
25	Westmoreland	WLF315	5062 Salton Sea	0.176	12.3	5.8

Single

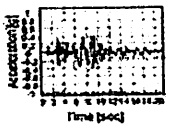

Multiple

Figure 2: Typical profile of ground motion records.

3. Result and Discussion

Figure 3 shows the base shear force, F_b acting on the frame for different value of behaviour factor, q. As mentioned before, the latter is used to reduce the forces obtained from linear analysis to take into account the nonlinear response of a structure. It can be clearly observed that the magnitude of base shear force, F_b is decreases as the value of behaviour factor, q increases. In this study, the magnitude of base shear force, F_b is in range of 466.5 kN to 194.7 kN. The decrement of base shear force, F_b is in range of 26% to 58% compared to the frame with the behaviour factor, q equal to 2.3. This means that the frames designed with higher value of behaviour factor, q tend to be weaker due to lower design forces which will produce lower bending moment, shear force, and axial load.

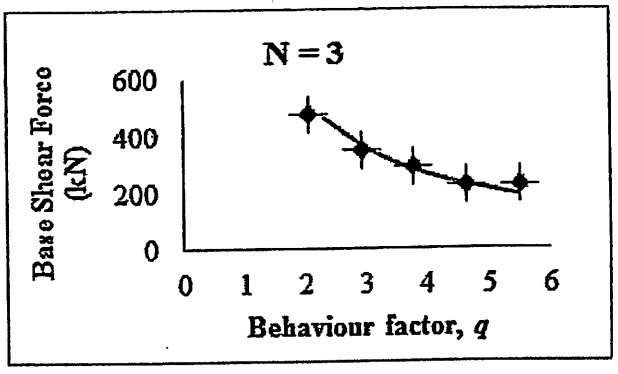

Figure 3: Comparison of base shear force, F_b acting on three storey frames.

In this study, the seismic performance of three storey hospital RC frame is evaluated based on the IDR. The latter is the relative horizontal displacement between two adjacent storey normalized to its storey height. In Performance-Based Earthquake Engineering (PBEE), there are four performance levels namely as Operational (OP), Immediate Occupancy (IO), Life Safety (LS), and Near Collapse (NC) that might be experienced by structures during earthquake [16]. According to FEMA 356 [17], all performance levels can be measured based on the IDR. Performance level of IO, LS, and NC correspond to the IDR equal to 1%, 2% and 4%, respectively. By referring to Eurocode 8 [1], the limitation of IDR for structures having non-structural elements of brittle materials attached to the structure can be determined as follow:

$$d_r \nu \leq 0.005h \tag{1}$$

where d_r is the design interstorey drift, h is the storey height, and ν is the reduction factor.

Since this study focus on hospital building in importance class IV, the value of reduction factor, ν is equal to 0.4 [1]. From equation (1), the IDR is limited to 1.25%.

Figure 4(a) presents the distribution of IDR along the height of three storey hospital RC frames subjected to the single earthquake. The magnitude of IDR is the mean value from 25 ground motion records. It can be clearly observed that the IDR experienced by frames designed with high value of behaviour factor, q is higher compared to the similar frame designed with low behaviour factor, q. As an example, The frame designed with behaviour factor, q equal to 5.5 experienced the IDR of 1.09% which is approximately around 65% higher compared to the frame with behaviour factor, q equal to 2.3 (IDR = 0.66%). As discussed in previous paragraph, high value of behaviour factor, q tends to produce weaker frame which will have higher lateral displacement due to earthquake excitation resulting in higher IDR. This result is in good agreement with previous study [18] which concluded that as the value of behaviour factor, q is increases, the magnitude of IDR also increases and tends to concentrate at specific storey. Due to single earthquake, it is observed that the IDR for all frames is still lower than the limit of 1.25%.

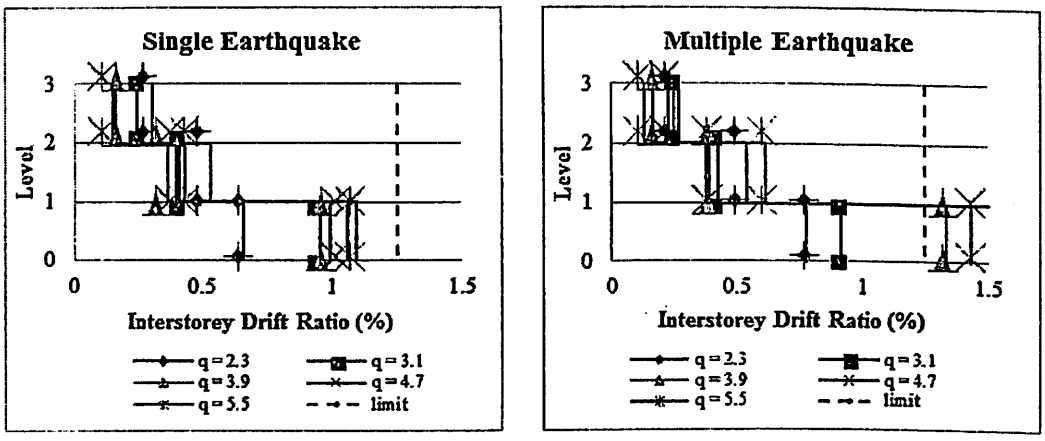

(a) (b)

Figure 4: IDR of three storey hospital RC frame (a) single earthquake (b) multiple earthquake

Figure 4(b) presents the distribution of IDR for all frames when subjected to multiple earthquakes. The response of three storey hospital RC frames is in similar pattern as being subjected to the single earthquake, where the frames designed with higher behaviour factor, q tend to have higher magnitude of IDR. The maximum IDR also concentrated at the same level, which is the bottom one. However, it can be clearly observed that the magnitude of IDR due to action of multiple earthquakes is relatively higher compared to the single earthquake. As an example, the IDR for frame designed with behaviour factor, q equal to 2.3 is 0.66% and 0.78% when subjected to the single and multiple earthquakes, respectively. This result is in line with previous finding which concluded that the IDR demand is higher when subjected to multiple earthquake compared to single earthquake [7]. In this study, it is also observed that the multiple earthquakes also cause the IDR of weaker frames ($q \geq 3.9$) exceed the limit of 1.25% as recommended by the code. Hence, the value of behaviour factor, q for multiple earthquakes should be lower than the one designed for single earthquake only.

4. Conclusion

This study presents the seismic response of three storey hospital RC frame subjected to single and multiple earthquakes. A typical frame had been designed repeatedly using five different

value of behaviour factor, q in ductility class medium which is equal to 2.3, 3.1, 3.9, 4.7, and 5.5. A total of 250 nonlinear time history analyses had been conducted on all frames to obtain the mean value of IDR. There are a few conclusions that can be drawn from this study as follow:

- The value of behaviour factor, q stongly influences the magnitude of base shear force, F_b acting on the frame. Higher value of behaviour factor, q produced lower magnitude of base shear force, F_b. As a result, frames designed with higher value of behaviour factor, q is weaker.
- When subjected to single earthquake, the frames designed with higher value of behaviour factor, q experienced higher IDR compared the similar frame designed with lower value of behaviour factor, q. Due to lower strength, the magnitude of IDR increase around 44% to 65% as the value of behaviour factor, q increases.
- The action of multiple earthquakes on frame tends to cause higher IDR compared to the action of single earthquakes. This pattern is observed for all frames regardless the value of behaviour factor, q. In this study, the action of multiple earthquakes on frames designed with behaviour factor, $q \geq 3.9$ exceed the limit of 1.25% as recommended. So, lower value of behaviour factor, q should be considered so that the building can survive the multiple earthquakes without structural damages.

5. Acknowledgement

The authors gratefully acknowledge the facilities provided by Universiti Sains Malaysia and financial support from MyBrain15, a scholarship provided by Ministry of Education Malaysia to accomplish this study.

6. References

[1] CEN Eurocode 8, Design of structures for earthquake resistance, *Part 1: General rules, seismic actions and rules for buildings*, Brussels, 2003.

[2] FEMA NEHRP, Recommended provisions for seismic regulations for new buildings and other structures, *Part 1: Provisions, FEMA 368, Building Seismic Safety Council for the Federal Emergency Management Agency*, 2000.

[3] C. Amadio, M. Fragiacomo, and S. Rajgelj, The effects of repeated earthquake ground motions on the non-linear response of SDOF systems, *Journal of Earthquake Engineering and Structural Dynamics* (32), 2003, pp. 291-308.

[4] G.D. Hatzigeorgiou, Behaviour factors for nonlinear structures subjected to multiple near-fault earthquakes, *Journal of Computers and Structures* (88), 2010, pp.309-321.

[5] Ade Faisal, T.A. Majid, and G.D. Hatzigeorgiou, Investigation of story ductility demands of inelastic concrete frames subjected to repeated earthquakes, *Journal of Soil Dynamics and Earthquake Engineering* (44), 2013, pp.42-53.

[6] G.D. Hatzigeorgiou, and D.E. Beskos, Inelastic displacement ratios for SDOF structures subjected to repeated earthquakes, *Journal of Engineering Structures* (31), 2009, pp.2744-2755.

[7] G.D. Hatzigeorgiou, and A.A. Liolios, Nonlinear behaviour of RC frames under repeated strong ground motions, *Journal of Soil Dynamics and Earthquake Engineering* (30), 2010, pp.1010-1025.

[8] FEMA NEHRP, Recommended provisions design examples, *Topic 7: Concepts of Seismic-Resistant Design, FEMA 451B, Building Seismic Safety Council for the Federal Emergency Management Agency,* 2006.

[9] ICC, *International Building Code*, United States of America, 2006.

[10] R.S. Jalali, and M.D. Trifunac, A note on strength-reduction factors for design of

structures near earthquake faults, *Journal of Soil Dynamics and Earthquake Engineering* (28), 2008, pp.212-222.
[11] J.W. Pappin, P.H.I. Yim, and C.H.R. Koo, 2011. An approach for seismic design in Malaysia following the principles of Eurocode 8, *Bulletin Jurutera* (10), 2011, pp.22-28.
[12] F. Mazza, and A. Vulcano, Nonlinear dynamic response of RC framed structures subjected to near-fault ground motions, *Bulletin of Earthquake Engineering* (8), 2010, pp.1331-1350
[13] MOSTI, Seismic and tsunami hazards and risks study in Malaysia, *Final Report*, 2009.
[14] A. Adnan, Hendriyawan, A. Marto, and P.N.N. Selvanayagam, Development of seismic hazard maps of east Malaysia, *Advances in Earthquake Engineering Applications,* 2008, pp.1-17.
[15] Pacific Earthquake Engineering Research Center, *PEER strong motion database*, [accessed 08.12.13] *http://peer.berkeley.edu/smcat*.
[16]M.N. Fardis, Seismic design, assessment, and retrofitting of concrete buildings, *Springer*, New York, 2009.
[17] FEMA NEHRP, Prestandard and commentary for the seismic rehabilitation of buildings, *FEMA 356, Building Seismic Safety Council for the Federal Emergency Management Agency,* 2000.
[18] J. Ruiz-Garica, and E. Miranda, Evaluation of residual demands in regular multi-storey frames for performance –based seismic assessment, *Journal of Earthquake Engineering and Structural Dynamics* (35), 2006, pp. 1609-1629.

The 5th Asia Conference on Earthquake Engineering
October 16-18, 2014

COST OPTIMIZATION OF SEISMIC DESIGN OF LOW RISE HOSPITAL RC FRAME IN MALAYSIA

Mohd Irwan Adiyanto[1], Taksiah A Majid[2] and Fadzli Mohamed Nazri[3]

ABSTRACT

Before 21st century, nobody in Malaysia, from government to public citizen worry about the earthquake because the country is situated relatively far from the active seismic fault region. Therefore, the construction practice never consider the earthquake load in design process. However, the catastrophic 2004 Aceh earthquake with magnitude Mw 9.0 which also triggered a disastrous Indian Ocean tsunami had became a wakeup call to the Malaysian to be aware for earthquake hazard. After the disaster, serious effort had been taken by the government, researchers, and engineers to face future earthquakes. A lot of researches had been conducted related to this field such as seismology, tsunami, disaster management, and seismic assessment on existing structures. For new structures, it is worth to consider seismic design for important structures located in medium to high seismic region. Since have lack of experience in dealing with seismic design, the uncertainties arises such as the level of ductility and appropriate behavior factor, q to be used. This paper investigates the effect of behavior factor, q on total cost of material for three storey reinforced concrete hospital building. The typical frame had been designed based on Eurocode 8 with five different value of behavior factor, q for ductility class medium. The result shows that the value of behavior factor, q used in design strongly influencing the amount of steel tonnage and total cost of materials. By selecting suitable value of behavior factor, q the cost of material can be saved up t0 22%.

Keywords: Hospital RC frame, seismic design, behavior factor, cost, ductility class medium

INTRODUCTION

Before 21st century, nobody in Malaysia, from government to public citizen worry about the earthquake because the country is situated relatively far from the active seismic fault region. Therefore, the construction practice never consider the earthquake load in design process. However, the catastrophic 2004 Aceh earthquake with magnitude Mw 9.0 which also triggered a disastrous Indian Ocean tsunami had became a wakeup call to the Malaysian to be aware for earthquake hazard. After the disaster, serious effort had been taken by the government, researchers, and engineers to face future earthquakes. A lot of researches had been conducted related to this field such as seismology, tsunami, disaster management, and seismic assessment on existing structures. For new structures, it is worth to consider seismic design for important structures located in medium to high seismic region (Mosti, 2009).

In order to implement seismic design, the designer has to deal with a concept known as behavior factor, q which is proposed to reduce the forces obtained from a linear analysis, in order to account for the nonlinear response of a structure (Eurocode 8, 2004). The proposed value of behavior factor, q had been re-evaluated for many times over the past few years. According to Gillie et al., (2010) the behavior factor, q resulting from forward directivity ground motion is smaller than those obtained from non-forward directivity ground motions. In addition, the European and American standards are too conservative where the ductility demand which corresponds to the behavior factor, q is higher than the ductility supply (Borzi and Elnashai, 2000). Since have lack of experience in dealing with seismic design, the uncertainties arises such as the level of ductility and appropriate behavior factor, q to be used for design in Malaysia. This paper investigates the effect of behavior factor, q on total cost of material for three storey reinforced concrete (RC) hospital building. The typical frame had been designed based on Eurocode 8 (2004) with five different value of behavior factor, q for ductility class medium (DCM).

[1] Postgraduate Student, School of Civil Engineering, Universiti Sains Malaysia, Penang, Malaysia, irwano_07@yahoo.com
[2] Disaster Research Nexus, School of Civil Engineering, Universiti Sains Malaysia, Penang, Malaysia, taksiah@usm.my
[3] Disaster Research Nexus, School of Civil Engineering, Universiti Sains Malaysia, Penang, Malaysia, cefmn@usm.my

FRAME MODEL AND DESIGN RESPONSE SPECTRUM

In this study, a typical frame for hospital building had been used to investigate the effect of behavior factor, q on cost of material. The typical RC frame has three equal bay of 5.0 m length and storey height of 3.3 m. The frame is regular in plan and elevation. Similar frame had been used in previous work (Adiyanto and Majid, 2014a). The value of behavior factor, q to be used in design depends on the materials, type of structures, and class of ductility. In Eurocode 8 (2004), the value of behavior factor, q for ductility class medium (DCM) of RC moment resisting frame is lies in range of 1.5 to 5.85 where the proposed value for such structure with multi bay is equal to 3.9. Therefore, the design process of typical frame had been conducted using five different value of behavior factor, q equal to 2.3, 3.1, 3.9, 4.7, and 5.5. As a result, a total of five different frames had been produced for comparison on cost. All frames had been designed by referring to Eurocodes (Eurocode 2, 2004; Eurocode 8, 2004) based on concrete compressive strength, f_{cu} and yield strength of steel, f_y equal to 30 N/mm^2 and 500 N/mm^2, respectively. The following load combination had been considered in structural analysis in order to get the bending moment, shear force, and column axial load for design purpose:

i. Combination 1 = $1.0G + \Psi_2 Q + 1.0E$ (1)
ii. Combination 2 = $1.0G + \Psi_2 Q + 1.0E$ (2)
iii. Combination 3 = $1.35G + 1.50Q$ (3)

where G is the dead load, Q is the live load, and E represents the earthquake load acting laterally on each storey joint. This concept is known as lateral force method (Eurocode 8, 2004). All load combination also had been used in previous work by Hatzigeorgiou and Liolios (2010). For hospital ward which is classified as Category A, the value of quasi-permanent of a variable action, Ψ_2 to be multiplied with the live load, Q in load combination 1 and load combination 2 is equal to 0.3 (Acun et al., 2012).

As mentioned before, the lateral force method had been used in the structural analysis. According to this method, the earthquake action on building is represented by horizontal forces which acting on each storey joints as shown in Fig. 1. First of all, the magnitude of total horizontal force namely as base shear force, F_b has to be determined by using the following equation:

$$F_b = m \cdot S_d(T_1) \cdot \lambda \tag{4}$$

where m is the total mass of the structure, $S_d(T_1)$ represents the ordinate of the design spectrum at period T_1, and λ corresponds to the correction factor which is equal to 0.85 for building with number of storey more than two (Eurocode 8, 2004).

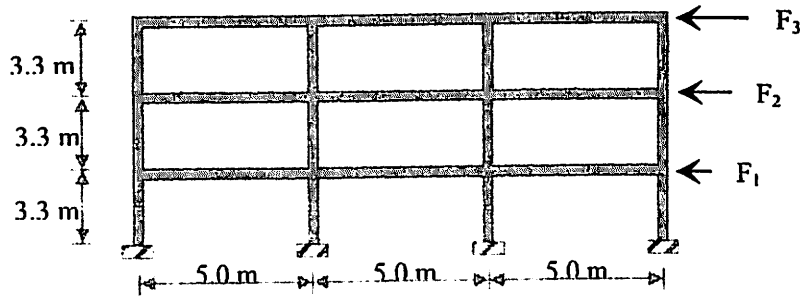

Figure 1. Action of horizontal forces on frame

Then, the designer has to distribute the base shear force, F_b proportionally into horizontal force at each storey by using this equation:

$$F_i = F_b \cdot \frac{z_i \cdot m_i}{\sum z_j \cdot m_j} \tag{5}$$

where F_i is the horizontal force on storey i, m_i and m_j represents the masses of storey i and j, respectively while the z_i and z_j are the height of the masses of m_i and m_j above the level of application of the seismic action, respectively.

In order to determine the ordinate of the design spectrum at period T_1, $S_d(T_1)$ the design response spectrum which is strongly influenced by behavior factor, q has to be developed. For this purpose, the Type 1 design spectrum which compatible with Soil D having average value of propagation velocity of S waves in the upper 30 m of the soil profile at shear strain of 10^{-5} or less, $v_{s,30}$ was chosen as proposed by Eurocode 8 (2004). This study focus on hospital building which is classified into importance classes IV. Therefore, the value of importance factor, γ_I is equal to 1.4. The magnitude of reference peak ground acceleration, a_{gR} for 500 years return period is 0.12g to represent the moderate seismic region in Malaysia (Adnan et al., 2008; Mosti, 2009). Fig. 2 depicts the design response spectrum for five different value of behavior factor, q.

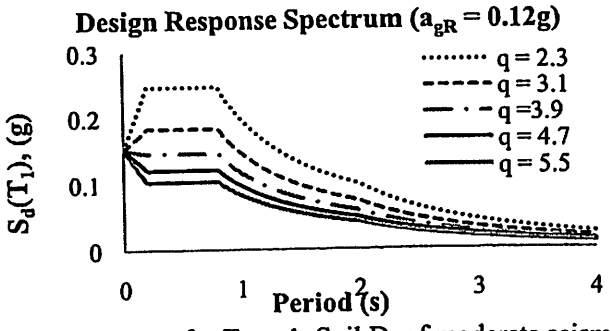

Figure 2. Design response spectrum for Type 1, Soil D, of moderate seismic region in Malaysia

RESULT AND DISCUSSION

In this study, a typical three storey frame representing hospital building had been designed based on five different value of behavior factor, q. As mentioned in previous section, the behavior factor, q directly influences the magnitude of the ordinate of the design spectrum at period T_1, $S_d(T_1)$. Indirectly, behavior factor, q influences the magnitude of base shear force, F_b and horizontal forces of storey joint as derived by equation (4) and (5). Table 1 presents the magnitude of base shear force, F_b and horizontal forces at each storey for all frames. It can be observed that the magnitude of base shear force, F_b and the corresponding horizontal forces at each storey, F_i are proportionally decrease when the value of behavior factor, q is increases. Therefore, in structural analysis frames with higher value of behavior factor, q had been subjected to lower magnitude of horizontal forces, F_i result in lower magnitude of bending moment, shear force, and axial load.

Table 1. Effect of behavior factor, q on base shear force, F_b and horizontal forces, F_i

	Horizontal forces, F_i (kN)				
Behavior factor, q	2.3	3.1	3.9	4.7	5.5
Storey 3	195.2	144.6	114.6	95.3	81.5
Storey 2	172.1	127.5	101.1	84.1	71.9
Storey 1	99.2	73.5	58.2	48.4	41.4
Base Shear Force, F_b (kN)	466.5	345.6	273.9	227.8	194.7

The art of RC design is quite unique because it requires the designer to play around with amount of concrete and steel reinforcement (Adiyanto and Majid, 2014b). This mean that the size of steel bar and its number alongside with the size of section have to be smartly adjusted by the designer. As an example, large size of section selected for design of beam and/or column element will result in high volume of concrete and lower tonnage of steel reinforcement and vice versa. The limitation of minimum and maximum percentage area of steel reinforcement as proposed by the codes (Eurocode 2, 2004; Eurocode 8, 2004) also have to be taken into account. In this study, all five frames had been designed with similar size of section as follow:

- Beam at top storey, RB = 250 mm x 550 mm
- Beam at first and second storey, FB = 300 mm x 600 mm
- Column at all storey, CA = 375 mm x 375 mm

Therefore, the total volume of concrete required for all frames is similar regardless the value of behavior factor, q. In addition, the dynamic characteristic of all frames is similar with fundamental period of vibration, T_1 is equal to 0.5 sec. Fig. 3 presents the comparison of steel tonnage used as flexural reinforcement for beam at first and second storey, FB.

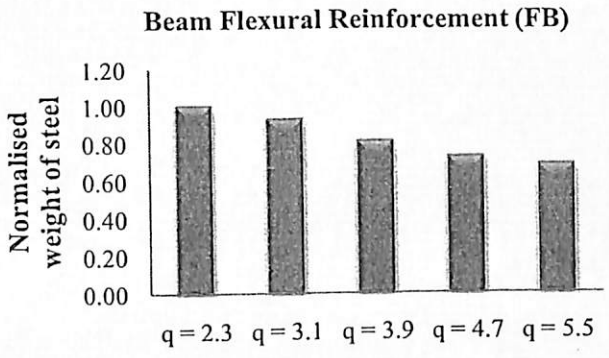

Figure 3. Effect of behavior factor, q on beam flexural reinforcement

The flexural reinforcement in beam section is the longitudinal reinforcement which is placed horizontally to resist the tensile stress resulting from bending moment. As mentioned before, the size of section, size of steel bar, and its number have to be adjusted smartly so the economic and safe design can be produced. Since the size of section of FB is maintained by 300 mm x 600 mm for all frames, the total weight of steel bar as flexural reinforcement are comparable. From Fig. 3, it is clearly observed that the total weight of steel bar is decreases as the value of behavior factor, q is increases. Frame designed based on behavior factor, q = 2.3 requires the highest amount of steel bar compared to the others. The amount of steel bar decreases around 7% to 32% when the value of behavior factor, q is increases from 3.1 to 5.5, respectively. This result can be explained by the effect of behavior factor, q on the base shear force, F_b and horizontal forces, F_i. As discussed in Table 1, the latter is lower for frames with higher value of behavior factor, q. Then, the bending moment also becomes lower resulting in lower tensile stress. Therefore, it requires lower amount of steel bar as flexural reinforcement.

For a beam element, the designer also has to design for shear reinforcement which is useful to resist stress resulting from shear force. The shear reinforcement is place vertically along the beam with specific spacing. It also known as link or transverse reinforcement. The effect of behavior factor, q on the total weight of steel bar used as shear reinforcement in FB is shown in Fig. 4.

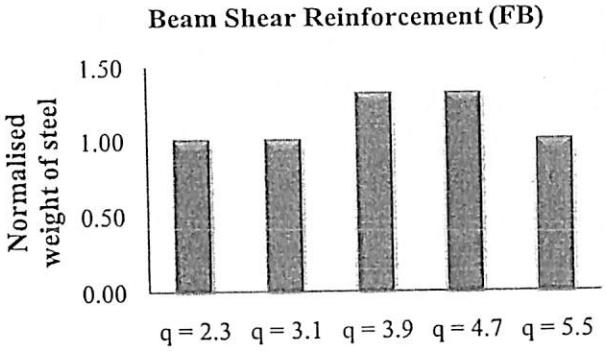

Figure 4. Effect of behavior factor, q on beam shear reinforcement

From Fig. 4, the total weight of steel bar used as shear reinforcement did not influenced by the value of behavior factor, q. It can be clearly observed that frames designed with behavior factor, q equal to 2.3, 3.1, and 5.5 have similar weight of steel bar as shear reinforcement. The same result also obtained for frames designed based on behavior factor, q equal to 3.9 and 4.7 which are the highest. It can be said that the there is no clear trend about the effect of behavior factor, q on the shear reinforcement. According to Eurocode 8 (2004), the spacing of shear reinforcement, s should be designed based on minimum among the 24 times diameter of shear reinforcement, d_{bw}, 8 times the minimum diameter of flexural reinforcement, d_{bL} and the quarter of the depth of beam section, h_w. It shall be not more than 225 mm as the following equation:

$$s = \min\{h_w / 4; 24d_{bw}; 225; 8d_{bL}\} \quad (6)$$

where the diameter of shear reinforcement, d_{bw} shall be not less than 6 mm. Therefore, the spacing of shear reinforcement, s can be increased if the diameter of shear reinforcement, d_{bw} diameter of flexural reinforcement, d_{bL} and the depth of beam section, h_w is increased. In this study, the shear reinforcement for FB of all frames using 6 mm diameter of steel bar. The beam size also similar as mentioned in previous paragraph. Therefore, the only parameter which influencing the spacing of shear reinforcement, s is only the diameter of flexural reinforcement, d_{bL}. Frames with behavior factor, q equal to 3.9 and 4.7 had been designed with smaller size of bar as flexural reinforcement compared to other frames. Therefore, the former require closer spacing of shear reinforcement, s which result in higher amount of steel bar.

For moment resisting frame system, the role of RC column is very important which is to support the beams and slabs before transferring the loads to the foundation (Subramaniam, 2011). In earthquake prone area, the RC column has to be designed and detailed properly to resist both gravity and lateral load. In DCM structures, the bending moment for design of column flexural reinforcement is derived from its corresponding beam strength. The design should fulfill the Strong Column ~ Weak Beam philosophy (Elnashai and Sarno, 2008). In this philosophy, the design moment of resistance of the column, M_{Rc} shall be equal to 1.3 times the design moment resistance of the corresponding beam, M_{Rb} (Eurocode 8, 2004). This philosophy is proposed to avoid the soft storey mechanism during earthquake. The comparison of total weight of steel bar used as flexural reinforcement (placed vertically) for column is shown in Fig. 5.

As explained in previous paragraph, the value of behavior factor, q strongly influencing the total weight of steel bar used as flexural reinforcement of beam element. In Fig. 5, the same trend can be observed where the total weight of steel bar used as column flexural reinforcement is decreases around 25% to 62% as the value of behavior factor, q increases. This is due to lower design moment of resistance of beam, M_{Rb} for frames with high behavior factor, q which contributes to lower design moment of resistance of column, M_{Rc}. This situation finally result in lower amount of steel bar for column flexural reinforcement. However, for frames designed based on behavior factor, q equal to 4.7 and 5.5, the total weight of steel bar is similar. This result is due to the requirement for column design

which states that the total area of steel bar as flexural reinforcement of primary column shall lies between 1% to 4% of the total area of column section (Eurocode 8, 2004; Acun et al., 2012). Therefore, although the column for frame with behavior factor, q = 5.5 can be designed with lower amount of steel bar, it has to follow the requirement of minimum 1% total area of column section to be provided. As a result, the number of steel bar has to be increased for column of that frame.

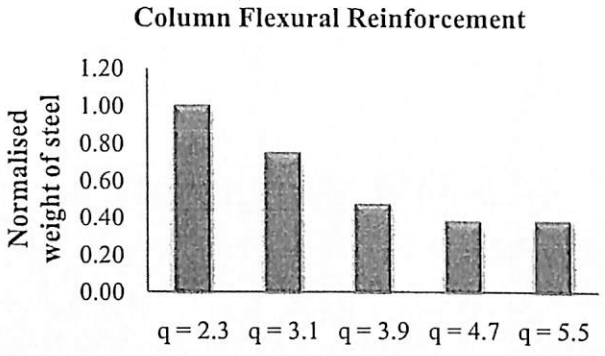

Figure 5. Effect of behavior factor, q on column flexural reinforcement

Just like the beam element, the design of RC column also did not complete without the shear reinforcement. The comparison of total weight of steel bar used as shear reinforcement for column is presented by Fig. 6. It can be clearly observed that the total weight of steel bar is rapidly increases as the value of behavior factor, q is increases. In this study, the increment is around 2.1 to 4.8 times the total weight of steel bar for frame with behavior factor, q = 2.3.

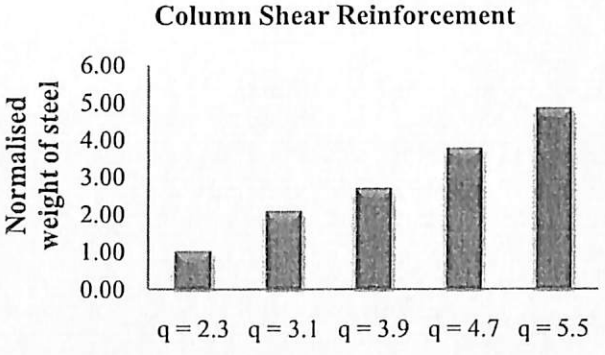

Figure 6. Effect of behavior factor, q on column shear reinforcement

This result is strongly associated with the requirement of confinement reinforcement for column as proposed by Eurocode 8 (2004). The requirement of confinement reinforcement is indicated by the required mechanical volumetric ratio of confining hoops within the critical region, $\omega_{wd\ req}$. The latter is influenced by the curvature ductility factor, μ_ϕ normalized design axial load, v_d gross cross-sectional width, b_c width of confined core, b_0 and design value of tension steel strain at yield, $\varepsilon_{sy,d}$. Higher value of behavior factor, q will increase the value of curvature ductility factor, μ_ϕ which result in higher required mechanical volumetric ratio of confining hoops within the critical region, $\omega_{wd\ req}$. As explained by Elghazouli (2009), the best solution to fulfill this requirement is the designer has to play around with the spacing of shear reinforcement, s. Decreasing the latter will decrease the required mechanical volumetric ratio of confining hoops within the critical region, $\omega_{wd\ req}$. At the same moment, this action will result in increase to the provided mechanical volumetric ratio of confining hoops within the critical region, $\omega_{wd\ prov}$. Using higher number and/or larger diameter of steel bar also can be considered as a solution. As a result, more amount of steel bar used as shear reinforcement has to be provided for frames with higher value of behavior factor, q.

In reality, every buildings tend to be a unique projects with different layout, function, and requirement (Booth and Key, 2006). Therefore, it is hard to establish the additional cost of providing the seismic resistance. However, it is worth to study about costing so the authority can have a guideline for future planning and development. From summation of cost of concrete and steel reinforcement, the total cost of material can be estimated. Fig. 7 presents the comparison of total cost of material for all frames.

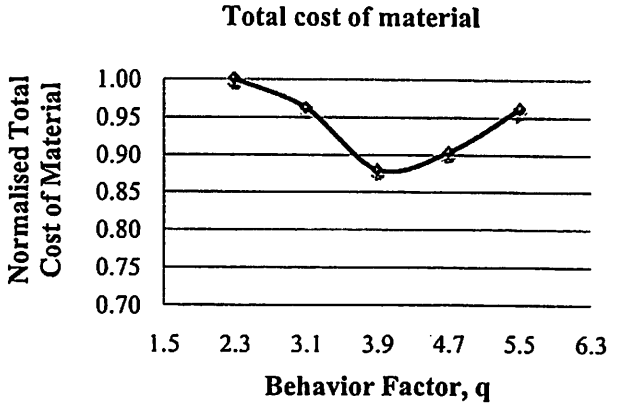

Figure 7. Effect of behavior factor, q on total cost of material

Form Fig. 7, it can be clearly observed that the total cost of material is strongly influenced by the value of behavior factor, q used for design. The most expensive frame is belong to the one which had been design with behavior factor, q = 2.3. Then, the total cost of material is decreases as the value of behavior factor, q is increases. This is due to lower magnitude of base shear force, F_b and horizontal forces, F_i acting on the frame. The total cost of material can be saved up to 22% when using behavior factor, q = 3.9. However, the former is increases as the behavior factor, q > 3.9 was used. This is due to rapid increasing in total weight of steel for column shear reinforcement to fulfill the requirement of confinement reinforcement as discussed in previous paragraph.

CONCLUSIONS

This paper investigates the effect of behavior factor, q on the total cost of material for seismic design of low rise RC hospital building. A typical three storey RC frame had been designed repeatedly by referring to Eurocode 8 (2004). Five value of behavior factor, q = 2.3, 3.1, 3.9, 4.7, and 5.5 had been used for DCM. The frame is assumed to be located at moderate seismic region in Malaysia where the reference peak ground acceleration, a_{gR} is equal to 0.12g. From this study, there are several conclusions can be drawn as follow:

- Total weight of steel bar used as flexural reinforcement for beam is decreases as the value of behavior factor, q is increases.
- The is no clear trend of the effect of behavior factor, q on total weight of steel bear used as shear reinforcement for beam. This is because the requirement of maximum spacing of shear reinforcement, s which has to be fulfilled.
- Total weight of steel bar used as flexural reinforcement for column is decreases as the value of behavior factor, q is increases. This is because the design of column flexural reinforcement is strongly related to the design of the flexural reinforcement of its corresponding beam.
- Total weight of steel bar for column shear reinforcement is rapidly increasing as the value of behavior factor, q is increases due to requirement of confinement reinforcement of ductile column.
- Finally, the total cost of material can be saved up to 22% when using behavior factor, q = 3.9 compared to the behavior factor, q = 2.3. However, the total cost of material is increasing when

the behavior factor, q > 3.9 due to rapid increasing of the total weight of steel bar for column shear reinforcement.

Therefore, the selection of behavior factor, q for design is very important since it will strongly influence the cost. It is worth to design economic structures without compromising safety. The evaluation of all frames used in this study with nonlinear time history analysis can be found elsewhere (Adiyanto and Majid, 2014a; Adiyanto et al., 2014c).

ACKNOWLEDGMENTS

The authors gratefully acknowledge the facilities provided by Universiti Sains Malaysia and financial support from MyBrain15, a scholarship provided by Ministry of Education Malaysia to accomplish this study. The authors also gratefully acknowledge the Institute of Postgraduate Studies Universiti Sains Malaysia for funding to attend the conference.

REFERENCES

Acun, B., A. Athanasopoulou, A. Pinto, E. Carvalho, and M. Fardis., (2012), "Eurocode 8: Seismic Design of Buildings Worked Examples," European Commission Joint Research Center, Ispra, Italy.

Adiyanto, M.I. and T.A. Majid., (2014a), "Seismic Performance of Three Storey Hospital RC Frame Subjected to Multiple Earthquake in Moderate Seismic Region," *Proceeding of International Congress on Natural Sciences and Engineering, Kyoto 2014*, 619-626.

Adiyanto, M.I. and T.A. Majid., (2014b), "Seismic Design of Two Storey Reinforced Concrete Building in Malaysia With Low Class Ductility," *Journal of Engineering Science and Technology*, 9(1), 27-46.

Adiyanto, M.I., T.A. Majid, and M.N. Fadzli., (2014c), "Nonlinear Response of Low Rise Hospital RC Building in Malaysia Due to Far and Near Field Earthquake," *Accepted for presentation and publication for Proceeding of Conference on the 3rd Geohazard Information Zone and the 5th Seminar and Short Course of HASTAG, Medan 2014.*

Adnan, A., Hendriyawan, A. Marto, and P.N.N. Selvanayagam., (2008), "Development of Seismic Hazard Maps of East Malaysia," *Advances in Earthquake Engineering Applications*, 1-17.

Booth, E. and D. Key, (2006). *Earthquake Design Practice for Buildings*, 2nd ed, Thomas Telford.

Borzi, B., and A.S. Elnashai., (2000), "Refined forced reduction factors for seismic design," *Journal of Engineering Structures*, 22, 1244-1260.

CEN., 2004. Eurocode 2: Design of Concrete Structures. Part 1-1: General Rules and Rules for Buildings, European Committee for Standardization, Brussels.

CEN., 2004. Eurocode 8: Design of Structures for Earthquake Resistance. Part 1: General Rules, Seismic Actions and Rules for Buildings, *Final Draft prEN 1998*, European Committee for Standardization, Brussels.

Elghazouli, A.Y., (2009). *Seismic Design of Buildings to Eurocode 8*, Taylor & Francis.

Elnashai, A.S. and L.D. Sarno, (2008). *Fundamentals of Earthquake Engineering*, 1st ed, John Wiley &Sons.

Gillie, J.L., A.R. Marek, and M.D. Cole., (2010), "Strength reduction factors for near-fault forward directivity ground motions," *Journal of Engineering Structures*, 32, 273-285.

Hatzigeorgiou, G.D. and A.A. Liolios., (2010), "Nonlinear Behaviour of RC Frames Under Repeated Strong Ground Motions," *Journal of Soil Dynamics and Earthquake Engineering*, 30, 1010-1025.

MOSTI., 2009. Seismic and Tsunami Hazards and Risk Study in Malaysia, *Final Report*, Ministry of Science, Technology, and Innovation of Malaysia.

Subramaniam, N., (2011), "Design of Confinement Reinforcement for RC columns," *The Indian Concrete Journal*, 1-8.

DUCTILITY DEMANDS OF INELASTIC STRUCTURES AFFECTED BY REPEATED EARTHQUAKES

FINAL REPORT

RU GRANT

(1001/PAWAM/814115)

By

Assoc. Prof. Dr. Taksiah A.Majid

UNIVERSITI SAINS MALAYSIA

December 2015

TABLE OF CONTENTS

LIST OF FIGURES

LIST OF FIGURES

LIST OF TABLES

LIST OF ABBREVIATIONS

2D	=	2 dimension
3D	=	3 dimension
ACI	=	American Concrete Institute
AISC	=	American Institute of Steel Construction
ANOVA	=	Analysis of Variance
ASCE	=	American Society of Civil Engineers
ATC	=	Applied Technology Council
BSSC	=	Building Seismic Safety Council
Comp.	=	component
Damp.	=	damping ratio
DCH	=	High Ductility
DCL	=	Low Ductility
DCM	=	Medium Ductility
Dir.	=	direction
Dist.	=	source-to-site distance
DOF	=	Degree of Freedom
EDP	=	Engineering Demand Parameter
Eff-Mass	=	modal effective mass
Epi.	=	epicentre
ESD	=	European Strong Motion Database
FDE	=	Near-Field Earthquake with Forward Directivity Effect
FEMA	=	Federal Emergency Management Agency
FFE	=	Far-Field Earthquake
FFGM	=	Far-Field Ground Motion
Freq.	=	frequency

GM	=	Ground Motion
ICC	=	International Code Council
IDA	=	Incremental Dynamic Analysis
Mag.	=	magnitude
MDOF	=	Multi Degree of Freedom
NFGM	=	Near-Fault Ground Motion
NSA	=	Nonlinear Static Analysis
NTHA	=	Nonlinear Time History Analysis
Part-Fact	=	modal participation factor of mass
PEER	=	Pacific Earthquake Engineering Research center
PEER NGA	=	Pacific Earthquake Engineering Research center: NGA database
PGA	=	Peak Ground Acceleration
PGV	=	Peak Ground Velocity
POA	=	Pushover Analysis
RC	=	Reinforced Concrete
RFDE	=	Residual motion from near-field earthquake with Forward Directivity Effect
SDOF	=	Single Degree of Freedom
SRSS	=	Square Root of the Sum of the Squares
X-Disp.	=	displacement at x-direction
x-dir	=	x direction of structure plan
Y-Rotn.	=	rotation at y-direction
Z-Disp.	=	displacement at z-direction
z-dir	=	*z*-direction of structure plan

LIST OF SYMBOLS

$\mathbf{C}$	=	damping matrix
$\mathbf{K_o}$	=	elastic (initial) stiffness matrix
$\mathbf{K_p}$	=	matrix of the change in stiffness that result from in elastic behaviour of the system due to material nonlinearity
$\mathbf{M}$	=	mass matrix
$\mathbf{r}$	=	displacement vector of the free DOFs due to a unit displacement of the base support
$\Delta\mathbf{Q}$	=	vector of incremental nodal loads and reactions
$\Delta\mathbf{u}$	=	vector of incremental nodal displacement

C20	=	concrete grade with 20 MPa of compressive strength
C_{ms}	=	modal seismic coefficient
C_t	=	coefficient for reinforced concrete moment resisting frame in Eurocode 8
E_b	=	Young modulus of beam
E_c	=	Young modulus of column
F_b	=	seismic base shear
F_e	=	elastic force
F_i	=	horizontal force acting on story i
$F_i(x)$	=	force at story i in x-direction
$F_i(z)$	=	force at story i in z-direction
F_m	=	modal force
F_{ratio}	=	significance level of regression analysis
F_{test}	=	significance level of F_{ratio} from analysis of variance
F_y	=	yield force
g	=	gravity (9.81 m/s^2)
H	=	total height
H	=	total height of building
H_i	=	story i height
I	=	moment of inertia
I_b	=	moment of inertia of beam
I_c	=	moment of inertia of column

ID_{max} = maximum interstory drift

ID_{uc} = ultimate interstory drift capacity

ID_y = yield interstory drift capacity

ID_{yc} = yield interstory drift capacity

I_{ef} = effective moment of inertia

I_g = gross moment of inertia

K = stiffness

K_e = elastic stiffness

K_o = elastic rotation stiffness of the member

L = length

L_b = length of beam

L_c = length of column

M = magnitude

m = total mass of building

M = bending moment

M_b = body wave magnitude

M_c = capping moment which is equal to maximum moment

M_{col} = moment at column

m_i = mass at story i

m_i, m_j = the story masses associated with all gravity load

M_L = local magnitude (Richter scale)

M_{max} = maximum moment

M_s = surface wave magnitude

M_w = moment magnitude

M_x = moment in x-direction

M_y = yield moment

M_{y-x} = yield moment in z-direction

M_{y-z} = yield moment in x-direction

M_z = moment in z-direction

N = number of story

n = dimensionless parameter to increase β_o

P = axial force

q = behaviour factor

q_o = behaviour factor without overstrength factor

R = source to site distance

r	=	post-yield stiffness ratio
R^2	=	coefficient of determination in regression analysis
$ri_{2/1}$	=	relative increment due to double event repeated earthquakes
$ri_{2\text{-}3/1}$	=	relative increment due to double and triple event repeated earthquakes
$ri_{3/1}$	=	relative increment due to triple event repeated earthquakes
r_K	=	ratio of global post-yield stiffness to elastic stiffness
ry	=	rotation at y-direction
$S(z/H)$	=	reduction stiffness along the height
S500	=	steel grade for 500 MPa of tensile strength
S_a	=	spectral acceleration
$S_a(T_i)$	=	spectral acceleration at period of mode i
S_d	=	design spectral acceleration of Eurocode 8
$S_d(T_1)$	=	ordinate of design spectrum of Eurocode 8 Type 1 at period T_1
S_e	=	elastic response spectrum
s_i	=	modal displacement at story i
s_i, s_j	=	displacement of masses m_i, m_j in the fundamental mode shape
$Sig.F_{ratio}$	=	significance level of F_{ratio} from analysis of variance
T	=	period
T_1	=	fundamental period of building
T_B	=	first corner period of the constant acceleration in elastic response spectrum of Eurocode 8
T_C	=	second corner period of the constant acceleration in elastic response spectrum of Eurocode 8
T_D	=	value defining the beginning of the constant displacement response range of the spectrum
T_P	=	pulse period of velocity ground motion
tx	=	translation at x-direction
tz	=	translation at z-direction
V_b	=	base shear
V_c	=	base shear capacity
V_d	=	base shear design
V_{fy}	=	base shear at first local yield
V_{max}	=	maximum base shear
V_y	=	yield base shear
W	=	weight of structure
W_{em}	=	effective weight of the structure

X_{ij} = i^{th} observation on the j^{th} independent variable

y_i = response in regression analysis

z = story height from ground floor

z/H = relative story height from ground floor

z/x = ratio of PGA of the components z to x from earthquake record

α = unloading parameter in Modified-Takeda hysteresis rule

α_c = mass proportional damping coefficient

α_1 = multiplier of horizontal seismic design action at formation of global plastic mechanism

a_g = design peak ground acceleration

α_o = dimensionless parameter to control degree of participation of overall shear deformations in a simplified model of multi-story building

α_u = multiplier of horizontal design seismic action at formation of first plastic hinge in the system

α_u/α_1 = overstrength factor

β_c = stiffness proportional damping coefficient

β = reloading parameter in Modified-Takeda hysteresis rule

β_p = regression intercept of variable j in regression analysis

δ = ratio of lateral stiffness at top of structure to the lateral stiffness at the base

Δ_{max} = maximum displacement

ΔQ = incremental nodal load

ΔQ_n = incremental nodal load at n stage

Δ_{roof} = roof displacement

Δt = time interval

Δu = incremental displacement vector over the time interval

$\Delta \dot{u}$ = incremental velocity vector over the time interval

$\Delta \ddot{u}$ = incremental acceleration vector over the time interval

Δu_{roof} = incremental nodal displacement at roof

$\Delta \ddot{u}_g$ = incremental ground motion acceleration vector over the time interval

ΔV_b = incremental base shear

Δ_y = yield displacement

Δ_{yield} = yield displacement

ε = regression error

ε_i = regression error of i^{th} observation

ϕ = curvature of the section due to flexural action

$\phi_{si/z}$ = modal displacement at z-direction

$\phi_{sj/x}$ = modal displacement at x-direction

η = damping correction factor with a reference value of $\eta = 1$ for 5% viscous damping

ϑ_c = ratio of story ductility to global ductility capacities

λ = correction factor in determining base shear in Eurocode 8

λo = dimensionless parameter that controls the variation of lateral stiffness along the height of structure (1 for linear variation, 2 for parabolic variation)

μ = ductility ratio

μ_Δ = roof ductility

$\mu_{\Delta,All\text{-}1}$ = predicted roof ductility demand for single event of FFE and FDE repeated earthquakes

$\mu_{\Delta,All\text{-}23}$ = predicted roof ductility demand for double and triple events of FFE and FDE repeated earthquakes

$\mu_{\Delta,D1}$ = predicted roof ductility demand for single event of FDE repeated earthquakes

$\mu_{\Delta,D2}$ = predicted roof ductility demand for double events of FDE repeated earthquakes

$\mu_{\Delta,D23}$ = predicted roof ductility demand for double and triple events of FDE repeated earthquakes

$\mu_{\Delta,D3}$ = predicted roof ductility demand for triple events of FDE repeated earthquakes

$\mu_{\Delta,F1}$ = predicted roof ductility demand for single event of FFE repeated earthquakes

$\mu_{\Delta,F2}$ = predicted roof ductility demand for double events of FFE repeated earthquakes

$\mu_{\Delta,F23}$ = predicted roof ductility demand for double and triple events of FFE repeated earthquakes

$\mu_{\Delta,F3}$ = predicted roof ductility demand for triple events of FFE repeated earthquakes

$\mu_{\Delta c}$ = roof ductility capacity

μ_{sc} = story ductility capacity

$\mu_{\theta,c}$ = ductility of plastic rotation capacity

$\mu_{\theta,u}$ = ultimate rotation ductility

μ_s = story ductility demand

$\mu_{s,All}$ = maximum story ductility demand for all cases of repeated earthquakes

$\mu_{s,D1}$ = predicted maximum story ductility demand for single event of FDE repeated earthquakes

$\mu_{s,D2}$ = predicted maximum story ductility demand for double events of FDE repeated earthquakes

$\mu_{s,D3}$ = predicted maximum story ductility demand for triple events of FDE repeated earthquakes

$\mu_{s,F1}$ = predicted maximum story ductility demand for single event of FFE repeated earthquakes

$\mu_{s,F2}$ = predicted maximum story ductility demand for double events of FFE repeated earthquakes

$\mu_{s,F3}$ = predicted maximum story ductility demand for triple events of FFE repeated earthquakes

$\mu_{s,max}$ = maximum story ductility

μ_{sc} = story ductility capacity

ω_i, ω_j = circular frequency of mode i and j

θ_c = capping rotation

θ_p = plastic rotation

θ_{pc} = post-capping rotation capacity

θ_{roof} = maximum roof drift ratio

θ_y = yield rotation

ρ = ratio of the stiffness of all beams at the mid-high story of the frame to the sum of the stiffness of all columns at the same story

$\rho_{M\&T}$ = ρ according Miranda and Taghavi (2005)

ξ = modal critical damping ratio

CHAPTER 1
INTRODUCTION

1.1 Background

Earthquakes usually do not occur as a single event, as mostly assumed in seismic design, but as a series of shocks. Strong earthquakes have more and larger aftershocks, sometimes foreshocks, and the sequences can last for years or even longer. Aftershocks are usually unpredictable and can be of a large magnitude which could cause collapse to buildings which already damaged from the main shock. Båth (1973) noted that in many instances the largest earthquake aftershock is about 1.2 less in magnitude than that of the main shock. Foreshock activity has been detected for about 40% of all moderate to large earthquakes, and up to 70% for events of M >7.0 (Kayal, 2008). They occur from a matter of minutes to days or even longer before the main shock. However, some large earthquakes show no foreshock activity at all.

The repetition of medium-strong earthquake ground motions after intervals of time is characterizing the repeated earthquake. Interval of time could be short or long which might take several minutes, hours, days, or even years, but not more than the structure lifetime (i.e. 50 years). The combination of foreshock, mainshock, and aftershock in seismic sequences is demonstrated in Figure 1.1 and listed in Table 1.1. Table 1.1 concludes that the seismic sequences are not the series of foreshock, mainshock and aftershock within 24 hours only. Furthermore, the repeated earthquake is not necessarily sourced from the same ruptured fault because it can be experienced by the site that situated near active faults having varies fault types and

ruptured mechanism (e.g. Tarzana, Los Angeles, US, see Griffith and Cook, 2004). It indicates repeated earthquakes can be a combination of near-field and far-field earthquakes containing ground motions with forward directivity (pulse-effect) and backward directivity (no pulse effect) effects. Based on the aforementioned quake events, it can be concluded that the seismic sequences is the series of foreshock, mainshock and aftershock within 24 hours, some days, or even some years.

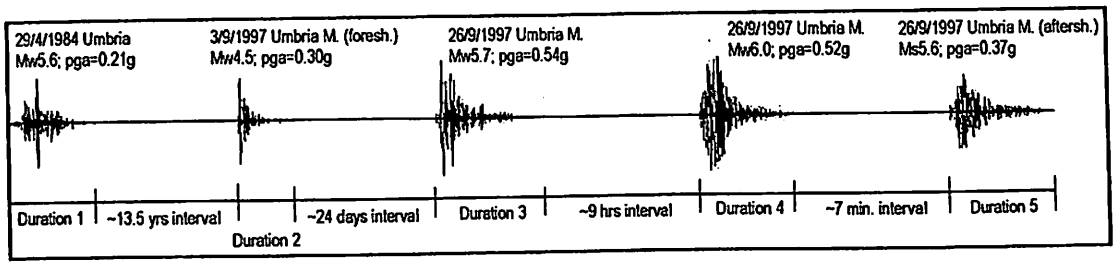

Figure 1.1: An example of repeated earthquake ground motions recorded from Norcera Umbra station, Italy

The repetition of medium-strong earthquake ground motions after short intervals of time is a character of repeated earthquakes (Amadio et al., 2003). It was recently observed in, Italy, Turkey and California, as previously listed in Table 1.1. In such cases, the structure that already damaged after the first earthquake ground motion and not yet repaired may become completely inadequate at the end of the seismic sequence (Elnashai et al., 1998; Muria Vila and Toro Jaramillo, 1998). Despite the seismic sequences hazard was clearly threatening, the effect of repeated earthquakes on the structures has not attracted much attention (Hatzigeorgiou and Beskos, 2009).

Table 1.1: Examples of repeated earthquake event around the world

No.	Station	Dir.	Earthquake name	Date	Time	Mag.	PGA(g)	Source
1	LDEO C0375VO, Turkey	NS	Duzce	7/11/1999	16:57	Mw7.2	0.919	ESD
		NS	Duzce (aftershock)	12/11/1999	16:54	Mw4.9	0.352	ESD
		NS	Duzce (aftershock)	13/11/1999	0:54	Ms4.5	0.304	ESD
		NS	Duzce (aftershock)	19/11/1999	19:59	Ms4.4	0.595	ESD
2	Izmit-Met. Istasyonu, Turkey	EW	Izmit	17/8/1999	11:55	Mw5.8	0.223	ESD
		EW	Izmit (aftershock)	13/9/1999	0:01	Mw7.6	0.317	ESD
3	Duzce-Met. Mudurlugu, Turkey	EW	Duzce	29/8/1999	10:15	Mw4.2	0.157	ESD
		EW	Izmit (aftershock)	12/11/1999	16:57	Mw7.2	0.513	ESD
4	IRIGM-Sta. No.496, Turkey	NS	Duzce (aftershock)	12/11/1999	17:16	Mb4.7	1.036	ESD
		NS	Duzce (aftershock)	12/11/1999	17:17	Mb5.2	0.747	ESD
		NS	Duzce (aftershock)	12/11/1999	17:46	Mb4.5	0.575	ESD
5	Colforito, Italy	NS	Umbria Marche	26/9/1997	0:33	Mw5.7	0.345	ESD
		NS	Umbria Marche	26/9/1997	9:40	Mw6.0	0.199	ESD
6	Norcera Umbra, Italy	NS	Umbria	29/4/1984	05:02	Mw5.6	0.209	ESD
		NS	Umbria Marche (foreshock)	3/9/1997	22:07	Mw4.5	0.295	ESD
		NS	Umbria Marche	26/9/1997	0:33	Mw5.7	0.538	ESD
		NS	Umbria Marche	26/9/1997	9:40	Mw6.0	0.524	ESD
		NS	Umbria Marche (aftershock)	26/9/1997	9:47	Ms5.6	0.372	ESD
7	Forgario-Comio, Italy	EW	Friuli (aftershock)	11/5/1976	22:44	Mw4.9	0.306	ESD
		EW	Friuli (aftershock)	11/9/1976	16:35	Mw5.5	0.232	ESD
		EW	Friuli (aftershock)	15/9/1976	3:15	Mw6.0	0.218	ESD
		EW	Friuli (aftershock)	15/9/1976	9:21	Mw6.0	0.336	ESD
		EW	Friuli (aftershock)	16/9/1977	23:48	Mw5.4	0.193	ESD
8	Nalband, Armenia	EW	Spitak (aftershock)	18/1/1989	13:09	Ms3.7	0.206	ESD
		EW	Spitak (aftershock)	18/1/1989	16:53	ML4.1	0.217	ESD
9	Kalamata-OTE Bldg., Greece	EW	Kalamata	13/9/1986	17:24	Ms6.2	0.240	ESD
		EW	Kalamata (aftershock)	15/9/1986	11:41	Ms5.4	0.240	ESD
10	IITR Berlongfer, India	NS	India-Burma Border, India	9/1/1990	18:51	Ms6.1	0.142	Cosmos
		NS	India-Burma Border, India	6/8/1988	0:36	Ms7.2	0.344	Cosmos
11	CHY080, Taiwan	EW	Chi-Chi	20/9/1999	17:47	Mw7.6	0.082	Cosmos
		EW	Chi-Chi (aftershock)	20/9/1999	18:03	Mw6.2	0.048	Cosmos
12	CSB19001 Jiashi, China	WE	Northwest China (foreshock)	5/4/1997	23:46	Mw5.9	0.233	Cosmos
		WE	Northwest China (foreshock)	6/4/1997	4:36	Mw5.9	0.144	Cosmos
		WE	Northwest China	11/4/1997	5:34	Mw6.1	0.273	Cosmos
		WE	Northwest China (aftershock)	15/4/1997	18:19	Mw5.8	0.239	Cosmos
13	Victoria, Baja, Mexico	SN	Mexico	11/3/1978	5:40	Mw4.4	0.504	Cosmos
		SN	Mexicali Valley	11/3/1978	23:57	ML4.8	0.459	Cosmos
		SN	Mexicali Valley	12/3/1978	0:30	ML4.5	0.418	Cosmos
		SN	Mexicali Valley	12/3/1978	18:42	ML4.8	0.570	Cosmos
14	Nahanni, NWT, Sta.1, Canada	NS	Nahanni, NWT	23/12/1978	5:16	Ms6.9	0.975	Cosmos
		NS	Nahanni, NWT (aftershock)	23/12/1978	5:48	Ms5.4	0.228	Cosmos
15	DGG Llolleo, Chile	NS	Valparaiso	3/3/1985	22:47	Ms7.8	0.712	Cosmos
		NS	Valparaiso (aftershock)	3/3/1985	23:38	Ms6.3	0.186	Cosmos
		NS	Valparaiso (aftershock)	8/4/1985	23:27	Ms5.0	0.204	Cosmos
16	Imperial Valley, Array 9, US	SN	El Centro	19/5/1940	4:36	Mw6.9	0.348	Cosmos
		SN	Borrego Mountain	9/4/1968	2:28	Mw6.5	0.130	Cosmos
		EW	Imperial Valley	15/10/1979	23:16	Mw6.5	0.236	Cosmos
		EW	Imperial Valley (aftershock)	15/10/1979	23:19	ML5.0	0.189	Cosmos
17	Cedar Hill NA, Tarzana, US	EW	Whittier Narrows	1/10/1987	14:42	Mw6.1	0.405	Cosmos
		EW	Northridge	17/1/1994	12:30	Mw6.7	1.778	Cosmos
		EW	Northridge (aftershock)	20/3/1994	21:20	Mw5.3	0.372	Cosmos
18	City Hall Annex, Hollister, US	WE	Hollister	9/4/1961	7:23	ML5.6	0.179	Cosmos
		WE	Hollister	28/11/1974	23:01	Mw5.2	0.166	Cosmos
		WE	Loma Prieta	18/10/1989	0:04	Mw7.0	0.221	Cosmos
19	24399 Mt Wilson-CIT Sta., US	NS	Whittier Narrows	1/10/1987	14:42	Mw6.0	0.186	PEER
		NS	Whittier Narrows (aftersh.)	4/10/1987	10:59	Mw5.3	0.158	PEER
20	Gavilan CGB, Gilroy, US	EW	Loma Prieta	18/10/1989	0:04	Mw7.0	0.356	Cosmos
		EW	Gilroy	14/5/2002	5:00	Mw4.9	0.213	Cosmos

NS=North-South; EW = East-West; WE = West-East; SN = South-North
ESD = European Strong-Motion Database (Ambraseys et al., 2001)
Cosmos = COSMOS Virtual Data Centre http://db.cosmos-eq.org/scripts/earthquakes.plx
PEER = PEER NGA Database http://peer.berkeley.edu/nga/

To the best of author's knowledge, there are few studies have examined the seismic sequences effect on the buildings. The recent studies published have not addressed the needs in engineering design properly. For instance, some of studies focused on single-of-degree-system (SDOF) having bilinear elasto-plastic hysteresis with no stiffness and strength degradation (Hatzigeorgiou and Beskos, 2009; Hatzigeorgiou, 2010a; Hatzigeorgiou, 2010b). In fact, the real structure is in multi-degree-of-freedom (MDOF) comprises of beam, column, and beam-column joint that can be deformed in different manners due to cyclic loading reversals propagated by earthquake ground motion.

Recently, Hatzigeorgiou and Liolios (2010) had tried to address the lack in MDOF issue. Unfortunately, they have used 2 reinforced concrete (RC) frame models to represent 2 type of fundamental period of vibration of structures with unvaried behaviour factor. All of those studies were carried out using ground motion that was characterized based on source-to-site distance only. In fact, the character of ground motion would be appropriately classified by its large pulse and permanent shifted containing in the motion (e.g. Somerville, 2003; Mavroeidis and Papageorgiou, 2003; Baker, 2007). These pitfalls could increase the uncertainty in nonlinear dynamic analysis. Therefore, more comprehensive study pertained the repeated earthquake hazard on the system having a broad range of fundamental period of vibration and strengths, as well as an appropriate classification of ground motion, is needed. Consequently, the result can be used as the general insight and tool in seismic engineering design and evaluation.

1.2 Objectives

The objectives of this study is as follows:

1. To identify the effect of FFGM and NFGM in repeated earthquakes on the ductility demand of the 3D generic MDOF systems.
2. To identify the effect of oscillatory character, γ, and pulse period, T_p, of repeated NFGM coupled orthogonally with non-pulse NFGM on the ductility demand of 3D generic MDOF systems.
3. To identify the effect of structure's fundamental period and number of story, force reduction factor, type of material of MDOF frame, on the ductility demand of 3D generic MDOF system.
4. To develop and propose empirical relation formula for ductility demand of 3D generic MDOF system due to repeated earthquake taking into account the effect of structure's fundamental period and number of story, force reduction factor, type of material of MDOF frame, repeated FFGM or NFGM, oscillatory character and pulse period of repeated NFGM, and seismic sequence cases.

CHAPTER 2
LITERATURE REVIEW

2.1 Earthquake Ground Motion

2.1.1 Near-Field Ground Motion

Seismic waves from near-field ground motion (NFGM) propagating massive devastation to the local buildings. The ruptured faults of NFGM transmit a unique seismic wave to the earth surface which is indicated by some large pulses in their ground motion records. The identified effects of this NFGM characteristic are forward directivity effect (FDE), fling effect, hanging wall effect and vertical effect, which are highly influenced by source mechanism, fault rupture direction, and fault rupture slip direction (Somerville, 2003).

Large pulses in long period of earthquake ground motion record, especially in velocity and displacement motions, may occur when the rupture of earthquake at dip-slip or strike-slip fault having source-to-site distance of about less than 20 km (Stewart et al., 2002; Bray and Rodriguez-Marek, 2004; Li and Xie, 2007). However, there was no universal consensus in definition of upper limit of the NFGM's distance. Hence Stewart et al. (2002) recommended that 20-60 km should be appropriate range for upper limit of distance which is followed by Li and Xie (2007). Velocity with large pulse in its long period is called as FDE or pulse-effect which could be occurred when the rupture front propagates toward the site.

FDE looks as a single large pulse of motion that occurred at the beginning of the record, which represents most of the seismic energy from the rupture caused by a velocity of the propagation of fault rupture toward a site which closes to the shear wave velocity. An example of FDE is demonstrated in the Rinaldi record of 1994

Northridge earthquake, as shown in Figure 2.1b, which is clearly indicating a large pulse compare to the Taft record of 1952 Kern County earthquake in Figure 2.1a. Large pulse of displacements with offset waveforms in NFGM is called as fling-step effect (e.g. the Sakarya-SKR record of 1999 Kocaeli earthquake as depicted in Figure 2.1c), which might be contained on the record at the site with slip-parallel and slip-normal directions for faults of strike-slip and dip-slip, respectively. Both effects could be occurred together on the site either near strike-slip or dip-slip faults.

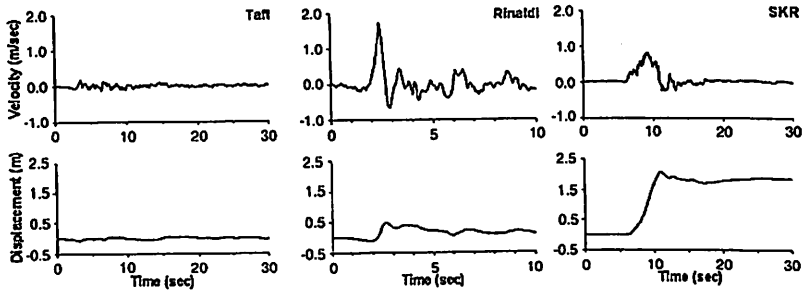

a) Far-field motion b) FDE motion c) Fling-step motion

Figure 2.1: Comparison of typical far- and near-field velocity and displacement (Kalkan and Kunnath, 2006)

Response of structure built in near-field site is much affected by FDE pulse motion. Therefore, many studies were reported by seismologist that dedicated to numerically simulate the pulse-like ground motion in order to describe the ground motions with FDE and to estimate the response of structure induced by this motion (Makris, 1997; Alavi and Krawinkler, 2001; Menun and Fu, 2002; and Mavroeidis and Papageorgeou 2003; Bray and Rodriguez-Marek, 2004; Kalkan and Kunnath, 2006; Baker, 2007).

2.1.2 Far-Field Ground Motion

In engineering practices, regular ground motion is widely used since the earthquake motion in California was successfully recorded and processed into digital format in forties. Before unique characters were found in some ground motions, all of regular motions were fall into group of far-field ground motion (FFGM). Therefore it can be defined that any ground motion which not possessed any unique character of NFGM is grouped as FFGM. However, the weak motion that recorded from distant earthquake is not considered as FFGM in this study. For comparison with NFGM, the velocity and displacement time histories of FFGM are depicted in Figure 2.1a.

2.2 Seismic Evaluation of Building

2.2.1 Simplified Model for MDOF System

In order to reduce computational and data management efforts in using the nonlinear static analysis (NSA) and nonlinear time history analysis (NTHA) methods in multi-degree of freedom (MDOF) system, the simplified model was introduced. Simplified model aims to consolidate the governed properties of detailed structural models into equivalent MDOF model, i.e., stick model, fish bone model, and generic frame model. The generic frame model is discussed separately in the next subsection.

The stick model (or continuum model) have been used since the work by Newmark (1959) or earlier. Stick model is a cantilever beam having a number of lumped masses that indicate the story. It reduced the number of DOF significantly compared with other simplified model. This model can represent flexural beam or shear beam. Flexural beam model is utilized when rotational coupling among various vertical flexural elements is negligible e.g., braced frames or cantilever shear walls.

The yield interstory displacement is identical for all stories. Shear beam model is used when story shear mechanisms are anticipated or when strong beam~weak column phenomena applied. It means the effect of hinge progress on the beams prior hinge of columns cannot be detected (Takada et al., 1988; FEMA, 2005). A stick model could be extended to dual cantilever model as demonstrated in by Basu et al. (1979), Basu and Dar (1982), Miranda (1999), Miranda and Reyes (2002), Taghavi and Miranda (2005). The model comprised of flexural cantilever beam and shear cantilever beam deforming in bending and shear deformations, respectively. Both beams connected by axially rigid member that transmit horizontal force so that the system undergoes the same lateral deformation.

Fish bone model is proposed by Nakashima et al. (2002) by assuming all rotations at beam-column joints lying at each floor are identical. The model also assumes the axial elongation and contraction of columns and beams are neglected. Therefore, the point of contra-flexure of all beams is restricted to their mid spans at each floor. Moreover, uniform cross-section for each member is assumed and effect of slab on beam stiffness and strength are excluded. At each floor, all beams can be condensed into one rotational spring, as well as all columns in each story can be represented by a column comprising a single mass, spring, and dashpot per floor.

2.2.2 Generic Frame Model for MDOF System

The use of generic frame structure model can be traced back to the work by Esteva and Ruiz (1989) and followed by Osteraas and Krawinkler (1990). They tuned the moment resisting frame model so that it matched with the designed building. This process was considering the geometry, gravity and lateral loading, drift criteria, member sizes, and structural capacity that complied with the code at

that time. The model was extended by Nassar and Krawinkler (1991) by introducing the plastic hinge (rotation spring) at beam or column members and at support to model the strong column~weak beam behaviour, weak column~strong beam behaviour, and soft story model as illustrated in Figure 2.2.

The Nassar and Krawinkler's model has been used for further studies e.g. to quantify the effect of vertical irregularities in mass, stiffness, or strength on seismic demands using column hinges only (Krawinkler and Al-Ali, 1996; Al-Ali and Krawinkler, 1998), to develop a simple tool for conceptual design of MDOF system using beam hinges only (Seneviratna and Krawinkler, 1997). Thus, the generic frame model was theoretically enhanced and verified using real 3, 9, and 20 stories steel structures using column hinges only through SAC project by Gupta and Krawinkler (1999, 2000). Furthermore, the Gupta and Krawinkler's model was modified to 3, 6, 9, 12, 15, 18 stories of steel structures to evaluate the seismic demands of nondeteriorating frame system due to regular ground motions (Medina and Krawinkler, 2003; Krawinkler et al., 2003; Medina and Krawinkler, 2005; Chintanapakdee and Chopra, 2003; Chopra and Chintanapakdee, 2001).

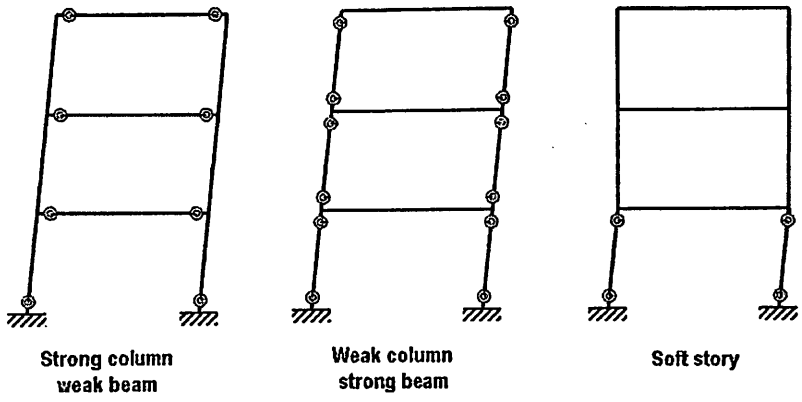

Figure 2.2: Generic frame model of inelastic structures used in Nassar and Krawinkler (1991)

Ruiz-Garcia and Miranda (2005) enhanced the two-dimensional single bay generic frame to be more versatile and realistic following the behaviour of moment resisting frame that containing flexure and shear deformation affected by earthquake. The strength and stiffness were adjusted differently with the previous generic frame models. Their model was also extended to three-bay generic frame by Zareian and Krawinkler (2009) in developing the simplified procedure of performance based design for reinforced concrete (RC) buildings. The idea of this extension was to include the interior beam-column joint, not exterior beam-column joint only as in single-bay generic frame, so that it became a model with more realistic seismic behaviour. Despite it needs more rigor processes, the aforesaid advantageous conclude that the Ruiz-Garcia and Miranda's generic frame model provide the most realistic result in structural earthquake engineering simulation compare with other simplified model i.e. stick model and fish bone model.

2.3 Seismic Response of Building

2.3.1 Effect of Fundamental Period of Vibration

In earthquake engineering, structural characteristic namely as fundamental period of vibration of system (or natural period) is very important, either for design or evaluation, because of its relation to the seismic hazard demand curve, i.e. design response spectrum. Mass, strength, and stiffness affect this fundamental period of vibration of building. Consequently, other important parameters, e.g. building height (or number of story), number of bays, structural regularity, section size are also governed the fundamental period of building. In seismic code, the relationship of fundamental period with building height is very common to help the engineer in estimating the design response spectrum. Commonly, the relationship of fundamental

period of building and building height was empirically determined based on real measurement on the building structure.

The stiffness of building decreases as the height of building increases. Therefore it leads the increment of displacement demands as the fundamental period of building increases. This condition was clearly demonstrated in Ruiz-Garcia and Miranda (2006). They evaluated generic flexible and rigid frames (represent bare and infilled frames) and found that as the fundamental period of vibration elongates the dispersion of displacement demand tends to increase and as the intensity of seismic motion increase. However, this increment of displacement demands was not in constant rate. Moreover, it demonstrated that despite buildings having the same number of stories (or height), but different fundamental period, the displacement demands would not be the same. The demands on the generic flexible frames were significantly larger than the demands on the generic rigid frames.

2.3.2 Effect of Behaviour Factor

Behaviour factor (denoted as q) is known as response modification coefficient (R) in ASCE 7-05. Some documents and references denoted this parameter as force (or strength) reduction factor. Behaviour factor is used for reducing the elastic design response spectrum and defined as the ratio of the elastic strength demand to the inelastic strength demand (Eurocode 8), as shown in Figure 2.3. Elastic strength demand is typically defined by the 5% damped elastic response spectrum, whereas inelastic strength demand is the strength required in the structure to response beyond the elastic range but within the selected ductility limits (Kappos, 1999).

The theoretical background of behaviour factor is approached by Eurocode 8 and US Code in different way as demonstrated in Kappos (1999), Borzi and Elnashai (2000), Fardis (2009). It made the value of behaviour factor is provided larger in US than in Europe due to the differences on the applied ground motion (Borzi and Elnashai, 2000; Mitropoulou et al., 2010). For instance moment resisting frame in ASCE 7-05 provides a range of behaviour factor from 3 to 8, whereas Eurocode 8 provides a range from 3 to 6.75. Therefore different levels of damage during earthquakes are likely to occur for the same structures designed according to these codes despite they provide the same strength of material. Moreover, it is important to underlined that higher behaviour factor do not necessarily lead to lighter structures because the loading scenarios may also affect the system (Borzi and Elnashai, 2000).

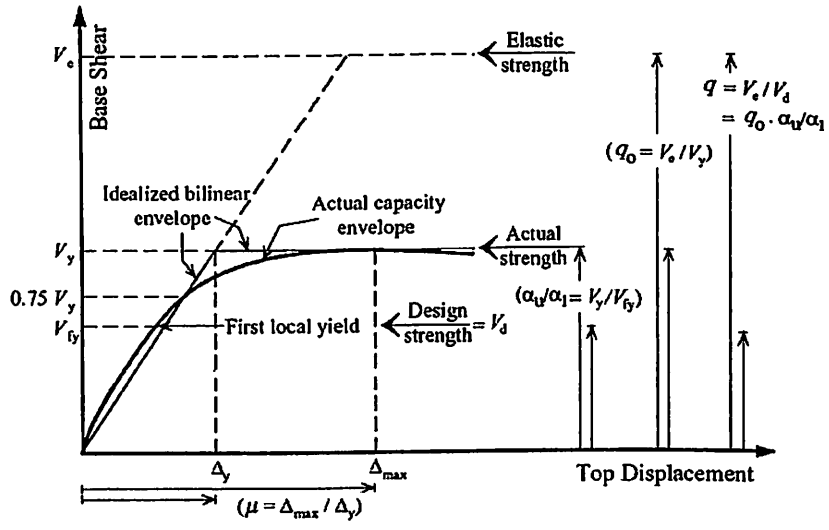

Figure 2.3: Definition of behaviour factor, q, overstrength factor, α_u/α_1, and displacement ductility, μ (modified from Elnashai and Di Sarno, 2008)

Many studies dedicated to investigate the suitable behaviour factor for many structural and ground motion type either based on single-degree of freedom (SDOF) system or MDOF system. In seventies the well-known behaviour factor was proposed as a function of ductility by Newmark and Hall (1973) and they considered that behaviour factor equal to the displacement ductility in the long period range of

system. It is because they observed that elastic and inelastic SDOF systems with the same initial stiffness reached almost the same displacement. The ductility is found higher than the behaviour factor for short period of system and hence the equal energy approach might be adopted to calculate force reduction. This work was refined and extended by Lai and Biggs (1980), in which computed the inelastic design spectra with the use of deamplification factor not only based on displacement ductility and spectral region, but also damping ratio.

Nassar and Krawinkler (1991) investigated the effect of strength hardening and bilinear and stiffness degrading hysteresis models effect on the behaviour factor. They found that stiffness degradation has negligible effect on the behaviour factor. Borzi and Elnashai (2000) has found the similar findings by using 364 ground motion records for the effect of strength hardening-softening and stiffness degradation in hysteresis model. Similar work using various hysteresis type and damping ratio was also done by Vidic et al. (1994), Cuesta and Ascheim (2001), Cuesta et al. (2003) and Karakostas et al. (2007). Using 124 ground motions for 5% damped bilinear SDOF system, Miranda and Bertero (1994) found that soft soil effect influenced the behaviour factor and proposed behaviour factor based on rock, alluvium, soft soil sites condition.

Effect of NFGM on the behaviour factor has been evaluated by Jalali and Trifunac (2008) using strength hardening elasto-plastic SDOF system. They considered the fault-normal and fault-parallel motions of NFGMs. It found that behaviour factor from FFGM was significantly not the same with the behaviour factor from NFGM and thus proposed a factor to solve this problem. Very recently Gillie et al. (2010) examines the influence of ground motions with FDE on the behaviour factor using bilinear SDOF system. It finds that FDE significantly affects

the behaviour factor (ranged from 0.5 to 3 s of period) and shows that behaviour factor is smaller than those from non-FDE motions, particularly in the constant velocity region which corresponds to the range of periods of FDE pulses. It means the use of behaviour factor obtained from non-FDE motions is unlikely safe for design of structures built at the region having FDE of earthquake.

In relation with MDOF system, Kappos (1999) has evaluated the actual behaviour factor based on inelastic time history analysis of MDOF system (up to five-story structures) represent the European code-designed RC buildings compared with the value provided by Eurocode 8. It showed that behaviour factor of Eurocode 8 is smaller than the predicted from MDOF system for most of short and intermediate periods. Using different behaviour factors to design steel moment resisting frames, Lee and Foutch (2006) found that the recommended value of behaviour factor in code provided conservative designs for some structures considered. Karavasilis et al. (2007) proposed a simple expression of behaviour factor for plane steel moment resisting frame (up to 20 stories) based on a statistical analysis on the maximum story ductility resulted from thousands of nonlinear time history analysis. They found that behaviour factor was heavily dependent on the number of story and capacity factor of the steel frame. They concluded that the behaviour factor of Eurocode 8 might be on the conservative side. Recently, Mitropoulou et al. (2010) examines the different values of behaviour factor from Eurocode 2 and 8 for safety design of 5 story irregular plan and 8 story regular plan RC structures. They conclude that the behaviour factor suggested by the Eurocode 8 does not lead to the most safely design, particularly for the considered RC buildings.

2.3.3 *Effect of Ground Motion Type*

Many studies show that inelastic demands of structures depend on the type of induced ground motion. Recently, the parameters governed the NFGM and its effect on the inelastic demand of structures have been extensively studied (e.g. Mavroedis and Papageorgiou, 2003, 2004; Alavi and Krawinkler, 2004; Kalkan and Kunnath, 2006).

In the 1970s, a pioneering work in investigating NFGM affecting a building was conducted by Bertero et al. (1978) and they concluded that the destruction of structures is caused by the 1.0 – 1.5 s pulse period of NFGM. The effect of NFGM on the structural response is further explored by Hall et al. (1995). The study found that the effect of NFGM can be very effective in causing damage in structure when the fundamental period of vibration of structure is comparable to the duration of the NFGM's pulse.

In the form of a response spectrum, Maholtra (1999) assessed the characteristic of two NFGM and one synthetic motion records that contain directivity pulse in comparison to one earthquake record that contained no directivity pulse. The study revealed pulse-like ground motions with a high PGV/PGA ratio, which have a wide acceleration-sensitive region in their elastic response spectrum. This affects the responses of structures in increasing the base shear and interstory drifts in high-rise buildings, increasing the ductility demand. The high PGV/PGA ratio might reduce the apparent flexibility of high-rise and base-isolated buildings, as well as the effectiveness of supplemental damping. Similarly, the spectra domain was presented by Chopra and Chintanapakdee (2001), who explored the earthquake response of SDOF structures to NFGM and FFGMs by considering the normal and parallel components of the motions.

Significant insights were introduced in some studies (Alavi and Krawinkler, 2001; Krawinkler et al., 2003; Krawinkler et al., 2005) that employed full-cycle and multiple-cycle square pulses with various periods and amplitudes as equivalent pulses to represent FDE affecting one-bay nine-storey generic frames. These studies revealed that large elastic storey shear forces in the upper storey of the structure were found to be generated by FDE with a fundamental period of the structure higher than the pulse period, $T_1 > T_p$. This, in turn, results in early yielding of upper storey when the structure is relatively strong. Storey ductility demands stabilize in the upper portion, and the maximum demand migrates to the base when the strength is reduced. The maximum storey ductility demands occur in the bottom portion regardless of the strength for the fundamental period of structure $T_1 < T_p$ (short period structure).

By using the real records of FDEs, studies were conducted by MacRae et al. (2001), Akkar et al. (2005), and Kalkan and Kunnath (2006) in exploring the response of generic multi-storey structures due to FDE. Their results support previous findings by Alavi and Krawinkler (2004). Additionally, Madan and Hashmi (2008) investigation on the designed RC infilled frame induced by real FDEs shows generally the same trend of result as well. These conclusion are in line with the result from a similar study conducted by Mavroeidis and Papageorgiou. (2004), which clearly demonstrated that the pulse period, T_p, significantly affects the elastic and inelastic responses of SDOF structures.

2.3.4 Effect of Repeated Ground Motion

There are few studies have examined the seismic sequences effect on the buildings. Elnashai et al. (1998) has predicted that the multiple earthquake ground motions can give ductility demand required significantly higher than that required by

a single event. Amadio et al. (2003) indicates that repeated earthquakes can imply a considerable accumulation of damage and a consequent reduction in the behaviour factor. The main factors affect the response namely structural period, type of earthquake ground motion, and level of available ductility.

Hatzigeorgiou and Beskos (2009) runs million nonlinear time history analyses on the elasto-plastic SDOF system with strain hardening and empirically introduced an expression to estimate the inelastic displacement ratio (defined as the ratio of maximum inelastic displacement and maximum elastic displacement) on the flexural-based RC and steel structures based on period of vibration, force reduction factor, site conditions, post-yield stiffness, and damping. They find the inelastic displacement ratio for all SDOF systems built at all soil types generally appear to be increased 2 times or more with respect to that obtained for the corresponding single earthquakes.

Similarly, Hatzigeorgiou (2010a) exposed the ductility demand of elasto-plastic SDOF system with strain hardening induced by repeated earthquakes. The induced earthquakes were grouped into FFGM and NFGM. The result supports their previous findings on the similar topic. Again, based on the same study, Hatzigeorgiou (2010b) proposed ductility demand controls, which is actually slightly different with his previous work. In this study he distinguished the ground motion based on the motion type and also soil condition of the recording station.

The use of non-degrading stiffness and strength of hysteresis model on the SDOF system done by (Hatzigeorgiou, 2010a, 2010b, 2010c) may yield uncorrected result as discussed in previous section. Therefore, to generalize the result from elasto-plastic SDOF system with non-degrading stiffness and strength to MDOF system that represents either RC or steel structures seems not adequate.

An extensive parametric study on the inelastic response of 8 RC planar frames induced by real and synthetic repeated ground motions sourced from stiff soil (soil type B) was done by Hatzigeorgiou and Liolios (2010). The RC frame models are assumed to be situated in Greece. It consists of 2 vertically regular frames (with natural periods of 0.64 s and 1.23 s) and 2 vertically irregular frames (with natural periods of 0.5 s and 0.97 s), which is each having 3 and 8 stories. Each model has 2 variants which are varied based on its behaviour factor (q = 3.1 and 3.9). The study examined local or global structural damage, maximum displacements, interstory drift ratios, and development of plastic hinges using NTHA.

The result for model using non-degrading stiffness and strength hysteresis rule and designed with q = 3.9 has demonstrated that the double events of repeated earthquakes has produced roof ductility demand ranged from 4.1 - 5.6 on the 3-story RC structure, whereas roof ductility demand of 4.5 – 5.7 on the structures with T_1 = 1.23 s. It is meant that the repeated earthquakes increased the roof ductility demand of 1.1 – 1.4 and 1.0 – 1.2 on both RC frames considered.

The study done by Hatzigeorgiou and Liolios (2010) has used few natural period types and behaviour factors only which is not adequate to represent a broad range of structures available in RC buildings. Commonly, parametric studies done to examine the seismic demands of inelastic structures have used broader range of natural period and behaviour factor as explained in e.g. Medina and Krawinkler (2003), Ruiz-Garcia and Miranda (2005), Zareian and Krawnikler (2009). The ground motion type has not considered in this study as well.

CHAPTER 3
METHODOLOGY

3.1 General

This chapter explains the procedure utilized for modelling the inelastic structures and ground motions as well as how to analyze the result. In general, the methodology used in this study is as illustrated in Figure 3.1. It is consist of development of inelastic structures varied by strength (behaviour factor), fundamental period of vibration, and plastic rotation capacity of member; development of synthetic ground motions, nonlinear analysis, determination of seismic demand, and development of empirical relationship through regression analysis.

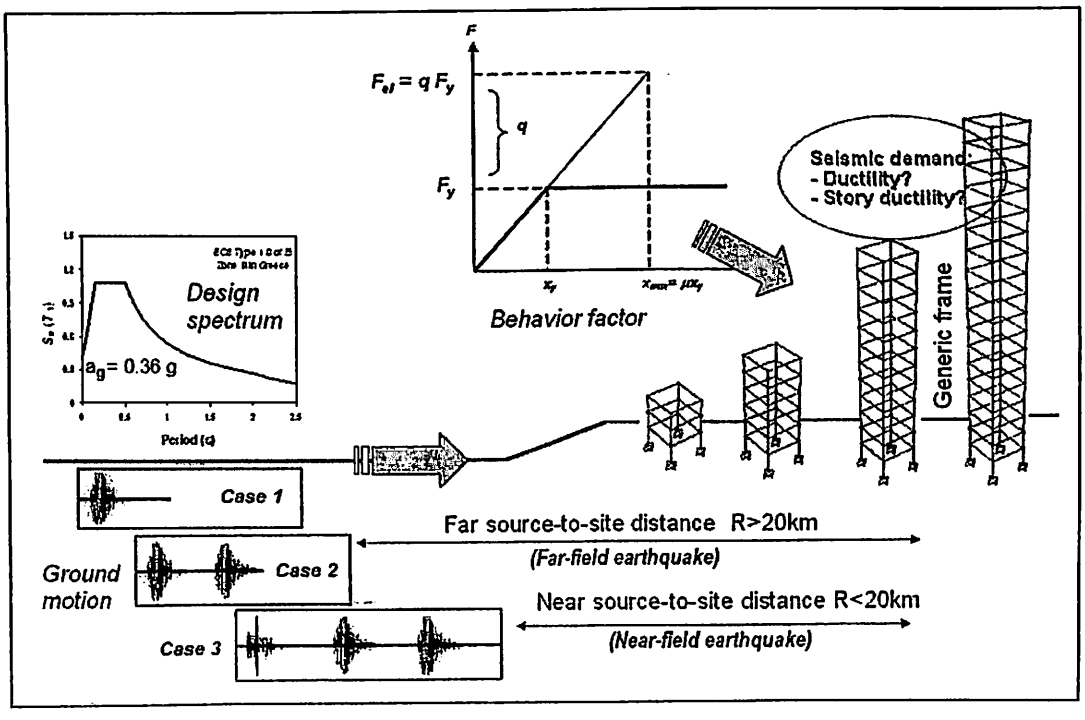

Figure 3.1: Illustration of general methodology used in this study

The methodology comprises of several procedures started from development of inelastic structures, selection and scaling of ground motion, assembling synthetic ground motion, nonlinear analysis, and statistical analysis. These procedures are depicted in Figure 3.2 and rigorously explained in the next sections.

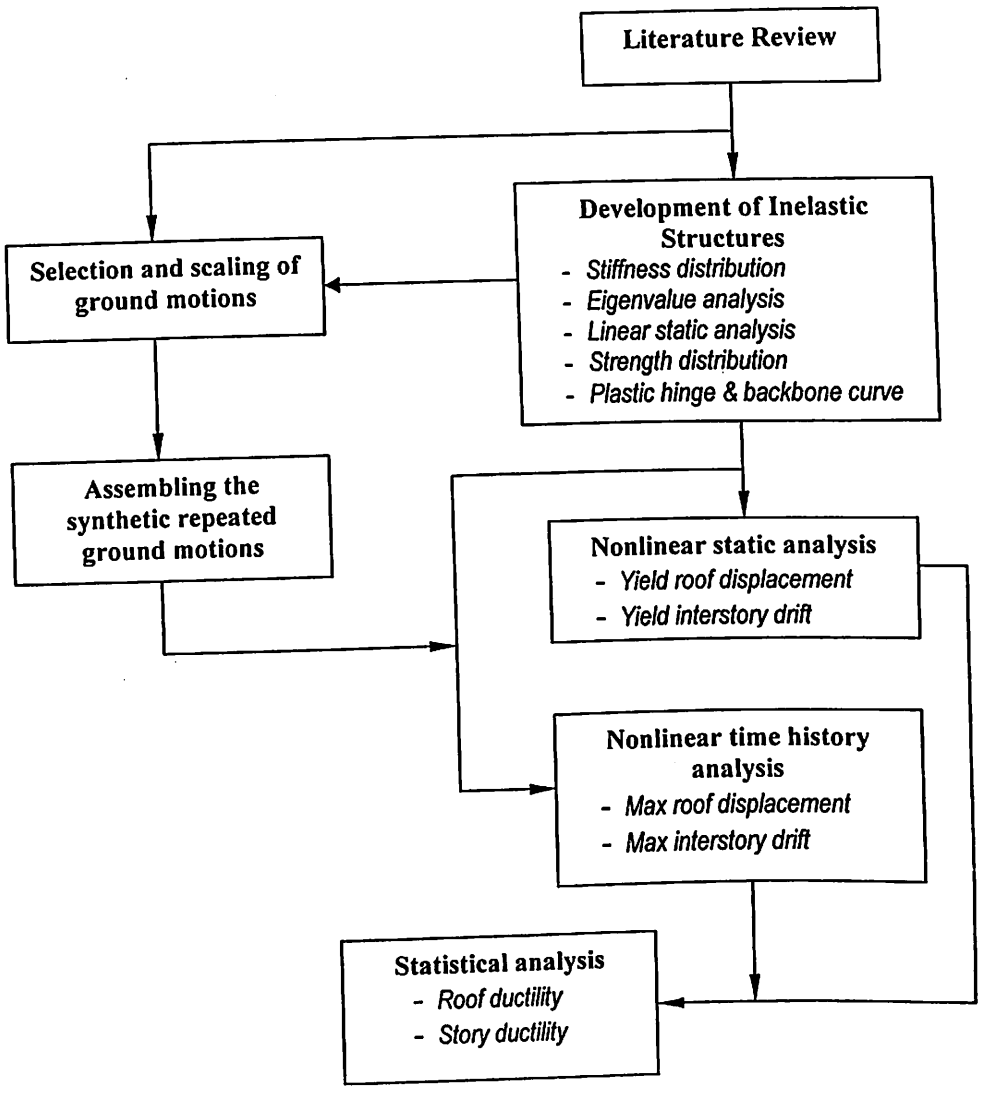

Figure 3.2: Flow chart of the methodology

3.2 Engineering Demand Parameters

In this study, roof ductility demand (μ_Δ) and story ductility demand (μ_s) are used as engineering demand parameters (EDP) of global ductility. The global ductility demand is selected because it is reflected the maximum displacement demand (Δ_{roof}) and its corresponding maximum roof drift ratio (θ_{roof} = Δ_{roof} / total height of system). The μ_Δ and θ_{roof} can be related to maximum displacement and global ductility demands of an equivalent single-degree of freedom (SDOF) system [i.e. standard nonlinear static analysis of BSSC (2000)] through behaviour factor (Ruiz-Garcia and Miranda, 2005). It is said so because the nonlinear behaviour of μ_Δ and θ_{roof} on the regular frames is dominated by first mode of vibration.

The story ductility is more sensitive than the global ductility in detecting structural damage of elements because it is related directly to the interstory drift (*ID*). The story ductility is also directly linked to the level of inelastic behaviour that system experiences (Medina and Krawinkler, 2003). The μ_Δ and μ_s are mostly employed in the parametric analysis of seismic demands of building structures (e.g. Medina and Krawinkler 2003, Ruiz-Garcia and Miranda (2005), Rigato and Medina (2007), Zareian and Krawinkler (2009). These two prameters can be calculated through the ratio of maximum displacement and displacement at yielding, respectively, as follows

$$\mu_\Delta = \Delta_{max}/\Delta_y \tag{3.1}$$

$$\mu_s = ID_{max}/ID_y \tag{3.2}$$

where Δ_{max} denotes maximum roof displacement defined through nonlinear time history analysis (NTHA), Δ_y is yield displacement defined through standard pushover analysis (POA), ID_{max} is maximum *ID* defined via NTHA, and ID_y denotes yield *ID*

resulted from POA. Since the analysis is done up to the collapse state where instability or excessive displacement response may occur, the EDPs are controlled by the same parameter defined through POA (so-called global ductility and story ductility capacities). These capacity parameters are defined analogously as the μ_Δ and μ_s.

3.3 Development of Inelastic Structures

3.3.1 Selection of the Simplified Model

In this study inelastic structure is moment resisting frame system using generic multi-degree of freedom (MDOF) model in 3-dimensional multi-storey single-bay system. This generic model is developed based on the 2D multi-storey single-bay models of Ruiz-Garcia and Miranda (2005). The modelling concept is previously proposed by Medina and Krawinkler (2003). The concept was also used in Ibarra and Krawinkler (2005) and Rigato and Medina (2007). The idea of using generic model (also called as theoretical model) is mainly because this study aims to propose something in theoretical perspective so that the result can be functioned in general manner.

3.3.2 Properties of the Model

Since this study focuses on the regular geometric system, horizontal dimension of the system in any story <130% of an adjacent story (ASCE, 2005) or no setback (Eurocode 8), the elevation and plan of 3D generic MDOF structure is as shown in Figure 3.3. Regular stiffness in elevation is used for the model. The weight is lumped at the centre of each story and arranged to remain constant at individual storey. It can be said that the model is having co-centric centers of strength, rigidity,

and mass at all levels, which is comply with Eurocode 8 and ASCE (2005) as a regular system in horizontal and elevation.

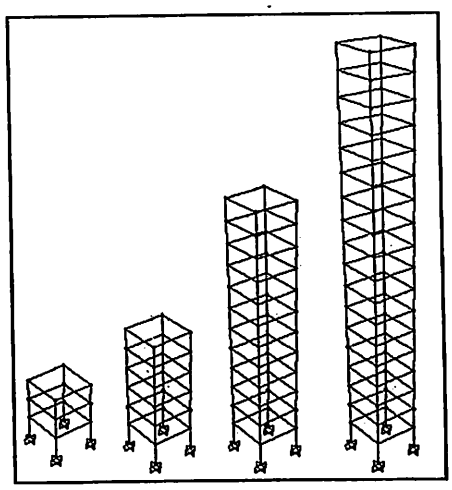

Figure 3.3: Models of 3D generic 3, 6, 12, and 18-story single-bay frames

The plan shape of floor and roof is squared plan size, H_i x H_i. By assuming ratio of the span to story height is equal to 2.0 for all stories of the generic model hence parameter H_i is equal to the twice of column height. To model the presence of rigid slab, a rigid diaphragm assumption of the floor/roof is utilized. It is meant all nodes at the same floor or roof are constrained so that the displacement in a direction performs in the same magnitude.

Five percent Rayleigh damping ratio is used at the 1st mode and the mode where 90% of mass participation attained. Columns and beams at each story have the same stiffness in order to reduce the uncertainty in modelling. Since the most of damage on the building due to earthquake occurred at the member ends, the inelasticity is modeled by flexural plastic hinges located at the member ends (full-hinge mechanism) and a 10% of member length from beam-column joint is assumed for plastic hinge length.

Considered fundamental periods of the 3D generic MDOF model are T_1 = 0.45, 0.75, 1.26, and 1.71 seconds for the 3, 6, 12, and 18 storey models, respectively. This fundamental periods can be classified as *stiff structures* (Medina and Krawinkler, 2003). The range of fundamental period is selected mainly because of multi-story moment resisting frame have fundamental period within that range, particularly for 3 to 20 stories of building (Goel and Chopra, 1997; Coburn and Spence, 2002). The selected periods relate to the number of story, N, following Eurocode 8 through

$$T_1 = 0.075\ (N\ H_i)^{3/4} \tag{3.3}$$

where N is number of story of the MDOF model viz. 3, 6, 12, and 18; and H_i is the story height. Value of 0.075 is coefficient C_t in Eurocode 8 which is assumed for reinforced concrete moment resisting frames in this study. The selection of T_1 and N are also dedicated to fulfil other criteria of period T_1 when employing static lateral method using Eurocode 8 as follows:

$$T_1 \leq \begin{cases} 4.T_C \\ 2.0s \end{cases} \tag{3.4}$$

where T_C is the upper limit of the period of the constant spectral acceleration branch (Type 1 in Eurocode 8), as shown in Figure 3.4.

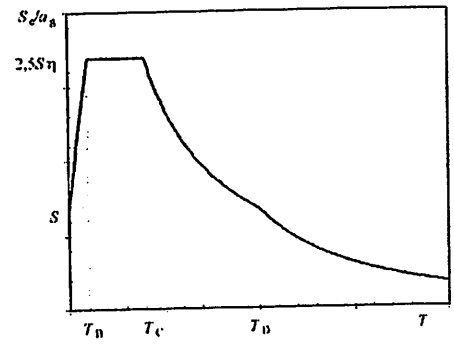

Figure 3.4: Elastic response spectrum of Eurocode 8

3.3.3 Stiffness Distribution

The generic frame models in this study are designed to exhibit a first-mode elastic deflected shape in order to be more realistic. For this, Taghavi and Miranda (2005) proposed the following empirical relationship of number of story (N) with the ratio of the stiffness of all beams at the mid-height story of the frame to the sum of the stiffness of all columns at the same story (ρ).

$$\rho = \frac{\alpha_o^2}{12N^2} \tag{3.5}$$

where ρ is Blume's (1966) ratio defined as follows

$$\rho = \frac{\sum\left(E_b I_b / L_b\right)}{\sum\left(E_c I_c / L_c\right)} \tag{3.6}$$

Parameters of I_b, I_c, L_b, and L_c are moment of beam and column, and length of beam and column, respectively. In this study, the length of beam is assumed to be two times the length of column (L_b=$2L_c$) with identical moment of inertia for beam and column (I_c=I_b), as listed in Table 3.1. The height of story is calculated based on empirical relationship of fundamental period and total building's height of Eurocode 8. Dimensionless parameter α_o is proposed by Miranda (1999) in order to control the degree of participation of overall flexural and overall shear deformations in a simplified model of multi-story buildings to predict *ID* demands. The parameter is also control the deflected shape of the model.

$$\left.\begin{array}{ll} \alpha_o = 0 & \text{represents pure flexural model,} \\ \alpha_o = \infty & \text{represents pure shear model.} \end{array}\right\} \tag{3.7}$$

Table 3.1: Parameters to define story height, beam length, and ratio of moment of inertia of beam and column

T_1	N	$H=L_c$	L_b	δ	$\rho_{M\&T}$
0.45 s	3	3.60 m	7.20 m	1.00	2.083
0.75 s	6	3.60 m	7.20 m	0.50	0.521
1.26 s	12	3.60 m	7.20 m	0.35	0.130
1.71 s	18	3.60 m	7.20 m	0.25	0.058

Miranda and Reyes (2002) notes that moment-resisting frame buildings based on detailed analytical building models usually have α_0 between 5 and 20. Therefore this study selects α_0=15 for the generic frame models to define ρ for number of story N = 3, 6, 12, and 18 so that it could deflect in flexural and shear model likewise on the real multi-story buildings, as proposed by Ruiz-Garcia and Miranda (2005). However, since three-dimensional moment-resisting frame is analyzed in this study, the value of ρ is defined as multiplication of plane frame's ρ, which is done by neglecting all of the transverse beams that perpendicular to the considered plane. The empirical ratio of stiffness beam and column at mid-height of structures ($\rho_{M\&T}$) is listed in Table 3.1.

Furthermore, Miranda and Reyes (2002) suggests a tool to tune stiffness distribution through the relationship of the ratio of the lateral stiffness at the top of the structure to the lateral stiffness at the base (δ) with the reduction stiffness along the height, $S(z/H)$, as follows

$$S(z/H) = 1 - [(1 - \delta)\,(z/H)^{\lambda o}] \qquad (3.8)$$

where z denotes story height, H is total height, λo is the dimensionless parameter that controls the variation of lateral stiffness along the height of the structure, which is λo equal to 1 and 2 corresponding to linear and parabolic variations, respectively.

The parameter δ is equal to 1 for uniform stiffness variation along height. By assuming $\lambda o = 2$ or parabolic variation along the height and adopting Ruiz-Garcia and Miranda's (2005) ratio of the lateral stiffness at the top of the structure to the lateral stiffness at the base (δ), the reduction stiffness along the height $S(z/H)$ is obtained and depicted in Figure 3.5. In order to have more realistically simulation, this study selects the decreasing stepwise distribution of lateral stiffness based on resulted parabolic variation. The lateral stiffness changes for every 3 stories as shown in Figure 3.6.

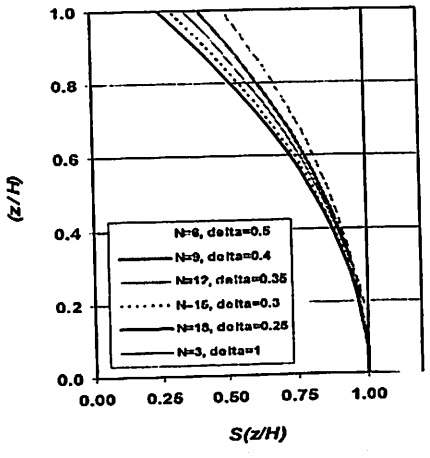

Figure 3.5: Distribution of lateral story stiffness along the height

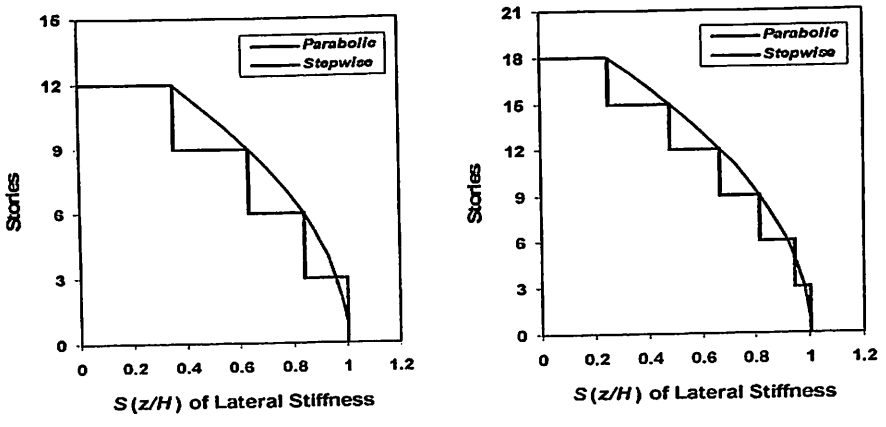

Figure 3.6: Lateral stiffness stepwise variation along the height for 12 and 18-story models

3.3.4 *Eigenvalue Analysis*

In order to make sure that the estimated fundamental period matches with fundamental period of vibration of the system, the Eigenvalue analysis is conducted. This analysis is parallel with modal analysis to determine the dynamic characteristics of the models namely frequency, damping, participation factor, mass participation factors, and modal displacement. The total weight as employed in Zareian and Krawinkler (2009) is utilized for thc started value of assumption of weight. Ratio damping equal to 5% is utilized. Ruaumoko 3D program developed by Carr (2008) was employed to run Eigenvalue analysis.

3.3.5 *Distribution of Strength*

Six type of ductility-related behaviour factor (q factor in Eurocode 8) namely q = 1, 1.5, 2, 4, and 6, are considered. It is done because most of earthquake resistant building designed based on Eurocode 8 for moment resisting frame were having behaviour factor within the range of $1.5 < q \leq 4$ for ductility class medium (denoted as DCM in Eurocode 8), whereas Ductility class high (DCH) within the range of $4 < q \leq 6$ (Fardis, 2009). To represent ductility class low (DCL) the behaviour factor of q = 1.5 is also selected in this study, whereas q = 1 is used as the starting point (elastic state) of the analysis. Definition of the plastic hinge is in line with the selected q using linear elastic analysis, as clearly explained in previous chapter. The q factor defines through the ratio of the ground motion intensity, $Sa(T_1)/g$, to the design lateral force in the structure, V_d, divided by the weight of the structure, W, as follows

$$q = \frac{Sa(T_1)/g}{V_d/W} \tag{3.9}$$

This definition is also employed by Medina and Krawinkler (2003), Ibarra and Krawinkler (2005), Ruiz-Garcia and Miranda (2005), Rigato and Medina (2007), Zareian and Krawinkler (2009).

Inelastic results obtained in the analysis by keeping the ground motion intensity constant and reducing the value of the design yield moments. The moment and rotation of this linear elastic analysis at q = 1 means that both are resulted from the same elastic and yield forces, $F_e = F_y$. It also can be said that the design yield moment in the MDOF system through q = 6 only needs to be 1/6 of the value required for q = 1.

Maximum moment resulted from linear elastic static lateral method is assigned as the yield moment (M_y) to the hinges location for POA and NTHA. The strength of member is proportioned from the lateral shear height-wise distribution calculated from the following Eurocode 8 provisions.

$$F_i = F_b \frac{s_i m_i}{\sum (s_j m_j)} \tag{3.10}$$

where

F_i = the horizontal force acting on story i,

s_i, s_j = displacements of massess m_i, m_j in the fundamental mode shape,

m_i, m_j = the story masses associated with all gravity loads.

F_b = the seismic base shear, defined as follows

$$F_b = S_d(T_1) m \lambda \tag{3.11}$$

This definition is also employed by Medina and Krawinkler (2003), Ibarra and Krawinkler (2005), Ruiz-Garcia and Miranda (2005), Rigato and Medina (2007), Zareian and Krawinkler (2009).

Inelastic results obtained in the analysis by keeping the ground motion intensity constant and reducing the value of the design yield moments. The moment and rotation of this linear elastic analysis at $q = 1$ means that both are resulted from the same elastic and yield forces, $F_e = F_y$. It also can be said that the design yield moment in the MDOF system through $q = 6$ only needs to be 1/6 of the value required for $q = 1$.

Maximum moment resulted from linear elastic static lateral method is assigned as the yield moment (M_y) to the hinges location for POA and NTHA. The strength of member is proportioned from the lateral shear height-wise distribution calculated from the following Eurocode 8 provisions.

$$F_i = F_b \frac{s_i m_i}{\sum (s_j m_j)} \tag{3.10}$$

where

F_i = the horizontal force acting on story i,

s_i, s_j = displacements of massess m_i, m_j in the fundamental mode shape,

m_i, m_j = the story masses associated with all gravity loads.

F_b = the seismic base shear, defined as follows

$$F_b = S_d(T_1) m \lambda \tag{3.11}$$

The analysis is conducted by keeping the ground motion intensity constant and reducing the value of the aforementioned design yield moments (Medina and Krawinkler, 2003; Ruiz-Garcia and Miranda, 2005). The moment and rotation of this linear elastic static analysis at $q = 1$ means that both result from the same elastic and yield forces, $F_e = F_y$.

To adopt strong-column-weak-beam mechanism in earthquake resistant system which aims to promote inelastic action in beam rather than in column, 1.3 strength ratios of column and beam is initially considered ($\Sigma M_b \leq 1.3\Sigma M_{col}$), as suggested by Eurocode 8, in obtaining the height-wise strength distribution. The strength is tuned and the mechanism is checked using POA by examining the plastic hinge progress. The illustration of column strength variation in the generic RC model is presented in Figure 3.8. The overstrength is added uniformly by a factor 1.3 of the available strength to represent the overstrength regulated in Eurocode 8 for real multi-story multi-bay structures.

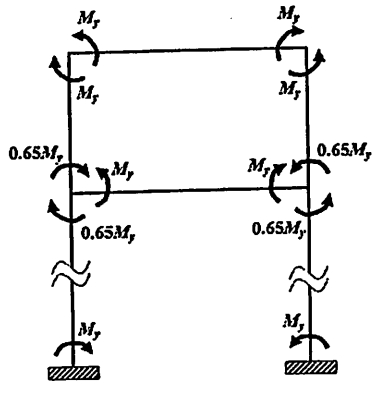

Figure 3.8: Column strength variation in the generic model

The bending moment of member at this stage is considered as the yield strength of member. This strength is considered having behaviour factor $q = 1$. Most of reinforced concrete structures are experiencing strength hardening as discussed in previous chapter. Therefore, the maximum strength of member is incorporated and

defined based on the empirical findings (Haselton et al., 2007). For other type of strength considered, it can be provided by simply dividing it with behaviour factor.

3.3.6 Plastic Hinge and Backbone Curve

The plastic hinge is represented by moment-rotation relationship, whereas the shear deformation as well as moment-axial interaction are disregarded as discussed in previous section. To simulate the cyclic behaviour of members in plastic hinge under load reversals, hysteresis rule is employed. For seismic design and evaluation of RC structure, Modified-Takeda model (Figure 3.9) was widely used (e.g., Loh et al., 2002; Priestley et al., 2007; Fardis, 2007). This is because of the model have been utilize to simulate the experimental testing by many investigators and implemented in many commercial software (Ruaumoko, SAP2000, ETABS, STAAD).

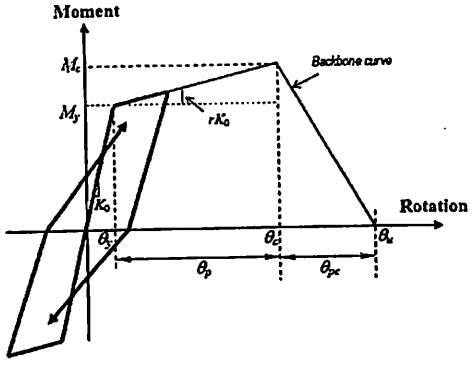

Figure 3.9: Modified-Takeda hysteresis and backbone curve

The unloading and reloading parameters (α and β) in Modified-Takeda hysteresis rule for beam member are selected based on some experimental works on RC structures, which is equal to 0.3 and 0.6 respectively, as suggested by Fardis (2007) and Priestley et al. (2007). This study also assumed $\alpha = 0.3$ and $\beta = 0.6$ for column whereas post-yield stiffness ratio of member (or bi-factor) is obtained following the method discussed in the next section.

3.3.7 Rotation Capacity

Haselton et al. (2007) has identified the rotation capacity of RC beam-column member based on evaluating and calibrating the database of experimental testing of RC columns. Therefore, this current study employs the rotation capacities within the range of capacity suggested by Haselton et al. (2007) so that it could represent the capacity of general RC structures.

The backbone curve proposed by Zaerian and Krawinkler (2009) that shaped the rotation capacity of the member ends is demonstrated by thin line in Figure 3.9. It shows that the yield rotation (θ_y) of member is obtained by the ratio of M_y with elastic rotation stiffness (K_0=6EI/L) of the member. In this study, post-yield stiffness ratio (r) of the member's hysteresis rule is estimated based on the ratio of capping moment and yield moment (M_c/M_y) and ductility of plastic rotation capacity ($\mu_{\theta,c}$), as follows

$$r = \frac{M_c - M_y}{K_0(\mu_{\theta,c} - 1)\theta_y} \tag{3.12}$$

where

$$\mu_{\theta,c} = \frac{\theta_c}{\theta_y} = \frac{\theta_y + \theta_p}{\theta_y} \tag{3.13}$$

$$\theta_y = M_y / K_0 \tag{3.14}$$

Ratio of M_c/M_y is assumed to be equal to 1.13 as suggested by FEMA-P695 (FEMA, 2009) for RC structures, which is based on recent work done by Haselton et al. (2007). Since the ratio of M_c/M_y reflects the capacity of member in strength hardening, hence M_c is also equal to maximum moment, M_{max}.

The range of rotation capacity, i.e. plastic rotation, θ_p, is provided in some references because plastic rotation capacity mostly affects the collapse capacity of the ductile system (Ibarra and Krawinkler, 2005; Ibarra et al., 2005). Recently, Haselton et al. proposed a range of rotation capacities as follows: θ_p = 0.015 to 0.082, post-capping rotation capacity, θ_{pc} = 0.015 to 0.10, and M_c/M_y = 1.11 to 1.20. Zareian and Krawinkler (2009) study on multistory RC frames has used the rotation capacities within the Haselton's et al. (2007) range after running probability of exceedance analysis to define common value used. Therefore this study follows Zareian and Krawinkler's (2009) rotation capacities to reflect low, medium, and high capacities of the member, as follows θ_p = 0.02, 0.04, and 0.06, respectively.

The post capping rotation, θ_{pc}, is a new parameter which is commonly presented by sharp drop (vertical drop) after capping point of rotation in some guidelines (e.g. BSSC, 2000). This study selects θ_{pc} = 0.06 based on average value of Zareian and Krawinkler's (2009) study, whereas ratio of M_c/M_y = 1.13 based on average value of Haselton et al. (2007).

3.4 Seismic input

3.4.1 Selection of Ground Motion Record

Since this study is intended to represent European buildings in the high seismic zone, the records from European earthquakes available in European Strong Motion Database (Ambraseys et al. 2001) are selected for far-fault ground motion (FFE). Moreover, it sources from earthquake with magnitude equal and more than 5.5. It is done because the selected design spectrum was Eurocode 8 design spectrum Type 1. Since ground motion record from station built on Soil B is majority used in

defining the amplification of Eurocode 8 spectrum (Iervolino, 2008), this study selects the record sourced from station built on Soil Type B of Eurocode 8 only.

However, ESD provides few records which contain large pulse, the unique motion in near-fault ground motion with forward directivity effect (FDE), based on list given by Baker (2007), Mavroedis and Papageorgiou (2003), and Bray and Rodriguez-Marek (2004). Therefore, FDE records are selected from Pacific Earthquake Engineering Research (PEER) Database using the same method as FFE, which is sourced from other regions around the world. This FDE record is commonly characterized based on the large pulse period, which is denoted as T_p. Number of selected strong motion records for each type of ground motion is 20 records.

To incorporate the FDE having a single component of large pulse in its horizontal components, 20 synthetic residual FDEs of Baker (2007), denotes RFDE, is also used. The motion is coupling with FDE having large pulse in bi-directional excitation to represent other horizontal component having no large pulse motion. This is inspired since the RFDE motion could reflect the same seismic source regimes with its FDE so that it would useful in the parametric study for a NFGM event with orthogonal component. Moreover, it is also because both motions would have the same oscillation period and duration (Baker, 2007).

3.4.2 Scaling Ground Motion

Spectrum acceleration at fundamental period of structure, denoted as $Sa(T_1)$, is utilized as intensity measure of ground motion using in nonlinear dynamic analysis. The scaling process focuses on this intensity measure following method proposed by Shome et al. (1998), by means all ground motions is scaled to the same pseudo-spectrum acceleration provided by Eurocode 8 at the first mode period of the

structure, T_1. It is employed since it involves simple process and provides a relative accuracy (Giovenale et al., 2004).

3.4.3 Assembling Ground Motion to Represent Repeated Earthquake

In this study, repeated earthquake presents in form of the combination of ground motion with single, double and triple events. The method of assembly is taken from Hatzigeorgiou and Beskos (2009). As the best of author's knowledge, no other method is found related to this issue. In this method, the amplitude ratio of assembled ground motion is scaled based on the ratio of peak ground acceleration (PGA), which is governed by magnitude within a consecutive earthquakes sourced from the same seismic region and recorded at the same site. The ratio of PGA is derived using the ratio of empirical attenuation functions, which varied in magnitude. Moreover, an interval motion with zero acceleration of amplitude and 100 seconds of duration length inserts in between two consecutive ground motions. This interval is absolutely enough to achieve the state of rest of any structure after vibrate due to its inherent damping, which is suggested by Hatzigeorgiou (2010b).

A total of 3 cases of earthquake excitation were considered as suggested by Hatzigeorgiou and Beskos (2009). Typical profile of each case is shown in Figure 3.10:

Single event, Case 1: (1.000, 0.000, 0.000)

Double events, Case 2: (1.000, 1.000, 0.000)

Triple events, Case 3: (0.853, 1.000, 0.853)

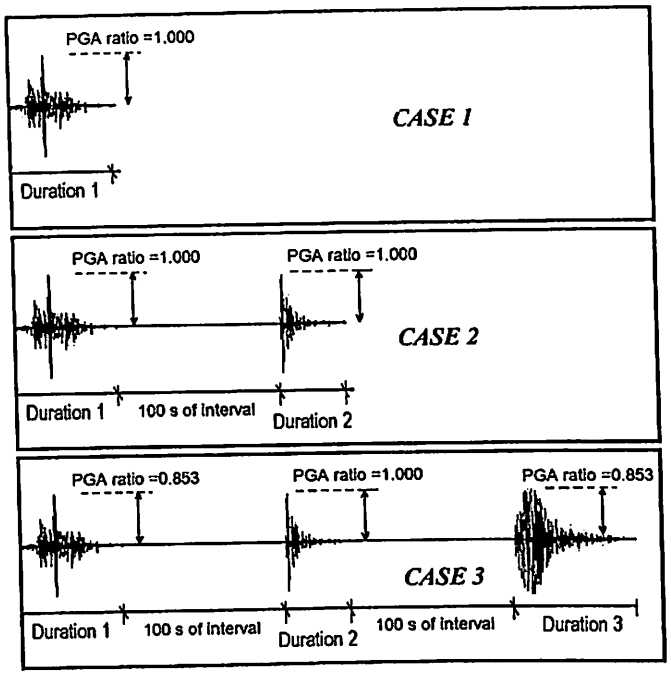

Figure 3.10: Illustration of assembling the ground motion to generate synthetic repeated earthquake used in this study

Each of FFE, FDE, and RFDE events is applied for GM Case 1 or single event. For GM Case 2 and 3 of FFE, repeated earthquakes are assembled from FFE plus other FFEs, which is randomly combined from different single FFE event. Repeated earthquake GM Case 2 and 3 of FDE are assembled from a single FDE event coupling with RFDE events. In these cases, RFDEs are randomly selected. The combination of ground motion (GM) is listed in Table 3.2 and 3.3. Matlab program is utilized for this assembling process. It should be noted that this assembling work is done after all the selected ground motions are scaled based on $Sa(T_1)$ as discussed in previous section.

Table 3.2: Combination of repeated earthquake for FFE

	GM Case 1			GM Case 2			GM Case 3		
Ratio of PGA	1.000	0	0	1.000	1.000	0	0.853	1.000	0.853
GM No.	FFE	-	-	FFE	FFE	-	FFE	FFE	FFE
1	1	-	-	1	17	-	9	1	17
2	2	-	-	2	3	-	4	2	3
3	3	-	-	3	7	-	16	3	7
4	4	-	-	4	4	-	18	4	4
5	5	-	-	5	6	-	1	5	6
6	6	-	-	6	8	-	13	6	8
7	7	-	-	7	10	-	4	7	10
8	8	-	-	8	5	-	12	8	5
9	9	-	-	9	20	-	20	9	20
10	10	-	-	10	12	-	3	10	12
11	11	-	-	11	13	-	10	11	13
12	12	-	-	12	14	-	19	12	14
13	13	-	-	13	9	-	12	13	9
14	14	-	-	14	1	-	15	14	1
15	15	-	-	15	12	-	3	15	12
16	16	-	-	16	8	-	1	16	8
17	17	-	-	17	19	-	15	17	19
18	18	-	-	18	8	-	13	18	8
19	19	-	-	19	4	-	5	19	4
20	20	-	-	20	10	-	14	20	10

Table 3.3: Combination of repeated earthquake for FDE

	GM Case 1			GM Case 2			GM Case 3		
Ratio of PGA	1.000	0	0	1.000	1.000	0	0.853	1.000	0.853
GM No.	FDE	-	-	FDE	RFDE	-	RFDE	FDE	RFDE
1	1	-	-	1	3	-	6	1	3
2	2	-	-	2	15	-	16	2	15
3	3	-	-	3	1	-	10	3	1
4	4	-	-	4	7	-	18	4	7
5	5	-	-	5	2	-	6	5	2
6	6	-	-	6	15	-	7	6	15
7	7	-	-	7	10	-	11	7	10
8	8	-	-	8	16	-	5	8	16
9	9	-	-	9	19	-	3	9	19
10	10	-	-	10	1	-	13	10	1
11	11	-	-	11	17	-	2	11	17
12	12	-	-	12	20	-	20	12	20
13	13	-	-	13	16	-	18	13	16
14	14	-	-	14	2	-	17	14	2
15	15	-	-	15	14	-	13	15	14
16	16	-	-	16	18	-	4	16	18
17	17	-	-	17	7	-	7	17	7
18	18	-	-	18	12	-	8	18	12
19	19	-	-	19	7	-	11	19	7
20	20	-	-	20	8	-	1	20	8

3.5 Nonlinear Static Analysis

To determine yield displacement, Δ_y, ultimate displacement, Δ_u, yield interstory drift (ID_y), and ultimate interstory drift (ID_u), nonlinear static analysis is conducted using standard POA (ATC-40, 1996). Those displacements are taken from roof and 1st story, and all stories for *ID*. The displacement from 1st story is selected because the seismic demand at lower part usually increases as the height of building increases.

The first modal shape is used as the height-wise distribution of incremental lateral loads because it is more practical and widely used since it is formalized in BSSC (2000). Moreover, this force distribution type could also produce approximately similar with SRSS modal distribution (Chopra, 2006). The selection of the first modal shape also gives a small error to the result of NTHA.

The gravity load is not included in POA since the effect of moment due to gravity load on the roof displacement is negligible as explained by Medina and Krawinkler (2003). Consequently, the turning point of strength in capacity curve from elastic to plastic state is become more apparent, which makes determination of global yield displacement is easier.

The base shear, V_b is defined as the summation of lateral nodal loads. As the result, the POA (so-called capacity curve) is commonly constructed in incremental base shear ($\Delta V_b = \Sigma \Delta Q_n$) versus incremental nodal displacement at roof, Δu_{roof}. From the capacity curve, the yield roof displacement, Δ_y, and maximum roof displacement, Δ_{max}, are determined using a method as discussed in the next section. Thus, global ductility capacity is defined as the ratio of maximum to the yield roof displacements. At the same time, the corresponding displacements of yield and maximum states at each story are recorded so that the *ID* could be defined. Similarly, the story ductility

capacity is determined as the ratio of ID_u to ID_y. The global post-yield stiffness ratio (i.e. post-yield stiffness normalized by initial stiffness) can be defined through capacity curve as well. SAP2000 software was used to conduct the standard POA.

3.5.1 Global Yield and Maximum Displacements

Global yield displacement of frame system can be obtained through few methods viz. bi-linear approximation of capacity curve (Paulay, 1998), ATC (1996) method, or first significant member yield (Yuksel and Polat, 2005). Common method used in the ductility demand analysis is bi-linear approximation (i.e. Medina and Krawinkler, 2003; Ruiz-Garcia and Miranda, 2005). In bi-linear approximation the linear relationship coincide up to the structural element developing approximately 75% of its nominal strength. In the traditional approximation, the displacement corresponding to this level of maximum base shear on the capacity curve can be accepted as the system yield strength (Park, 1988; Elnashai and Di Sarno, 2008) as shown in Figure 3.11. Therefore, this study uses bi-linear approximation in obtaining global yield displacement (Δ_y).

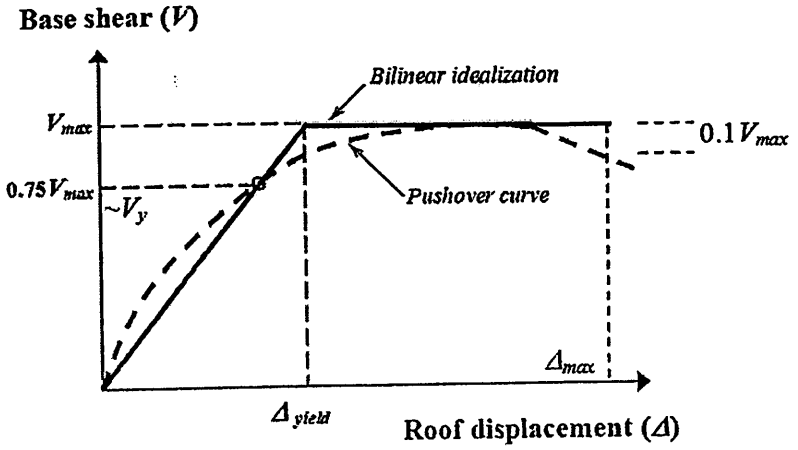

Figure 3.11: Pushover curve, global yield, and maximum displacement definitions used in this study

Global maximum displacement (displacement at collapse) of capacity curve through POA (Δ_{max}) is defined as the maximum point of roof displacement. If the strength deterioration occurred, the maximum displacement is taken as a point where the 10% of maximum strength drop (Park, 1988; Elnashai and Di Sarno, 2008).

3.5.2 Ratio of Global Ductility Capacity

Global ductility capacity under consideration in this study consists of roof ductility and maximum story ductility. Based on the capacity curve of POA, the roof ductility capacity could be derived based on Eq. 3.1 (Figure 3.11), whereas maximum story ductility is defined as the maximum value of the story ductility determined through Eq. 3.2. Thus, the ratio of global ductility capacity is determined as the ratio of maximum story ductility to the roof ductility.

3.5.3 Global Post-Yield Stiffness Ratio

In this study, the stiffness exceeded the elastic stiffness in capacity curve of POA denotes global post-yield stiffness. The global post-yield stiffness can be defined by comparing the hardening base shear (maximum base shear minus yield base shear) to the elasto-plastic displacement capacity ($\Delta_{max} - \Delta_y$). Therefore, post-yield stiffness ratio could be determined as the ratio of post-yield stiffness to the elastic stiffness. The global elastic stiffness is simply defined by comparing the yield base shear and yield displacement.

3.6 Nonlinear Time History Analysis

NTHA is conducted to define the maximum displacement at roof (Δ_{max}) and maximum *ID* (ID_{max}) due to ground motions of earthquake. Determination of EDP

namely μ_Δ and μ_s needs these two parameters in combination with Δ_y and ID_y resulted from POA.

The NTHA of MDOF system can be represented by the well-known equation of motion in incremental form as follow:

$$\mathbf{M}\,\Delta\ddot{u} + \mathbf{C}\,\Delta\dot{u} + \mathbf{K}_{\Delta t}\Delta u = -\mathbf{M}\,\mathbf{r}\,\Delta\ddot{u}_g \qquad (3.15)$$

where **M** is the mass matrix, Δu represents the incremental displacement vector during the time interval (Δt), $\mathbf{K}_{\Delta t}$ is the stiffness matrix for the current time interval, **C** denotes the damping matrix consisting of elements representing damping coefficients used for the current time interval, **r** corresponds to the displacements vector of the free DOFs due to a unit displacement of the corresponding base support, and $\Delta\ddot{u}_g$ is the incremental ground motion acceleration vector over the time interval. In that equation of motion, the stiffness is sourced from force-deformation relationship which contains the nonlinearities of material and geometry. Further detail explanation in conducting NTHA can be found in many textbooks (e.g. Hart and Wong, 1999; Datta, 2010).

The displacement result of NTHA and its corresponding *ID* is taken from the major direction of the model, induced by the major component of orthogonal ground motions, which is produced the dominant results. Ruaumoko 3D program by Carr (2008) is used as tool in conducting this NTHA.

3.6.1 Rayleigh Damping

Inappropriate modelling of structural damping in NTHA could lead to inaccurate estimate of displacements and internal forces. This effect is clearly apparent when the Rayleigh damping is mixed with lumped plasticity model adopted

for the plastic hinge at members ends of MDOF system. The critical damping ratios used in practice vary anywhere from 1 to 10% of critical (Taranath, 2005) whereby the upper end values are for seismic design. However, the use of 5% as critical damping is widely accepted for moment resisting frame, particularly in theoretical model or simplified model (Chopra, 2006; Hart and Wong, 1999; Datta, 2010). Therefore, the critical damping ratio (ξ) of 5% is used at the first mode and also at the mode where the 90% of mass participation attained.

3.7 Data and Statistical Analysis

3.7.1 Data Management

Data considered in this study is EDP as discussed previously. The EDP consists of roof ductility and story ductility which is defined based on the result of NTHA and POA. The entire ductility results were filtered using maximum ductility value based on nonlinear static analysis. It is assumed beyond this maximum deformation level the result achieves near collapse or even collapse already. Therefore all ductility results beyond this maximum level were disregarded. Each single data of roof ductility and maximum story ductility for each condition considered in this study is taken from the mean value of the results due to 20 ground motions.

3.7.2 Statistical Analysis

Linear multiple regression analysis is conducted in order to produce simple empirical relationship of ductility demands of MDOF system using common parameters in seismic design and evaluation namely the structure period, behaviour factor, and hysteresis model. In general, linear multiple regression analysis can be

expressed in form of response (y_i), predictor variables (x_{ij}), and regression intercept (β) as follows:

$$y_i = \beta_0 + \beta_1 x_{i1} + \beta_1 x_{i2} + ... + \beta_p x_{ij} + \varepsilon_i \quad (3.16)$$

where x_{ij} is the i^{th} observation on the j^{th} independent variable. Least square method is commonly used to solve this general linear equation. It should be noted that predictor variables is only those that have strong correlations with the dependent variables (response), which is determined based on standard statistical significance level test.

In regression work, the dependent or independent variables data can be transformed to other mathematical form in order to have the adequacy of fit of the coefficient of determination, denoted as R^2. Further detail mathematical explanation of regression analysis and its variables correlation analysis can be found in many standard statistical textbooks (e.g. Draper and Smith, 1998; Chatterjee and Hadi, 2006). As a tool, SPSS software is used in this regression analysis.

3.8 Summary of Methodology

3.8.1 Summary of Procedure

To have clear picture on the methodology, the following steps are listed as the summary of the methodology used in this study.

1. Modelling the inelastic structures in term of story stiffness distribution and dynamic properties:
    a) assuming the considered fundamental period and number of story of structures,
    b) defining the height of structures using empirical expression of fundamental period in Eurocode 8,

c) assuming the started value of moment of inertia of members which is identical for column and beam,

d) estimating the distribution shape of story stiffness. Moment of inertia of members are tuned while adjusting the story stiffness;

e) assuming the started value of story weight.

f) running the Eigenvalue analysis to check whether the predicted fundamental period is correct or not. At this step, story weight, modulus of elasticity, and moment of inertia might be tuned. The dynamic properties of the structures resulted from this analysis are recorded.

2. Modelling the inelastic structures in term of strength distribution:

a) defining the base shear using EC 8 design spectrum and distributing the equivalent lateral force to all stories following the first mode shape;

b) running the linear static analysis and noting the flexure bending moment at member ends;

c) adjusting the ratio of bending moment of column and beam at each joint of frame to adopt strong column weak beam behaviour of Eurocode 8;

d) adding the uniformly overstrength to all bending moment of members. The bending moment of member at this stage is considered as the yield strength of member.

e) assuming the maximum strength of member considering the strength hardening based on empirical findings;

f) the strength result at this stage is considered having behaviour factor equal to 1. For other type of strength considered, simply reducing the strength by dividing it with behaviour factor.

3. Modelling the inelastic structures in term of the deformation capacity of member:
    a) based on yield moment, modulus of elasticity, and moment of inertia, determining the yield rotation of member ends;
    b) defining the capping and collapse rotations and converting to curvatures;
    c) defining the curvature ductility,
    d) repeating the procedure from step a) for other behaviour factor type.
4. Scaling and assembling the ground motion:
    a) selecting ground motion based on soil type and ground motion type,
    b) scaling the ground motion refer to design spectrum and to the ratio of seismic sequences considered,
    c) assembling the repeated ground motion.
5. Nonlinear analysis:
    a) POA,
    b) NTHA,
6. Determining the seismic drift demand, and
7. Regression analysis

3.8.2 Summary of Investigation Setting

In this study, the investigation setting of the considered variables is as follow:

1. 4 types fundamental period of moment resisting frame, T_1 = 0.45, 0.75, 1.26, and 1.71 seconds.
2. 4 type number of story, N = 3, 6, 12, and 18.
3. Length of beam twice of column length, $L_b = 2L_c$.

4. Moment of inertia column equal to moment of inertia of beam, $I_c = I_b$.
5. Identical lumped weights on each story of a model.
6. Eurocode 8 Type 1 design spectra for Soil B in Greece's highest seismic zone.
7. 5 types ductility related behaviour factor, q = 1, 1.5, 2, 4, 6. Includes with strength adjustment $\Sigma M_b \leq 1.3\Sigma M_{col}$ and overstrength $\alpha_u/\alpha_1 = 1.3$.
8. Flexure bending moment as strength in plastic hinge definition. Excludes shear, axial, as well as interaction of axial, shear and moment.
9. Line element with lumped plasticity model for plastic hinge.
10. 3 type of backbone curve model based on plastic rotation capacity, θ_p = 0.02, 0.04, and 0.06; post-capping rotation capacity, θ_{pc} = 0.06; and ratio M_c/M_y = 1.13.
11. Modified-Takeda hystresis rule with $\alpha = 0.3$, $\beta = 0.6$, and strength deterioration to represent cyclic behaviour of RC members.
12. 5% of critical viscous damping ratio using Rayleigh damping with modified initial stiffness model.
13. 3 cases of seismic repetition (single, double and triple events).
14. 60 pairs input ground motion (20 real FFE, 20 real FDE, and 20 synthetic RFDE) to be assembled for synthetic repeated earthquake motion.
15. After assembling, 140 synthetic repeated earthquake motions in total (60 motions for Case 1, 2, and 3 of FFE; 60 motions for Case 1, 2, and 3 of FDE; and 20 motion for Case 1 of RFDE).
16. Roof ductility and story ductility as seismic demand parameter derived from roof displacements and *ID*, respectively.
17. A total of 8400 NTHA runs in this study.

CHAPTER 4
RESULT AND DISCUSSION

4.1 Inelastic Structure Models

4.1.1 Dynamic Characteristic

Dynamic characteristics of all generic frame models based on Eigenvalue analysis are presented in Table A.1 to A.4 in Appendix A. It showed that all models produce identical fundamental periods at mode 1 and mode 2 as expected. The modal displacement demonstrated no rotation at these modes, which meant translation at orthogonal horizontal directions governed. The case of no rotation deformations also occurred at mode 4 to 7. These fundamental periods and modal displacements are clearly indicated that the models are regular in plan and torsionally balanced. Mass participation is achieved 90% at mode 5 and 7 for models with 3, 6, and 12, 18 stories, respectively. To cover the response contributions of the most of natural modes of vibration, this study considered the mass participation up to 95%.

4.2 Ground Motions

Selected ground motions for far-field (FFE) and near-field earthquakes (FDE), as well as residual of near-field earthquake (RFDE), are presented in Table C.1 to C.6 (Appendix C) sourced from seismic station built in stiff soil. The FFE ground motion is mainly dominated from Italy, Greece, and Turkey, with magnitude and source-to-site distance ranged from M5.6 to M7.2 and from 21 to 80 km, respectively. The peak ground acceleration (PGA) of selected motions is ranged from 0.112g to 0.505g. FDE motions are dominated by California and Taiwan earthquakes and mainly from source-to-site distance less than 10 km and magnitude larger than

M6.0. It shows that all normal component of record tend to produce higher velocity than its parallel component, which is not the case in acceleration motion component. It is indicating that the motion having a significant large pulse is reflecting the FDE.

The spectrums acceleration and velocity of selected FFE, FDE, and RFDE motions are depicted in Figure C.2, C.3, C.5, and C.6 (Appendix C). From the mean spectrum acceleration in Figure 4.1, it shows that the amplitude of spectrum FFE and RFDE tends to decrease in the same shape at period of $T \geq 1.0$ s compares with spectrum FDE motion. It indicates that the pulse content in longer period of the RFDE motion is missing (extracted). It is also apparent in the velocity spectrum at the same longer period. These conditions explain that large pulse in FDE governs in the longer period as stated in many studies (e.g. Somerville, 2003; Mavroedis and Papageorgiou, 2003, Baker, 2007). The scaling factor of selected ground motions to the corresponding fundamental period of models [$Sa(T_1)$] is presented in Table C.4 to C.6 (Appendix C).

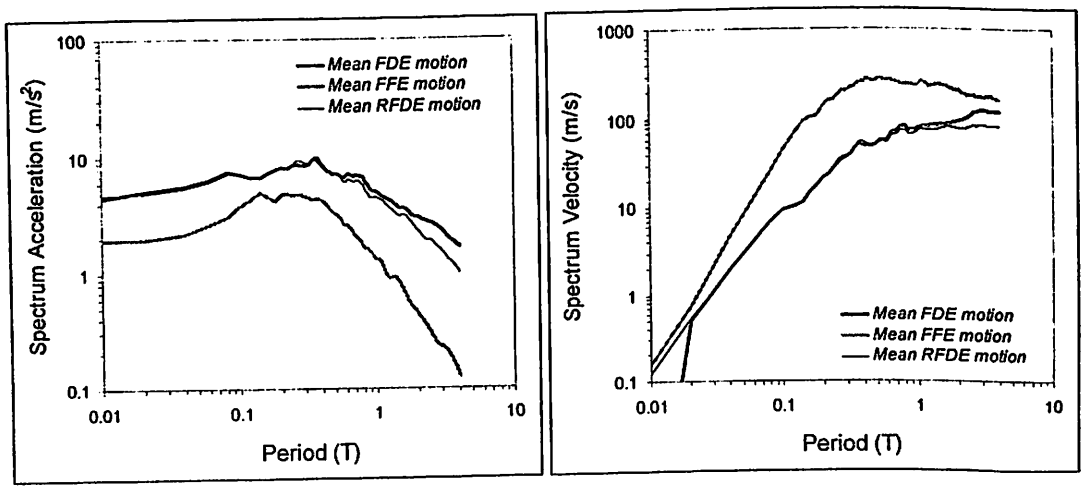

Figure 4.1: Mean spectrums acceleration and velocity of selected FDE, FFE, and RFDE motions

4.3 Global Ductility and Post-Yield Stiffness Ratio Capacities

In this section, the ductility and post-yield stiffness ratio are resulted from nonlinear static analysis or pushover analysis (POA). The models are in condition where plastic hinges occur in many beams, not in column, at a loading step prior to structure loss its global stiffness or analysis stops. It is meant all models are in strong column~weak beam condition. Examples of plastic hinge distribution of this condition are depicted in Figure D.1 in Appendix D.

The example of capacity curve resulted from POA is depicted in Figure 4.2 and Figure 4.3 for models having plastic rotation capacity Rot. = 0.04, that monitored from roof and first story, respectively (Figure D.2 to D.5 in Appendix D). In this case, the inclusion of first story in monitoring the capacity was mainly because as the number of story of building increases the amplification of drift demand increases at lower part of building, particularly for 12-story building or taller (Medina and Krawinkler, 2003). The figures show as the number of story increases the global strength (base shear) and lateral displacement increases, as expected. This is also explained that the roof and first story displacement ductility, denoted as global ductility ($\mu_{\Delta c}$) and story ductility capacities (μ_{sc}), respectively, are performed in the same condition, as demonstrated in Figure 4.4 and Table D.1 and D.2 in Appendix D. Figure 4.4 also shows that the slope of post-elastic stiffness decreases as behaviour factor increases and it is close to zero at $q = 6$.

The global ductility capacity of inelastic structure models for behaviour factor $q = 1.5$ is found equal to 4.59, 5.14, 5.08, and 6.70 for models with 3, 6, 12, and 18-story, respectively.

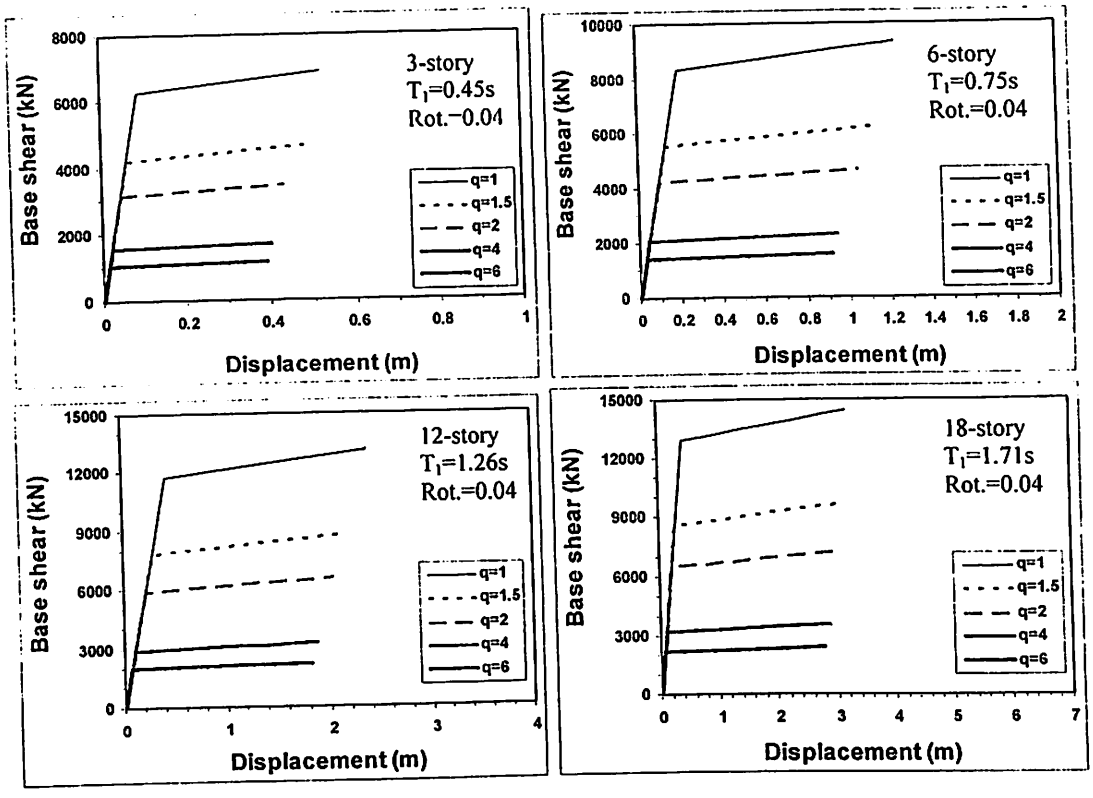

Figure 4.2: Roof displacement of models with 0.04 of plastic rotation capacity based on pushover analysis

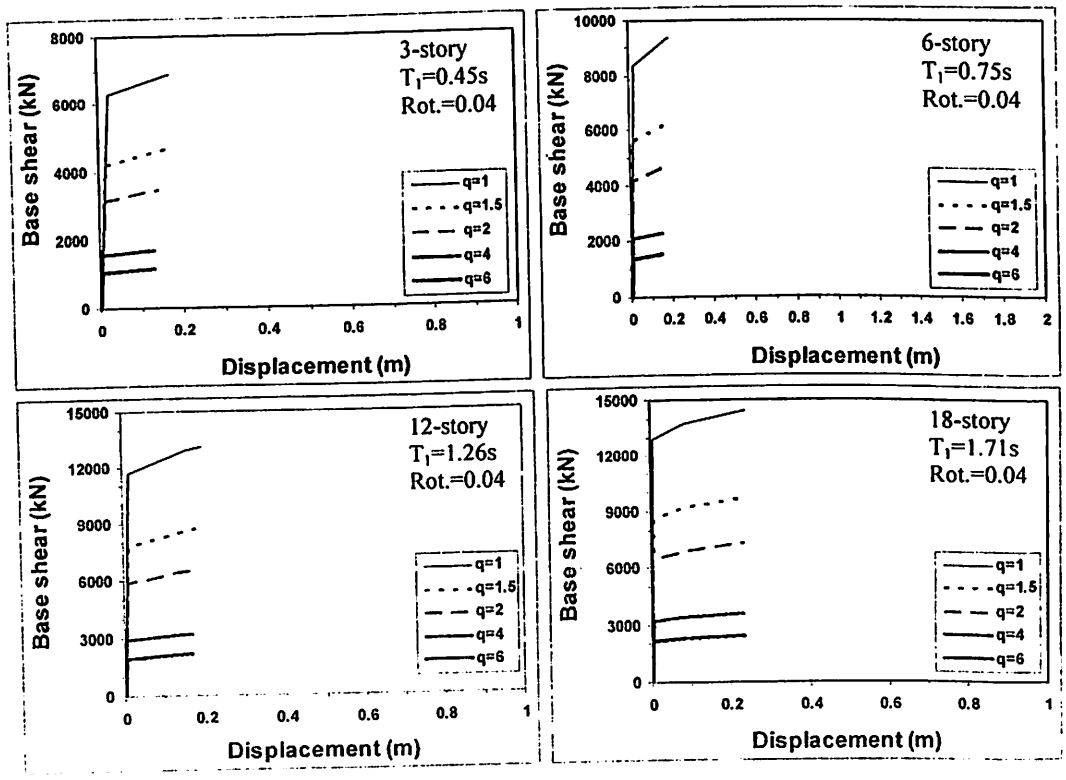

Figure 4.3: First floor displacement of models with 0.04 of plastic rotation capacity based on pushover analysis

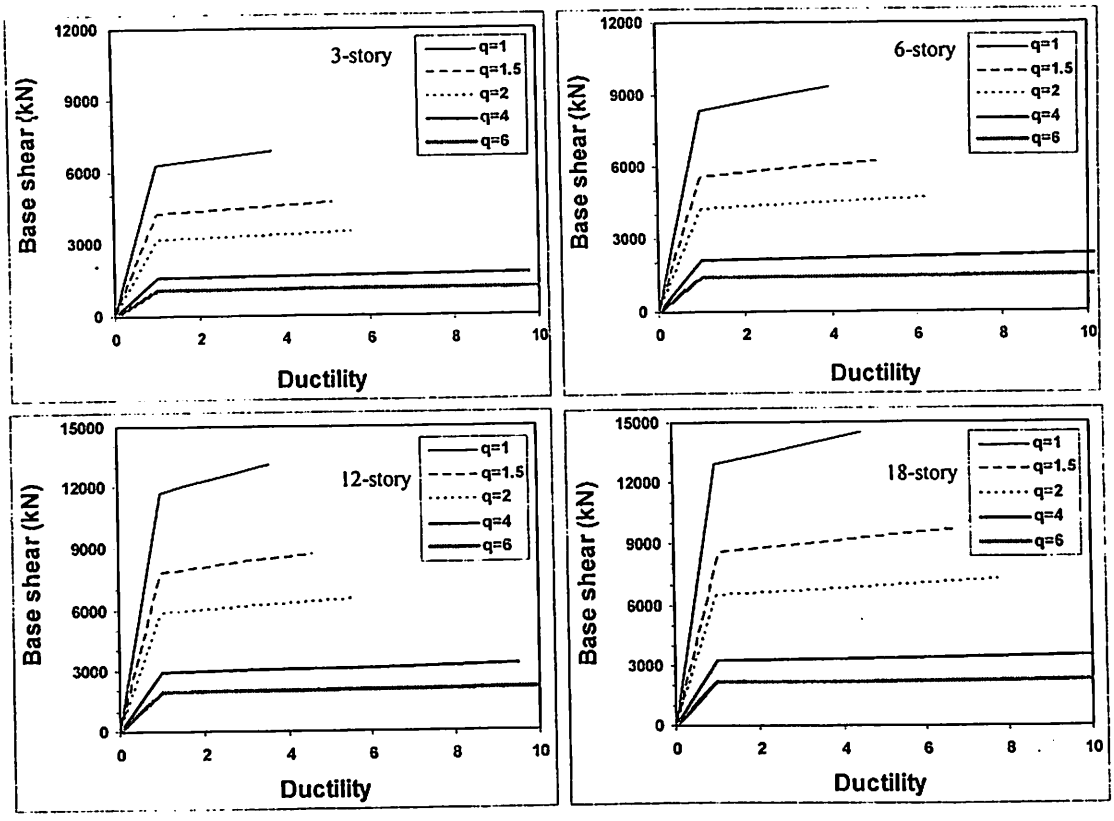

Figure 4.4: Variations of global ductility with behaviour factor for 0.02 of plastic rotation capacity

These global ductility capacities reached about 8 times for all models, in average, for behaviour factor q = 6, the global ductility reach 37.23, 38.88, 41.69, and 58.54 for the 3, 6, 12, and 18-story models, respectively. To relate the global ductility capacity with the story ductility capacity, the ratio of story ductility and global ductility capacities denoted as ϑ_c, were introduced and listed in Table D.3 in Appendix D. In average, the inelastic models having behaviour factor ranged from 1.5 to 6 have ϑ_c equal to 1.22, 1.69, 2.06, and 4.57 for models with 3, 6, 12, and 18-story, respectively.

The variation of ductility affected by the number of story (or fundamental period) is presented in Figure D.2 to D.5 in Appendix D. The figure clearly demonstrated as the number of story increases, the global strength and ductility increases. This study also found that the plastic rotation capacity affects

proportionally the global post-yield stiffness ratio, as expected (see Figure D.6 and D.7 in Appendix D). For instance, 18-story models with q = 4 and plastic rotation capacity 0.02, 0.04, and 0.06 have exhibited the global post-yield stiffness ratios equal to 0.96%, 0.46%, and 0.31%, respectively (Figure 4.5). For 3-story model with the same q and plastic rotation capacity, the global post-yield stiffness ratio equal to 1.13%, 0.58%, and 0.39%, respectively. It can be said as the plastic rotation capacity increases 3 times the global post-yield stiffness ratio decreases about 3 times, as well. Similar trends are reported in Zareian and Krawinkler (2009).

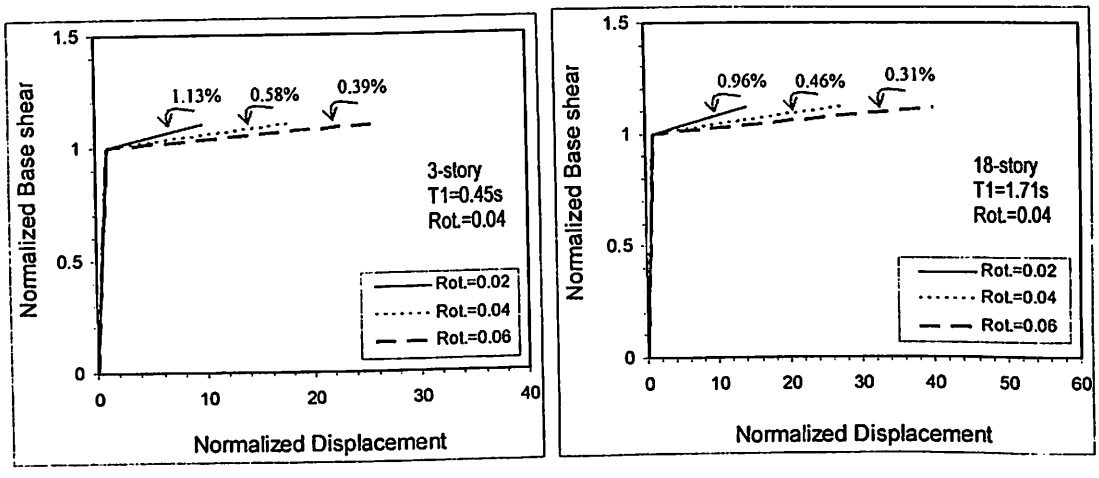

Figure 4.5: Example of post-yield stiffness ratio on the 3- and 18-story models

The interstory drift capacities at yield (ID_{yc}) and ultimate state (ID_{uc}) is presented in Figure D.8 to D.9 in Appendix D. The maximum ID_{yc} tends to perform at the middle part of stories and thus shifts to upper part, particularly on the 18-story models. It also shows that ultimate interstory drift (ID_{uc}) on the 3 and 6-story models occur mainly in the middle part of stories. It migrates to the lower part of stories as the number of story increases, particularly on the 18-story model. Moreover, the story ductility capacity increases as number of story (and fundamental period)

increases. These all agree well with the generic model of Medina and Krawinkler (2003).

4.4 Roof Ductility Demands

Global ductility demand is defined after 8400 nonlinear analyses were performed. The result is taken from the roof displacement at major direction of the system, which has produced the dominant results. Global ductility demands consist of roof ductility, μ_Δ, and story ductility, μ_s. Three case scenarios of repeated earthquake are represented by GM Case1, Case 2, and Case 3, which are denoted for single, double and triple earthquake ground motions sequences, respectively. All are done for FFE and FDE, included the RFDE.

4.4.1 Effect of Behaviour Factor and Fundamental Period

For regular earthquake analysis or single event earthquake, denotes as GM Case 1, the variation of roof ductility demand as a function of behaviour factor and plastic rotation capacity is depicted in Figure 4.6 and Figure 4.7. This ductility demand is an average result using each 20 ground motions representing FFE and FFE. The figure presents the ductility demands for 3, 6, 12, and 18-story models or model having fundamental period (T_1) equal to 0.45, 0.75, 1.26, and 1.71 seconds, respectively. It clearly shows that behaviour factor affects the ductility demands for all models, particularly significant for models having $q \geq 4$ (i.e. high ductility class in Eurocode 8). This influence is more apparent when FDE affects the models (Figure 4.6).

Table 4.1 presents the minimum to maximum range of roof ductility demands based on average plastic rotation capacity and the behaviour factor, which ranges for medium ductility class (DCM) and high ductility class (DCH) of Eurocode 8 ($1.5 < q \leq 4$ and $4 < q \leq 6$, respectively). It explains that models having DCM and DCH induced by FFE produce 4.3 and 6.4 of maximum roof ductility demands, respectively, whereas models induced by FDE reach to 5.9 and 9.9, respectively. In RFDE, behaviour factor tends to affect roof ductility demand following the FDE trend. This result shows that behaviour factor affect the roof ductility demand significantly.

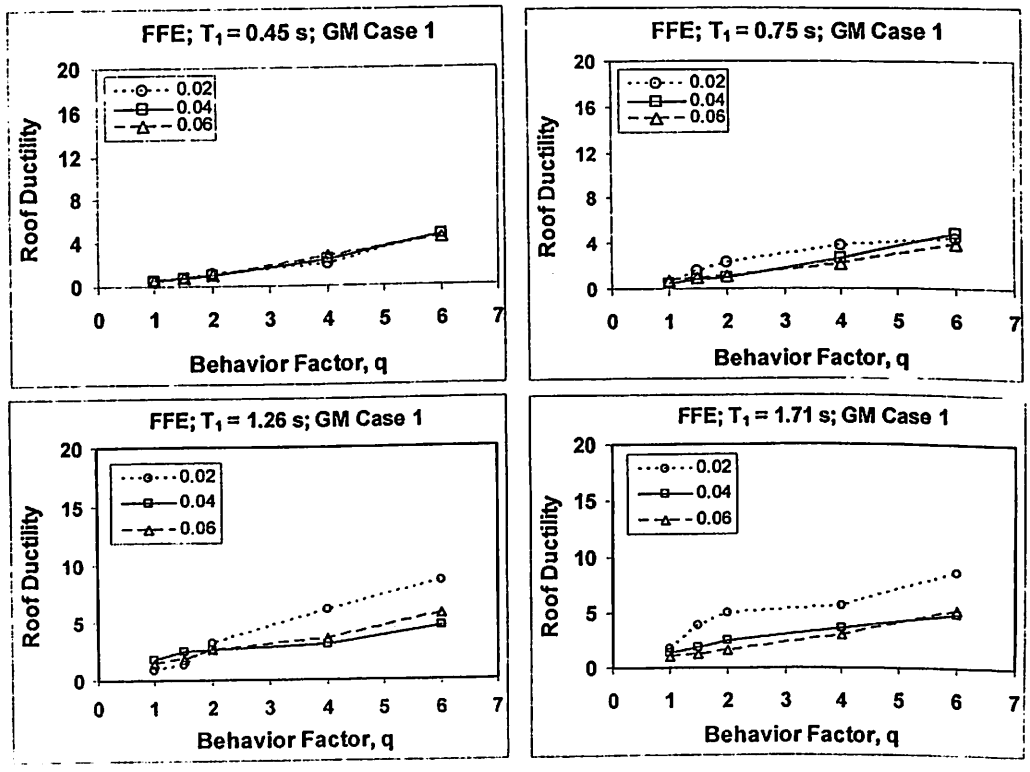

Figure 4.6: Roof ductility demands as a function of behaviour factor and plastic rotation capacity, affected by single event of FFE

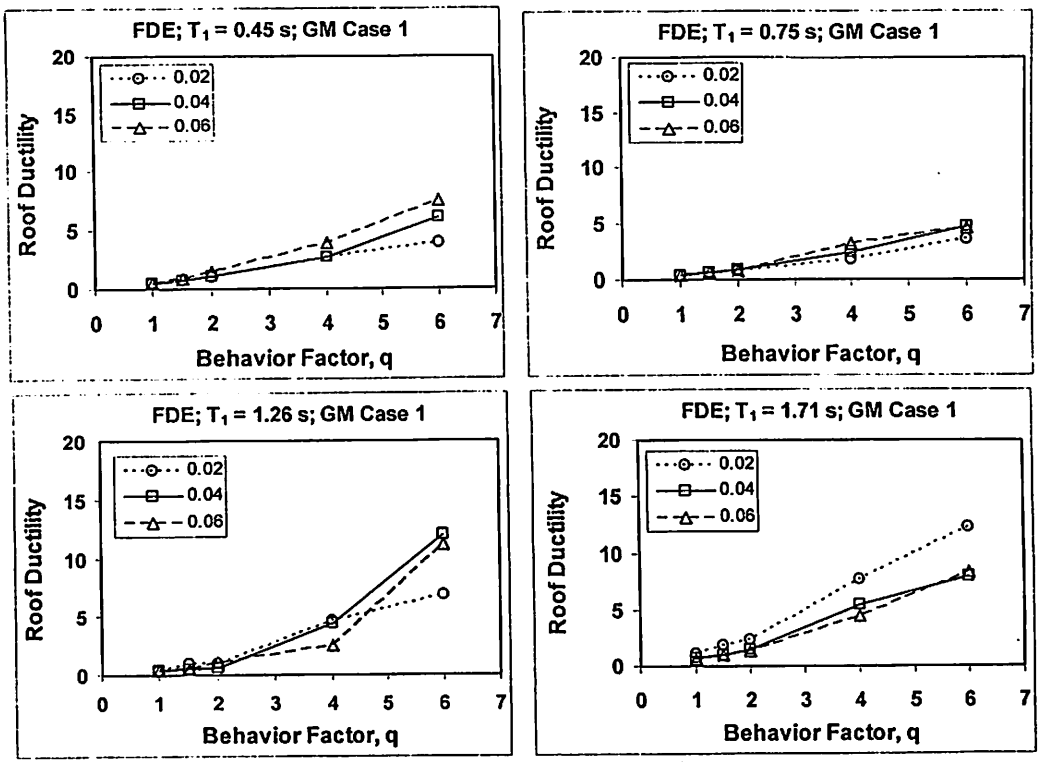

Figure 4.7: Roof ductility demands as a function of behaviour factor and plastic rotation capacity, affected by single event of FDE

Table 4.1: Roof ductility demands based on average plastic rotation capacity and single events (GM Case 1) of FFE and FDE

Models	q	Roof Ductility Demands, μ_Δ		
		FFE	FDE	Residual FDE
3-story model (T_1 = 0.45 s)	$1.5 < q \leq 4$	1.0 - 2.5	1.0 - 3.1	1.0 - 2.8
	$4 < q \leq 6$	2.5 - 4.6	3.1 - 5.8	2.8 - 5.4
6-story model (T_1 = 0.75 s)	$1.5 < q \leq 4$	1.1 - 2.9	1.0 - 2.4	1.0 - 1.4
	$4 < q \leq 6$	2.9 - 4.4	2.4 - 4.3	1.4 - 2.9
12-story model (T_1 = 1.26 s)	$1.5 < q \leq 4$	1.9 - 4.3	1.0 - 3.9	1.0 - 2.9
	$4 < q \leq 6$	4.3 - 6.4	3.9 - 9.9	2.9 - 6.9
18-story model (T_1 = 1.71 s)	$1.5 < q \leq 4$	2.3 - 4.1	1.3 - 5.9	1.3 - 3.7
	$4 < q \leq 6$	4.1 - 6.2	5.9 - 9.5	3.7 - 6.3

The results of this study were compared with Hatzigeorgiou (2010b), which has been conducting an extensive study using elasto-plastic SDOF system induced by near-field earthquake in evaluating the behaviour factor. The criteria of near-field earthquake used by Hatzigeorgiou was based on source-to-site distance less than 10

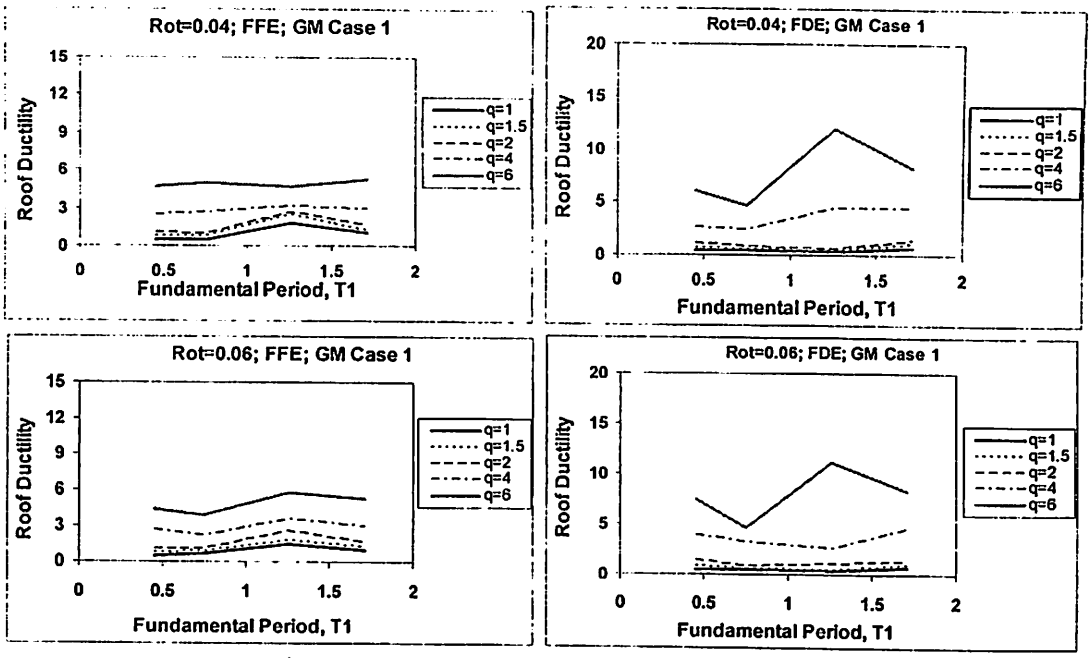

Figure 4.8: Roof ductility demand as a function of fundamental period and behaviour factor. Models are induced by single event (GM Case 1) of FFE and FDE

4.4.2. Effect of Global Post-Yield Stiffness Ratio

Effect of global post-yield stiffness ratio, r_K, on the roof ductility demand, μ_Δ, can be seen in Figure 4.9 and Figure 4.10. Figure 4.9 explains the roof ductility demand as a function of global post-yield stiffness ratio and plastic rotation capacity (denotes Rot.=0.02, 0.04, and 0.06). It demonstrates that the post-yield stiffness ratio decreases as the roof ductility demand increases. This mechanism is correct because when the fundamental period of system under the same strength increases, the global stiffness decreases (more flexible), hence roof and story drifts increases. In Figure 4.9, each point of post-yield stiffness ratio also represents a behaviour factor of the system, which explains the change in ductility class (e.g. DCM to DCH in Eurocode 8) affects the post-yield stiffness and thus it influences the roof ductility demand due to its post-yield stiffness ratio.

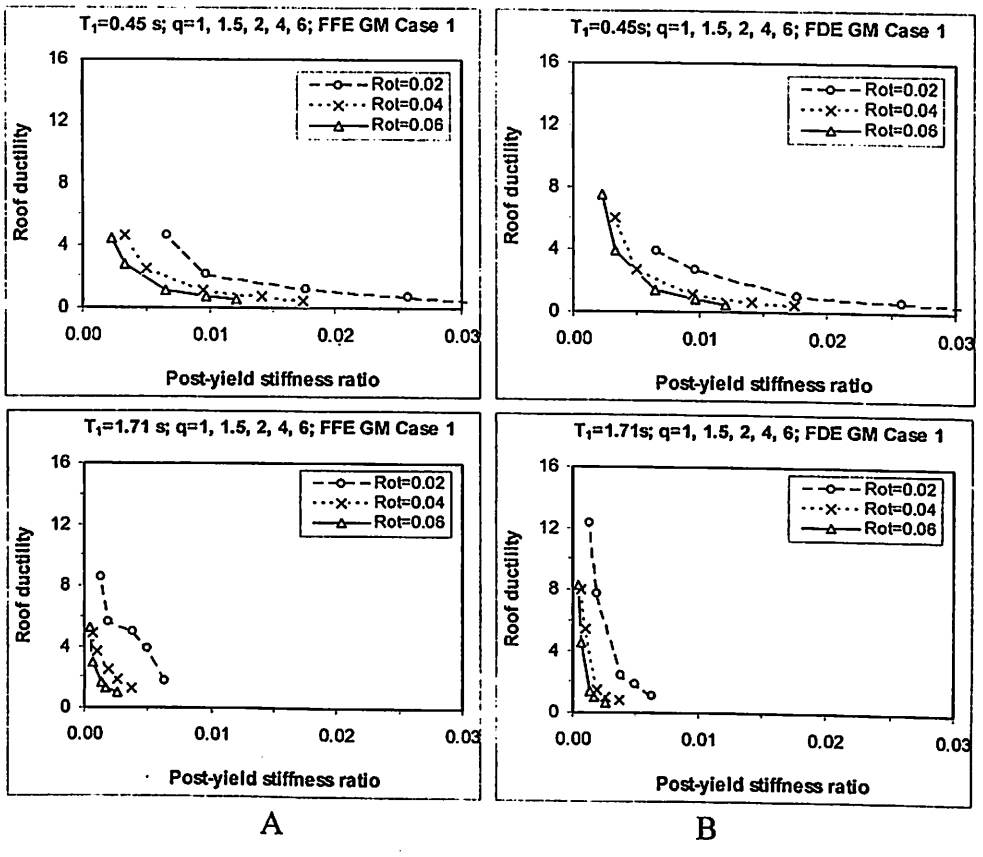

Figure 4.9: Mean roof ductility demand as a function of global post-yield stiffness ratio and plastic rotation capacity. Each point represents a behaviour factor. Models with T_1 = 0.45 and 1.71 s induced by GM Case 1 of a) FFE, and b) FDE

Figure 4.10 depicts the of ductility demand as a function of global post-yield stiffness ratio and behaviour factor for two types of plastic rotation capacity (Rot.=0.02 and 0.06). Each point in this figure represents fundamental period of models under consideration and hence the trend follows the same way as previously discussed. It is evident that no regular trend is demonstrated as the post-yield stiffness ratio is changed. In this case, the irregularity of effect post-yield stiffness ratio on the roof ductility demand explains its dependency to fundamental period since its shape of line indicates the same trend as in Figure 4.8. In general, effect of behaviour factor on the trend of roof ductility demand in Figure 4.10 is superior to the effect of post-yield stiffness ratio.

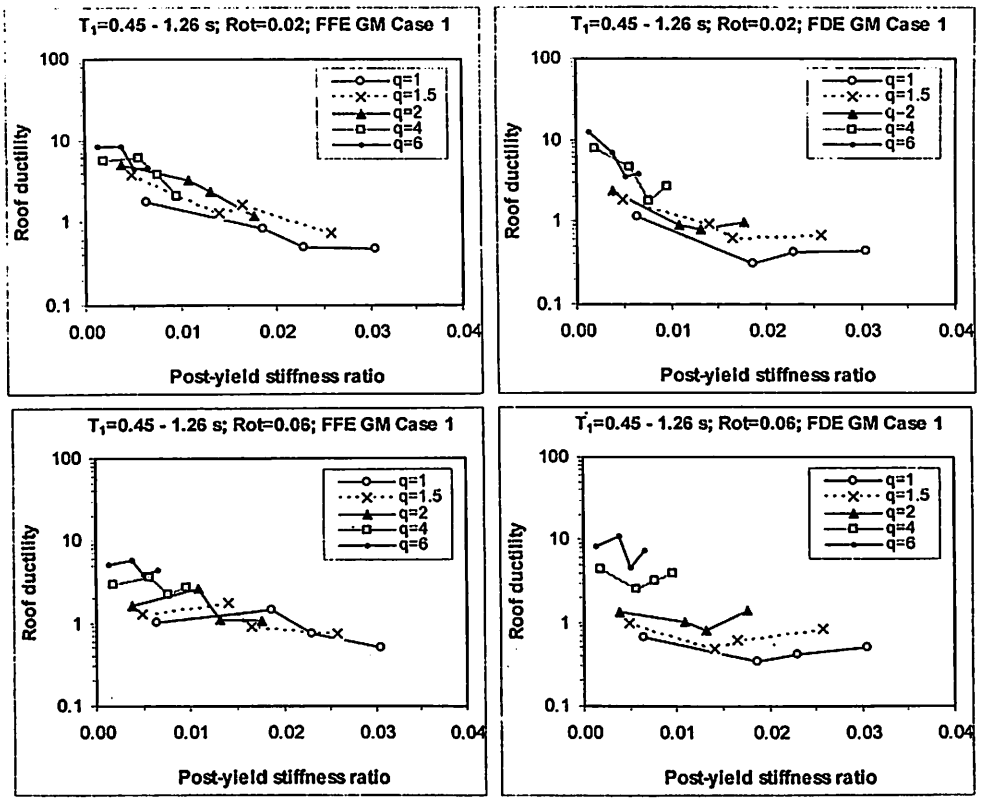

Figure 4.10: Mean roof ductility demand as a function of global post-yield stiffness ratio and behaviour factor. Each point represents fundamental period of models T_1 = 0.45, 0.75, 1.26 and 1.71 s. Models induced by GM Case 1 of FFE and FDE

It should be noted that the variation of post-yield stiffness ratio of the system under the same behaviour factor or ductility class is reflecting the variation of strength (i.e. flexural strength) of the elements represented by the ratio of maximum bending moment to the yield moment (M_o/M_y). It is because the M_o/M_y of elements has involved in the formation of the backbone curve of the hysteresis system, which in turn has participated in the global backbone curve. Unfortunately, the effect of M_o/M_y on the roof ductility ratio could not be presented since this parameter was not varied in designing the model. However, the variation of post-yield stiffness ratio in this study could reflect the variation of M_o/M_y by assuming a single value of plastic rotation capacity is used. Therefore, it can be said that as the M_o/M_y of element in the

system under the same plastic rotation capacity increases, the post-yield stiffness ratio increases and hence the roof ductility demand decreases.

4.4.3. Effect of Repeated Ground Motion

Repeated ground motion, represented by GM Case 1, 2, and 3 for single, double, and triple events, respectively, was expecting to enlarge the seismic demands as discussed in Chapter 2. The influence of repeated earthquakes on the roof ductility demands of models having fundamental period of 0.45, 0.75, 1.26, and 1.71 s and average plastic rotation capacity are demonstrated in Figure 4.11 to Figure 4.14. It is clearly apparent that the repeated earthquake affects the roof ductility demands in almost all conditions considered. For all models with lower behaviour factor (i.e. $q <$ 2), the effect of repeated FDE looks insignificant and can be negligible. This is only the case for 3-story model induced by repeated FFE.

The figures also explain that repeated earthquake of GM Case 3 mainly dominate in affecting the roof ductility demand. However, the gap of roof ductility demands under repeated FDE of GM Case 2 and 3 on the models having $T_1 \geq 0.75$ s and $q \leq 4$ is relatively small and hence can be neglected (Figure 4.13). The effect of repeated earthquake in form of roof ductility demand due to GM Case 2 or 3 normalized to GM Case 1, denotes as relative increment of repeated earthquake, is introduced in Table 4.2. Figure E.1 and E.2 in Appendix E further explains how superior GM Case 2 or 3 to GM Case 1.

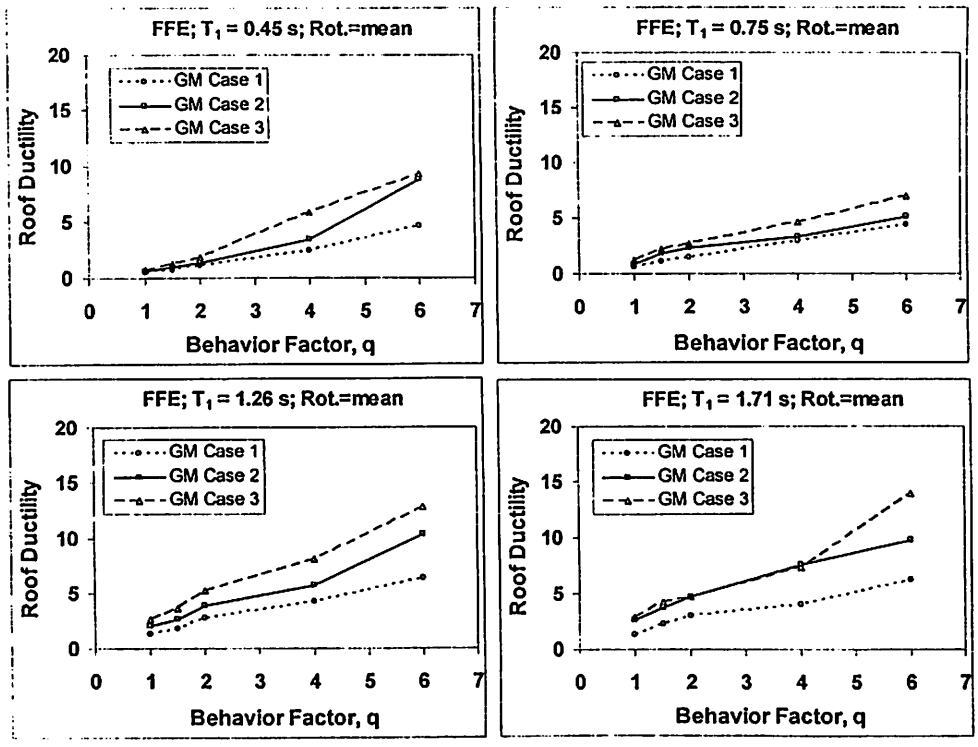

Figure 4.11: Roof ductility demand as a function of behaviour factor and mean plastic rotation capacities of models induced by repeated FFE

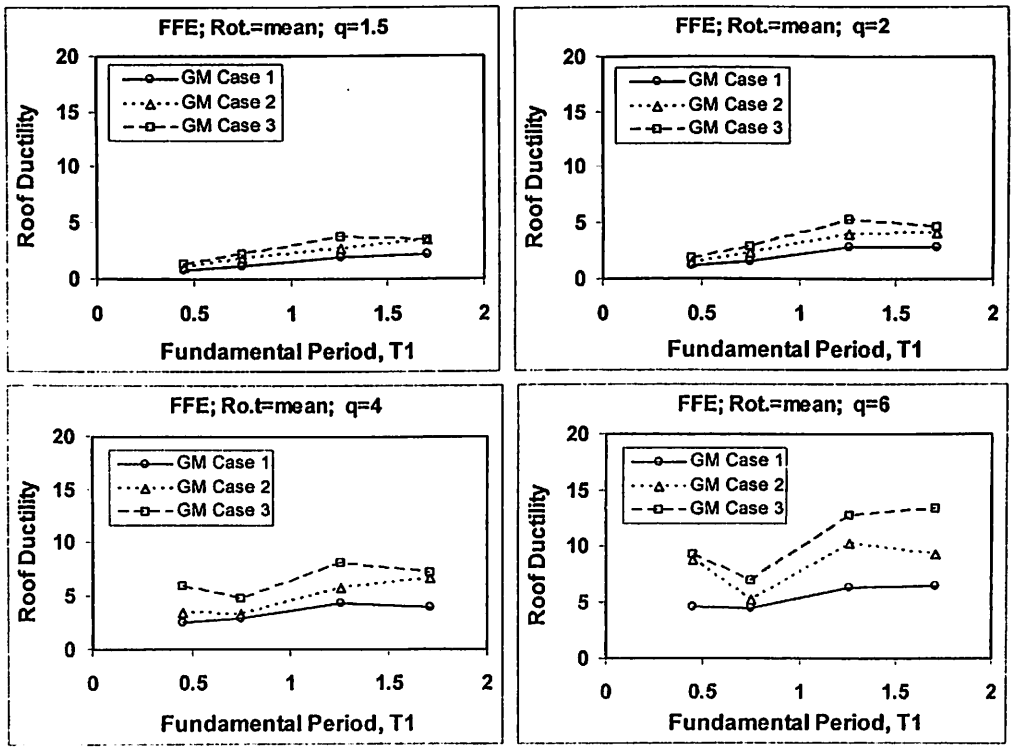

Figure 4.12: Roof ductility demand as a function of fundamental periods and mean plastic rotation capacities of models with q = 1.5 to 6 induced by repeated FFE

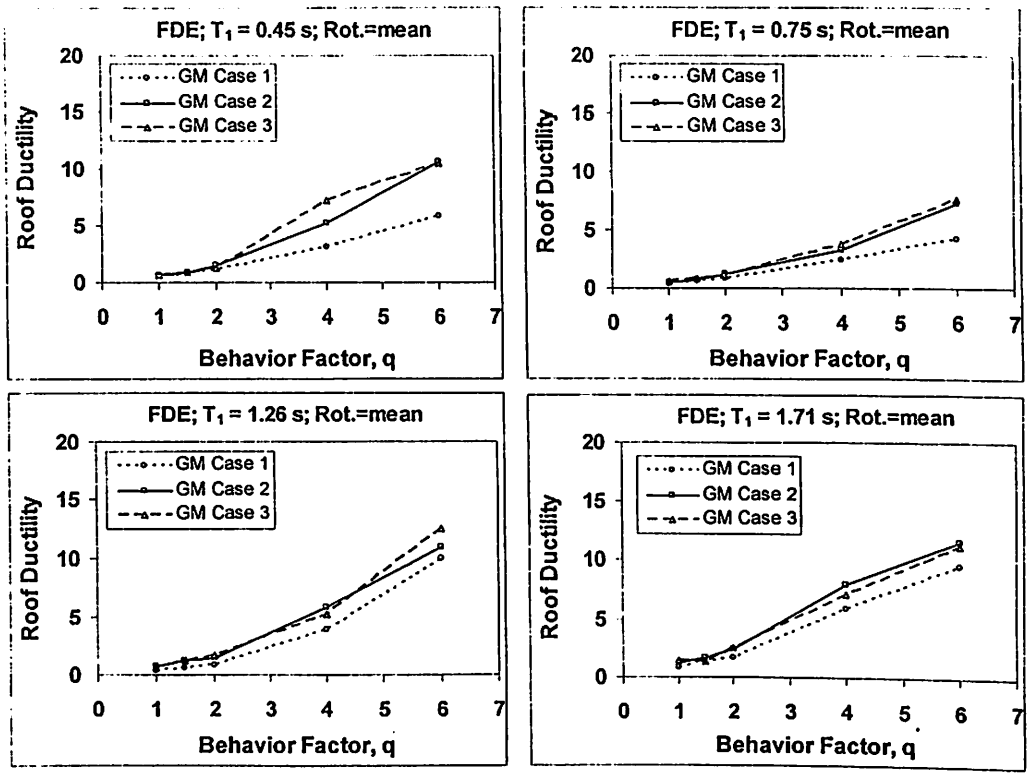

Figure 4.13: Roof ductility demand as a function of behaviour factor and mean plastic rotation capacities of models induced by repeated FDE

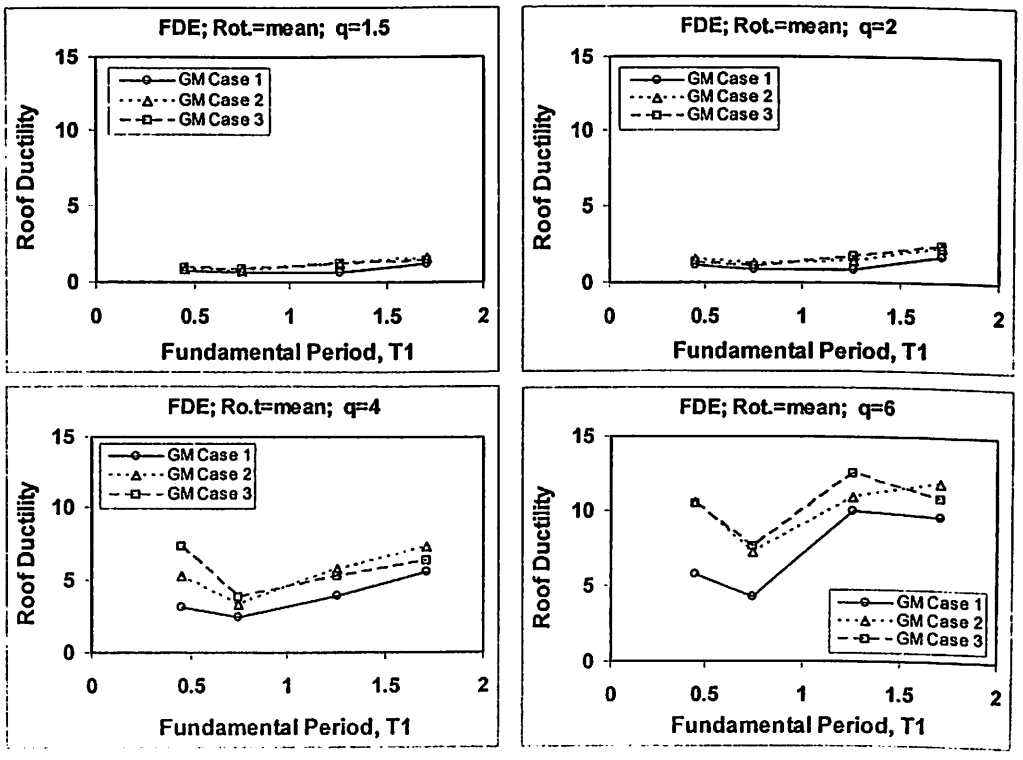

Figure 4.14: Roof ductility demand as a function of fundamental periods and mean plastic rotation capacities of models with q = 1.5 to 6 induced by repeated FDE

It is very interesting to note that repeated FDE does not dominant compare with FFE as commonly resulted from regular seismic analysis using single events. For instance, the roof ductility demand affected by GM Case 1 of FDE reached 1.5 times higher than the roof ductility demand affected by GM Case 1 of FFE, as shown in Table 4.1. In repeated earthquake cases, both ground motion types is relatively the same in influencing the roof ductility demand, which means the effect is not significantly differ, particularly on the 3 and 6-story models having $q \geq 4$.

Table 4.2: Relative increment of roof ductility demand on the models with $q \geq 1.5$ and average plastic rotation capacity induced by repeated earthquake

Models	Repeated GM case	FFE				FDE			
		q=1.5	q=2	q=4	q=6	q=1.5	q=2	q=4	q=6
3-story model (T_1 = 0.45 s)	GM Case 2	1.3	1.2	1.4	1.9	1.2	1.3	1.7	1.8
	GM Case 3	1.6	1.6	2.4	2.0	1.2	1.1	2.4	1.8
6-story model (T_1 = 0.75 s)	GM Case 2	1.6	1.6	1.1	1.2	1.3	1.5	1.4	1.7
	GM Case 3	1.9	1.8	1.6	1.6	1.3	1.3	1.6	1.8
12-story model (T_1 = 1.26 s)	GM Case 2	1.5	1.4	1.3	1.6	1.9	1.7	1.5	1.1
	GM Case 3	2.0	1.8	1.9	2.0	2.0	2.1	1.3	1.3
18-story model (T_1 = 1.71 s)	GM Case 2	1.6	1.6	1.9	1.6	1.3	1.4	1.3	1.2
	GM Case 3	1.8	1.6	1.8	2.2	1.1	1.5	1.2	1.2

It is worth to note that behaviour factor slightly affects the relative increment of roof ductility demand of 12 and 18-story models induced by repeated FFE, as indicates in Table 4.2. Such of cases show that the increase of behaviour factor tends to decrease the relative increment as demonstrated by the 12-story models induced by GM Case 2 and 3 of FDE and 6-story models induced by GM Case 2 and 3 of FFE. In general, the trend of relative increment is arbitrary due to the presence of behaviour factor.

Fundamental period of system has influenced the relative increment of roof ductility demand in such of way, which shaped in similar trend with roof ductility demand of the models induced by single event of earthquake as discussed in previous section. Models with $q \geq 4$ induced by GM Case 2 and 3 of FDE have demonstrated that the relative increment was reduced by the increase of number of story of models (or fundamental period). It can be said that as the flexibility of building with DCH increases, the effect of repeated earthquake on the roof ductility demand decreases. For lower behaviour factor such as $q < 4$ (DCM), the repeated earthquake GM Case 2 and 3 of FDE have increased the relative increment of roof ductility demand on the 3-story models up to 12-story models and then decreased significantly on the 18-story models. Note that the aforementioned conditions are strictly applied for repeated FDE contain a ground motion with large pulse (in main-shock) in its seismic sequences.

In average, the relative increment of roof ductility due to the repeated earthquake GM Case 2 and GM Case 3, reached 1.5 and 1.7 times, respectively, higher than GM Case 1 earthquake regardless the type of ground motion. If ground motion type is considered, the presence of repeated FFE have increased 1.6 and 1.7 times the roof ductility demands of the models designed with DCM and DCH, respectively, compared with the single earthquake effect, as used commonly in regular seismic design and evaluation. These effects could be higher for particular cases such as on the 3 and 12-story models designed with DCM, as well as 3, 12, and 18-story models designed with DCH. For the models designed with DCM and DCH, the effect of repeated FDE is found identically reach to 1.5 times, in average, higher than the single earthquake effect. As repeated FFE, such cases of models may experience larger amplification of roof ductility when repeated FDE induced (see

Table 4.2). Unlike the effect given by the single event earthquake case, these findings explain that repeated FDE is inferior to repeated FFE of about 9% in affecting the roof ductility demand of the considered models. It should be noted that these results are valid for regular reinforced concrete moment resisting frame that the gravity load has not affected the system significantly.

Findings of this study were compared with Hatzigeorgiou and Liolios (2010), which involved 3 and 8-story RC moment resisting frames (T_1 = 0.64 and 1.23 s, respectively) having q = 3.9, which was designed according to Eurocode 8. They induced the model with few records of repeated earthquakes regardless the type of ground motion. They found that double events of repeated earthquakes has produced roof ductility demand ranged from 4.1 to 5.6 on the 3-story RC structure, whereas from 4.5 to 5.7 for roof ductility demand on the structures with T_1 = 1.23 s. Their results were larger than the result of current study on the 3-story model, which has produced in the range of 3.4 – 4.0 of roof ductility demand after experiencing double event of repeated earthquakes. However, results for roof ductility demands were very close with them namely 4.2 – 5.7 on the model with T_1 = 1.26 s after experiencing double event of repeated earthquakes. Hatzigeorgiou and Liolios (2010) has found lower increment of roof ductility demand reached to 1.1 – 1.4 and 1.0 – 1.2 for 3-story model and for model with T_1 = 1.23 s, respectively, due to double event of repeated earthquake, whereas the current study has found the relative increment reached 1.6 – 1.7 for 3-story model and 1.5 – 1.8 for model with T_1 = 1.23 s. The different seems to be realistic since the deterioration of strength and stiffness in the hysteresis model has not been incorporating in Hatzigeorgiou and Liolios (2010). This effect would significantly apparent for system with shorter period such as Hatzigeorgiou and Liolios' models (e.g. Medina and Krawinkler, 2004).

Since the models considered in this study is regular in horizontal and elevation, i.e. response is dominant by the first mode of vibration of the system, a comparison can be made with the SDOF system from previous studies. As discussed in Chapter 2, Hatzigeorgiou and Beskos (2009) conducted the similar topic on the nonlinear SDOF system and they found that repeated earthquake has increased the ductility demand up to 2 times, in average, which is larger 25% than the average result of this study. However, this average result was based on elasto-plastic SDOF system having damping ratio from 1 to 10%, post-yield stiffness ratio from 0% to 5%, no overstrength of system, and the system built on all soil types (Soil A, B, C, and D), which was covering too wide range of system compared with current study. If their empirical relationship was used specifically with the scenario considered in this study, it is found that 1.2 and 1.4 increment of ductility due to the GM Case 2 and 3, respectively, which is 23% lesser than the aforementioned result of this study. The study done by Hatzigeorgiou (2010) regarding the effect of repeated earthquake on the elasto-plastic strength hardening SDOF system has demonstrated approximately similar result. This time he grouped the ground motion into near-field and far-field earthquakes. By using his empirical relationship of ductility demand, it is found the amplification due to repeated earthquake only reached 1.2 times higher than the effect of single earthquake event.

Nevertheless, the Hatzigeorgiou and Beskos (2009) and Hatzigeorgiou (2010a) studies were based on the non-degrading stiffness and strength system and without overstrength factor. The system using hysteresis rule with strength and stiffness degradations could produce larger peak displacement response compare with system using elasto-plastic hystresis rule (e.g. Medina and Krawinkler, 2004;

Ruiz-Garcia and Miranda, 2005). This is why both of their results tend to significantly lower than the result of current study.

Using the roof ductility demand result of the current study included with its considered parameters, the behaviour factor utilizing the empirical relationship proposed by Hatzigeorgiou (2010b) were calculated. The relationship was developed using the same elasto-plastic SDOF model as Hatzigeorgiou and Beskos (2009) and Hatzigeorgiou (2010a), which induced by NFGM only. The results were compared due to GM Case 1, 2, and 3 and listed in Table 4.3. It shows that the behaviour factor on the system having $0.45 < T_1 < 1.86$ s due to single event earthquake (GM Case 1) is lower than the behaviour factor of Hatzigeorgiou (2010b).

Table 4.3: Comparison of behaviour factor with Hatzigeorgiou's (2010b) results for system with $0.45 < T_1 < 1.86$ s induced by near-field ground motions

Hatzigeorgiou's (2010b)	This study		
GM Case 1, 2, 3	GM Case 1	GM Case 2	GM Case 3
1	1	1	1
1.5	1.4	1.7	1.4
2	1.6	1.8	1.8
4	3.8	4.8	4.9
6	5.7	6.6	6.7

Moreover, the current study tends to produce larger behaviour factor on the system induced by GM Case 2 and 3 of repeated earthquake. In general, the behaviour factor from the current study was reasonably close with his study by considering the type of degree of freedom of the system as well as the differences in using hysteresis model. The other problem might attribute to this difference was sourced from the selected NFGM of Hatzigeorgiou (2010b), which was taken based on source-to-site distance (≤ 10 km) while the current study was mainly based on large-pulse criteria.

4.5 Story Ductility Demands

As stated previously story ductility demand, μ_s, is one of the important engineering demand parameter (EDP) in performance based earthquake engineering. This parameter is a relative drift between two adjacent stories on the inelastic models. Since the inelastic models were induced by 20 ground motions for each variant studied, herein the considered EDP is a mean value of μ_s. In this section μ_s is also presented in maximum story ductility demand. The repeated earthquake case considered is identical with roof ductility demand.

The examples of story ductility demands of inelastic structures with 0.04 of plastic rotation capacity due to regular earthquake event (GM Case 1) are depicted in logarithmic form in Figure 4.15 to Figure 4.18. The figures indicate that most of the story drift extremely exhibit at lower part of stories, especially at first story of model having number of story of 6, 12, and 18 with $q > 1.5$. Similar trend was also found in story drift on the 9, and 18-story models Ruiz-Garcia and Miranda (2005), as well as on the 8, and 12-story models done by Ruiz-Garcia and Negrete-Manriquez (2011). This condition appears as a logic consequence of the migration of maximum value over the height of story drift from top to bottom as the intensity level of motion increases (Medina and Krawinkler, 2003; Ruiz-Garcia and Miranda, 2005). As explained in previous chapter, seismic hazard used in this study was considered as the highest for Greece and even Europe, which made the motion intensity level considered high as well.

It is also apparent that the story ductility level at bottom stories increased significantly as the story number of models increased, especially for $q \geq 4$. The presence of this condition is because the structure P-Delta effect governs the response of models (Medina and Krawinkler, 2003; Ruiz-Garcia and Miranda, 2005).

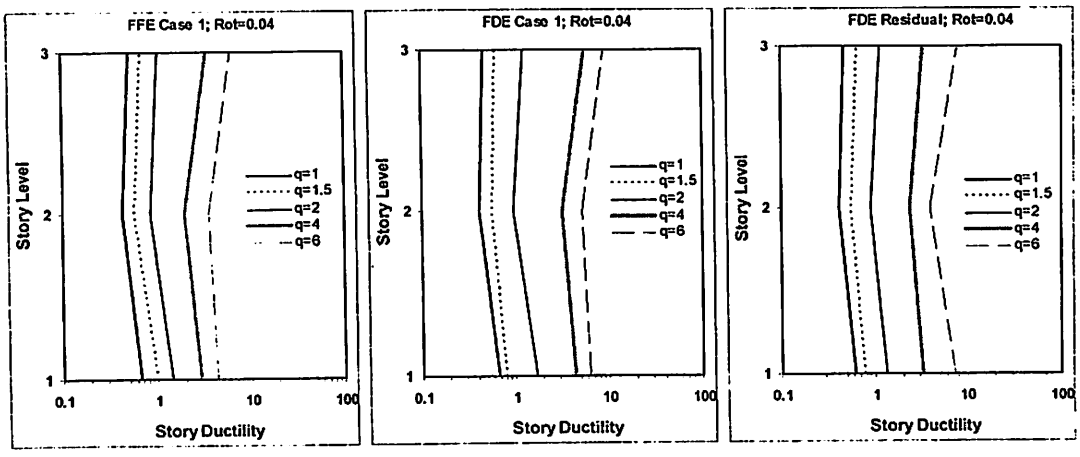

Figure 4.15: Story ductility demands of 3-story inelastic structures due to repeated earthquakes GM Case 1 FFE and FDE, and residual FDE

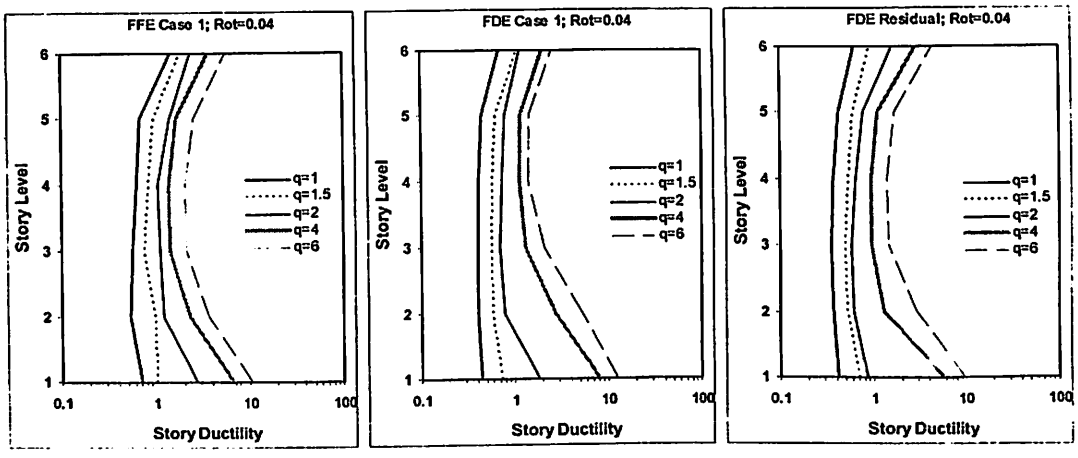

Figure 4.16: Story ductility demands of 6-story inelastic structures due to repeated earthquakes GM Case 1 FFE and FDE, and residual FDE

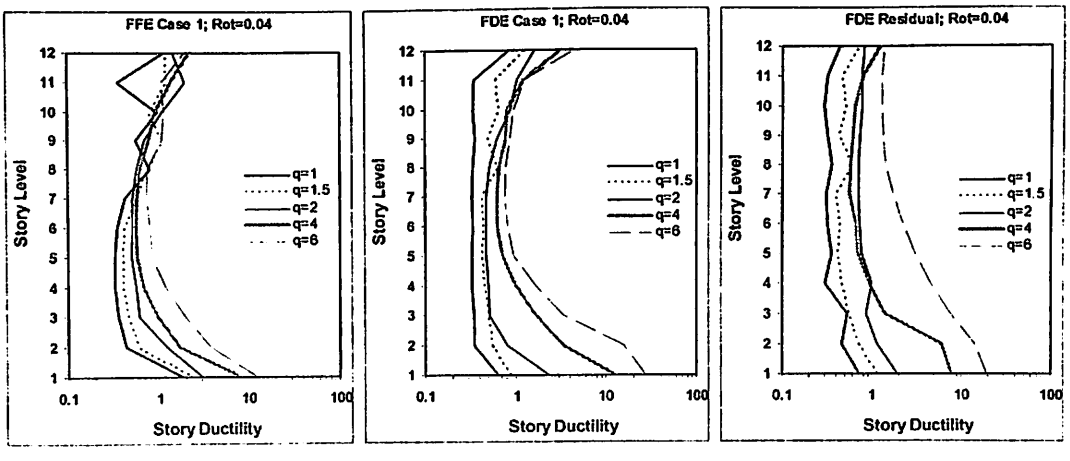

Figure 4.17: Story ductility demands of 12-story inelastic structures due to repeated earthquakes GM Case 1 FFE and FDE, and residual FDE

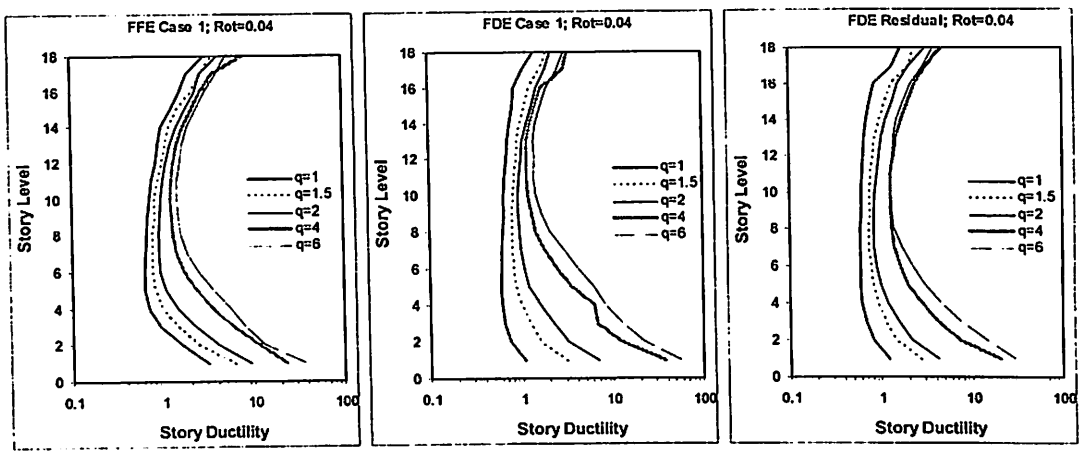

Figure 4.18: Story ductility demands of 18-story due to repeated earthquakes GM Case 1 FFE and FDE, and residual FDE

The maximum story ductility demand for models considered after affected by regular earthquake (GM Case 1) of FFE, FDE, and residual FDE is presented in logarithmic form in Figure 4.19 and Figure 4.20. Figure 4.19 explains the maximum story ductility demand in a function of fundamental period and behaviour factor, whereas Figure 4.20 depicts the story ductility demand of model with $0.45 < T_1 < 1.71$ s in a function of behaviour factor and plastic rotation capacity. Further discussion related to these figures is placed in the next sections.

4.5.1 Effect of Behaviour Factor and Fundamental Period

Similar with roof ductility demands, story ductility demands is increased as behaviour factor increased at almost all of story of all models. Few models have indicated that this trend were not applied at some stories, i.e. at mid height to the top part of the 12-story and 18-story (plastic rotation capacity of 0.02) models. Similar problem have occurred on the taller models in the studies done by Alavi and Krawinkler (2001), Medina and Krawinkler, Ruiz-Garcia and Miranda (2005). In the first two studies, the jagged-like pattern of story ductility is believed due to the large

pulse content in NFGM having FDE. It makes the system having low q tends to give high story drift at upper level and low story drift at lower level, whereas the system with high q performs in opposite way. It can be seen that the maximum drift is shifted from upper to lower stories as the q increased.

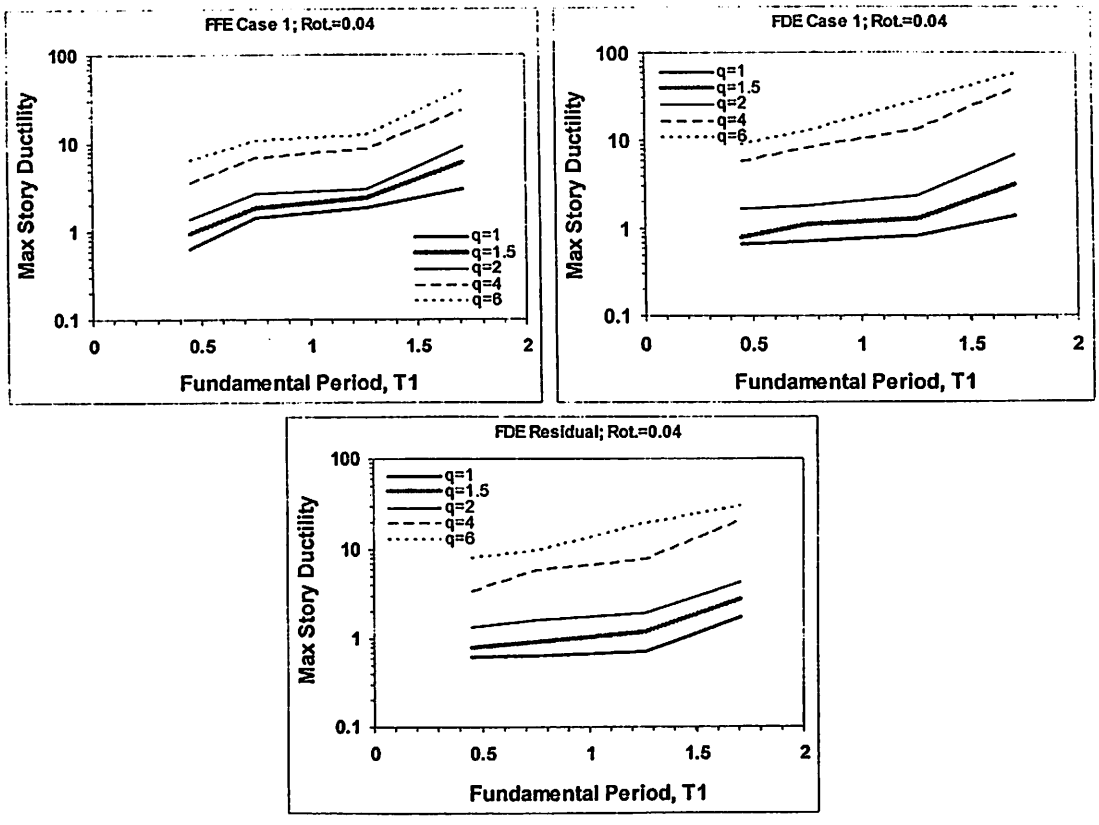

Figure 4.19: Maximum story ductility demands of inelastic structures affected by repeated earthquakes GM Case 1of FFE, FDE and Residual FDE

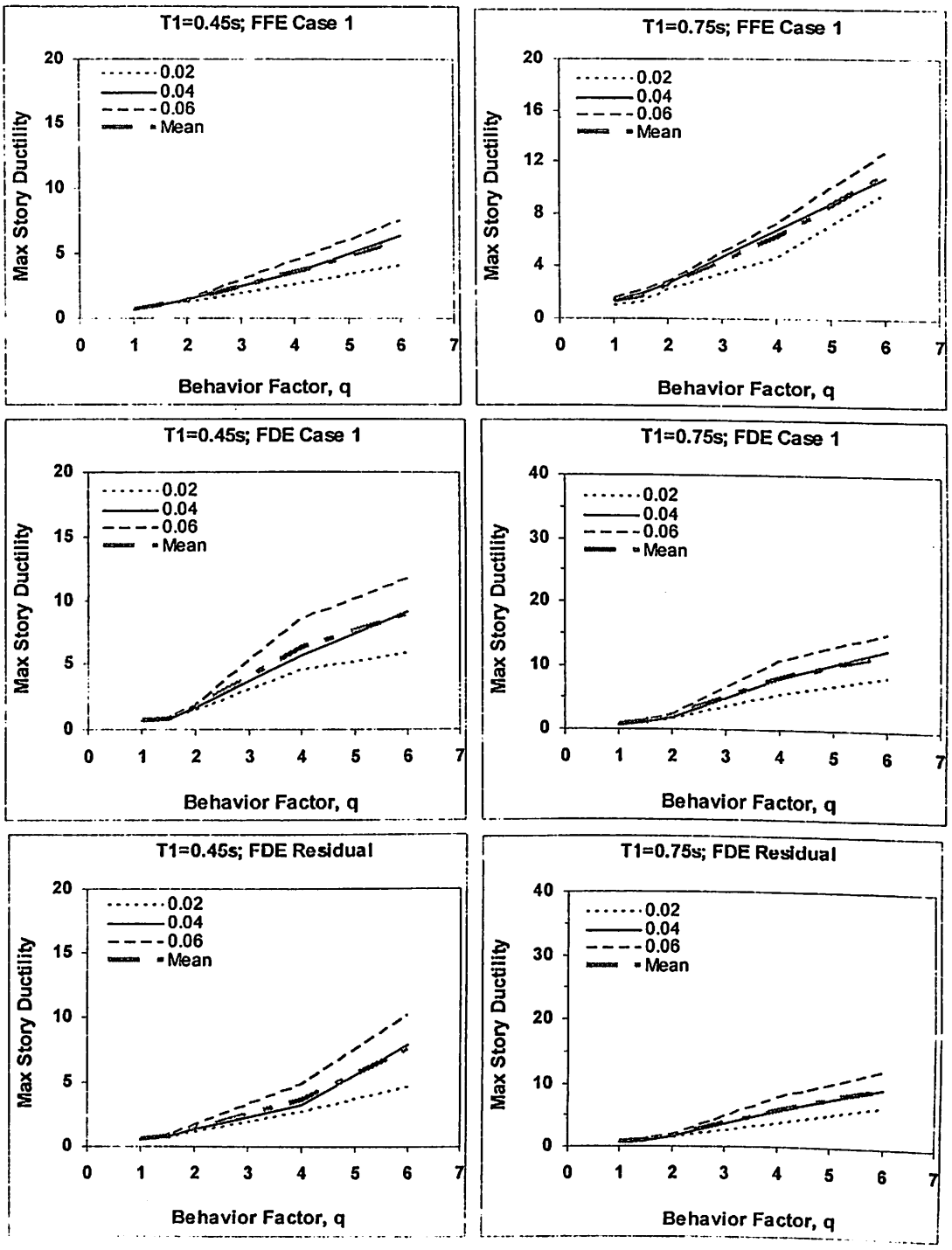

Figure 4.20: Maximum story ductility demands of inelastic structures as a function of behaviour factor and plastic rotation capacities (0.02, 0.04, and 0.06) due to GM Case 1 of FFE, FDE, and residual FDE

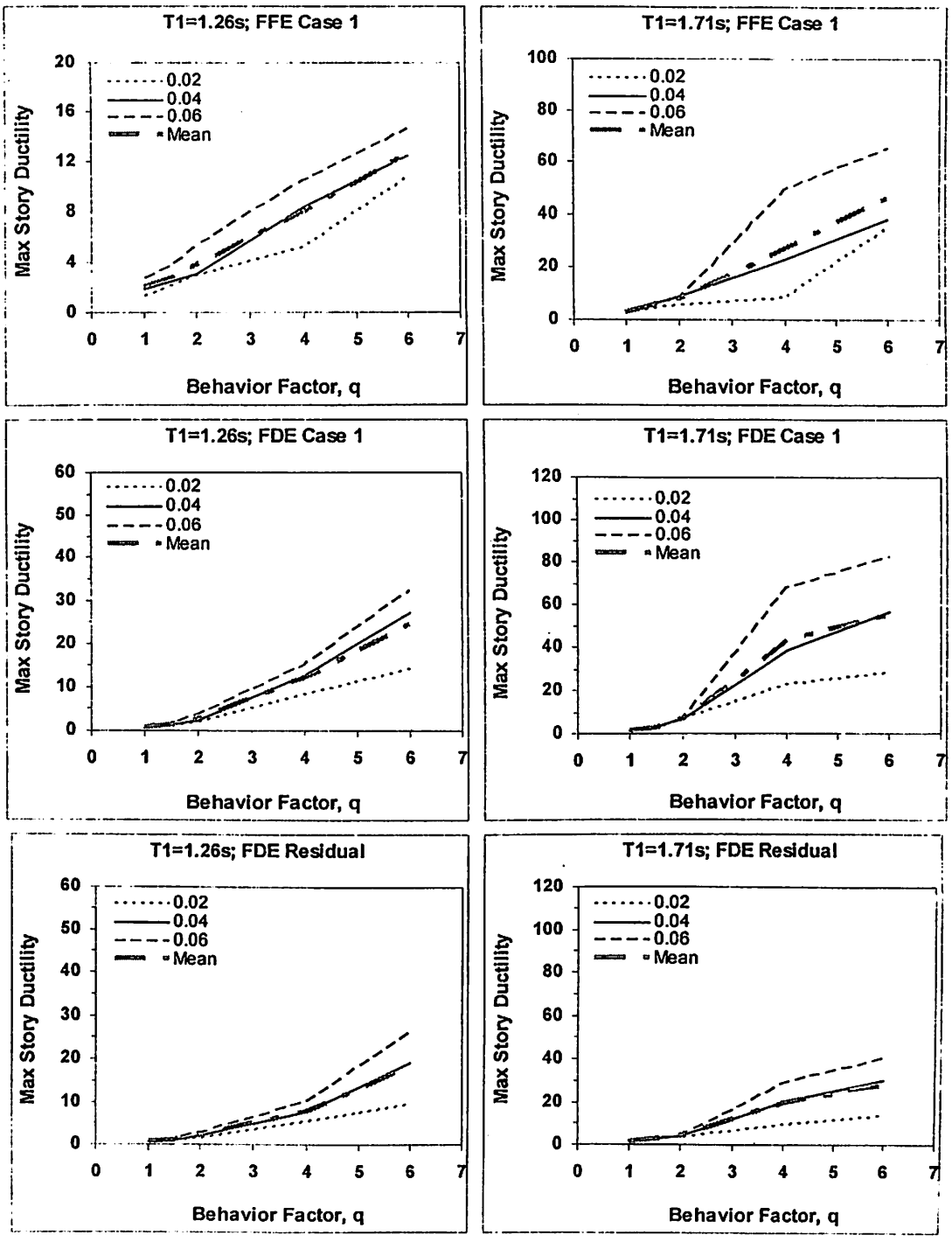

Figure 4.20: *Continued*

It is found that the jagged-like pattern of story ductility not only occurred in models induced by FDE, but also on the models affected by FFE, which indicated that pulse content seemed not entirely control those pattern. The change of governing story from top to bottom in story ductility due to FDE was also not exhibited in the current studies as well in Ruiz-Garcia and Miranda (2005). The way of modelling strong-column-weak-beam might be attributed to this problem since their models were using beam-hinge mechanism (plastic hinge at beam only), whereas models of Ruiz-Garcia and Miranda (2005) and the current study were developed with full-hinge mechanism (plastic hinge at all element ends). It is also evident that the secondary story ductility concentration tends to exhibit in the upper stories, which is more apparent as the number of story of model increases and the strength decreases. This is a consequence of higher-mode effect, which is not apparent on the system built with beam-hinge mechanism (Ruiz-Garcia and Miranda, 2005; Alavi and Krawinkler, 2001; Medina and Krawinkler, 2003).

Figure 4.16 to 4.19 explain the story ductility profile changes as the number of stories (fundamental period) increases. Despite the magnitude of story ductility demands is varied, the story ductility profiles tend to perform in similar trend, i.e. the lower amplitude of story ductility occurs in intermediate stories, as the same trend as reported by Ruiz-Garcia and Miranda (2005). Figure 4.20 depicts how the considered fundamental period of vibration of the models affects the maximum story ductility arbitrarily. It can be seen that the influence of fundamental period was less significant to the maximum story ductility in the range of $0.45 < T_1 < 1.71$ s for all type of ground motion considered. For FDE and residual FDE ground motions, the less significance of fundamental period on the maximum story ductility is more broaden namely $T_1 < 1.71$ s, particularly for models with $q \leq 2$.

4.5.2 Effect of Global Post-Yield Stiffness Ratio

Figure 4.21 depicts graphs of mean maximum story ductility demand versus global post-yield stiffness ratio. The trend is identical with the graphs of mean roof ductility demand versus post-yield stiffness ratio, as discussed in previous section.

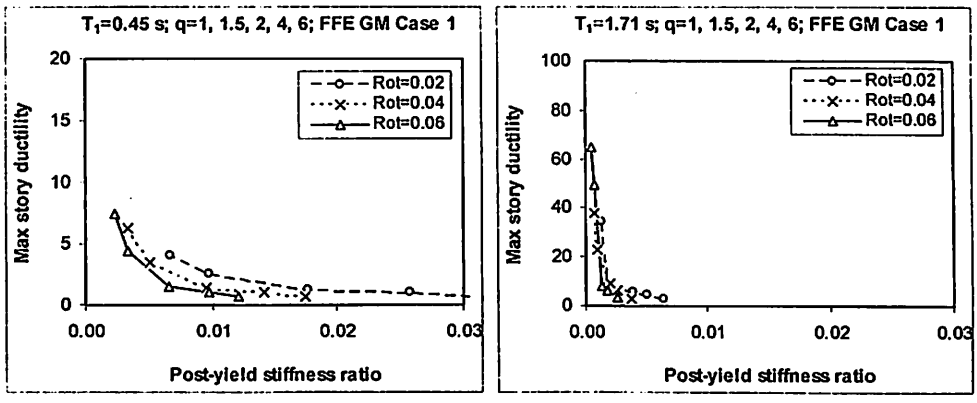

(a) (b)

Figure 4.21: Mean maximum story ductility demand as a function of global post-yield stiffness ratio and plastic rotation capacity (0.02, 0.04, and 0.06). Each point represents a behaviour factor. Models with a) T_1 = 0.45, and b) 1.71 s, induced by GM Case 1 of FFE

The increasing function of global post-yield stiffness ratio as a function of the decreasing of behaviour factor, the decreasing of plastic rotation capacity, and the decreasing of fundamental period of vibration would deteriorate the maximum story ductility demand. The same mechanism occurred for the effect of post-yield stiffness ratio on the maximum story ductility demand due to FDE.

4.5.3 Effect of Repeated Ground Motions

In this section the influence of repeated FFE and FDE on the story ductility demands of inelastic structures having several types of fundamental periods of vibration, behaviour factor, and plastic rotation capacity are discussed. Figure 4.22 and Figure 4.23 portrays the trend of story ductility demand, μ_s, along the height

under seismic sequences GM Case 1, 2, and 3. For shorter period of system, i.e. 3-story model, the maximum story ductility demand due to GM Case 1, 2, and 3 of FFE tends to exhibit at the top story for the model with low q. This maximum demand then migrates to the bottom story as the strength decreases (q increases). The similar trend is also occurred on the 3-story models induced by FDE. At the same time, the 6-story model induced by repeated FFE and FDE tends to give the contrary pattern of story ductility demand. For taller models, all of the extreme story ductility demand due to GM Case 1 to 3 is situated at the bottom story, regardless the type of behaviour factor and ground motion. It means the dispersion of maximum story ductility of the inelastic structures induced by repeated earthquake of GM Case 2 and 3 follows the same trend like GM Case 1, as discussed in previous section. It can be said that the influence of repeated earthquake to the dispersion of maximum story ductility demands is negligible.

The similar trend was also found for the story drift on the 3 and 8-story RC frame models, which was used by Hatzigeorgiou and Liolios (2010) in evaluating the repeated earthquakes. Using different type of material (i.e. steel) and non-degrading strain hardening bilinear hysteresis rule, Ruiz-Garcia and Negrete-Manriquez (2011) has indicated that the story drift on the 4, 8, and 12- story inelastic models was performed in the same trend as well. These two studies have supported the previous findings mentioned that the repeated earthquakes were not affecting the dispersion of maximum story ductility along the height.

In general, the relative increment of story ductility demand on the system due to repeated FFE (GM Case 2 or 3) tends to decrease as the behaviour factor increases. This trend is clearly evident as the number of story of models (or fundamental period) increases, particularly on the 6- and 12-story models, as plotted

in Figure 4.23. It should be note that this is not the case for all stories along the height. For the models induced by repeated FDE, the trend of relative increment of story ductility demand tends to experience contrarily, except for 12-story models. This indicates that the behaviour factor increases (the strength decreases) as the relative increment of story ductility increases. The significance of various fundamental periods of models on the relative increment of story ductility demand due to repeated FDE is not apparent.

The maximum story ductility demand, $\mu_{s,max}$, of considered inelastic structures is depicted as a function of behaviour factor in Figure 4.24 and 4.25. It is evident that the behaviour factor affects the increment of maximum story ductility demands. The increase of behaviour factor tends to raise the relative increment of $\mu_{s,max}$ regardless the types of fundamental period and ground motions. Although in few cases GM Case 2 is found dominant, i.e. models with $T_1 < 1.71$ s and $q = 6$, repeated earthquake GM Case 3 generally produced higher influence on the increment of $\mu_{s,max}$ than GM Case 2 for all type of ground motions. Moreover, the effect of repeated FFE and FDE on the $\mu_{s,max}$ of models having $q \leq 2$ tends to small and can be neglected. It can be said that only $\mu_{s,max}$ on the structures with high q (i.e. $q = 4$ and 6) are affected by the presence of repeated earthquake. This condition is clearly apparent on the case of repeated FDE, as depicted in Figure 4.25.

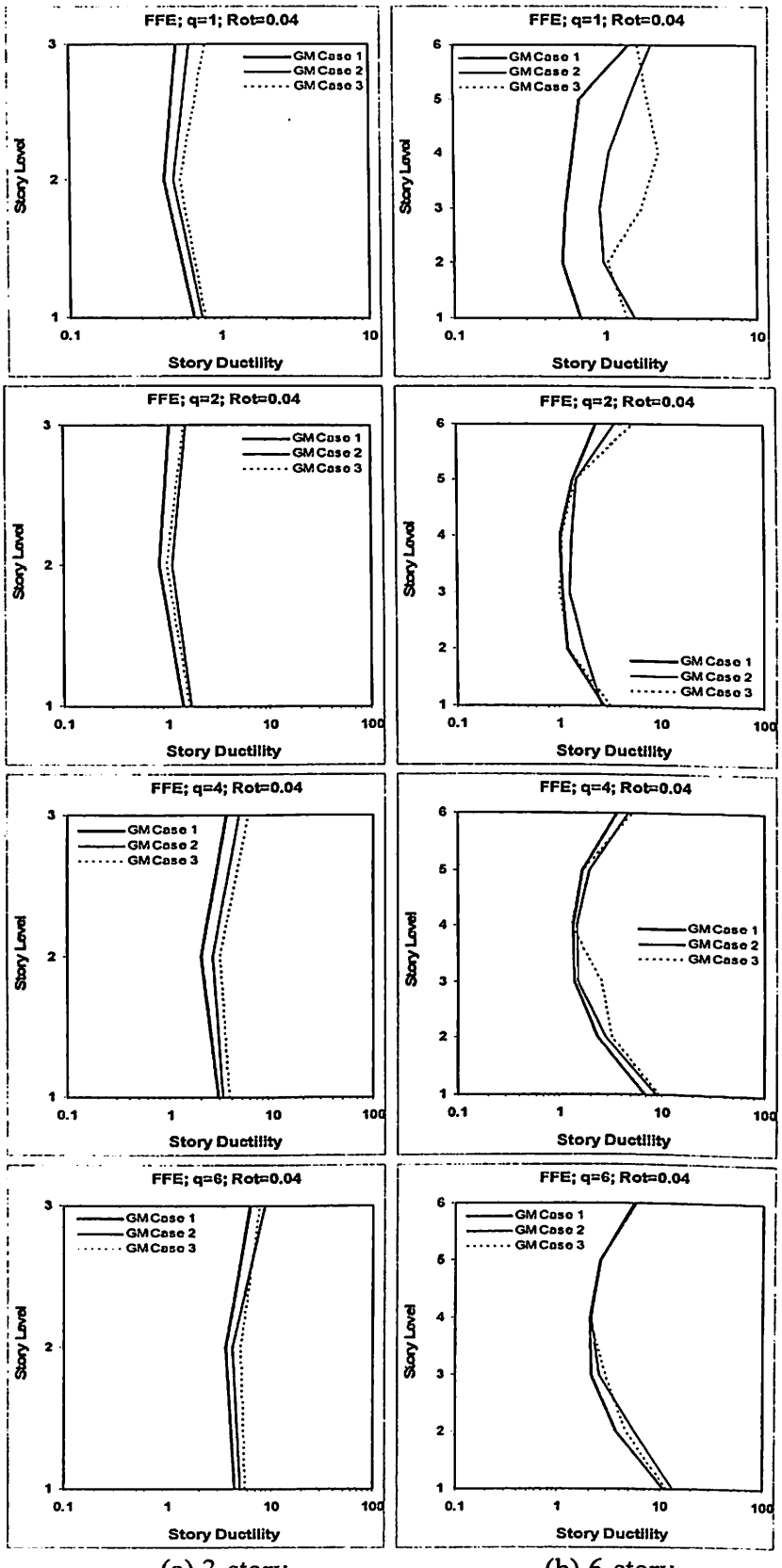

(a) 3-story (b) 6-story

Figure 4.22: Story ductility demands of 3, 6, 12, and 18-story inelastic structures with plastic rotation capacity of 0.04 affected by GM Case 1, 2, and 3 of repeated FFE

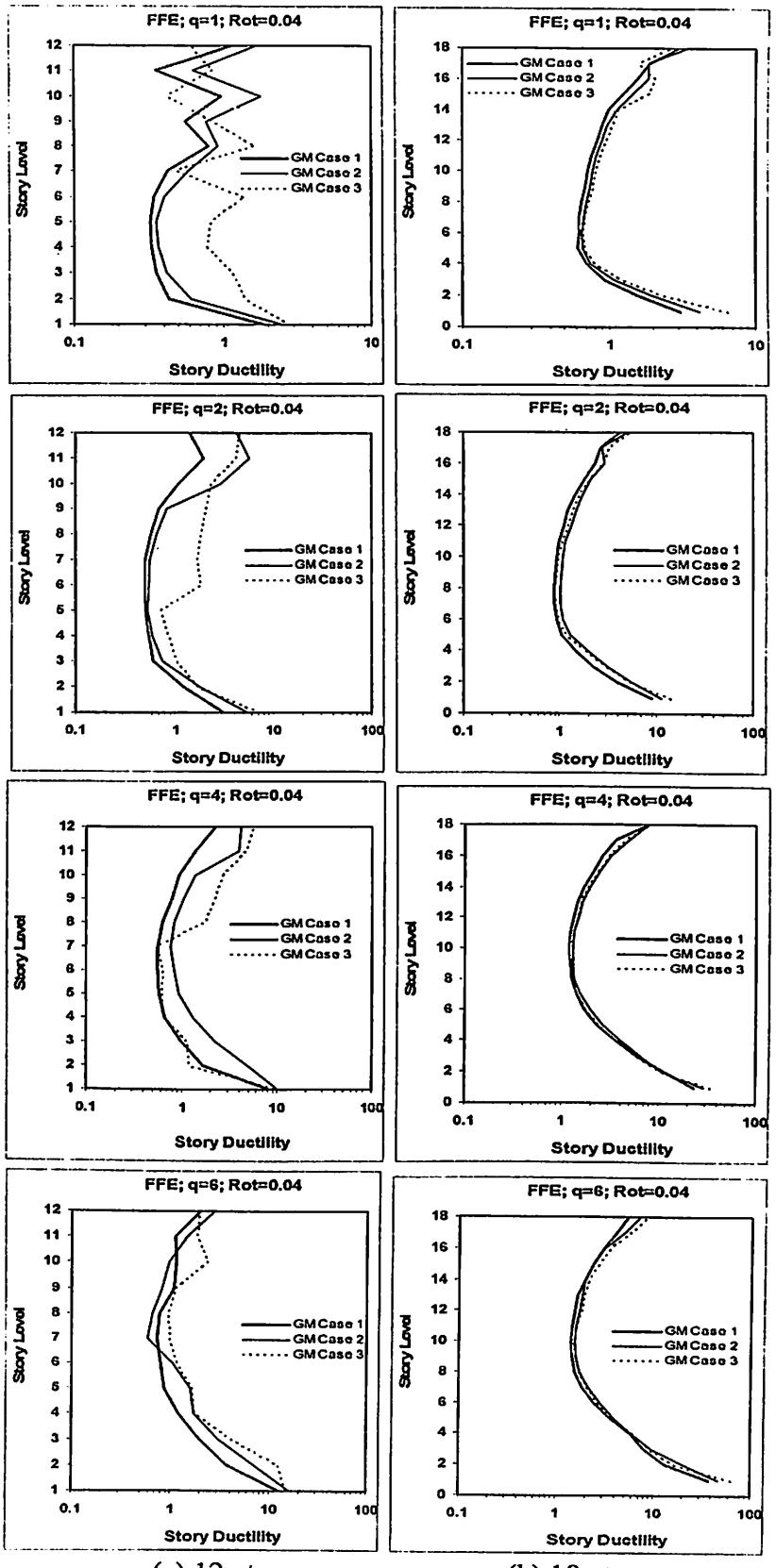

(a) 12-story (b) 18-story

Figure 4.22: *Continued*

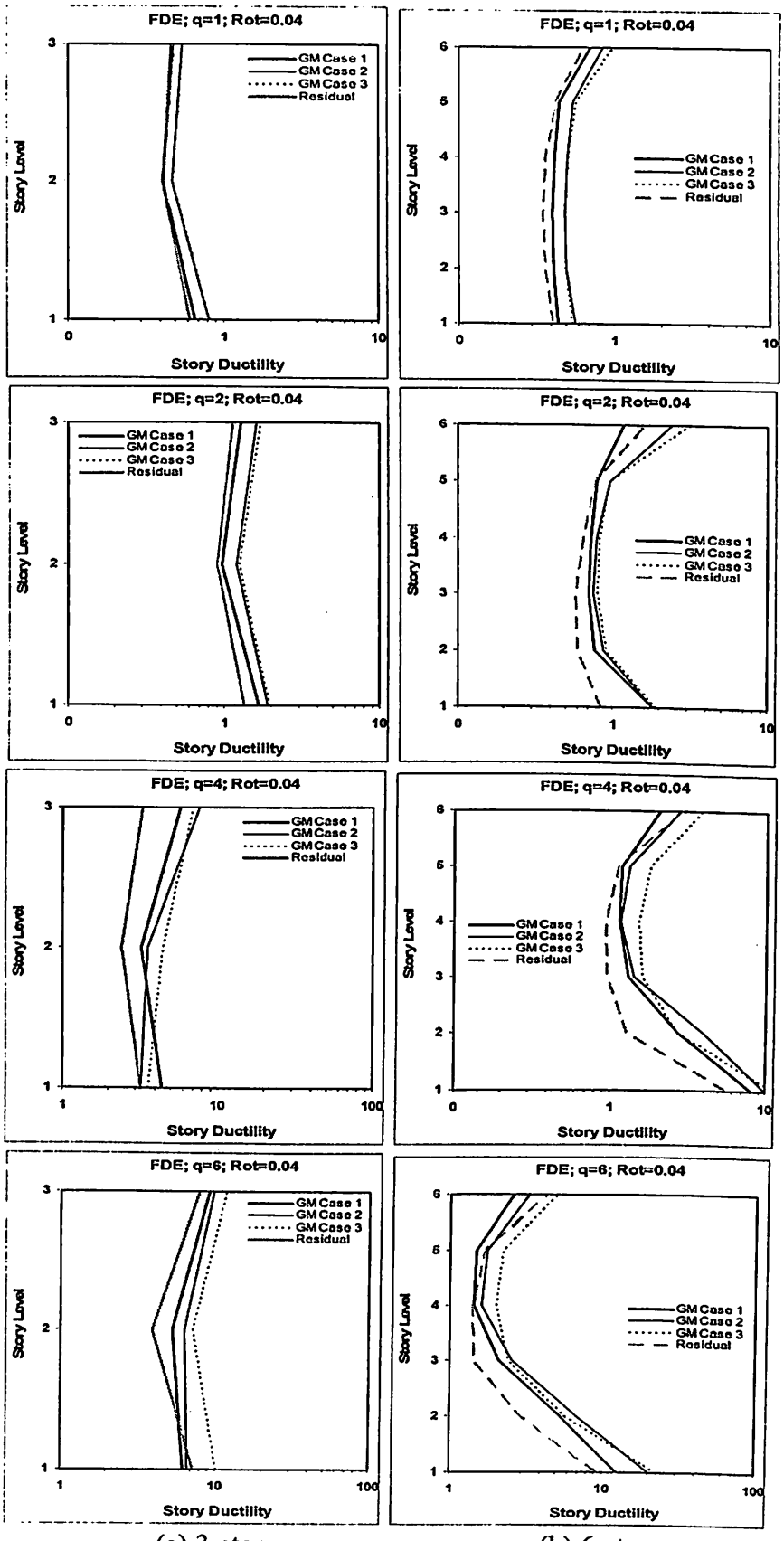

(a) 3-story (b) 6-story

Figure 4.23: Story ductility demands of 3, 6, 12, and 18-story inelastic structures with plastic rotation capacity of 0.04 affected by GM Case 1, 2, and 3 of repeated FDE

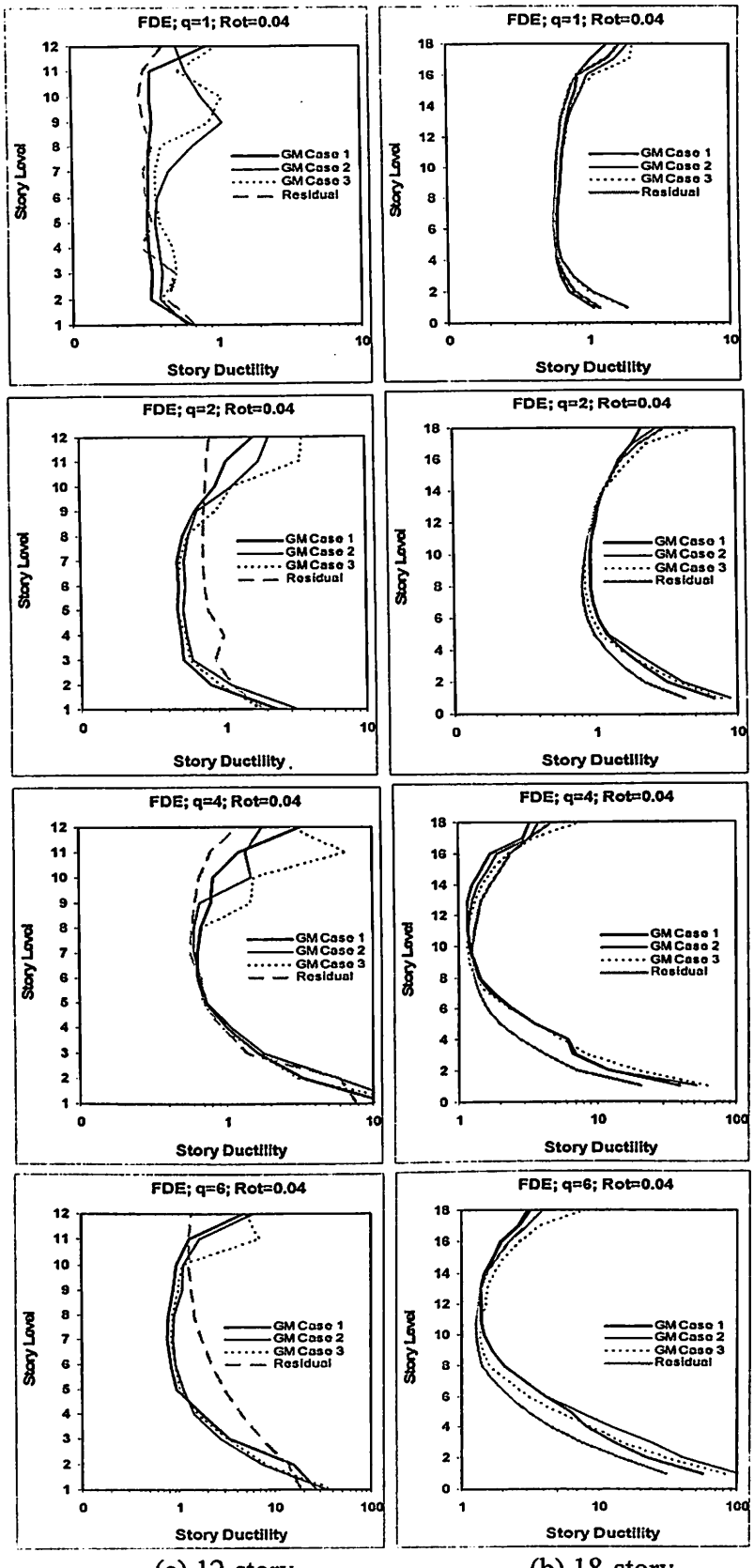

(a) 12-story (b) 18-story

Figure 4.23: *Continued*

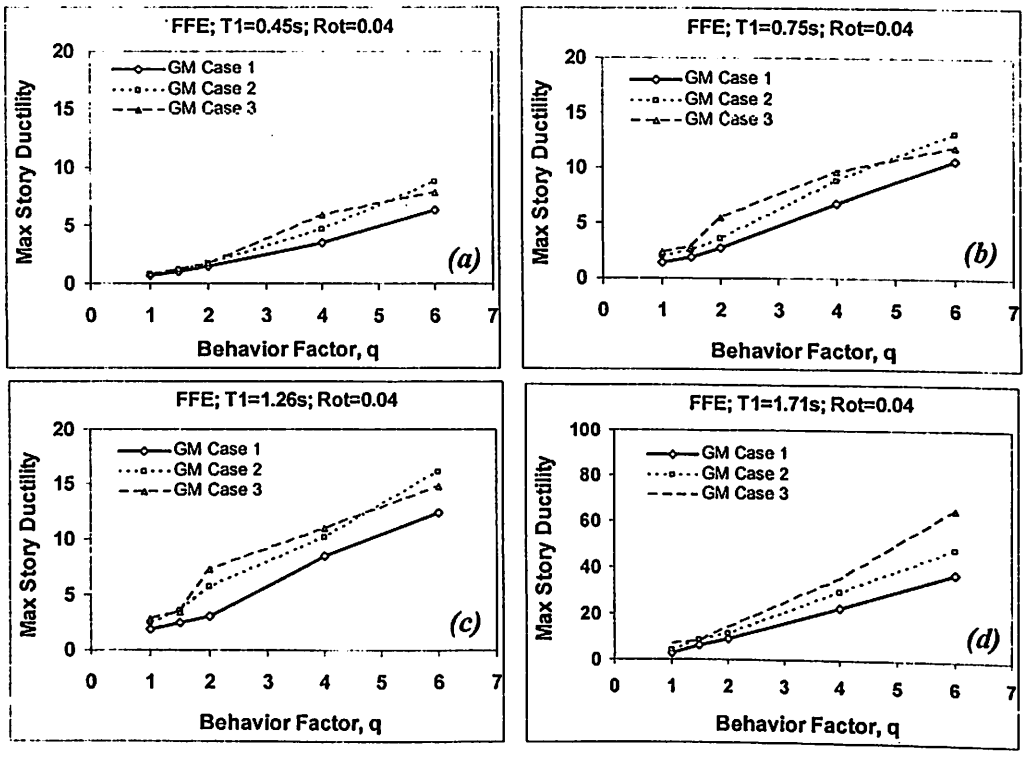

Figure 4.24: Maximum story ductility demand of 3, 6, 12 and 18-story inelastic structures with 0.04 of plastic rotation capacity due to repeated FFE

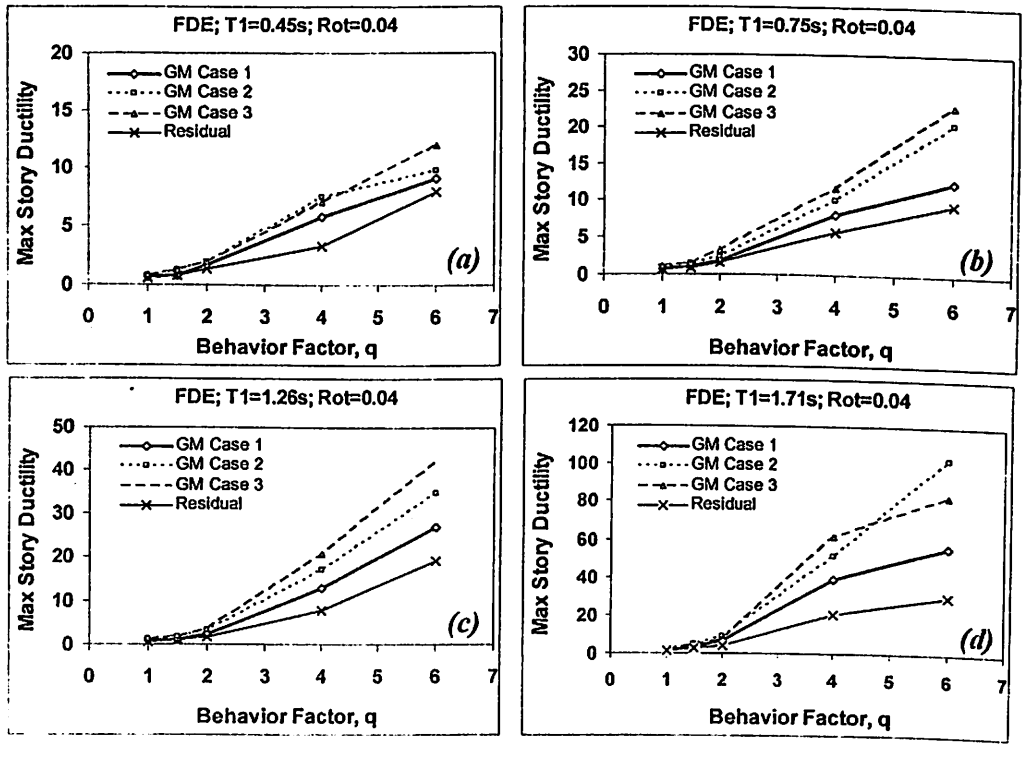

Figure 4.25: Maximum story ductility demand of 3, 6, 12 and 18-story inelastic structures with 0.04 of plastic rotation capacity due to repeated FDE

The relative increment of maximum story ductility demand, $\mu_{s,max}$, on the models with fundamental period $0.45 \leq T_1 \leq 1.71$ s (or system having 3 to 18 of number of story) with average plastic rotation capacity and $q \geq 1.5$ is listed in Table 4.4. For this range of model, the relative increments of $\mu_{s,max}$ due to repeated FFE, regardless GM Case 2 or 3, are found within the range of 1.2 to 1.9 and 1.1 to 1.6 for the system designed with DCM and DCH, respectively. It means the system designed with DCM experiences higher increment of $\mu_{s,max}$ than the system designed with DCH. These are found contrary with the models affected by repeated FDE which produced relative increment of $\mu_{s,max}$ with range of 1.1 to 1.8 and 1.2 to 2.0 for system designed with DCM and DCH, respectively.

In general, GM Case 3 has propagated the increment of $\mu_{s,max}$ on the considered inelastic structures of 16% larger than GM Case 2. On the system with DCM and DCH, the gap of increment of $\mu_{s,max}$ between GM Case 3 and 2, regardless the ground motion type, have reached 19.2% and 12.8 %, respectively. Therefore, it can be said that the maximum story ductility on the system with DCM could be increased higher than the system with DCH when the seismic sequences exhibited.

Table 4.4: Relative increment of maximum story ductility demand on the models with average plastic rotation capacity and $q \geq 1.5$ induced by repeated earthquakes

Models	Repeated GM case	FFE				FDE			
		q=1.5	q=2	q=4	q=6	q=1.5	q=2	q=4	q=6
3-story model	GM Case 2	1.2	1.2	1.4	1.4	1.5	1.1	1.3	1.2
(T_1 = 0.45 s)	GM Case 3	1.3	1.2	1.4	1.3	1.5	1.3	1.2	1.4
6-story model	GM Case 2	1.5	1.3	1.3	1.1	1.3	1.3	1.4	1.8
(T_1 = 0.75 s)	GM Case 3	1.7	1.9	1.4	1.1	1.3	1.6	1.4	2.0
12-story model	GM Case 2	1.4	1.6	1.2	1.3	1.4	1.4	1.4	1.4
(T_1 = 1.26 s)	GM Case 3	1.3	1.8	1.3	1.1	1.5	1.5	1.8	1.8
18-story model	GM Case 2	1.5	1.4	1.2	1.2	1.5	1.4	1.3	1.6
(T_1 = 1.71 s)	GM Case 3	1.5	1.7	1.6	1.5	1.5	1.3	1.3	1.5

As the best of author knowledge, the similar studies that evaluate the maximum story ductility demand on the various type of fundamental period of vibration, plastic rotation capacity and behaviour factor were not available yet. Therefore the comparison of maximum story ductility is hardly possible to make. Nevertheless, Hatzigeorgiou and Liolios (2010) and Ruiz-Garcia and Negrete-Manriquez (2011) have studied the effect of repeated earthquake on the few models. The former have been focussing on the roof ductility of 3 and 8-story regular RC frame having q = 3.9. This article graphically explained that the maximum interstory drift on the 8-story RC frame with T_1 = 1.23 s was increased about 1.4 to 1.75 times due to seismic sequences. It is meant that the maximum story ductility of that structure increased in the same range of value due to repeated earthquake. Unfortunately, there was no information regarding the type of ground motion they used. Hence, it is assumed that their result was based on general ground motion type so that comparison can be made with current models that having T_1 = 1.26 s and q = 4. Results show that the increment of maximum story ductility demand was within the range of 1.20 to 1.60.

Ruiz-Garcia and Negrete-Manriquez (2011) evaluated 3, and 8-story steel structures (T_1 = 1.23 and 1.95 s) under real and synthetic repeated earthquake. This study graphically demonstrated that the increment of maximum interstory drift reached about 1.23 and 1.14 when synthetic earthquake induced the models with T_1 = 1.23 and 1.95 s, respectively. Unfortunately, there was no information pertain the behaviour factor they have used in the article. Therefore, the average maximum story ductility demand of system having high ductile system i.e. q = 4 to 6 were used and it is found that the increment of about 1.43 due to repeated FDE for system with T_1 = 1.26 s. This result is reasonable since the Ruiz-Garcia and Negrete-Manriquez's

result was based on slightly shorter fundamental period than the current study. Moreover they were using the elasto-plastic strength degrading system as the hysteresis rule of the elements, which was not the same with the system used in the current study. The maximum interstory drift on the model considered in Hatzigeorgiou and Liolios (2010) and Ruiz-Garcia and Negrete-Manriquez (2011) were exhibited in the lower stories, which are well agreed with the current study.

4.6 Prediction of Ductility Demand due to Repeated Earthquake

4.6.1 Roof Ductility Demand

This section explains the prediction of roof ductility demand due to repeated earthquake on the considered inelastic structures using the method discussed in previous chapter. It is found that some parameters namely fundamental period (number of story) and behaviour factor strongly affect the roof ductility demands when repeated earthquake exhibited. Therefore, the data for regression analysis is arranged by fundamental period, T_1, and behaviour factor, q. Although the effect of plastic rotation capacity, θ_p, on the roof ductility demand was indicated its dependency to the other parameters, i.e. T_1 and q, θ_p was used it in order to get clearer picture based on statistical analysis. Two nonlinear parameters of structure to be incorporated namely the ratio of post-yield stiffness, r_K, and the ratio of roof ductility to maximum story ductility capacities, ϑ_c. The parameter r_K reflect the stiffness condition of the system in linear and nonlinear states. It is representing a condition as the building more flexible when the r_K decreases. How much P-Delta affecting the system can also be explained by this parameter, since P-Delta effect on the ratio of post-yield stiffness is increased as the height of building increased. In

regression model, the type of ground motion (FFE and FDE) is not used because they were considered as qualitative variables.

Linear multiple regression analysis is used to obtain regression intercepts (β_0 to β_5) in each bin. Five predictor variables in a first-order regression model are fitted to the mean roof ductility, that affected by repeated FFE, in each bin, as shown in the following equation:

$$Ln(\mu_\Delta) = \beta_0 + \beta_1.T_1 + \beta_2.q + \beta_3.\theta_p + \beta_4.r_K + \beta_5.\vartheta_c + \varepsilon \qquad (4.3)$$

Using least square method, the regression error, ε, obtained for each bin is a zero mean random variable with variance of squared standard deviation.

Before regression analysis conducted, correlation analyses between dependent and predictors variables were preceded in order to define which variables were statistically significance to the considered dependent variable. It is found that the variable of plastic rotation capacity, θ_p, has nothing to do with mean roof ductility demands of inelastic structures affected by repeated FFE and hence this variable was negligible. For repeated FDE, the statistically negligible variables was added with fundamental period of vibration, T_1, and ratio capacity of maximum story ductility to roof ductility, ϑ_c. The model of regression analysis in the next paragraphs was based on the significance level of F-ratio $\approx$ 0.00. The subscripts j and n in notation of maximum story ductility demand, $\mu_{\Delta jn}$, indicate the type of ground motion and case of repetition of earthquake, respectively, which is F for far-field earthquake, D for near-field earthquake having FDE, and 1 to 3 for repeated GM Case 1 to 3, respectively.

As the result, this study proposed empirical relationships to estimate mean roof ductility demand, μ_{Δ}, for inelastic structures affected by repeated FFE GM Case 1, 2, and 3, respectively as follows:

$$Ln(\mu_{\Delta,F1}) = 1.031T_1 + 0.326q - 7.428r_K - 0.188\vartheta_c + 0.809 \quad (4.4)$$

$$Ln(\mu_{\Delta,F2}) = 0.843T_1 + 0.303q - 25.363r_K - 0.082\vartheta_c - 0.281 \quad (4.5)$$

$$Ln(\mu_{\Delta,F3}) = 1.051T_1 + 0.318q - 19.864r_K - 0.190\vartheta_c - 0.082 \quad (4.6)$$

where T_1 is fundamental period of vibration of system within the range of $0.45 \leq T_1 \leq 1.71$ s, q is from 1 to 6, which denotes behaviour factor (so-called force reduction factor or response modification factor), r_K is ratio of global post-yield stiffness to elastic stiffness (0.0004 to 0.0305), and ϑ_c is capacity ratio of story ductility to roof ductility (1.17 to 4.89). Variables of r_K and ϑ_c are determined using POA or using Eq. 2.1 and 2.2 for practical purpose in engineering design and evaluation. The coefficients of determination, R^2, for Eq. 4.4 to Eq. 4.6 are 0.828, 0.844, and 0.844, respectively. As explained previously, R^2 = 1.0 theoretically indicates the best correlation between the analytical and the prediction model variables, and irrelevant predictor variables lead to small values for this coefficient of determination. Moreover, Eq. 4.5 and 4.6 can be presented in the following format, when the repeated earthquake cases of FFE (general case of repeated earthquake) are disregarded (R^2 = 0.876).

$$Ln(\mu_{\Delta,All-1}) = 0.460T_1 + 0.426q - 3.397r_K + 0.025(\vartheta_c) - 1.174 \quad (4.12)$$

$$Ln(\mu_{\Delta,All-23}) = 0.579T_1 + 0.423q - 13.201r_K - 0.036(\vartheta_c) - 0.519 \quad (4.13)$$

It is very important to correlate all data between predicted model with analytical result in order to detect the outliers and the dispersion of correlation data. Therefore, the data based on analytical result (exact) and predicted formula in Figure 4.26 and Figure 4.27 were plotted. The data scatteration in these figures is clearly evident, particularly ductility demand on the system induced by FDE. The scattered data is more apparent as the ductility demand increases. However, the scattered data in evaluating the ductility demand, as shown in these figures, was reasonably accepted because it could not be avoided. The nature of nonlinearity on the considered structures and uncertainty in ground motions are believed as the main parameters influenced to this scattered data (Miranda, 1993; Lam et al., 1998; Hatzigeorgiou, 2010).

The correlation between predicted model and analysis result is depicted in Figure 4.28. It is apparent that the scattered data within the range of $3 \leq \mu_\Delta \leq 6$ of GM Case 1 shows in Figure 4.26a and 4.27a decreases in Figure 4.28a. Similarly, the scattered data within the range of $5 \leq \mu_\Delta \leq 11$ in Figure 4.26b and 4.26c as well as in Figure 4.27b and 4.27c are evidently decreased in Figure 4.28b. The predicted model for RC frames affected by single event earthquake done by Hatzigeorgiou and Liolios (2010) has shown in similar pattern.

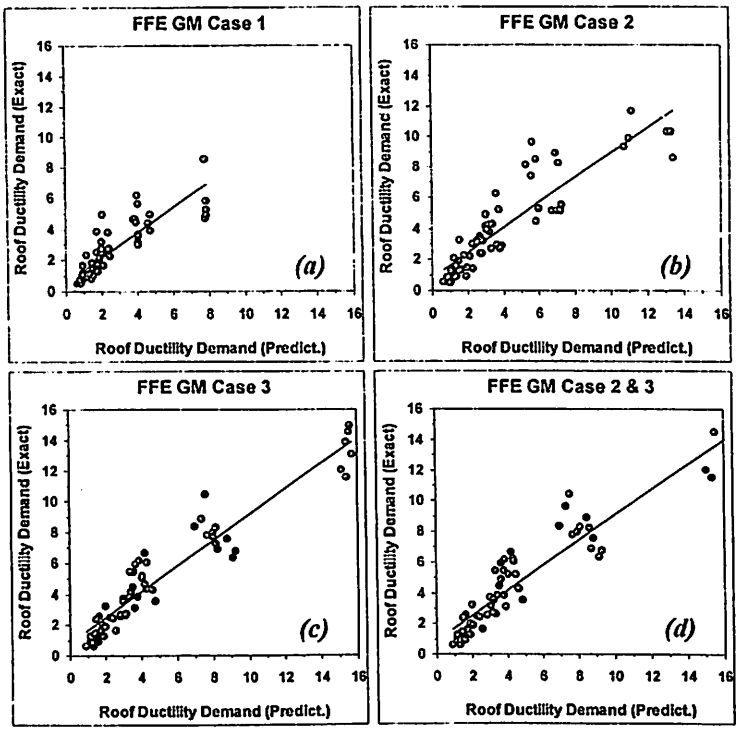

Figure 4.26: Comparison of prediction model with analytical result (exact) of mean roof ductility demand of inelastic structures, μ_Δ, due to repeated FFE

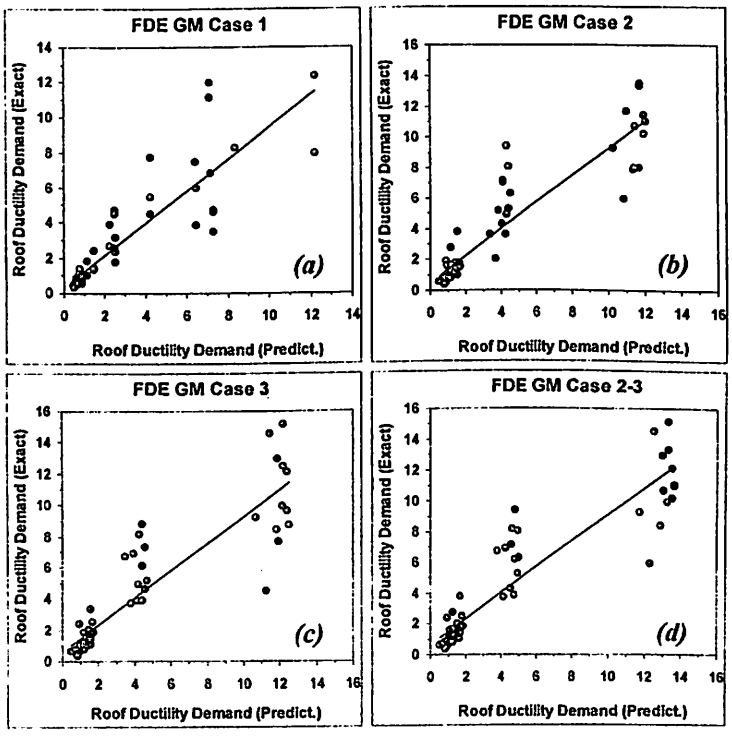

Figure 4.27: Comparison of prediction model with analytical result (exact) of mean roof ductility demand of inelastic structures, μ_Δ, due to repeated FDE

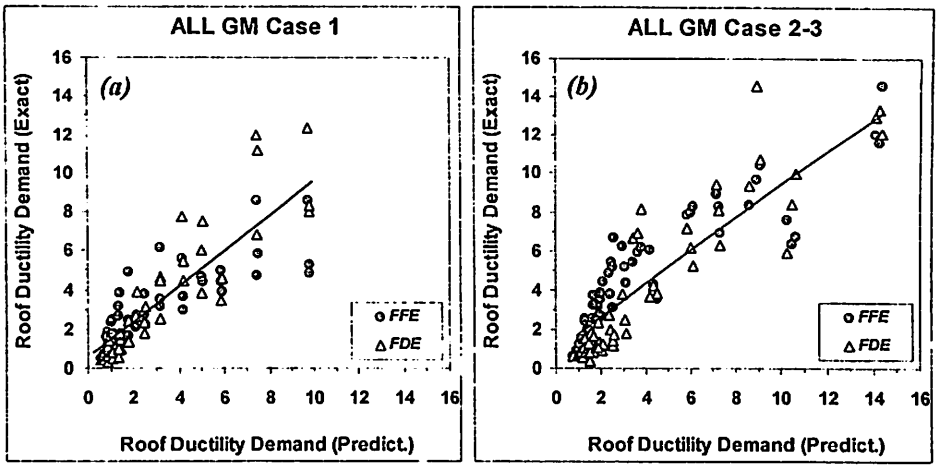

Figure 4.28: Comparison of prediction model with analytical result (exact) of mean roof ductility demand, μ_Δ, due to all type of repeated earthquakes

It is evidence that uncertainty in ground motion (i.e. ground motion type) can affect the dispersion of ductility demand data, as discussed in previous paragraph. From this result, it can be said that the scattered data problem within the range of $3 \leq \mu_\Delta \leq 6$ for the system induced by single event of earthquake can be reduced by the appropriate selection of ground motion type. This insight can be extended to the scattered data problem due to seismic sequences within the range of $5 \leq \mu_\Delta \leq 11$ as well. For higher roof ductility demand, i.e. $\mu_\Delta \geq 11$, other factor influencing the scattered data problem is dominant such as the nonlinearity problem (e.g. P-Delta effect) of the structures.

Sensitivity analysis based on Pearson correlation are found that behaviour factor, q and ratio of post-yield stiffness, r_K, are mainly governed the mean roof ductility demand of the considered inelastic structures affected by FFE as well as FDE in Eq. 4.4 to 4.13. In this case, q is relatively higher than r_K in affecting μ_Δ and both works contrary. It is meant as q increases, the μ_Δ increases, whereas as r_K increases, the μ_Δ decreases. Theoretically, it reflects a correct mechanism, despite the Pearson correlation cannot be used fully to decide the causal relationship between to

random variables, because the drift of system will reduce when the stiffness of system (i.e. r_K) is increased, whereas the drift of system increases as the ductility of system increases (i.e. higher q).

The fundamental period of vibration of system, T_1, and capacity ratio of story ductility to roof ductility, ϑ_c, have weak correlations to μ_Δ and hence their influences are lesser than q and r_K. Both parameters are influencing μ_Δ in the same way, which means the μ_Δ will increase as T_1 and ϑ_c increase. Again, these conditions are theoretically correct because as the height of system (with same stiffness) increases the fundamental period increases and then the drift at roof consequently will increase. Moreover, effect of T_1 and ϑ_c on the system induced by FDE, particularly for seismic sequences GM Case 2 and 3, are very weak and hence negligible as the same as plastic rotation capacity, θ_p. Indirectly, T_1 and θ_p have, however, moderately influenced to the ratio of post-yield stiffness, r_K. This is the case for ϑ_c as well. It is worth to noting that parameters r_K and ϑ_c have strong correlations with T_1, whereas only ϑ_c has strong correlation with q.

In most practical engineering design and evaluation, it is more convenience to have a tool in form of ratio in assessing the effect of two factors on the seismic performance of structures. Therefore the effect of repeated earthquake on the roof ductility demand of inelastic structures can be easily understood in form of the ratio of ductility demand due to repeated earthquakes GM Case 2 or 3 (or both) to the ductility demand induced by repeated earthquakes GM Case 1 [i.e. $ri_{2/1} = Ln(\mu_\Delta)_2 / Ln(\mu_\Delta)_1$; and $ri_{3/1} = Ln(\mu_\Delta)_3 / Ln(\mu_\Delta)_1$, respectively]. Having this ratio, the increment on the drift of structures affected by repeated earthquakes can be simply estimated after conducting a regular procedure in seismic design or evaluation (e.g. multiplying the drift result of linear time history analysis by this ratio).

4.6.2 Maximum Story Ductility Demand

The empirical formulas to estimate of mean maximum story ductility demand, denotes $\mu_{s,jn}$, are found and proposed in this section in the same way as the aforesaid roof ductility demand. The subscripts j and n indicate the terms as mentioned previously. The $\mu_{s,jn}$ of inelastic structures for system induced by repeated far-field earthquake GM Case 1, 2 and 3 can be predicted as follow:

$$Ln(\mu_{s,F1}) = 0.545T_1 + 0.380q - 30.673r_K + 0.220\vartheta_c - 0.585 \quad (4.14)$$

$$Ln(\mu_{s,F2}) = 0.480T_1 + 0.339q - 44.574r_K + 0.230\vartheta_c - 0.053 \quad (4.15)$$

$$Ln(\mu_{s,F3}) = 0.361T_1 + 0.315q - 50.818r_K + 0.318\vartheta_c + 0.135 \quad (4.16)$$

where R^2 of these relationships are found to be 0.926, 0.920, and 0.901, respectively. For the system induced by seismic repetition GM Case 2 or 3, Eq. 4.15 and 4.16 can be merged to the relationship in Eq. 4.17 with $R^2 = 0.910$, as follows:

$$Ln(\mu_{s,F23}) = 0.361T_1 + 0.315q - 51.132r_K + 0.295\vartheta_c + 0.147 \quad (4.17)$$

For the inelastic structures induced by repeated near-field earthquakes with FDE for GM Case 1, 2, and 3, respectively:

$$Ln(\mu_{s,D1}) = 0.274T_1 + 0.589q - 21.812r_K + 0.272\vartheta_c - 1.183 \quad (4.18)$$

$$Ln(\mu_{s,D2}) = 0.355T_1 + 0.601q - 21.019r_K + 0.280\vartheta_c - 1.015 \quad (4.19)$$

$$Ln(\mu_{s,D3}) = 0.518T_1 + 0.620q - 21.693r_K + 0.191\vartheta_c + 0.963 \quad (4.20)$$

Eq. 4.18 to 4.19 are fitted with R^2 equals to 0.898, 0.908, and 0.915, respectively. For the system affected by either double or triple events of seismic sequences FDE, the following expression can be used ($R^2 = 0.912$).

$$Ln(\mu_{s,D23}) = 0.442T_1 + 0.620q - 23.514r_K + 0.229\vartheta_c + 0.931 \quad (4.21)$$

To predict mean maximum story ductility demand of inelastic structures induced by general ground motion type and general repetition case of earthquake (single event and multiple events of earthquakes, respectively), the following relationships for GM Case 1 and GM Case 2-3 are introduced ($R^2 = 0.883$ and 0.870, respectively).

$$Ln(\mu_{s,All-1}) = 0.410T_1 + 0.485q - 26.243r_K + 0.246\vartheta_c - 0.884 \quad (4.22)$$

$$Ln(\mu_{s,All-23}) = 0.402T_1 + 0.467q - 37.323r_K + 0.262\vartheta_c - 0.392 \quad (4.23)$$

The correlation of predicted model in Eq. 4.14 to 4.24 with the analytical result is plotted in Figure 4.29 to 4.31. In general, the scattered data appears in the range of $\mu_{s,max} > 20$ for all GM Cases, which is inevitable, especially at higher ductility level. Nevertheless, it is evident in any case that the results from predicted

4.6.2 Maximum Story Ductility Demand

The empirical formulas to estimate of mean maximum story ductility demand, denotes $\mu_{s,jn}$, are found and proposed in this section in the same way as the aforesaid roof ductility demand. The subscripts j and n indicate the terms as mentioned previously. The $\mu_{s,jn}$ of inelastic structures for system induced by repeated far-field earthquake GM Case 1, 2 and 3 can be predicted as follow:

$$Ln(\mu_{s,F1}) = 0.545T_1 + 0.380q - 30.673r_K + 0.220\vartheta_c - 0.585 \quad (4.14)$$

$$Ln(\mu_{s,F2}) = 0.480T_1 + 0.339q - 44.574r_K + 0.230\vartheta_c - 0.053 \quad (4.15)$$

$$Ln(\mu_{s,F3}) = 0.361T_1 + 0.315q - 50.818r_K + 0.318\vartheta_c + 0.135 \quad (4.16)$$

where R^2 of these relationships are found to be 0.926, 0.920, and 0.901, respectively. For the system induced by seismic repetition GM Case 2 or 3, Eq. 4.15 and 4.16 can be merged to the relationship in Eq. 4.17 with $R^2 = 0.910$, as follows:

$$Ln(\mu_{s,F23}) = 0.361T_1 + 0.315q - 51.132r_K + 0.295\vartheta_c + 0.147 \quad (4.17)$$

For the inelastic structures induced by repeated near-field earthquakes with FDE for GM Case 1, 2, and 3, respectively:

$$Ln(\mu_{s,D1}) = 0.274T_1 + 0.589q - 21.812r_K + 0.272\vartheta_c - 1.183 \quad (4.18)$$

$$Ln(\mu_{s,D2}) = 0.355T_1 + 0.601q - 21.019r_K + 0.280\vartheta_c - 1.015 \quad (4.19)$$

$$Ln(\mu_{s,D3}) = 0.518T_1 + 0.620q - 21.693r_K + 0.191\vartheta_c + 0.963 \quad (4.20)$$

Eq. 4.18 to 4.19 are fitted with R^2 equals to 0.898, 0.908, and 0.915, respectively. For the system affected by either double or triple events of seismic sequences FDE, the following expression can be used ($R^2 = 0.912$).

$$Ln(\mu_{s,D23}) = 0.442T_1 + 0.620q - 23.514r_K + 0.229\vartheta_c + 0.931 \quad (4.21)$$

To predict mean maximum story ductility demand of inelastic structures induced by general ground motion type and general repetition case of earthquake (single event and multiple events of earthquakes, respectively), the following relationships for GM Case 1 and GM Case 2-3 are introduced ($R^2 = 0.883$ and 0.870, respectively).

$$Ln(\mu_{s,All-1}) = 0.410T_1 + 0.485q - 26.243r_K + 0.246\vartheta_c - 0.884 \quad (4.22)$$

$$Ln(\mu_{s,All-23}) = 0.402T_1 + 0.467q - 37.323r_K + 0.262\vartheta_c - 0.392 \quad (4.23)$$

The correlation of predicted model in Eq. 4.14 to 4.24 with the analytical result is plotted in Figure 4.29 to 4.31. In general, the scattered data appears in the range of $\mu_{s,max} > 20$ for all GM Cases, which is inevitable, especially at higher ductility level. Nevertheless, it is evident in any case that the results from predicted

model obtained from this study are in good agreement with those obtained from the well-accepted dynamic inelastic analyses.

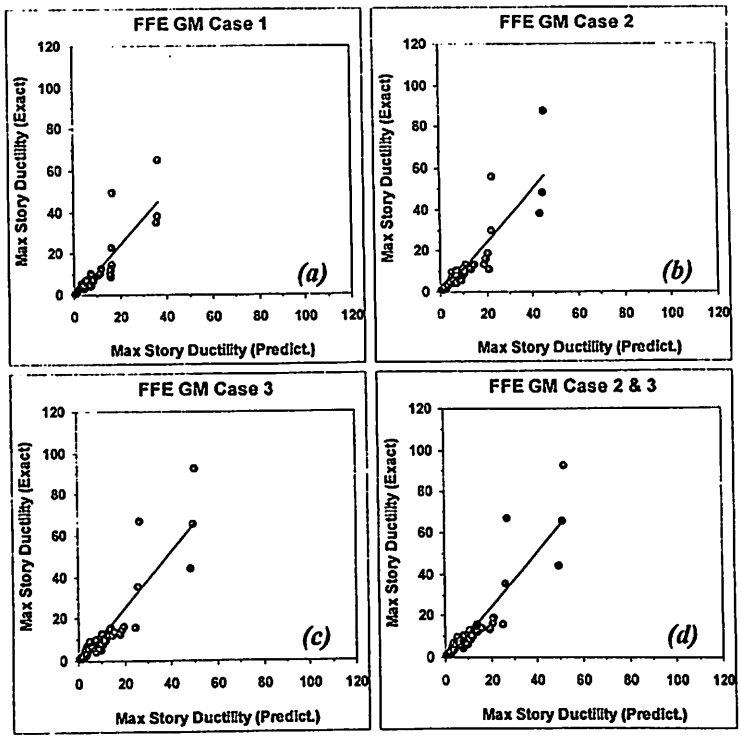

Figure 4.29: Comparison of prediction model with analytical result (exact) of mean roof ductility demand of inelastic structures, $\mu_{s,max}$, due to repeated FFE

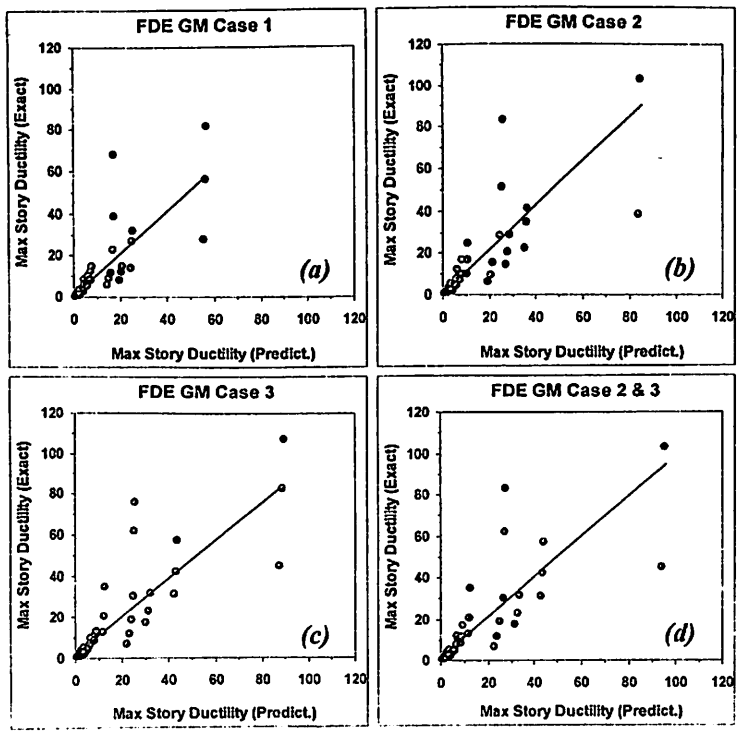

Figure 4.30: Comparison of prediction model with analytical result (exact) of mean roof ductility demand of inelastic structures, $\mu_{s,max}$, due to repeated FDE

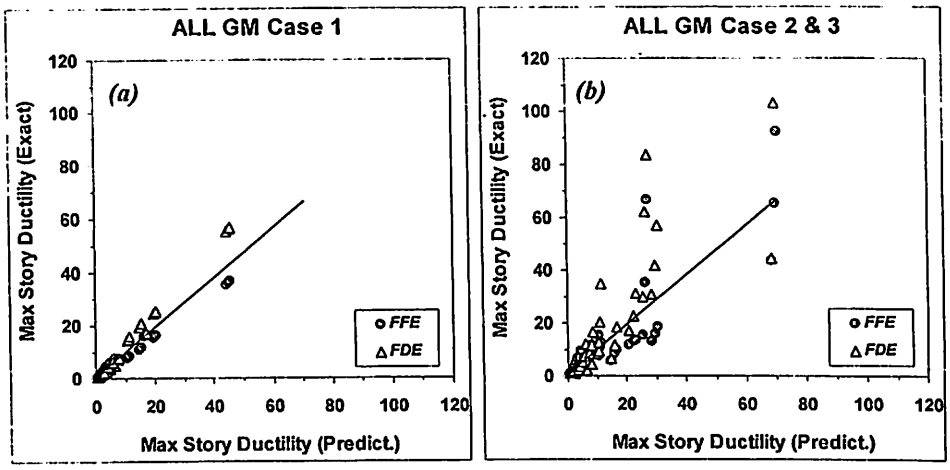

Figure 4.31: Comparison of prediction model with analytical result (exact) of mean maximum story ductility of inelastic structures, $\mu_{s,max}$, due to all type of repeated earthquakes

The sensitivity analysis for the predicted model to define maximum story ductility has found that q and r_K are also play the main roles, as in roof ductility demand. Whilst, the predictor variables of T_1 and ϑ_c have less effect to the mean roof ductility demand of the considered inelastic structures affected by repeated earthquakes.

CHAPTER 5
CONCLUSIONS

5.1 Conclusions

This study investigated the effect of repeated far-field ground motion (FFGM) and near-field ground motion (NFGM) on the ductility demand on the 3D generic multi-degree of freedom (MDOF) systems. The FFGM represented by non-pulse like ground motion namely as far-field earthquake (FFE). The NFGM represented by pulse like ground motion namely as forward directivity effect (FDE). A total of 5 value of behaviour factor representing ductility class low (DCL), ductility class medium (DCM), and ductility class high (DCH) had been considered in developing the 3D generic MDOF frames. The standard pushover analysis (POA) and nonlinear time history analysis (NTHA) had been conducted on the 3D generic MDOF frames. The following subsections describe the conclusions of this study based on all four objectives:

5.1.1 The effect of FFGM and NFGM in repeated earthquakes on the ductility demand of the 3D generic MDOF systems

1. The repeated earthquakes are found to be significantly influenced the roof ductility demand of inelastic structures under consideration. In this case, triple events of repeated earthquake (GM Case 3) is superior to double events of repeated earthquake (GM Case 2).
2. In average, the relative increment of roof ductility due to the repeated earthquake GM Cases 2 and 3, reached 1.5 and 1.7 times, respectively, higher

than the single event earthquake (GM Case 1) regardless the type of ground motion.

3. In average, the relative increment of roof ductility demand due to repeated earthquake FFE is found reach to 1.64 and 1.72 for DCM and DCH behaviour factors, respectively. For the effect of repeated FDE, the relative increment of roof ductility demand is reached 1.48 and 1.52 for DCM and DCH, respectively.

4. The maximum story ductility demand of inelastic structures under consideration is found significantly affected by the repeated earthquakes, as the same as the roof ductility demand. However, the effect of repeated earthquake on the maximum story ductility of models having DCM of $q < 2$ tends to small and can be neglected.

5. The extreme story ductility demand on the structures induced by repeated earthquakes tends to exhibit in the upper level for short structure i.e. 3-story model, with low behaviour factor, regardless the type of ground motion. This maximum demand then migrates to the bottom story as the strength decreases (behaviour factor increases).

6. For taller models, i.e. 6, 12, and 18-story model, all of the extreme story ductility demand due to GM Case 1, 2 and 3 is situated at the bottom story, regardless the type of behaviour factor and ground motion. It is meant the influence of repeated earthquake on the dispersion of maximum story ductility demands is negligible.

7. In average, the repeated earthquake FFE made the relative increment of maximum story ductility demand reached 1.4 and 1.3 times for DCM and DCH behaviour factors, respectively. For the effect of repeated FDE, the

relative increment of maximum story ductility demand experienced 1.4 and 1.5 times for DCM and DCH, respectively

5.1.2 *The effect of oscillatory character, γ, and pulse period, T_p, of repeated NFGM coupled orthogonally with non-pulse NFGM on the ductility demand of 3D generic MDOF systems.*

1. The existence of high velocity pulse in NFE with forward directivity effect clearly requires greater demand compared to residual (ordinary) earthquake. The maximum IDR caused by NFE with forward directivity effect is in range of 0.86% to 94% and from 4% to 102% higher than that caused by residual earthquake for 3 and 18 storey models, respectively.
2. For both 3 and 18 storey models, the difference of maximum IDR between NFE with forward directivity effect and its residual earthquake is increases as further decreasing of strength (high R-factor). It was observed that the magnitude of maximum IDR was clearly amplified as the pulse period, T_p approaching the fundamental period of building, T_1 due to effects of resonance.

5.1.3 *The effect of structure's fundamental period and behaviour factor on the ductility demand of 3D generic MDOF system.*

1. The relative increment of roof ductility demand due to repeated earthquake is not mainly governed by fundamental period of vibration or number of story of the structures. It is meant that short structures having DCM might have relative increment of roof ductility demand larger than tall structures having DCM or DCH and vice versa.

2. In general, the trend of relative increment of roof ductility demand due to repeated earthquakes is arbitrary due to the presence of behaviour factor. However, such cases indicate that the increase of behaviour factor tends to decrease the relative increment as demonstrated by the 12-story models (T_1 = 1.26 s) induced by GM Case 2 and 3 of repeated FDE and 6-story models induced by GM Case 2 and 3 of repeated FFE.

3. The behaviour factor affects the relative increment of maximum story ductility demands due to repeated earthquake. The increase of behaviour factor tends to increase the maximum story ductility demands regardless the types of fundamental period and ground motions.

4. For such case, the relative increment of maximum story ductility demand on the system due to repeated FFE GM Case 2 and 3 tends to decrease as the behaviour factor increases. This trend is clearly evident as the number of story of models (fundamental period) increases, particularly on the 6 and 12-story models.

5. It is not apparent the significance of the change of fundamental period of the models on the relative increment of maximum story ductility demand due to repeated FDE.

6. Structures with DCM behaviour factor induced by repeated FFE experienced higher relative increment of maximum story ductility demand than the structures with DCH behaviour factor. These are found contrary with the structures affected by repeated FDE

5.1.4 *The empirical relation formula for ductility demand of 3D generic MDOF system*

1. The roof ductility demand of inelastic structures affected by GM Case 1, 2, and 3 of repeated FFE and FDE can be predicted through the following expression.

$$Ln(\mu_{\Delta})_n = \beta_0 + \beta_1.T_1 + \beta_2.q + \beta_3.r_K + \beta_4.\vartheta_c \qquad (5.1)$$

where μ_{Δ} is roof ductility demand depend on the type of ground motion and case of seismic sequences of n as listed in Table 5.1, β_0 to β_5 denote coefficients of regression as listed in Table 5.1, T_1 is fundamental period of vibration with the range of application from 0.45 to 1.71 · seconds or equivalent to building having number of story from 3 to 18 using empirical relationship in Eurocode 8, q denotes behaviour factor within the range 1 to 6, r_K denotes global post-yield stiffness ratio, and ϑ_c is global ductility capacity. Parameters of r_K and ϑ_c can be defined through capacity curve of pushover analysis, or predicted using empirical relationship in Eq. 5.2 and 5.3 for practical purpose, respectively.

$$Log(r_K) = -0.508T_1 - 0.135q - 11.252\theta_p - 0.952 \qquad (5.2)$$

$$\vartheta_c = 6.177T_1^3 - 17.543T_1^2 + 16.450T_1 - 3.210 \qquad (5.3)$$

Table 5.1: Coefficients of regression for Eq. 5.1

n	Ground motion type and repeated earthquake cases	β_0	β_1	β_2	β_3	β_4
1	FFE GM Case 1	-0.809	1.031	0.326	-7.482	-0.188
2	FFE GM Case 2	-0.281	0.843	0.303	-25.363	-0.082
3	FFE GM Case 3	-0.082	1.051	0.318	-19.864	-0.190
2-3	FFE GM Case 2/3	-0.106	1.022	0.317	-19.498	-0.160
1	FDE GM Case 1	-1.538	-0.112	0.527	0.688	0.237
2	FDE GM Case 2	-0.411	0	0.486	-27.953	0
3	FDE GM Case 3	-0.381	0	0.487	-28.208	0
2-3	FDE GM Case 2/3	-0.346	0	0.496	-26.660	0
1	FFE/FDE GM Case 1	-1.174	0.460	0.426	-3.397	0.025
2-3	FFE/FDE GM Case 2/3	-0.519	0.579	0.423	-13.201	-0.036

where θ_p denotes plastic rotation capacity in backbone curve of element's plastic hinge definition with the range of application (0.02 to 0.06). It is recommended to use high θ_p for the well-detailed reinforcement of RC system.

2. The effect of repeated earthquake GM Case 2 and 3, or 2-3 on the roof ductility demand can be presented in the relative increment as follows:

$$ri_{2/1} = Ln(\mu_\Delta)_2 / Ln(\mu_\Delta)_1 \quad (5.4)$$

$$ri_{3/1} = Ln(\mu_\Delta)_3 / Ln(\mu_\Delta)_1 \quad (5.5)$$

$$ri_{2\text{-}3/1} = Ln(\mu_\Delta)_{2\text{-}3} / Ln(\mu_\Delta)_1 \quad (5.6)$$

3. The maximum story ductility demand of inelastic structures affected by GM Case 1, 2, and 3 of repeated earthquake FFE and FDE can be estimated through the following expression.

$$Ln(\mu_{s,max})_n = a_0 + a_1.T_1 + a_2.q + a_3.r_K + a_4.\vartheta_c \quad (5.7)$$

where $\mu_{s,max}$ is maximum story ductility demand depend on the type of ground motion. The rest of parameters are the same as aforesaid in previous section, but a_0 to a_5 denote coefficients of regression are listed in Table 5.2.

Table 5.2: Coefficients of regression for Eq. 5.7

n	Ground motion type and repeated earthquake cases	a_0	a_1	a_2	a_3	a_4
1	FFE GM Case 1	-0.585	0.545	0.380	-30.673	0.220
2	FFE GM Case 2	-0.053	0.480	0.339	-44.574	0.230
3	FFE GM Case 3	0.135	0.309	0.309	-50.818	0.318
2-3	FFE GM Case 2/3	0.147	0.361	0.315	-51.132	0.295
1	FDE GM Case 1	-1.183	0.247	0.589	-21.812	0.272
2	FDE GM Case 2	-1.015	0.355	0.601	-21.019	0.280
3	FDE GM Case 3	-0.963	0.518	0.620	-21.693	0.191
2-3	FDE GM Case 2/3	-0.931	0.442	0.620	-23.514	0.229
1	FFE/FDE GM Case 1	-0.884	0.410	0.485	-26.243	0.246
2-3	FFE/FDE GM Case 2/3	-0.392	0.402	0.467	-37.323	0.262

4. The effect of repeated earthquake GM Case 2 and 3, or 2-3, on the roof ductility demand can be predicted in the relative increment as the same as explained in previous paragraphs.

5. The aforesaid empirical relationships are valid only within the range considered in this study namely structures with fundamental period of vibration of $0.45 \leq T_1 \leq 1.71$ s (or 3 to 18 of number of story), DCM and DCH behaviour factors of $1.5 \leq q \leq 6$, plastic rotation capacity of $0.02 \leq \theta_p \leq 0.06$, ratio of maximum story ductility to roof ductility capacities of $1.17 \leq \vartheta_c \leq 4.89$, post-yield stiffness ratio of $3.05\% \leq r_K \leq 0.04\%$, seismic sequences with not more than triple events, and repeated FDE containing single event having motion with pulse effect.

5.3 Suggestion for Future Studies

Although some works have been published recently, the study under the topic of seismic performance of structures induced by repeated earthquakes is still lack and needs more enhancements. Therefore, some suggestions for future studies are as follows:

1. The effect of record-to-record variability of ground motion can be considered.
2. The effect of pulse period in ground motion having forward directivity effect will give benefit to the enhancement of ductility demand prediction.
3. The similar study is also important for other type of structures (e.g. dual-system).
4. The similar study can be carried out using double or triple events seismic sequences with all motion containing large pulse. It is because there was some cases indicated double events of FDE having large pulse.
5. Torsional unbalanced system induced by repeated earthquake can also be considered. It is because many short structures having torsional system.
6. Similar studies focused on elements responses are also important to be considered.

REFERENCES

Akkar, S., Yazgan, U., and Gulkan, P. (2005). Drift estimates in frame buildings subjected to near-fault ground motions. *Journal of Structural Engineering, 131*(7), 1014-1024.

Al-Ali, A. K. A., and Krawinkler, H. (1998). *Effects of vertical irregularities on seismic behaviour of building structures*. Stanford.: Report No. 130, John A. Blume Earthquake Engineering Center, Stanford University.

Alavi, B., and Krawinkler, H. (2001). *Effects of near-fault ground motions on frame structures*: Report No.138, John A. Blume Earthquake Engineering Center, Stanford University.

Alavi, B., and Krawinkler, H. (2004). Behavior of moment-resisting frame structures subjected to near-fault ground motions. *Earthquake Engineering and Structural Dynamics, 33*(6), 687-706.

Amadio, C., Fragiacomo, M., and Rajgelj, S. (2003). The effects of repeated earthquake ground motions on the non linear response of SDOF systems. *Earthquake Engineering and Structural Dynamics, 32*(2), 291-308.

Ambraseys, N., Smit, P., Sigbjörnsson, R., Suhadolc, P., and Margaris, B. (2001). Internet-Site for European Strong-Motion Data. <http://www.isesd.cv.ic.ac.uk>, EVR1-CT-1999-40008.

ASCE. (2005). *Minimum design loads for buildings and other structures, ASCE/SEI 7-05*. Reston, VA.: ASCE.

ATC. (1996). *Seismic Evaluation and Retrofit of Concrete Buildings, ATC-40*. Redwood City: Applied Technology Council.

Baker, J. W. (2007). Quantitative classification of near-fault ground motions using wavelet analysis. *Bulletin of the Seismological Society of America, 97*(5), 1486-1501.

Basu, A. K., and Dar, G. Q. (1982). Dynamic characteristics of coupled wall frame systems. *Earthquake Engineering and Structural Dynamics, 10*(4), 615-631.

Basu, A. K., Guliani, A. K., Bajaj, R. S., and Nagpal, A. K. (1979). Dynamic characteristics of coupled shear walls. *Journal of the Structural Division, 105*(8), 1637-1652.

Bath, M. (1973). *Introduction to seismology*: Springer, Birkhäuser.

Bertero, V. V., Stephen, A. M., and Ricardo, A. H. (1978). Aseismic design implications of near-fault san fernando earthquake records. *Earthquake Engineering and Structural Dynamics, 6*(1), 31-42.

Borzi, B., and Elnashai, A. S. (2000). Refined force reduction factors for seismic design. *Engineering Structures, 22*(10), 1244-1260.

Bray, J. D., and Rodriguez-Marek, A. (2004). Characterization of forward-directivity ground motions in the near-fault region. *Soil dynamics and earthquake engineering, 24*(11), 815-828.

BSSC. (2000). *Prestandard and Commentary for the Seismic Rehabilitation of Buildings, FEMA-356,* . Washington, DC: Federal Emergency Management Agency.

Carr, A. (2008). 3D Ruaumoko: inelastic three-dimensional dynamic analysis program. *Department of Civil Engineering, University of Canterbury, Christchurch.*

CEN. (2004). *Eurocode 8: Design of structures for earthquake resistance. Part 1: General rules, seismic actions and rules for buildings* (Vol. 1). Brussels.: European Committee for Standardization.

Chatterjee, S., and Hadi, A. S. (2006). *Regression analysis by example.* Hoboken: John Wiley and Sons, Inc.

Chintanapakdee, C., and Chopra, A. K. (2003). Evaluation of modal pushover analysis using generic frames. *Earthquake Engineering and Structural Dynamics, 32*(3), 417-442.

Chopra, A., K. , and Chintanapakdee, C. (2001). Comparing response of SDF systems to near-fault and far-fault earthquake motions in the context of spectral regions. *Earthquake Engineering and Structural Dynamics, 30*(12), 1769-1789.

Chopra, A. K. (2006). *Dynamics of structures: theory and applications to earthquake engineering* (3rd ed.). Upper Saddle River,: Prentice Hall.

Coburn, A., and Spence, R. (2002). *Earthquake Protection, 2nd Ed.* Chichester: John Wiley and Sons, Ltd.

Cuesta, I., and Aschheim, M. A. (2001). Isoductile strengths and strength reduction factors of elasto plastic SDOF systems subjected to simple waveforms. *Earthquake Engineering and Structural Dynamics, 30*(7), 1043-1059.

Cuesta, I., Aschheim, M. A., and Fajfar, P. (2003). Simplified R-factor relationships for strong ground motions. *Earthquake spectra, 19*, 25.

Datta, T. K. (2010). *Seismic analysis of structures.* Singapore: John Wiley and Sons (Asia) Pte Ltd.

Draper, N. R., and Smith, H. (1998). *Applied Regression Analysis.* New York: Wiley-Interscience.

Elnashai, A. S., Bommer, J. J., and Martinez-Pereira, A. (1998). *Engineering implications of strong-motion records from recent earthquakes.* Paper presented at the 11th European Conference on Earthquake Engineering.

Elnashai, A. S., and Di Sarno, L. (2008). *Fundamentals of earthquake engineering.* Chichester: John Wiley and Sons.

Esteva, L., and Ruiz, S. E. (1989). Seismic failure rates of multistory frames. *Journal of Structural Engineering, 115*, 268.

Fardis, M. N. (Ed.). (2007). *Guidelines for displacement-based design of buildings and bridges* (Vol. LESSLOSS Report No. 2007/05). Pavia: IUSS Press.

Fardis, M. N. (2009). *Seismic design, assessment and retrofitting of concrete buildings: based on EN-Eurocode 8* (Vol. 8). New York: Springer.

Ibarra, L., and Krawinkler, H. (2005). Global collapse of frame structures under seismic excitations. Report No. 2005/06, Pacific Earthquake Engineering Research Center, University of California at Berkeley.

Ibarra, L. F., Medina, R. A., and Krawinkler, H. (2005). Hysteretic models that incorporate strength and stiffness deterioration. *Earthquake Engineering and Structural Dynamics, 34*(12), 1489-1511.

Iervolino, I., Maddaloni, G., and Cosenza, E. (2008). Eurocode 8 compliant real record sets for seismic analysis of structures. *Journal of Earthquake Engineering, 12*(1), 54-90.

Jalali, R. S., and Trifunac, M. D. (2008). A note on strength-reduction factors for design of structures near earthquake faults. *Soil dynamics and earthquake engineering, 28*(3), 212-222.

Kalkan, E., and Kunnath, S., K. . (2006). Effects of fling step and forward directivity on seismic response of buildings. *Earthquake Spectra, 22*(2), 367-390.

Kappos, A. J. (1999). Evaluation of behaviour factors on the basis of ductility and overstrength studies. *Engineering Structures, 21*(9), 823-835.

Karakostas, C. Z., Athanassiadou, C. J., Kappos, A. J., and Lekidis, V. A. (2007). Site-dependent design spectra and strength modification factors, based on records from Greece. *Soil dynamics and earthquake engineering, 27*(11), 1012-1027.

Karavasilis, T. L., Bazeos, N., and Beskos, D. E. (2007). Behavior factor for performance-based seismic design of plane steel moment resisting frames. *Journal of Earthquake Engineering, 11*(4), 531-559.

Kayal, J. R. (2008). *Microearthquake seismology and seismotectonics of South Asia*. New York: Springer Verlag.

Krawinkler, H., and Al-Ali, A. (1996). Seismic demand evaluation for a 4 story steel frame structure damaged in the Northridge earthquake. *The Structural Design of Tall Buildings, 5*(1), 1-27.

Krawinkler, H., Alavi, B., and Zareian, F. (2005). *Impact of near-fault pulse on engineering design.*

Krawinkler, H., Medina, R., and Alavi, B. (2003). Seismic drift and ductility demands and their dependence on ground motions. *Engineering Structures, 25*(5), 637-653.

Lai, S. S. P., and Biggs, J. M. (1980). Inelastic response spectra for aseismic building design. *Journal of the Structural Division, 106*(6), 1295-1310.

Lee, K., and Foutch, D. A. (2006). Seismic evaluation of steel moment frame buildings designed using different R-values. *Journal of Structural Engineering, 132*, 1461.

Li, S., and Xie, L. (2007). Progress and trend on near-field problems in civil engineering. *Acta Seismologica Sinica, 20*(1), 105-114.

Loh, C. H., Wan, S., and Liao, W. I. (2002). Effects of hysteretic model on seismic demands: consideration of near fault ground motions. *The Structural Design of Tall Buildings, 11*(3), 155-169.

MacRae, G. A., Morrow, D. V., and Roeder, C. W. (2001). Near-fault ground motion effects on simple structures. *Journal of Structural Engineering, 127*(9), 996-1004.

Madan, A., and Hashmi, A. K. (2008). Analytical prediction of the seismic performance of masonry infilled reinforced concrete frames subjected to near-field earthquakes. *Journal of Structural Engineering, 134*(9), 1569-1581.

Makris, N. (1997). Rigidity-plasticity-viscosity: can electrorheological dampers protect base-isolated structures from near-source ground motions? *Earthquake Engineering and Structural Dynamics, 26*(5), 571-591.

Mavroeidis, G. P., and Papageorgiou, A. S. (2003). A mathematical representation of near-fault ground motions. *Bulletin of the Seismological Society of America, 93*(3), 1099-1131.

Mavroeidis, G. P., and Papageorgiou, A. S. (2004). Effect of fault rupture characteristics on near-fault strong ground motions. *Bulletin of the Seismological Society of America, 100*(1), 37-58.

Medina, R. A., and Krawinkler, H. (2003). *Seismic demands for non-deteriorating frame structures and their dependence on ground motions*: Report No. TR 144, John A. Blume Earthquake Engineering Centre, Stanford University.

Medina, R. A., and Krawinkler, H. (2005). Evaluation of drift demands for the seismic performance assessment of frames. *Journal of Structural Engineering, 131*(7), 1003-1013.

Menun, C., and Fu, Q. (2002). *An analytical model for near-fault ground motions and the response of SDOF systems.* Paper presented at the Proceedings 7th U.S. National Conference on Earthquake Engineering, Boston, Massachusetts.

Miranda, E. (1999). Approximate seismic lateral deformation demands in multistory buildings. *Journal of Structural Engineering, 125*(4), 417-425.

Miranda, E., and Bertero, V. V. (1994). Evaluation of strength reduction factors for earthquake-resistant design. *Earthquake spectra, 10*, 357-357.

Miranda, E., and Reyes, C. J. (2002). Approximate lateral drift demands in multistory buildings with nonuniform stiffness. *Journal of Structural Engineering, 128*(7), 840-849.

Mitropoulou, C. C., Lagaros, N. D., and Papadrakakis, M. (2010). Building design based on energy dissipation: a critical assessment. *Bulletin of Earthquake Engineering, 8*, 1375–1396.

Muria Vila, D., and Toro Jaramillo, A. M. (1998). *Effects of several events recorded at a building founded on soft soil.* Paper presented at the 11th European Conference on Earthquake Engineering.

Nakashima, M., Ogawa, K., and Inoue, K. (2002). Generic frame model for simulation of earthquake responses of steel moment frames. *Earthquake Engineering and Structural Dynamics, 31*(3), 671-692.

Nassar, A. A., and Krawinkler, H. (1991). *Seismic demands for SDOF and MDOF systems*: Report No. TR 144, John A. Blume Earthquake Engineering Centre, Stanford University.

Newmark, N. M. (1959). A method of computation for structural dynamics. *Journal of Engineering Mechanics Division, 85*, 67-94.

Newmark, N. M., and Hall, W. J. (1973). Seismic design criteria for nuclear reactor facilities. Report No. 46, Building Practices for Disaster Mitigation, National Bureau of Standards, U. S. Department of Commerce.

Osteraas, J., and Krawinkler, H. (1990). Behavior of steel buildings. *Earthquake spectra, 5*(1), 51-88.

Park, R. (1988). Ductility evaluation from laboratory and analytical testings. *Proceedings of 9th World Conference on Earthquake Engineering*, Tokyo-Kyoto, 605-616.

Paulay, T. (1998). Torsional mechanisms in ductile building systems. *Earthquake Engineering and Structural Dynamics, 27*(10), 1101-1121.

PEER. (2010). PEER NGA Database. from http://peer.berkeley.edu/nga/

Priestley, M. J. N., Calvi, G. M., and Kowalsky, M. J. (2007). *Displacement-based seismic design of structures*. Pavia: IUSS Press.

Rigato, A. B., and Medina, R. A. (2007). Influence of angle of incidence on seismic demands for inelastic single-storey structures subjected to bi-directional ground motions. *Engineering Structures, 29*(10), 2593-2601.

Ruiz-Garcia, J., and Miranda, E. (2005). *Performance-based assessment of existing structures accounting for residual displacements*. Stanford.: Report No. 153, John A. Blume Earthquake Engineering Center, Stanford University.

Ruiz-García, J., and Miranda, E. (2006). Residual displacement ratios for assessment of existing structures. *Earthquake Engineering and Structural Dynamics, 35*(3), 315-336.

Ruiz-García, J., and Negrete-Manriquez, J. C. (2011). Evaluation of drift demands in existing steel frames under as-recorded far-field and near-fault mainshock-aftershock seismic sequences. *Engineering Structures, 33*(2), 621-634.

Salomos, G., Pinto, A., and Dimova, S. (2008). *A review of the seismic hazard zonation in national building codes in the context of Eurocode 8*. Ispra: EUR 23563 EN - 2008, Joint Research Centre.

Seneviratna, G., and Krawinkler, H. (1997). *Evaluation of inelastic MDOF effects for seismic design*: The John A. Blume Earthquake Engineering Center, Stanford University.

Shome, N., Cornell, C. A., Bazzurro, P., and Carballo, J. E. (1998). Earthquakes, records, and nonlinear responses. *Earthquake spectra, 14*(3), 469-500.

Sommerville, P. G. (2003). *Characterization of near fault ground motions for design.* Paper presented at the 5th International Conference: Seismic Bridge Design and Retrofit for Earthquake Resistance, Hilton La Jolla Torrey Pines - La Jolla, California.

Stewart, J. P., Chiou, S. J., Bray, J. D., Graves, R. W., Somerville, P. G., and Abrahamson, N. A. (2002). Ground motion evaluation procedures for performance-based design. *Soil dynamics and earthquake engineering, 22*(9-12), 765-772.

Takada, T., Hwang, H. H. M., and Shinozuka, M. (1988). *Response modification factor for multiple-degree-of-freedom systems*. Paper presented at the Proceedings of Ninth World Conference of Earthquake Engineering.

Taghavi, S., and Miranda, E. (2005). Approximate floor acceleration demands in multistory buildings. II: Applications. *Journal of Structural Engineering, 131*(2), 212-220.

Taranath, B. S. (2005). *Wind and earthquake resistant buildings: structural analysis and design*. New York: Marcel Dekker.

Vidic, T., Fajfar, P., and Fischinger, M. (1994). Consistent inelastic design spectra: strength and displacement. *Earthquake Engineering and Structural Dynamics, 23*(5), 507-521.

Wood, S. L. (1992). Seismic response of R/C frames with irregular profiles. *Journal of Structural Engineering, 118*(2), 545-566.

Yuksel, I., and Polat, Z. (2005). Yield state investigation of reinforced concrete frames from a new point of view. *Engineering Structures, 27*(1), 119-127.

Zareian, F., and Krawinkler, H. (2009). *Simplified performance-based earthquake engineering*. Stanford: Report No. 169, John A. Blume Earthquake Engineering Center, Stanford University.

BSSC. (2000). *Prestandard and Commentary for the Seismic Rehabilitation of Buildings, FEMA-356,* . Washington, DC: Federal Emergency Management Agency.

Carr, A. (2008). 3D Ruaumoko: inelastic three-dimensional dynamic analysis program. *Department of Civil Engineering, University of Canterbury, Christchurch.*

CEN. (2004). *Eurocode 8: Design of structures for earthquake resistance. Part 1: General rules, seismic actions and rules for buildings* (Vol. 1). Brussels.: European Committee for Standardization.

Chatterjee, S., and Hadi, A. S. (2006). *Regression analysis by example.* Hoboken: John Wiley and Sons, Inc.

Chintanapakdee, C., and Chopra, A. K. (2003). Evaluation of modal pushover analysis using generic frames. *Earthquake Engineering and Structural Dynamics, 32*(3), 417-442.

Chopra, A., K. , and Chintanapakdee, C. (2001). Comparing response of SDF systems to near-fault and far-fault earthquake motions in the context of spectral regions. *Earthquake Engineering and Structural Dynamics, 30*(12), 1769-1789.

Chopra, A. K. (2006). *Dynamics of structures: theory and applications to earthquake engineering* (3rd ed.). Upper Saddle River,: Prentice Hall.

Coburn, A., and Spence, R. (2002). *Earthquake Protection, 2nd Ed.* Chichester: John Wiley and Sons, Ltd.

Cuesta, I., and Aschheim, M. A. (2001). Isoductile strengths and strength reduction factors of elasto plastic SDOF systems subjected to simple waveforms. *Earthquake Engineering and Structural Dynamics, 30*(7), 1043-1059.

Cuesta, I., Aschheim, M. A., and Fajfar, P. (2003). Simplified R-factor relationships for strong ground motions. *Earthquake spectra, 19*, 25.

Datta, T. K. (2010). *Seismic analysis of structures.* Singapore: John Wiley and Sons (Asia) Pte Ltd.

Draper, N. R., and Smith, H. (1998). *Applied Regression Analysis.* New York: Wiley-Interscience.

Elnashai, A. S., Bommer, J. J., and Martinez-Pereira, A. (1998). *Engineering implications of strong-motion records from recent earthquakes.* Paper presented at the 11th European Conference on Earthquake Engineering.

Elnashai, A. S., and Di Sarno, L. (2008). *Fundamentals of earthquake engineering.* Chichester: John Wiley and Sons.

Esteva, L., and Ruiz, S. E. (1989). Seismic failure rates of multistory frames. *Journal of Structural Engineering, 115*, 268.

Fardis, M. N. (Ed.). (2007). *Guidelines for displacement-based design of buildings and bridges* (Vol. LESSLOSS Report No. 2007/05). Pavia: IUSS Press.

Fardis, M. N. (2009). *Seismic design, assessment and retrofitting of concrete buildings: based on EN-Eurocode 8* (Vol. 8). New York: Springer.

FEMA. (2005). *Improvement of nonlinear static seismic analysis procedures, FEMA 440.* Washington, DC: Federal Emergency Management Agency.

FEMA. (2009). *Quantification of building seismic performance factors, FEMA P695.* Washington, DC: Federal Emergency Management Agency.

Gillie, J.L., Marek, A.R., and Cole, M.D. (2010). Strength reduction factors for near-fault forward-directivity ground motions. *Journal of Engineering Structures*, 32, pp.273-285.

Goel, R. K., and Chopra, A. K. (1997). Period formulas for moment-resisting frame buildings. *Journal of Structural Engineering, 123*(11), 1454-1461.

Griffith, W. A., and Cooke, M. L. (2004). Mechanical validation of the three-dimensional intersection geometry between the Puente Hills blind-thrust system and the Whittier fault, Los Angeles, California. *Bulletin of the Seismological Society of America, 94*(2), 493.

Gupta, A., and Krawinkler, H. (1999). *Seismic demands for the performance evaluation of steel moment resisting frame structures*: Report No. 132, The John A. Blume Earthquake Engineering Center, Stanford University.

Gupta, A., and Krawinkler, H. (2000). Estimation of seismic drift demands for frame structures. *Earthquake Engineering and Structural Dynamics, 29*(9), 1287-1305.

Hall, J. E., Heaton, T. H., Hailing, M. W., and Wald, D. J. (1995). Near-source ground motion and its effects on flexible buildings. *Earthquake Spectra, 11*, 569-606.

Hart, G. C., and Wong, K. F. (1999). *Structural Dynamic for Structural Engineers*, John Wiley and Sons New York.

Haselton, C. B., Liel, A. B., Lange, S. T., and Deierlein, G. G. (2007). *Beam-column element model calibrated for predicting flexural response leading to global collapse of RC frame buildings.* Berkeley: Report No. 2007/03, Pacific Earthquake Engineering Research Center, University of California at Berkeley.

Hatzigeorgiou, G. D. (2010a). Damping modification factors for SDOF systems subjected to near-fault, far-fault and artificial earthquakes. *Earthquake Engineering and Structural Dynamics, 39*(11), 1239-1258.

Hatzigeorgiou, G. D. (2010b). Ductility demand spectra for multiple near- and far-fault earthquakes. *Soil dynamics and earthquake engineering, 30*(4), 170-183.

Hatzigeorgiou, G. D. (2010c). Behavior factors for nonlinear structures subjected to multiple near-fault earthquakes. *Computers and Structures, 88*(5-6), 309-321.

Hatzigeorgiou, G. D., and Beskos, D. E. (2009). Inelastic displacement ratios for SDOF structures subjected to repeated earthquakes. *Engineering Structures, 31*(11), 2744-2755.

Hatzigeorgiou, G. D., and Liolios, A. A. (2010). Nonlinear behaviour of RC frames under repeated strong ground motions. *Soil dynamics and earthquake engineering, 30*(10), 1010-1025.

Ibarra, L., and Krawinkler, H. (2005). Global collapse of frame structures under seismic excitations. Report No. 2005/06, Pacific Earthquake Engineering Research Center, University of California at Berkeley.

Ibarra, L. F., Medina, R. A., and Krawinkler, H. (2005). Hysteretic models that incorporate strength and stiffness deterioration. *Earthquake Engineering and Structural Dynamics, 34*(12), 1489-1511.

Iervolino, I., Maddaloni, G., and Cosenza, E. (2008). Eurocode 8 compliant real record sets for seismic analysis of structures. *Journal of Earthquake Engineering, 12*(1), 54-90.

Jalali, R. S., and Trifunac, M. D. (2008). A note on strength-reduction factors for design of structures near earthquake faults. *Soil dynamics and earthquake engineering, 28*(3), 212-222.

Kalkan, E., and Kunnath, S., K. . (2006). Effects of fling step and forward directivity on seismic response of buildings. *Earthquake Spectra, 22*(2), 367-390.

Kappos, A. J. (1999). Evaluation of behaviour factors on the basis of ductility and overstrength studies. *Engineering Structures, 21*(9), 823-835.

Karakostas, C. Z., Athanassiadou, C. J., Kappos, A. J., and Lekidis, V. A. (2007). Site-dependent design spectra and strength modification factors, based on records from Greece. *Soil dynamics and earthquake engineering, 27*(11), 1012-1027.

Karavasilis, T. L., Bazeos, N., and Beskos, D. E. (2007). Behavior factor for performance-based seismic design of plane steel moment resisting frames. *Journal of Earthquake Engineering, 11*(4), 531-559.

Kayal, J. R. (2008). *Microearthquake seismology and seismotectonics of South Asia.* New York: Springer Verlag.

Krawinkler, H., and Al-Ali, A. (1996). Seismic demand evaluation for a 4 story steel frame structure damaged in the Northridge earthquake. *The Structural Design of Tall Buildings, 5*(1), 1-27.

Krawinkler, H., Alavi, B., and Zareian, F. (2005). *Impact of near-fault pulse on engineering design.*

Krawinkler, H., Medina, R., and Alavi, B. (2003). Seismic drift and ductility demands and their dependence on ground motions. *Engineering Structures, 25*(5), 637-653.

Lai, S. S. P., and Biggs, J. M. (1980). Inelastic response spectra for aseismic building design. *Journal of the Structural Division, 106*(6), 1295-1310.

Lee, K., and Foutch, D. A. (2006). Seismic evaluation of steel moment frame buildings designed using different R-values. *Journal of Structural Engineering, 132*, 1461.

Li, S., and Xie, L. (2007). Progress and trend on near-field problems in civil engineering. *Acta Seismologica Sinica, 20*(1), 105-114.

Loh, C. H., Wan, S., and Liao, W. I. (2002). Effects of hysteretic model on seismic demands: consideration of near fault ground motions. *The Structural Design of Tall Buildings, 11*(3), 155-169.

MacRae, G. A., Morrow, D. V., and Roeder, C. W. (2001). Near-fault ground motion effects on simple structures. *Journal of Structural Engineering, 127*(9), 996-1004.

Madan, A., and Hashmi, A. K. (2008). Analytical prediction of the seismic performance of masonry infilled reinforced concrete frames subjected to near-field earthquakes. *Journal of Structural Engineering, 134*(9), 1569-1581.

Makris, N. (1997). Rigidity-plasticity-viscosity: can electrorheological dampers protect base-isolated structures from near-source ground motions? *Earthquake Engineering and Structural Dynamics, 26*(5), 571-591.

Mavroeidis, G. P., and Papageorgiou, A. S. (2003). A mathematical representation of near-fault ground motions. *Bulletin of the Seismological Society of America, 93*(3), 1099-1131.

Mavroeidis, G. P., and Papageorgiou, A. S. (2004). Effect of fault rupture characteristics on near-fault strong ground motions. *Bulletin of the Seismological Society of America, 100*(1), 37-58.

Medina, R. A., and Krawinkler, H. (2003). *Seismic demands for non-deteriorating frame structures and their dependence on ground motions*: Report No. TR 144, John A. Blume Earthquake Engineering Centre, Stanford University.

Medina, R. A., and Krawinkler, H. (2005). Evaluation of drift demands for the seismic performance assessment of frames. *Journal of Structural Engineering, 131*(7), 1003-1013.

Menun, C., and Fu, Q. (2002). *An analytical model for near-fault ground motions and the response of SDOF systems.* Paper presented at the Proceedings 7th U.S. National Conference on Earthquake Engineering, Boston, Massachusetts.

Miranda, E. (1999). Approximate seismic lateral deformation demands in multistory buildings. *Journal of Structural Engineering, 125*(4), 417-425.

Miranda, E., and Bertero, V. V. (1994). Evaluation of strength reduction factors for earthquake-resistant design. *Earthquake spectra, 10*, 357-357.

Miranda, E., and Reyes, C. J. (2002). Approximate lateral drift demands in multistory buildings with nonuniform stiffness. *Journal of Structural Engineering, 128*(7), 840-849.

Mitropoulou, C. C., Lagaros, N. D., and Papadrakakis, M. (2010). Building design based on energy dissipation: a critical assessment. *Bulletin of Earthquake Engineering, 8*, 1375–1396.

Muria Vila, D., and Toro Jaramillo, A. M. (1998). *Effects of several events recorded at a building founded on soft soil.* Paper presented at the 11th European Conference on Earthquake Engineering.

Nakashima, M., Ogawa, K., and Inoue, K. (2002). Generic frame model for simulation of earthquake responses of steel moment frames. *Earthquake Engineering and Structural Dynamics, 31*(3), 671-692.

Nassar, A. A., and Krawinkler, H. (1991). *Seismic demands for SDOF and MDOF systems*: Report No. TR 144, John A. Blume Earthquake Engineering Centre, Stanford University.

Newmark, N. M. (1959). A method of computation for structural dynamics. *Journal of Engineering Mechanics Division, 85*, 67-94.

Newmark, N. M., and Hall, W. J. (1973). Seismic design criteria for nuclear reactor facilities. Report No. 46, Building Practices for Disaster Mitigation, National Bureau of Standards, U. S. Department of Commerce.

Osteraas, J., and Krawinkler, H. (1990). Behavior of steel buildings. *Earthquake spectra, 5*(1), 51-88.

Park, R. (1988). Ductility evaluation from laboratory and analytical testings. *Proceedings of 9th World Concference on Earthquake Engineering*, Tokyo-Kyoto, 605-616.

Paulay, T. (1998). Torsional mechanisms in ductile building systems. *Earthquake Engineering and Structural Dynamics, 27*(10), 1101-1121.

PEER. (2010). PEER NGA Database. from http://peer.berkeley.edu/nga/

Priestley, M. J. N., Calvi, G. M., and Kowalsky, M. J. (2007). *Displacement-based seismic design of structures*. Pavia: IUSS Press.

Rigato, A. B., and Medina, R. A. (2007). Influence of angle of incidence on seismic demands for inelastic single-storey structures subjected to bi-directional ground motions. *Engineering Structures, 29*(10), 2593-2601.

Ruiz-Garcia, J., and Miranda, E. (2005). *Performance-based assessment of existing structures accounting for residual displacements*. Stanford.: Report No. 153, John A. Blume Earthquake Engineering Center, Stanford University.

Ruiz-García, J., and Miranda, E. (2006). Residual displacement ratios for assessment of existing structures. *Earthquake Engineering and Structural Dynamics, 35*(3), 315-336.

Ruiz-García, J., and Negrete-Manriquez, J. C. (2011). Evaluation of drift demands in existing steel frames under as-recorded far-field and near-fault mainshock-aftershock seismic sequences. *Engineering Structures, 33*(2), 621-634.

Salomos, G., Pinto, A., and Dimova, S. (2008). *A review of the seismic hazard zonation in national building codes in the context of Eurocode 8*. Ispra: EUR 23563 EN - 2008, Joint Research Centre.

Seneviratna, G., and Krawinkler, H. (1997). *Evaluation of inelastic MDOF effects for seismic design*: The John A. Blume Earthquake Engineering Center, Stanford University.

Shome, N., Cornell, C. A., Bazzurro, P., and Carballo, J. E. (1998). Earthquakes, records, and nonlinear responses. *Earthquake spectra, 14*(3), 469-500.

Sommerville, P. G. (2003). *Characterization of near fault ground motions for design.* Paper presented at the 5th International Conference: Seismic Bridge Design and Retrofit for Earthquake Resistance, Hilton La Jolla Torrey Pines - La Jolla, California.

Stewart, J. P., Chiou, S. J., Bray, J. D., Graves, R. W., Somerville, P. G., and Abrahamson, N. A. (2002). Ground motion evaluation procedures for performance-based design. *Soil dynamics and earthquake engineering, 22*(9-12), 765-772.

Takada, T., Hwang, H. H. M., and Shinozuka, M. (1988). *Response modification factor for multiple-degree-of-freedom systems*. Paper presented at the Proceedings of Ninth World Conference of Earthquake Engineering.

Taghavi, S., and Miranda, E. (2005). Approximate floor acceleration demands in multistory buildings. II: Applications. *Journal of Structural Engineering, 131*(2), 212-220.

Taranath, B. S. (2005). *Wind and earthquake resistant buildings: structural analysis and design*. New York: Marcel Dekker.

Vidic, T., Fajfar, P., and Fischinger, M. (1994). Consistent inelastic design spectra: strength and displacement. *Earthquake Engineering and Structural Dynamics, 23*(5), 507-521.

Wood, S. L. (1992). Seismic response of R/C frames with irregular profiles. *Journal of Structural Engineering, 118*(2), 545-566.

Yuksel, I., and Polat, Z. (2005). Yield state investigation of reinforced concrete frames from a new point of view. *Engineering Structures, 27*(1), 119-127.

Zareian, F., and Krawinkler, H. (2009). *Simplified performance-based earthquake engineering*. Stanford: Report No. 169, John A. Blume Earthquake Engineering Center, Stanford University.

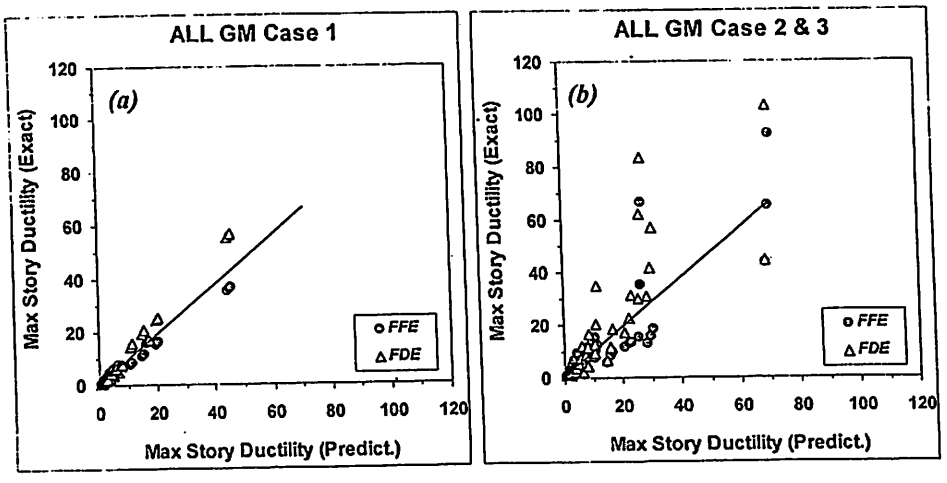

Figure 4.31: Comparison of prediction model with analytical result (exact) of mean maximum story ductility of inelastic structures, $\mu_{s,max}$, due to all type of repeated earthquakes

The sensitivity analysis for the predicted model to define maximum story ductility has found that q and r_K are also play the main roles, as in roof ductility demand. Whilst, the predictor variables of T_1 and ϑ_c have less effect to the mean roof ductility demand of the considered inelastic structures affected by repeated earthquakes.